WORLD METEOROLOGICAL ORGANIZATION

INSTRUMENTS AND OBSERVING METHODS
REPORT No. 106

# WMO FIELD INTERCOMPARISON OF THERMOMETER SCREENS/SHIELDS AND HUMIDITY MEASURING INSTRUMENTS

*Ghardaïa, Algeria, November 2008 – October 2009*

M. Lacombe (France)
D. Bousri (Algeria)
M. Leroy (France)
M. Mezred (Algeria)

WMO/TD-No. 1579
2011

Chairperson, Publications Board
World Meteorological Organization (WMO)
7 bis, avenue de la Paix
P.O. Box 2300
CH-1211 Geneva 2, Switzerland

Tel.: +41 (0) 22 730 84 03
Fax: +41 (0) 22 730 80 40
E-mail: Publications@wmo.int

## FOREWORD

The WMO Combined Intercomparison of Temperature Screens/Shields in Conjunction with Humidity Measuring Instruments was carried out in Ghardaïa, Algeria from November 2008 to October 2009, at the kind invitation of the Algerian Meteorological Service and under the leadership of CIMO. This intercomparison allowed testing the performance of the instruments in desert conditions, in a dry, hot and dusty environment. It was planned to carry out a follow-up intercomparison of similar instruments in an arctic environment at a later stage.

The main objectives of this intercomparison were to gain knowledge on the performance characteristics and operational factors of radiation screens/shields and humidity sensors. This included especially the reliability, accuracy and long-term stability of tested humidity sensors and the estimation of impact of radiation, wind speed, precipitation on humidity measurements inside the different screens/shields. An International Organizing Committee was set up to determine and agree on the rules of the intercomparison and to support its preparation and execution. The IOC was also tasked to agree on the procedures used for the evaluation of the results and to review and agree on their presentation in the final report of the intercomparison.

This report presents in a detailed manner the procedures followed for the data acquisition and the analysis and a comparison of the performance of the instruments relative to the reference. It also contains datasheets for each of the participating instruments, which provide exhaustive information on their performances throughout the intercomparison period, and as a function of different parameters. A number of recommendations were drawn from the results and are directed to users (such as the type of shields to be preferred in desert conditions), to manufacturers, as well as to CIMO for its future activities and conduction of the follow-up intercomparison in arctic environment.

I wish to express my since appreciation, and that of CIMO, to the Algerian Meteorological Service, for hosting this intercomparison, providing suitable facilities and for the support provided by its staff members, in particular to Mrs Djazia Bousri and Mr Mohamed Mezred. I should also like to mention and acknowledge the significant work done by MeteoFrance in analysing the results of the intercomparison, in particular to Mrs Muriel Lacombe and Mr Michel Leroy. Finally, I would like to thank the members of the IOC, who provided regular advice and feed-back on the conduction of the intercomparison and its evaluation.

I am confident that WMO Members and other network managers, as well as data users and manufacturers of such instruments will find this report very useful. It will provide a better understanding of their characteristics and potential use and will contribute to improving temperature and humidity measurements in desert conditions that are of crucial importance among other for climate change monitoring.

B. Calpini

(Prof. B. Calpini)

President
Commission for Instruments and
Methods of Observation

This page left intentionally blank.

# EXECUTIVE SUMMARY

CONDITIONS OF THE COMBINED INTERCOMPARISON

The WMO Field intercomparison of thermometer screens and humidity measuring instruments was held from the 1st of November 2008 to the 31st of October 2009, at the meteorological station of Ghardaïa, Algeria.

The need of a combined intercomparison of thermometer screens/shields and humidity measuring instruments in hot desert conditions was identified in 2003. The site of Ghardaïa, Algeria, was proposed by the Algerian National Weather Service (ONM) and accepted by the ET & IOC in 2006.

This intercomparison hosted:

- 18 different types of screens/shields both ventilated (7) and non-ventilated (11), most of them installed in pairs (the total number being 29);
- 2 wind sensors from the manufacturer Thies (Germany) for evaluating ultrasonic temperature measurement (proposed by DWD);
- 8 different types of humidity sensors, most of them installed in pairs (the total number being 17)

Météo-France supplied calibrated Pt100 probes for most of the screens. All humidity sensors were delivered to Trappes for calibration in agreement with the manufacturers. An on-site calibration was also performed for a subset of the hygrometers.

The ONM prepared the experimental field and installed 36 platforms for the selected screens/shields and the ancillary sensors (radiation sensors, 2-meter wind, ground temperature…).

All data were filtered with quality control procedures. Over the 12 months period of the intercomparison, more than 500 000 minutes of data are available for the majority of the screens and hygrometers, allowing a deep data analysis.

Generally the intercomparison was successful. It experienced problems in its schedule, due to customs constraints and electrical grounding problems at the beginning.

SCREENS/SHIELDS INTERCOMPARISON

All screens were compared to a temperature probe installed in an Eigenbrodt screen (Germany). This probe appeared to be the most convenient after an analysis was done to determine the working reference. But it was warmer than some other screens during periods with high solar radiation and low wind speed. This shows that this screen, though selected as the working reference, also suffered from some radiation error.

The group of four large Stevenson type screens provided very good results though most of them reacted slower than the working reference.

Some small passive multi-plate screens exhibited warmer temperatures than the reference (~0.5℃). Two had results close to the reference. O nly one model gave surprisingly good results, with colder measurements than the reference in case of high solar radiation.

Artificially ventilated screens gave disappointing results, with quite warm temperatures in case of high solar radiation. This may be due to their design and/or some faults in the ventilation during the test (dust and sand reducing the ventilation efficiency).

The air temperature calculated from the Thies ultrasonic anemometers was much colder than all other screens, the absolute difference increasing with solar radiation and decreasing with the wind speed. This indicates that this instrument could be less influenced by radiation than the screens, and thus could be a good candidate for use as a reference. However, a systematic difference between the two sensors, including some scattering, shows either a calibration problem or a principle limitation of the system for measuring air temperature.

Extra analysis gave results during a sand blowing event.

Results are available for an artificially-ventilated screen whose ventilation did not work.

HUMIDITY MEASURING INSTRUMENTS INTERCOMPARISON

Two references were needed for the analysis of humidity measuring sensors. The dew-point hygrometer Thygan was chosen to be the reference initially. After a failure of the transmission module of the Thygan sensors in May 2009, another working reference was chosen: the average of two Vaisala HMP45D installed in the same Eigenbrodt screen. The whole study was conducted with respect to both references.

Though significant differences of temperature were seen between screens, no clear influence on the relative humidity values was detected.

Five models gave very good results over the test period, with no drift (< 0.5%) and more than 98% of the data within ± 3% of the reference. These results are much better than what could be expected from the current knowledge about the state of the art. In addition to the “quality” of the sensors, an explanation may be the mainly dry conditions experienced during the intercomparison. Only few events close to saturation were encountered.

Two models gave medium results.

RECOMMENDATIONS

In desert conditions, non-aspirated, naturally ventilated radiation shields or weather screens may perform better. Aspirated screens using fans tend to be blocked in dusty or sandy environments and may need more frequent maintenance. Manufacturers of artificially ventilated radiation shields are recommended to provide a clear indication of the fan status directly at the screen or its control unit, or the datalogger.

It is recommended that further investigation be conducted on the potential of using ultrasonic devices such as sonic anemometers, as temperature reference systems for screen intercomparisons.

CIMO and manufacturers should aim for a standard laboratory test method to determine the radiation error of weather screens and radiation shields. The proposal is to evaluate the radiation error for a maximum global radiation of 1000W/m$^2$ and a wind speed of 1m/s.

Field intercomparisons of humidity sensors should be performed by using one type of screen for all sensors. They should use a condensation hygrometer as reference system that measures the dew point (or frost point) directly.

Manufacturers of humidity probes should provide a clearly represented quick installation guide (or card) to assist the user in the first phase of operation.

It should be planned to have at least two meetings for each intercomparison: one meeting before the start and one after the end for finalizing the intercomparison report.

Some of the well-performing screens in this intercomparison should also be used in a follow up intercomparison in arctic regions to have a link between both experiments.

In the CIMO guide, a clear distinction should be made between percentages of relative humidity and percentages as an expression for any other quotient.

## ACKNOWLEDGEMENTS

Thanks to all our colleagues of the International Organizing Committee that took part in this intercomparison: Dr Eckhard Lanzinger, Ms Rodica Nitu, Dr Bruce Baker. Their contribution and their expertise during the writing of the final report were precious.

Thanks to all people in Météo-France that were involved in this intercomparison, from calibration of instruments to transportation and customs affairs services.

Thanks to Dr Jérôme Duvernoy, Météo-France, who performed an on-site visit and calibration in Ghardaïa in June 2008 and helped for the beginning of the intercomparison.

Thanks to all people at the ONM in Algiers that were involved in this intercomparison.

Thanks to all the staff of the CNIM that were involved in this intercomparison, for installation, maintenance and customs affairs.

Thanks are extended to the technicians and the observers in Ghardaïa and DRMSE for their precious collaboration.

Thanks to the local authorities of Ghardaïa.

Thanks to the support of CIMO, especially Dr Isabelle Rüedi for organizing all the teleconferences, her predecessor Dr Miroslav Ondráš and Dr Igor Zahumenský for managing the meeting in Ghardaïa, in March 2007.

The authors

This page left intentionally blank.

## TABLE OF CONTENTS

# 1 INTRODUCTION

## 1.1 BACKGROUND

Several intercomparisons of radiation screens/shields with respect to temperature measurements were organized by National Meteorological Services in temperate climatic regions (see for example [10]). Except an EUMETNET test program in icing conditions (EUMETNET SWS II project [7]), no such intercomparison was held in artic and tropical regions. Knowledge of the characteristics of temperature measurements in these regions is particularly important for climatological studies and climate change. As a result of an increasing implementation of automatic weather stations many new screen designs are introduced in the networks.

The effect of screen design was in particular evaluated in WMO IOM report No. 66 [9]. Methods for comparing the performance of thermometer shields/screens are defined in an ISO standard (ISO 17714). [4]

Since the last humidity sensor intercomparison was held by WMO in the period 1985-1989, there was a need to update the knowledge about sensors that are available on the market and are widely used.

This intercomparison was organized by WMO under the auspices of the Commission for Instruments and Methods of Observation (CIMO). An International Organizing Committee (IOC) was setup to overview the conduction of the intercomparison. The measurement period lasted from 1 November 2008 to 30 August 2010.

## 1.2 OBJECTIVES

Defined during the first meeting of the International Organizing Committee (IOC) on Surface Based Intercomparisons held in Trappes in 2003 [1], the main objectives of this intercomparison were agreed on as follows:

a) To update the knowledge on performance characteristics and operational factors of radiation screens/shields tested in the intercomparison;

b) To update the knowledge on performance characteristics and operational factors of humidity sensors tested in the intercomparison;

c) To analyse performance characteristics (especially reliability, accuracy and long-term stability) of tested humidity sensors;

d) To estimate an impact of radiation, wind speed, precipitation on humidity measurements inside the different screens/shields;

e) To improve the accuracy of the humidity measurements using the tested radiation screens/shields;

f) To make available the summary of initial results of the intercomparison within three months after the end of the testing period and to publish the Final Report of the intercomparison within the WMO IOM Report Series within twelve months after the testing is finished;

g) To draft recommendations for consideration by CIMO.

## 1.3 SITE SELECTION

The first joint of the CIMO Expert Team on Surface-based Instrument Intercomparisons and Calibration Methods (ET) and IOC meeting in Trappes (2003) defined and agreed on the organization of the combined intercomparison of thermometer screens/shields, in conjunction with humidity measurements, in various climatic regions. But it was difficult was to find a WMO Member ready to organize such an intercomparison.

Several Regional Instrumentation Centres (RIC) exist and have been set up for various tasks, including international instrument comparisons and evaluations.

Algiers (Algeria) is one of these centres and was willing to develop its activities. In the framework of a bilateral cooperation (France-Algeria), M. Leroy went to Algeria in September 2005, to check with the Algerian Meteorological Service (Office National de Météorologie, ONM), the possibility to host an international intercomparison of thermometer screens/shields including humidity measurements. The organization of such an intercomparison was thought to be an opportunity both to develop the expertise of the RIC of Algiers and to fulfil the objective of the intercomparison. The proposed assistance of another experienced RIC (e.g. Trappes) was seen to be a great advantage, to organize technically the Intercomparison and/or to calibrate the sensors.

Several potential sites were visited in South Algeria : Ghardaïa, El Goléa, Ouargla and Hassi Messaoud. Though not having the most extreme conditions, the site of Ghardaïa appeared to be the most convenient place to organize an intercomparison:

- a large protected test field,
- 2 kilometres from the airport,
- a new observing station and building,
- a local team with a visible motivation for such an operation.

The other sites were directly located on airports and had constraints due to local military activities on the airport.

The climatology of Ghardaïa indicates maximum temperature up to 46℃ in July, relative humidity ranging from less than 10% to 100% during the year.

During the second meeting of the ET & IOC in Geneva in December 2005 [2], these sites were described. The ET & IOC recognized the interest of a test site in Algeria.

WMO wrote a letter to the permanent representative of Algeria to ask for the possibility of hosting an intercomparison. Algeria answered positively. Therefore, the site of Ghardaïa was selected at the beginning of 2006.

# 2 INSTRUMENTS

## 2.1 SELECTION PROCEDURE

The ET/IOC agreed on the procedures for the selection of the participating instruments. It prepared two questionnaires (see Annex 9.1 and 9.2) to assist in the selection procedure. The first one aimed at receiving proposals on potential participants from WMO Members. The second one seeking more detailed information on selected instruments.

Thirty-six responses were received from 19 different countries. Preferences were given to:
- Original physical principles
- Sensors currently used by NWS in hot desert conditions
- Automatic sensors, not manual
- Sensors used in a large number of sites
- Two instruments should be provided

Due to custom problems concerning temporary export to Algeria, the selection was modified in order to have the largest possible number of sensors evaluated during this intercomparison.

Eighteen candidate screens and/or hygrometers were selected during the meeting of the 4th session of the ET/IOC [3].

Screens from manufacturer Metspec could not be delivered in time to Algiers. As ventilated Davis screens had been delivered at the beginning of the test of the acquisition system, it was decided to include them in the participating instruments list, instead of the Metspec screens.

A humidity probe (HMP45DB from Vaisala) was delivered by the Bureau of Meteorology with their screen. As it was possible to log data from the sensor on the data acquisition system, it was decided to include it in the list of participating RH sensors.

The final selection of instruments that participated in this intercomparison included:
- 16 different types of screens/shields both ventilated (7) and non-ventilated (9), most of them installed in pairs (the total number being 29)
- 2 extra wind sensors from manufacturer Thies (Germany) to evaluate ultrasonic temperature measurement, proposed by DWD (see [11]). This would allow to measure the acoustic virtual temperature (no influence from solar radiation) from the sensor. This would also allow the calculation of the air temperature, with additional relative humidity and pressure information
- 8 different types of humidity sensors most of them installed in pairs (the total number being 17)

The list of instruments is available in table 1 and table 2 and in annex 9.3 for a more complete version.

**Table 1. List of participating screens/shields**

| Member country | Manufacturer | Type | Number | Acronym |
|---|---|---|---|---|
| Algeria | Socrima | Large Stevenson Screen | 1 | LSOC |
| Australia | BoM | Small Stevenson screen | 1 | LBOM |
| Austria | Lanser | | 2 | LLAN |
| France | Socrima | BMO1195D | 2 | SSOC |
| Germany | Fischer | 431411 | 2 | VFIS |

| Member country | Manufacturer | Type | Number | Acronym |
|---|---|---|---|---|
| Germany | Vaisala | DTR13 (HMT 330 MIK) | 2 | SVAI |
| Germany | Eigenbrodt | LAM630 | 2 | VEIG |
| Italy | CAE | TU20AS | 2 | SCAE |
| Sudan | Casella | Stevenson Screen | 1 | LCAS |
| Switzerland | Meteolabor | Thygan VTP37 Airport<br>Thygan VTP37 Thermohygrometer | 1<br>1 | VTHY |
| Switzerland | Rotronic | AG/RS12T | 2 | VROT |
| UK/HMEI | Windspeed | T351-PX-D/3 | 2 | SWIN |
| USA | Davis | PN7714 | 2 | SDAV |
| USA | Davis | 07755 | 2 | VDAV |
| USA/HMEI | Young | 41003 | 2 | SYOU |
| USA/HMEI | Young | 43502 | 2 | VYOU |

**Table 2. List of participating RH sensors**

| Member country | Manufacturer | Type in type of screen | Number | Acronym |
|---|---|---|---|---|
| Australia | BoM | HMP45D in BoM screen (LBOM) | 1 | LBOM |
| Germany | Fischer | 431411in Fischer screen (VFIS) | 2 | VFIS |
| Germany | Vaisala | HMT337 | 2 | SVAI |
| Germany | Vaisala | HMP45D in Eigenbrodt screen (VEIG) | 4 | UHMP |
| Germany | Testo | AG/63379742 in small Socrima screen (SSOC) | 2 | UTES |
| Italy | CAE | TU20AS | 2 | SCAE |
| Switzerland | Meteolabor | Thygan VTP37 Airport<br>Thygan VTP37 Thermohygrometer | 1<br>1 | VTHY |
| Switzerland | Rotronic | Hygroclip S3 in Rotronic screen (VROT) | 2 | VROT |

The combined instruments or set of instruments, measuring both the air temperature and the relative humidity, are named with the same acronym in these tables and the various graphs in this report. In the data base, the names of the parameters are suffixed by _T for air temperature and _RH for relative humidity, so they are different. In this report, only the prefix, such as SVAI, was used to shorten the text. As each graph in this report deals with either Air Temperature or RH, there is no real ambiguity with the use of the “common” prefix or acronym. For example, the Vaisala set of instruments (HMT337 + DTR13) is labelled by SVAI. The air temperature analysis deals with temperature SVAI_T, measured in the DTR13 screen. The RH analysis deals with relative humidity, SVAI_RH, measured and calculated from the HMT337 dew point sensor and the DTR13 screen.

## 2.2 PHYSICAL PRINCIPLES

It is well known that temperature and humidity measurements are influenced by a number of environmental parameters, such as:

1. direct and indirect short-wave radiation
2. direct and indirect infrared radiation
3. insufficient natural or artificial ventilation of the air inside the screen
4. psychrometric cooling due to wet surfaces on the screen and/or the sensor
5. the deposit of sand on the outside and inside of the screen and on the sensor especially in Saharan climate.

Humidity probes are also prone to hysteresis effects, i.e. the course of the humidity time series has influence on the humidity measurement as well.

Manufacturers design shields that are made to provide an enclosure with an internal temperature that is both uniform and the same as that of the outside air. It should completely surround the thermometers and exclude radiant heat, precipitation and other phenomena that might influence the measurement.

For these reasons, all the tested screens can be classified as follows.

### 2.2.1 Classification of screens

#### 2.2.1.1 By shape

a) Louvred (caged) screens: These screens are typically Stevenson wooden screens with louvers. The following participating instruments belong to this group: LBOM BoM (Australia); LLAN Lanser (Austria); LCAS Casella (Sudan); LSOC Socrima (Algeria).

b) Round shaped multi-plate screens: These shields are composed of 7 to 12 plates stacked one on another; the plates are mostly round and some of them rectangular. The following participating instruments belong to this group: SDAV and VDAV Davis (USA); VFIS Fischer (Germany); VEIG Eigenbrodt (Germany); SVAI Vaisala (Germany); SYOU 41003 Young (USA); SSOC Socrima (France); SWIN Windspeed (UK).

c) Specific design: These shields have different designs. The following participating instruments belong to this group: VTHY Thygan (Switzerland), SCAE TU20AS (Italy); VROT Rotronic (Switzerland); VYOU 43502 Young (USA).

#### 2.2.1.2 By size

a) Large screens: These are screens with a large internal volume. The following participating instruments belong to this group: LBOM BoM (Australia); LLAN Lanser (Austria); LCAS Casella (Sudan); LSOC Socrima (Algeria).

b) Smaller screens: These are screens with a diameter of 14 to 33cm and a height of 14 to 50cm. The following participating instruments belong to this group: SDAV & VDAV Davis (USA); VFIS Fischer (Germany); VEIG Eigenbrodt (Germany); SVAI Vaisala (Germany); SYOU 41003 Young (USA); SSOC Socrima (France); VTHY Thygan (Switzerland), SCAE TU20AS (Italy); VROT Rotronic (Switzerland); VYOU 43502 Young (USA).

c) Miniature screens: One candidate screen has a diameter of 7.5cm and a height of 15cm: SWIN Windspeed (UK)

2.2.1.3 By ventilation

a) Naturally ventilated screens: These screens are designed so that the air inside is renewed by ambient wind (natural convection). The following participating instruments belong to this group: LBOM BoM (Australia); LCAS Casella (Sudan); LSOC & SSOC Socrima (Algeria); SCAE TU20AS (Italy); SDAV 07714 Davis (USA); SVAI Vaisala (Germany); SYOU 41003 Young (USA); SWIN Windspeed (UK).

b) Artificially ventilated screens: These screens are equipped with a fan that aspirate the air into the screen (forced convection). If the ventilation is well designed, these screens give colder measurements for large irradiance. The following participating instruments belong to this group: VTHY Thygan (Switzerland), VROT Rotronic (Switzerland); VYOU 43502 Young (USA); VDAV 07755 Davis (USA); VFIS Fischer (Germany).

c) Hybrid screens: these screens have ventilation both natural and artificial. This is the case of VEIG Eigenbrodt (Germany) and LLAN Lanser (Austria).

2.2.1.4 By Material

a) Wood: The following participating instruments belong to this group: LBOM BoM (Australia); LCAS Casella (Sudan); LSOC Socrima (Algeria); LLAN Lanser (Austria).

b) Plastic: The following participating instruments belong to this group: SWIN Windspeed (UK); VEIG Eigenbrodt (Germany); SVAI Vaisala (Germany); SSOC Socrima (France); SDAV & VDAV Davis (USA); SYOU & VYOU Young (USA).

c) Metal: The following participating instruments belong to this group: VFIS Fischer (Germany); VTHY Thygan (Switzerland); SCAE TU20AS (Italy); VROT Rotronic (Switzerland).

2.2.2 Classification of hygrometers

The participating humidity sensors can be classified in two main groups:

a) Capacitive sensors: The active part of the humidity sensor consists of a polymer foil sandwiched between two electrodes to form a capacitor. The electrical impedance of this capacitor provides a measure of the relative humidity. The following participating instruments belong to this group: VFIS 431401Fischer (Germany); UTES Testo (Germany); SCAE TU 20AS (Italy); VROT Hygroclip S Rotronic (Switzerland), UHMP HMP45D (Germany), LBOM HMP45DB (Australia), SVAI HMT337 Vaisala (Germany)

b) Dew point sensors: The dewpoint hygrometer is used to measure the temperature at which moist air, when cooled, reaches saturation and a deposit of dew can be detected on a surface at constant pressure. The temperature of this surface is then by definition the dewpoint temperature from which relative humidity can be calculated for any given air temperature. Only VTHY VTP37 Thygan (Switzerland) belongs to this group.

## 2.3 ANCILLARY MEASUREMENTS

The field intercomparison site was equipped with additional meteorological measurements to evaluate the effects of wind and radiation on temperature and humidity measurements.

The meteorological data were provided by the following ancillary measurements (see part 4.2 for positioning of instruments).

### 2.3.1 Wind measurements

Wind measurements at 2-meter height were done using three 2D ultrasonic wind sensors:

- two Thies ultrasonic anemometers
- one Gill Windsonic

**Figure 1. Thies ultrasonic anemometer**

**Figure 2. Gill ultrasonic anemometer**

### 2.3.2 Radiation measurements

Global and infrared radiation was measured with one pyranometer (CM11 from Kipp&Zonen) and one pyrgeometer (CGR4 from Kipp&Zonen) respectively.

An albedometer (CMA11 from Kipp&Zonen) was also installed.

**Figure 3. Albedometer & Pyrgeometer**

**Figure 4. Pyranometer**

The sunshine duration was measured by an heliograph CE181 from Cimel Electronique.


**Figure 5. Heliograph**

### 2.3.3 Additional temperature measurements

Extra temperature probes were installed on the ground, at 10cm and 50 cm-height above the ground.

**Figure 6. Ground, +10cm, +50cm-height temperature probes**

### 2.3.4 Local measurements

Ghardaïa station measurements are made with a Degreane Automatic Weather Station (Xaria). The following parameters are measured: pressure, precipitation, sun duration, wind at 10-meter height, temperature and humidity (1.5-meter height). Pressure, wind and relative humidity were made available for data analysis.

Ghardaïa is also a 24h-manned station. Local observations (present weather, cloudiness) were also available for data analysis.

## 2.4 MAJOR PROBLEMS ENCOUNTERED

### 2.4.1 TU20AS CAE

This screen has a double shield to protect the sensors against the radiation. To improve the natural ventilation, the external shield is partly opened in one direction and must be oriented towards north (in northern hemisphere), to avoid any direct solar radiation on the internal shield.
Though this constraint was indicated in the documentation, the two sensors were mistakenly oriented towards south and the results obtained are not significant at all. Therefore, it was decided in agreement with the manufacturer to skip any data from these screens and the results, non significant at all of this equipment, are excluded from this report, both for temperature and relative humidity.

### 2.4.2 YOUNG artificially ventilated screens (43502)

The data analysis and the field controls showed that the artificial ventilation of these screens was not operative during the first 11 months of the intercomparison. The field control performed on 30$^{th}$ of September 2009 showed that the power supply was out of order. Therefore it was decided to use only the remaining month (October 2009) for the “normal” data analysis. The period with the non operative artificial ventilation was used to illustrate the errors occurring in such conditions.

### 2.4.3 Grounding problems

The organizer had some grounding problems related to the main power supply. It was one reason for the delayed beginning of the intercomparison and the first two months, some problems remained. These problems were identified in the dataset and some small periods with such problems were discarded during the QA process.

### 2.4.4 Acquisition system for sensors with serial outputs

The main acquisition system was suitable only for analog inputs (from the majority of instruments). Some instruments had a numerical output on a serial line, with some specific formats and protocols. For these sensors, a specific software was developed and run on a separate PC with a multiport serial card. It appeared that an internal bug lead to the irregular stopping of the software after few hours or days, needing a manual re-launching of the acquisition program. This drawback explained many missing data from the instruments with a serial output (ATHI, SVAI, VTHY).

# 3 INSTRUMENT CALIBRATION

Prior to the beginning of the field intercomparison almost all temperature and humidity sensors were calibrated at the metrology laboratory of the RIC in Trappes (France). Météo-France had provided calibrated Pt100 probes that are suitable with most of the selected screens/shields. The probes were calibrated in a stirred bath for the following four points: -20℃, 0℃, 20℃ and 40℃. This calibration showed that all probes were within +/- 0.05 K. Therefore, it was decided not to apply any correction to the temperature measurements from these probes. Nevertheless, when available, each datasheet includes information about the calibration of the temperature probe used in the screen.

The temperature probe delivered by Météo-France were mainly calibrated during the beginning of 2006. The instruments delivered by the participants were calibrated during the beginning of 2007, well before the official start of the intercomparison (November 2008).

The calibration results are in the annex 9.4.1. and 9.4.2.

Screens that do not suit the proposed Pt100 were shipped to Trappes, to calibrate the temperature sensor provided by the manufacturers. This was done in agreement with the manufacturer.

All humidity sensors were also delivered to Trappes for calibration. Humidity calibration was carried out in a generating bath. The calibration was made for the following five points of relative humidity: 11%, 33%, 55%, 75% and 90% at two points of temperature: 23℃ and 40℃.

The calibration results are in the annex 9.4.3 and 9.4.4.

It was decided that calibration data would be used to interpret results and not to correct the measurements.

Due to the delayed start of the intercomparison, a limited calibration has been performed on site, with a portable humidity generator (General Eastern Model C1-RH generator) and two relative reference hygrometers (Vaisala HMI31 and HMP35A). Dr J. Duvernoy, responsible of the metrology laboratory of the RIC of Trappes, brought this equipment and performed this calibration in Ghardaïa, during June 2008. Due to the limited time, only a subset of the hygrometers could be calibrated, on a limited numbers of points, corresponding to the calibration points in laboratory of the reference hygrometers.

The calibration results are in the annex 9.4.5.

It was planned to re-calibrate the temperature probes and the hygrometers in the RIC of Trappes, after the end of the intercomparison. But the very long delays due to custom problems to get back the instruments did not allow it before the compilation of the final report.

Therefore, especially for hygrometers, the period of available calibration data is well outside the common limits for hygrometers and reduces the validity of this data to understand possible drifts of the sensors.

# 4 METHODOLOGY AND ORGANIZATION

## 4.1 SITE DESCRIPTION

The city of Ghardaïa is located at 640 km southward of the capital Algiers. The location of Ghardaïa is indicated by the “A” letter on the figure 7.


**Figure 7. General situation of Ghardaïa**

The Intercomparison campaign was held at the meteorological station of Ghardaïa (32°24 N, 03°48 E, 468 meters above the sea level). It is located near the airport of Noumerate, 20 km to the south east of the city center.

To the North-West of the meteorological station lies the town of Ghardaïa (20km); to the East is the airport of Noumerate (1500m); to the North is an open terrain and in the South the national road No. 1. The soil texture is rocky.

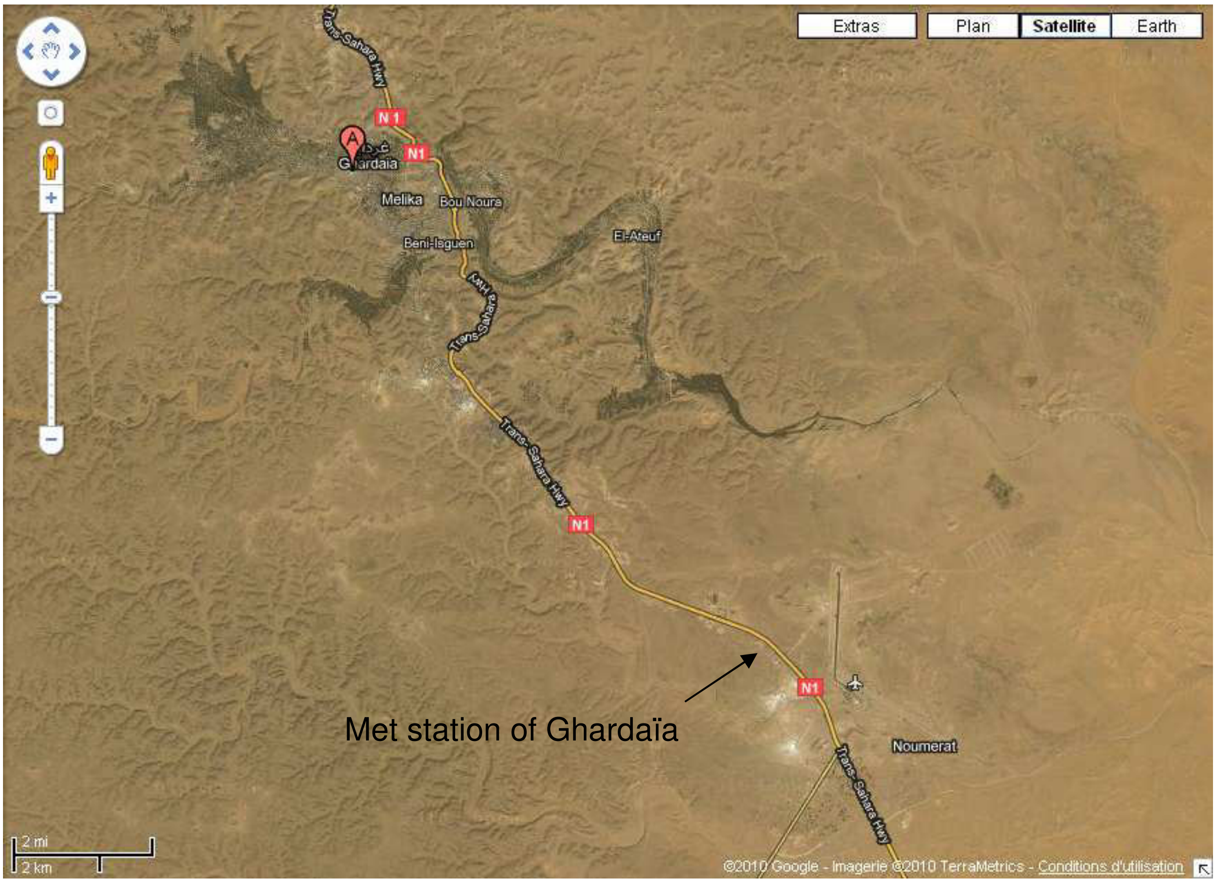


**Figure 8. Satellite view of the Ghardaïa region**

The climate of the city of Ghardaïa is characterized by low annual precipitation, which is extremely variable, varying from 1 mm to over 100 mm.

The annual distribution of temperature is fairly uniform. The average temperatures of summer vary from 40°C to 45°C, and the absolute max imum temperature recorded in Ghardaïa is 47°C in July 2005.

The maximum winds are about 15 m/s, occurring during the spring season, and their directions are predominantly from north-northeast.

In the last decade, the annual average temperatures has shown a slight increase which has a direct impact on the socio-economic life and environment of the area.

The Intercomparison site (figure 9) is a flat area of 1120m$^2$ and it is equipped with 36 small concrete platforms. Each platform is supplied with a power supply of 220 VDC.

**Figure 9. Intercomparison field – Ghardaïa, Algeria**

## 4.2 POSITIONING OF INSTRUMENTS AND INSTALLATION PROCEDURES

The intercomparison site is an area of 1120 $m^2$, configured over a stony and regular soil, which is a feature of the region around Ghardaïa.

The experimental area is situated at more than 30 meters from the meteorological station building, so chosen as to avoid the influence that the building could generate.

The screens and shields under test have been arranged on a rectangular grid with 4 meters between adjacent instruments, as shown on figure 10.

All screens and shields were installed so that the temperature measurement would be at 1.50-meter height above ground level, except for the two LLAN which were installed at 1.80-meter height (the screens were delivered with their stands). For all screens, the maximum tolerance was ± 5% of the height.

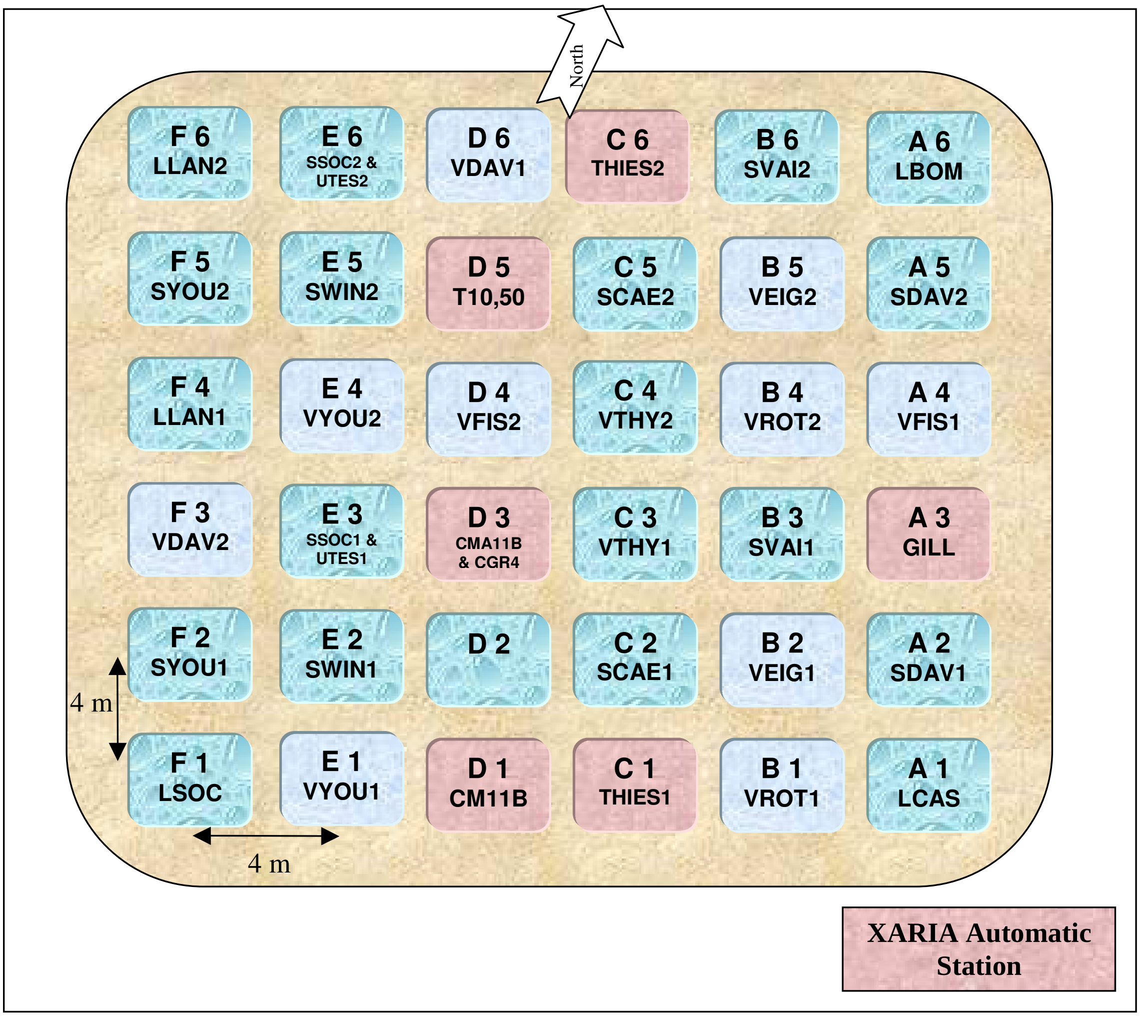


**Screens**

A1 : Casella
A2, A5 : Davis
A4, D4 : Fischer
A6: Stevenson
B1, B4: RS 12T Rotronic
B2, B5: LAM 630 Eigenbrodt
B3, B6: HMT 330 Vaisala
C2, C5: TU 20 AS CAE
C3, C4: VTP 37 Thygan
D6, F3: Davis
E1, E4: Young
E2, E5: T351 Windspeed
E3, E6: Socrima
F1: Large Socrima
F2, F5: Young
F4, F6: Lanser

Ventilated Non-Ventilated

**Ancillary measurements**

A3: Windsonic Gill
C1, C6: Ultrasonic Anemometer 2D
D1: Pyranometer CM11B
D3: Albedometer CMA11 B & pyrgeometer CGR4
D5 : Ground, +10 +50 cm temperatures
Xaria : (P,T,U,RR,SD)

**Figure 10. Positioning of instruments**

The figure 11 gives an overview of the field test before the installation of the instruments.

At each location a small cable box (figure 12) is available, with power and signal cables. Cables are connected to the row connecting box (figure 13). All cables from the test field are eventually connected to the main box (figure 14), before going to the station building. The cable box inside the building is shown on figure 15.

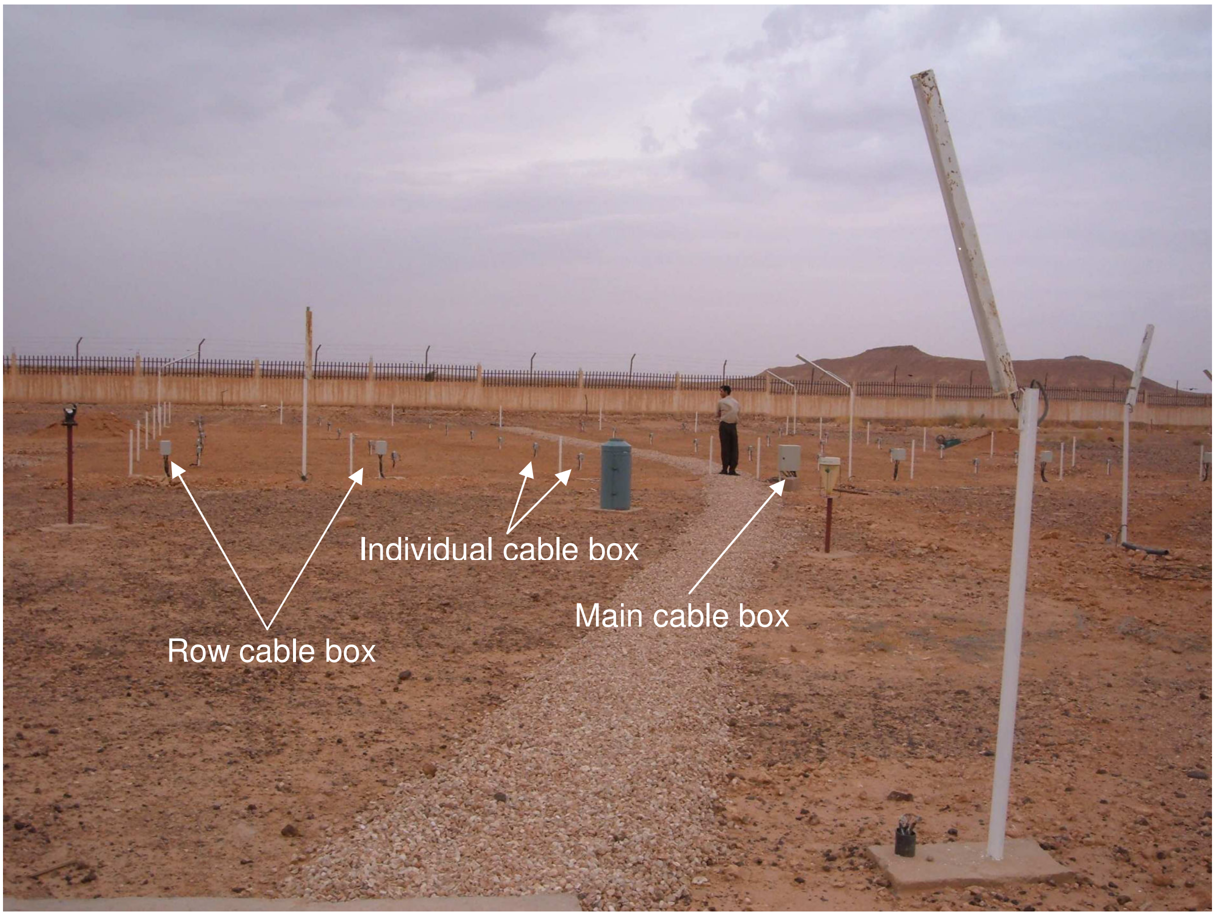


**Figure 11. Overall view of the experimental field**

**Figure 12. Individual box**

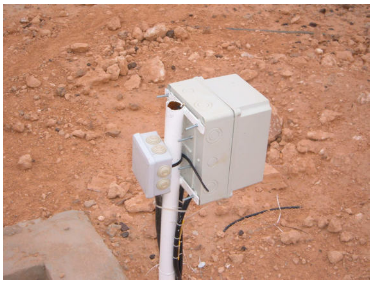

**Figure 13. Row box**

**Figure 14. Main box**

**Figure 15. Main box inside the building**

## 4.3 DATA ACQUISITION

The acquisition of data from sensors and systems under test was done using two systems: one for analogue sensors (data acquisition system) and the other for digital sensors (multi-channel cards).

### 4.3.1 Acquisition of analogue sensors

The acquisition of data from the analogue sensors for the intercomparison was done using a data acquisition system (DAS) manufactured by Yokogawa (Japan). In order to reduce the loss of data, an extra identical DAS has been used for the intercomparison. The main DAS did not experience any trouble during the intercomparison.

The Yokogawa DAS is a complex system that enables the acquisition of analog and digital signals. Each DAS is composed of the following modules:

- three main units, model MW100,
- five universal input modules, model MX110-UNV-M10
- seven four-wire RTD input modules MX110-4VR-M06
- one high speed digital input module model MX115-D05-H10

The system is equipped with a battery and an inverter, as back up for the main power system, to ensure its continuity in operations. To protect data acquisition against mains power failure, PCs and experimental field power are connected to a generator set. This generator switches on automatically in case of a power failure.

Each main unit comes with a Web server function, allowing users to easily enter settings and monitor measured data from a PC using a web browser. The time of the DAS is automatically synchronized with the master PC. Each DAS unit provides daily log files.

The main unit MW100 has a capacity of maximum 6 modules per unit. The measurement interval could vary from 10 ms to 60 s; up to three different intervals can be defined per unit. The unit has one slot for a Compact Flash Type II card, which could store the measurement data, the processed data, and the unit configuration.

The five universal input modules, MX110-UNV-M10 have been used for the acquisition of measurements from sensors with a DC voltage output. Each of these modules has 10 inputs. The highest resolution is 100 µV for 2V measurement range.

The seven four-wire RTD input modules MX110-4VR-M06 were used for the acquisition of data from the Pt100 temperature sensors. Each module has 6 inputs. The maximum resolution is 0.01℃.

The digital input module, model MX115-D05-H10, have 10 inputs per module. The input type is non-voltage contact of 5V level.

**Figure 16. One of the two Data Acquisition Systems**

### 4.3.2 Acquisition of digital sensors

The acquisition of data from the digital instruments was done using two multiport acquisition cards model AccelePort Xr920, manufactured by Digi International. Each of these cards has eight RS232 serial ports, with baud rates up to 921600 bps. Given the fact that the distance between sensors and the acquisition computer exceeds 15 meters, RS232/RS485 converters were used, to ensure the quality of data received.

**Figure 17. AccelePort Xr920 Card**

**Figure 18. RS 232/RS485 Converter**

A dedicated software was developed by Météo-France to acquire the data from all digital sensors.

The acquisition rate for the wind sensors (Thies and Gill) was 2 samples per second. The software processed and recorded one-minute messages with 2-minute and 10-minute averages.

The Thies temperature measurements were stored every 10 seconds and the virtual air temperature was processed later.

### 4.3.3 Synopsis of the system

The figure 19 represents the synopsis of data acquisition.

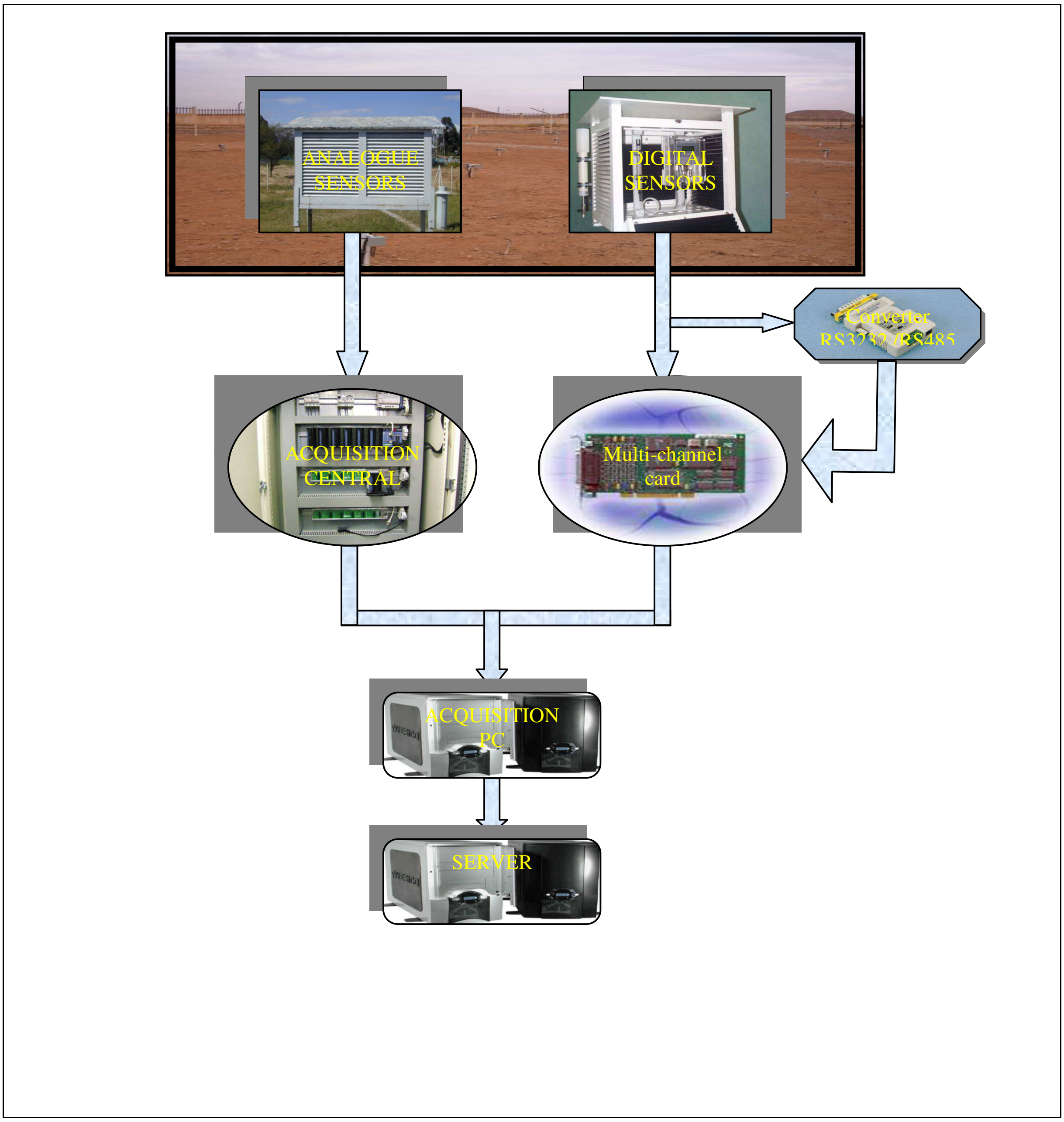


**Figure 19. Synopsis of the acquisition collect**

### 4.3.4 Acquisition during the intercomparison period – Storage procedure

Where feasible, the data sampling interval for the digital sensors and on the data acquisition unit was ten seconds (six samples per minute) .

The acquisition data system was configured to collect and store measurement data in CSV or ASCII format.

The Thygan sensors output one measurement only every ten minutes. For ancillary wind measurement, data sampling rate was two samples per second. Ten-minute and two-minute averages and wind gusts were processed and stored, every minute.

The data collected directly from the sensors has been referred to as the “raw data”. All data were entered in a local BDDGEN database. In March 2007, the ET/IOC agreed to use the specific software package "BDDGEN" to handle and analyze large volume of data. This database system was developed by Météo-France. It is based on binary files.

The raw data and the database binary files were stored on the master computer and on an external hard disk in Ghardaïa. In addition to that, the database binary files were downloaded in Trappes by modem line every month during the intercomparison period.

### 4.4 QUALITY ASSURANCE AND SUPERVISION OF INSTRUMENTS

The local staff performed a daily visual check using the MW100 viewer and the software developed by Météo-France.

Once per month, radiation sensors and solar panels were cleaned. Pictures of the instruments were taken.

All information on visual inspection, maintenance and repair were stored in an electronic local logbook.

### 4.5 DATA POLICY

The following are the guiding principles for data policy of the intercomparison that was agreed by the ET/IOC:

The WMO has the copyright on the intercomparison dataset.

The complete intercomparison dataset is kept by WMO Secretariat, the ET/IOC chair, the Project Leader. WMO may, if requested by the ET/IOC, export whole or part of the comparison dataset on to the CIMO/IMOP website, or other website controlled by the ET/IOC members, as soon as the Final Report is published. In particular, the Data Sheets prepared for each of the instrument involved can be published on the Web site as soon as the Final Report is published.

After the Intercomparison, every participant could get a copy of the comparison dataset, containing any further raw data obtained during the tests, related to its own instruments.

The WMO authorizes the Project Leader with the agreement of the ET/IOC chair, to publish full results in a Final Report of the intercomparison on behalf of the ET/IOC.

The ET/IOC members may publish their partial scientific results if demanded by the scientific community before the end of the intercomparison, provided the publication was authorized by the Project Leader and that the participating instruments remain anonymous in that publication.

The comparison dataset may be provided to other parties for the purpose of scientific studies on the subject. This requires an approval of the ET/IOC chair, and is possible only after the full results of the intercomparison have been published.

For publication and for presentation to third parties, the participants are only allowed to use data of their own instrument. In doing so, they will avoid qualitative assessment of their instruments in comparison with other participating instruments.

# 5 DATA ANALYSIS AND RESULTS

## 5.1 DATA PROCESSING AND QUALITY CONTROL

Data processing for the intercomparison is provided by both BDDGEN software (in Météo-France) and MySQL server (in Algeria).

### 5.1.1 Processing of the 10-second data

The ASCII files generated by the DAS and the numerical sensors acquisition software were locally processed to generate 10-second data. These database binary files were transferred from Ghardaïa to Trappes by modem line every month during the intercomparison period.

Météo-France has developed a specific software to process one-minute averages and quality control for all parameters from the 10-second data. The quality control of data was processed according the specifications of CBS-IOS ET-AWS-4 final report [6]. The main criteria of this report are recalled below.

All data were flagged using five QC categories:

- "0" - good (accurate; data with errors less than or equal to a specified value);
- "1" - inconsistent (one or more parameters are inconsistent; the relationship between different elements does not satisfy defined criteria);
- "2" - doubtful (suspect);
- "3" - erroneous (wrong; data with errors exceeding a specified value);
- "7" - missing data (for any reason).

There should be at least 66% (2/3) of the samples available to compute an instantaneous (one-minute) value. If less than 66% of the samples were available in one minute, the value was flagged as missing.

The table 3 gives the acceptable range and maximum allowed variability for instantaneous values. If a data were outside the acceptable limit, it was flagged as erroneous. The maximum allowed variability of the instantaneous values are also shown for each parameter.

**Table 3. Limits for instantaneous values**

| | | Temperature (°C) | Relative humidity (%) | Global radiation (W/m$^2$) |
|---|---|---|---|---|
| Acceptable range | Minimum value | -5 | 0 | -50 |
| | Maximum value | 50 | 125 | 1600 |
| Maximum variability | Limit for doubtful | 3 | 10 | 800 |
| | Limit for erroneous | 5 | 15 | 1000 |

The software also processed the temperature data from Thies sensors. Their virtual air temperature was corrected with the AWS pressure and relative humidity according to an algorithm developed by the DWD (see References section for more details).

### 5.1.2 MySQL database

MySQL server is a relational database management system that runs as a server providing multi-user access several databases. The server is accompanied by several related scripts that perform setup operations when you install or provide assistance to administer the server.

Single language for describing, manipulating, controlling access and query relational databases is SQL (Structured Query Language). It is a declarative language.

Data are imported into MySQL server. PHP is used to manage, visualizing data imported and to analyze the experimental data according to ISO 17714. Programs in PHP were developed on the website http://www.meteo.dz/meteo.dz/station/index_gha.php. It works with the browser Mozilla Firefox.

### 5.1.3 BDDGEN database

This specific software package called "BDDGEN" was developed by Météo-France to handle and analyze large volume of data.

It includes many programs, such as:

- Visualisation of time series
- Statistical processing: calculation of minima, maxima, sums…
- Statistical charts: histograms, box plots…
- Useful tools: sun height and azimuth processing, filters…

## 5.2 SUMMARY OF AVAILABLE DATA

The field intercomparison has been continuously managed for 12 months in all weather conditions. It was conducted from the 1st of November, 2008 to the 31st of October, 2009.

### 5.2.1 Screens/shields

Figure 20 gives a summary of available temperature data for the intercomparison period for the different quality levels. Numerical values are available in table 4.

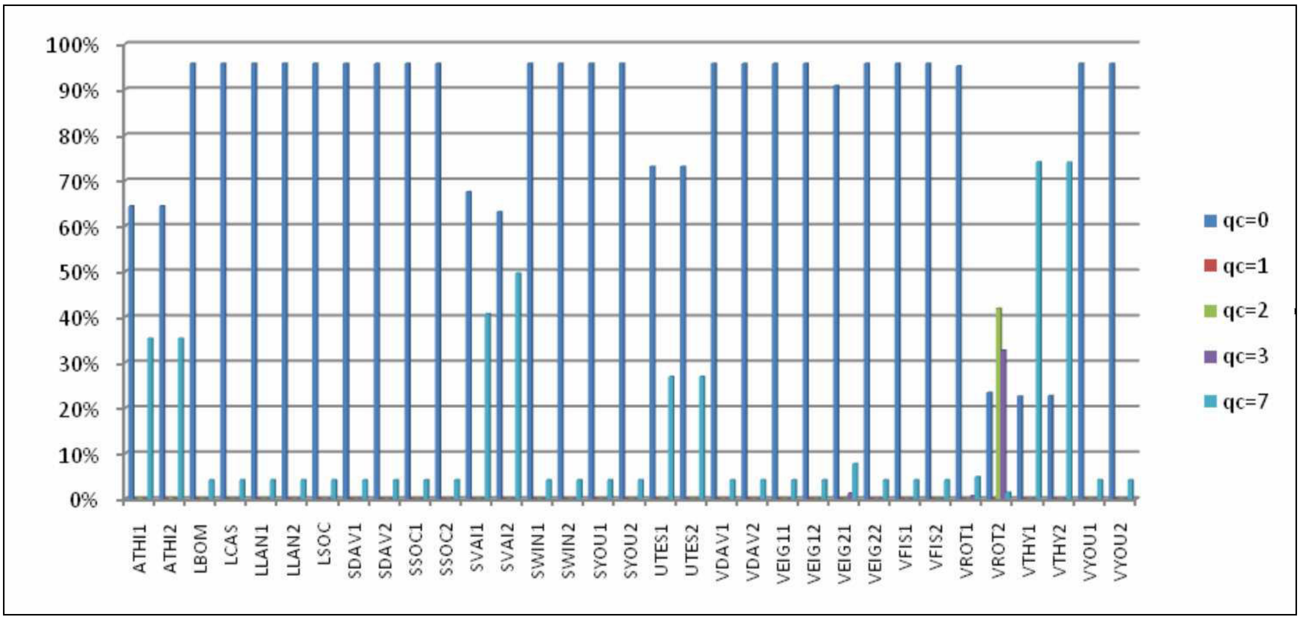


**Figure 20. Temperature quality control information**

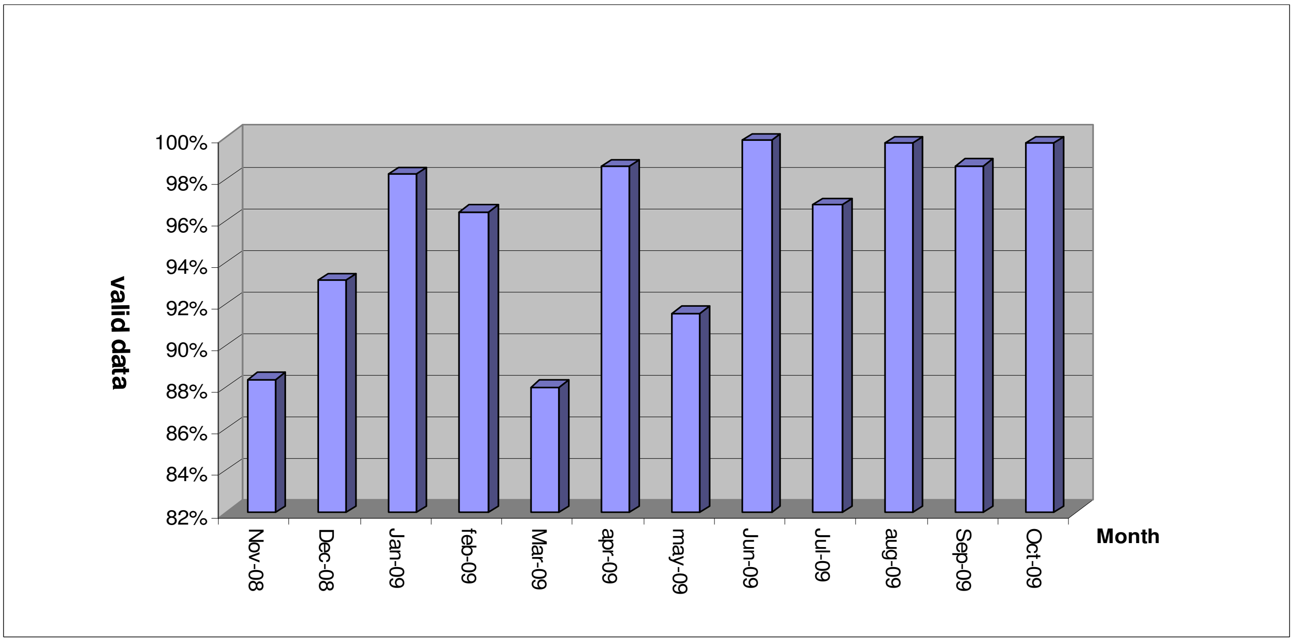


**Figure 21. Data validation by month**

Figure 20 reveals some problems:

– The VROT2 screen provided a signal that was not correlated with temperature. No explanation was found. Therefore, VROT2 is no longer taken into account in the following text;
– The VTHY sensors suffered some critical malfunctions: both gave no values after May 2009 due to a problem of overvoltage.

According to the QC daily reports the maximum total availability of valid data was 95.75%. The following screens gave the highest percentage (95.75%) of valid data for temperature measurements corresponding to more than 500000 minutes for almost each of the screens : LBOM, VFIS1, VDAV2, LCAS, SDAV1 VFIS2, SDAV2, VEIG11, VEIG12, VYOU1, SWIN1, SSOC1, VYOU2, SWIN2, SSOC2, LSOC, SYOU1, VDAV1, LLAN1, SYOU2, LLAN2.

**Table 4. Data availability for screens/shields**

| Screen | QC=0 valid | QC=1 inconsistent | QC=2 doubtful | QC=3 erroneous | QC=7 missing |
|---|---|---|---|---|---|
| ATHI1 | 64.4% | 0.0% | 0.3% | 0.0% | 35.3% |
| ATHI2 | 64.4% | 0.0% | 0.3% | 0.0% | 35.3% |
| LBOM | 95.7% | 0.0% | 0.0% | 0.0% | 4.2% |
| LCAS | 95.7% | 0.0% | 0.0% | 0.0% | 4.2% |
| LLAN1 | 95.7% | 0.0% | 0.0% | 0.0% | 4.2% |
| LLAN2 | 95.7% | 0.0% | 0.0% | 0.0% | 4.2% |
| LSOC | 95.7% | 0.0% | 0.0% | 0.0% | 4.2% |
| SDAV1 | 95.7% | 0.0% | 0.0% | 0.0% | 4.2% |
| SDAV2 | 95.7% | 0.0% | 0.0% | 0.0% | 4.2% |
| SSOC1 | 95.7% | 0.0% | 0.0% | 0.0% | 4.2% |
| SSOC2 | 95.7% | 0.0% | 0.0% | 0.0% | 4.2% |

| Screen | QC=0 valid | QC=1 inconsistent | QC=2 doubtful | QC=3 erroneous | QC=7 missing |
|---|---|---|---|---|---|
| SVAI1 | 67.5% | 0.0% | 0.0% | 0.0% | 40.7% |
| SVAI2 | 63.1% | 0.0% | 0.0% | 0.0% | 49.6% |
| SWIN1 | 95.7% | 0.0% | 0.0% | 0.0% | 4.2% |
| SWIN2 | 95.7% | 0.0% | 0.0% | 0.0% | 4.2% |
| SYOU1 | 95.7% | 0.0% | 0.0% | 0.0% | 4.2% |
| SYOU2 | 95.7% | 0.0% | 0.0% | 0.0% | 4.2% |
| VDAV1 | 95.7% | 0.0% | 0.0% | 0.0% | 4.2% |
| VDAV2 | 95.7% | 0.0% | 0.0% | 0.0% | 4.2% |
| VEIG11 | 95.7% | 0.0% | 0.0% | 0.0% | 4.2% |
| VEIG12 | 95.7% | 0.0% | 0.0% | 0.0% | 4.2% |
| VEIG21 | 90.8% | 0.0% | 0.0% | 1.3% | 7.8% |
| VEIG22 | 95.7% | 0.0% | 0.0% | 0.0% | 4.2% |
| VFIS1 | 95.7% | 0.0% | 0.0% | 0.0% | 4.2% |
| VFIS2 | 95.7% | 0.0% | 0.0% | 0.0% | 4.2% |
| VROT1 | 95.2% | 0.0% | 0.0% | 0.7% | 4.9% |
| VTHY1 | 22.6% | 0.0% | 0.0% | 0.0% | 74.1% |
| VTHY2 | 22.7% | 0.0% | 0.0% | 0.0% | 74.0% |
| VYOU1 | 95.7% | 0.0% | 0.0% | 0.0% | 4.2% |
| VYOU2 | 95.7% | 0.0% | 0.0% | 0.0% | 4.2% |

The average percentage of missing data for the SVAI and ATHI sensors is around 38%. The main reason is frequent failures of the acquisition software, not problems of the sensors. We note more than 73% of missing values for Thygan sensors, due to frequent failures of the acquisition software and the stop of transmission from Thygan sensors from May 2009..

For the above reasons the data of SVAI1, SVAI2, VTHY1, VTHY2, ATHI1 and ATHI2 can only be used for a restricted analysis.

For the screen/shield data analysis, periods lasting at least six hours with steady conditions of cloudiness during day or night were identified. Clear sky is defined by cloudiness less or equal to 1 okta. Overcast sky is defined by cloudiness greater or equal to 7 okta. Table 5 gives the number of events and the total duration for each specific condition.

**Table 5. Identification of specific periods**

| | Day | Night |
|---|---|---|
| Clear sky | 131 events ↔ 1205 hours | 182 events ↔ 1648 hours |
| Overcast | 21 events ↔ 150 hours | 24 events ↔ 187 hours |

The distribution of these events is shown in figure 22. The number of events that occurred during the considered month is indicated above each bar.

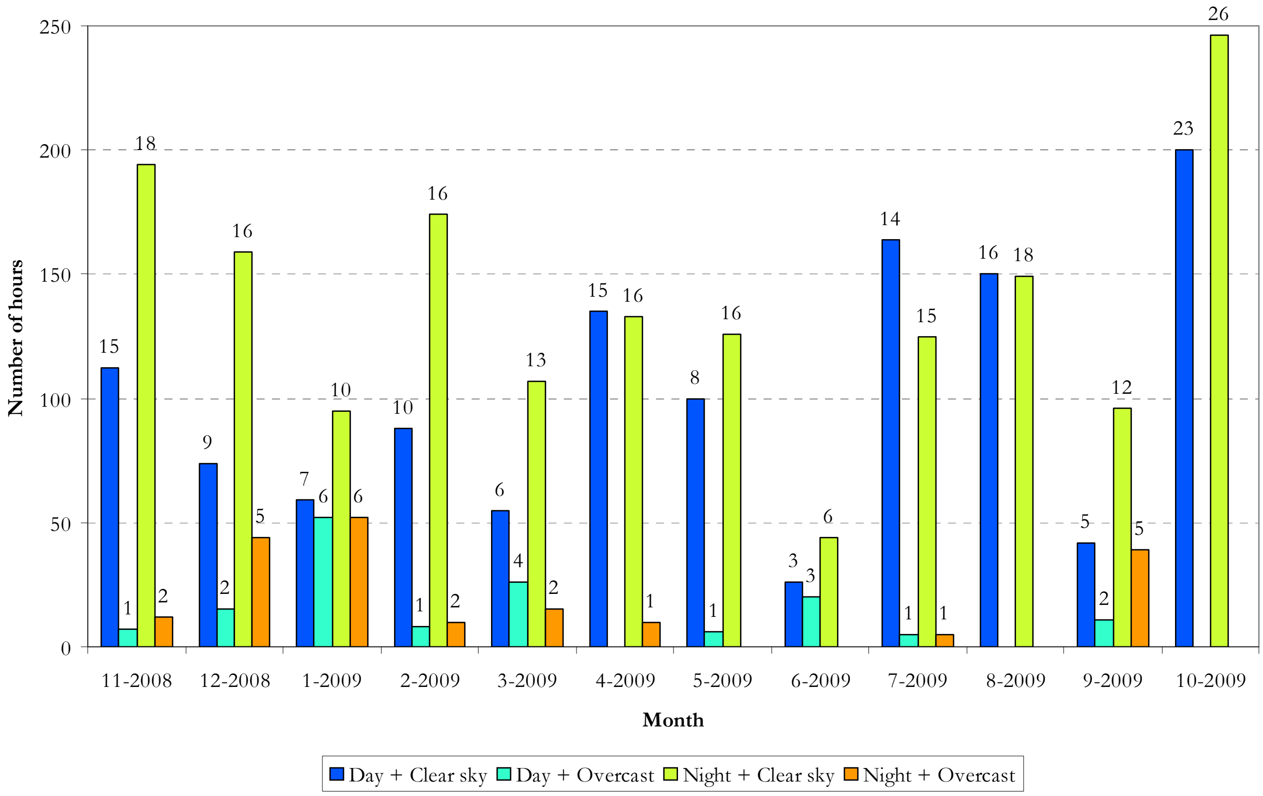


**Figure 22. Distribution of long periods with specific sky conditions.**

### 5.2.2 Humidity sensors

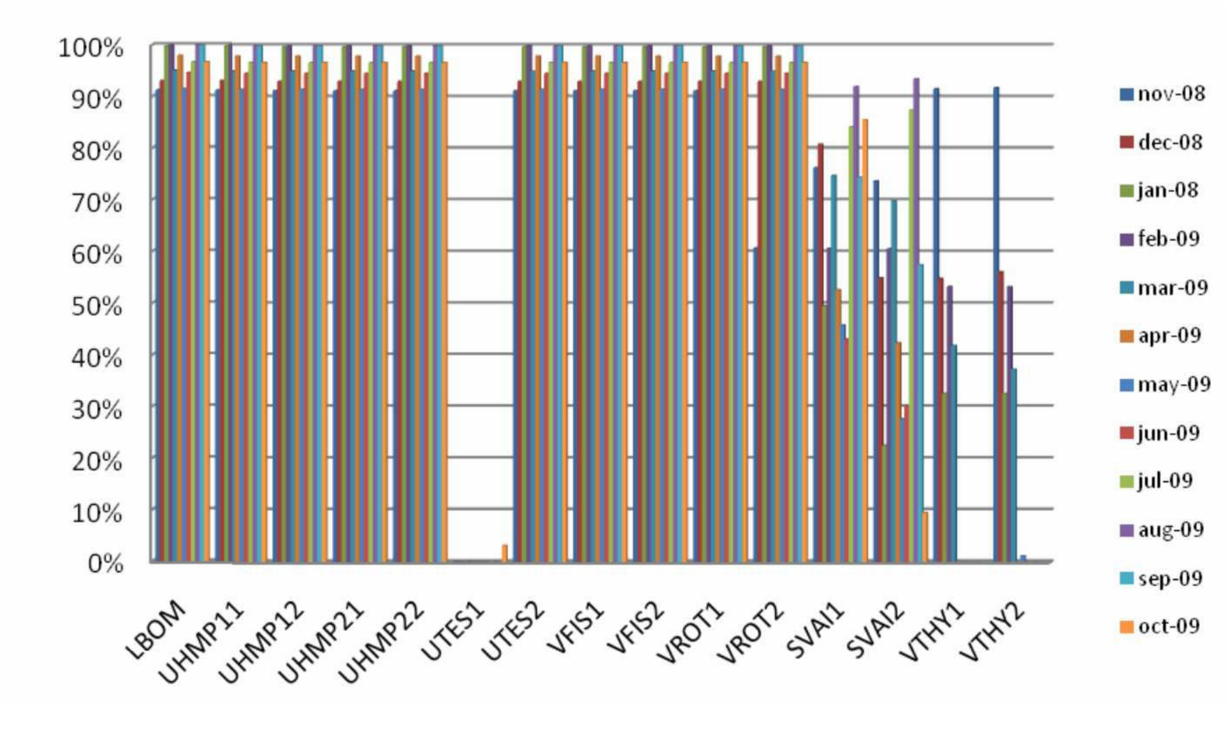


**Figure 23. Total availability for relative humidity sensors**

As shown in figure 23, some critical malfunctions were found:

- UTES1: humidity sensor failed during the whole period of the intercomparison The suspected reason for this fault is a problem of power supply and connection;
- SVAI2: few data received on January, February, April, May and June 2009;
- The dew point hygrometers VTHY1 and VTHY2 suffered from some critical malfunctions: both gave no values after May 2009 due to a problem of overvoltage.

Figure 24 gives a summary of available relative humidity data for the intercomparison period for the different quality levels. Numerical values are available in table 6.

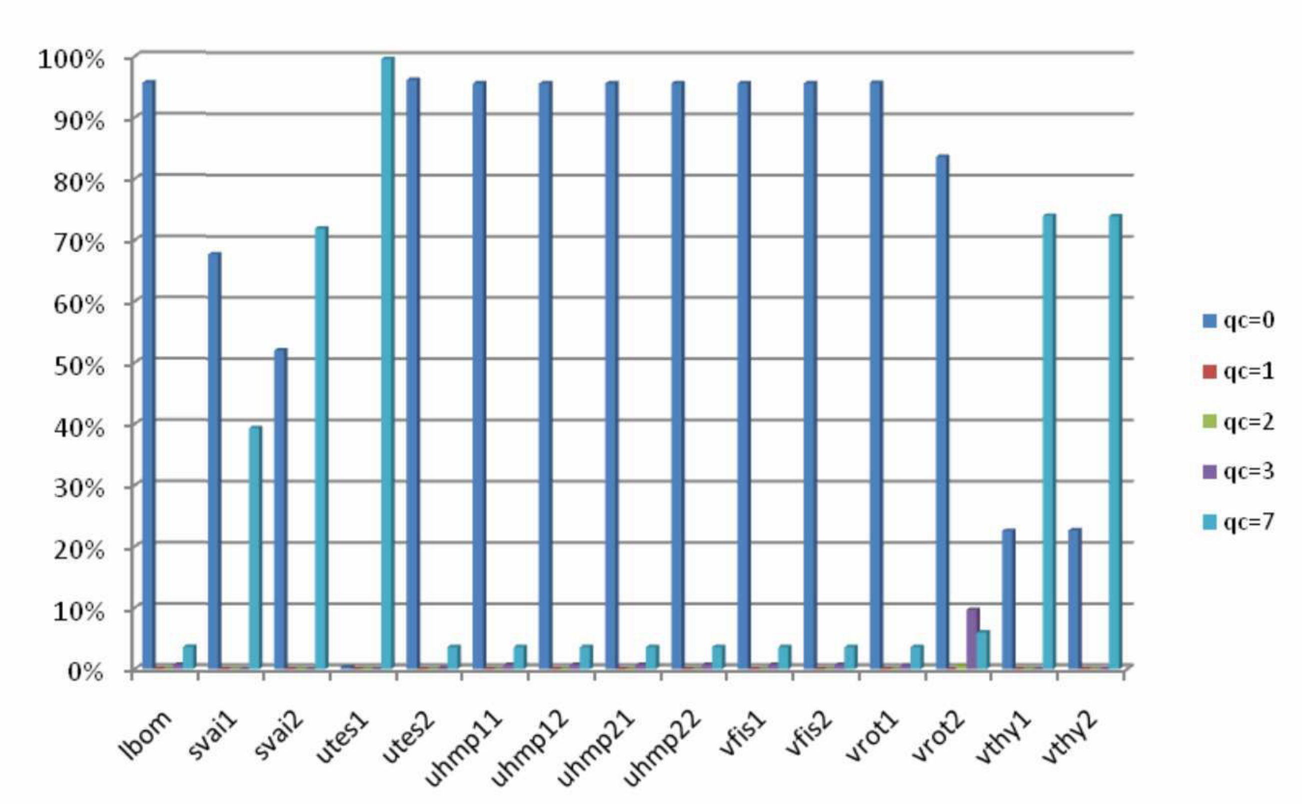


**Figure 24. QC flags of relative humidity sensors**

The percentage of missing data for the screens SVAI1 and SVAI2 amount to 35% up to 59%. The main reason is frequent failures of the acquisition software, not problems of the sensors. Due to these problems and the stop of transmission from Thygan sensors from May 2009, the percentage of missing data for both Thygans is more than 73%.

For this reason the data of the humidity sensors UTES1, VTHY1, VTHY2 and SVAI2 can only be used for a restricted analysis.

**Table 6. Data availability for relative humidity sensors**

| Sensor | QC=0 | QC=1 | QC=2 | QC=3 | QC=7 |
|---|---|---|---|---|---|
| | valid | inconsistent | doubtful | erroneous | missing |
| LBOM | 95.7% | 0.0% | 0.0% | 0.7% | 3.6% |
| SVAI1 | 67.8% | 0.0% | 0.0% | 0.0% | 39.4% |
| SVAI2 | 52.1% | 0.0% | 0.0% | 0.0% | 72.0% |
| UTES1 | 0.0% | 0.0% | 0.0% | 0.0% | 100.0% |
| UTES2 | 96.3% | 0.0% | 0.0% | 0.1% | 3.6% |
| UHMP11 | 95.7% | 0.0% | 0.0% | 0.7% | 3.6% |
| UHMP12 | 95.7% | 0.0% | 0.0% | 0.7% | 3.6% |

| Sensor | QC=0 | QC=1 | QC=2 | QC=3 | QC=7 |
|---|---|---|---|---|---|
| | valid | inconsistent | doubtful | erroneous | missing |
| UHMP21 | 95.7% | 0.0% | 0.0% | 0.7% | 3.6% |
| UHMP22 | 95.7% | 0.0% | 0.0% | 0.7% | 3.6% |
| VFIS1 | 95.7% | 0.0% | 0.0% | 0.7% | 3.6% |
| VFIS2 | 95.7% | 0.0% | 0.0% | 0.7% | 3.6% |
| VROT1 | 95.8% | 0.0% | 0.0% | 0.6% | 3.6% |
| VTHY1 | 22.6% | 0.0% | 0.0% | 0.0% | 74.1% |
| VTHY2 | 22.7% | 0.0% | 0.0% | 0.0% | 74.0% |

### 5.2.3 Ancillary sensors

In figure 25 and figure 26 data availability is shown for each month during the period of intercomparison for global radiation and the wind speed measured by the Gill ultrasonic anemometer.

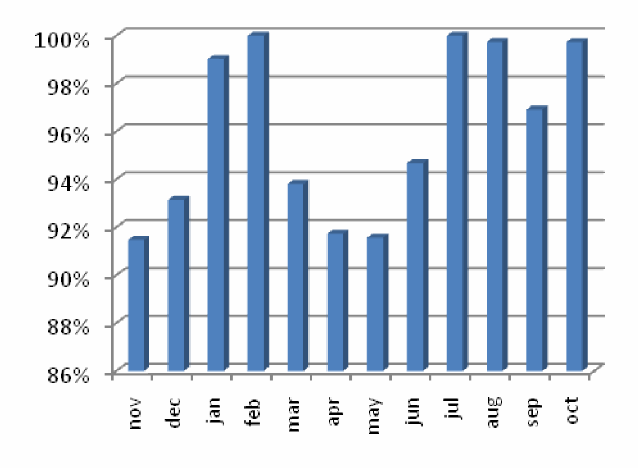


**Figure 25. Total availability for the global radiation**

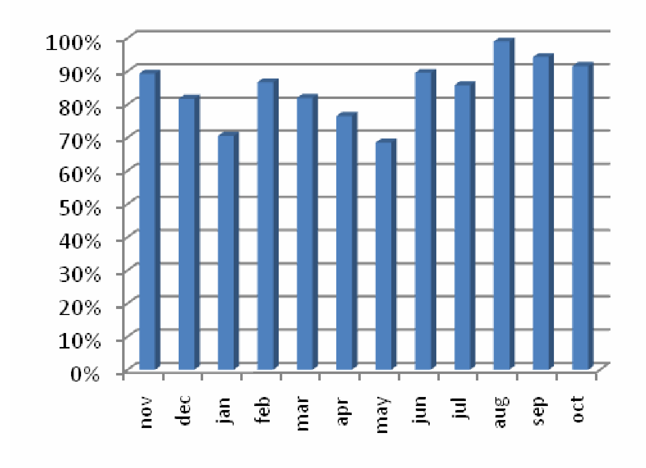


**Figure 26. Total availability for the Gill wind speed**

## 5.3 CLIMATOLOGY OF THE TEST PERIOD

### 5.3.1 Temperatures and relative humidity

The monthly mean temperature of Ghardaïa is 10.4 °C in January and 36.3 °C in July, as shown in figure 27. As shown in figure 28, monthly mean amplitudes of temperatures are more moderate in the winter than in the summer (average 11°C in winter and 13.5°C in summer). They fluctuate around 20°C.

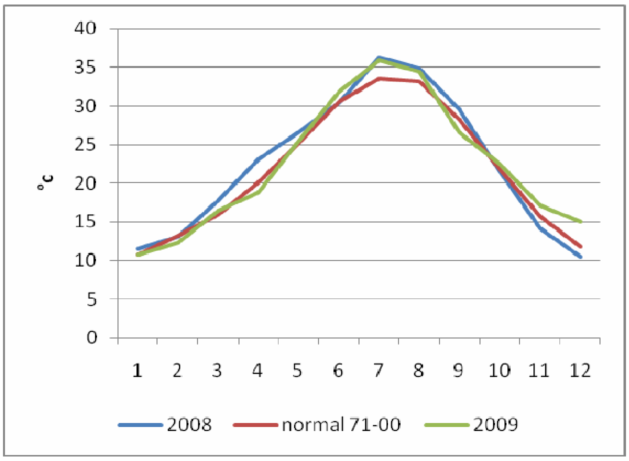


**Figure 27. Monthly mean temperatures**

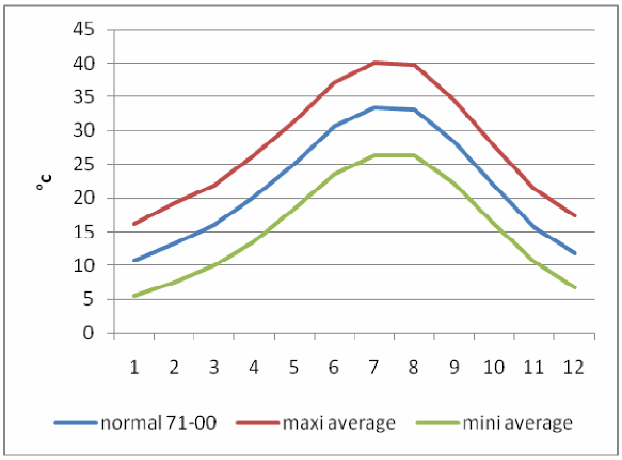


**Figure 28. Monthly mean thermal amplitudes**

The daily extreme temperatures are calculated from the valid 1-minute values.

The maximum temperature Tx of day D is the warmest temperature between day D 06:01 and day D+1 06:00.

The minimum temperature Tn of day D is the coldest temperature between day D-1 18:01 and day D 18:00.

Each day, both Tn and Tx are validated when at least 1430 of the 1440 possible values are valid (QC=0). A special rule is applied to SVAI screens: due to acquisition problems, about 10% of their 1-minute values are not available (about one missing value every 10 minutes), so Tn and Tx are computed if at least 1300 of the 1440 daily 1-minute values are valid.

The plot of the daily maximum and minimum temperatures during the test period is given in the figure 29. These data were measured by the VEIG22 temperature sensor.

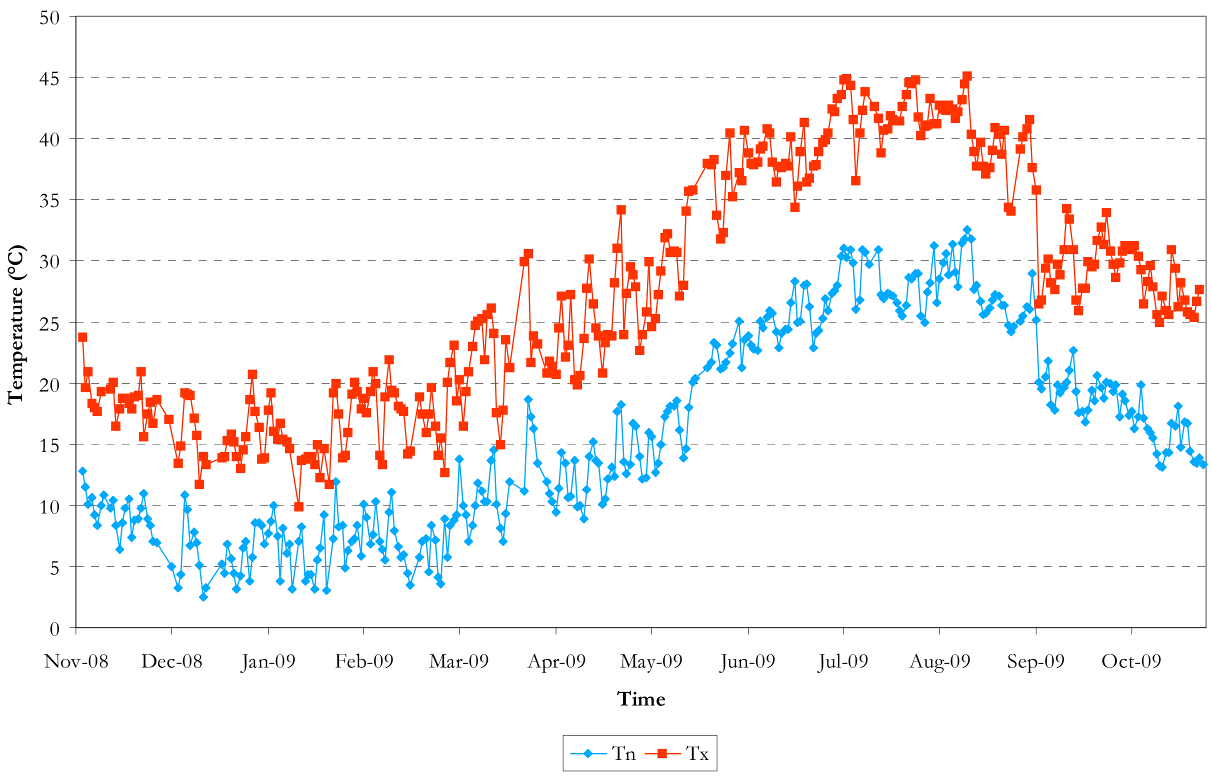


**Figure 29. Daily extreme temperatures**

The daily extreme values of relative humidity are calculated from the valid 1-minute values.

Maximum (resp. minimum) relative humidity RHx (resp. RHn) of day D is the highest (resp. lowest) relative humidity between day D 00:01 and day D+1 00:00.

Each day, both RHn and RHx are validated when at least 1430 of the 1440 possible values are valid (QC=0). A special rule is applied to SVAI screens: due to acquisition problems, about 10% of their 1-minute values are not available (about one missing value every 10 minutes), so RHn and RHx are computed if at least 1300 of 1440 daily 1-minute values are valid.

The plot of the daily maximum and minimum relative humidity during the intercomparison is given in figure 30. These are data from the UHMP22 sensor.

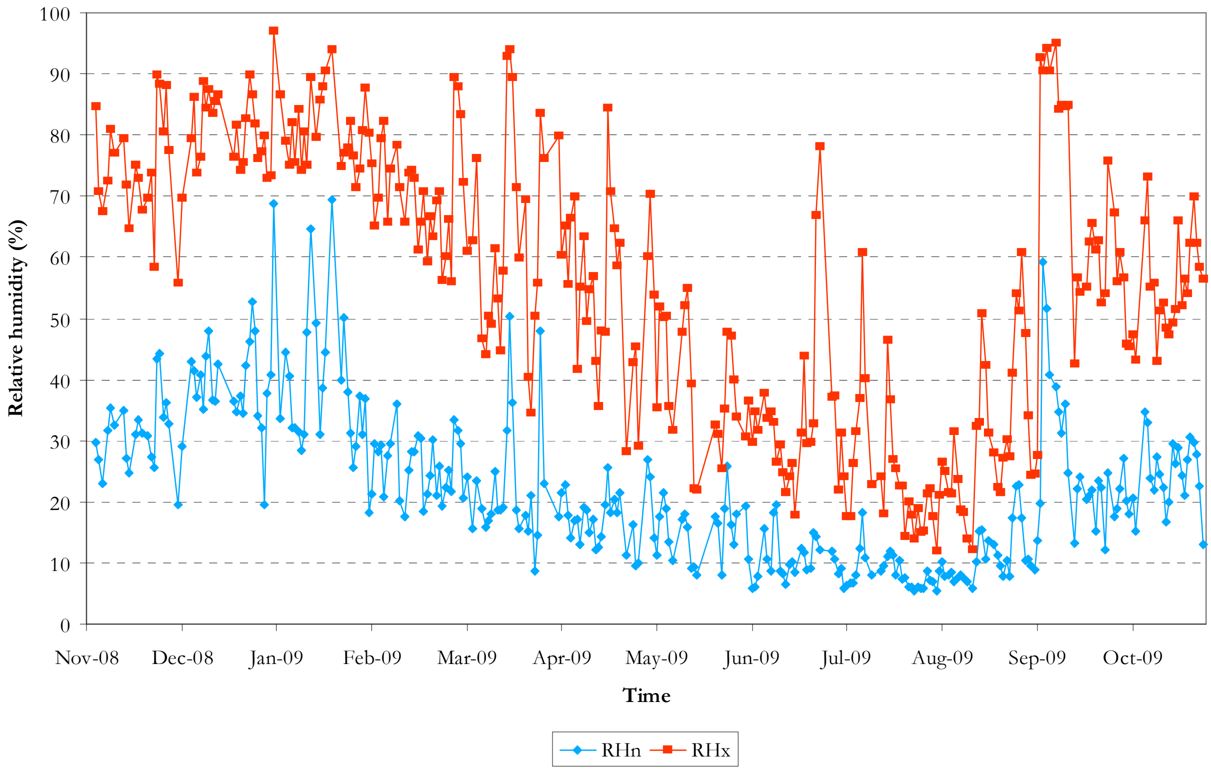


**Figure 30. Daily extreme values of relative humidity**

### 5.3.2 Wind

Stronger winds in the region of Ghardaïa are mostly prevailing during the period from March to June. On average 3.3 days of dust storms and 49 blowing sand events occur per year.

The average wind speed is around 5 m/s to 6 m/s; blowing between 9h and 18h and generally occurring from April to June (see figure 31). The maximum wind speeds are generally between 6 m/s and 10 m/s occurring from September to January. Wind maxima exceeding 20 m/s (over 75 km/h) are also quite frequent and can mainly be observed from February to May.

The maximum number of days of calm winds was noted in July and August and at night as shown in figure 31.

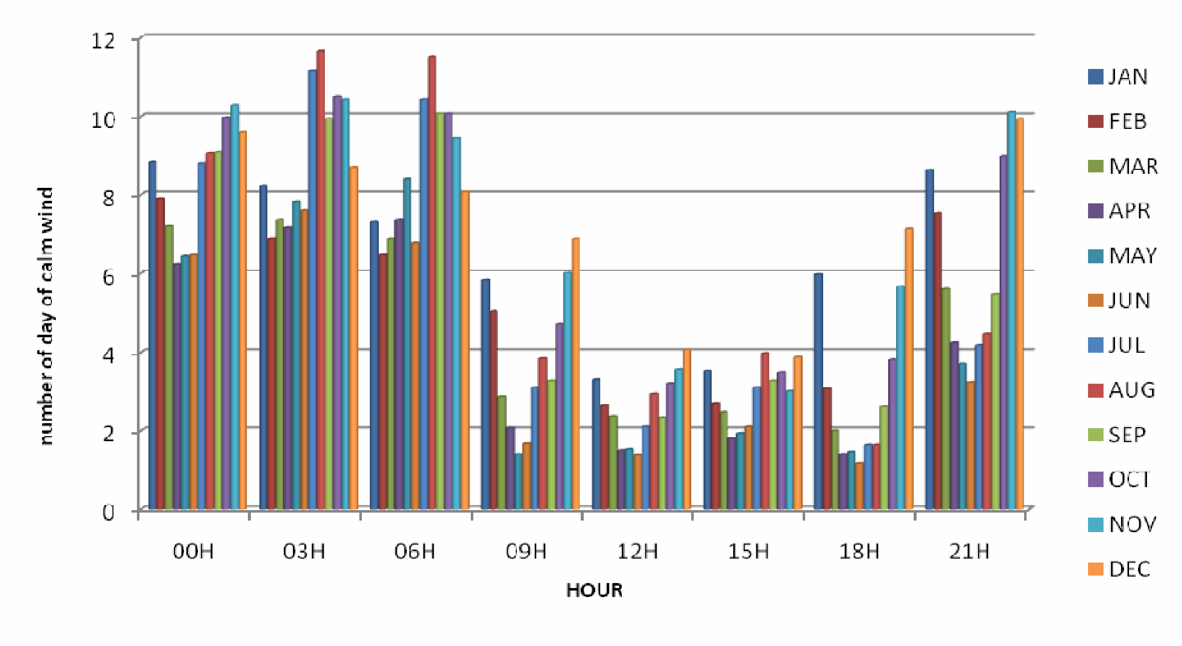


**Figure 31. Average number of days of calm winds during the period 1971-2000**

Prevailing wind direction in winter and spring is North to North East, with average speeds up to 10 m/s and 13 m/s respectively. In summer wind directions are mainly North East to South with average speeds up to 12 m/s. In late autumn wind directions are changing to North West, East and South, with average speeds up to 11 m/s as shown in figure 32.

The most frequent wind speed is between 5 to 9m/s which can also be recognized on the figure 33. Wind directions from North to North-East are dominant with frequencies of 14.8% and 11.6% respectively.

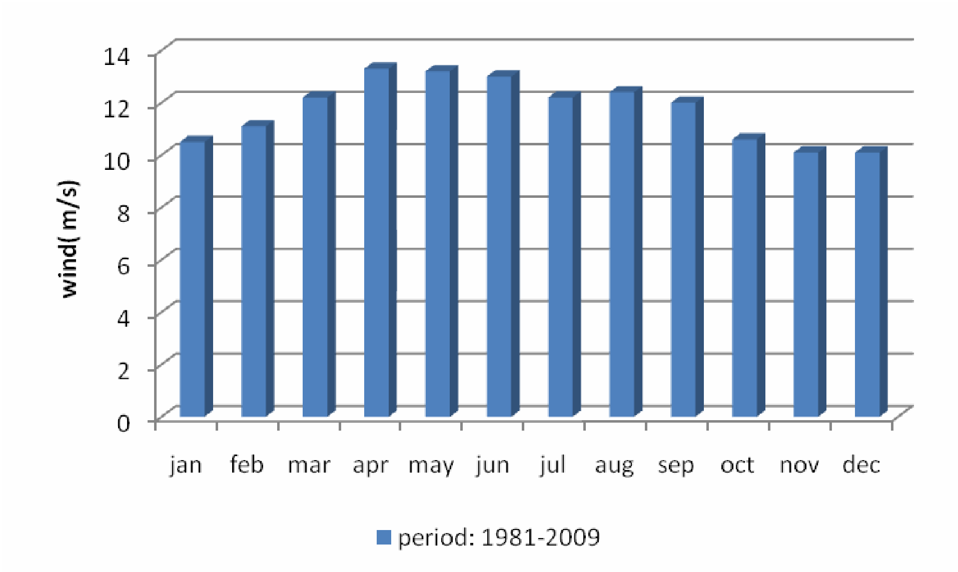


**Figure 32. Average maximum wind speed**

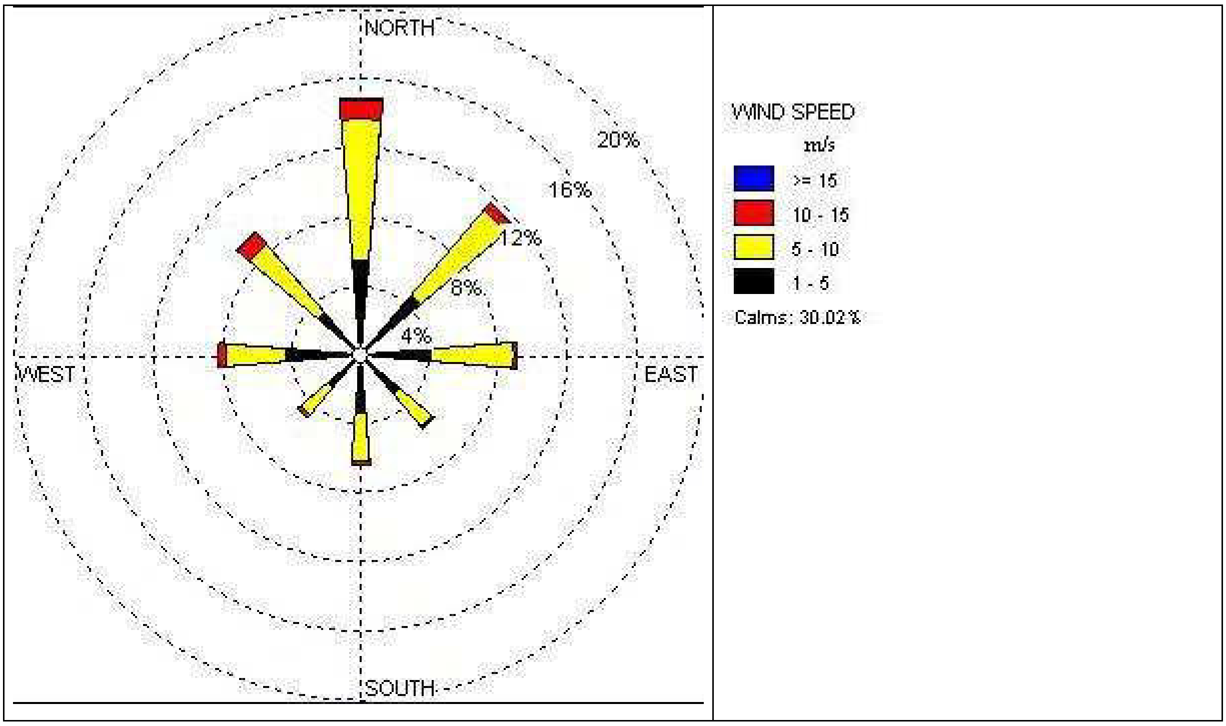


**Figure 33. Mean annual frequency of wind directions for wind speed classes (1998-2008).**

### 5.3.3 Sunshine duration

The mean monthly totals of sunshine duration show a maximum of 350 hours in May 2009 and a minimum of 195 hours in January 2009. April, May and October 2009 had significantly greater values of monthly sunshine duration than the normal. The yearly maximum event occurred in May and not in August as usual as shown on figure 34.

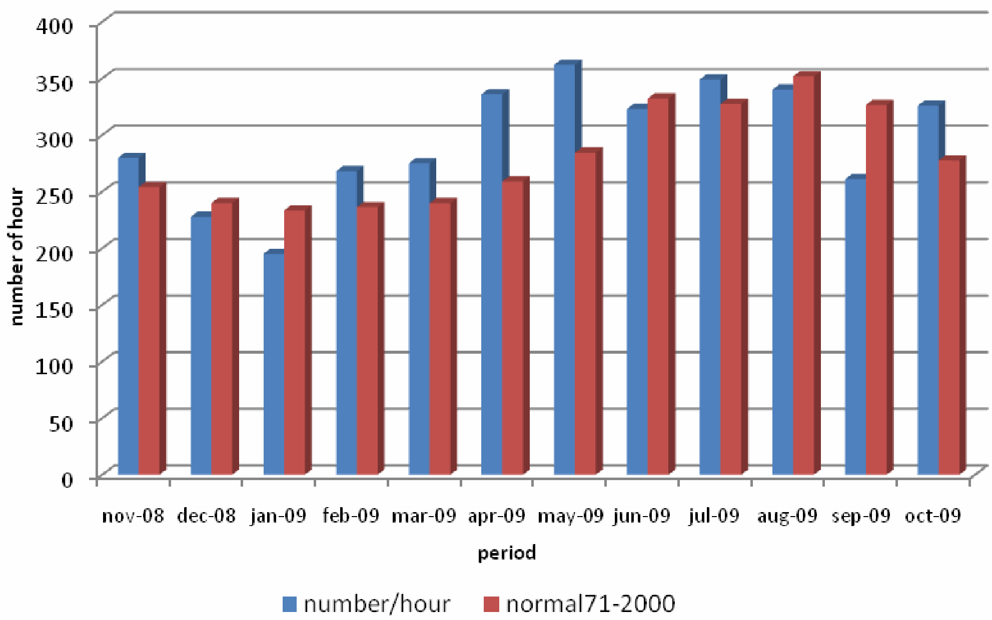


**Figure 34. Sunshine duration**

### 5.3.4 Albedo measurements

The albedo is the ratio between the reflected radiation and the incident radiation. It was measured by the albedometer CMA11. In Ghardaïa, it is around 0.38 when the soil is dry, between 0.28 and 0.29 when it is humid. The figure 35 shows the albedo (top chart), on the 18th and 19th of January, 2009. The first day was sunny, the soil was dry. On the second day, a strong shower is recorded from 07:00 to 8:40. Here the albedo is calculated for valid values of reflected and incident radiation. Moreover, only values above 50 W/m$^2$ were considered, in order to avoid out of range values, coming from the ratio of small radiation values.

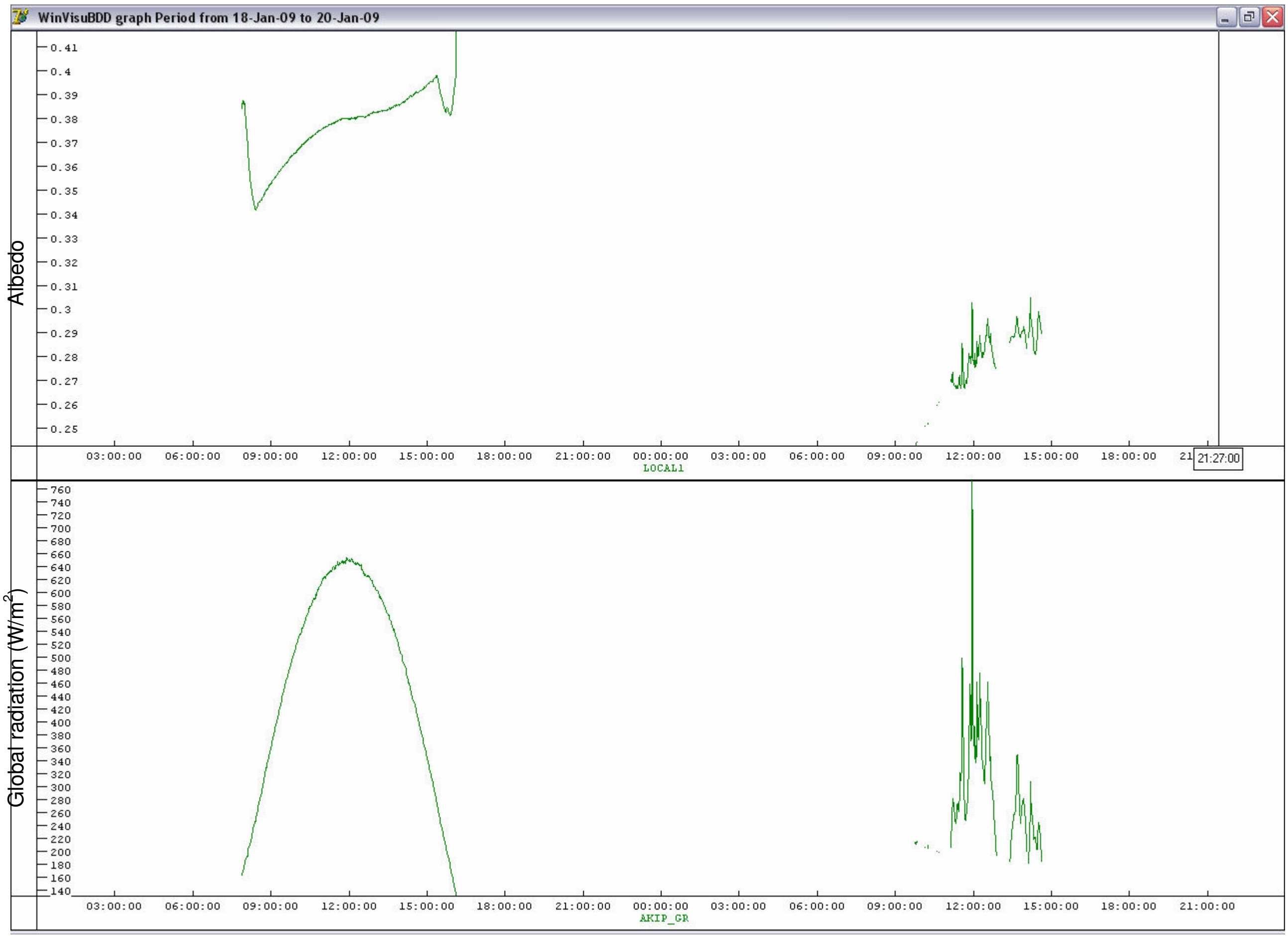


**Figure 35. Albedo measurements**

### 5.3.5 Precipitations

Rainfall events in Ghardaïa may be compared to Mediterranean-type or arid tropics rainfall events: they are highly variable from 1 to 100 mm/h when violent thunderstorms occur.

During the winter and spring of 2008 the amount of rainfall was relatively small, as depicted in figure 36. At the end of September 2008, an episode of torrential rain (150mm within one hour) hit the city of Ghardaïa causing exceptionally large floods. In January and September 2009, two peaks appeared in the monthly rainfall statistics where the monthly rainfall amount exceeded the long term climate normal.

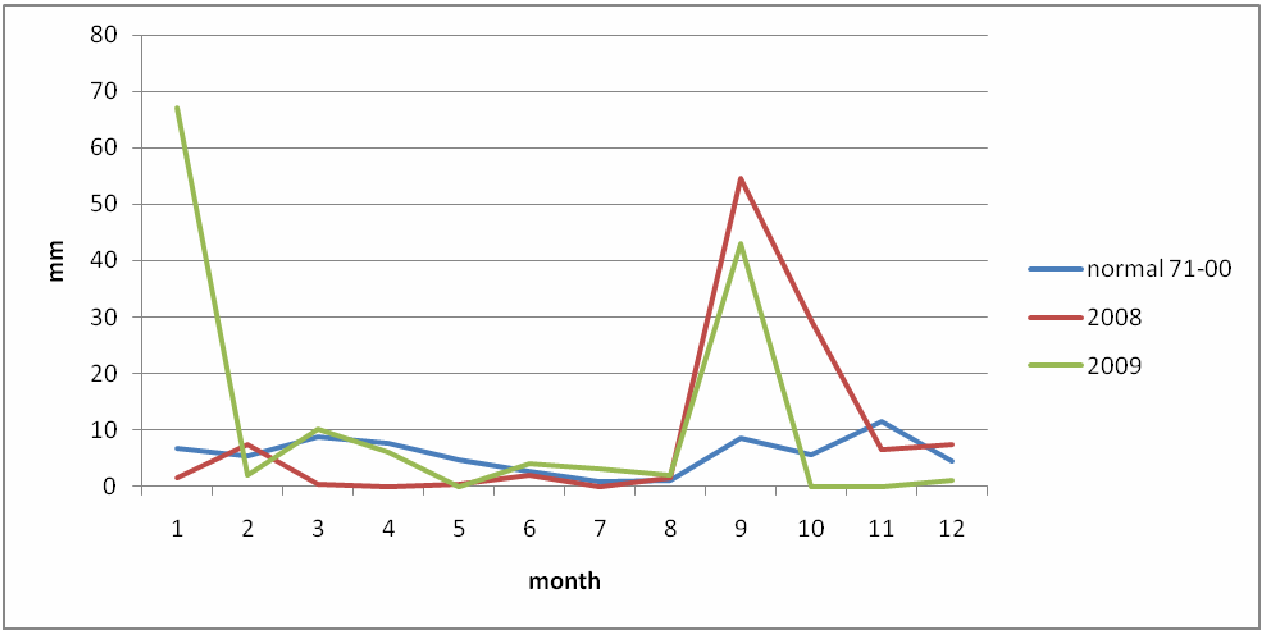


**Figure 36. Monthly rainfall amounts in Ghardaïa**

## 5.4 SCREENS

### 5.4.1 Choice of the reference

According to standard ISO17714:2007, screens “that are cooler during the day and warmer during the night are likely to be giving measurements that are closest to the truth”. Therefore, screens that give the coolest/lowest daily maximum temperatures are examined here.

For the selection of the reference screen, the screens performance in reporting the maximum and minimum temperature, relative to each other, was examined.

Each day, the median of maximum temperatures of all screens is computed. The following two plots show the distribution of differences between the maximum temperature reported from each screen and the computed median maximum temperature, for the whole period of the intercomparison.

The median maximum temperature was processed separately for the naturally ventilated screens and for those artificially ventilated, and the plots were organized function of the ventilation type of the screens.

Due to ventilation problems, only data in October 2009 are considered for VYOU screens. A separate study considering measurements of VYOU screens with no artificial ventilation is available in annex 9.6.

In each case, the warmer screens are above the y=0 line, while the cooler screens are below it.

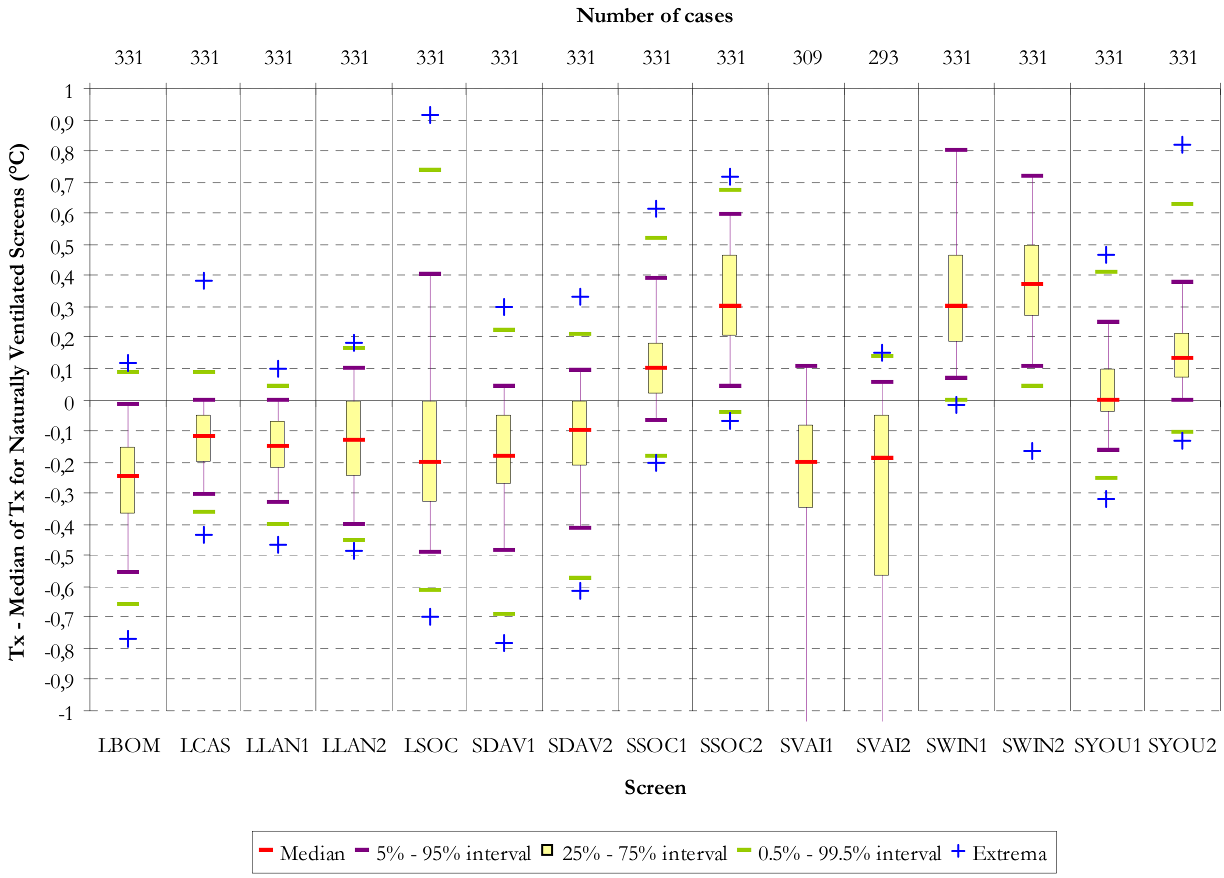


**Figure 37. Daily maximum temperatures of naturally ventilated screens**

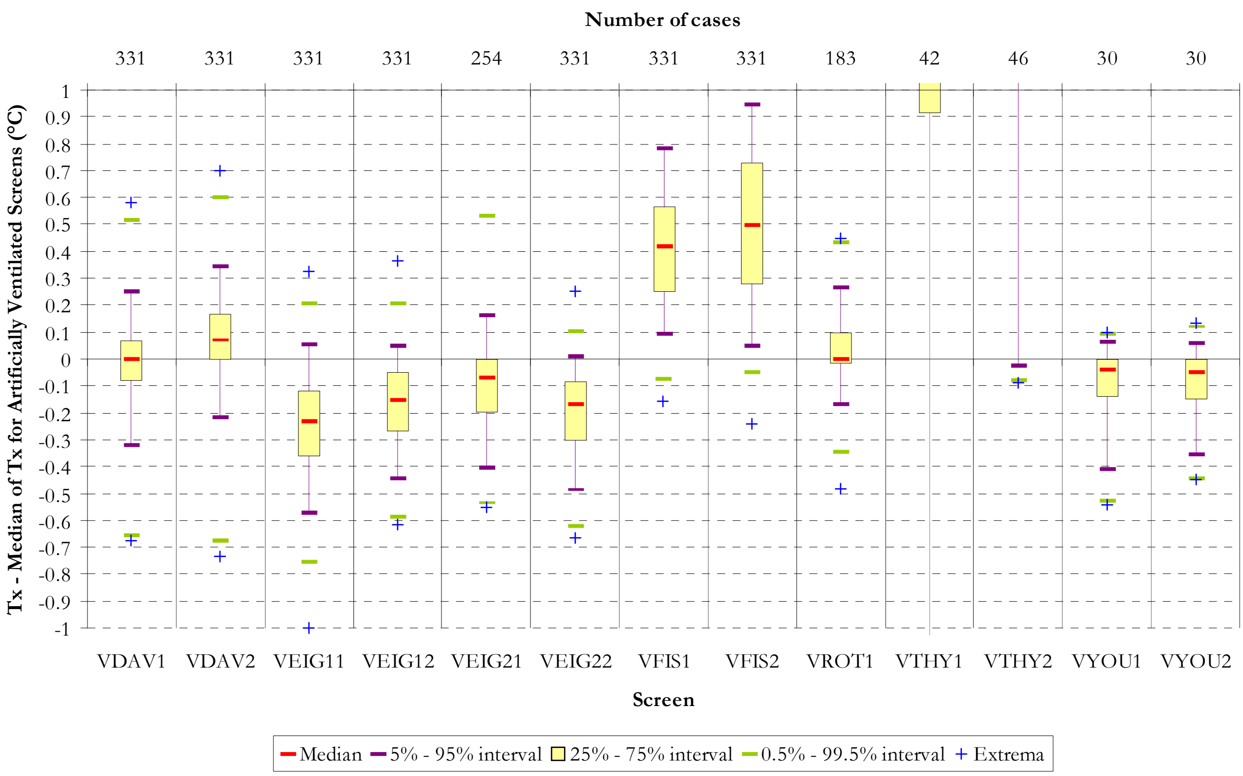


**Figure 38. Daily maximum temperatures of artificially ventilated screens**

The comparison between the median of daily maximum temperatures of naturally versus artificially ventilated screens shows that both are very close to the y=x line, with a y-intercept of -0.2°C.

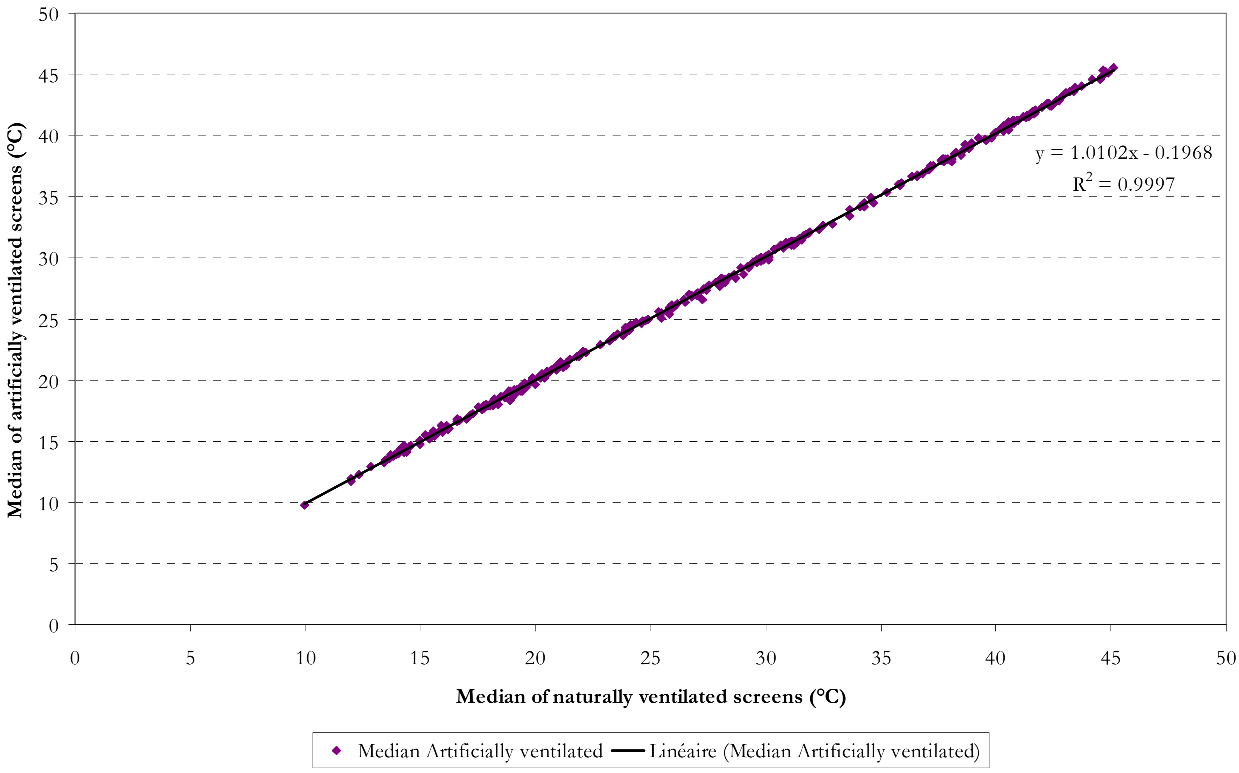


**Figure 39. Comparison between naturally and artificially ventilated screens for daily maximum temperatures**

The group of large Stevenson screens shows colder values. But it is suspected that this could be due to the time lag of these screens. The figure 40 shows one day of temperature measurements from two screens, VEIG11 (artificially ventilated) and LSOC (large Stevenson, naturally ventilated). The signal from LSOC is smoothed and delayed compared to VEIG11.


**Figure 40. Case study: 27th of August, 2009**

A similar analysis is conducted for the daily minimum temperatures, by plotting the differences between the minimum temperature reported from each screen and the computed median minimum temperature, for the whole period of the intercomparison.

The plots were organized function of the ventilation type of the screens.

In each case, the warmer screens are above the y=0 line, while the cooler screens are below it.

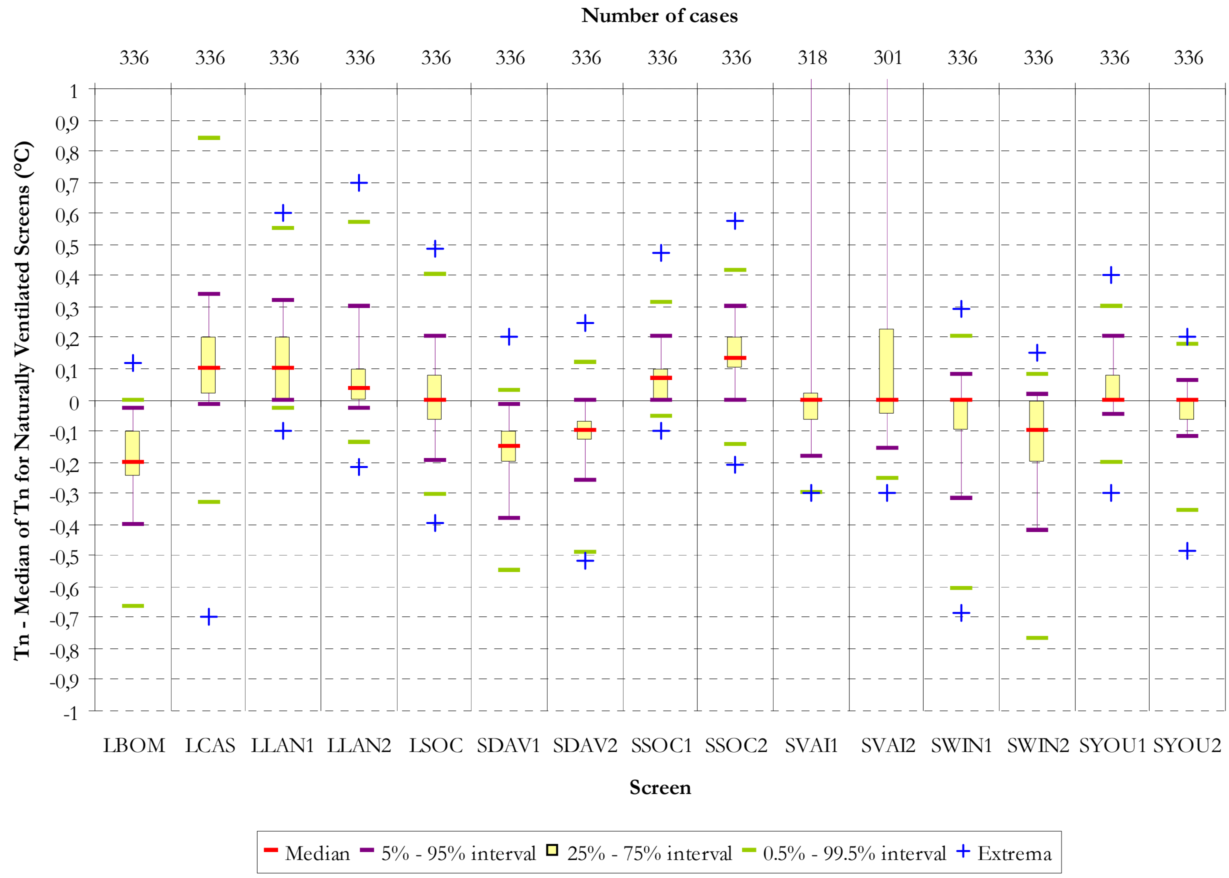


**Figure 41. Daily minimum temperatures of naturally ventilated screens**

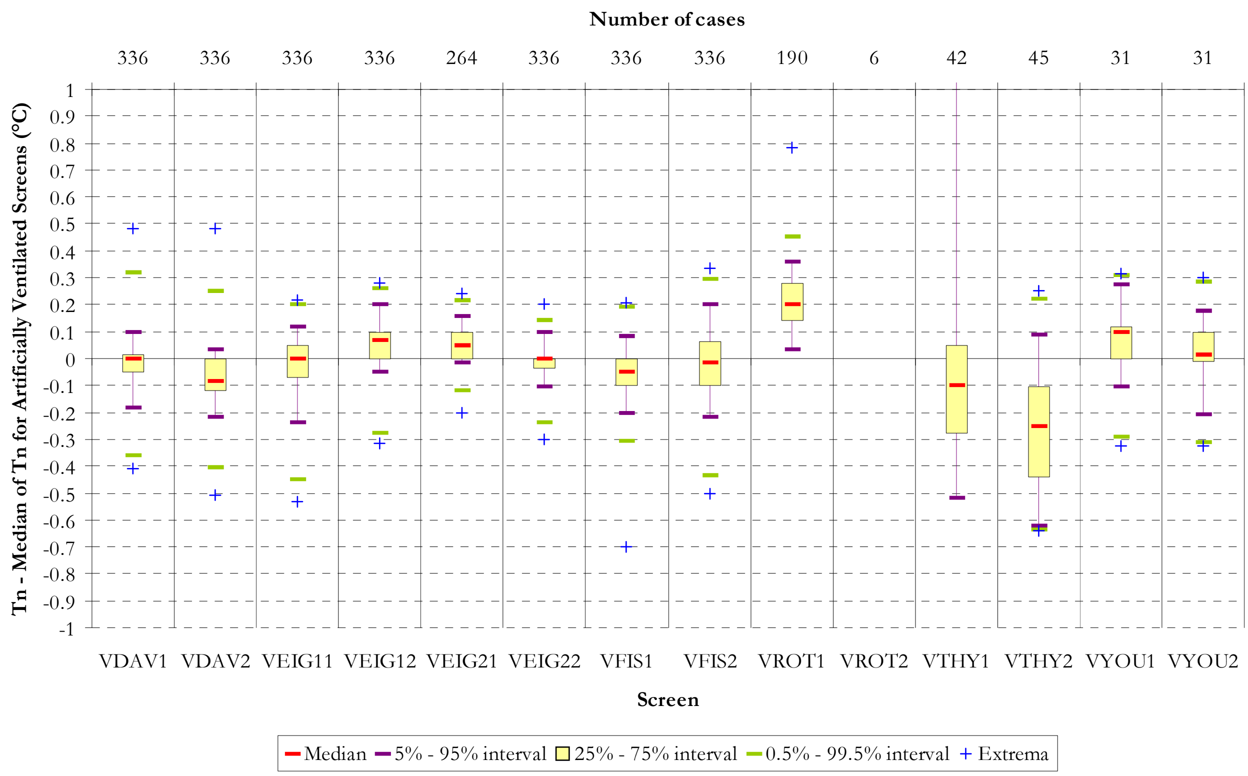


**Figure 42. Daily minimum temperatures of artificially ventilated screens**

Similar to the reporting of the maximum temperature, the two medians for the two types of screens show that they are very close to the y=x line, a slope very close to 1, and with a higher y-intercept than for maximum temperatures, -0.14℃.

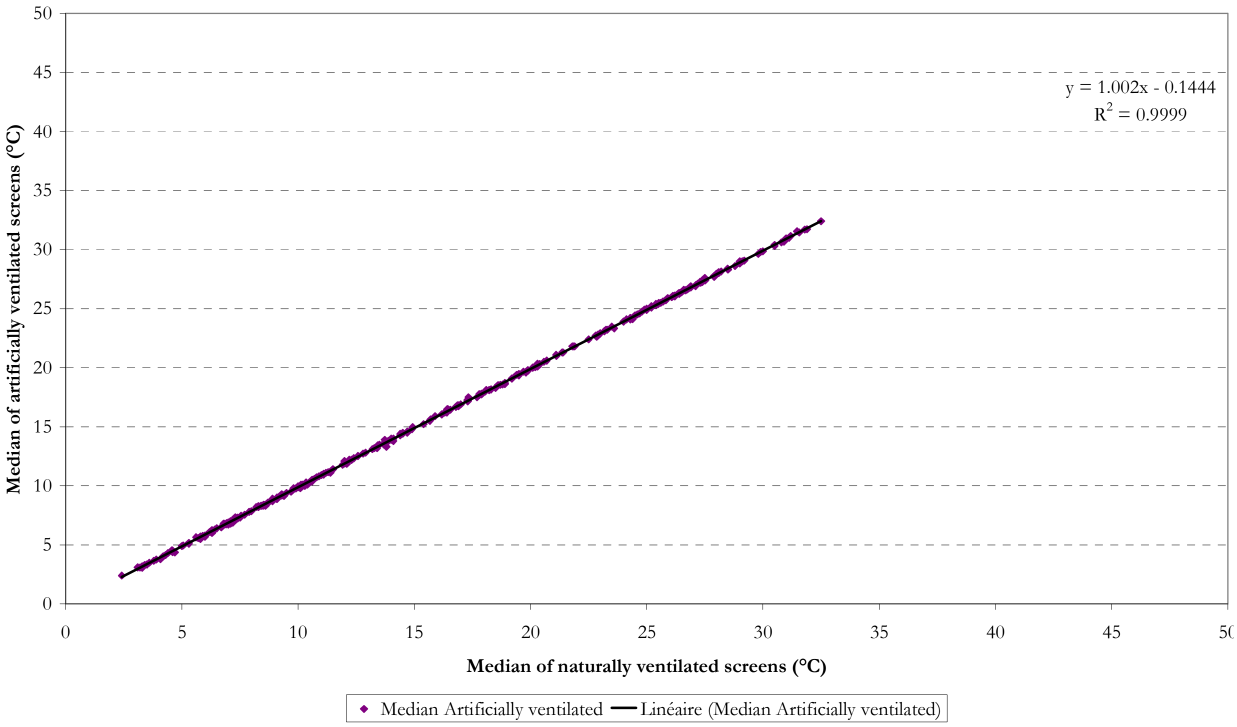


**Figure 43. Comparison between naturally and artificially ventilated screens for daily minimum temperatures**

The reference screen should ideally have a fast response which is generally the case for artificially ventilated screens.

Given the performance during the intercomparison, the following screens should not be chosen as the reference:

- VROT and VTHY have a very low number of data points,
- VDAV, VFIS and VYOU were warmer than the median temperature in at least 50% of the cases

Based on the information available, the VEIG screens are the most legitimate to be chosen as reference. Each VEIG screen has two temperature probes, which offers the option of selecting one of these probes as the reference, or the average of the two probes in the same screen. In each screen, one probe in installed towards North, the other towards South.

In order to see if the position of the sun could influence the probes inside VEIG screens, the distribution of the differences VEIG12-VEIG11 and VEIG22-VEIG21 are plotted, classified according the azimuth of the sun. Here are considered only the data where the sun elevation is positive.

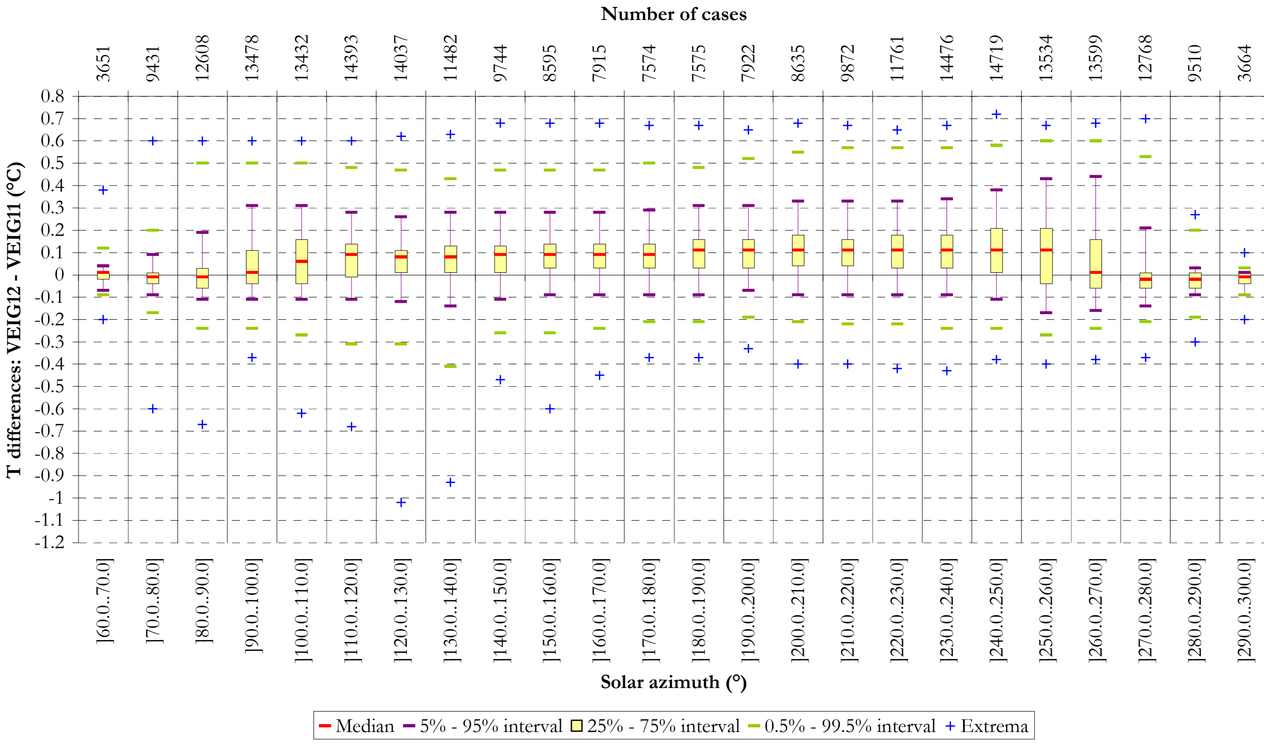


**Figure 44. Temperature differences of the two probes of VEIG1 screen**

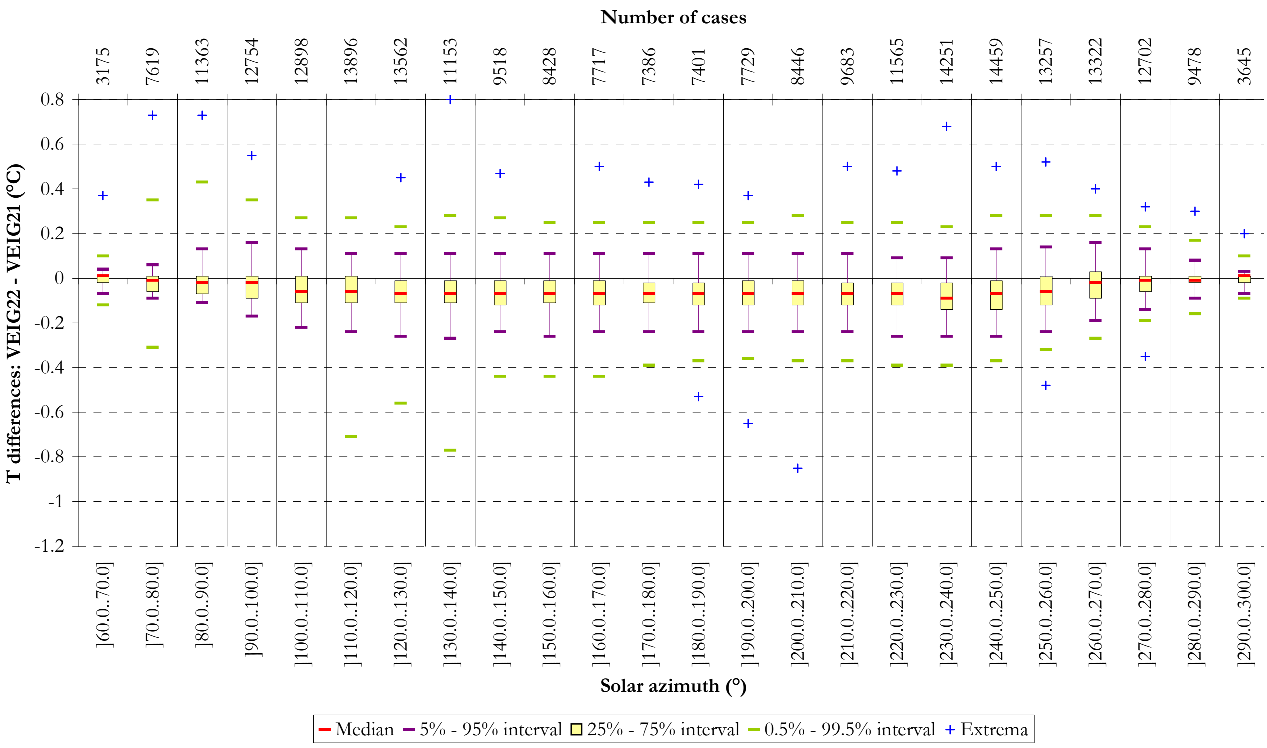


**Figure 45. Temperature differences of the two probes of VEIG2 screen**

On both plots a difference can be seen, corresponding to the east and west positions of the sun, compared to the south position. The plots are quite symmetric. The differences are smaller for the cases when the sun elevation is very low, for the classes (60..100) and (260..300): This could be interpreted as the absence of a radiation effect. No real difference can be seen between the east and west position of the sun.

The VEIG2 probes show less dispersion than VEIG1 probes. This recommends the probes in the VEIG2 as more suitable as the screens reference.. Of the two probes in VEIG2, VEIG22 has a higher number of available data, and is also colder than VEIG21.

**Therefore the VEIG22 probe is considered as the working reference for temperature measurement.**

### 5.4.2 Data analysis

This part includes general analysis for all screens. Detailed individual results are available in the datasheets.

#### 5.4.2.1 Global radiation data

Very high values of global radiation were measured during the intercomparison period. The pyranometer was calibrated before and after the experiment by the calibration service of the NWS of Algeria. The calibration coefficient has changed by only 2.4% during the experiment from 5.17µV/(W $m^{-2}$) to 5.05µV/(W $m^{-2}$).

For the evaluation, global radiation was processed with an average coefficient of 5.1µV/(W.$m^{-2}$).

Extremely high values of global radiation (greater than 1100W/$m^2$ and up to 1300W/$m^2$) could be found on partly cloudy days. These peak values are caused by scattered sunlight from the surface of very white clouds leading to high values of diffuse radiation in addition to maximum values of direct radiation.

Figure 46 shows two consecutive days: the first one is a partly cloudy day where global radiation values are above usual values, followed by a clear sky day where global radiation values do not exceed 1020W.$m^{-2}$.

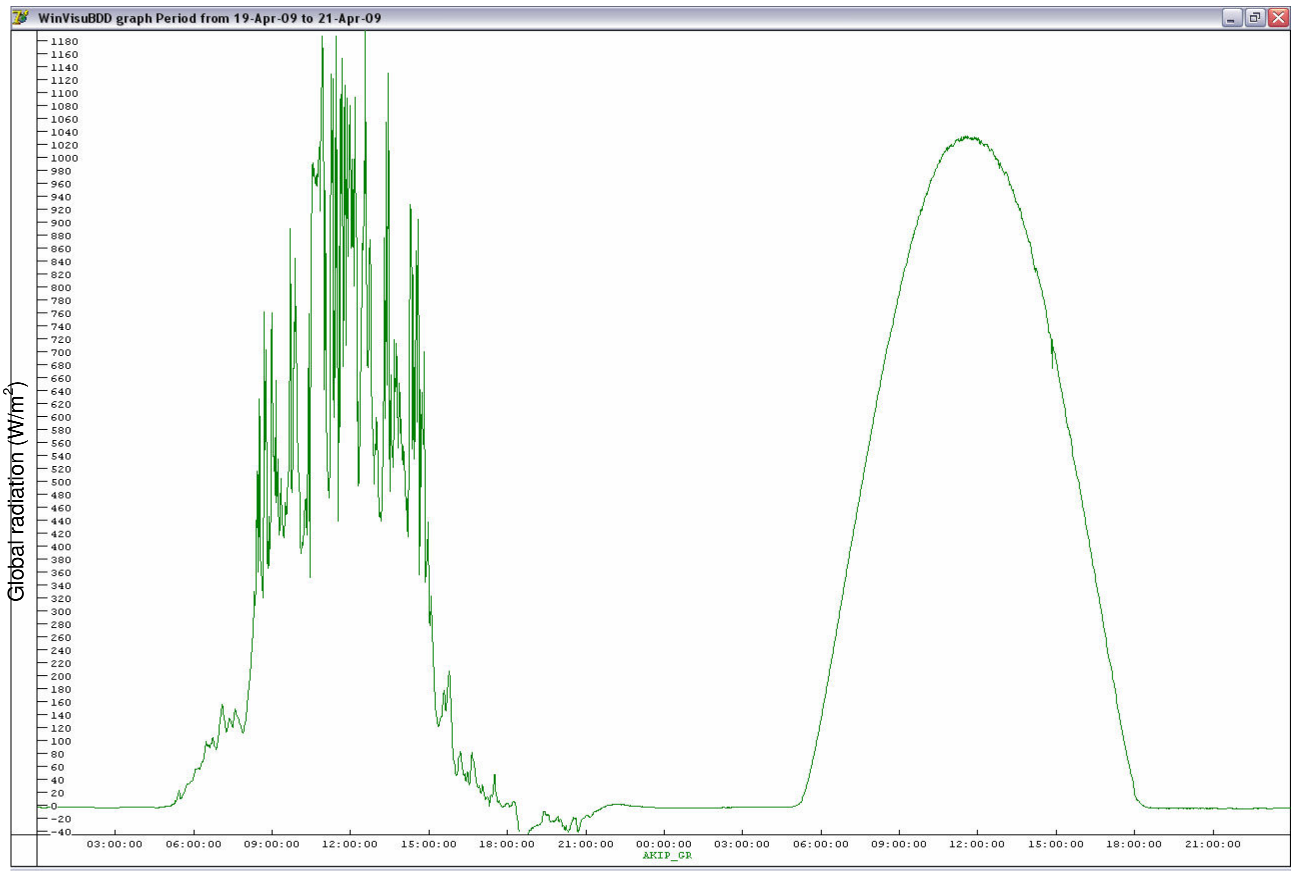


**Figure 46. Global radiation: very high values during partly cloudy days**

#### 5.4.2.2 Wind and global radiation

Figure 47 shows the distribution of wind speeds for different classes of global radiation.

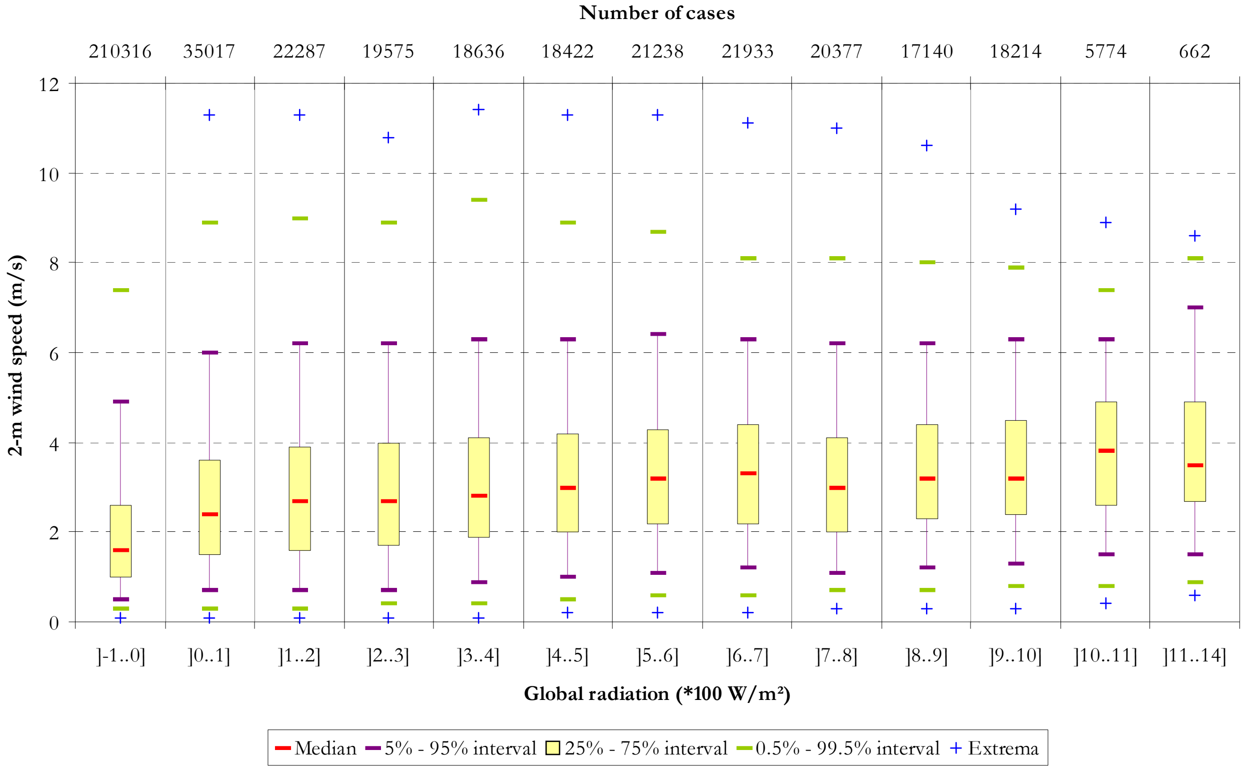


**Figure 47. Distribution of wind speed vs global radiation**

In every global radiation class, a wide range of wind speeds is available in the data set. However for high radiation values, large wind speeds (above 10m/s) and calm winds (below 1m/s) did not occur during the test period.

5.4.2.3 Method of data analysis and first results

For each sensor, its mode (most frequent value) and its mean are plotted. The figure 48 shows for most screens the differences are symmetric about zero (the mode varies between -0.2℃ and +0.2℃). A bell shape is not det ected. It is not the case for VROT1, VTHY1 et VTHY2: the graphical representation is not symmetrical. The average is -0.57℃ for the ATHY2 values.

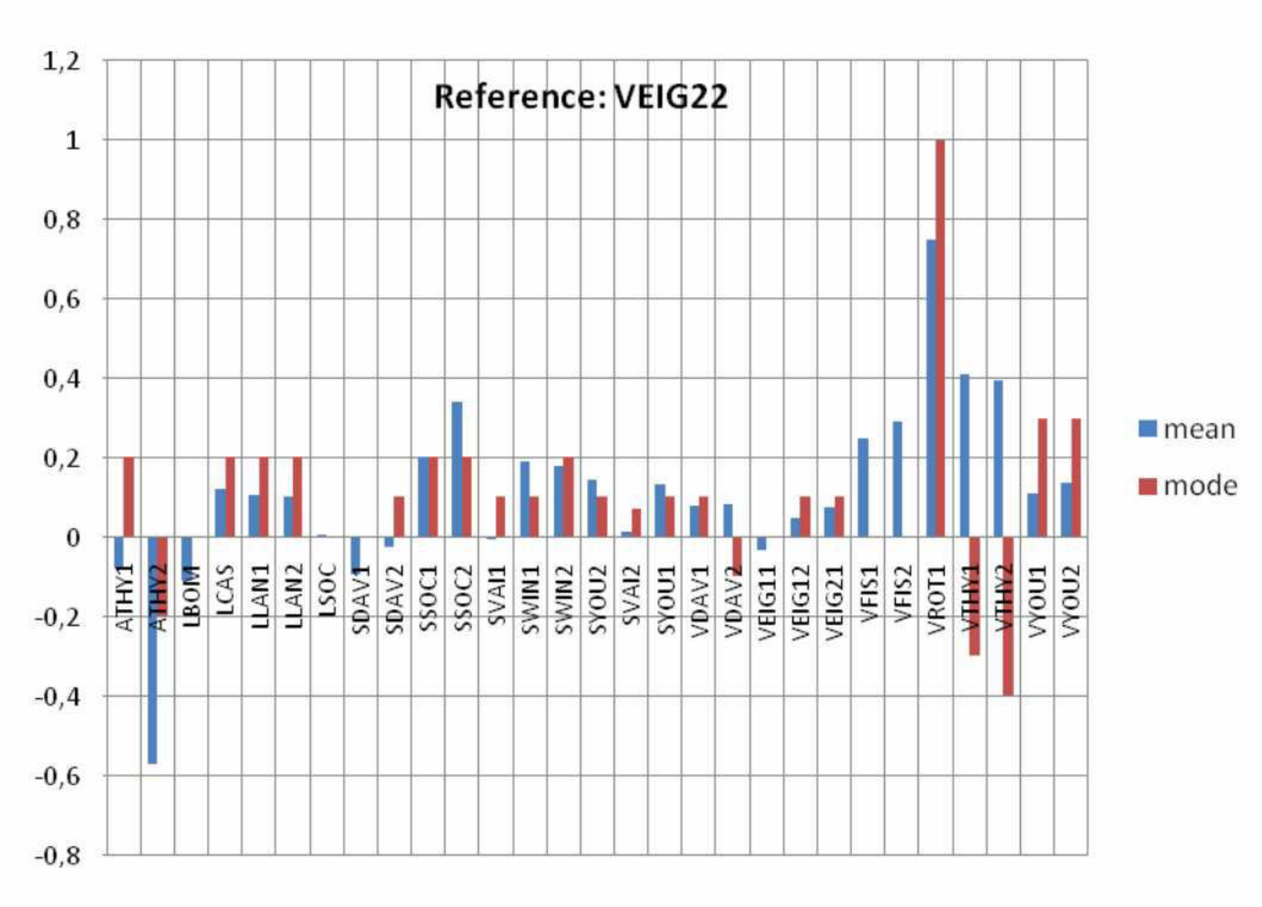


**Figure 48. Screen diagram with VEIG22 reference**

A detailed analysis of histograms is available in annex 9.5.

### 5.4.2.4 Distribution of differences with VEIG22 reference

The figure 49 shows the distribution of the differences with the reference, for each screen. It is based on 1-minute data.

The figure 50 is the same plot as the one before, but zoomed in, in order to emphasize details around 0.

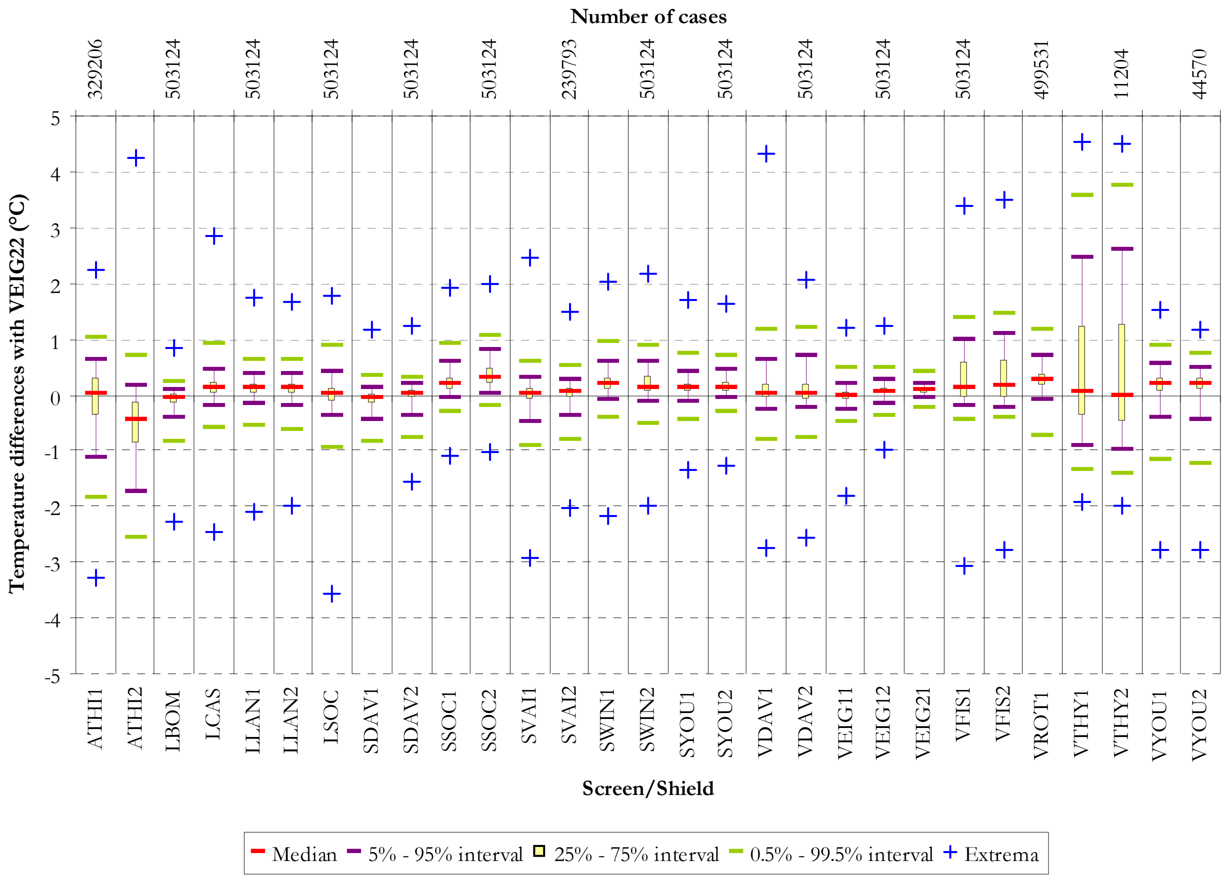


**Figure 49. Temperature differences with the reference (1-minute data)**

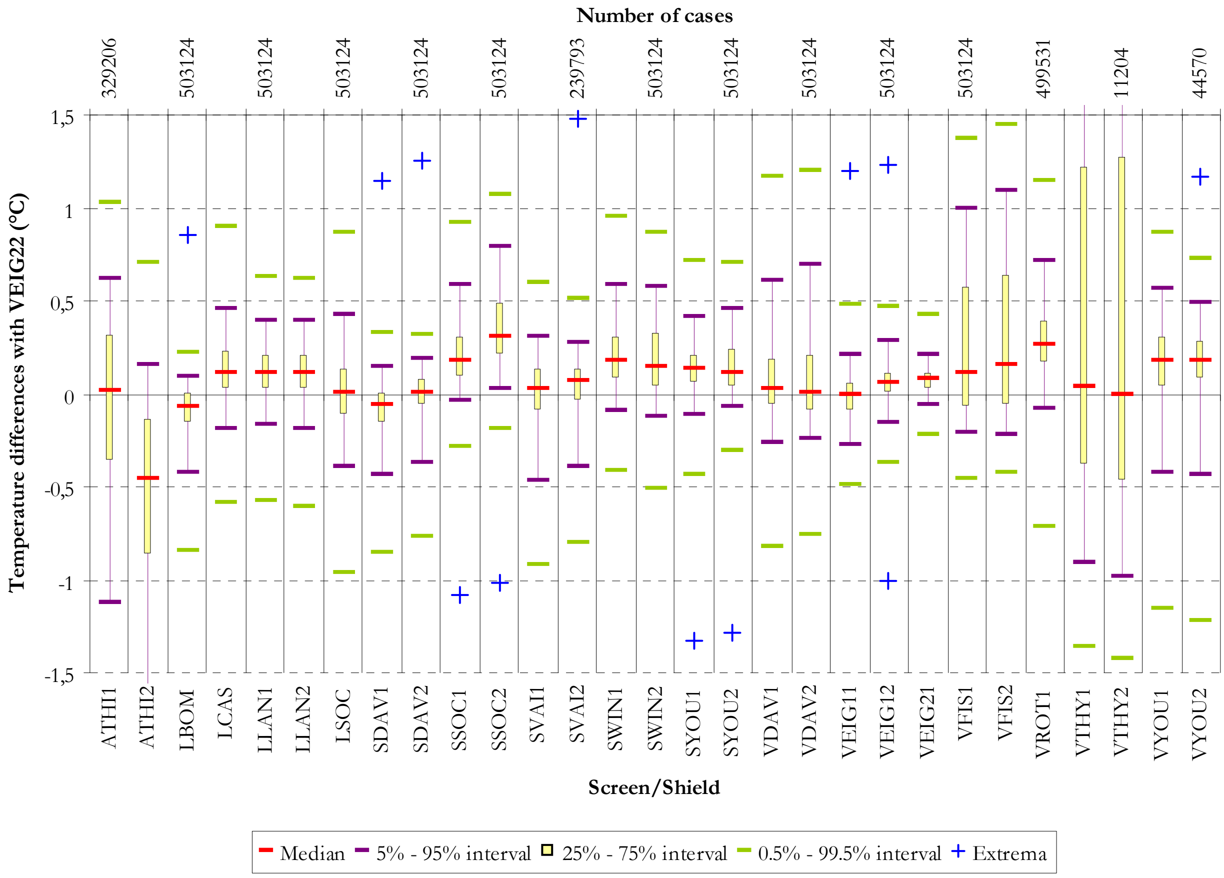


**Figure 50. Temperature differences with the reference (1-minute data), zoomed in**

### 5.4.2.5 Determination of time lag of the screens

To evaluate the time lag of the screens, during the calculation of daily maximum and minimum temperatures, the corresponding times when they occurred were also recorded. The distribution of the time differences in minutes when Tx occurred for the reference and for the other screens/shields is plotted in figure 51. A positive difference means that the maximum temperature of the screen under consideration occurs delayed with respect to the reference. Thus a negative difference corresponds to an earlier occurrence of the extreme value.

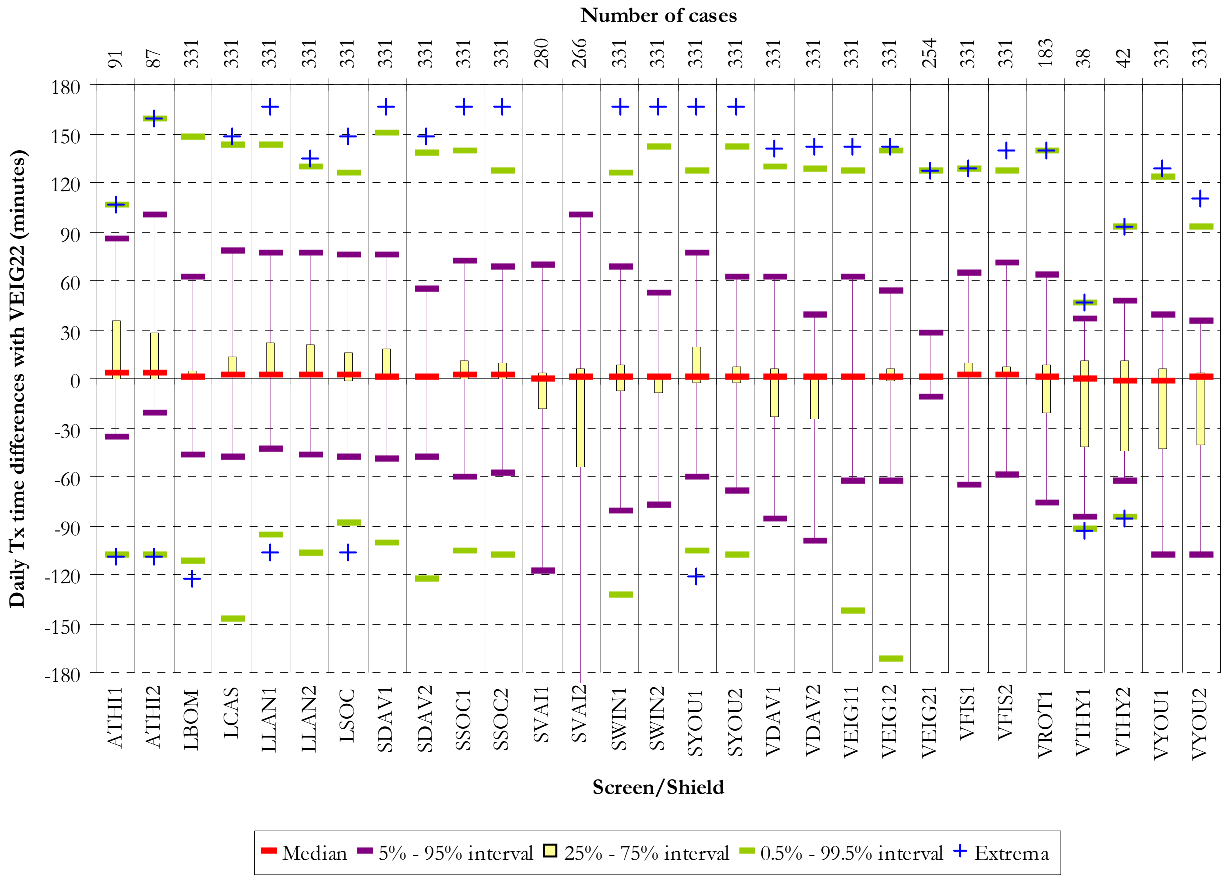


**Figure 51. Distribution of the differences in the time of occurrence of daily maximum temperatures**

A first conclusion is that many screens/shields have medians around 0, i.e. most screens are reporting Tx at the same time. On the other hand some extreme differences occurred with more than 180 minutes in some cases corresponding to days where the screens have recorded their Tx at completely different times compared to the reference.

More than the median values, yellow boxes (intervals with 50% of values) may be most representative of a screen's temporal behaviour. All large screens show a delay with their yellow boxes shifted to positive values. Some ventilated screens show an advance.

A similar chart for daily minimum temperatures Tn is shown in figure 52. Yellow boxes are very small: the majority of Tn occurred at the same time. This is due to the fact that the majority of Tn appears at the end of the night, with a slow decrease of temperature.

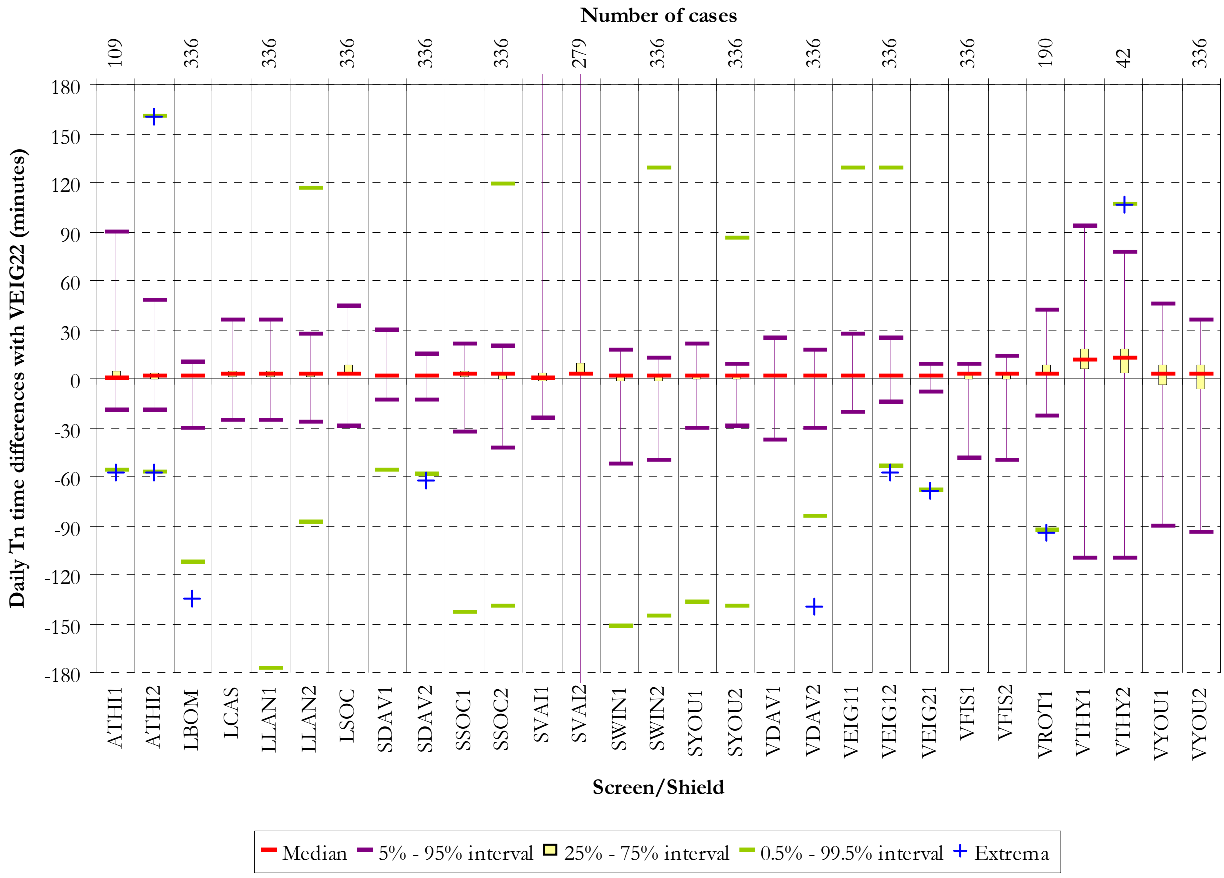


**Figure 52. Distribution of the differences in the time of occurrence of daily minimum temperatures**

### 5.4.2.6 Behaviour of all screens for low wind speeds

Figure 53 shows the distribution of temperature differences with the reference during clear days and wind speeds at 2-meter height below 2m/s (2-minute average), for the whole period of the intercomparison. In these cases the screens are more affected by high solar radiation in combination with low natural ventilation which could reveal a possible radiation error. A wind speed threshold of 1 m/s would be better, but the number of points would be too low. The analysis was done, and results were not so different.

The ATHI sensors are significantly colder than the reference by about 1℃. The VTHY screens are significantly warmer. Artificially-ventilated screens are not colder, as could be expected in such conditions. On the contrary, some small naturally-ventilated screens are colder than the reference: SDAV, SVAI.

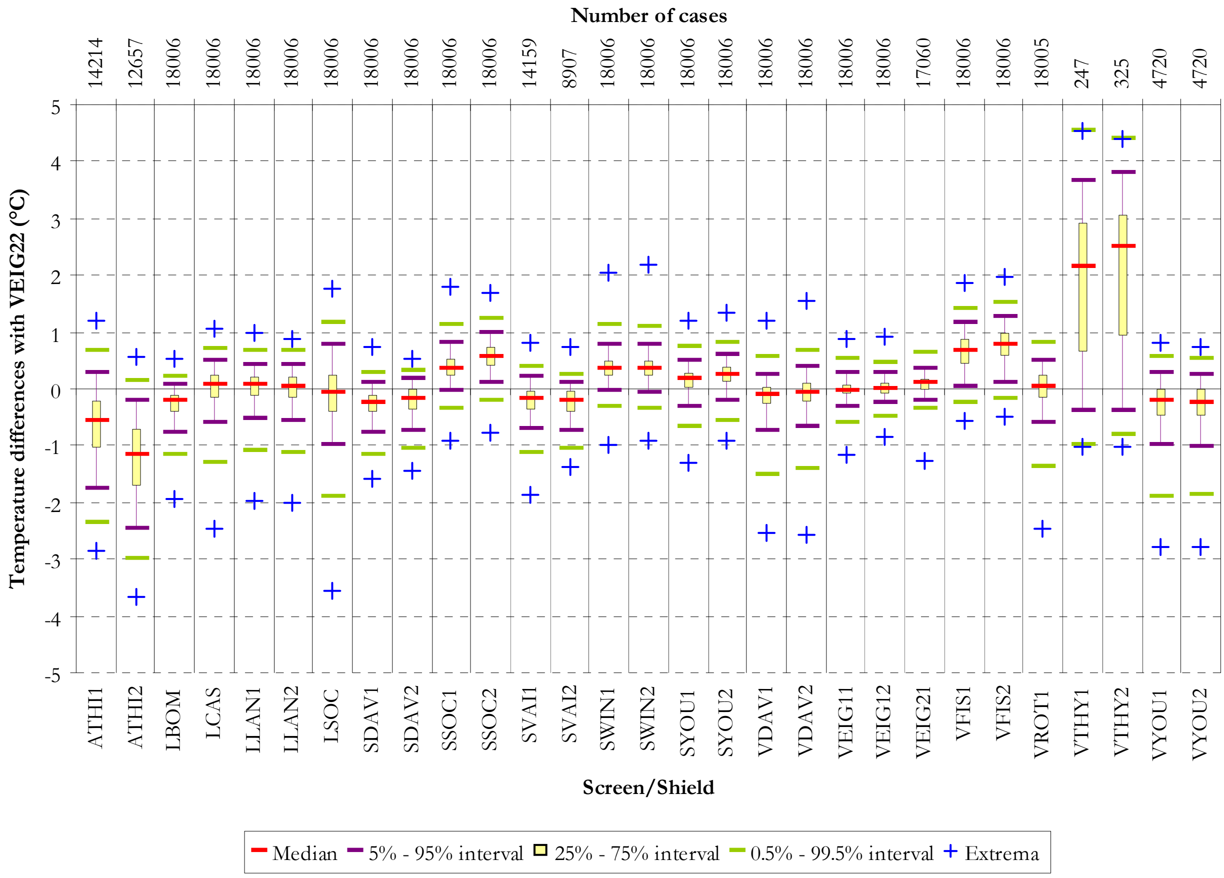


**Figure 53. Temperature differences during clear days and wind speeds below 2m/s**

### 5.4.2.7 Behaviour of screens during a sand blowing event

The complete study is available in annex 9.7.

## 5.5 HYGROMETERS

### 5.5.1 Choice of the reference

An Assmann Aspiration Psychrometer [8] could be used as a reference, but was not available in this intercomparison. The CIMO guide [5], section 4.4, considers that "the chilled-mirror hygrometer is used for meteorological measurements and as a reference instrument both in the field and in the laboratory". So, in previous meetings, the reference of humidity measurement was designated to be the Thygan from MeteoLabor. During the intercomparison it turned out that both Thygan sensors were not able to send valid measurements from May 2009 until the end of the measurement period (because of data acquisition system failure). Therefore only five months of reference data are available for analysis. As a consequence, Thygan sensors were used as a primary reference to choose another sensor as a working reference. This could be the sensor that gives the closest measurements to the Thygan during the first five months.

In order to choose the working reference, the measurements from both Thygan sensors are considered. They give very close results and so VTHY2 was selected as the primary reference as it gave a larger number of data.

From this point, the unit used to express a difference of relative humidity is "%", as it is in the CIMO guide. This is a difference expressed in % of RH. Therefore, a positive difference of 2% between one sensor and a reference measuring a relative humidity of 50%, means that this sensor has measured a relative humidity of 52%.

For each valid measurement, the differences between a given sensor (quality checked 1-minute values) and VTHY2 are computed. Figure 54 depicts the distribution of these differences. "Average 11 12" are the averages of UHMP11 and UHMP12 both being installed in the same screen VEIG1. "Average 21 22" represents the averages of UHMP21 and UHMP22 installed in screen VEIG2. These averages are computed only when the absolute difference between both measures is less than 1%.

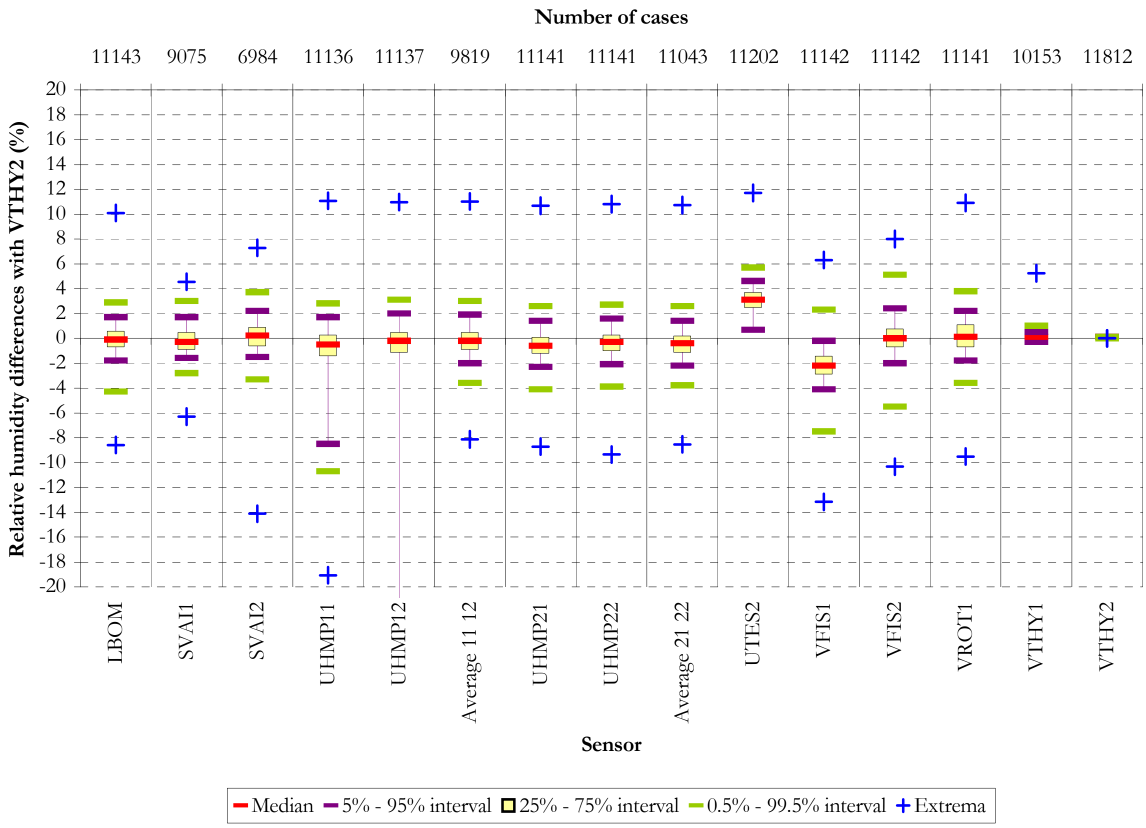


**Figure 54. Distribution of differences with VTHY2 for all relative humidity sensors**

Many sensors gave low differences with the Thygan, which is quite a good surprise. These sensors can not be chosen as a reference:

- LBOM because this probe was added in the intercomparison after the meeting in Ghardaïa (March 2007) and the results of the calibration performed before the intercomparison were not known. Nevertheless, this sensor gave quite good results!
- SVAI because they gave a low number of valid data (because of data acquisition system failure)
- UTES, VROT because differences with VTHY2 are quite scattered

For the above reasons the second working reference should preferably be chosen among the VFIS or UHMP sensors. UHMP sensors were selected, since two probes are installed in each of the VEIG screens. Under the condition that the difference between both probes is less than 1%, their average can be considered as a safe value. Probes in screen VEIG2 gave more data than those in screen VEIG1. Moreover, they are in the same screen than the temperature probe that was chosen for the temperature reference measurement.

**Therefore it was decided that the second working reference for humidity measurements, after VTHY2, is processed by averaging UHMP21 and UHMP22, when their absolute difference is less than 1%.** When the absolute difference was larger, data was discarded.

With these assumptions, the distribution of reference humidity measurements over the whole period of the intercomparison can be plotted (see figure 55).

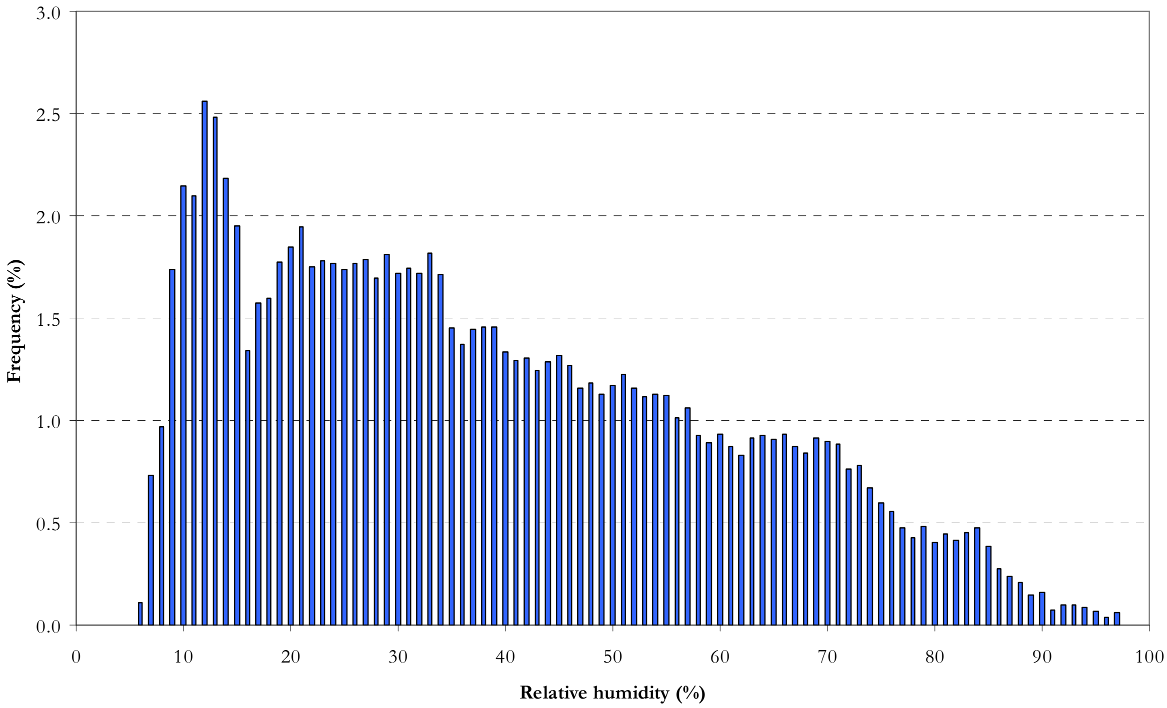


**Figure 55. Distribution of relative humidity measured by the reference over the whole period of intercomparison**

464168 values of the working reference (UHMP) are available over the period, out of the 525600 possible values, giving a data availability of 88.3%. These missing values are mainly explained by the fact that UHMP sensors had grounding problems during several days in May and October 2009. These erroneous data could easily be filtered out because every time when these problems occurred, both sensors differed by more than 1 %.

The minimum value of 5.6% was obtained on the 4th August 2009 at 15:03. The maximum value of 96.7% was measured on the 20th January 2009 at 08:22. The median humidity value is 34.2%.

The distribution of relative humidity against classes of temperature is plotted in figure 56. High values of relative humidity were obtained for low temperatures. Low values of relative humidity were obtained during hot periods.

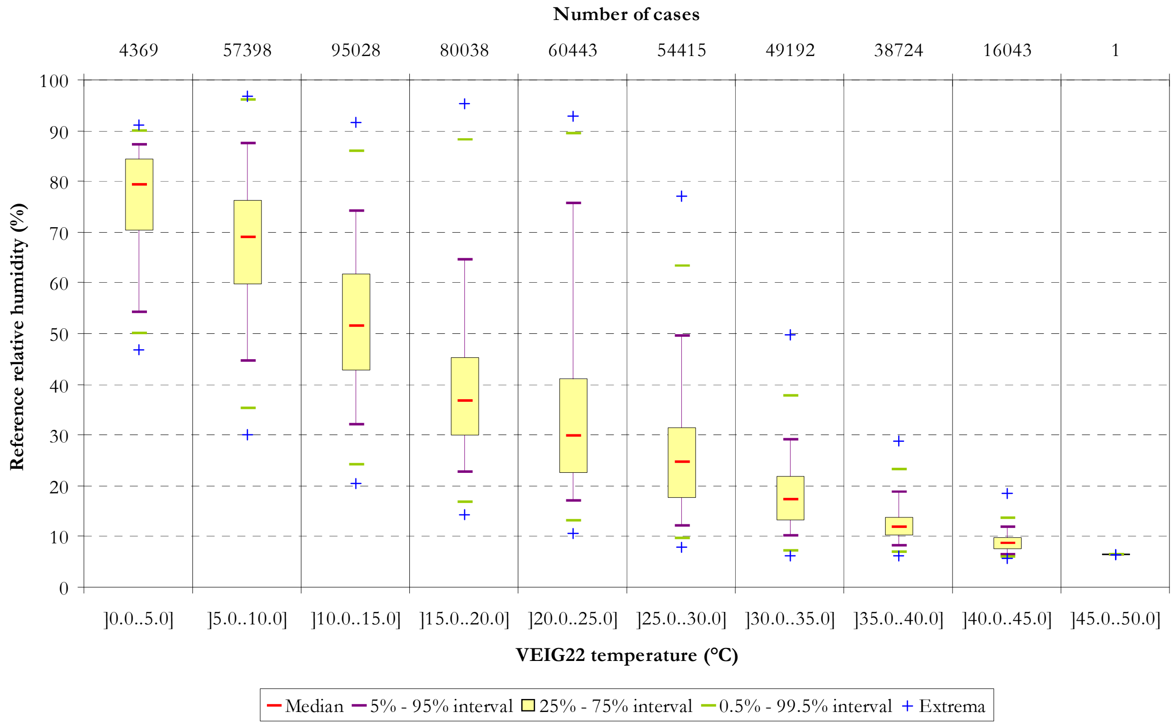


**Figure 56. Distribution of relative humidity against temperature classes**

### 5.5.2 Data analysis

This part includes general analysis for all relative humidity sensors. Detailed individual results are available in the datasheets.

#### 5.5.2.1 Consequences of an overestimation of temperature on relative humidity

As screens/shields may induce errors on temperature measurements, it is relevant to estimate what would be the error on relative humidity if the temperature is overestimated by 1℃, for a given dew point.

According the CIMO Guide, the relative humidity *U* (in %) is defined by:

$$U(t,t_d,p) = 100\frac{e_w^{'}(p,t_d)}{e_w^{'}(p,t)}$$

where *t* is the air temperature, $t_d$ is the dew point temperature, *p* is the atmospheric pressure and $e'_w$ is the saturation vapour pressure with respect to water.

The error on relative humidity if there is an overestimation of 1℃ on temperature, for a given dew point is given by:

$$\Delta = U(t+1,t_d,p) - U(t,t_d,p) = U(t,t_d,p)\left(\frac{e_w^{'}(p,t)}{e_w^{'}(p,t+1)} - 1\right)$$

In addition, the saturation vapour pressure is given by the formula:

$$e_w^{'}(p,t) = \left(1.0016 + 3.15\cdot 10^{-6}p - \frac{0.074}{p}\right)\cdot 6.112e^{\frac{17.62t}{243.12+t}}$$

The figure 57 gives the result, for the atmospheric pressure of 950 hPa. This value is chosen because the atmospheric pressure varied from 943 to 975 hPa during the intercomparison period.

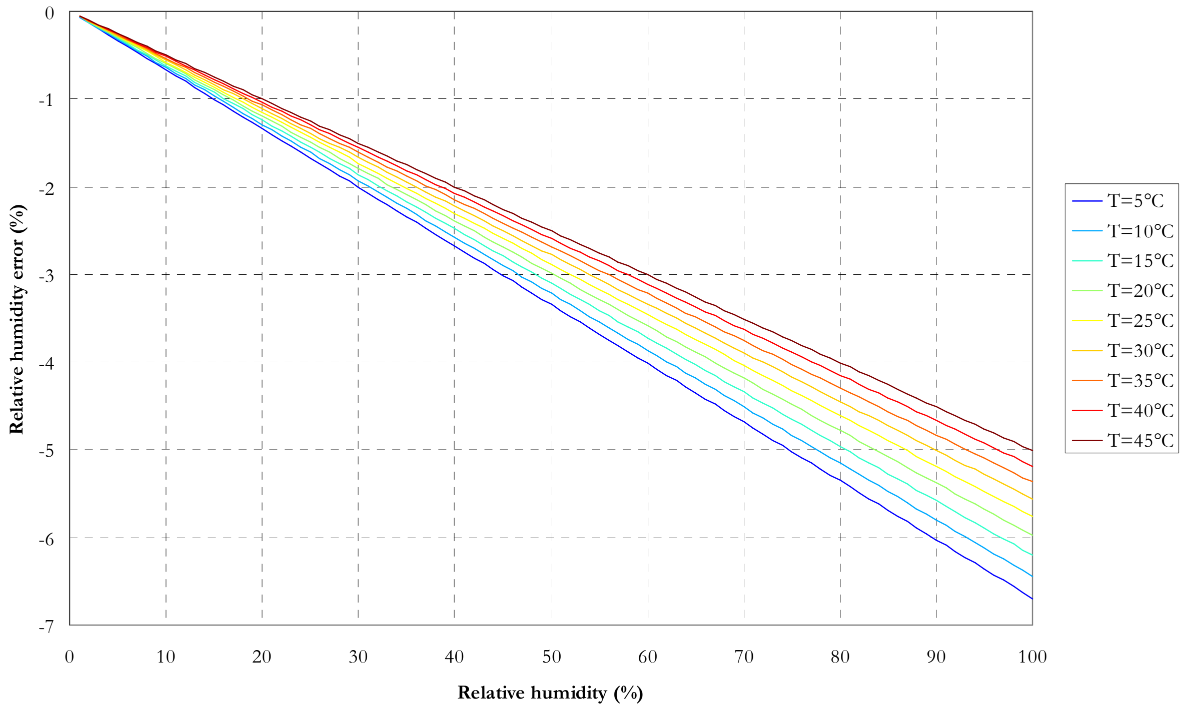


**Figure 57. The error on relative humidity for an overestimation of temperature of 1°C**

As expected, the influence of temperature is larger for high values of relative humidity: the relative humidity is 6% lower at saturation if the temperature is 21°C instead of 20°C. For low values of humidity, an overestimation of 1°C of temperature leads to an underestimation of humidity of about 1% at 45°C and 15% of relative humidity.

Therefore, differences of temperature inside various screens may generate differences of relative humidity of few percents. But the detailed analysis of relative humidity shown in the datasheets did not exhibit many differences. This may be due to the fact that the larger differences in temperature occurred during periods of high solar radiation, which occurred with low values of relative humidity. The influence of an error of temperature is reduced to 2 or 3% in such conditions.

### 5.5.2.2 Method of data analysis and first results

For each sensor, its mode and its mean (most frequent value) are plotted, for both working references (cf figure 58 and figure 59). For most sensors the differences are symmetric about zero without a bell shape. The graphical representation is not symmetrical for sensors UTES2, VFIS1.

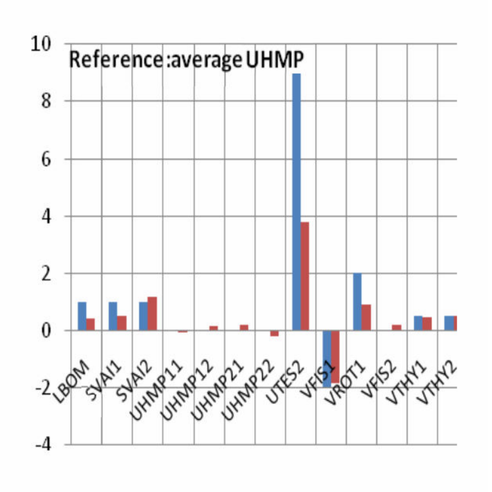


Figure 58. Diagram with UHMP reference

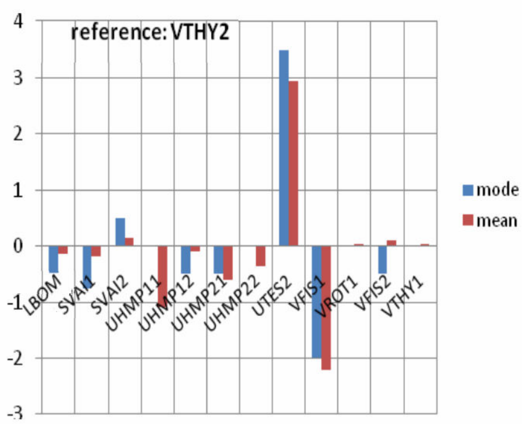


Figure 59. Diagram with VTHY2 reference

### 5.5.2.3 Distribution of differences with UHMP2 reference

For each valid measurement, the differences between a given sensor (quality checked 1-minute values) and UHMP2 are computed. The figure 60 shows the distribution of these differences.

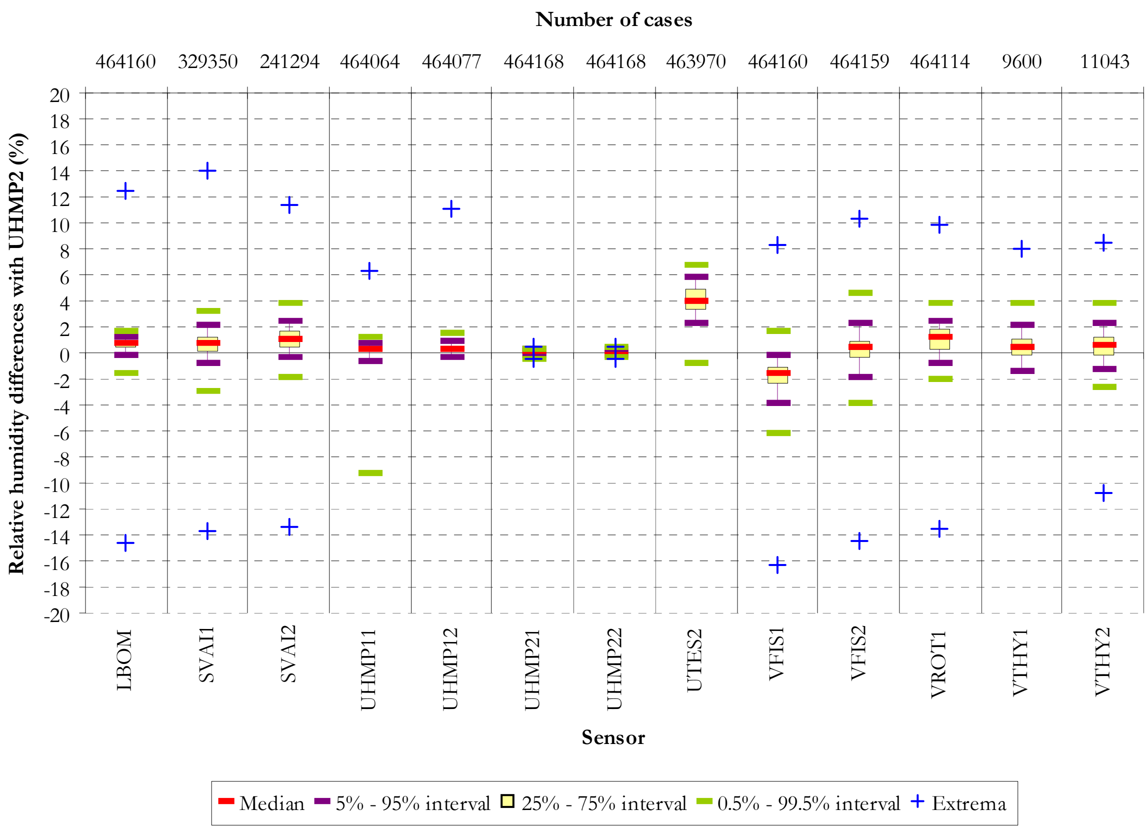


Figure 60. Distribution of differences with UHMP2 reference

### 5.5.2.4 Behaviour of sensors for very low values of relative humidity

The figure 61 shows the distribution of differences with UHMP2 when the reference relative humidity is below 20% and the temperature is above 30℃.

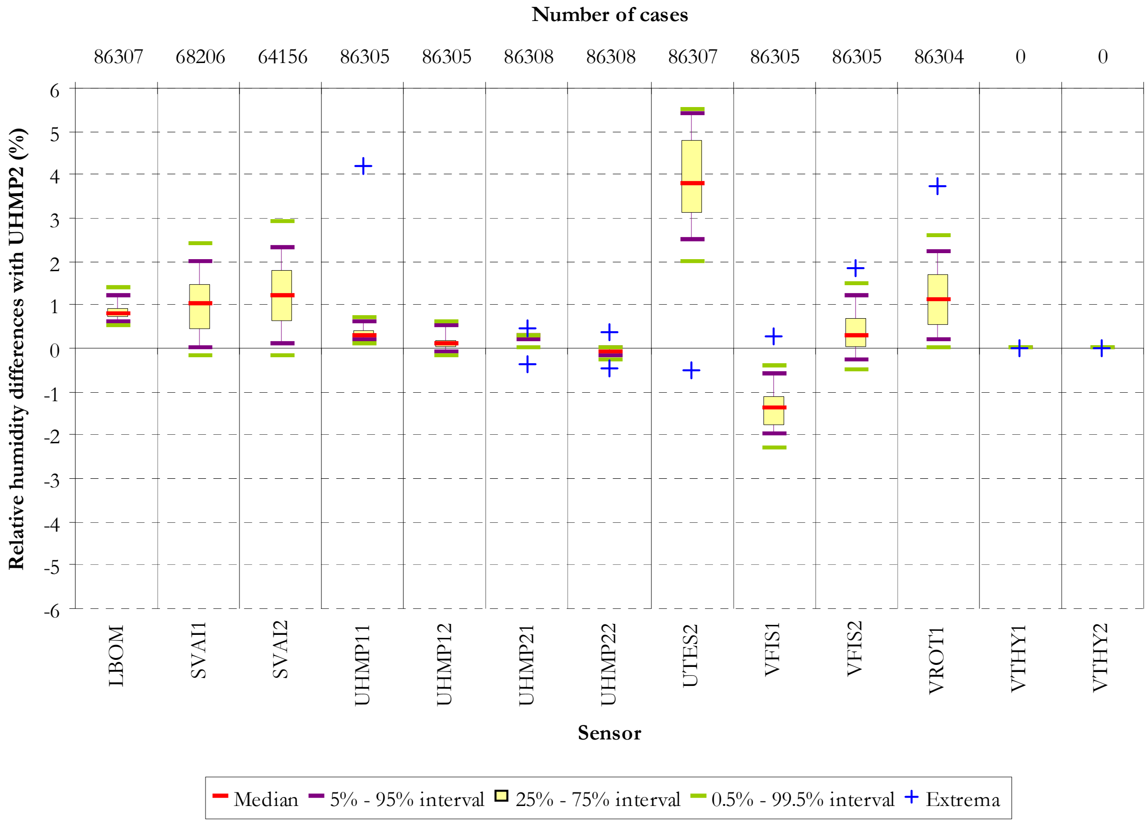


**Figure 61. Distribution of differences for relative humidity below 20%**

# 6 CONCLUSIONS

## 6.1 GENERAL

- Despite the difficulties encountered, the intercomparison was successful.
- The Ghardaïa Intercomparison experienced problems in its schedule, due to customs constraints and electrical grounding problems at the beginning.
- The data acquisition software and system for sensors with a numerical output experienced some problems, leading to gaps in the dataset.
- Nevertheless, over the 12 months period of the intercomparison, more than 500 000 minutes of data are available for the majority of screens and hygrometers, allowing a deep data analysis.

## 6.2 SCREENS

- Some uncertainties exist concerning the efficiency of the artificial ventilation of some screens, which might not have been working correctly.
- The Eigenbrodt LAM630, a multi-plate screen with artificial ventilation, was selected as a working reference, but was warmer than some other screens in case of high solar radiation and low wind speed. This shows that this screen, though selected as the working reference, also suffers from some radiation error.
- The air temperature calculated from the Thies ultrasonic anemometers was much colder than all other screens, the absolute difference increasing with solar radiation and decreasing with the wind speed. This indicates that this instrument could be less influenced by radiation than the screens, and thus could be a good candidate for use as a reference. However, a systematic difference between the two sensors, ranging from 0.4 to 0.7℃ with some scattering, shows either a calibration problem or a principle limitation of the system for measuring air temperature. Due to these issues, this sensor was not used as a reference.
- The group of four large Stevenson type screens provided very good results. They reacted slower than the working reference, though the BoM design exhibited a surprisingly fast response (in comparison to its size).
- Some small passive multi-plate screens exhibited warmer temperatures than the reference (~0.5℃). Two had results close to the reference. One model, the DAVIS 07714, gave surprisingly good results, with colder measurements than the reference in case of solar radiation. This result of DAVIS is surprising because past intercomparisons in other environments did not exhibit so good results in some other tests, done by individual members.
- Other artificially ventilated screens gave disappointing results, with quite warm temperatures in case of solar radiation. This may be due to their design and/or some faults in the ventilation during the test (dust and sand reducing the ventilation efficiency). For example, the ventilated DAVIS gave worst results (warmer temperatures during day) than the passive DAVIS, which was not expected.
- A summary of the performances found during the intercomparison is given in table 7. A rating of the performances, <u>in comparison to the working reference</u>, seen during <u>this intercomparison</u> is proposed, ranging from one star (*) to five stars (*****). The rating principles are given in annex 9.8.
- The working reference was found to be warmer than some other screens during high solar radiation and low wind speed, showing that this working reference was not the

“best” screen in all circumstances. Therefore the rating in comparison to the working reference is also completed by an additional and more “absolute” rating, taking into account the characteristics of the reference screen itself.

**Table 7. Global results for screens**

| Acronym | Screen name | Consistency between screens | System time response compared to the reference | Radiation error | % within ± 0.5℃ of the reference | Comment | Comparison with the working reference (VEIG) | More "absolute" Rating |
|---|---|---|---|---|---|---|---|---|
| LSOC | Socrima, abri grand modèle | NA | slower | 0.2℃ colder, downto 0.5℃ for high GR and low WS | 94% T<br>99% TN<br>87% TX | Globally colder. Warmer only during day and high WS | **** | **** |
| LBOM | BOM | NA | slower | 0.2℃ colder, downto 0.5℃ for high GR and low WS | 96% T, TX<br>98% TN | Globally cooler than the reference, low dispersion of differences. | ***** | ***** |
| LLAN | Lanser | ± 0.2℃ | slower | 0.2℃ warmer for low and medium GR.<br>0.2℃ colder for high GR and low WS | 98% T, TX<br>97% TN | Close to the reference with both colder and warmer T° | ***** | **** |
| LCAS | Casella, Stevenson screen | NA | slower | 0.2℃ warmer for low GR and low WS | 96% T, TN<br>> 99% TX | Close to the reference. No day-night and clear sky-overcast differences | ***** | **** |
| | | | | | | | | |
| SSOC | Socrima BMO 1195 | ± 0.4℃ with a systematic 0.2℃ difference | slower | 0.5℃ warmer with maximum for medium GR | 80% T<br>98% TN<br>62 - 92% TX | Low influence of WS on radiation error | *** | *** |
| SVAI | Vaisala DTR13 | ± 0.5℃ | faster for T↓<br>slower for T↑ | 0.3℃ colder for high GR<br>0.1℃ warmer for other GR | 95% T<br>76% TN<br>85% TX | Colder for high GR and low WS | *** | **** |

| Acronym | Screen name | Consistency between screens | System time response compared to the reference | Radiation error | % within ± 0.5℃ of the reference | Comment | Comparison with the working reference (VEIG) | More "absolute" Rating |
|---|---|---|---|---|---|---|---|---|
| SWIN | Windspeed T351-PX-D3 | ± 0.3℃ | slower for T↓<br>faster for T↑ | 0.4℃ | 92% T<br>98% TN<br>60% TX | Warmer than the reference during day, with no influence of the WS | *** | *** |
| SDAV | Davis 07714 | ± 0.3℃ | faster | 0.2℃ colder, down to 0.5℃ colder for high GR and low WS | 97% T<br>>99% TN<br>99% TX | Surprisingly good results for a low cost screen. Better than the VDAV | ***** | ***** |
| SYOU | Young 41003 | ± 0.3℃ | slower for T↓<br>= for T↑ | ~0.2℃ Colder for high GR and low WS | 97% T<br>>99% TN<br>92% TX | 0.2℃ warmer than the reference during day | **** | *** |
| | | | | | | | | |
| VFIS | Fisher 439102 | ± 0.3℃ | slower | up to 1℃ | 70% T<br>>99% TN<br>30% TX | Radiation error decreases with increasing WS. Fan ventilation OK | ** | ** |
| VEIG | Eigenbrodt LAM 630 | ± 0.2℃ | = reference | = reference | >99% T, TN<br>~98% TX | | ***** | **** |
| VTHY | Thygan VTP37 | ± 0.1℃ | | up to 2℃ | ~50% T, TN<br><3% TX | Unexpected results : flow rate of the ventilation reduced ? | ** | * |
| VROT | Rotronic RS12T | NA | slower | up to 1℃ | 85% T, TX<br>97% TN | Cooler than the reference for low WS, warmer for high WS | *** | *** |

| Acronym | Screen name | Consistency between screens | System time response compared to the reference | Radiation error | % within ± 0.5℃ of the reference | Comment | Comparison with the working reference (VEIG) | More "absolute" Rating |
|---|---|---|---|---|---|---|---|---|
| VDAV | Davis 07755 | ± 0.2℃ | slower for T↓<br>faster for T↑ | up to 1℃ | 90% T<br>99% TN<br>85% TX | Cooler than the reference for low WS, warmer for high WS | *** | *** |
| VYOU | Young 43502 | ± 0.2℃ | slower for T↓<br>faster for T↑ | 0.6 ℃ colder for low WS, up to 0.7℃ warmer when WS increases above 3 m/s. | 90% T<br>100% TN<br>91% TX | No ventilation the first 11 months. Analysis only over the last month | **** | **** |
| | | | | | | | | |
| ATHI | THIES CLIMA Ultrasonic anemometer 2D | ± 0.3℃ with a systematic 0.5℃ difference | | up to 2℃ colder | 60% T, TN<br>30-60% TX | Much colder than the reference. Differences decrease when WS increases | ** | ** |

## 6.3 HYGROMETERS

- The Meteolabor VTP37 (Thygan) chilled mirror hygrometer was the preferred reference chosen by the IOC. But after an electric overload, no data were available since May 2009.
- Therefore a second working reference was defined as the mean value of two HMP45D hygrometers installed inside the Eigenbrodt screen. This working reference was available during the whole period.
- Five (5) models gave very good results over the test period, with no drift (< 0.5%) and more than 98% of values within ± 3% of the reference. These results are much better than what could be expected from the current knowledge about the state of the art. In addition to the “quality” of the sensors, an explanation may be the dry conditions mainly experienced during the intercomparison. Only few events of high RH close to saturation were encountered.
- Two (2) models gave medium results with deviations up to 4%.
- One (1) model gave poor results with deviations up to 12%.
- In principle, if the temperature inside the screen with an installed hygrometer is different from the temperature of the screen of the reference, an influence of several % (up to 6% close to saturation) should occur on the RH measurement. Though significant differences of temperature were seen between screens, no clear influence on the RH values was detected.
- A summary of the performances found during the intercomparison is given in table 8. A rating of the performances, <u>in comparison to the working reference and the Thygan</u>, seen during <u>this intercomparison</u> is proposed, ranging from one star (*) to five stars (*****). The rating principles are given in the annex 9.8.

**Table 8. Global results for hygrometers**

| Acronym | Hygrometer name | Screen | Consistency between hygrometers | Annual drift | Influence of temperature (5°--> 45℃) | Influence of RH (5% --> 100%) | % within ± 3% of the reference | Comment | "Quality" of the hygrometer |
|---|---|---|---|---|---|---|---|---|---|
| LBOM | Vaisala HMP45 | BOM | NA | < 0.5% | no influence | no influence | 98% Thygan 99.7% UHMP2 | HMP45 delivered and calibrated by BOM in 2007. Same type than UHMP2. | ***** |
| VFIS | Fisher&co 431411 | Fisher | dispersion < 1% around differences of about 2.5% | < 0.5% | 5% | 4% | 80% sensor 1 96% sensor 2 | Sensor 1 drier by 2% | ** |
| SVAI | Vaisala HMT337 | Vaisala HMT330 MIK | ± 1.5% | < 0.5% | < 2% | < 2% | 98.5% | | **** |
| UHMP | Vaisala HMP45 | Eigenbrodt/LAM630 | ± 1% | < 0.5% | no influence | no influence | 98% Thygan 99.6% UHMP2 | Same type than UHMP2. ~2% drier than Thygan above 85% RH | ***** |
| UTES | Testo AG 63379742 | Small Socrima | NA | ~1.5 % | ~3% | ~2% | 52% Thygan 18% UHMP2 | Over-estimation of about 4%, not consistent with laboratory and site calibration | ** |
| VTHY | Meteolabor VTP37 | Meteolabor VTP37 | ± 0.5% | NA | no influence | no influence | 98% UHMP2 | | ***** |
| VROT | Rotronic AG/C94 | Rotronic RS12T | NA | < 0.5% | 2% | 4% | 98% | Output of sensor 2 not recognized | **** |

# 7 RECOMMENDATIONS

1. In desert conditions, non-aspirated, naturally ventilated radiation shields or weather screens may perform better. Aspirated screens using fans tend to be blocked in dusty or sandy environments and may need more frequent maintenance.
2. It is recommended that further investigation be conducted on the potential of using ultrasonic devices, such as sonic anemometers, as temperature reference systems for screen intercomparisons.
3. Manufacturers of artificially ventilated radiation shields are recommended to provide a clear indication (e.g. a LED light) of the fan status directly at the screen or its control unit, or the datalogger. This would allow maintenance staff to check whether the fan is functioning properly by visual inspection. Additionally the fan status and preferably the fan speed should be provided in the data output for automatic monitoring purposes.
4. CIMO and manufacturers should aim for a standard laboratory test method to determine the radiation error of weather screens and radiation shields. From the result of this intercomparison, the proposal is to evaluate the radiation error for a maximum global radiation of 1000W/m$^2$ and a wind speed of 1m/s. This could stimulate improvements in screen design and provide valuable information prior to field intercomparisons.
5. Field Intercomparisons of humidity sensors should use a condensation hygrometer as reference system that measures the dew point (or frost point) directly. If several screens are used in an intercomparison of humidity sensors, temperature differences can have an influence on the measured relative humidity values.
6. Field Intercomparisons of humidity sensors should be performed by using one type of screen for all sensors. Whenever possible several humidity sensors should be installed in one screen in order to provide nearly the same air temperature for all tested sensors.
7. Manufacturers of humidity probes should provide a clearly represented quick installation guide (or card) to assist the user in the first phase of operation.
8. It is recommended for future intercomparisons to separate the data acquisition of sensors planned to be used as references (at least cabling, if possible the acquisition system itself): if a failure occurs on one sensor, it should not affect another sensor.
9. For future intercomparisons, it should be planned to have an on-site meeting, shortly after the official beginning of the intercomparison, to check on site all the instruments, data acquisition system and procedures, preferably with all the participants wishing to participate and to check their instruments.
10. For future intercomparisons it should be planned to have at least two meetings for each intercomparison: one meeting before the start of the intercomparison and one after it for finalizing the intercomparison report. This is necessary to provide the final report promptly. Even an extensive use of telephone conferences cannot replace direct communication.
11. Some of the well-performing screens in this intercomparison should also be used in a possible follow up intercomparison of thermometer screens and humidity measuring instruments in arctic regions to have a link between both experiments.
12. In the CIMO guide a clear distinction should be made between percentages of relative humidity and percentages as an expression for any other quotient.

# 8 REFERENCES


*[1] WMO Final Report of the first session of the CIMO Expert Team Meeting SBII&CM*, Trappes (France), 24-28 November 2003

*[2] WMO Final Report of the second session of the CIMO Expert Team Meeting SBII&CM*, Geneva (Switzeland), 5-9 December 2005

*[3] WMO Final Report of the forth (reduced) session of the CIMO Expert Team Meeting SBII&CM*, Ghardaïa (Algeria), 19-23 March 2007

[4] ISO 17714:2007 Standard: Meteorology - Air temperature measurements - *Test methods for comparing the performance of thermometer shields/screens and defining important characteristics*, 2007

All the WMO reports are available at this page: http://www.wmo.int/pages/prog/www/IMOP/reports.html

[5] Guide to Meteorological Instruments and Methods of Observation ("CIMO Guide"), WMO publication n°8, 7th edition, 2008, available at: http://www.wmo.int/pages/prog/www/IMOP/publications/CIMO-Guide/CIMO Guide 7th Edition, 2008/CIMO_Guide-7th_Edition-2008.pdf

*[6] WMO Final Report of the forth session of the CBS-IOS Expert Team on the Requirements for Data from Automatic Weather Stations*, Geneva (Switzeland), 20-24 March 2006, available at: http://www.wmo.int/pages/prog/www/CBS-Reports/IOS-index.html

[7] Tammelin, B., Heimo, A., Leroy, M., Rast, J. and Säntti, K., 2001. Meteorological measurements under icing conditions - EUMETNET SWS II project. Reports 2001:6. Finnish Meteorological Institute. 52 p.

[8] World Meteorological Organization, 1989*a*: *WMO Assmann Aspiration Psychrometer Intercomparison* (D. Sonntag). Instruments and Observing Methods Report No. 34, WMO/TDNo. 289, Geneva.

[9] World Meteorological Organization, 1998*a*: *Recent Changes in Thermometer Screen Design and their Impact* (A. Barnett, D.B. Hatton and D.W. Jones). Instruments and Observing Methods Report No. 66, WMO/TD-No. 871, Geneva.

[10] World Meteorological Organization, 1989*b*: *WMO International Hygrometer Intercomparison* (J. Skaar, K. Hegg, T. Moe and K. Smedstud). Instruments and Observing Methods Report No. 38, WMO/TD-No. 316, Geneva.

[11] Lanzinger E., Langmack H., *Measuring Air Temperature by using an Ultrasonic Anemometer*, Poster presented at TECO-2005, Bucharest, Romania, available at: http://www.wmo.int/pages/prog/www/IMOP/publications/IOM-82-TECO_2005/Posters/P3(09)_Germany_4_Lanzinger.pdf (in World Meteorological Organization, 2005: Instruments and Observing Methods Report No. 82, WMO/TD-No. 1265, Geneva).

# 9 ANNEXES

## 9.1 QUESTIONNAIRE 1

**WORLD METEOROLOGICAL ORGANIZATION**

**QUESTIONNAIRE I**

to potential participants

of the WMO Combined Intercomparison of Thermometer Screens/Shields

in Conjunction with Humidity Measuring Instruments

Ghardaïa**,** Algeria

1. Member Country: ……………………………………………………………………………..
2. Expert (point-of-contact) for the intercomparison:
   Name, First Name:…………………………………………………………………………….
   Address: ……………………………………………………………………………………
   Tel./Fax: ……………………………………………………………………………………
   E-mail: ………………………………………………………………………………………
3. Basic information on the humidity sensor or screen/shield foreseen in the intercomparison: (1), (2)
   Thermometer screen/shield natural ventilated [ ]
   Thermometer screen/shield artificially ventilated [ ]
   Humidity sensor [ ]

3.1 Short description of the proposed humidity sensor or screen/shield:

…………………………………………………………………………………………………
…………………………………………………………………………………………………
…………………………………………………………………………………………………
…………………………………………………………………………………………………

3.2 Type of the humidity sensor or screen/shield:

a) Model/Type:………………………………………………………………………………
b) Manufacturer:……………………………………………….
   Country:…….…………………………
c) Number of sites where the sensor or screen/shield is in operational use or is intended to be in your country: ………………………………..………………………………………………….
d) Will you submit **one [ ]** or **two [ ]** identical instruments (2), (3)

3.3 Detailed information on the sensor or screen/shield:

3.3.1 **Thermometer screen/shield**:

- Performance characteristic (operating range): ……………………..………………
- Estimated radiation error:………………………………………………………………
- Material used (construction):……..……………………………………………………….
- Aspiration rate (in case of artificially ventilated screen/shield):……………………
- Suitable for the described temperature probe(4) [ ] or must be used with a particular type [ ] (2)
  - If only for a particular, please specify the sensor or limits:

……..…………………………………………………………………………………..
….……………………………………………………………………………………...
………………………………………………………………………………………...

- Suitable for any type of humidity sensor [ ] or only a particular type [ ] (2)
  - If only for a particular, please specify the sensor or limits:

    ……..…………………………………………………………………………………..
    ….……………………………………………………………………………………...
    …………………………………………………………………………………………

3.3.2 **Humidity sensor:**

- Parameter reported: Relative humidity [ ] Dew-point temperature [ ] (2)
- Principle of measurement:………………………………………………………………
- Measuring range:…………………………………………………………………...
- Performance characteristic (operating range): …………………………....……..
- Uncertainty: …………………………………………………………………………
- Time constant:………………………..……………………………………………...
- Resolution:…………………………...………………………………………………
- Long-term stability:………………………..……………………………………………..
- Sampling interval (internal or recommended):…...……………………………...
- Averaging interval (internal or recommended):……………………………………….
- Time resolution (if applicable):…………………………………………………………
- Output averaging time (if applicable): …………………………………………………

Date ______________ Signature of the Permanent Representative ______________

**NOTES:**

Further information on organizational and technical issue for the preparation of the intercomparison will be distributed in due course to the experts designated by you, as appropriate.

It is intended to calibrate the temperature probes and the humidity sensors in laboratory before and after the intercomparison. Meteo-France offered to do this calibration in its laboratory in Trappes (near Paris). Nevertheless, the sensors must be calibrated and adjusted by the manufacturer or the member country proposing the sensors.

(1) In case it is intended to submit more types of sensors, attach another completed copy(ies) of this questionnaire.

(2) Please tick the appropriate box.

(3) To achieve more confidence in the results, preferences will be given to testing of two identical instruments; however this is not a condition for participation.

(4) For the intercomparison of the screens, it is preferred to use the same type of temperature probe. Meteo-France (MF) has offered calibrated temperature probes, with characteristics given in the Attachment. Such a probe will be used in each screen with which it is compatible. Therefore, the compatibility between the MF probe and the proposed screen must be indicated. If there is any reason for not

using the MF probe (size, probe characteristics, calibration uncertainty, etc., this should be indicated.

Please return the completed questionnaire, as soon as possible,
but not later than **17 April 2006** to the WMO Secretariat, to the attention of:

Dr Miroslav Ondráš

Senior Scientific Officer, Observing System Division

World Weather Watch Department

P.O. Box 2300

1211 Geneva 2, Switzerland

Tel.: +(41 22) 730 8409

Fax: +(41 22) 730 8021

E-mail: mondras@wmo.int

**Attachment to Questionnaire I**

## Pt100 temperature sensor used by Meteo-France for air temperature measurements in the operational network

Technical parameters

Measuring range: - 40 ℃ to + 60 ℃.

Uncertainty: ± 0.1 ℃.

Metallic sheathed cable (4 wires) silver-welded on sensitive part. Cable length: 5 m.

Sense current must not exceed 3 mA (AC efficient current).

Metrology

Platinum wire resistance is equal to:

92.16 ± 0.04 ohms at - 20 ℃

100.00 ± 0,03 ohms at 0 ℃

107.79 ± 0.04 ohms at + 20 ℃

115.54 ± 0.04 ohms at + 40 ℃.

For the intercomparison, the probes will be selected to fall in these limits, equivalent to ± 0.1 ℃.

**Technical diagram** (all dimensions are in mm)

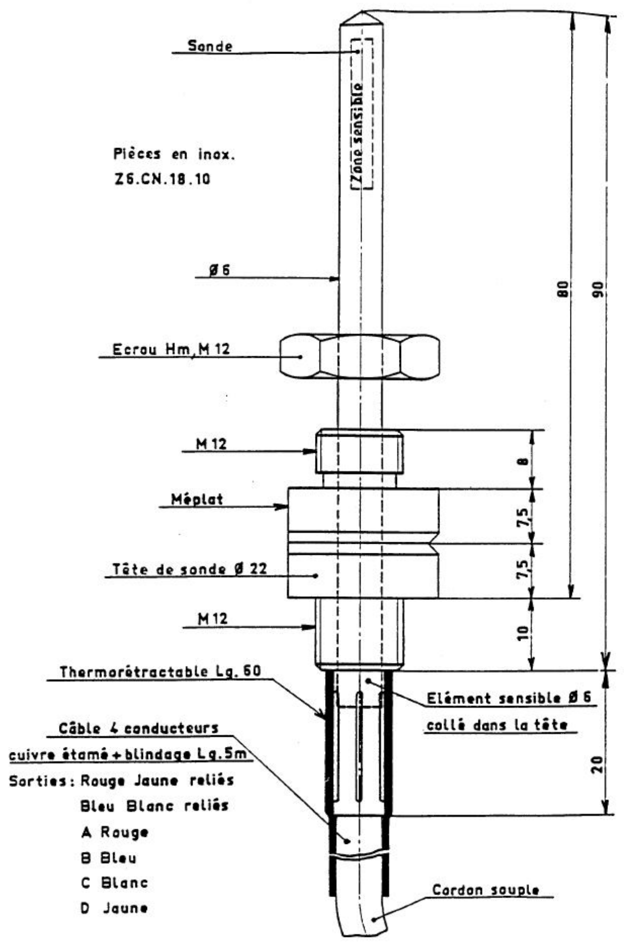

## 9.2 QUESTIONNAIRE 2

**WORLD METEOROLOGICAL ORGANIZATION**

**QUESTIONNAIRE II**

Addressed to Selected Participants of the

***WMO Combined Intercomparison of Thermometer Screens/Shields,***

***in Conjunction with Humidity Measurements, in Various Climatic Regions,***

***Ghardaïa, Algeria, January - October 2007***

*Note: Please complete a separate questionnaire for each type of Sensor.*
*If necessary, attach additional pages.*

*Electronic version of the Questionnaire is available at:*
*http://www.wmo.int/web/www/IMOP/intercomparisons.html*

| | |
|---|---|
| 1. | Member country |

| | |
|---|---|
| 2. | Name of participating institution/company |
| | Address |

| | | |
|---|---|---|
| 3. | Person responsible for the intercomparison | |
| | Surname | First name |
| | Tel.: | Fax: |
| | E-mail: | Other: |

| | | |
|---|---|---|
| 4. | Alternative contact person | |
| | Surname | First name |
| | Tel.: | Fax: |
| | E-mail: | Other: |

| | |
|---|---|
| 5. | Name of manufacturer *(if different from no above)* same ☐ different ☐ |
| | Address |

| | | |
|---|---|---|
| 6. | **Shipment of participating instruments** | |
| | Approx. commercial value Euro | Total weight of consignment kg |
| | Number of boxes | Overall volume of boxes $cm^3$ |
| | Overall dimension, in cm (i.e. for storage purposes)<br>Length x Width x Height cm | |
| | Other information concerning shipping | |

| | | |
|---|---|---|
| 7. | **Instrument specifications**<br>*Please enclose in a separate sheet a diagram showing, preferably, the different elements (photos are welcomed).*<br>***Please supply a technical documentation to allow the best evaluation by the organizer of all the constraints related to the installation, data acquisition and calibration.***<br>***Please indicate a representative point of the sensor or screen/shield.*** | |
| | Instrument name | Model/Type |
| | Number of sites where the instrument is in operational use or intended to be in your country: | Could you submit One ☐ or Two ☐ identical instruments? (Two identical instruments are preferred - one as backup.) |
| | Principle of operation: | |

| | | |
|---|---|---|
| 8. | **Information for field installation** | |
| | ***Notes on the power supply:*** Sensors should be able to operate on 220V AC, 50 Hz or unregulated 12V DC (if power supply is necessary); *For other voltages, converters must be provided.* | |
| | Overall dimensions of the instrument, in cm<br>Length x Width x Height cm | Total weight<br>kg |
| | Power supply/Voltage required | Maximum total power consumption (watts) |

| | | |
|---|---|---|
| 9. | **Sensor siting requirements** | |
| | Installation alignment required Yes ☐ No ☐ | |
| | Maximum distance to the data logger m | Cable length m |
| | Will an expert from the Member country assist with the installation of the Sensor Yes ☐ No ☐ | |
| | Will an installation tools kit accompany the shipment? Yes ☐ No ☐ | |
| | Any special tools required for the installation? Yes ☐ No ☐<br>Please describe | |

| 11. | **Calibration** |
|---|---|
| | Calibration reference |
| | Recommended calibration intervals |
| | Procedure |

| 12. | **Sensor Output** | | | |
|---|---|---|---|---|
| | *Analogue* | | Yes ☐ No ☐ | Voltage or current |
| | *Digital* | RS232 | Yes ☐ No ☐ | |
| | | Other | Yes ☐ No ☐ | Please specify |
| | Or propose and clearly describe an interface for data acquisition | | | |

| 13. | **Any other relevant information** |
|---|---|
| | |

Date

Name of person who completed this form

Please return an electronic copy the completed questionnaire, as soon as possible, but not later than **14 July 2006** to:

Dr Miroslav Ondráš

Senior Scientific Officer, Observing System Division

World Weather Watch Department

P.O. Box 2300

1211 Geneva 2, Switzerland

Tel.: +(41 22) 730 8409

Fax: +(41 22) 730 8021

E-mail: mondras@wmo.int

## 9.3 LIST OF SELECTED INSTRUMENTS

| Member country | Manufacturer | Type | Number | Acronym |
|---|---|---|---|---|
| Algeria | Socrima | Large Stevenson Screen | 1 | LSOC |
| Australia | BoM | Small Stevenson screen | 1 | LBOM |
| Austria | Lanser | | 2 | LLAN |
| France | Socrima | BMO1195D | 2 | SSOC |
| Germany | Fischer | 431411 | 2 | VFIS |
| Germany | Vaisala | HMT337 & HMT 330 MIK | 2 | SVAI |
| Germany | Eigenbrodt / Vaisala | HMP45D / LAM630 | 2 | VEIG UHMP |
| Germany | Testo | AG/63379742 | 2 | UTES |
| Italy | CAE | TU20AS | 2 | SCAE |
| Sudan | Casella | Stevenson Screen | 1 | LCAS |
| Switzerland | Meteolabor | Thygan VTP37 Airport | 1 | VTHY |
| Switzerland | Meteolabor | Thygan VTP37 Thermohygrometer | 1 | |
| Switzerland | Rotronic | AG/RS12T & Hygroclip S3 | 2 | VROT |
| UK/HMEI | Windspeed | T351-PX-D/3 | 2 | SWIN |
| USA | Davis | PN7714 | 2 | SDAV |
| USA | Davis | | 2 | VDAV |
| USA/HMEI | Young | 41003 | 2 | SYOU |
| USA/HMEI | Young | 43502 | 2 | VYOU |

## 9.4 CALIBRATION INFORMATION

### 9.4.1 Temperature calibrations by Meteo-France

| Installed in screen | Serial Number of the probe | Calibration date | Temperature (°C) | | | |
|---|---|---|---|---|---|---|
| | | | -20 | 0 | 20 | 40 |
| LCAS | T77 | 24-Jan-2006 | 0.0146 | -0.0175 | -0.0411 | -0.0632 |
| LLAN1 | T79 | 24-Jan-2006 | 0.0227 | -0.0032 | -0.0263 | -0.0408 |
| LLAN2 | T70 | 1-Feb-2006 | 0.0100 | -0.0184 | -0.0382 | -0.0542 |
| LSOC | T47 | 30-Jan-2006 | 0.0558 | 0.0286 | 0.0066 | -0.0112 |
| SDAV1 | UT68 | 3-May-2004 | 0.0850 | 0.0450 | 0.0160 | -0.0120 |
| SDAV2 | UT46 | 1-Apr-2004 | 0.0590 | 0.0200 | -0.0080 | -0.0380 |
| SSOC1 | T44 | 30-Jan-2006 | 0.0160 | -0.0124 | -0.0319 | -0.0473 |
| SSOC2 | T45 | 9-Feb-2006 | 0.0337 | 0.0072 | -0.0113 | -0.0267 |
| SYOU1 | T53 | 3-Feb-2006 | 0.0246 | -0.0032 | 0.0216 | -0.0346 |
| SYOU2 | T51 | 7-Feb-2006 | 0.0304 | 0.0031 | -0.0131 | -0.0261 |
| VDAV1 | 772 | 6-Jan-2006 | 0.0827 | 0.0544 | 0.0299 | 0.0087 |
| VDAV2 | 728 | 10-Jan-2006 | 0.1022 | 0.0756 | 0.0522 | 0.0216 |
| VEIG11 | T49 | 9-Feb-2006 | 0.0273 | -0.0022 | -0.0230 | -0.0383 |
| VEIG12 | T74 | 26-Jan-2006 | 0.0019 | -0.0247 | -0.0439 | -0.0598 |
| VEIG21 | T64 | 3-Feb-2006 | 0.0520 | 0.0201 | -0.0047 | -0.0268 |
| VEIG22 | T73 | 26-Jan-2006 | 0.0230 | -0.0057 | -0.0297 | -0.0477 |
| VYOU1 | T54 | 7-Feb-2006 | 0.0241 | -0.0030 | -0.0189 | -0.0307 |
| VYOU2 | T55 | 1-Feb-2006 | 0.0157 | -0.0128 | -0.0294 | -0.0435 |

| Sensor | Calibration date | Calibration temperature (°C) | | | |
|---|---|---|---|---|---|
| | | -20 | 0 | 20 | 40 |
| Tground | 27-Jul-2004 | 0.0520 | 0.0490 | 0.0540 | 0.0620 |
| T@10cm | 24-Jan-2006 | -0.0262 | -0.0520 | -0.0695 | -0.0839 |
| T@50cm | 24-Jan-2006 | 0.0207 | -0.0110 | -0.0343 | -0.0541 |

### 9.4.2 Temperature calibrations by manufacturers

| Screen | SN | Calibration date | Temperature (°C) | | | | |
|---|---|---|---|---|---|---|---|
| | | | -20 | 0 | 20 | 22 | 40 |
| SVAI1 | B494000 | 4-Jan-2007 | | | | -0.04 | |

| Screen | SN | Calibration date | Temperature (℃) | | | | |
|---|---|---|---|---|---|---|---|
| | | | -20 | 0 | 20 | 22 | 40 |
| | 9 | | | | | | |
| SVAI2 | B494001<br>0 | 4-Jan-2007 | | | | -0.04 | |
| SWIN1 | 1398 | 14-Mar-2007 | 0.0145 | -0.0335 | -0.0727 | | -0.1070 |
| SWIN2 | 1397 | 14-Mar-2007 | 0.0148 | -0.0381 | -0.0825 | | -0.1232 |
| VFIS1 | 188 | 19-Apr-2007 | | | 0.2 | | |
| VFIS2 | 189 | 19-Apr-2007 | | | 0.1 | | |
| VTHY1 | 338 | 1-Jun-2005 | | | | -0.03 | |
| VTHY2 | 339 | 1-Jun-2005 | | | | -0.05 | |

### 9.4.3 Relative humidity laboratory calibrations by Météo-France

| Sensor | Calibration date | T=23℃ | | | | | T=40℃ | | | | |
|---|---|---|---|---|---|---|---|---|---|---|---|
| | | 10% | 33% | 55% | 75% | 90% | 10% | 33% | 55% | 75% | 90% |
| SVAI1 | 12-Feb-2007 | 0.3 | -0.7 | -0.4 | -1.1 | -2.6 | 0.3 | 0.8 | 3.7 | -2.3 | 2.2 |
| SVAI2 | 12-Feb-2007 | -0.2 | 0.3 | -0.5 | -0.9 | -1.3 | 0.3 | 0.6 | 0.5 | 0.4 | 0.9 |
| UHMP11 | 09-Jan-2007 | 0.0 | 1.8 | 0.9 | 0.9 | 2.0 | 0.5 | 2.3 | 1.0 | 0.9 | 1.5 |
| UHMP12 | 09-Jan-2007 | -0.3 | 1.4 | 0.3 | 0.5 | 1.7 | 0.0 | 2.3 | 1.6 | 2.1 | 3.1 |
| UHMP21 | 09-Jan-2007 | -0.1 | 1.7 | 1.0 | 1.0 | 2.1 | 0.5 | 2.8 | 2.2 | 2.7 | 3.5 |
| UHMP22 | 09-Jan-2007 | -0.3 | 1.7 | 0.6 | 0.6 | 1.8 | 0.2 | 2.4 | 1.6 | 1.8 | 2.8 |
| UTES1 | 22-Dec-2006 | -0.6 | -0.4 | -0.2 | 0.7 | 1.4 | -0.8 | -0.8 | -1.1 | 0.0 | 1.2 |
| UTES2 | 22-Dec-2006 | -0.2 | 0.2 | 0.5 | 1.2 | 1.9 | -0.4 | -0.4 | -0.5 | 0.6 | 1.4 |
| VROT1 | 08-Mar-2007 | -1.7 | -0.1 | 0.7 | 0.7 | 1.3 | -0.7 | 0.1 | 0.7 | 1.3 | 3.1 |
| VROT2 | 08-Mar-2007 | -1.4 | 0.0 | 0.6 | 0.9 | 1.2 | -0.5 | 0.1 | 0.7 | 1.1 | 2.7 |

### 9.4.4 Relative humidity laboratory calibrations by manufacturers

| Sensor | Calibration date | T=22℃ | T=23℃ | | |
|---|---|---|---|---|---|
| | | 50% | 33% | 75% | 90% |
| VFIS1 | 19-Apr-2007 | | 0.3 | 0.8 | -1.5 |
| VFIS2 | 19-Apr-2007 | | 0.0 | -0.1 | -1.8 |
| VTHY1 | Jun-2005 | 0.4 | | | |
| VTHY2 | Jun-2005 | 0.4 | | | |

### 9.4.5 Relative humidity on-site calibrations by Météo-France

This calibration was processed on the 5th of June, 2008.

| Sensor | T=23℃ | | | | |
|---|---|---|---|---|---|
| | 10% | 33% | 50% | 80% | 90% |
| UHMP11 | 0.1 | 1.6 | 2.3 | | 1.7 |
| UHMP12 | -0.1 | 1.8 | 3.6 | | 3.5 |
| UHMP21 | 0.3 | 2.4 | 4.0 | | 4.7 |
| UHMP22 | -0.2 | 1.6 | 0.7 | | 0.6 |
| UTES2 | | -2.7 | | -0.3 | |
| VROT1 | -0.7 | 0.6 | 0.6 | | 0.1 |
| VROT2 | -0.3 | 0.7 | -0.7 | | 1.0 |

## 9.5 DETAILED ANALYSIS OF SCREENS HISTOGRAMS

The diagrams that show whether the distribution of the differences to normal are plotted in the following histograms. Almost all screens can be seen as having a normal distribution. This result is confirmed by the Q-Q plot (Quantile Quantile plot is a graphical technique for determining if two data sets come from populations with a common distribution). It is generally a more powerful approach than the common technique of comparing histograms.

The q-q plot is similar to a probability plot. For a probability plot, the quantiles for one of the data samples are replaced with the quantiles of a theoretical distribution.

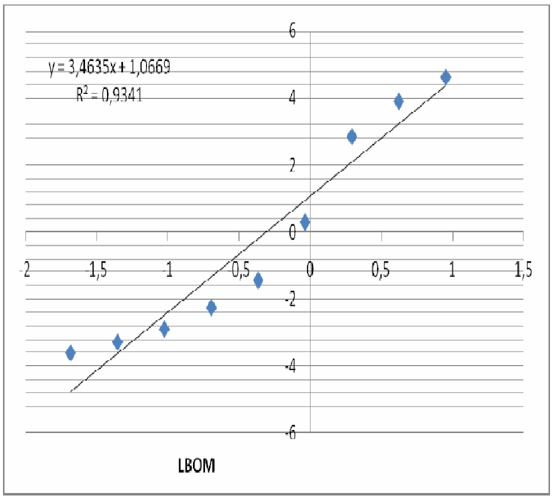


**Figure 62. Q-Q plot for LBOM-VEIG22**

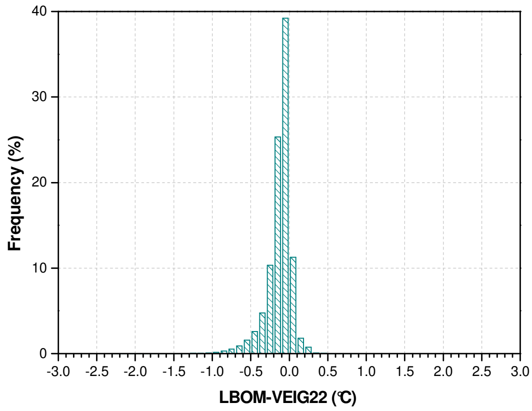


**Figure 63. Histogram for LBOM-VEIG22**

In terms of tail length, the histogram shown above would be characteristic of a "long-tailed" distribution and the majority of values (82%) are in the range [-0.2℃;+0.2℃] in figure 63. The same indication is found on figure 62: the points follow a strongly nonlinear pattern, suggesting that the data are non symmetric.

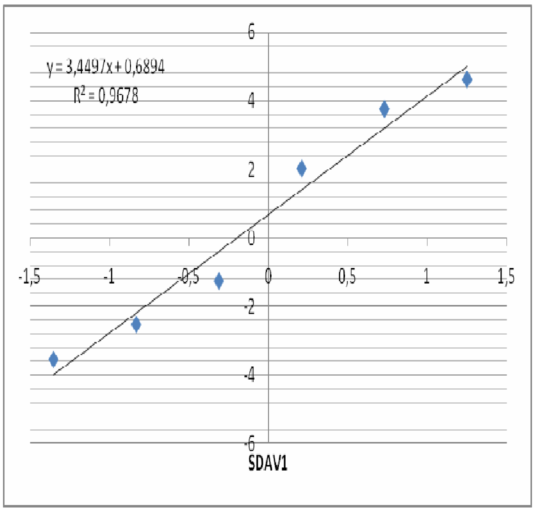


Figure 64. Q-Q plot for SDAV1-VEIG22

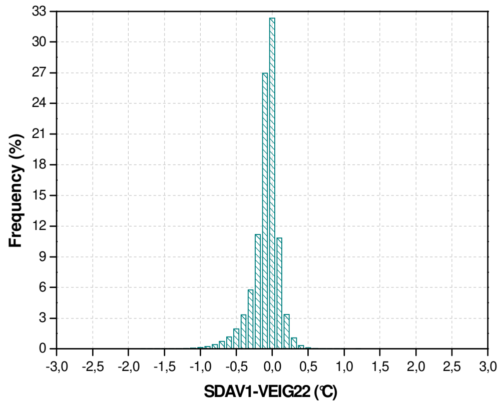


Figure 65. Histogram for SDAV1-VEIG22

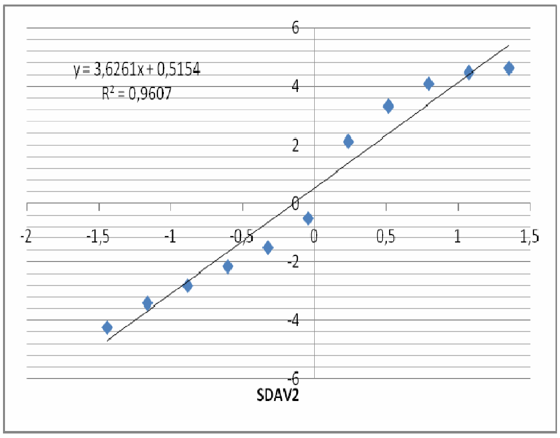


Figure 66. Q-Q plot for SDAV2-VEIG22

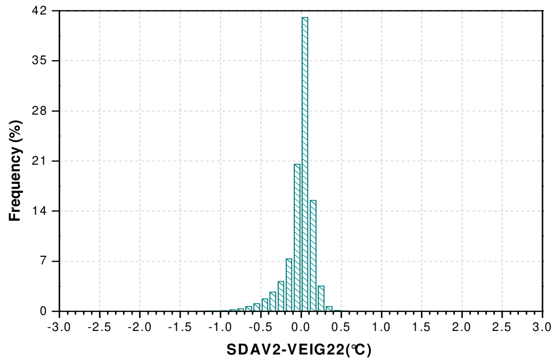


Figure 67. Histogram for SDAV2-VEIG22

Figure 66 and figure 64 show the linearity of the points suggesting that the data are normally distributed and figure 65 and figure 67 show that these two histograms are skewed to the left, suggesting that the data are not symmetric.

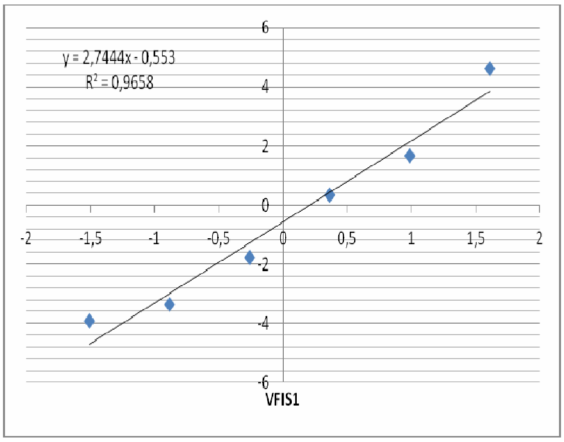


Figure 68. Q-Q plot for VFIS1-VEIG22

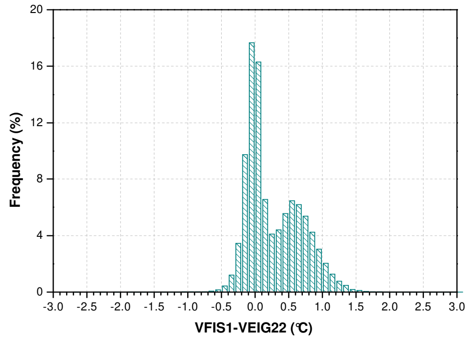


Figure 69. Histogram for VFIS1-VEIG22

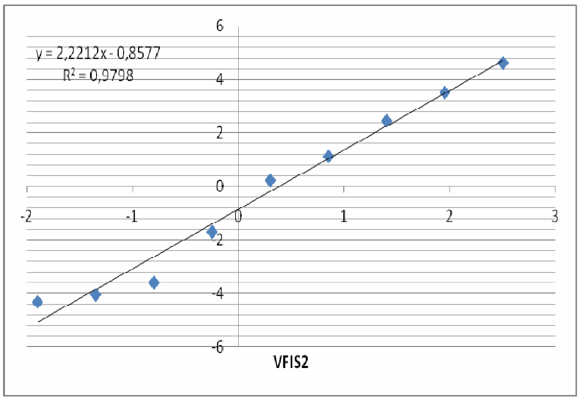


Figure 70. Q-Q plot for VFIS2-VEIG22

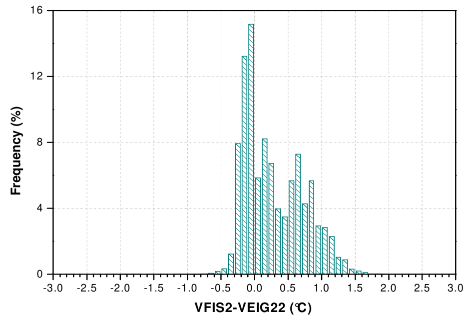


Figure 71. Histogram for VFIS2-VEIG22

This graph (Figure 69) illustrates bimodality due to a mixture of probability modes. In this case, each of the modes appears to have a roughly bell-shaped component. One could easily imagine the above histogram being generated by a process consisting of two normal distributions with the same standard deviation but with two different locations (one centred at 0 and the other centred at approximately 0.5).

Approximately 50% of the values are in the range [-0.2℃;+0.2℃]. The normal probability plot in figure 68 shows a reasonably linear pattern in the center of the data.

The figure 70 shows the linearity of the distribution but the graph of figure 71 shows that the histogram is non symmetric.

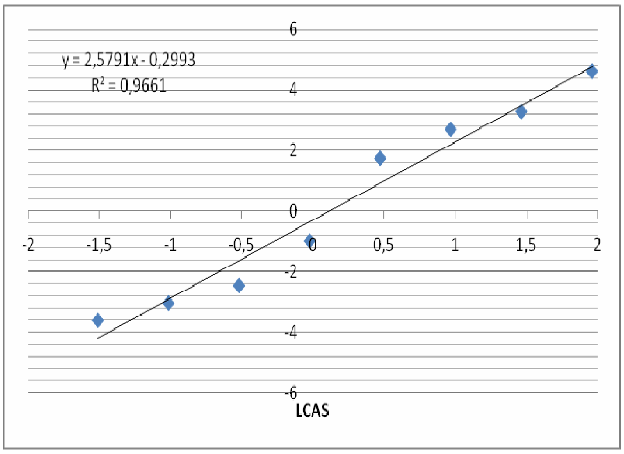


Figure 72. Q-Q plot for LCAS-VEIG22

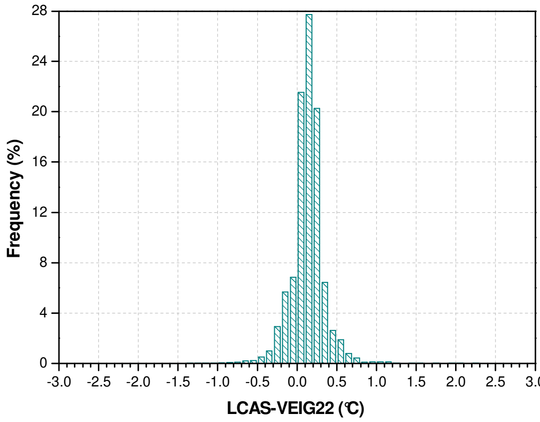


Figure 73. Histogram for LCAS-VEIG22

The graph in figure 72 shows the linearity of the points and suggests that the data are normally-distributed. This linearity is confirmed by the coefficient of adjustment $R^2$, equal to 0.97, very close to 1. A symmetric distribution is one in which the 2 "halves" of the histogram (Figure 73) appear as mirror-images of one another. The example in Figure 74 and Figure 75 is symmetric. And approximately 70% of values are in the range [-0.2°C; +0.2°C].

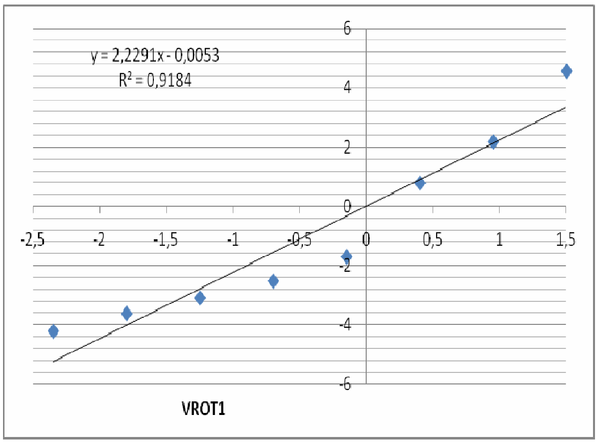


Figure 74. Q-Q plot for VROT1-VEIG22

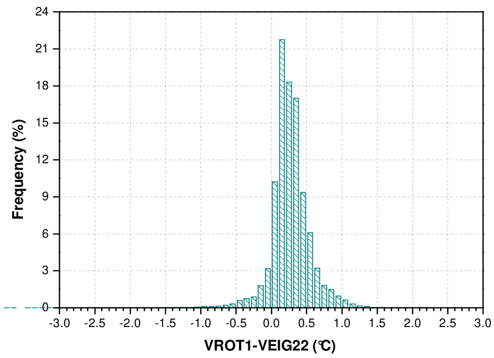


Figure 75. Histogram for VROT1-VEIG22

Figure 74 shows a reasonably linear pattern in the center of the data. However, the tails, particularly the upper tail, show departures from the fitted line and figure 75 shows that the histogram is skewed to the right, thus non symmetric.

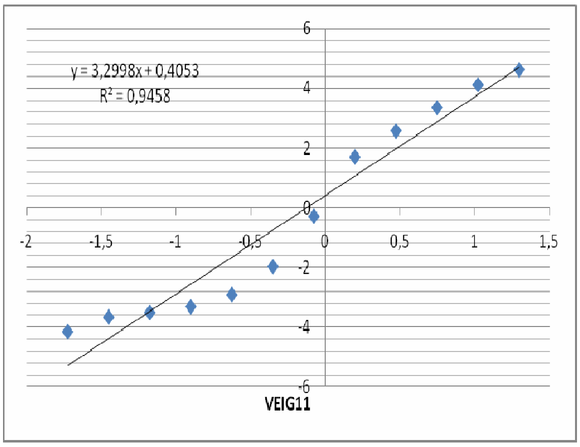


Figure 76. Q-Q plot for VEIG11-VEIG22

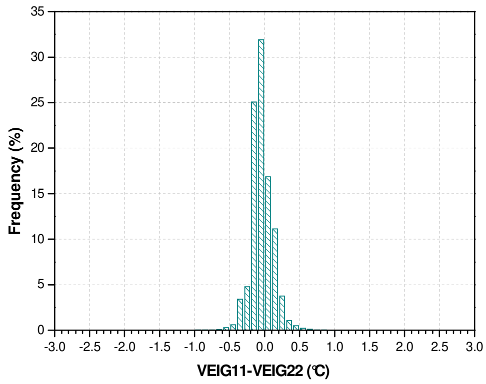


Figure 77. Histogram for VEIG11-VEIG22

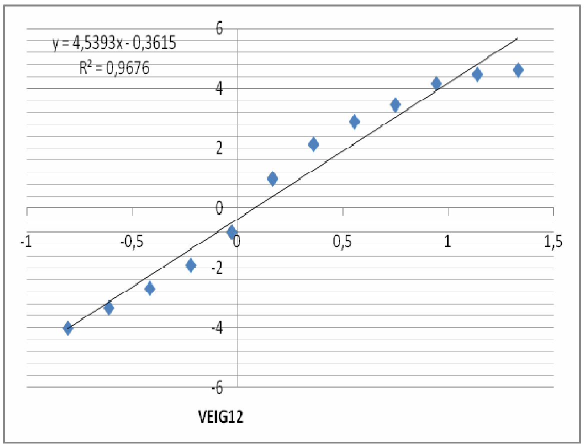


Figure 78. Q-Q plot for VEIG12-VEIG22

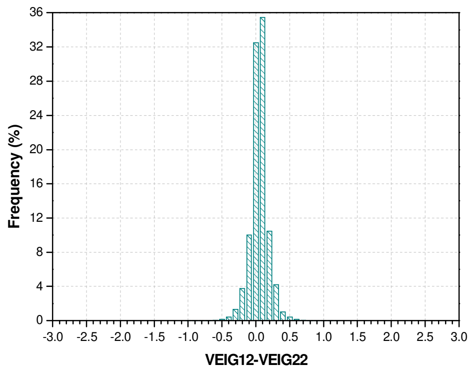


Figure 79. Histogram for VEIG12-VEIG22

Figure 76 shows the linearity of the points and approximately 86 % of values are in the range [-0.2℃;+0.2℃] , at first sight the distribu tion therefore appears symmetrical

Figure 78 shows a best linearity of the points in the center of the data. The upper tail, shows departures from the fitted line and 89% of values are in the range [-0.2℃;+0.2℃]. It confirms that this screen is symmetric.

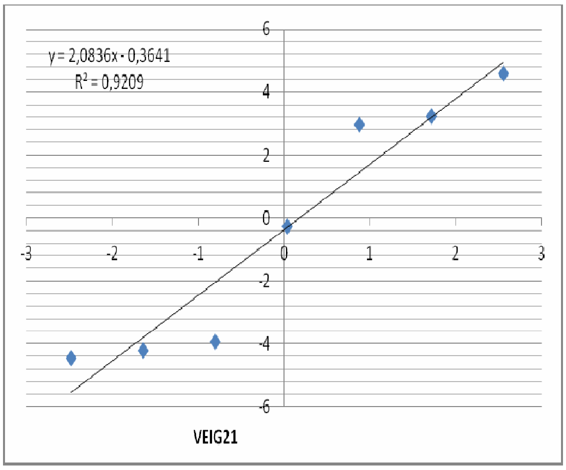


Figure 80. Q-Q plot for VEIG21-VEIG22

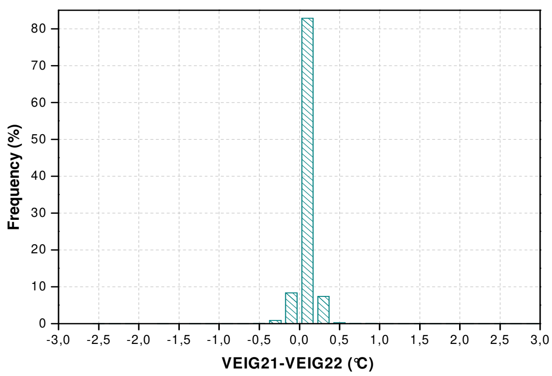


Figure 81. Histogram for VEIG21-VEIG22

The histogram in figure 81 shows that the majority of values approximately 95% are in the range [-0.2℃;+0.2℃]. The distribution appears sym metrical although it is not show in the curve of Q-Q plot (Figure 80) because of the high concentration of data in the range [0℃, +0.1℃].

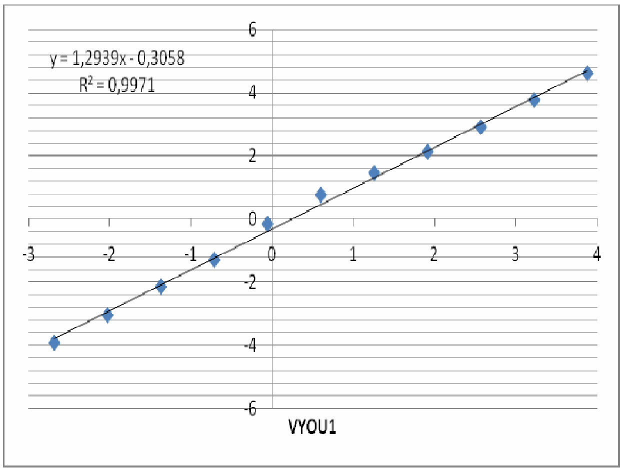


Figure 82. Q-Q plot for VYOU1-VEIG22

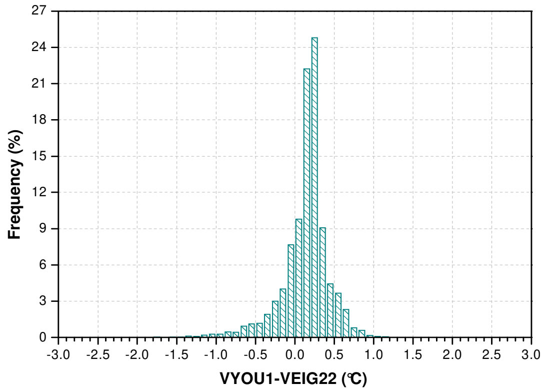


Figure 83. Histogram for VYOU1-VEIG22

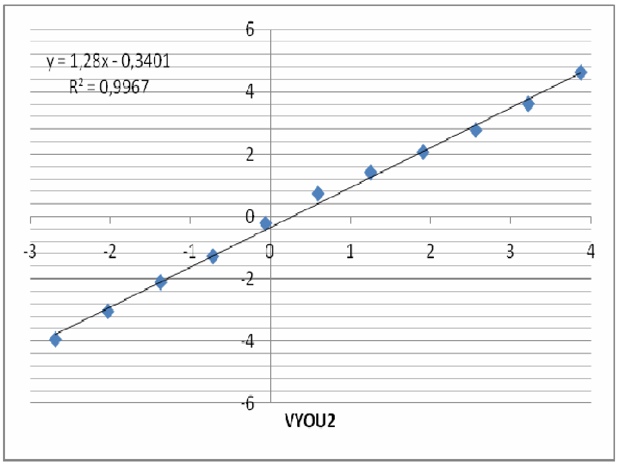


Figure 84. Q-Q plot for VYOU2-VEIG22

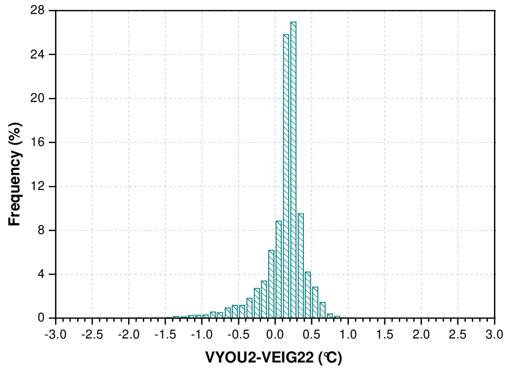


Figure 85. Histogram for VYOU2-VEIG22

The points are perfectly aligned on the graphs represented in the figure 82 and figure 84 and this linearity is confirmed by the coefficient of adjustment $R^2$, very close to 1. The two histograms in figure 83 and figure 85 show that two screens are approximately symmetrically distributed around the reference, and with a large dispersion around zero. The mode is centered at approximately 0.3 and 55% of values are in the interval [-0.2°C, +0.2°C]

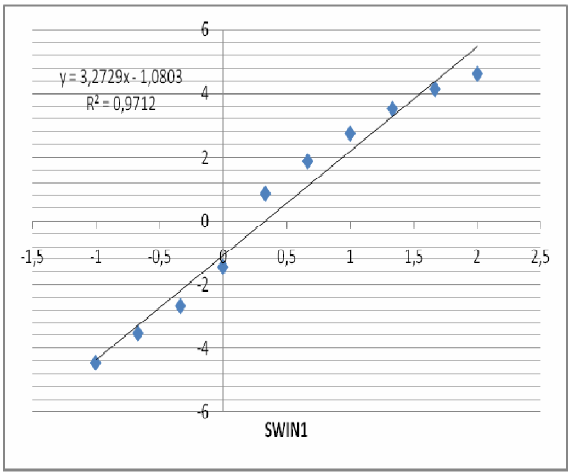


**Figure 86. Q-Q plot for SWIN1-VEIG22**

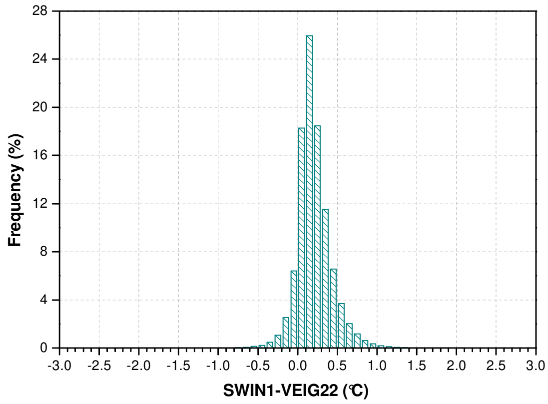


**Figure 87. Histogram for SWIN1-VEIG22**

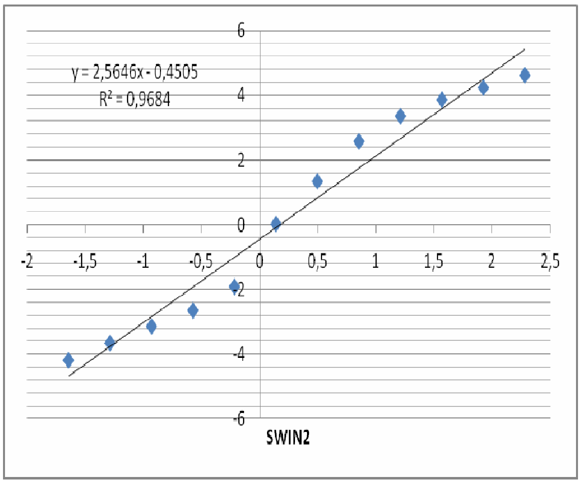


**Figure 88. Q-Q plot for SWIN2-VEIG22**

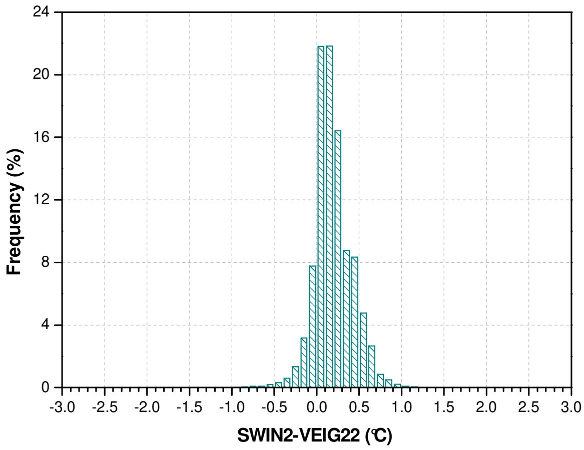


**Figure 89. Histogram for SWIN2-VEIG22**

Overall, for both SWIN screens the points are relatively aligned in the center of the data but skewed in the both extremities, as shown on the graphs represented in the figure 86 and figure 88, with the mode of the differences between 0℃ and 0.2℃, and symmetrical distributions about the modes being 0 and 0.1 respectively.

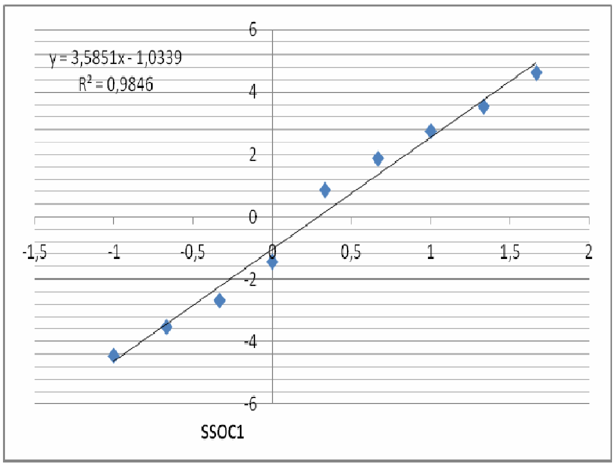


Figure 90. Q-Q plot for SSOC1-VEIG22

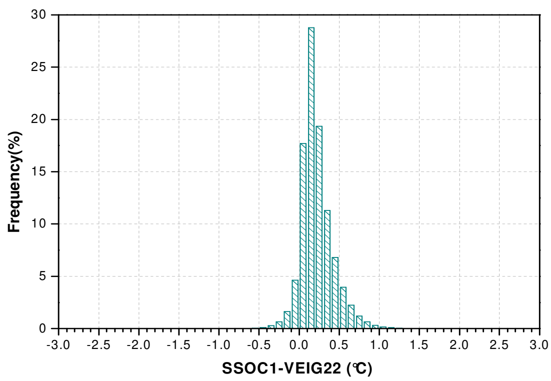


Figure 91. Histogram for SSOC1-VEIG22

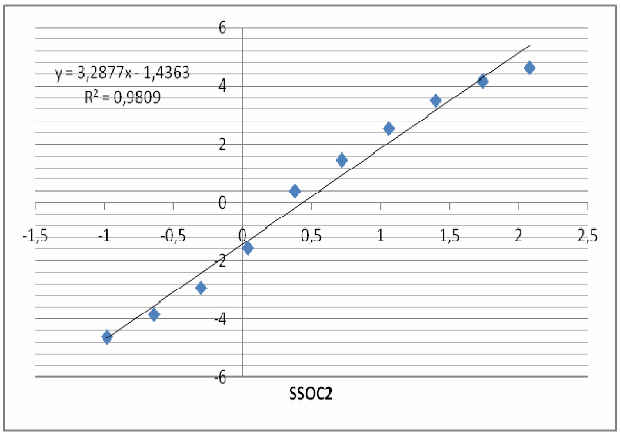


Figure 92. Q-Q plot for SSOC2-VEIG22

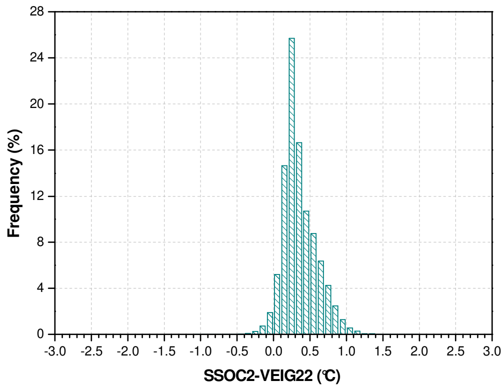


Figure 93. Histogram for SSOC2-VEIG22

For both SSOC screens the points are relatively aligned on the graphs represented in the figure 90 and figure 92, but the histogram in figure 91 and figure 93 shows they are skewed to the right then non symmetric.

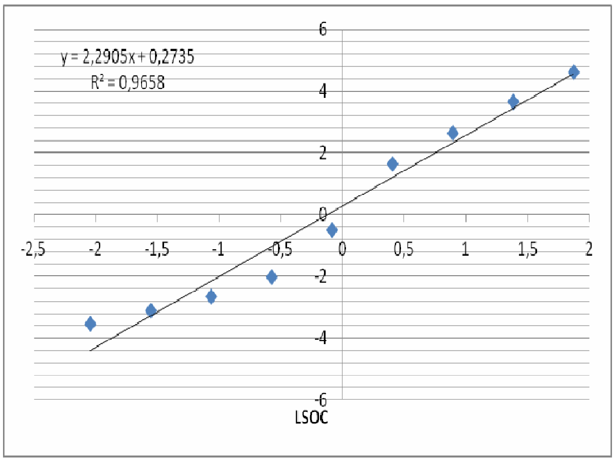


Figure 94. Q-Q plot for LSOC-VEIG22

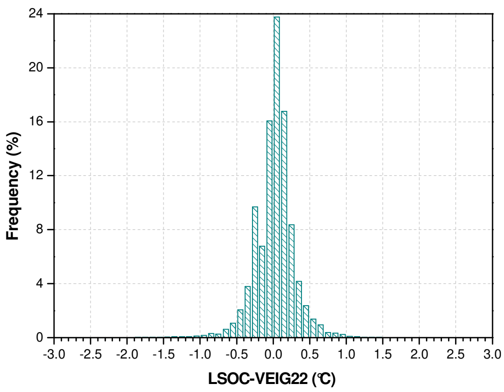


Figure 95. Histogram for LSOC-VEIG22

Figure 94 shows the linearity of the points and approximately 70 % of values are in the range [-0.2°C;+0.2°C. The mode and the mean are cen tred around zero and at first sight the distribution therefore appears symmetrical.

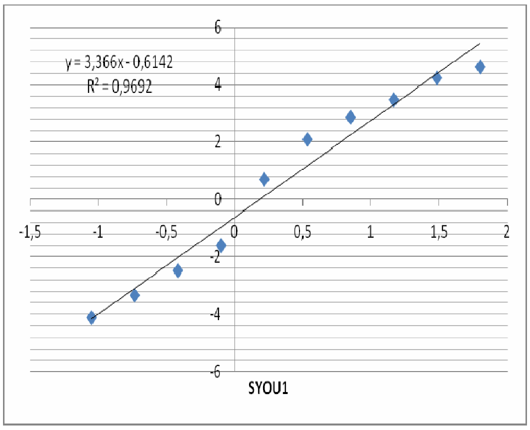


Figure 96. Q-Q plot for SYOU1-VEIG22

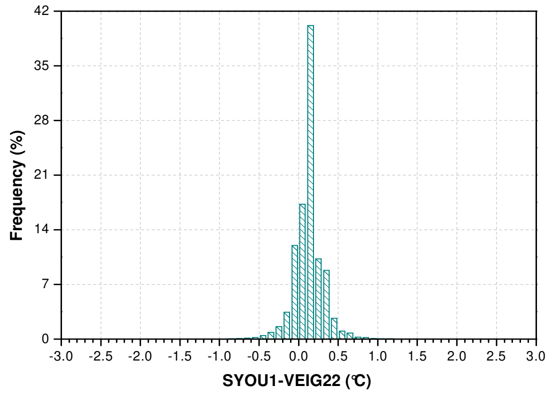


Figure 97. Histogram for SYOU1-VEIG22

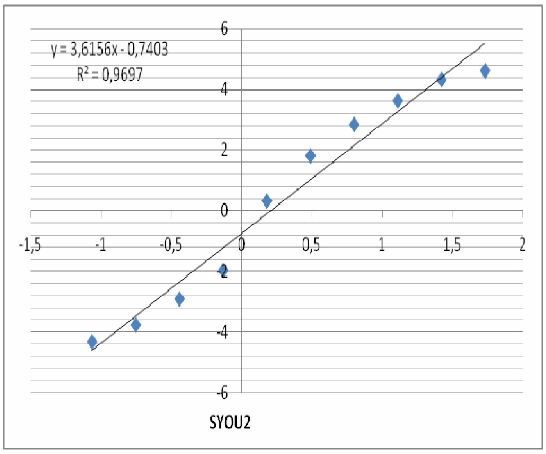


Figure 98. Q-Q plot for SYOU2-VEIG22

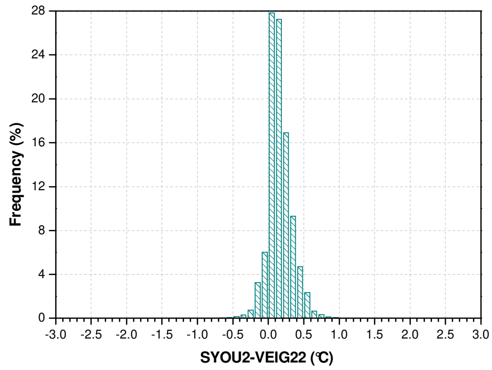


Figure 99. Histogram for SYOU2-VEIG22

For both SYOU screens the points are relatively aligned on the graph represented in the figure 96 and figure 98. Relative to the reference, approximately 70% of the data points being in the range [-0.2℃;+0.2℃]. For both screen s, the distribution of the differences is symmetrical around the highest frequency at 0.1°C and 0.2°C.

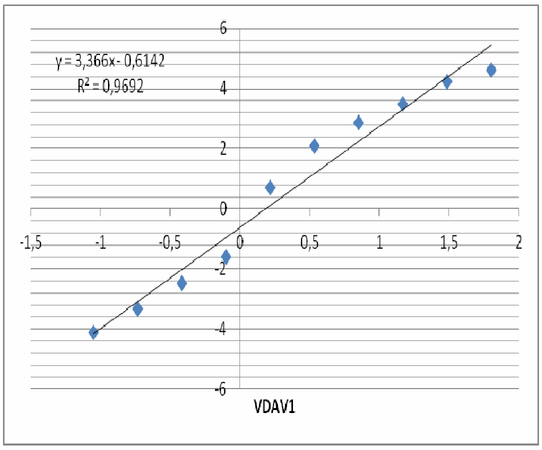


Figure 100. Q-Q plot for VDAV1-VEIG22

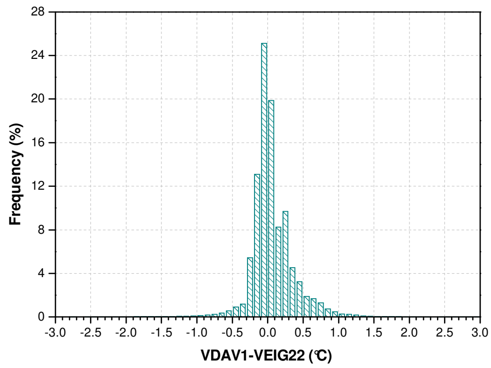


Figure 101. Histogram for VDAV1-VEIG22

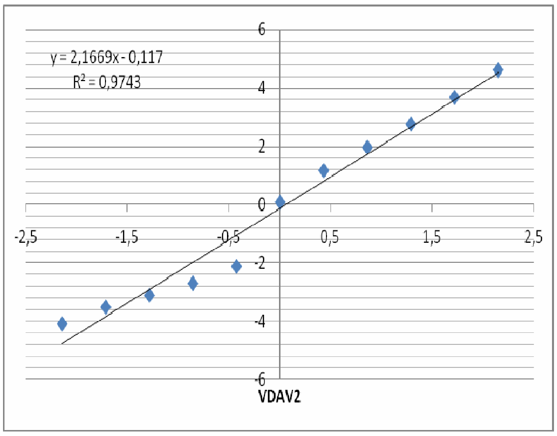


Figure 102. Q-Q plot for VDAV2-VEIG22

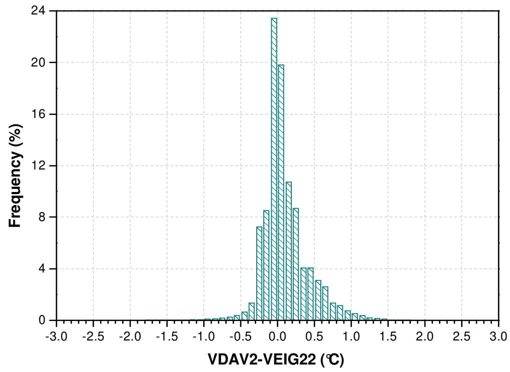


Figure 103. Histogram for VDAV2-VEIG22

The figure 100 and figure 102 show the linearity of the distribution but the graphs in figure 101 and figure 103 show that these two histograms are skewed to the right. Therefore the distributions of the differences are non symmetric.

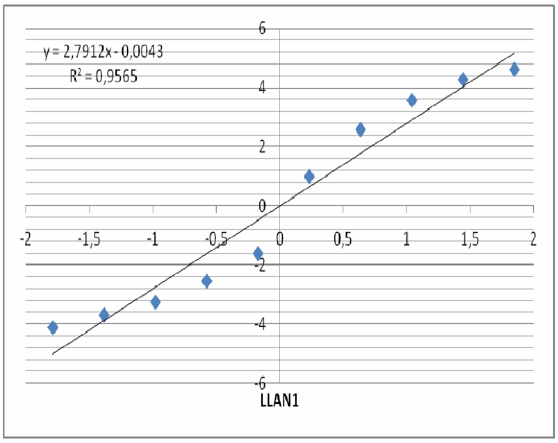


Figure 104. Q-Q plot for LLAN1-VEIG22

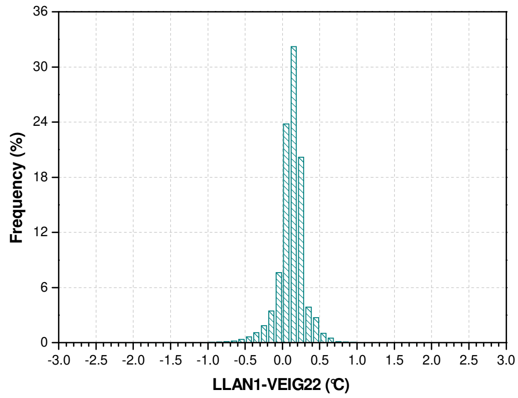


Figure 105. Histogram for LLAN1-VEIG22

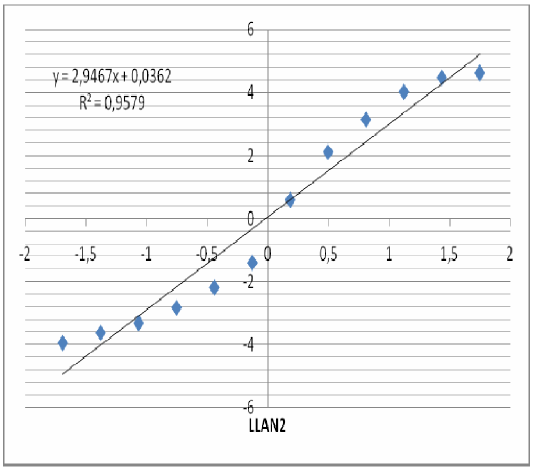


Figure 106. Q-Q plot for LLAN2-VEIG22

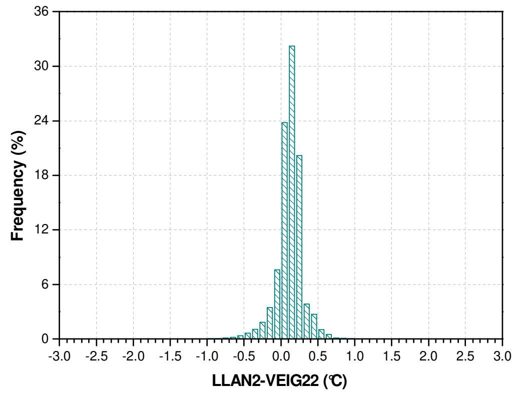


Figure 107. Histogram for LLAN2-VEIG22

For both LLAN screens the points are relatively aligned on the graphs represented in the figure 104 and figure 106, with approximately 75% of the data points in the range [-0.2℃;+0.2℃]. For both screens, the distribution o f the differences is symmetrical around the highest frequency at 0.1°C and 0.2°C.

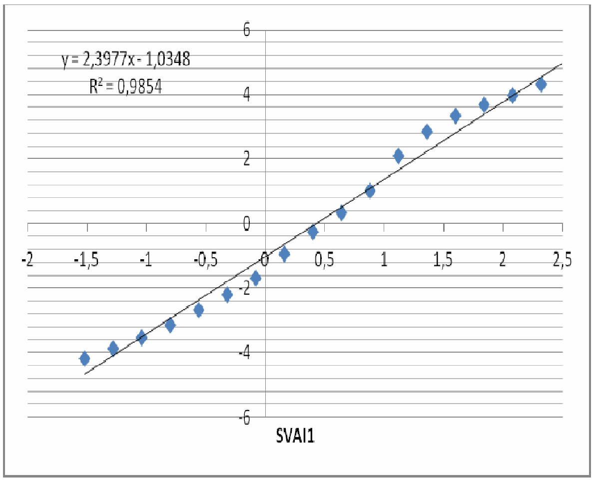


Figure 108. Q-Q plot for SVAI1-VEIG22

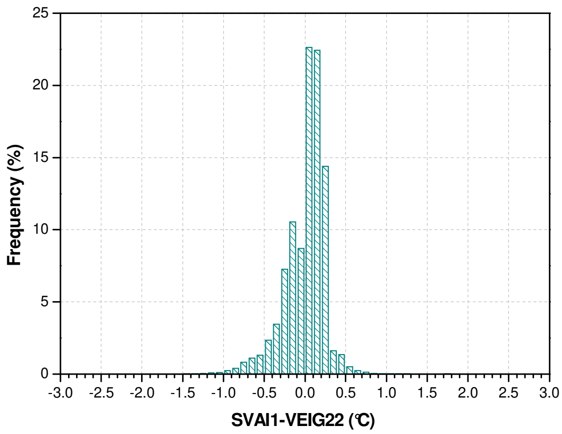


Figure 109. Histogram for SVAI1-VEIG22

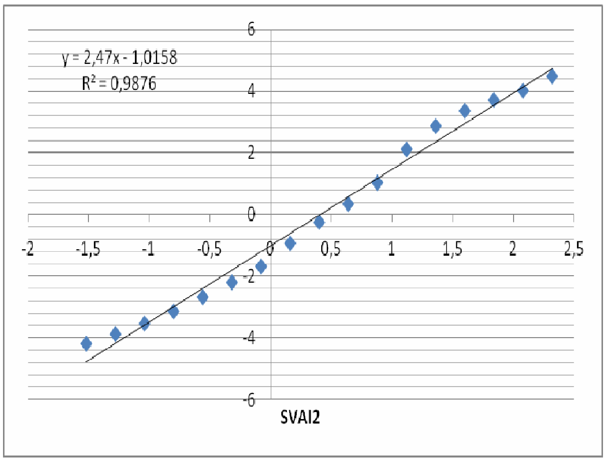


Figure 110. Q-Q plot for SVAI2-VEIG22

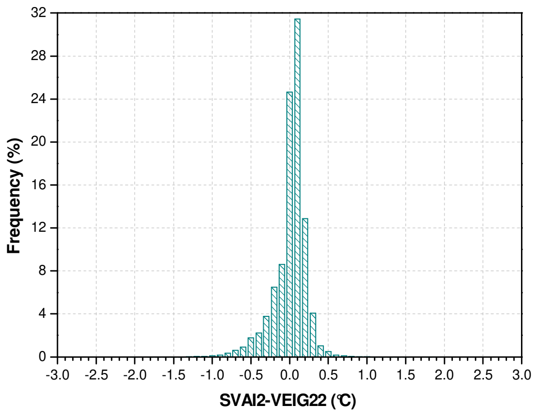


Figure 111. Histogram for SVAI2-VEIG22

Figure 108 and figure 110 show the linearity of the points and figure 109 and figure 111 show that these two histograms are skewed to the left, suggesting that the distribution of the differences is non symmetric.

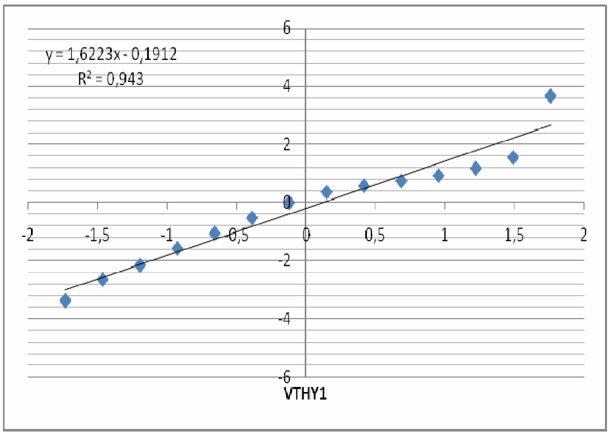


Figure 112. Q-Q plot for VTHY1-VEIG22

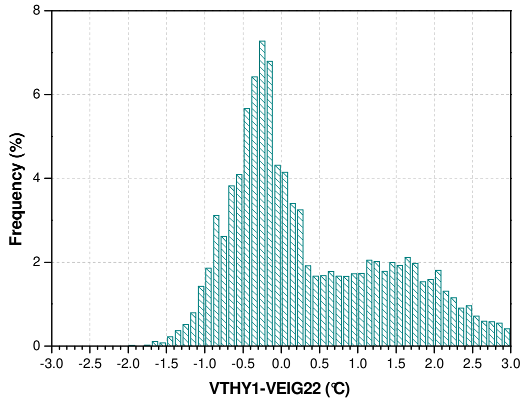


Figure 113. Histogram for VTHY1-VEIG22

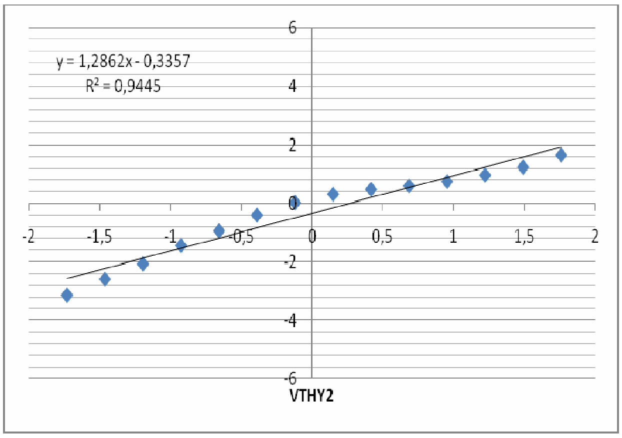


Figure 114. Q-Q plot for VTHY2-VEIG22

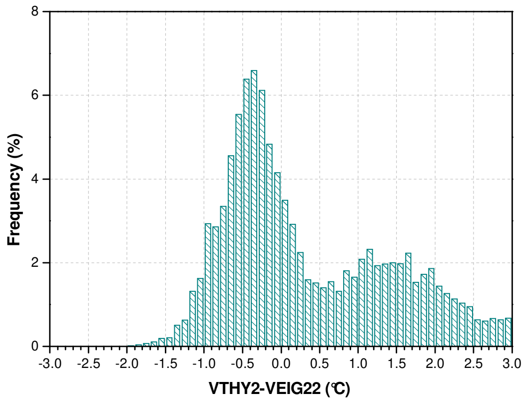


Figure 115. Histogram for VTHY1-VEIG22

Figure 112 and figure 114 show the linearity of the points although the tails, particularly the upper tail, show departures from the fitted line in figure 55. The two histograms in figure 113 and figure 115 show that they are skewed to the right, suggesting that the distribution of the differences are non symmetric.

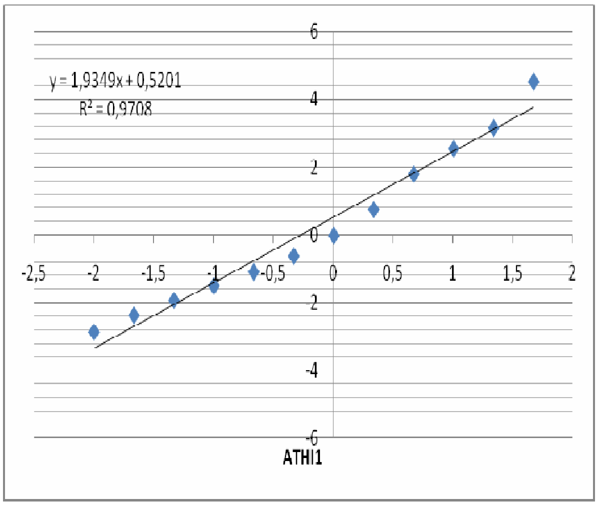


**Figure 116. Q-Q plot for ATHY1-VEIG22**

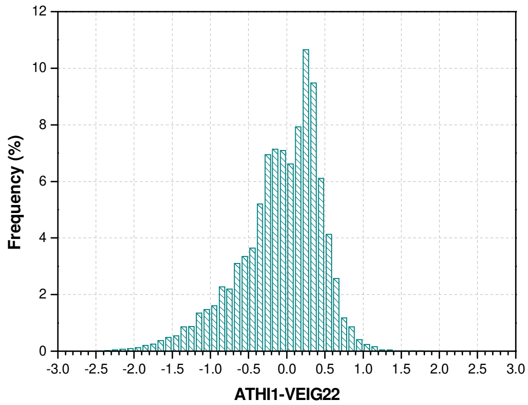


**Figure 117. Histogram for ATHY1-VEIG22**

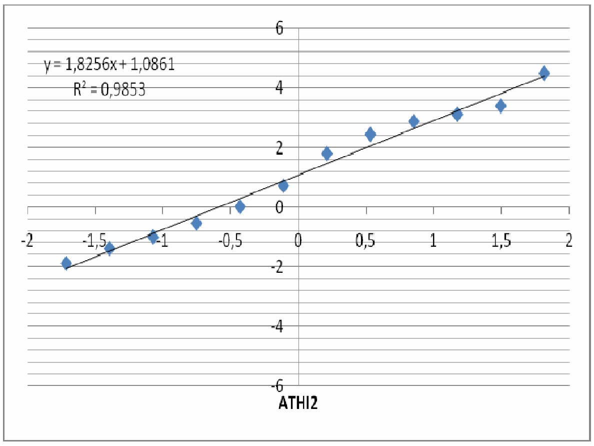


**Figure 118. Q-Q plot for ATHY2-VEIG22**

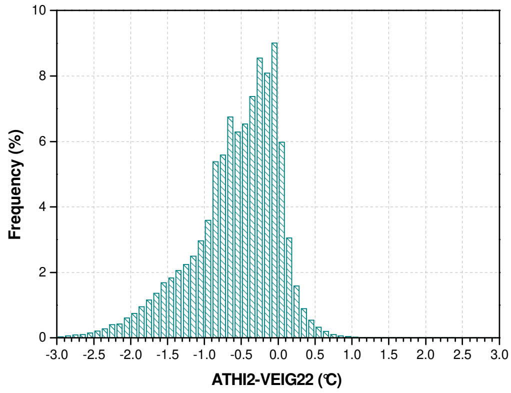


**Figure 119. Histogram for ATHY2-VEIG22**

Figure 116 shows the linearity of the points and figure 117 and figure 119 show that these two histograms are skewed to the left, suggesting that the distribution of the differences is non symmetric.

## 9.6 EFFECT OF NON-WORKING ARTIFICIAL VENTILATION

The two VYOU screens show a pronounced radiation error of about 1.8 K at low wind speeds and high irradiance during the period when the ventilation was not working.

In order to see the effect of the ventilation, the figure 120 shows on the top the evolution of temperature of both VYOU screens and the reference VEIG22, during 2 days before the operation of maintenance (when the power supply was repaired), and two days after. The chart in the middle is the global radiation, the one in the bottom is the 2-meter wind speed (2-minute average). The improvement due to the ventilation is clearly seen.

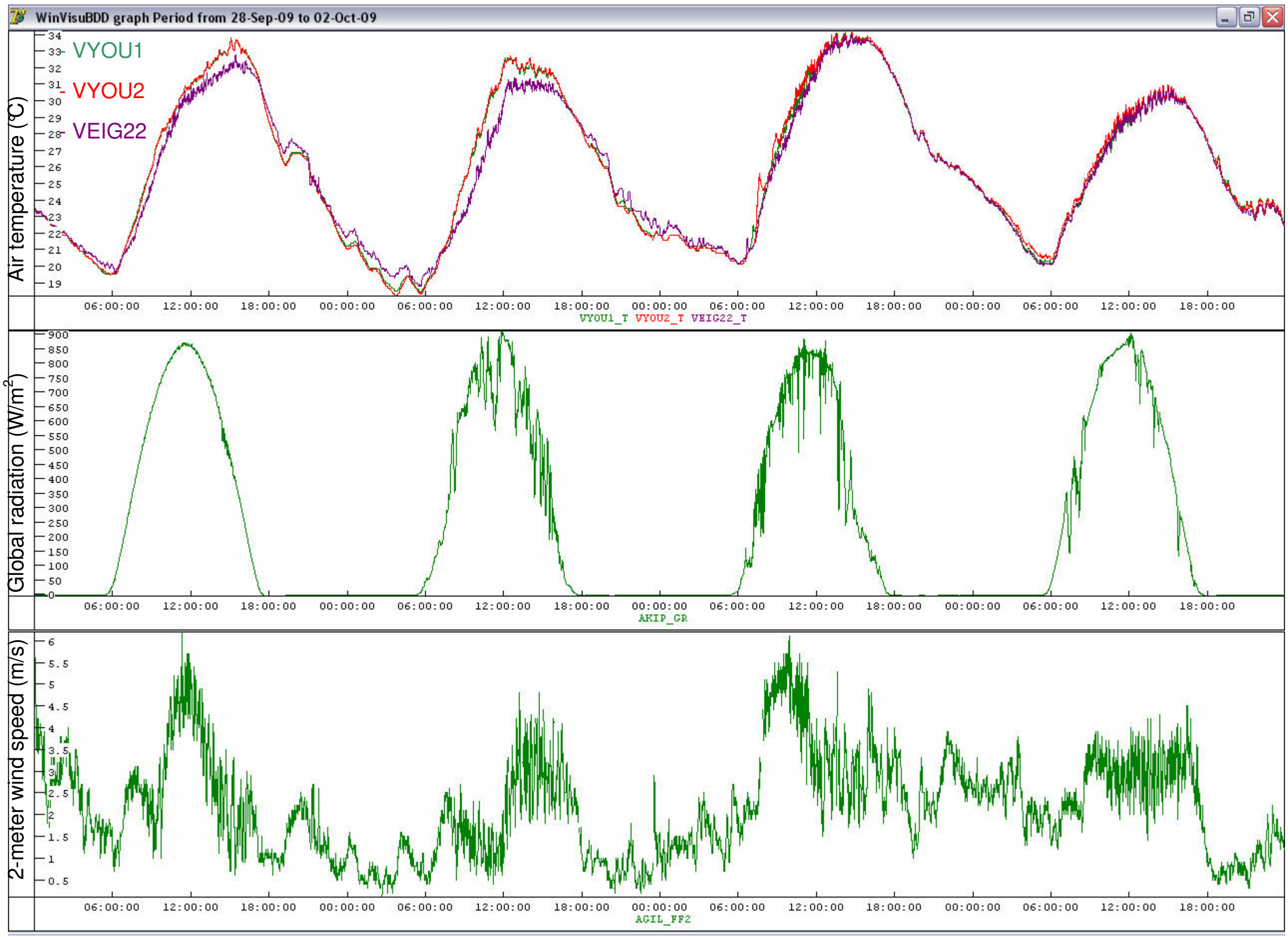


**Figure 120. Situation of the 28th of September to the 1st of October, 2009**

It is difficult to establish when the ventilation was shut off. Indeed, even in the beginning of the intercomparison period, VYOU screens showed radiation effect during day and during night. The figure 121 shows the same parameters as before, during the first days of the intercomparison period. So it was considered that the ventilation was not on during the first eleven months of the intercomparison.

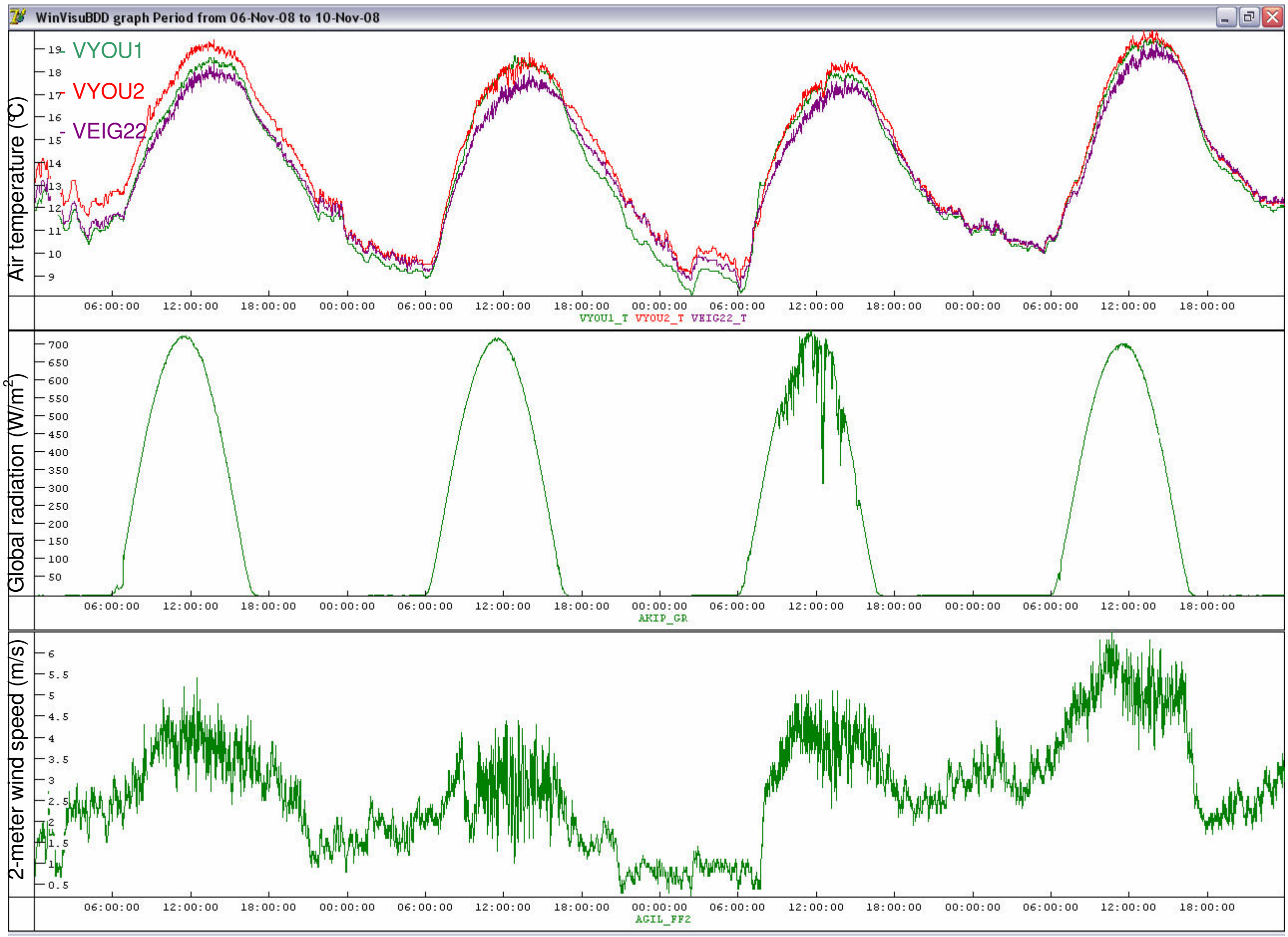


**Figure 121. Situation at the beginning of the intercomparison period**

The figure 122 and figure 123 show the histograms of differences with the reference before and after the cleaning operation. Both histograms after this operation are much less dispersed than histograms before it. For both screens the maximum frequency is obtained for the class of 0.2℃. For both screens the median s of the distributions after the cleaning is 0.18℃.

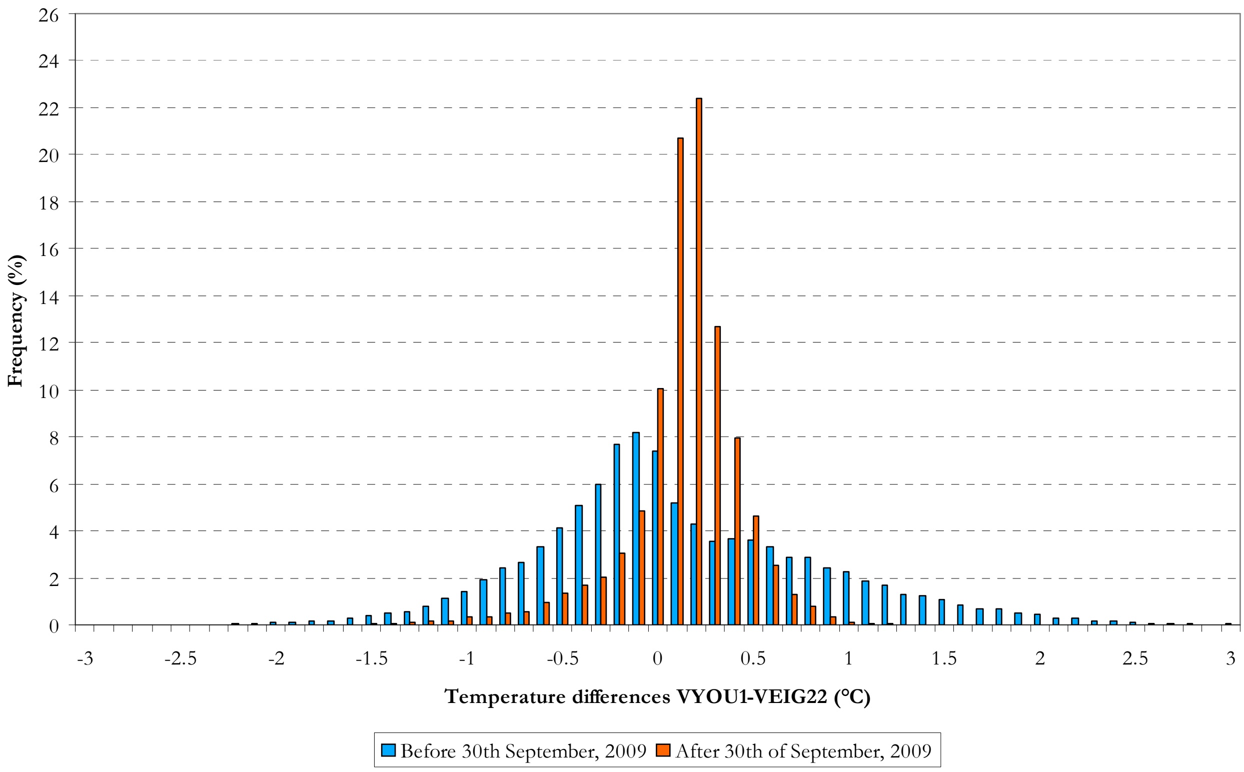


**Figure 122. Comparison before and after the maintenance operation for VYOU1 screen**

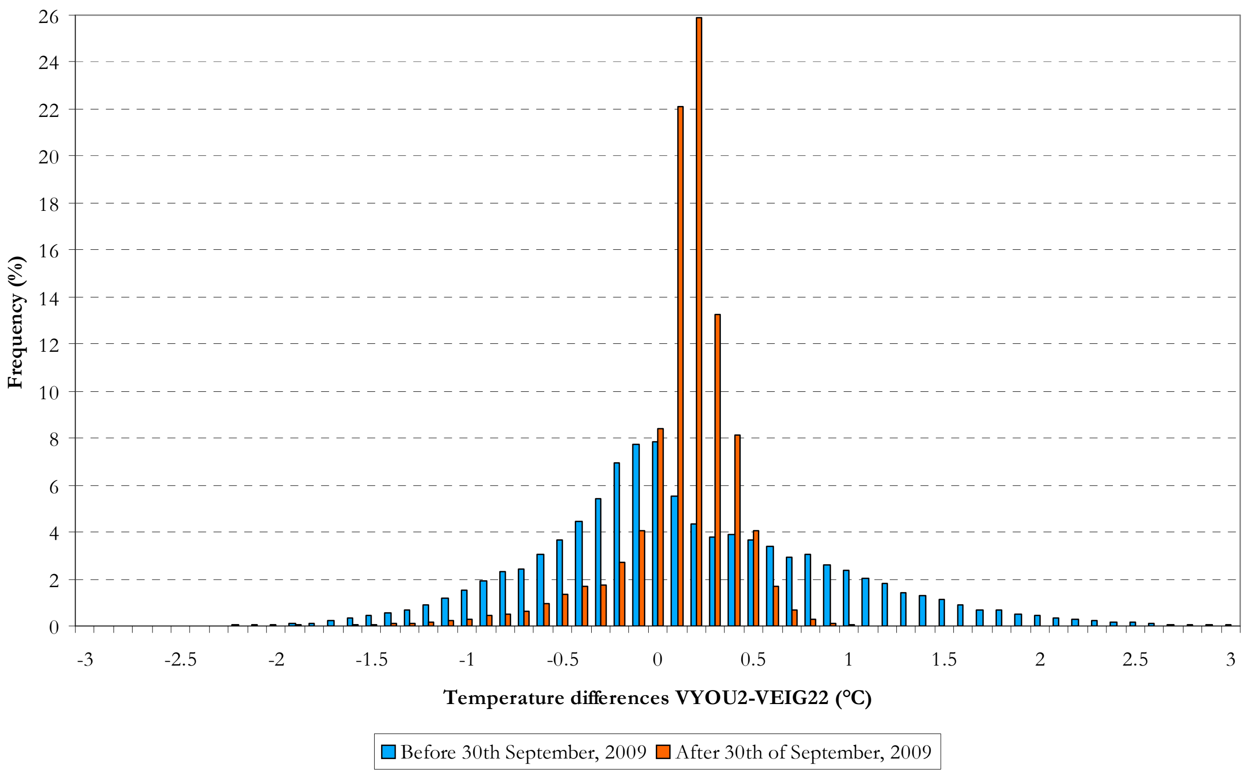


**Figure 123. Comparison before and after the maintenance operation for VYOU2 screen**

The table 9 gives numerical values of data that differ by less than 0.2°C (and 0.5°C) from the reference, before and after the cleaning.

**Table 9. Numerical values of histograms**

| | [-0.2°..0.2°] | [-0.5°..0.5°] |
|---|---|---|

| | | [-0.2°..0.2°] | [-0.5°..0.5°] |
|---|---|---|---|
| VYOU1 | before | 32.7 | 58.7 |
| | after | 61.0 | 91.4 |
| VYOU2 | before | 32.4 | 57.3 |
| | after | 63.2 | 93.4 |

The table 10 shows the contour plots obtained for both sensors before and after the maintenance operation. Charts after the operation are processed with less than one month of data, which may be not enough: most points represent less than 1000 data.

**Table 10. Contour plots for VYOU screens before and after maintenance operation**

| | Before operation | After operation |
|---|---|---|
| VYOU1 | 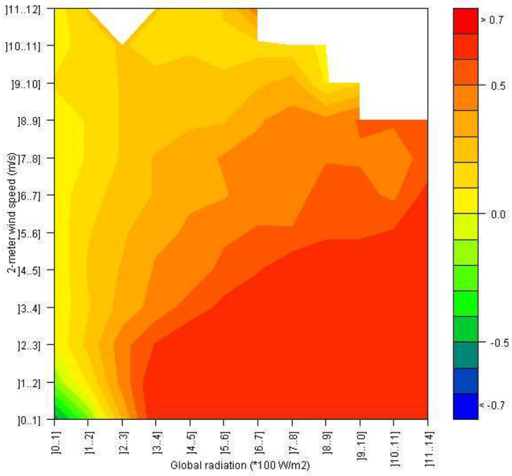 | 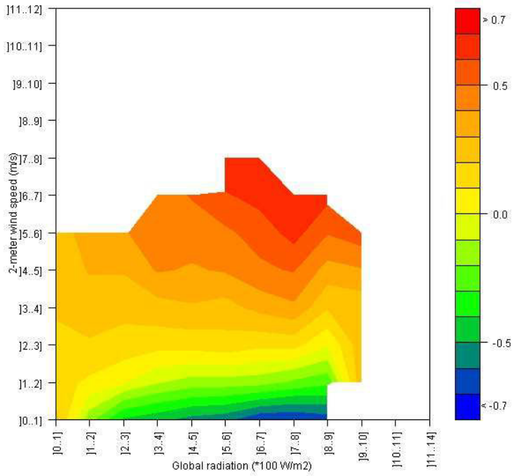 |
| VYOU2 | 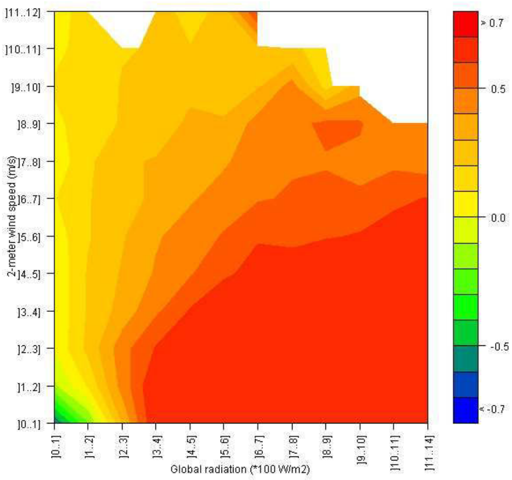 | 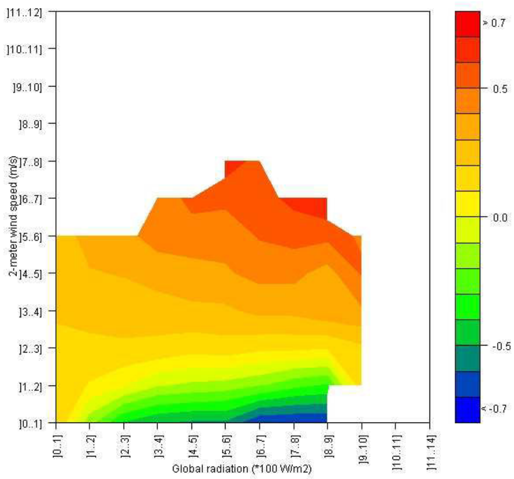 |

## 9.7 SAND BLOWING EVENT: BEHAVIOUR OF SCREENS

Many sand blowing events occurred from the 4th to the 7th of March, 2009. From the global meteorological point of view, the situation is very dynamic in the upper atmosphere: the North-Westerly jet stream is above Ghardaïa during the whole period. It brings cold air in higher altitudes and generates instable conditions at the ground level.

During this period, many fast variations of temperature and relative humidity occurred, as seen on figure 124. These events may be useful for a better understanding of the behaviour of screens/shields and relative humidity sensors in dynamic conditions.

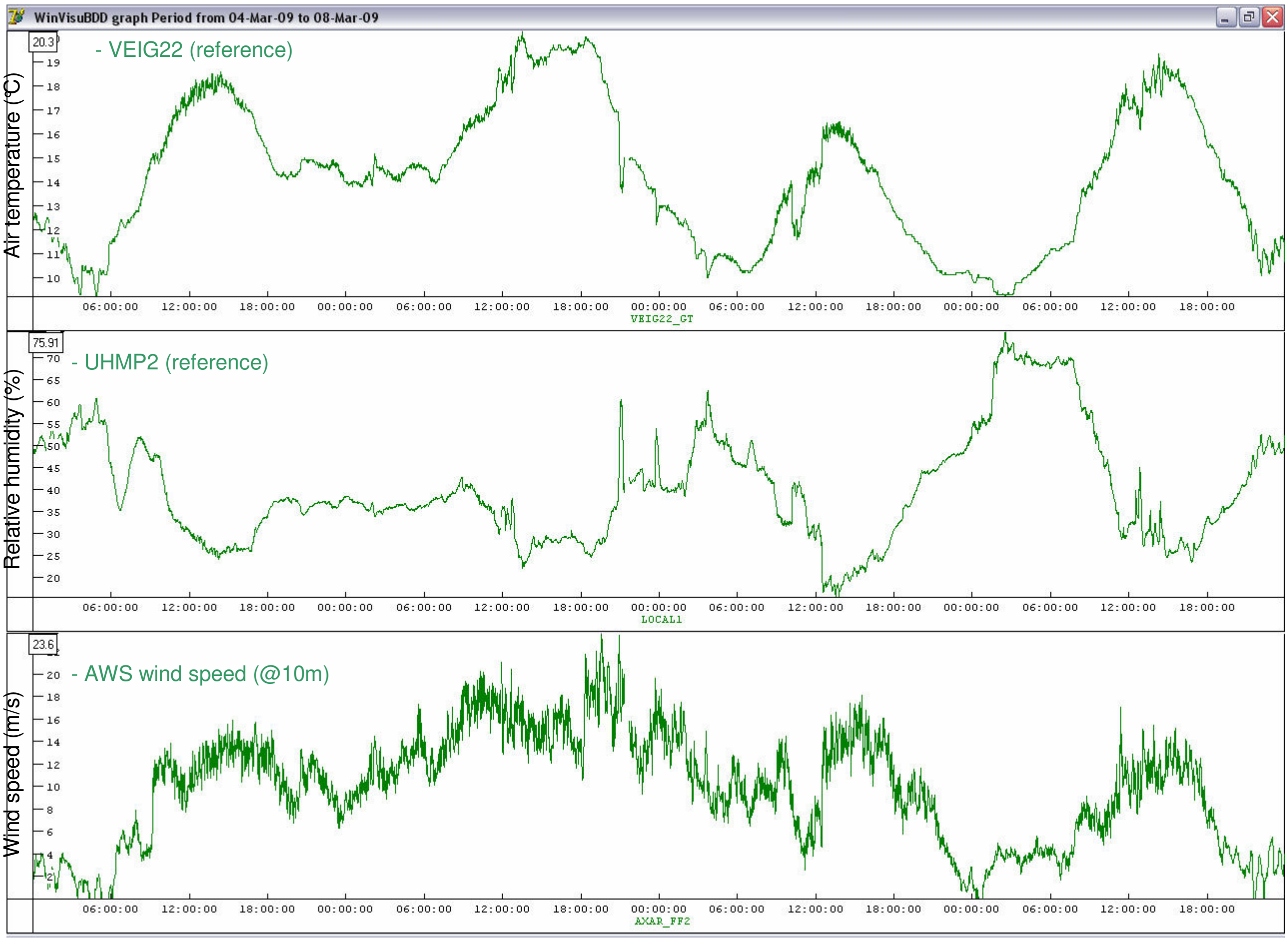


**Figure 124. Temperature, relative humidity and wind speed from the 4th to the 7th of March, 2009**

### 9.7.1 Large naturally-ventilated screens

LBOM gives very close results with the reference. LCAS and LSOC show an inertia: they show some delay regarding the reference and maxima (respectively minima) are underestimated (resp. overestimated), as shown on figure 125.


**Figure 125. Behaviour of LBOM, LCAS and LSOC screens**

### 9.7.2 Large artificially-ventilated screens

Like LCAS and LSOC in the section above, LLAN screens show an inertia versus the reference, cf figure 126.

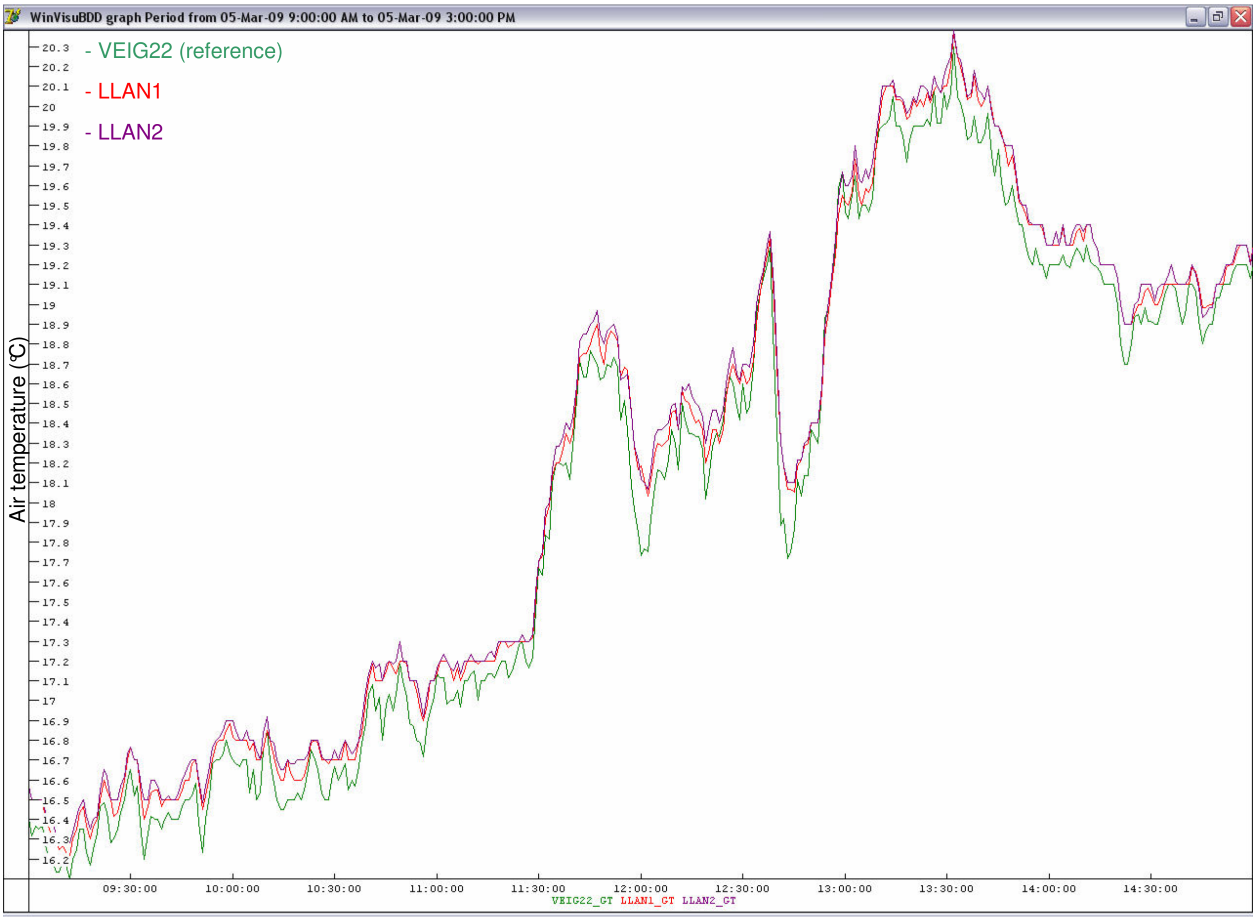


**Figure 126. Behaviour of LLAN screens**

### 9.7.3 Small naturally-ventilated screens

Nearly all small naturally-ventilated screens are in relative good agreement with the reference during these days. As an example the figure 127 shows the SYOU measurements.


**Figure 127. Behaviour of SYOU screens**

### 9.7.4 Small artificially-ventilated screens

Artificially-ventilated Davis screens showed some delay during these days, as shown in the figure 128.


**Figure 128. Behaviour of VDAV screens**

The four temperature probes in the VEIG screens showed very good agreement.

The figure 129 and the figure 130 respectively show the measurements from the VFIS and VROT sensors. On both figures, a delay in the temperature signal can be seen, but there is no delay on the relative humidity signal.

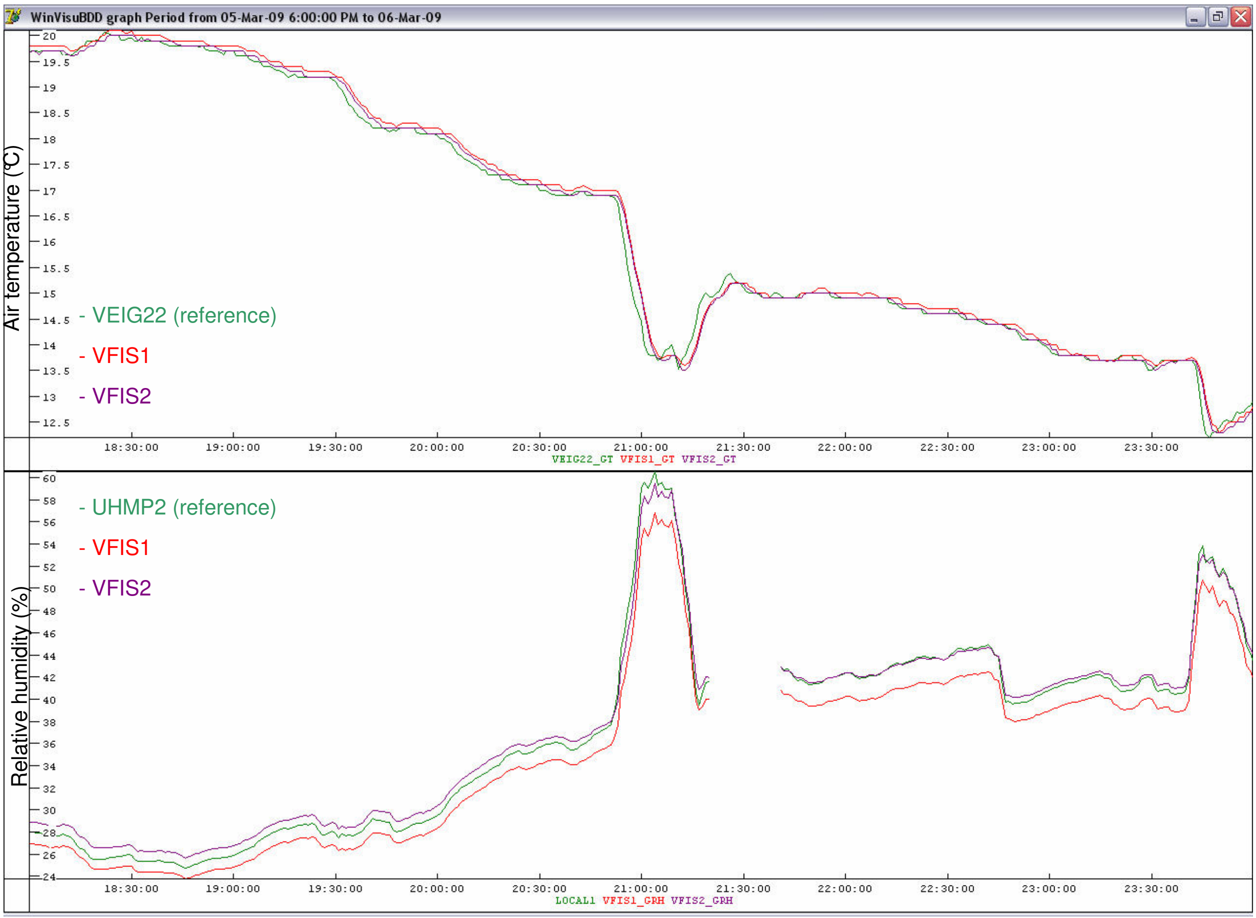


**Figure 129. Behaviour of VFIS screens**

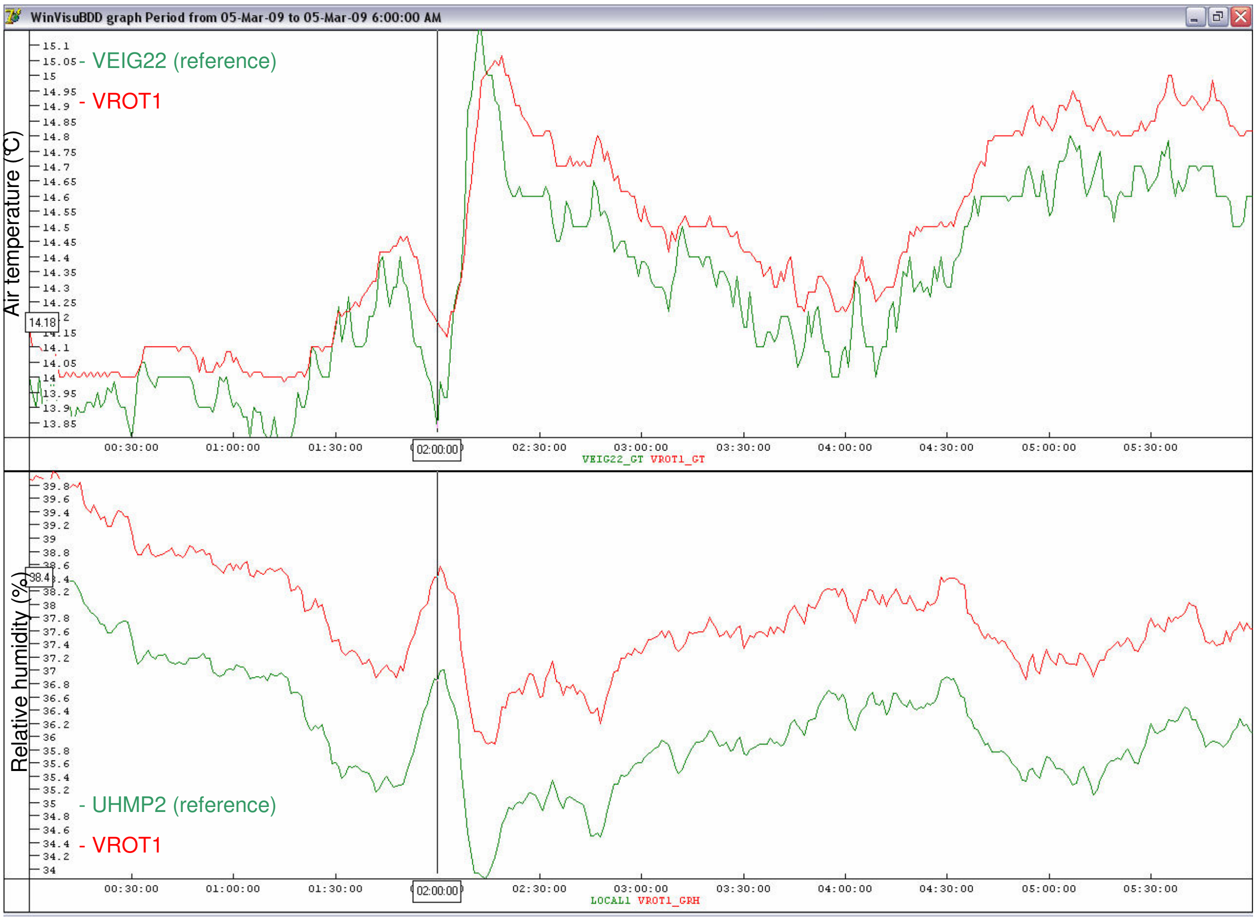


**Figure 130. Behaviour of VROT1 screen**

#### 9.7.5 Thies ultrasonic wind sensors

Unfortunately these sensors did not work during these days.

#### 9.7.6 Thygan sensors

Unfortunately these sensors did not work during these days.

## 9.8 RULES FOR RATINGS

### 9.8.1 Rules for rating the screens

A rating is proposed, based on the following conventions:

- The consistency between two identical screens is taken into account. If the absolute value of the limits contains 90% of the differences and is equal or lower than 0.1℃, 4 points are counted; 3 points for 0.2℃; 2 points for 0.3℃; 1 point for 0.5℃; 0 point above.
- The solar radiation error is evaluated from the datasheets. If for high solar radiation and low wind speed, the screen is colder than the reference, it gets 4 points; 3 points if warmer up to 0.2℃; 2 points if warmer up to 0.5℃; 1 point if warmer up to 1℃; 0 point for larger differences.
- The percentage of the differences of the minutely temperatures between the screen and the reference lying between –0.5℃ and +0.5℃ i s calculated (see datasheets). If this percentage is higher than 98%, the screen gets 4 points; 3 points if the percentage is higher than 95%; 2 points for 90%; 1 point for 80%; 0 point below.
- The same calculation is made for the percentage of the daily max temperatures (Tx) and for the daily min. temperature (Tn).
- If only one screen was present, the consistency is not taken into account. The total number of points is therefore multiplied by 5/4, to compensate the missing points from consistency section.
- If the total number of points is greater than 16, 5 stars are allocated (*****); if the total is greater than 12, 4 stars are allocated (****); greater than 8, 3 stars (***); greater than 4, 2 stars (**); less, 1 star (*).
- To take into account the imperfect characteristics of the working reference screen itself, one star is also added or removed in the last column of the table to get a more “absolute” rating.

The table 11 gives the raw rating for each screen.

**Table 11. Ratings of the screens**

| Screen acronym | Rating |
|---|---|
| LSOC | 11/16 → 13.75/20 |
| LBOM | 14/16 → 17.5/20 |
| LLAN | 17/20 |
| LCAS | 13/16 → 16.25/20 |
| SSOC | 10/20 |
| SVAI | 9/20 |
| SWIN | 10/20 |
| SDAV | 17/20 |
| SYOU | 15/20 |
| VFIS | 7/20 |
| VEIG | 18/20 |

| Screen acronym | Rating |
|---|---|
| VTHY | 4/20 |
| VROT | 6/15 |
| VDAV | 11/20 |
| VYOU | 12/20 |
| ATHI | 4/20 |

### 9.8.2 Rules for rating the hygrometers

A rating is proposed, based on the following conventions:

- The consistency between two identical hygrometers is taken into account. If the absolute value of the limits contain 90% of the differences and is equal or lower than 1%, 3 points are counted; 2 points for 2%; 1 point for 3%; 0 point above.
- The annual drift is evaluated from the datasheets. If the drift is evaluated to be less than 0.5% (or non significant), the hygrometer gets 3 points; 2 points for a drift less than 1.5%; 1 point for a drift less than 2.5%; 0 point for a larger drift.
- The maximum influence of temperature on the relative humidity is evaluated from the datasheets, for a range of temperature between 5 and 45℃. This maximum influence generally occurred close to 50% of RH, either due to the characteristics of the hygrometer itself or due to the range of temperature and RH experienced during the test period. If the influence of temperature over this 40℃ range is lower than 1%, the hygrometer gets 3 points. 2 points if the influence is lower 2%; 1 point if the influence is lower than 4%; 0 point above.
- The maximum influence of RH itself on the relative humidity measured by a hygrometer itself is evaluated from the datasheets, for a range of RH between 5 and 100%. This maximum influence generally occurred close to a temperature of 10℃, either due to the characteristics of the hygr ometer itself or due to the range of temperature and RH experienced during the test period. If the influence of RH over this 95% RH range is lower than 1%, the hygrometer gets 3 points. 2 points if the influence is lower than 2%; 1 point if the influence is lower than 4%; 0 point above.
- The percentage of the differences of the minutely RH between the hygrometer and the reference lying between –3% and +3% of RH is calculated (see datasheets). If this percentage is higher than 98%, the hygrometer gets 3 points; 2 points if the percentage is higher than 95%; 1 point for 90%; 0 point below.
- If only one screen was present, the consistency is not taken into account. The total number of points is therefore multiplied by 5/4, to compensate the missing points from consistency section.
- If the total number of points is greater then 12, 5 stars are allocated (*****); if the total is greater than 9, 4 stars are allocated (****); greater than 6, 3 stars (***); greater than 3, 2 stars (**); less, 1 star (*).

The table 12 gives the raw rating for each hygrometer.

**Table 12. Ratings of hygrometers**

| Hygrometer acronym | Rating |
|---|---|
| LBOM | 12/12 |
| VFIS | 6/15 |
| SVAI | 12/15 |
| UHMP | 15/15 |
| UTES | 5/12 |
| VTHY | 12/12 |
| VROT | 9/12 |

# APPENDICES

**Thermometer Screens**

LSOC
LBOM
LLAN
LCAS
SSOC
SVAI
SWIN
SDAV
SYOU
VFIS
VEIG
VTHY
VROT
VDAV
VYOU
ATHI
SCAE

**Humidity Measuring Instruments**

LBOM
VFIS
SVAI
UHMP
UTES
VTHY
VROT
SCAE

*This page left intentionally blank.*

# APPENDIX 1

## Thermometer Screens

LSOC
LBOM
LLAN
LCAS
SSOC
SVAI
SWIN
SDAV
SYOU
VFIS
VEIG
VTHY
VROT
VDAV
VYOU
ATHI
SCAE

*This page left intentionally blank.*

# BM0 1151 A0000 SOCRIMA
# – Algeria –
# LSOC

## TECHNICAL SPECIFICATIONS (PROVIDED BY THE MANUFACTURER)

Dimensions: Length 135 cm x Width 75 cm x Height 100 cm

Weight: 100 kg

Material/Structure: plastic

Estimated radiation error:

Aspiration rate (in case of artificially ventilated screen/shield): naturally ventilated

Power supply: none

**Figure 1**

## OVERVIEW

The LSOC screen is quite close to the reference: more than 90% of the differences between both are less than 0.5°C. The differences between LSOC and the reference 1-minute data are quite symmetrical: 50% of positive differences, 50% negative. Daily minimum temperatures are warmer than the reference in 70% of the cases. Daily maximum temperatures are cooler than the reference in about 64% of the cases. This may be explained by the inertia of this screen: it is a large plastic screen.

The medians of differences are quite stable when global radiation increases.

This screen behaves the same during day and night compared to the reference, except for clam winds: LSOC is about 0.15°C cooler by day than by night when wind speed is less than 1m/s.

During daytime, LSOC is very close to the reference for winds between 1 and 6m/s in overcast or clear sky conditions. For calm winds, LSOC is more than 0.3°C colder than the reference when the sky is clear whereas it is nearly 0.1°C warmer during overcast conditions. When the wind speed is above 6m/s, LSOC is close to the reference during overcast periods, but it is warmer than the reference during clear sky periods.

During night time, there is no clear difference between clear sky or overcast periods: LSOC screen is close to the reference, with exception of points with low number of data.

For calm winds, LSOC is close to the reference when the sun is high in the sky. It is about 0.25°C colder for low sun elevations, and more than 0.55°C colder for intermediate values of sun elevations. This may be explained by the thermal inertia of the LSOC screen: when the sun is rising, this screen is still cold from the night temperature drop.

The contour plot is uniform, the LSOC screen is about 0.1°C warmer than the reference. It is colder than the reference for calm winds and global radiation values lower than 500W/m$^2$.

Differences with the reference are mainly positive for negative gradients, and negative for positive gradients. This clearly illustrates a delay of LSOC screen compared to the reference.

## CALIBRATION INFORMATION

The calibration of the probe was performed in Trappes.

**Table 1**

| Screen | Location | Pt100 probe serial number | Calibration date | Instrument bias (°C) | | | |
|---|---|---|---|---|---|---|---|
| | | | | -20°C | 0°C | 20°C | 40°C |
| LSOC | F1 | T47 | 30-Jan-2006 | 0.0558 | 0.0286 | 0.0066 | -0.0112 |

The result of calibration of reference VEIG22 is available in the main report of the intercomparison, section 5.4.1.

## COMPARISON WITH THE REFERENCE

### HISTOGRAM OF DIFFERENCES

The histogram of differences between LSOC and the reference VEIG22 is plotted, using 1-minute quality checked data for the whole period of the intercomparison. Differences are plotted by steps of 0.1K. The vertical axis is the frequency in percent for each class of differences.

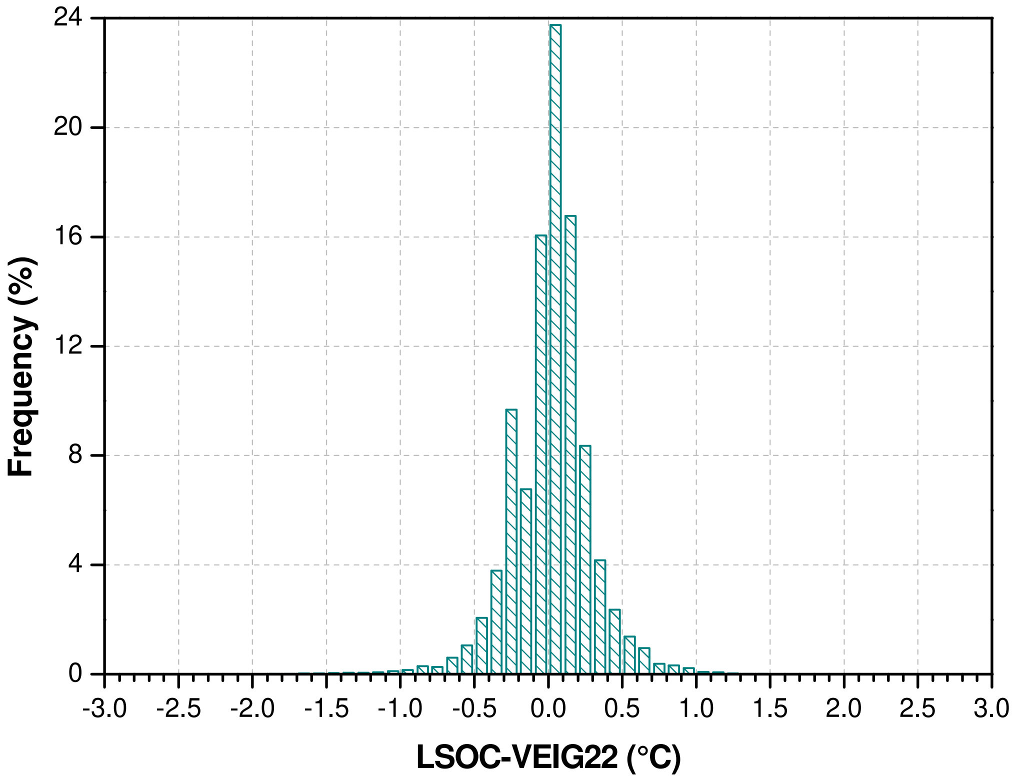


**Figure 2**

This screen is quite close to the reference: more than 90% of the differences between both are less than 0.5°C.

CUMULATIVE HISTOGRAMS OF DIFFERENCES OF DAILY EXTREME VALUES

The cumulative histograms of differences with the reference VEIG22 of T (1-minute quality checked data), Tn (daily minimum temperature) and Tx (daily maximum temperature) are plotted, for the whole period of the intercomparison. Differences are plotted by steps of 0.1K.

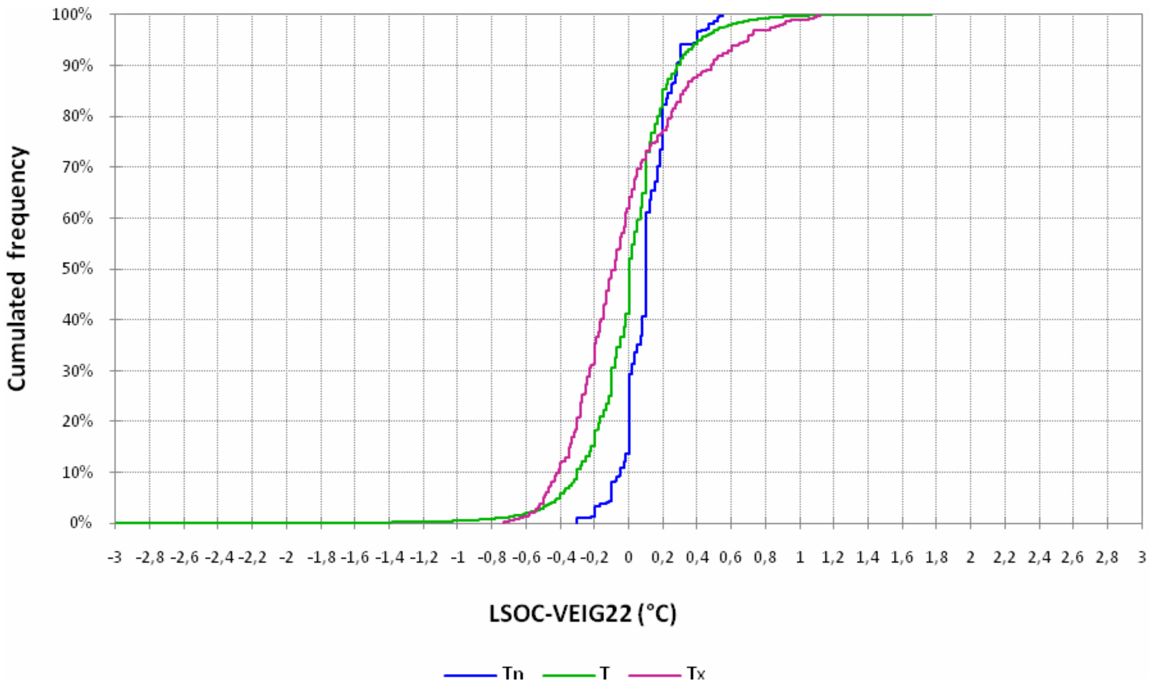


**Figure 3**

The differences between LSOC and the reference 1-minute data are quite symmetrical: 50% of positive differences, 50% negative. Daily minimum temperatures are warmer than the reference in 70% of the cases. Daily maximum temperatures are cooler than the reference in about 64% of the cases. This may be explained by the inertia of this screen: it is a large plastic screen.

TABLE

The table 2 indicates the percentage of data that differ by less than 0.2°C (and 0.5°C) from the reference.

**Table 2**

| | | [-0.2°..0.2°] | [-0.5°..0.5°] |
|---|---|---|---|
| LSOC | T | 70.2 | 94.1 |
| | Tn | 80.1 | 98.8 |
| | Tx | 43.2 | 87.3 |

## INFLUENCE OF GLOBAL RADIATION

The distribution of differences between LSOC and the reference VEIG22 is plotted, using 1-minute quality checked data for the whole period of the intercomparison. Differences are classified according global radiation.

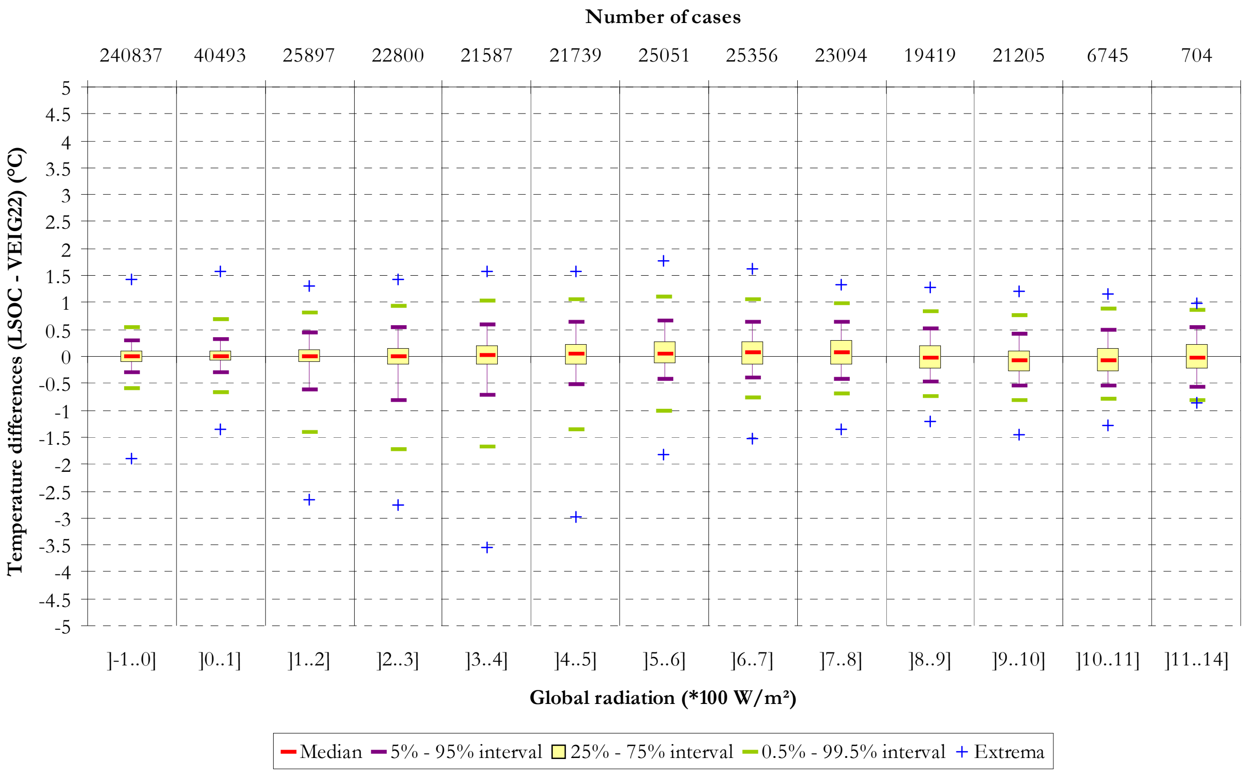


**Figure 4**

The medians of differences are quite stable when global radiation increases.

## RADIATION EFFECT

### DIFFERENCES BETWEEN DAY AND NIGHT BEHAVIOUR

The median of differences between LSOC and VEIG22 is plotted, using 1-minute quality checked data for the whole period of the intercomparison. We filter data for which sun elevation is above -1° (day) or below -1° (night). Differences are classified according 2-meter wind speed (2-minute average).

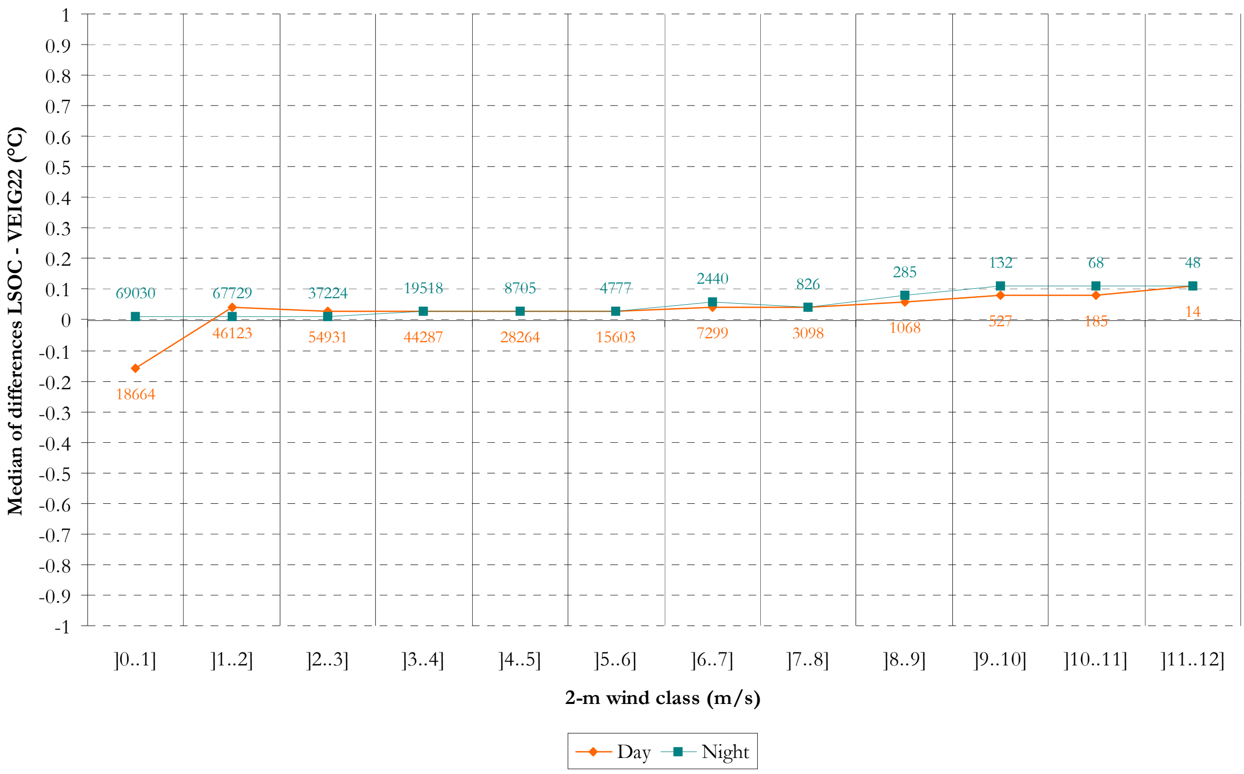


**Figure 5**

This screen behaves the same during day and night compared to the reference, except for clam winds: LSOC is about 0.15°C cooler by day than by night when wind speed is less than 1m/s.

## DIFFERENCES BETWEEN CLEAR SKY AND OVERCAST SKY DURING DAYTIME

The median of differences between LSOC and VEIG22 is plotted, using 1-minute quality checked data. Here, we consider periods lasting six hours at least where cloudiness is less or equal to 1 (clear sky) or more or equal to 7 (overcast sky), during daytime (sun elevation above -1°). Differences are classified according 2-meter wind speed (2-minute average).

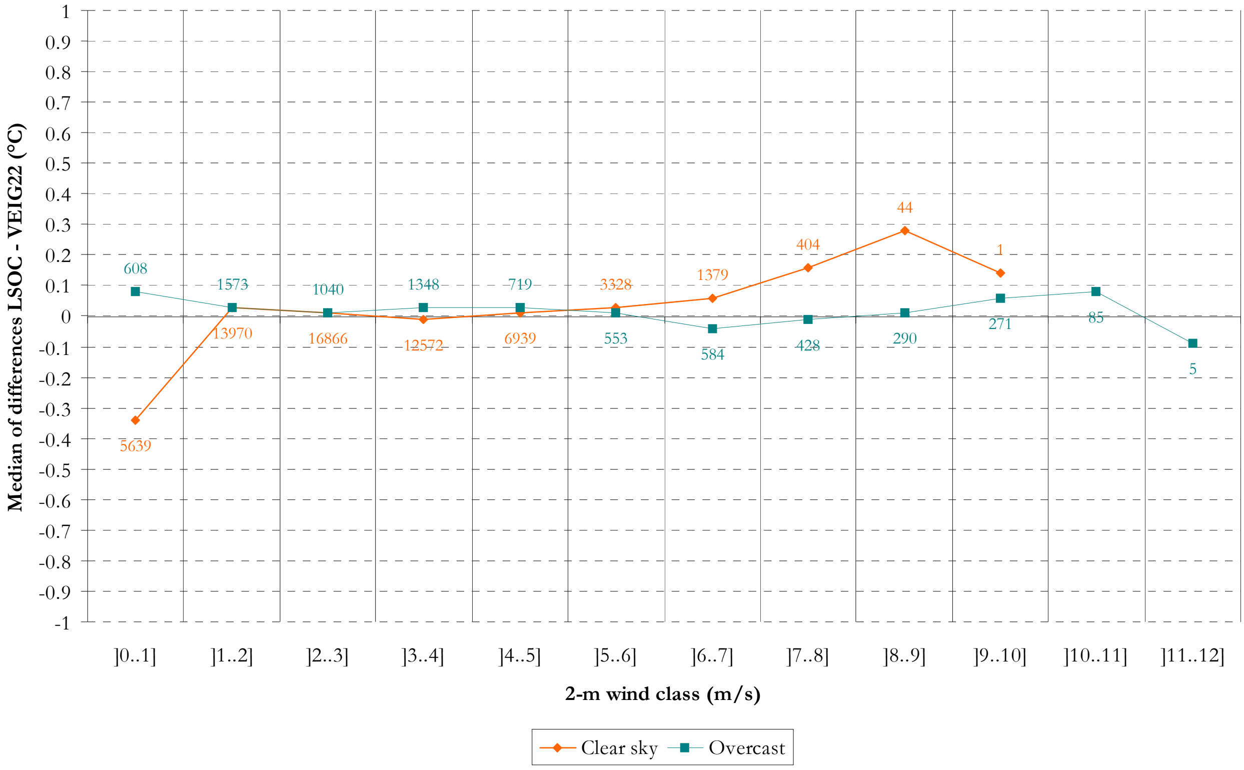


**Figure 6**

During daytime, LSOC is very close to the reference for winds between 1 and 6m/s in overcast or clear sky conditions. For calm winds, LSOC is more than 0.3°C colder than the reference when the sky is clear whereas it is nearly 0.1°C warmer during overcast conditions. When the wind speed is above 6m/s, LSOC is close to the reference during overcast periods, but it is warmer than the reference during clear sky periods.

## DIFFERENCES BETWEEN CLEAR SKY AND OVERCAST SKY DURING NIGHT TIME

The median of differences between LSOC and VEIG22 is plotted, using 1-minute quality checked data. Here, we consider periods lasting six hours at least where cloudiness is less or equal to 1 (clear sky) or more or equal to 7 (overcast sky), during night time (sun elevation below -1°). Differences are classified according 2-meter wind speed (2-minute average).

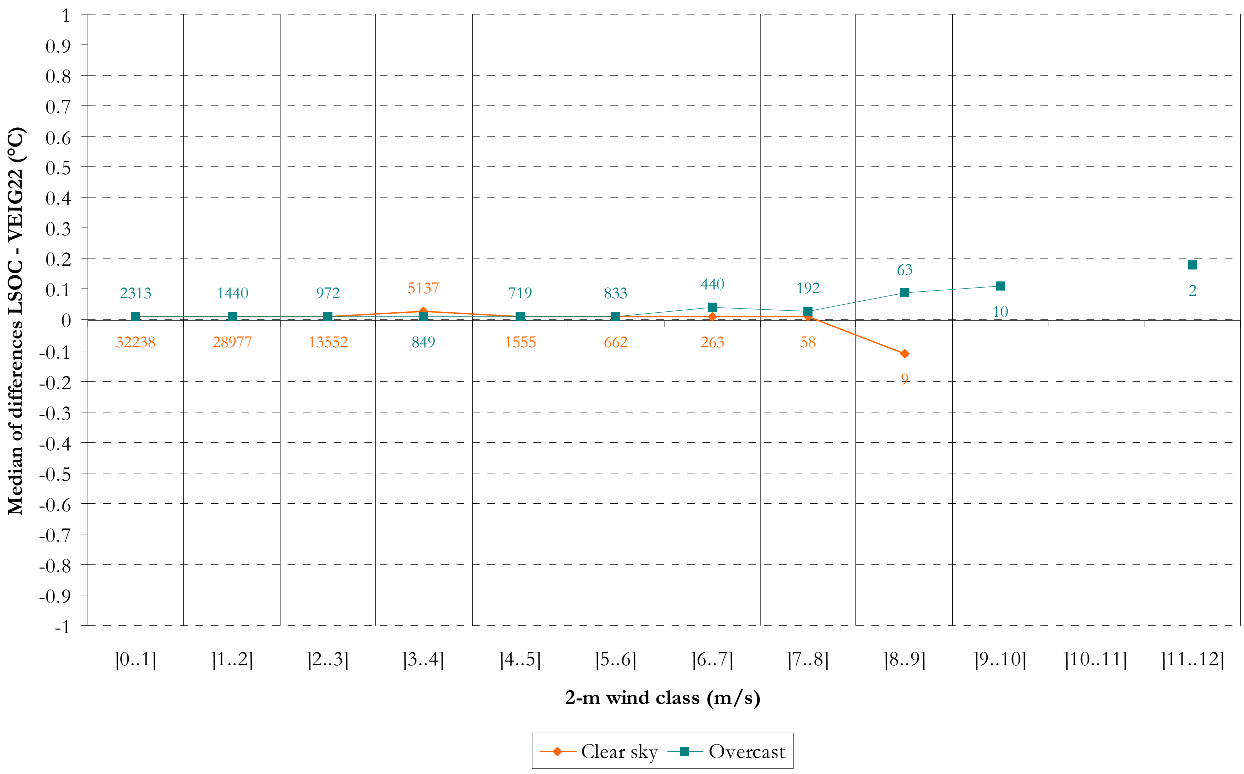


**Figure 7**

During night time, there is no clear difference between clear sky or overcast periods: LSOC screen is close to the reference, with exception of points with low number of data.

## EFFECT OF SUN ELEVATION

The median of differences between LSOC and VEIG22 is plotted, using 1-minute quality checked data. Here, we consider periods lasting six hours at least where cloudiness is less or equal to 1 (clear sky), during daytime (sun elevation above -1°). We filter data where sun elevation is low (below 10°), medium (between 10° and 45°) or high (above 45°). Differences are classified according 2-meter wind speed (2-minute average).

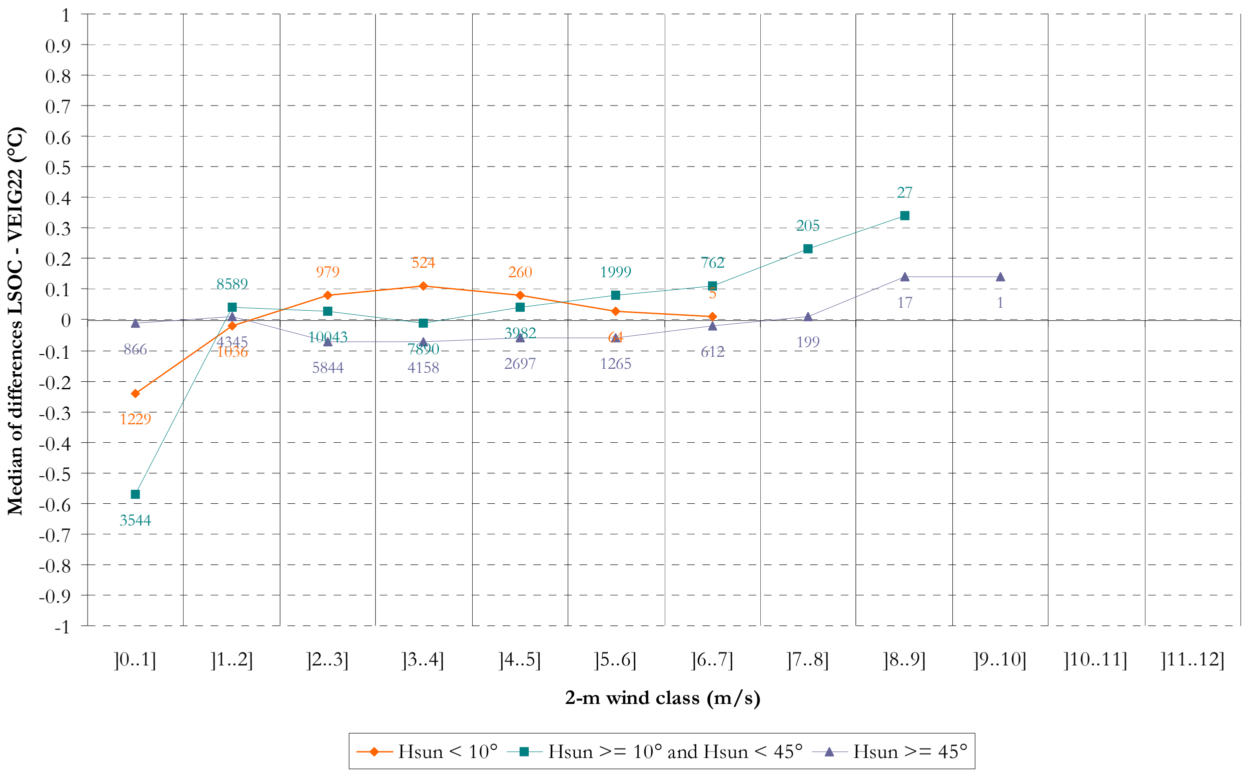


**Figure 8**

The three curves are quite closed one to another for winds above 1m/s. For calm winds, LSOC is close to the reference when the sun is high in the sky. It is about 0.25°C colder for low sun elevations, and more than 0.55°C colder for intermediate values of sun elevations. This may be explained by the thermal inertia of the LSOC screen: when the sun is rising, this screen is still cold from the night temperature drop.

## COMBINED EFFECT OF WIND AND GLOBAL RADIATION

The medians of differences between LSOC and VEIG22 are represented here with a contour plot. The global radiation values are on the X-axis and on the Y axis is the 2-meter wind speed value (2-minute average). Medians are used in all cases, providing that at least one data is available for both conditions on radiation and wind considered.

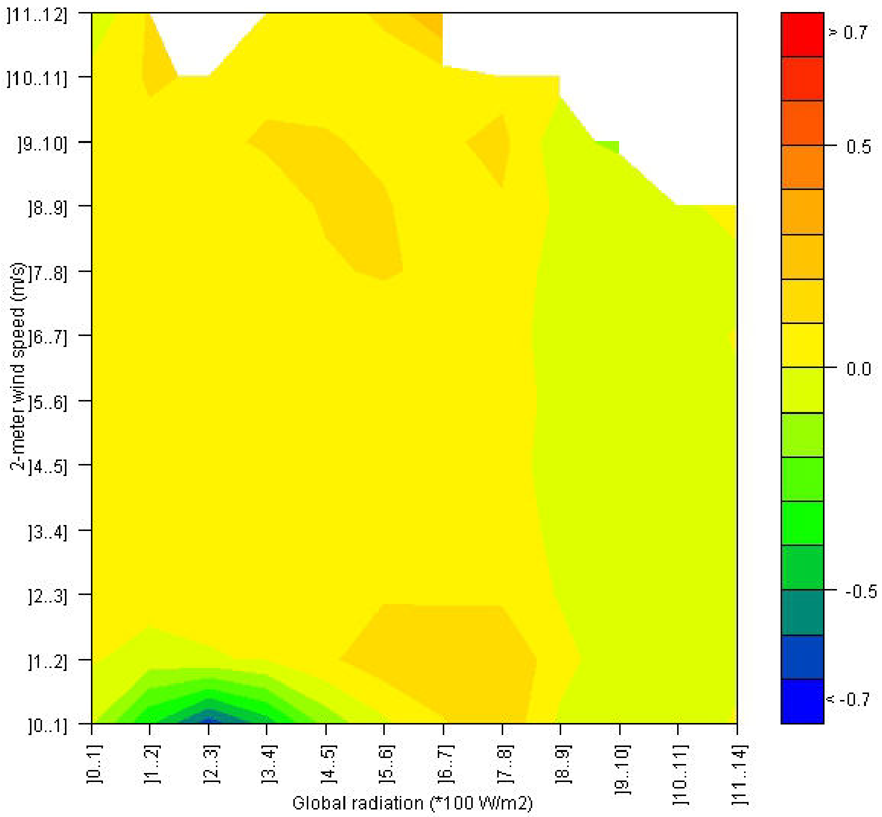


**Figure 9**

The contour plot is uniform, the LSOC screen is about 0.1°C warmer than the reference. It is colder than the reference for calm winds and global radiation values lower than 500W/m$^2$.

## BEHAVIOUR DURING INCREASE/DECREASE OF TEMPERATURE

The distribution of differences between LSOC and the reference VEIG22 is plotted, using 1-minute quality checked data for the whole period of the intercomparison. Differences are classified according the temporal gradient of reference temperature over 1 minute. A screen faster (or slower, respectively) than the reference would be warmer (cooler) for positive gradient, cooler (warmer) for negative ones.

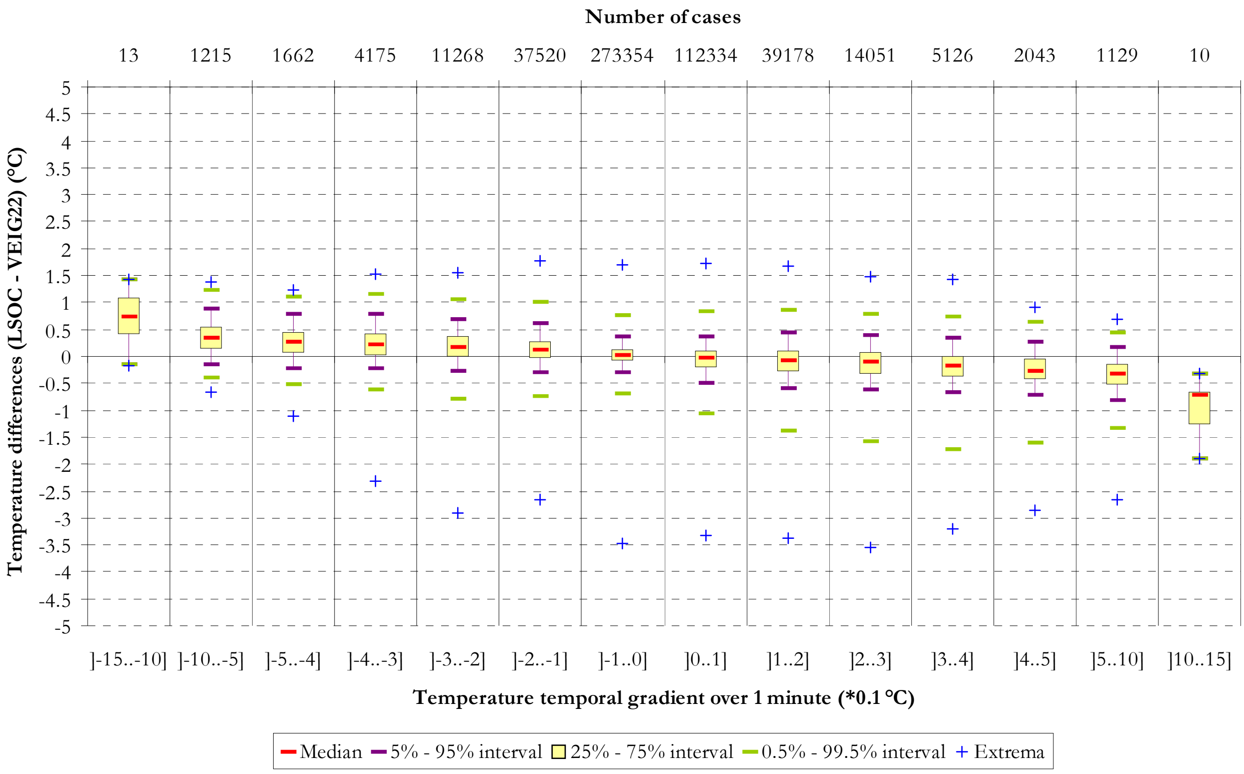


**Figure 10**

Differences with the reference are mainly positive for negative gradients, and negative for positive gradients. This clearly illustrates a delay of LSOC screen compared to the reference.

## QUALITY CONTROL INFORMATION

### DATA AVAILABILITY

The intercomparison period extends from the 1st of November 2008 to the 1st of November 2009. The theoretical number of 1-minute data is 525600.

The next table sums up the total number of data for each possible QC flag.

**Table 3**

| **QC flag** | LSOC |
|---|---|
| 0 (good) | 503266 |
| 1 (inconsistent) | 0 |
| 2 (doubtful) | 0 |
| 3 (erroneous) | 0 |
| 7 (missing) | 22334 |

### MAINTENANCE

No action done during the intercomparison period.

# Small Stevenson Screen
# WEATHER STATIONS AUSTRALIA
# – Australia –
# LBOM

**TECHNICAL SPECIFICATIONS (PROVIDED BY THE MANUFACTURER)**

Dimensions: Length 66.2 cm x Width 40.3 cm x Height 68 cm

Weight: 35 kg

Material/Structure: wood

Estimated radiation error:

Aspiration rate (in case of artificially ventilated screen/shield): naturally ventilated

Power supply: none

**Figure 1**

## OVERVIEW

The LBOM screen is globally cooler than the reference: nearly 86% of the 1-minute data are below the reference. The differences on daily extrema vary: 96% of minimum temperatures are below the reference, while 77% of the maximum temperatures.

For high radiation values, the LBOM screen is globally cooler than the reference. This may be a drawback of the reference.

During daytime, absolute differences are more important than during night time, except for wind speeds above 9 m/s. During overcast periods, absolute differences with the reference are very low for wind speeds below 6 m/s. Above this value, they are higher. During clear sky periods, absolute differences for low values of wind speed (below 3 m/s) are much higher than above 3 m/s.

During night time, differences are very small in clear sky conditions. They do not depend on wind speed. In overcast conditions they are slightly higher for some wind speed classes, but number of data is quite low.

LBOM screen gives measurements close to the reference for low sun elevation. The higher the sun, the cooler LBOM screen is in absolute value. Increasing wind speed reduces the difference with the reference.

The highest absolute differences are obtained for high radiation values and low wind speeds. This underlines the excellent ventilation of this screen.

The LBOM screen is globally cooler than the reference both in increasing or decreasing of temperature.

## CALIBRATION INFORMATION

None

The result of calibration of reference VEIG22 is available in the main report of the intercomparison, section 5.4.1.

## COMPARISON WITH THE REFERENCE

### HISTOGRAM OF DIFFERENCES

The histogram of differences between LBOM and the reference VEIG22 is plotted, using 1-minute quality checked data for the whole period of the intercomparison. Differences are plotted by steps of 0.1K. The vertical axis is the frequency in percent for each class of differences.

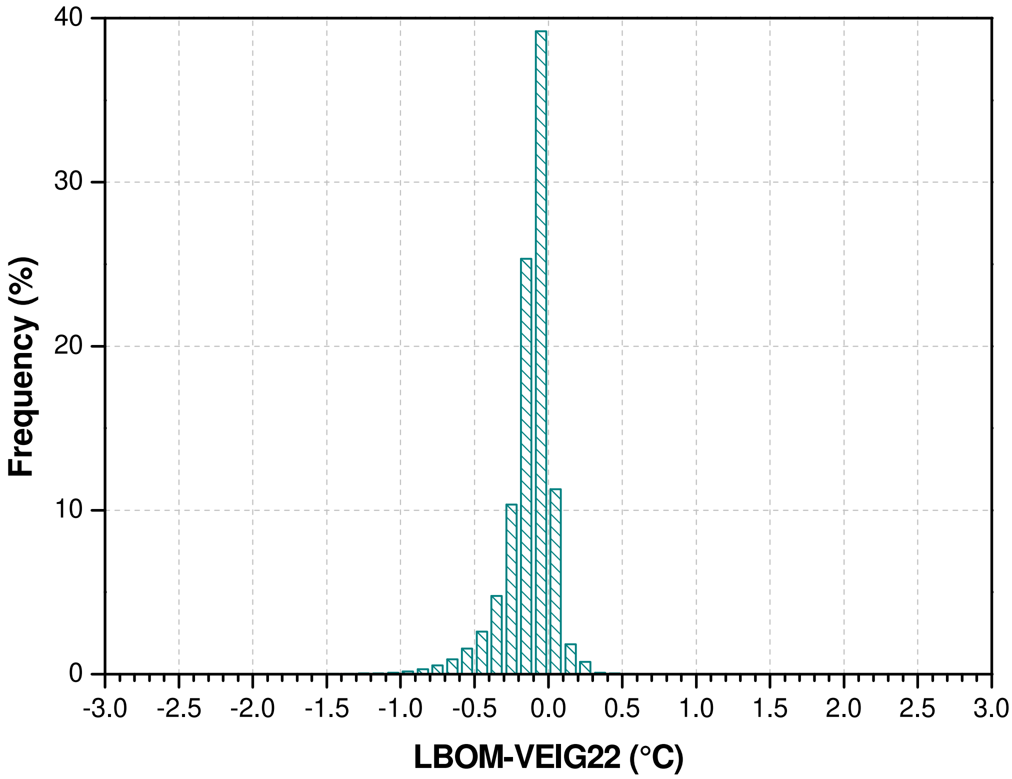


**Figure 2**

CUMULATIVE HISTOGRAMS OF DIFFERENCES OF DAILY EXTREME VALUES

The cumulative histograms of differences with the reference VEIG22 of T (1-minute quality checked data), Tn (daily minimum temperature) and Tx (daily maximum temperature) are plotted, for the whole period of the intercomparison. Differences are plotted by steps of 0.1K.

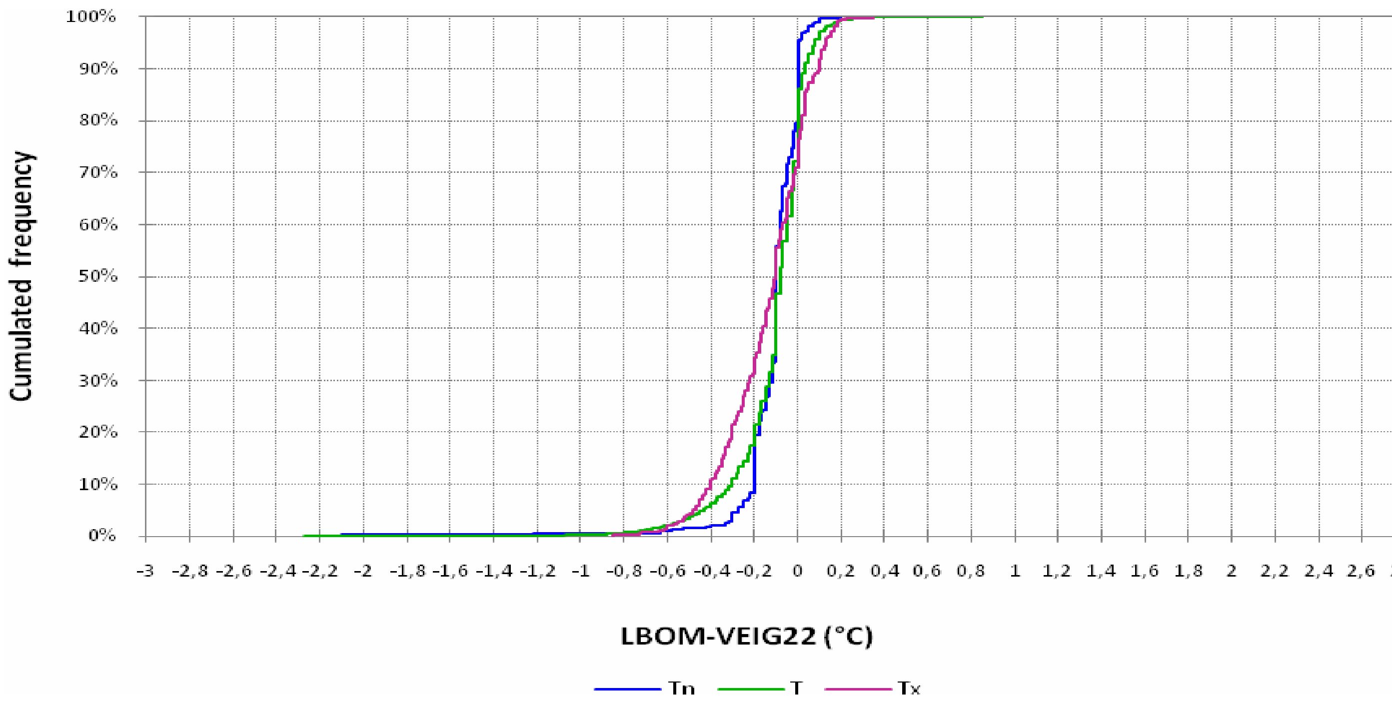


**Figure 3**

The LBOM screen is globally cooler than the reference: nearly 86% of the 1-minute data are below the reference. The differences on daily extrema vary: 96% of minimum temperatures are below the reference, while 77% of the maximum temperatures.

TABLE

The table 1 indicates the percentage of data that differ by less than 0.2°C (and 0.5°C) from the reference.

**Table 1**

| | | [-0.2°..0.2°] | [-0.5°..0.5°] |
|---|---|---|---|
| LBOM | T | 82.0 | 96.6 |
| | Tn | 87.9 | 98.4 |
| | Tx | 66.5 | 95.8 |

## INFLUENCE OF GLOBAL RADIATION

The distribution of differences between LBOM and the reference VEIG22 is plotted, using 1-minute quality checked data for the whole period of the intercomparison. Differences are classified according global radiation.

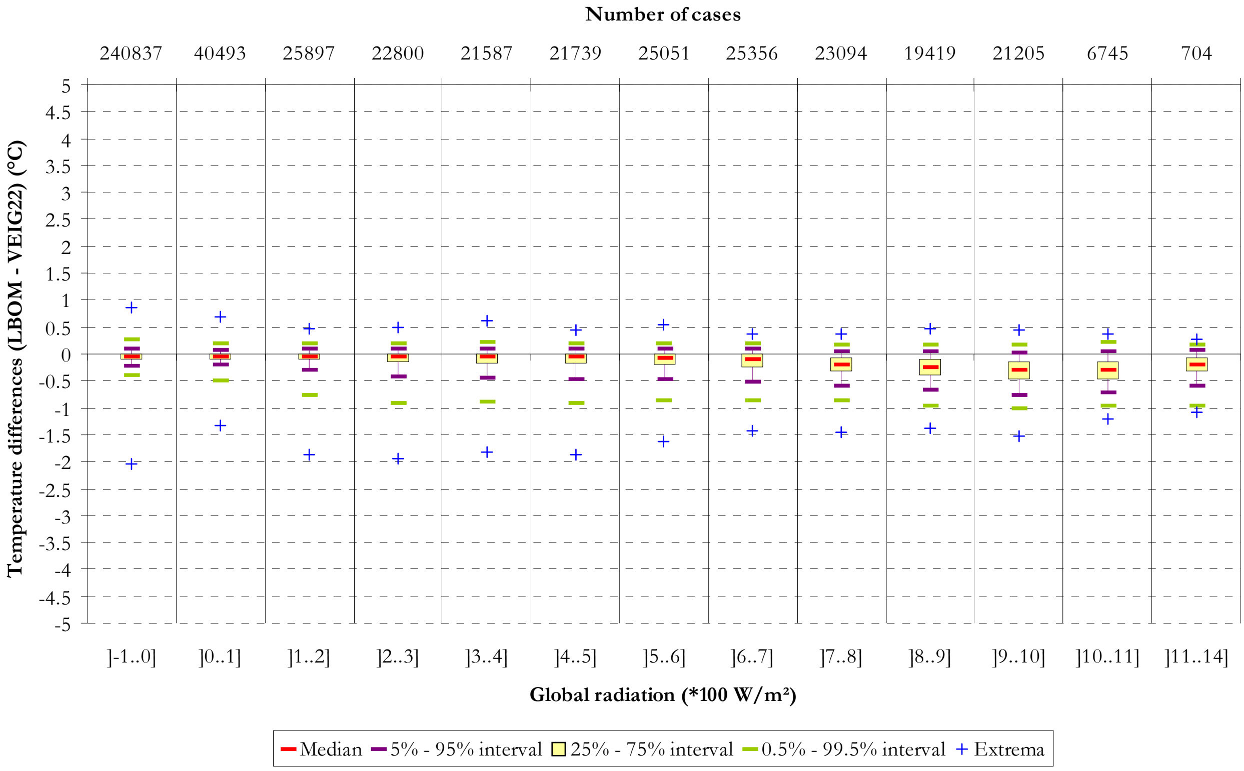


**Figure 4**

For high radiation values, the LBOM screen is globally cooler than the reference. This may be a drawback of the reference.

## RADIATION EFFECT

### DIFFERENCES BETWEEN DAY AND NIGHT BEHAVIOUR

The median of differences between LBOM and VEIG22 is plotted, using 1-minute quality checked data for the whole period of the intercomparison. We filter data for which sun elevation is above -1° (day) or below -1° (night). Differences are classified according 2-meter wind speed (2-minute average).

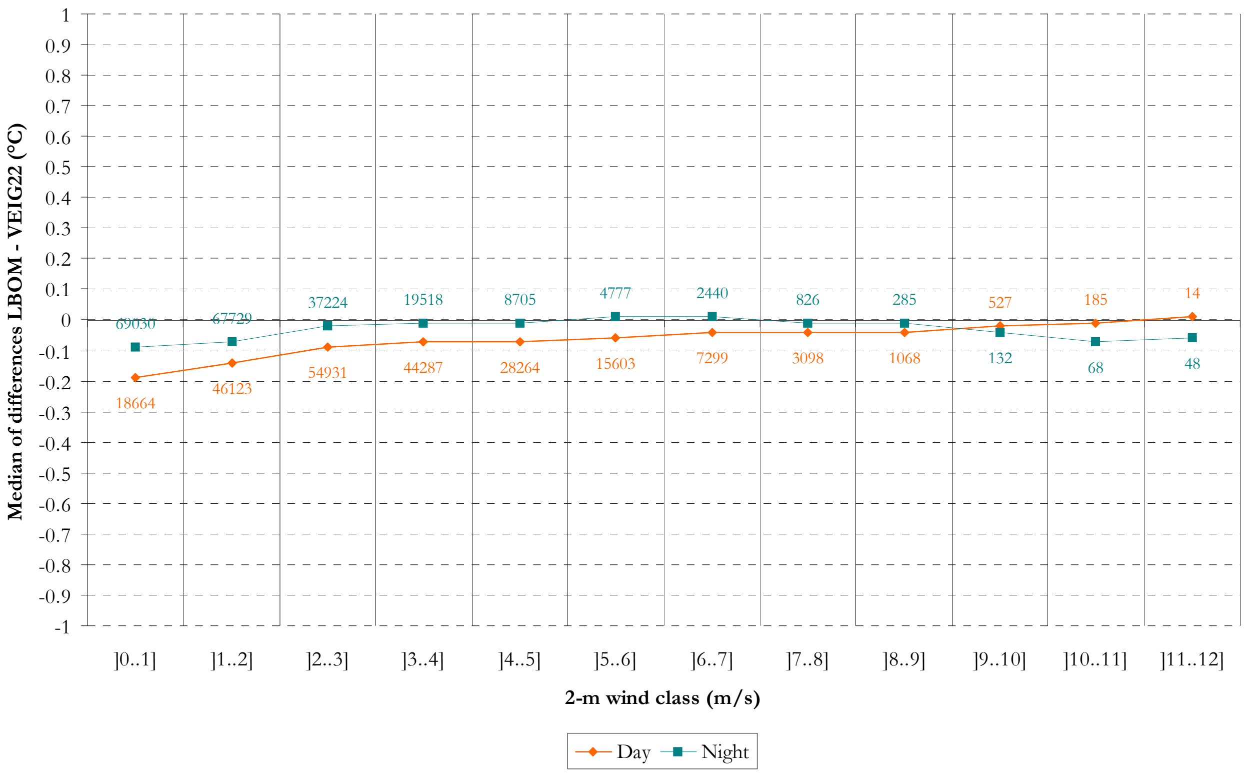


**Figure 5**

During daytime, absolute differences are more important than during night time, except for wind speeds above 9 m/s.

## DIFFERENCES BETWEEN CLEAR SKY AND OVERCAST SKY DURING DAYTIME

The median of differences between LBOM and VEIG22 is plotted, using 1-minute quality checked data. Here, we consider periods lasting six hours at least where cloudiness is less or equal to 1 (clear sky) or more or equal to 7 (overcast sky), during daytime (sun elevation above -1°). Differences are classified according 2-meter wind speed (2-minute average).

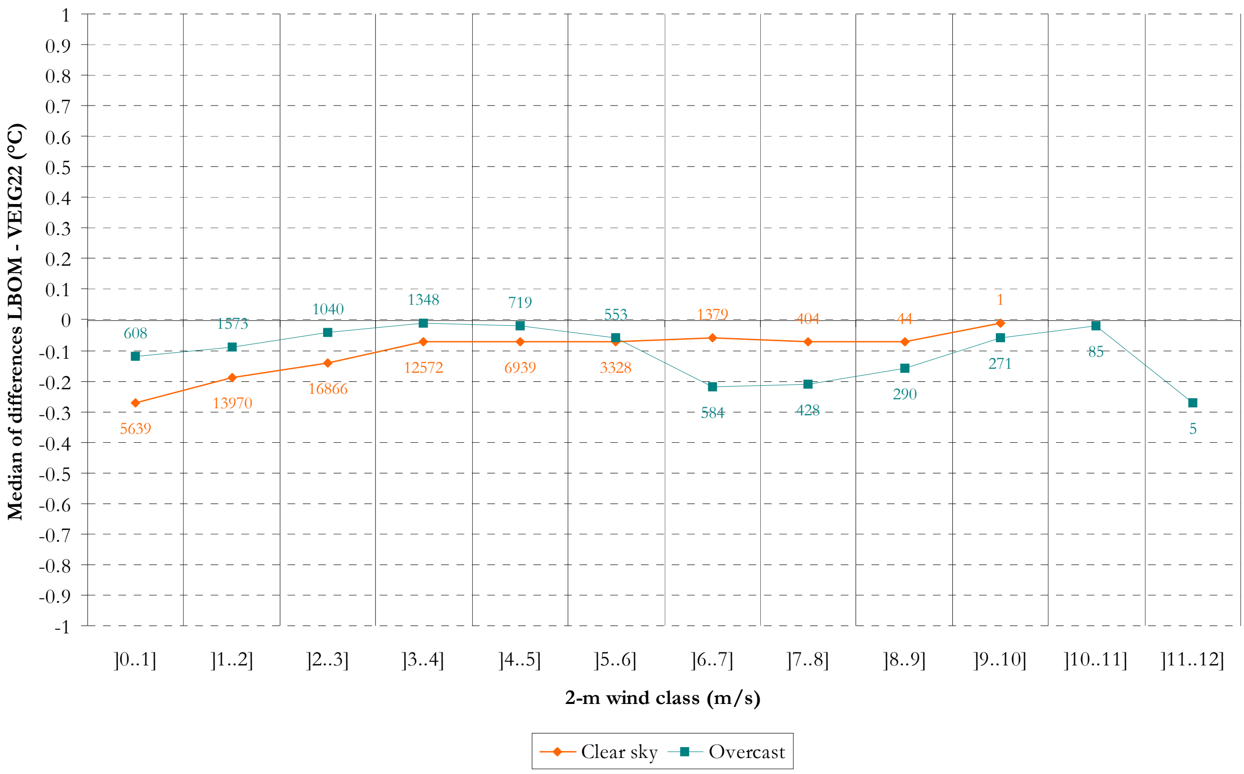


**Figure 6**

During overcast periods, absolute differences with the reference are very low for wind speeds below 6 m/s. Above this value, they are higher.

During clear sky periods, absolute differences for low values of wind speed (below 3 m/s) are much higher than above 3 m/s. As an example, the next figure shows temperature evolution during the 4th and the 5th of August, 2009, two sunny and hot summer days. The top chart is the 10-minute average temperature for sensors LBOM, VEIG22 and Thies sensors ATHI1 ATHI2. In the middle chart is the global radiation. On the bottom chart is the 2-meter wind speed (2-minute average).

The first day, the wind is quite calm, LBOM and VEIG22 measurements differ by about 0.6°C. On the second day, the wind is stronger, around 6 m/s, and both sensors give close measurements. Both days, Thies sensors are much cooler. They are not affected by wind speed.

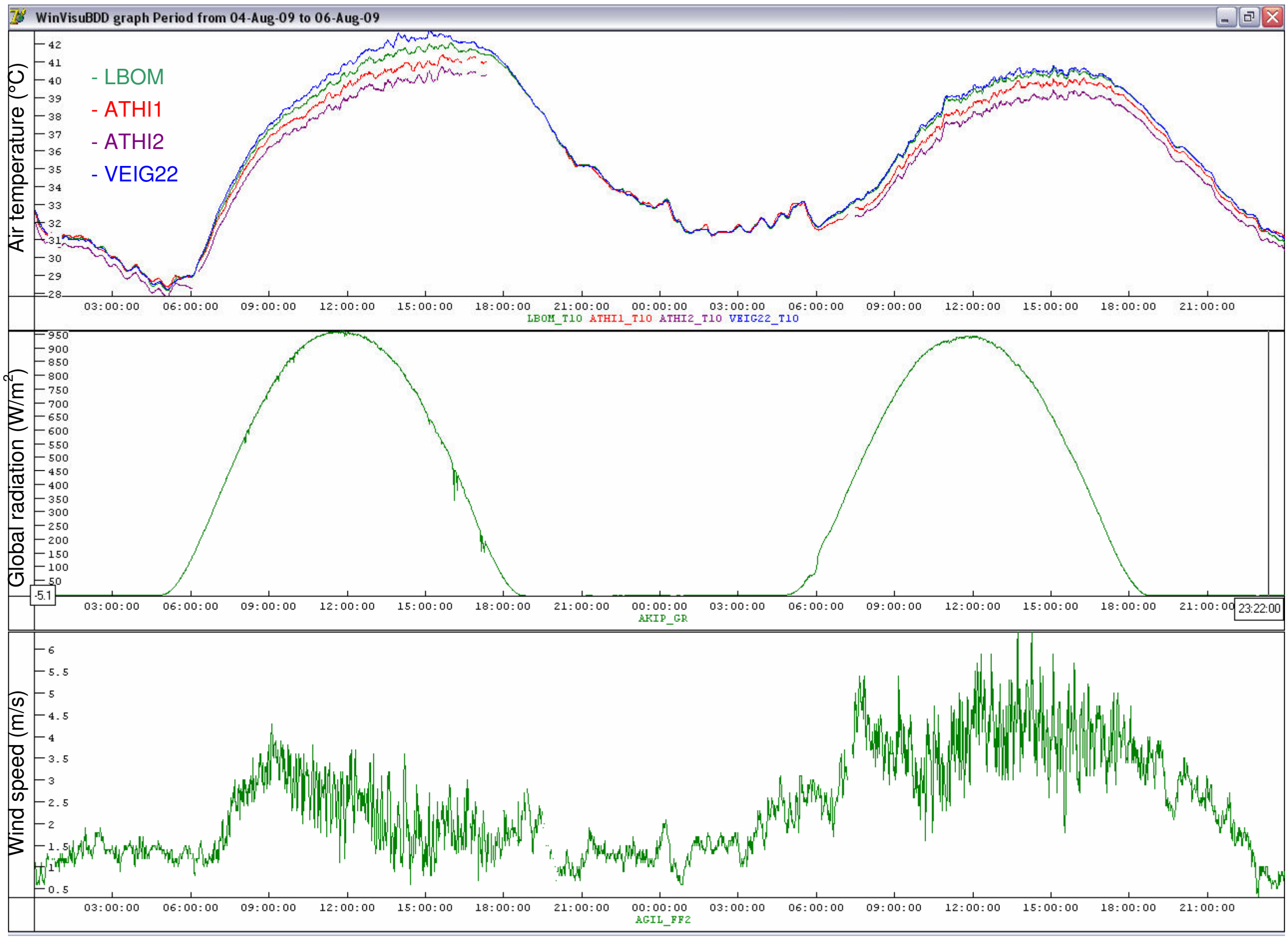


**Figure 7**

DIFFERENCES BETWEEN CLEAR SKY AND OVERCAST SKY DURING NIGHT TIME

The median of differences between LBOM and VEIG22 is plotted, using 1-minute quality checked data. Here, we consider periods lasting six hours at least where cloudiness is less or equal to 1 (clear sky) or more or equal to 7 (overcast sky), during night time (sun elevation below -1°). Differences are classified according 2-meter wind speed (2-minute average).

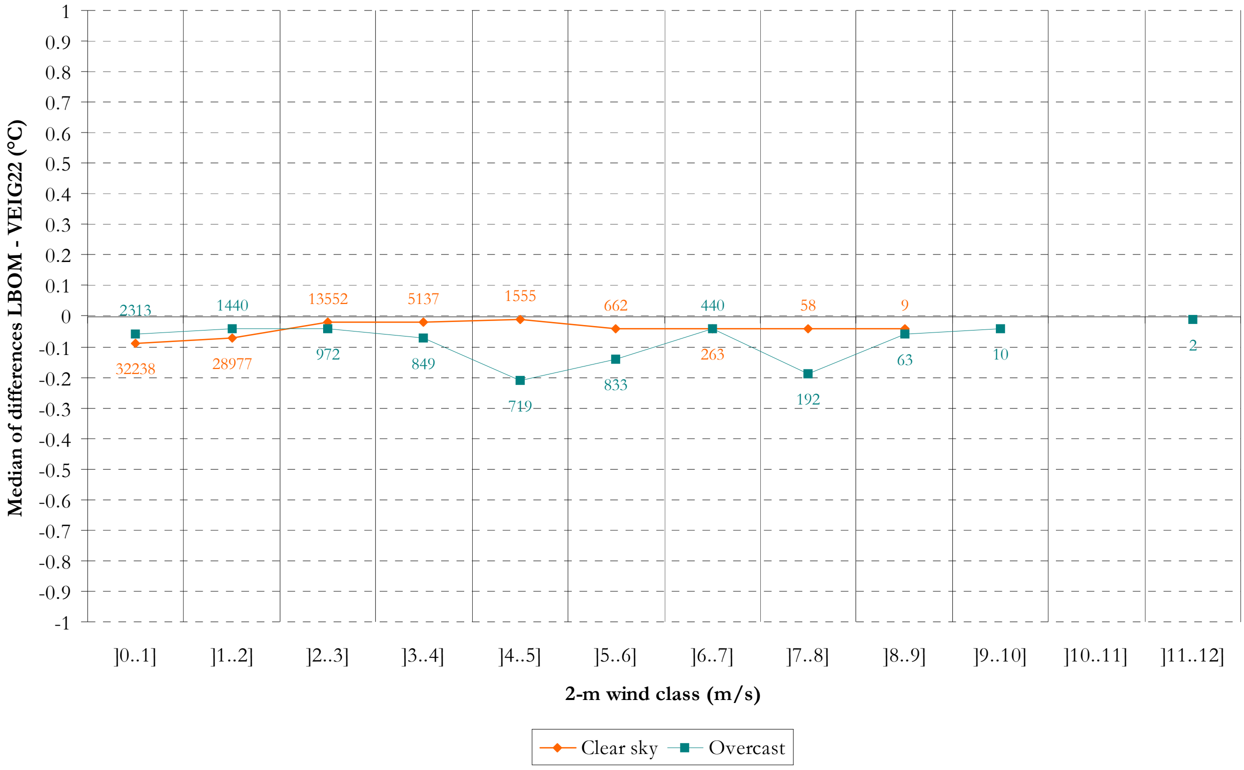


**Figure 8**

During night time, differences are very small in clear sky conditions. They do not depend on wind speed. In overcast conditions they are slightly higher for some wind speed classes, but number of data is quite low.

## EFFECT OF SUN ELEVATION

The median of differences between LBOM and VEIG22 is plotted, using 1-minute quality checked data. Here, we consider periods lasting six hours at least where cloudiness is less or equal to 1 (clear sky), during daytime (sun elevation above -1°). We filter data where sun elevation is low (below 10°), medium (between 10° and 45°) or  high (above 45°). Differences are classified according 2-meter wind speed (2-minute average).

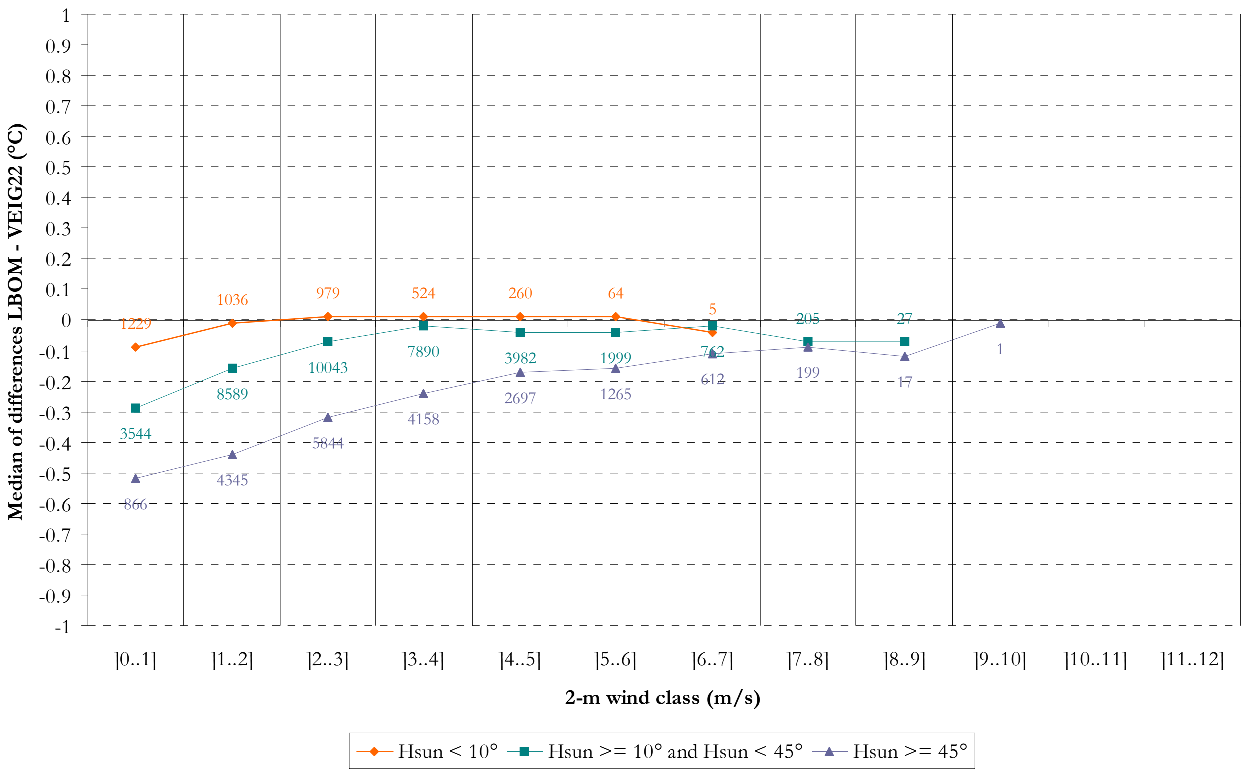


**Figure 9**

LBOM screen gives measurements close to the reference for low sun elevation. The higher the sun, the cooler LBOM screen is in absolute value. Increasing wind speed reduces the difference with the reference.

## COMBINED EFFECT OF WIND AND GLOBAL RADIATION

The medians of differences between LBOM and VEIG22 are represented here with a contour plot. The global radiation values are on the X-axis and on the Y axis is the 2-meter wind speed value (2-minute average). Medians are used in all cases, providing that at least one data is available for both conditions on radiation and wind considered.

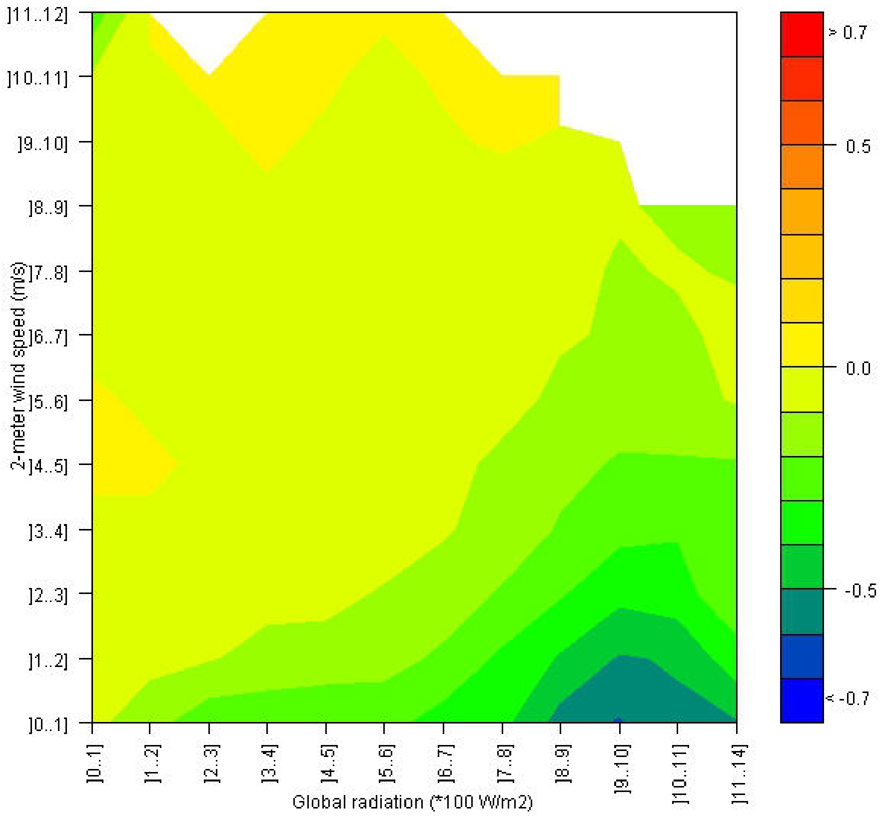


**Figure 10**

This screen is globally cooler than the reference. The highest absolute differences are obtained for high radiation values and low wind speeds. This underlines the excellent ventilation of this screen.

## BEHAVIOUR DURING INCREASE/DECREASE OF TEMPERATURE

The distribution of differences between LBOM and the reference VEIG22 is plotted, using 1-minute quality checked data for the whole period of the intercomparison. Differences are classified according the temporal gradient of reference temperature over 1 minute. A screen faster (or slower, respectively) than the reference would be warmer (cooler) for positive gradient, cooler (warmer) for negative ones.

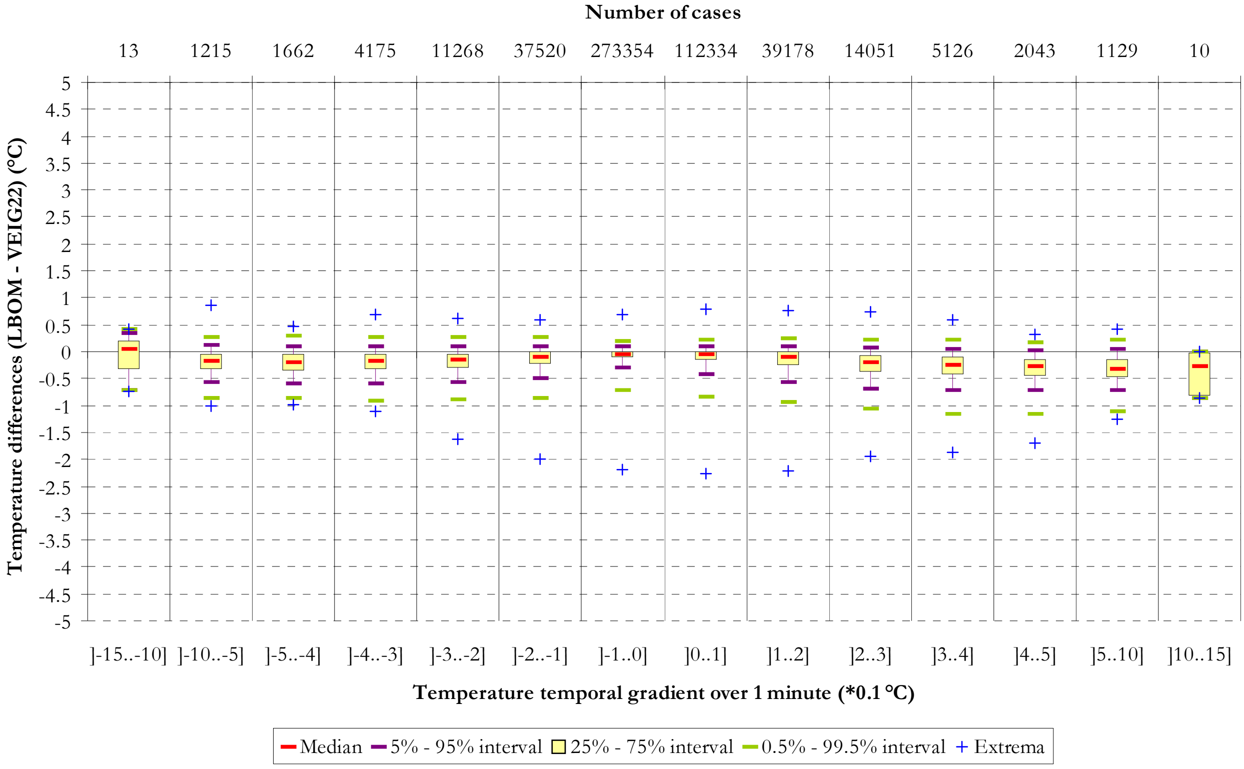


**Figure 11**

The LBOM screen is globally cooler than the reference both in increasing or decreasing of temperature.

## QUALITY CONTROL INFORMATION

DATA AVAILABILITY

The intercomparison period extends from the 1st of November 2008 to the 1st of November 2009. The theoretical number of 1-minute data is 525600.

The next table sums up the total number of data for each possible QC flag.

**Table 2**

| QC flag | LBOM |
|---|---|
| 0 (good) | 503266 |
| 1 (inconsistent) | 0 |
| 2 (doubtful) | 0 |
| 3 (erroneous) | 0 |
| 7 (missing) | 22334 |

MAINTENANCE

No action done during the intercomparison period.

# LANSER
# – Austria –
# LLAN

**TECHNICAL SPECIFICATIONS (PROVIDED BY THE MANUFACTURER)**

Dimensions: Length 50 cm x Width 50 cm x Height 60 cm

Weight: 14 kg

Material/Structure: wood

Estimated radiation error:

Aspiration rate (in case of artificially ventilated screen/shield): 2 m/s

Power supply: 12 V

**Table 1**

**Figure 1**

**Figure 2**

In this screen, the temperature probe is installed at 1.80-meter height, instead of 1.50 meter in other screens.

## OVERVIEW

The absolute differences between both screens are very low, they are most of the time lower than 0.5°C.

These screens are slightly warmer than the reference, 0.1°C in average. Daily minimum temperatures are generally warmer. Absolute differences in daily maximum temperatures exceed 0.2°C in more than 35% of the cases and 0.5°C in less than 3% of the cases.

Clear sky and overcast conditions give similar results, during day time or night time, except for calm winds. In that case, the median of differences is 0.1°C warmer in overcast conditions than in clear sky conditions.

The sun elevation has a small influence. Lanser screens are 0.2°C cooler than the reference for high sun elevation and low wind speed.

The highest absolute differences are obtained for low wind speeds and high radiations. Lanser screens are then cooler than the reference.

These screens are slightly slower than the reference.

## CALIBRATION INFORMATION

The calibration of both probes was performed in Trappes.

**Table 2**

| Screen | Location | Pt100 probe serial number | Calibration date | Instrument bias (°C) | | | |
|---|---|---|---|---|---|---|---|
| | | | | -20°C | 0°C | 20°C | 40°C |
| LLAN1 | F4 | T79 | 24-Jan-2006 | 0.0227 | 0.0032 | 0.0263 | 0.0408 |
| LLAN2 | F6 | T70 | 1-Feb-2006 | 0.0100 | 0.0184 | 0.0382 | 0.0542 |

The result of calibration of reference VEIG22 is available in the main report of the intercomparison, section 5.4.1.

## COMPARISON OF BOTH SENSORS

The distribution of differences between screen 1 and screen 2 is plotted, using 1-minute quality checked data for the whole period of the intercomparison. Differences are classified according screen 1 temperature.

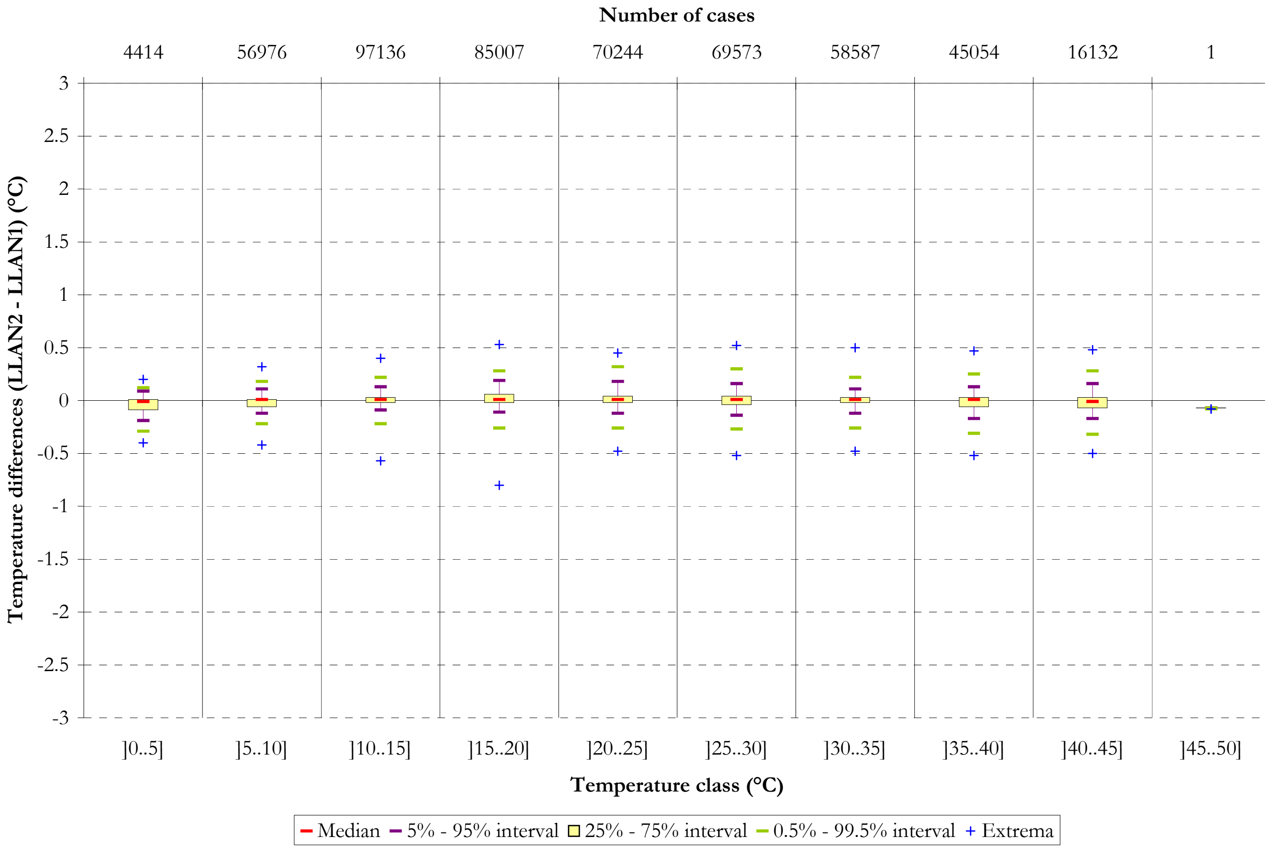


**Figure 3**

The absolute differences between both screens are very low, they are most of the time lower than 0.5°.

There is no influence of the temperature on these differences.

## COMPARISON WITH THE REFERENCE

### HISTOGRAM OF DIFFERENCES

The histogram of differences between LLAN and the reference VEIG22 is plotted, using 1-minute quality checked data for the whole period of the intercomparison. Differences are plotted by steps of 0.1K. The vertical axis is the frequency in percent for each class of differences.

Screen #1:

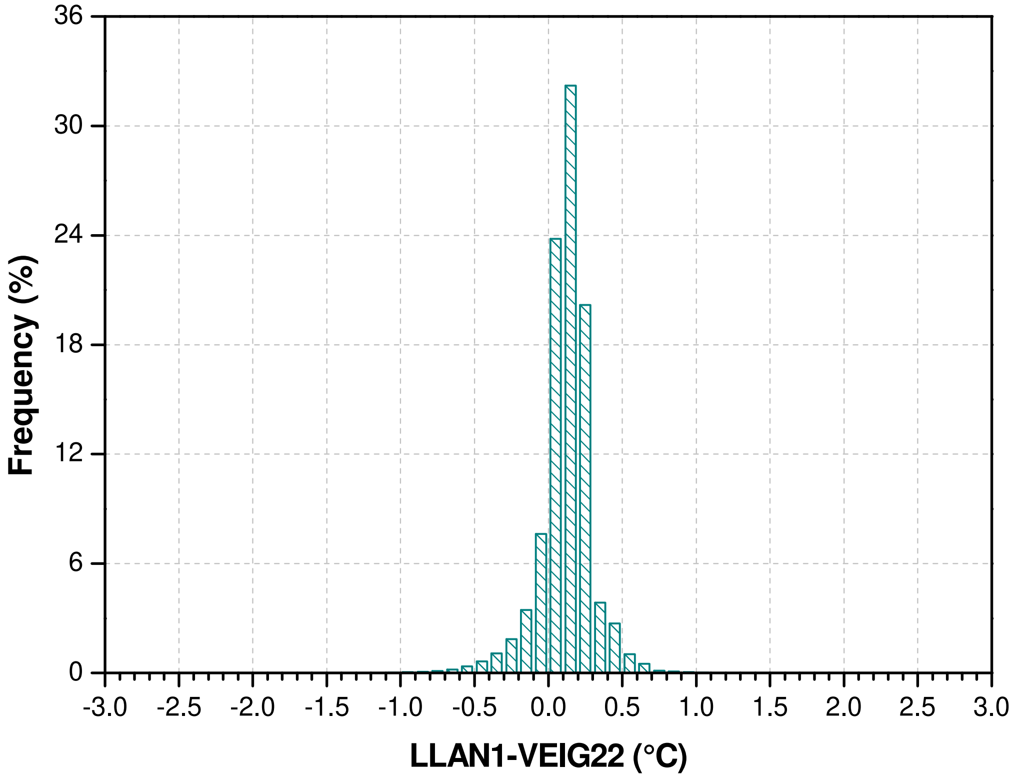


**Figure 4**

Screen #2 :

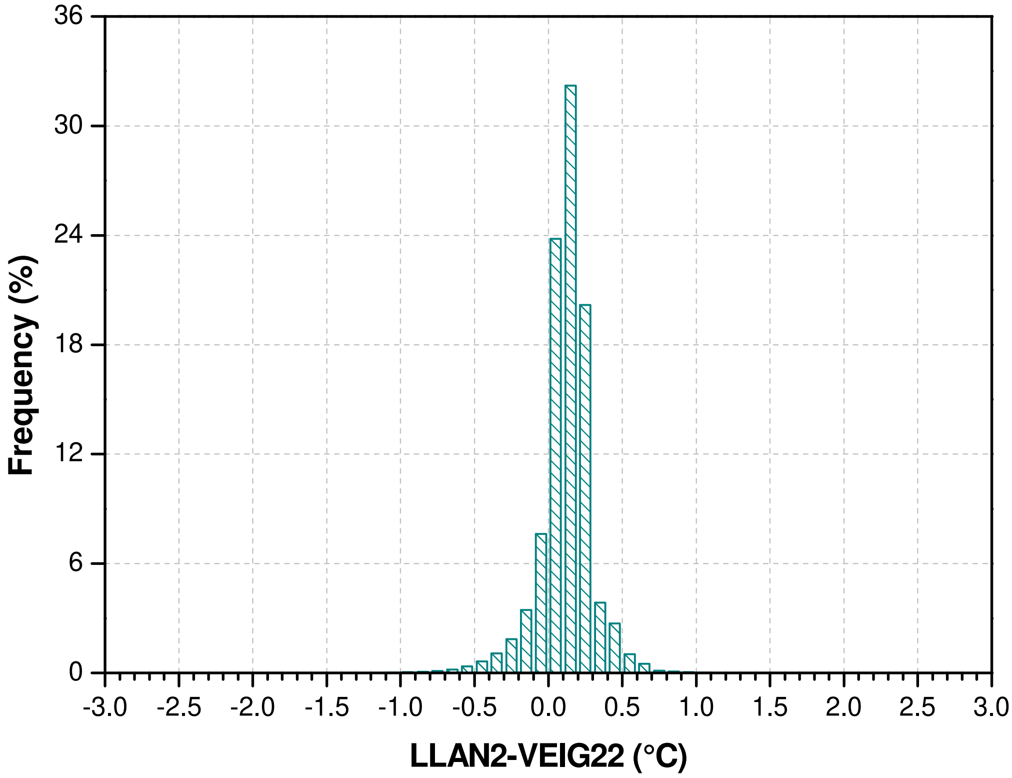


**Figure 5**

CUMULATIVE HISTOGRAMS OF DIFFERENCES OF DAILY EXTREME VALUES

The cumulative histograms of differences with the reference VEIG22 of T (1-minute quality checked data), Tn (daily minimum temperature) and Tx (daily maximum temperature) are plotted, for the whole period of the intercomparison. Differences are plotted by steps of 0.1K.

Screen #1:

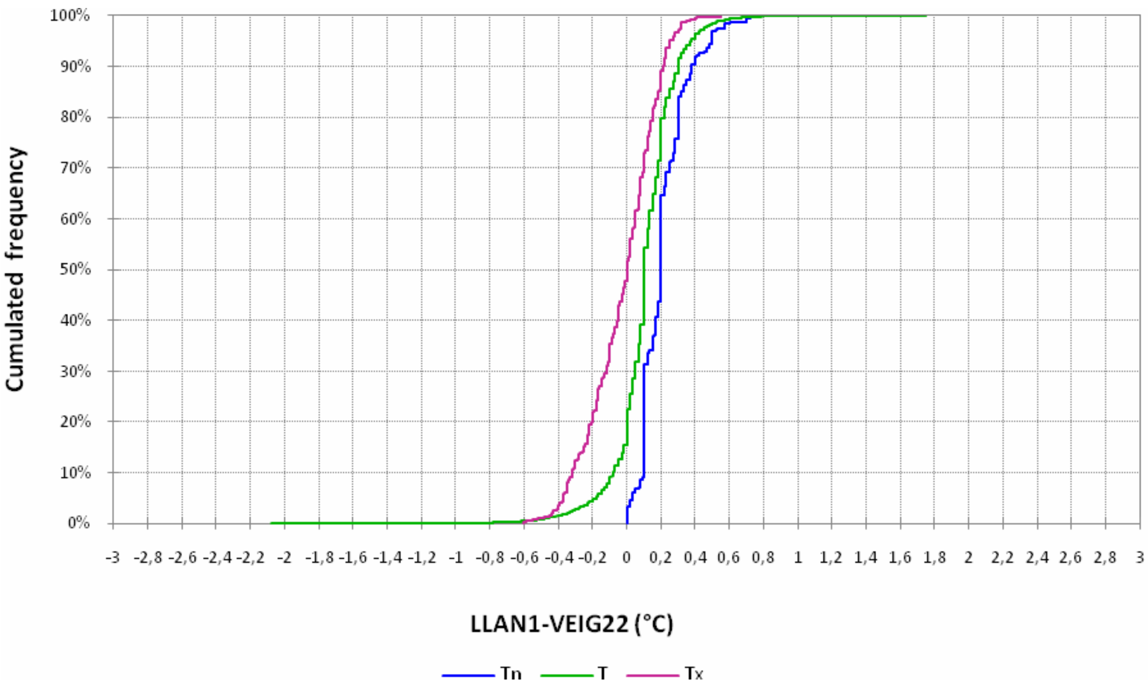


**Figure 6**

Screen #2:

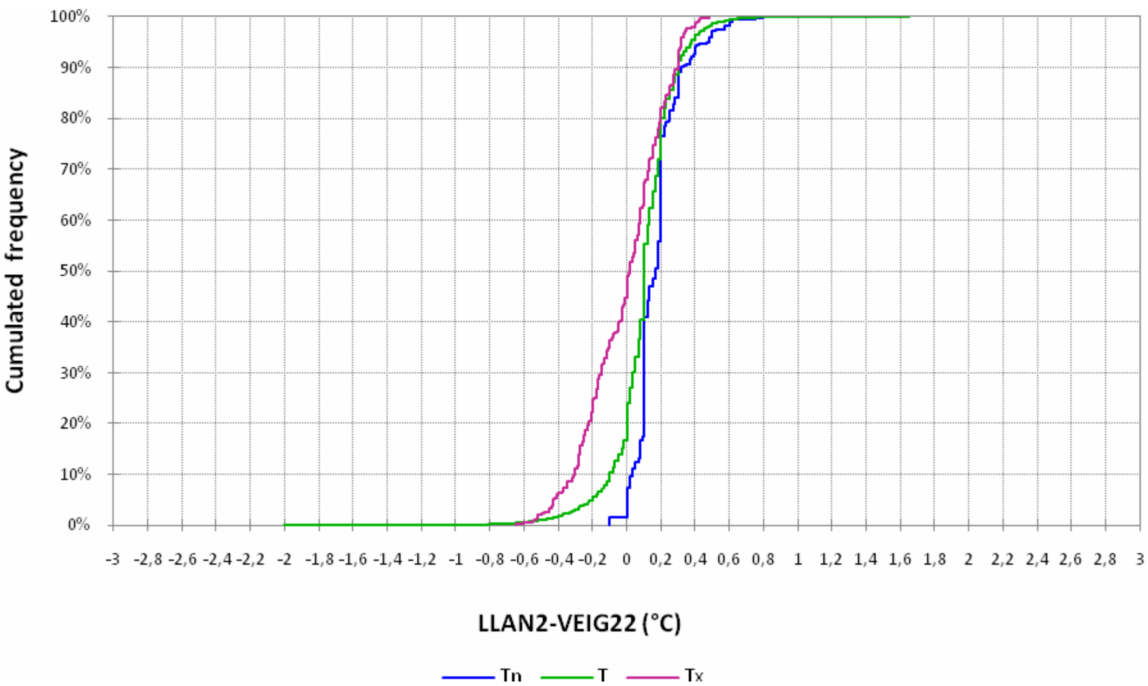


**Figure 7**

Daily minimum temperatures are generally warmer than those of the reference (in 95% of the cases). Daily maximum temperatures are well distributed, half part is below the reference, the other half is above it. Absolute differences exceed 0.2°C in more than 35% of the cases. They exceed 0.5°C in less than 3% of the cases.

TABLE

The table 3 indicates the percentage of data that differ by less than 0.2°C (and 0.5°C) from the reference.

**Table 3**

| | | [-0.2°..0.2°] | [-0.5°..0.5°] |
|---|---|---|---|
| LLAN1 | T | 75.5 | 97.8 |
| | Tn | 60.6 | 96.6 |
| | Tx | 67.9 | 98.6 |
| LLAN2 | T | 75.1 | 97.7 |
| | Tn | 72.4 | 0.0 |
| | Tx | 57.3 | 98.1 |

## INFLUENCE OF GLOBAL RADIATION

The distribution of differences between LLAN and the reference VEIG22 is plotted, using 1-minute quality checked data for the whole period of the intercomparison. Differences are classified according global radiation.

<u>Screen #1:</u>

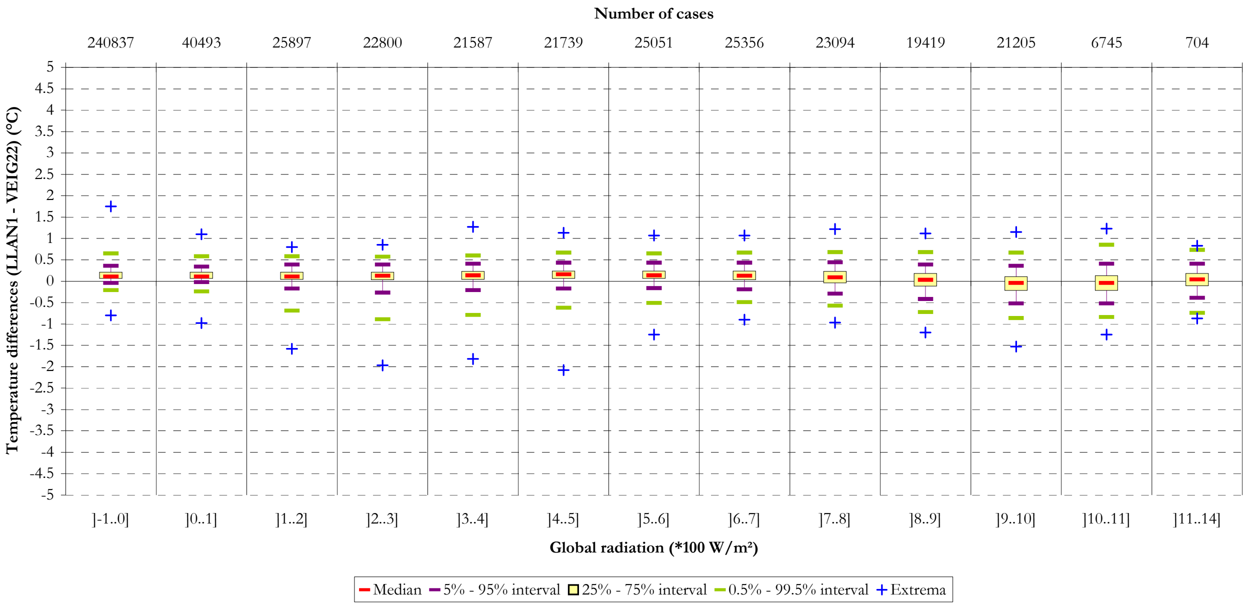


**Figure 8**

Screen #2:

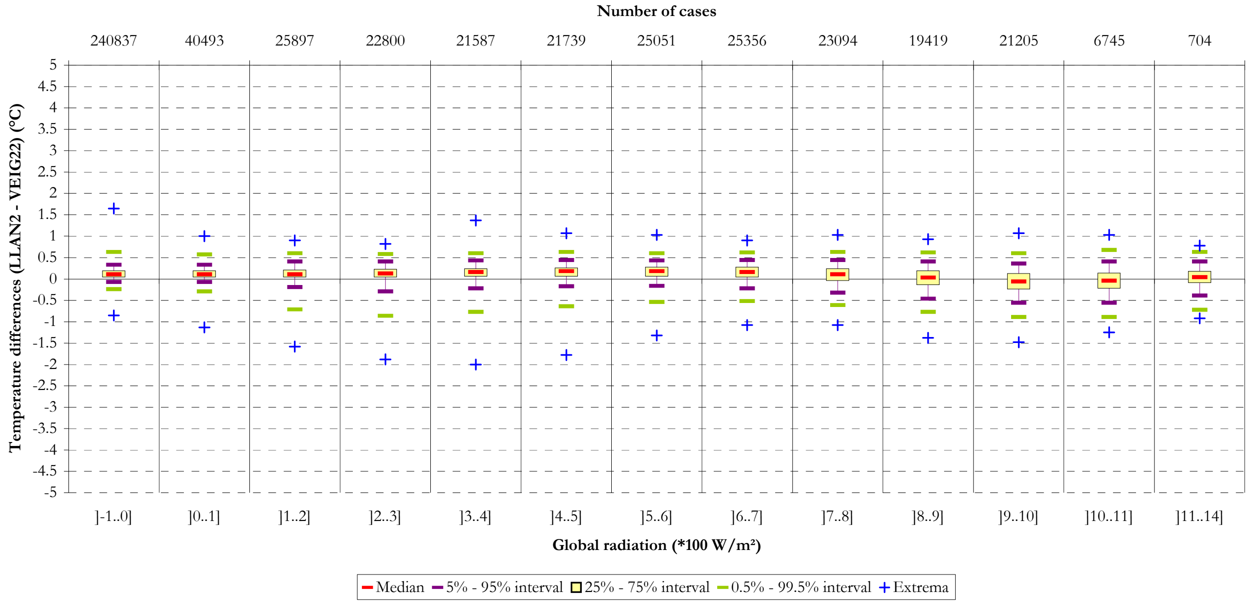


**Figure 9**

There is a small effect of global radiation on the differences regarding the reference: for very high values of radiation, differences are closer to zero and they are also more dispersed.

## RADIATION EFFECT

### DIFFERENCES BETWEEN DAY AND NIGHT BEHAVIOUR

The median of differences between LLAN and VEIG22 is plotted, using 1-minute quality checked data for the whole period of the intercomparison. We filter data for which sun elevation is above -1° (day) or below -1° (night). Differences are classified according 2-meter wind speed (2-minute average).

Screen #1 :

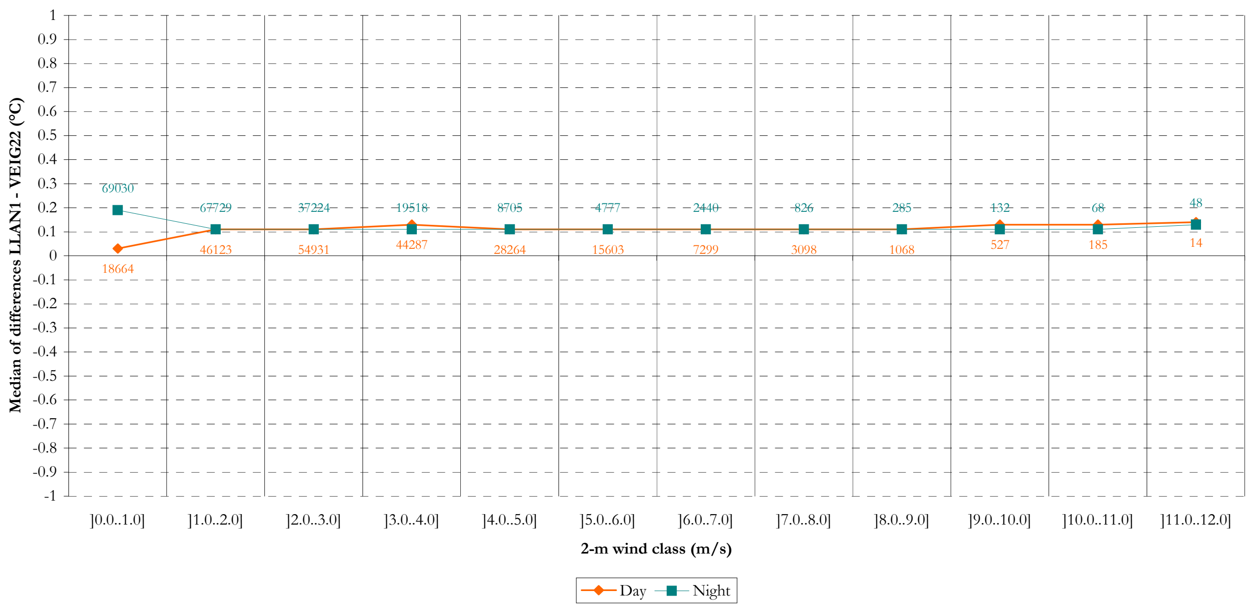


**Figure 10**

Screen #2 :

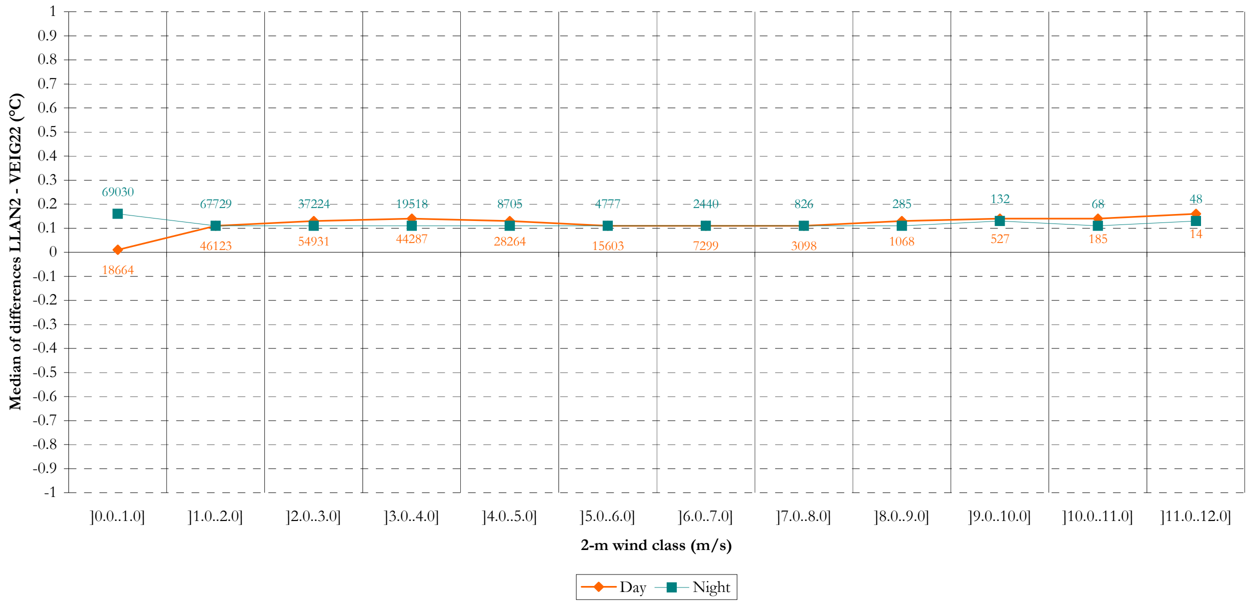

**Figure 11**

For calm winds (less than 1 m/s), the screens are about 0.2° warmer than the reference during the night, and give temperatures close to the reference during the day. For winds above 1 m/s, the behaviour of these screens is the same than the reference during the day or during the night, about 0.1° warmer than the reference.

DIFFERENCES BETWEEN CLEAR SKY AND OVERCAST SKY DURING DAYTIME

The median of differences between LLAN and VEIG22 is plotted, using 1-minute quality checked data. Here, we consider periods lasting six hours at least where cloudiness is less or equal to 1 (clear sky) or more or equal to 7 (overcast sky), during daytime (sun elevation above -1°). Differences are classified according 2-meter wind speed (2-minute average).

Screen #1 :

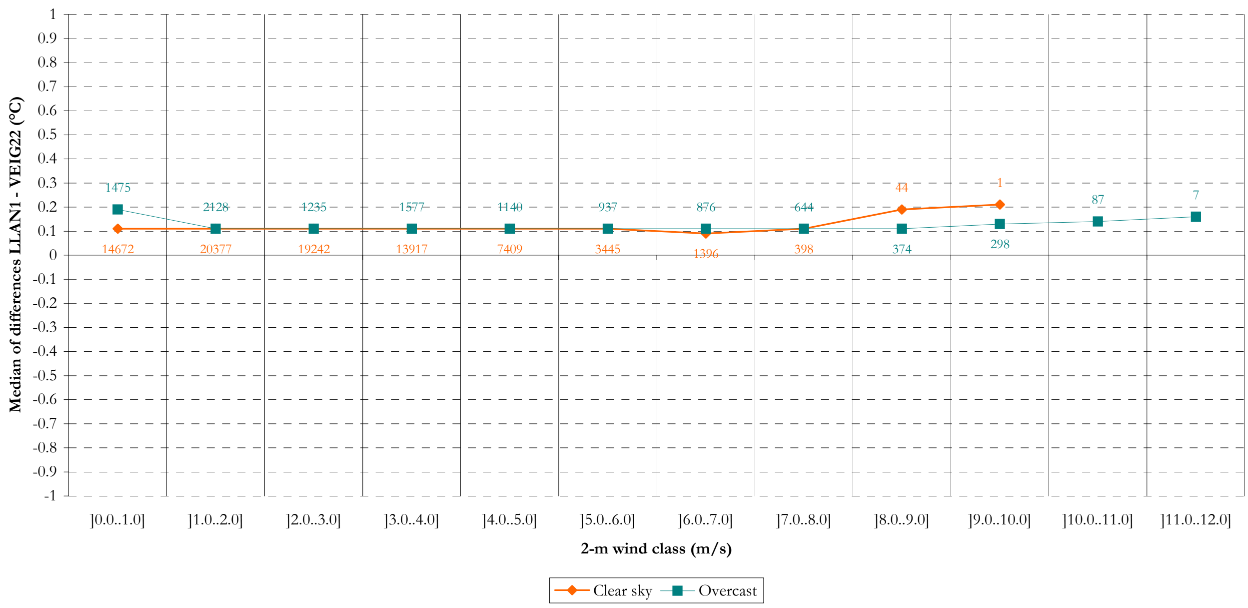

**Figure 12**

Screen #2 :

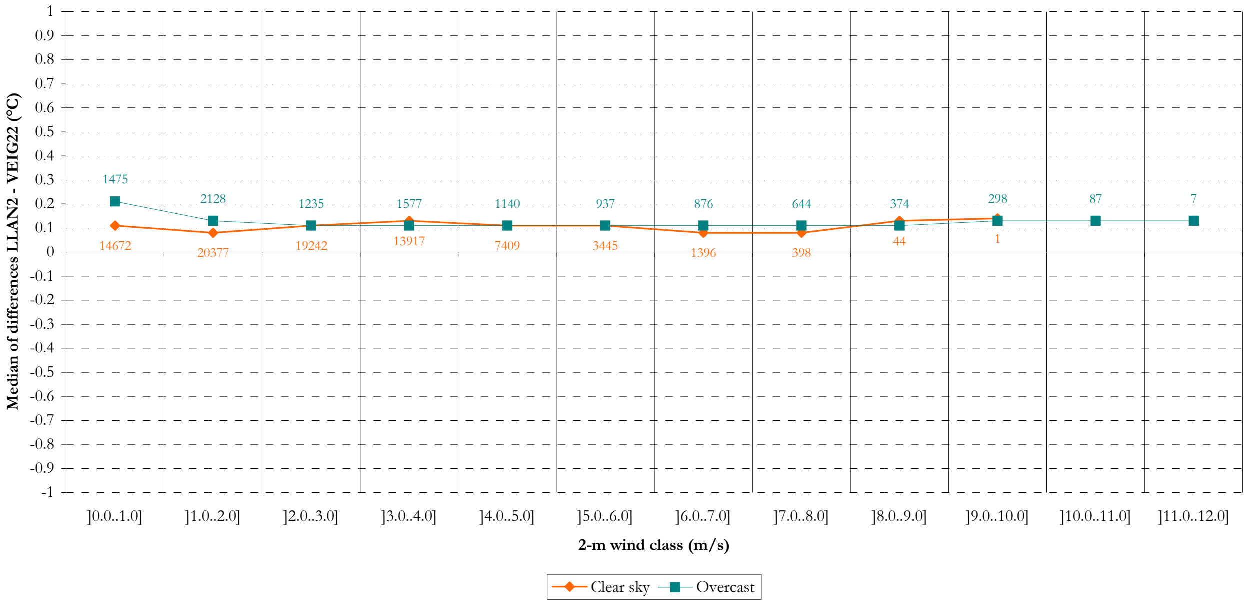


**Figure 13**

Clear sky and overcast conditions give similar results for both screens, except for calm winds. In that case, the median of differences is 0.1°C warmer in overcast conditions than in clear sky conditions.

DIFFERENCES BETWEEN CLEAR SKY AND OVERCAST SKY DURING NIGHT TIME

The median of differences between LLAN and VEIG22 is plotted, using 1-minute quality checked data. Here, we consider periods lasting six hours at least where cloudiness is less or equal to 1 (clear sky) or more or equal to 7 (overcast sky), during night time (sun elevation below -1°). Differences are classified according 2-meter wind speed (2-minute average).

Screen #1 :

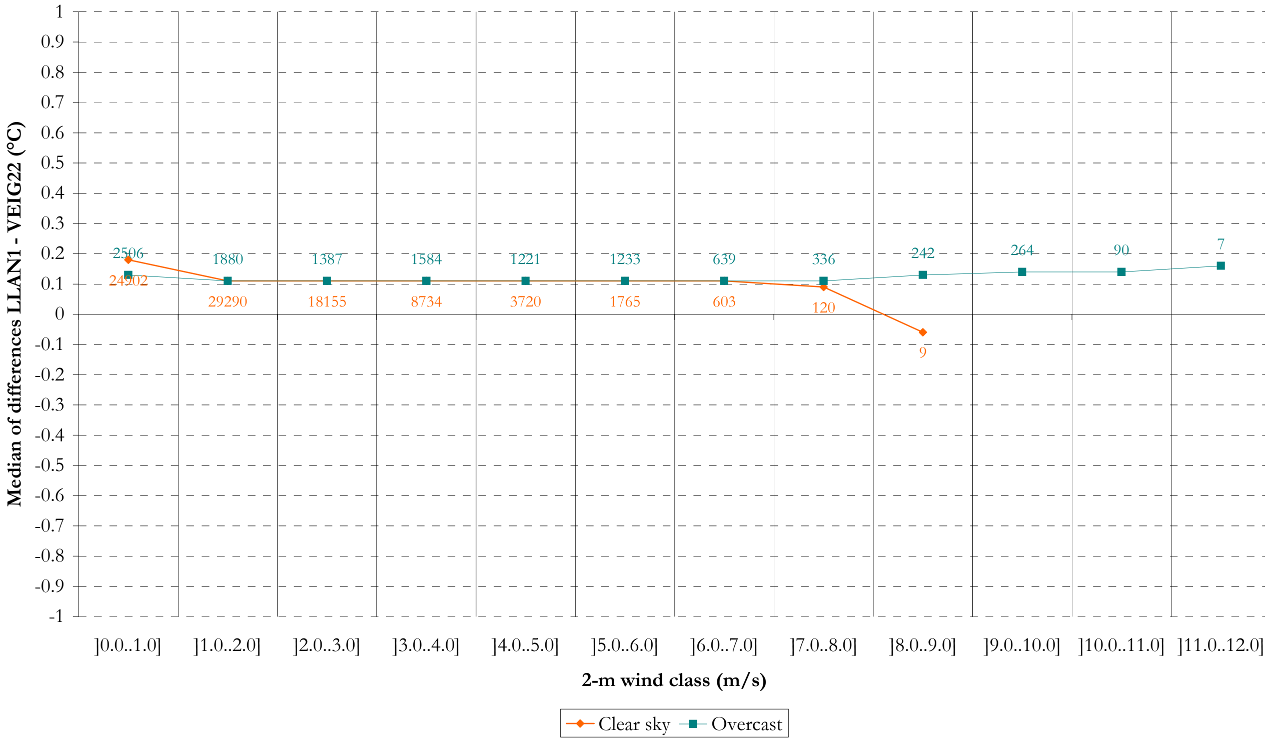


**Figure 14**

Screen #2 :

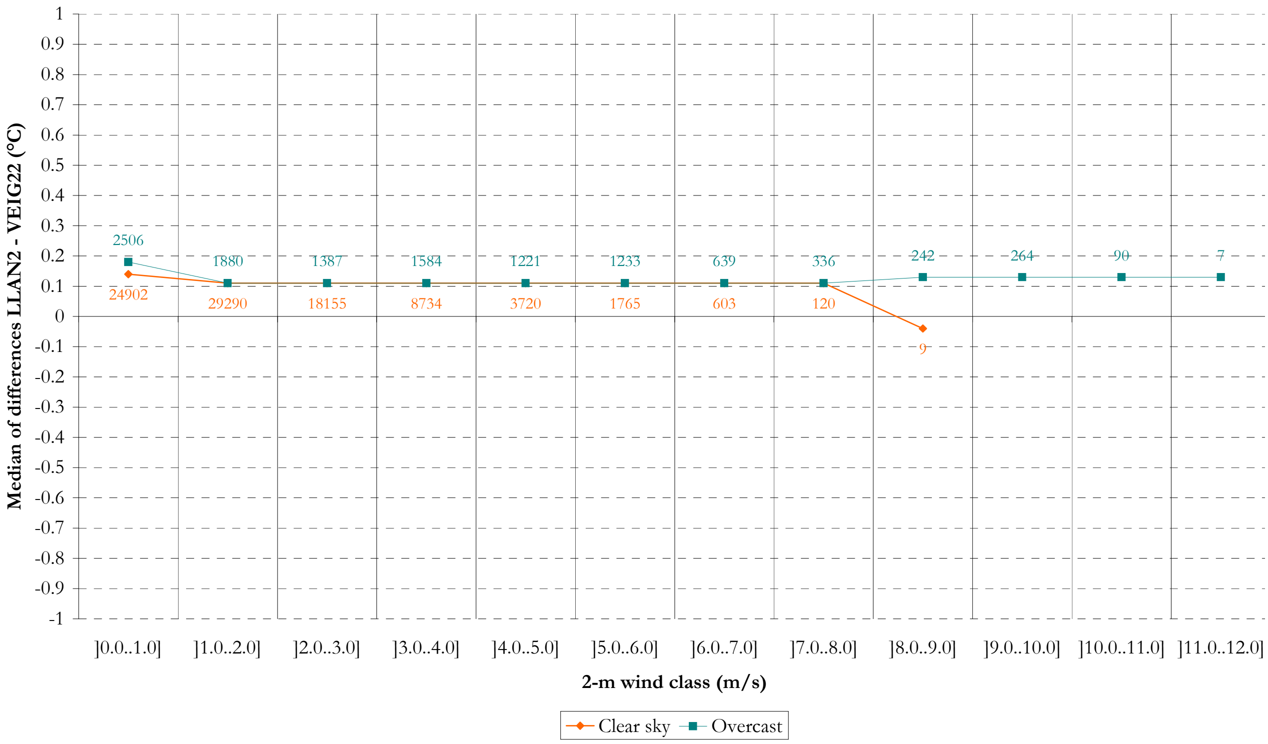


**Figure 15**

Conclusions for night time periods are very similar to day time. Differences between clear sky and overcast periods are even smaller for winds below 2 m/s.

## EFFECT OF SUN ELEVATION

The median of differences between LLAN and VEIG22 is plotted, using 1-minute quality checked data. Here, we consider periods lasting six hours at least where cloudiness is less or equal to 1 (clear sky), during daytime (sun elevation above -1°). We filter data where sun elevation is low (below 10°), medium (between 10° and 45°) or high (above 45°). Differences are classified according 2-meter wind speed (2-minute average).

<u>Screen #1 :</u>

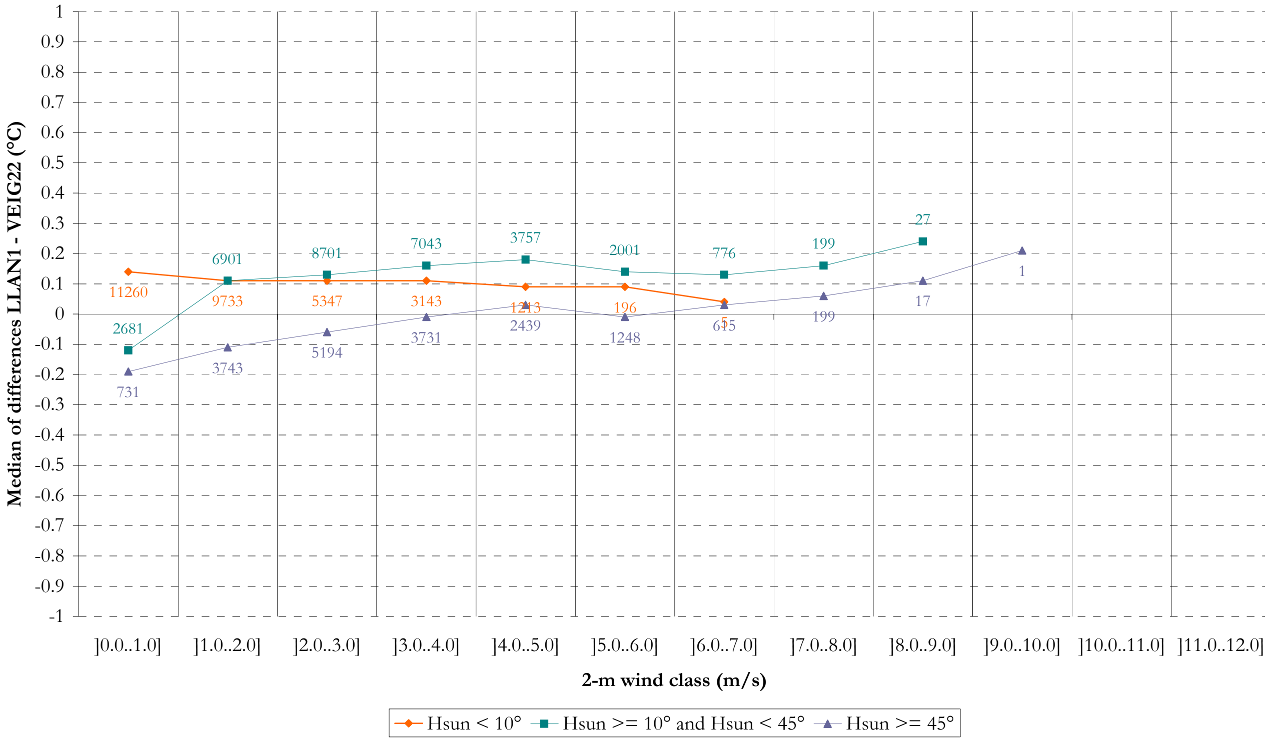


**Figure 16**

Screen #2 :

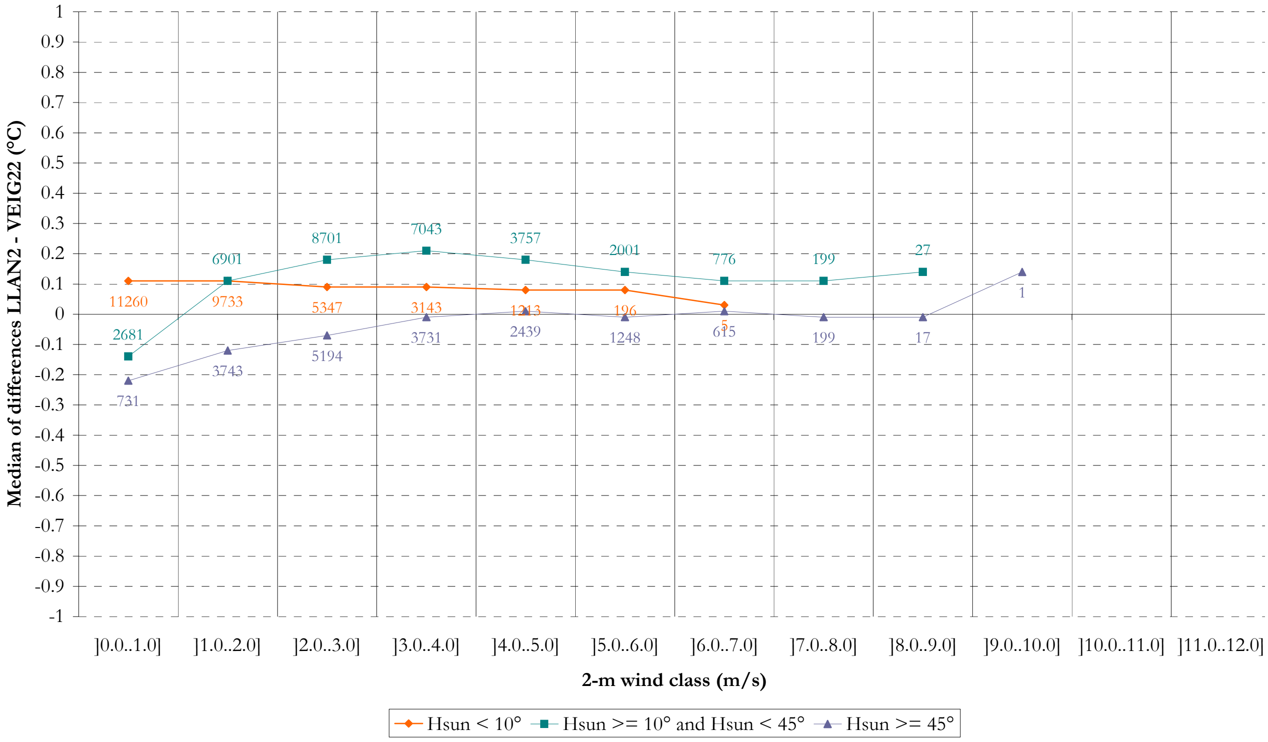


**Figure 17**

The curves for low sun heights show no influence of the wind speed: differences with the references is constant: about 0.1°C warmer. When the sun is higher in the sky (above 45°), differences depend on the wind speed: for low wind speed Lanser screens are 0.2 °C cooler than the reference. When the wind speed is higher, the difference with the reference becomes closer to zero. For intermediate values of sun elevation, the difference is also negative for calm winds, and becomes positive. It even reaches 0.2°C for winds around 4 m/s.

## COMBINED EFFECT OF WIND AND GLOBAL RADIATION

The medians of differences between LLAN and VEIG22 are represented here with a contour plot. The global radiation values are on the X-axis and on the Y axis is the 2-meter wind speed value (2-minute average). Medians are used in all cases, providing that at least one data is available for both conditions on radiation and wind considered.

Screen #1:

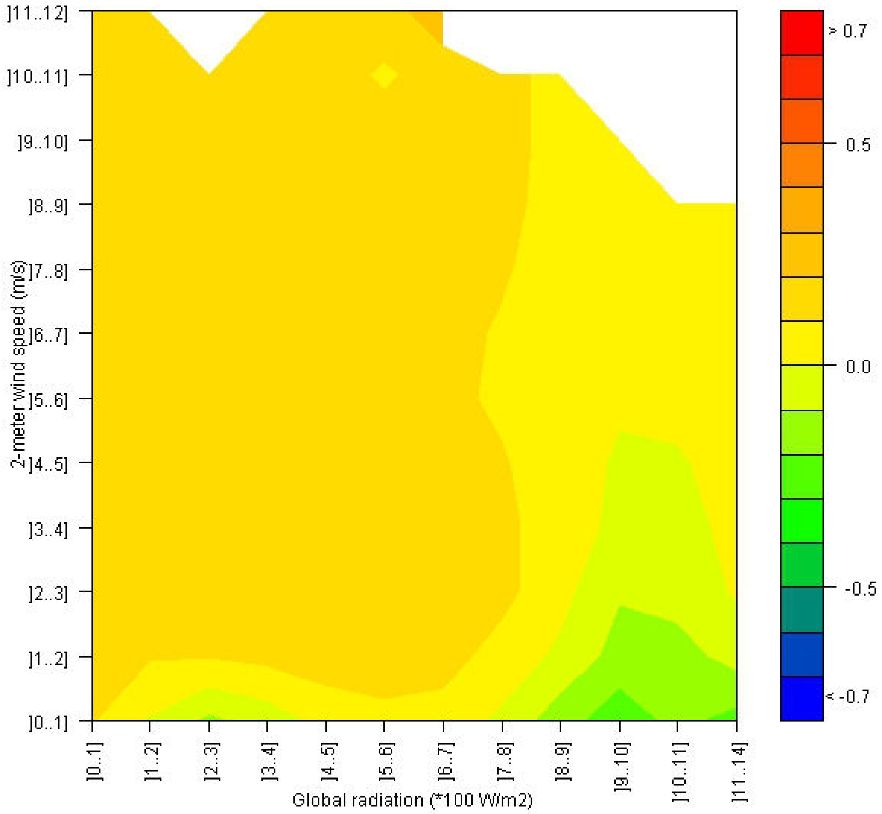


**Figure 18**

Screen #2:

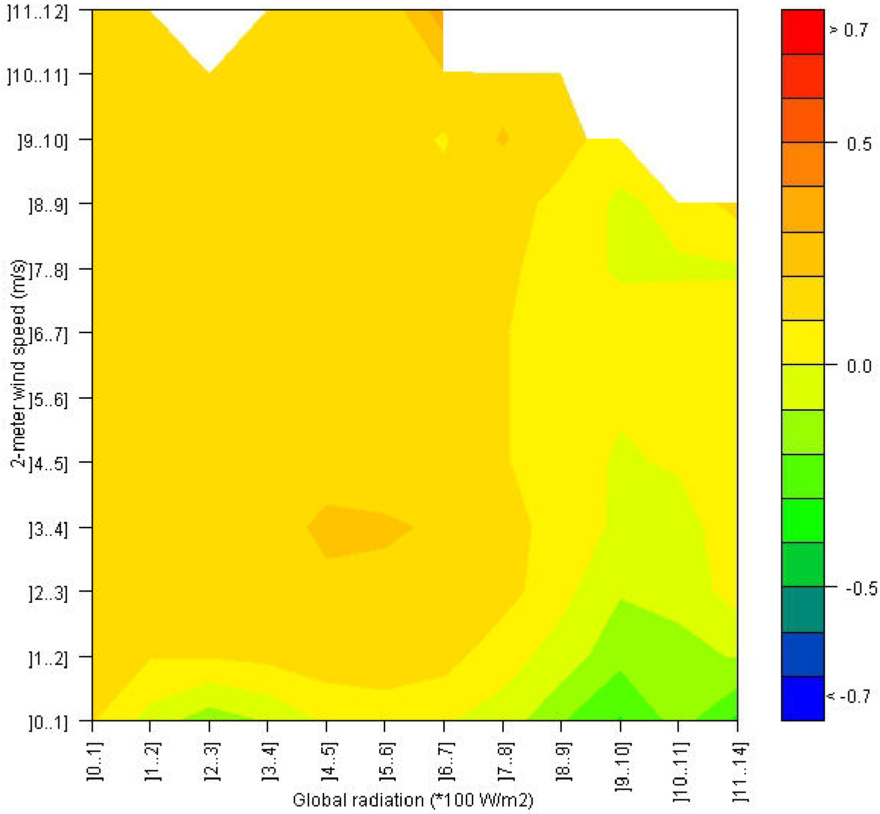


**Figure 19**

The highest absolute differences are obtained for low winds and high radiations.

## BEHAVIOUR DURING INCREASE/DECREASE OF TEMPERATURE

The distribution of differences between LLAN and the reference VEIG22 is plotted, using 1-minute quality checked data for the whole period of the intercomparison. Differences are classified according the temporal gradient of reference temperature over 1 minute. A screen faster (or slower, respectively) than the reference would be warmer (cooler) for positive gradient, cooler (warmer) for negative ones.

## Screen #1 :

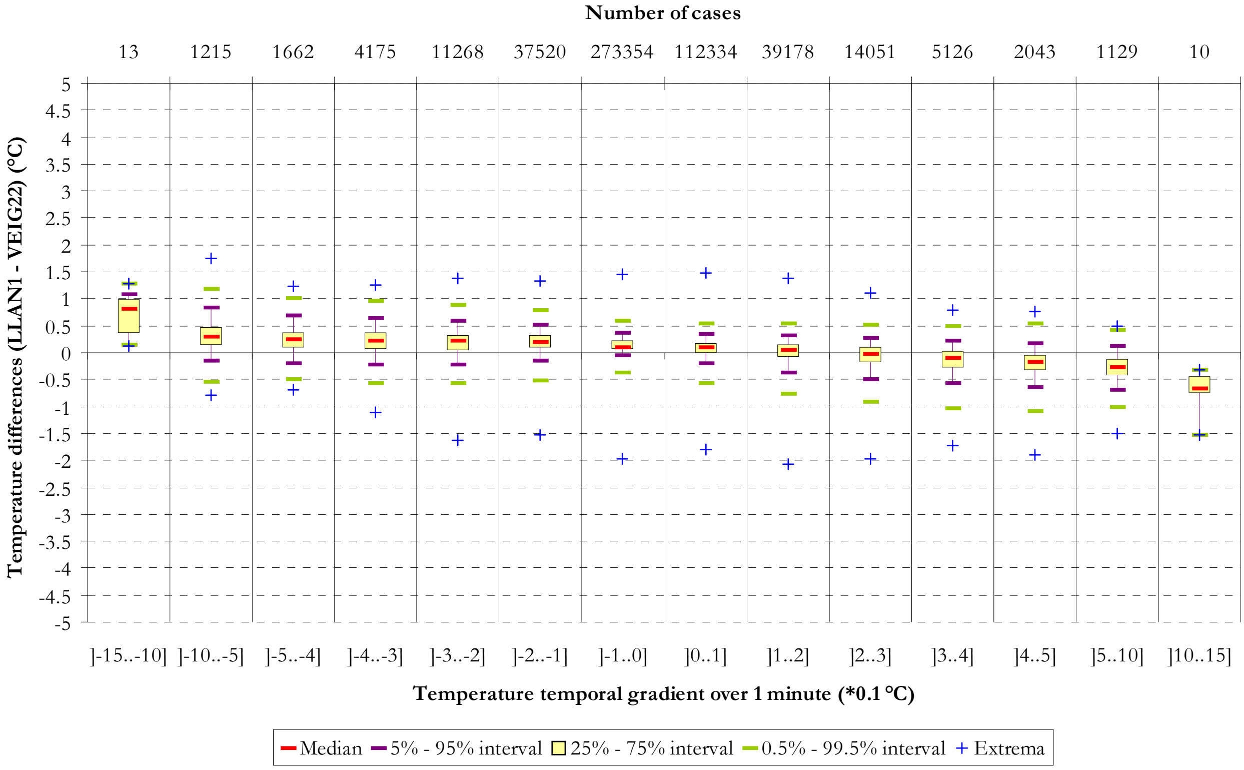


**Figure 20**

## Screen #2 :

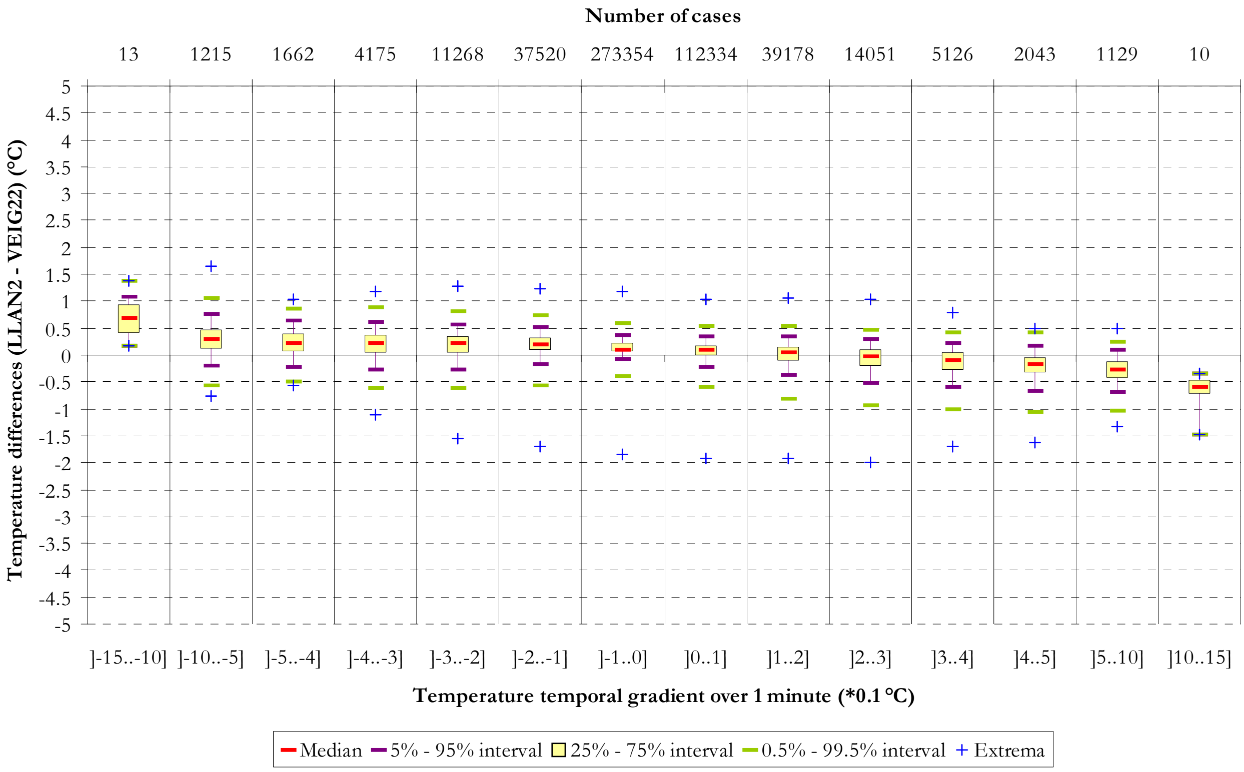


**Figure 21**

These screens are slightly slower than the reference.

## QUALITY CONTROL INFORMATION

### DATA AVAILABILITY

The intercomparison period extends from the 1st of November 2008 to the 1st of November 2009. The theoretical number of 1-minute data is 525600.

The next table sums up the total number of data for each screen and for each possible QC flag.

**Table 4**

| **QC flag** | LLAN**1** | LLAN**2** |
|---|---|---|
| 0 (good) | 503266 | 503266 |
| 1 (inconsistent) | 0 | 0 |
| 2 (doubtful) | 0 | 0 |
| 3 (erroneous) | 0 | 0 |
| 7 (missing) | 22334 | 22334 |

### MAINTENANCE

No action done during the intercomparison period.

# STEVENSON CASELLA
# – Sudan –
# LCAS

**TECHNICAL SPECIFICATIONS (PROVIDED BY THE MANUFACTURER)**

Dimensions: Length 80cm x Width 80 cm x Height 80 cm

Weight: 65 kg

Material / Structure: wood

Estimated radiation error:

Aspiration rate (in case of artificially ventilated screen/shield): naturally ventilated

Power supply: none

**Figure 1**

## OVERVIEW

The LCAS screen is globally 0.1°C warmer than the reference. The dispersion is quite low. The medians of the differences between this screen and the reference for Tn, T and Tx are around 0.2°C, 0.1°C and 0°C respectively.

There is no influence of the global radiation. Most of the differences (5-95% interval) are within -0.6 and +0.6°C for all classes of global radiation. The medians are stable around 0.1°C.

There is no clear difference between night and day, except for calm winds: LCAS screen is 0.2°C warmer during night for calm wind conditions, whereas it is close to the reference during daytime. For winds above 1m/s, LCAS is 0.1°C warmer than the reference during day or night conditions.

During daytime, for winds above 2m/s, LCAS screen is warmer than the reference. Medians of the differences are slightly greater for clear sky conditions than for overcast conditions. When the wind is less than 2m/s, it is the contrary: medians of differences for clear sky are less than for overcast conditions. LCAS screen is even colder than the reference for clear sky conditions and calm winds. During night time, clear sky and overcast conditions give similar results, with the exception of winds above 7m/s where the number of data is too low. For winds between 1 and 7m/s, LCAS is warmer than the reference by 0.1°C. For calm winds, it is warmer by 0.2°C.

Differences are mainly positive for negative temperature gradients, and slightly negative for positive gradients: this shows a slight delay when temperature increases and a more sensitive delay when temperature decreases, maybe due to the thermal inertia of this screen (quite large dimensions, in wood).

## CALIBRATION INFORMATION

The calibration of the probe was performed in Trappes.

**Table 1**

| Screen | Location | Pt100 probe serial number | Calibration date | Instrument bias (°C) | | | |
|---|---|---|---|---|---|---|---|
| | | | | -20°C | 0°C | 20°C | 40°C |
| LCAS | A1 | T77 | 24-Jan-2006 | 0.0146 | 0.0175 | 0.0411 | 0.0632 |

The result of calibration of reference VEIG22 is available in the main report of the intercomparison, section 5.4.1.

## COMPARISON WITH THE REFERENCE

### HISTOGRAM OF DIFFERENCES

The histogram of differences between LCAS and the reference VEIG22 is plotted, using 1-minute quality checked data for the whole period of the intercomparison. Differences are plotted by steps of 0.1K. The vertical axis is the frequency in percent for each class of differences.

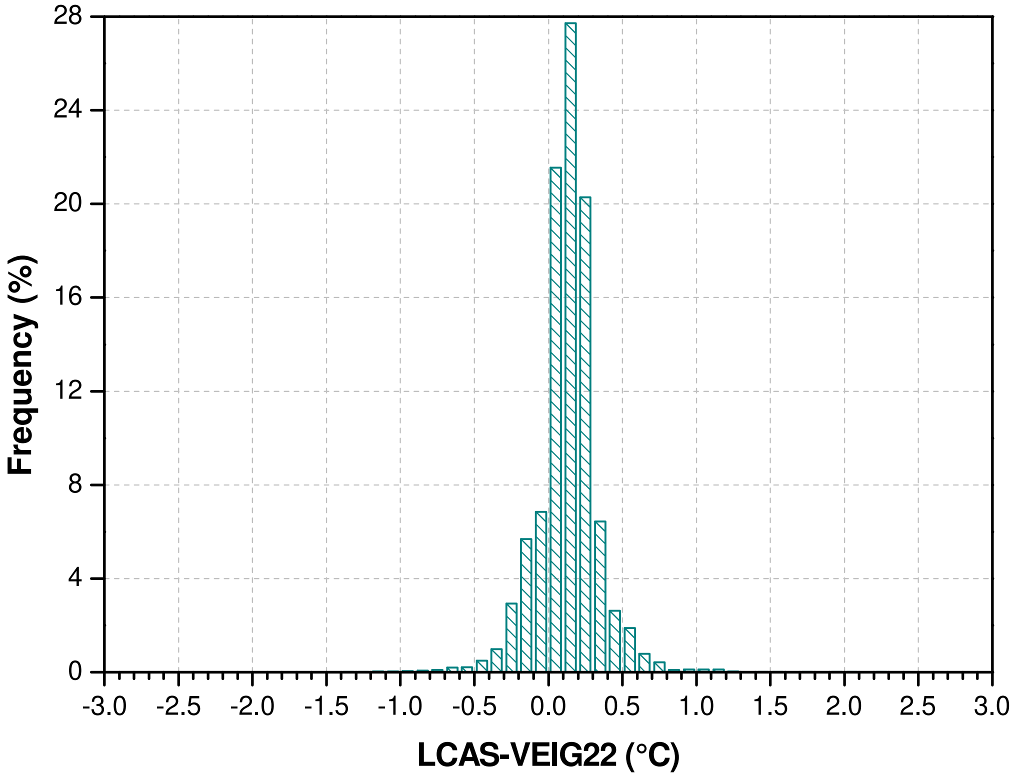


**Figure 2**

This screen is slightly warmer than the reference. The dispersion is quite low.

CUMULATIVE HISTOGRAMS OF DIFFERENCES OF DAILY EXTREME VALUES

The cumulative histograms of differences with the reference VEIG22 of T (1-minute quality checked data), Tn (daily minimum temperature) and Tx (daily maximum temperature) are plotted, for the whole period of the intercomparison. Differences are plotted by steps of 0.1K.

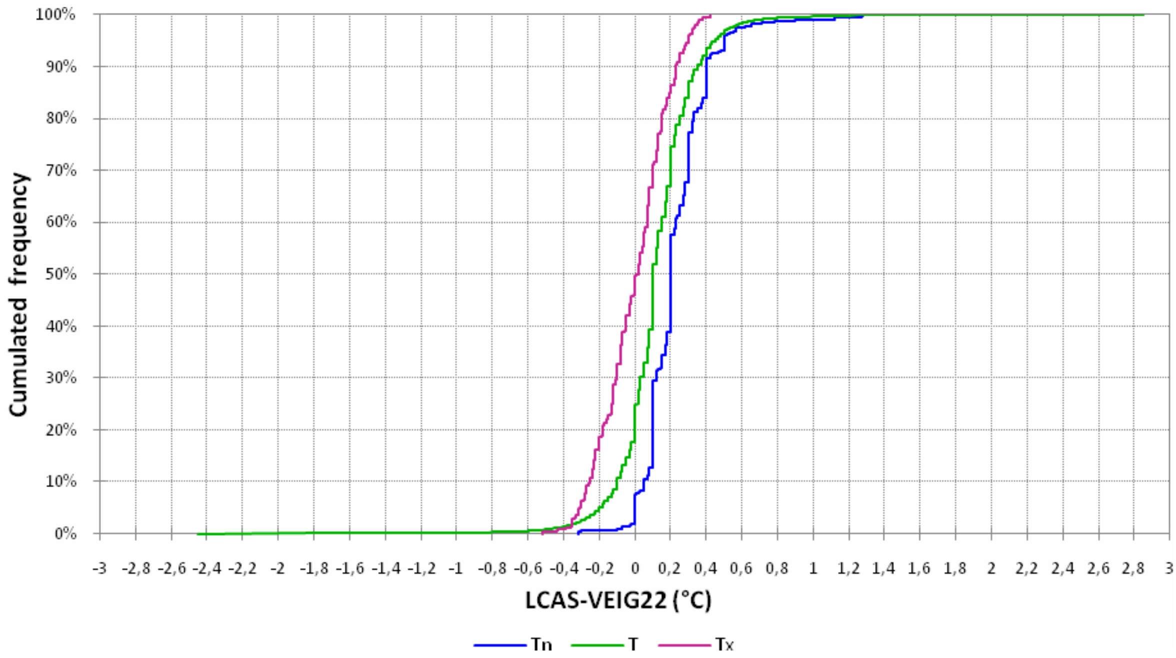


**Figure 3**

The medians of the differences between this screen and the reference for Tn, T and Tx are around 0.2°C, 0.1°C and 0°C respectively.

TABLE

The table 2 indicates the percentage of data that differ by less than 0.2°C (and 0.5°C) from the reference.

**Table 2**

| | | [-0.2°..0.2°] | [-0.5°..0.5°] |
|---|---|---|---|
| LCAS | T | 70.5 | 96.2 |
| | Tn | 53.7 | 96.0 |
| | Tx | 68.4 | 99.7 |

## INFLUENCE OF GLOBAL RADIATION

The distribution of differences between LCAS and the reference VEIG22 is plotted, using 1-minute quality checked data for the whole period of the intercomparison. Differences are classified according global radiation.

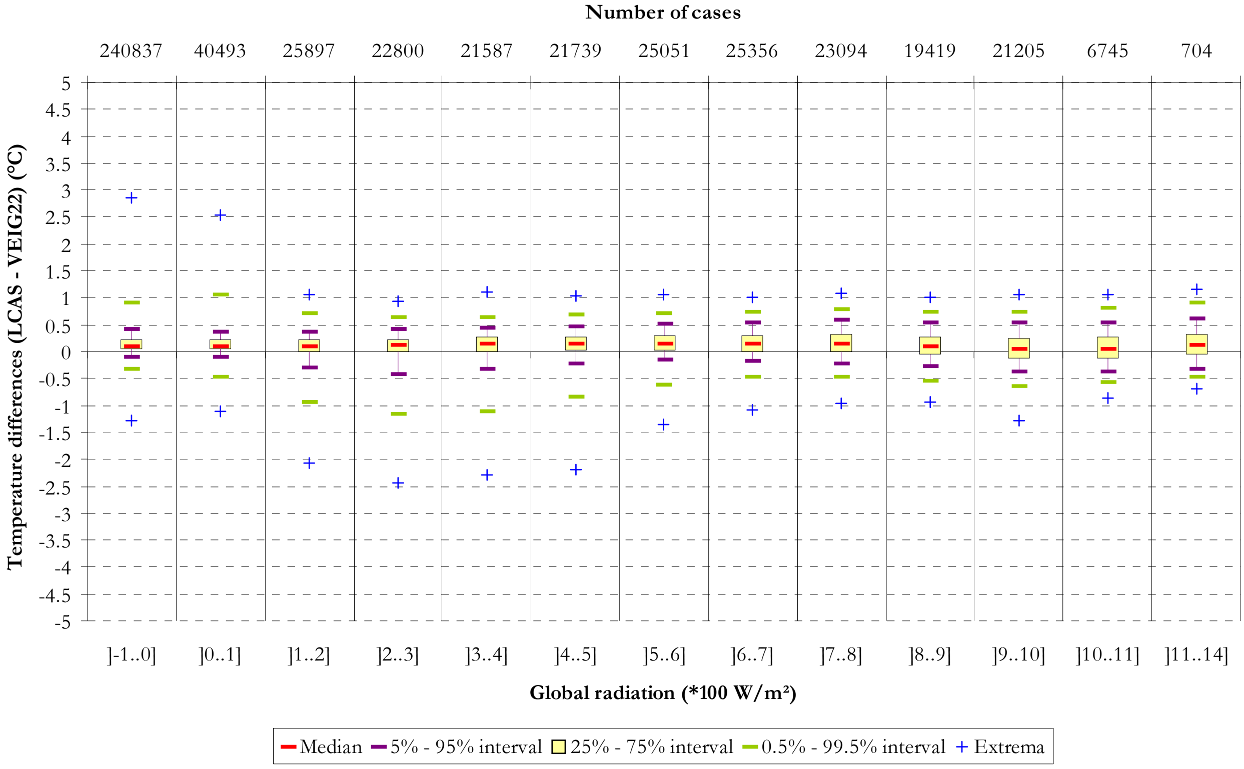


**Figure 4**

There is no influence of the global radiation on the differences with the reference. Most of the differences (5-95% interval) are within –0.6 and +0.6°C for all classes of global radiation. The medians are stable around 0.1°C.

## RADIATION EFFECT

### DIFFERENCES BETWEEN DAY AND NIGHT BEHAVIOUR

The median of differences between LCAS and VEIG22 is plotted, using 1-minute quality checked data for the whole period of the intercomparison. We filter data for which sun elevation is above -1° (day) or below -1° (night). Differences are classified according 2-meter wind speed (2-minute average).

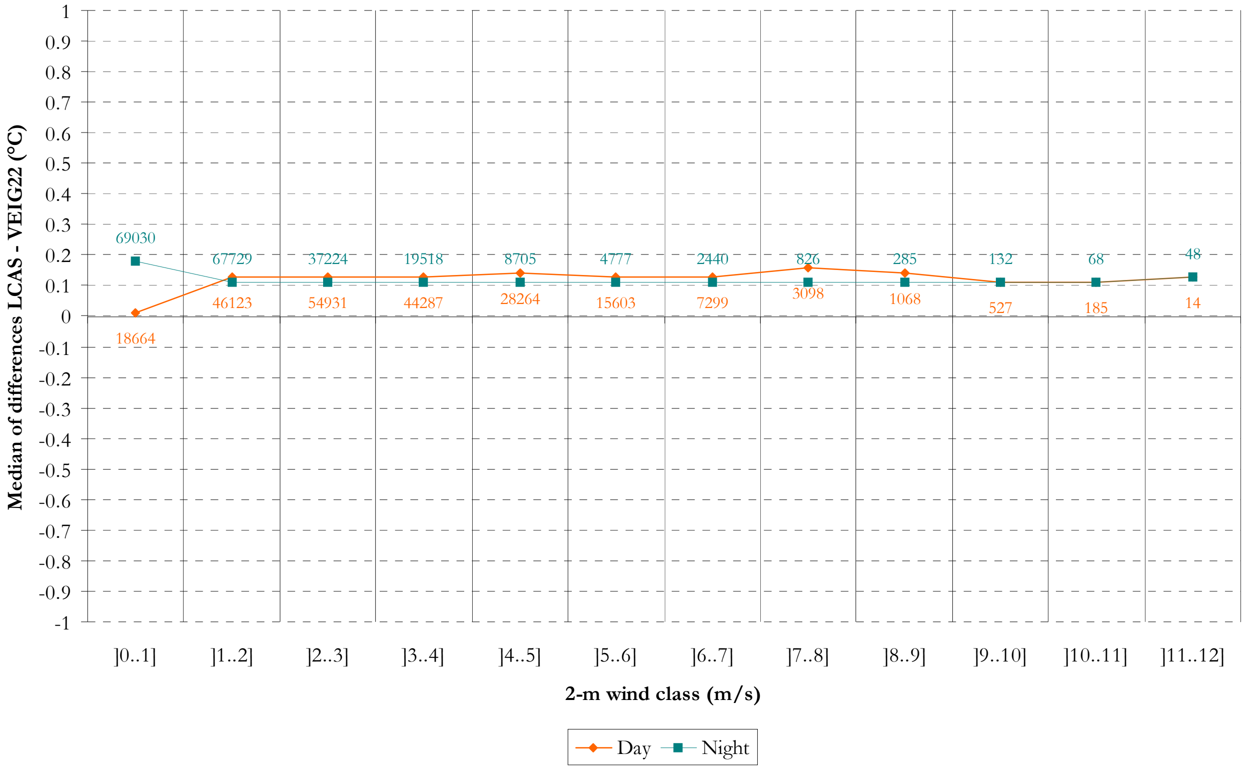


**Figure 5**

There is no clear difference between night and day, except for calm winds: LCAS screen is 0.2°C warmer during night for calm wind conditions, whereas it is close to the reference during daytime. For winds above 1m/s, LCAS is 0.1°C warmer than the reference during day or night conditions.

DIFFERENCES BETWEEN CLEAR SKY AND OVERCAST SKY DURING DAYTIME

The median of differences between LCAS and VEIG22 is plotted, using 1-minute quality checked data. Here, we consider periods lasting six hours at least where cloudiness is less or equal to 1 (clear sky) or more or equal to 7 (overcast sky), during daytime (sun elevation above -1°). Differences are classified according 2-meter wind speed (2-minute average).

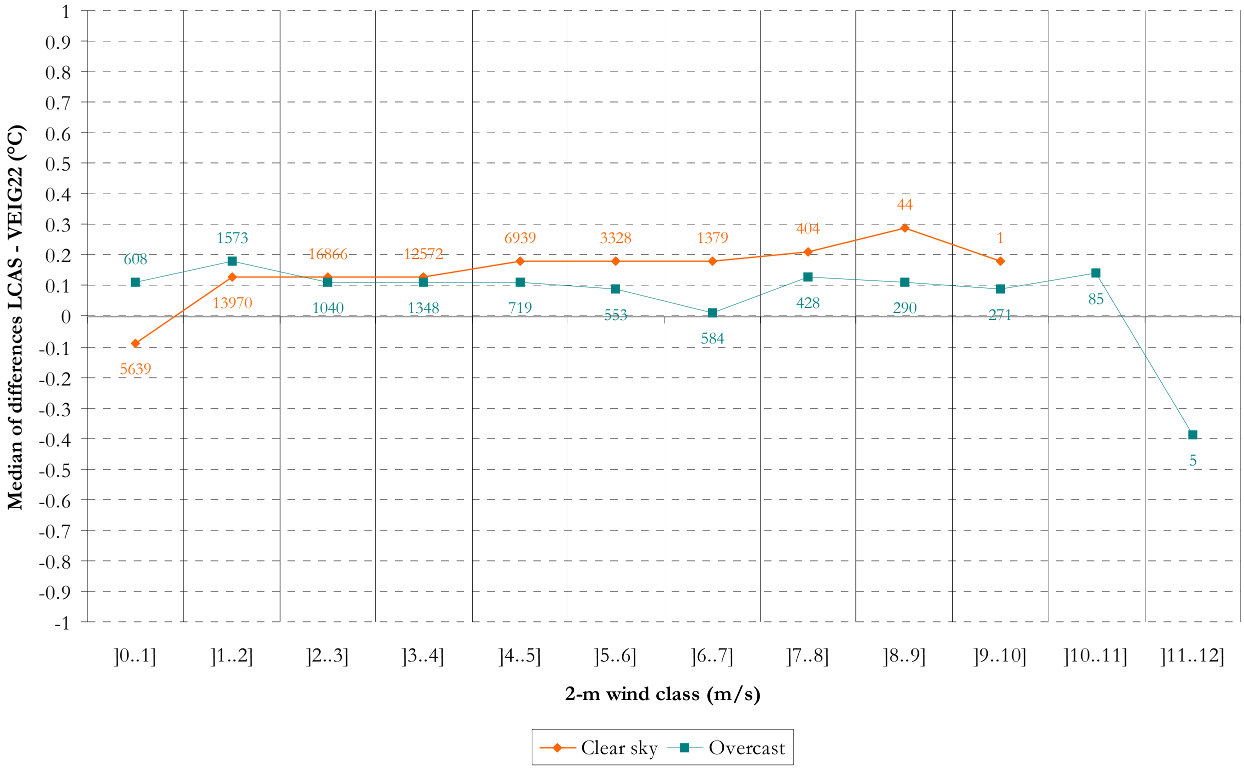


**Figure 6**

During daytime, for winds above 2m/s, LCAS screen is warmer than the reference. Medians of the differences are slightly greater for clear sky conditions than for overcast conditions. When the wind is less than 2m/s, it is the contrary: medians of differences for clear sky are less than for overcast conditions. LCAS screen is even colder than the reference for clear sky conditions and calm winds. These conditions often occurs in the morning, after sunrise. The figure 7 shows time evolution of LCAS temperature and the reference on the 27th of November, 2008 (top chart). The chart in the middle is the global radiation, and in the bottom is the 2-meter wind speed (2-minute average). Between 7:00 and 9:00, LCAS is colder than the reference. The wind is calm. After 9:00 the wind speed increases, LCAS is close to the reference.

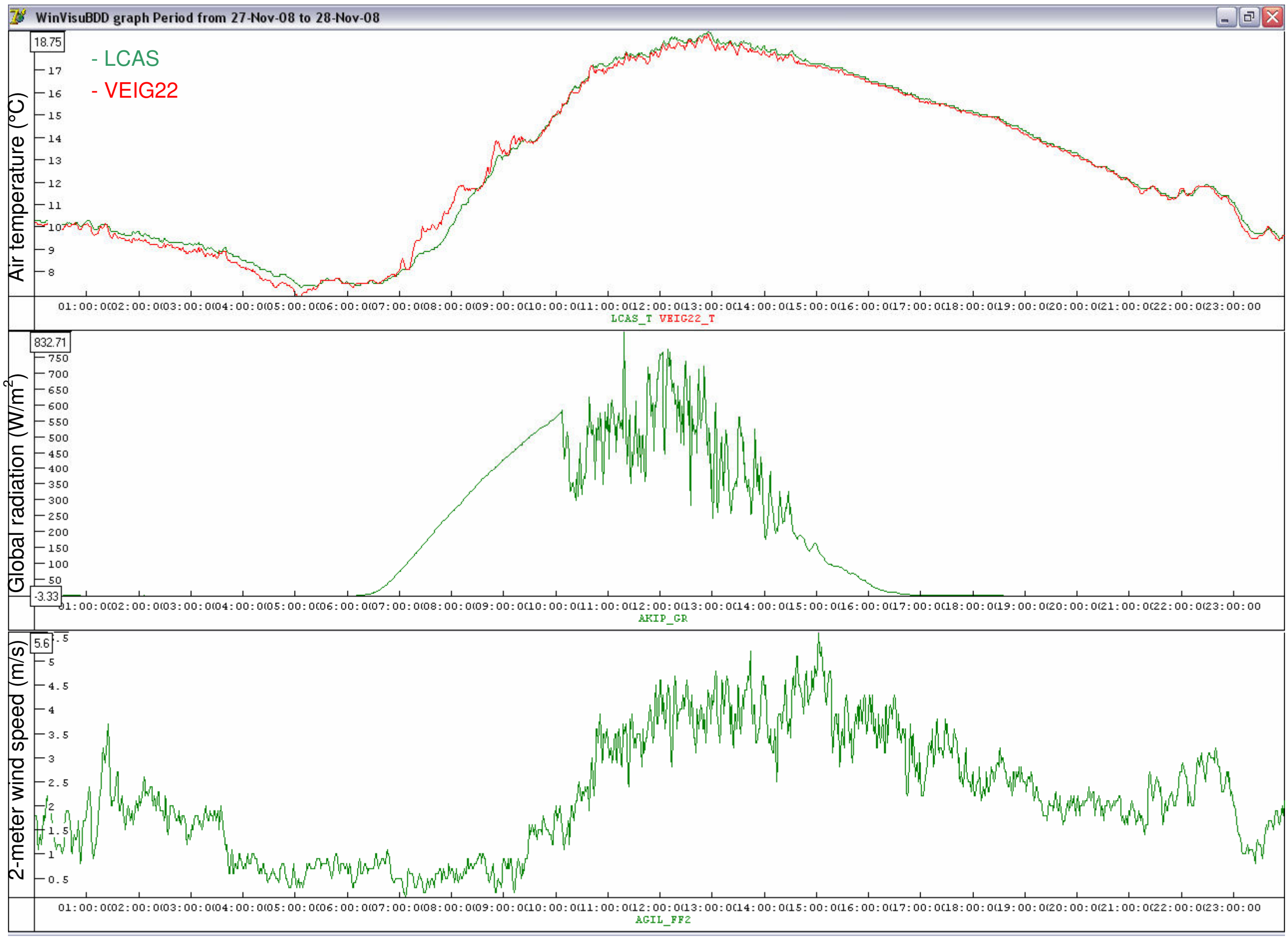


**Figure 7**

DIFFERENCES BETWEEN CLEAR SKY AND OVERCAST SKY DURING NIGHT TIME

The median of differences between LCAS and VEIG22 is plotted, using 1-minute quality checked data. Here, we consider periods lasting six hours at least where cloudiness is less or equal to 1 (clear sky) or more or equal to 7 (overcast sky), during night time (sun elevation below -1°). Differences are classified according 2-meter wind speed (2-minute average).

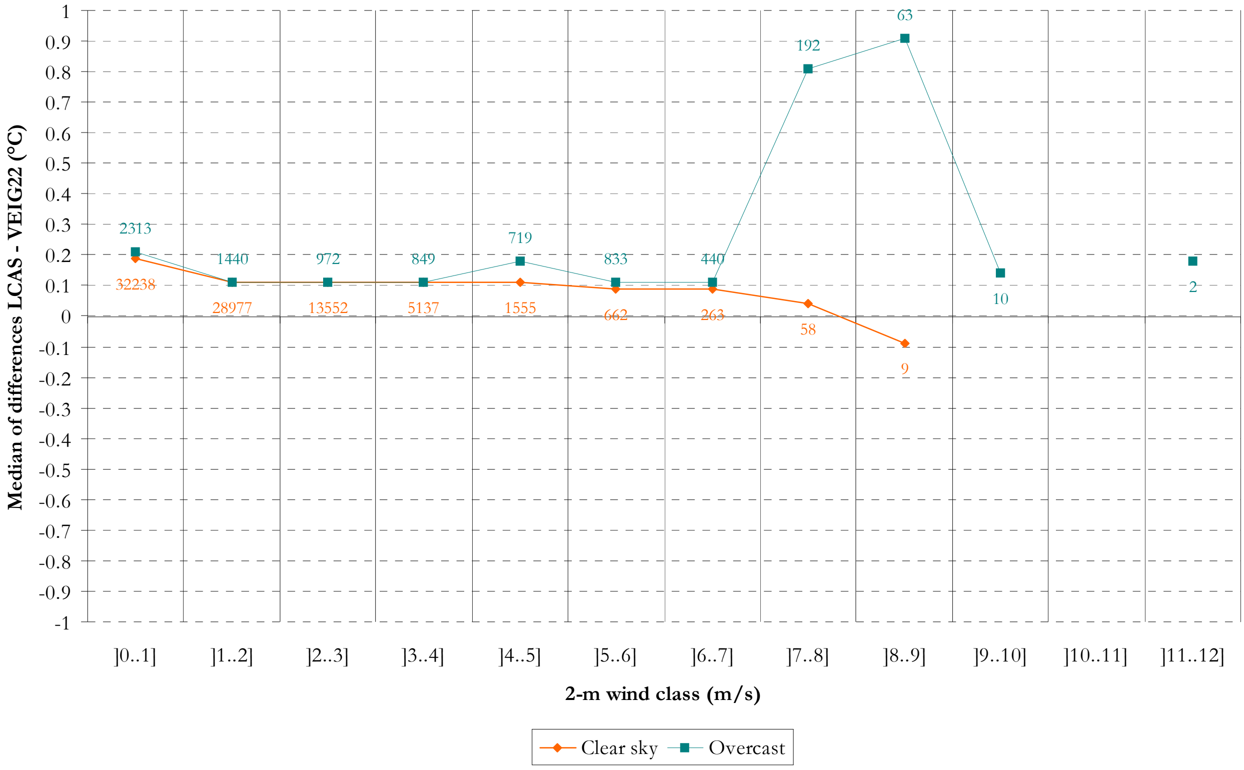


**Figure 8**

During night time, clear sky and overcast conditions give similar results, with the exception of winds above 7m/s where the number of data is too low. For winds between 1 and 7m/s, LCAS is warmer than the reference by 0.1°C. For calm winds, it is warmer by 0.2°C.

## EFFECT OF SUN ELEVATION

The median of differences between LCAS and VEIG22 is plotted, using 1-minute quality checked data. Here, we consider periods lasting six hours at least where cloudiness is less or equal to 1 (clear sky), during daytime (sun elevation above -1°). We filter data where sun elevation is low (below 10°), medium (between 10° and 45°) or high (above 45°). Differences are classified according 2-meter wind speed (2-minute average).

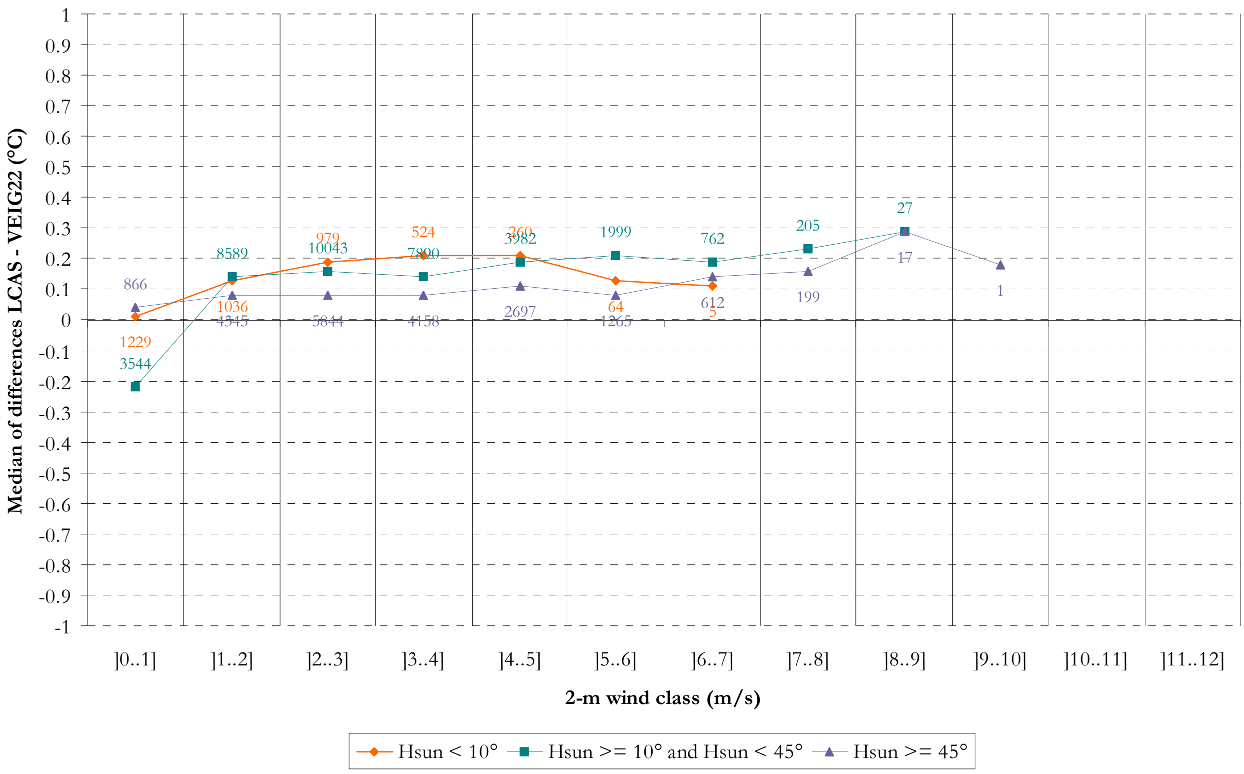


**Figure 9**

The three curves are very close one to another: for winds above 1m/s, LCAS screen is warmer by 0.1 to 0.2°C than the reference. For calm winds, it is close to the reference for high and low sun elevations. For medium values of sun elevation, LCAS is 0.2°C colder than the reference.

## COMBINED EFFECT OF WIND AND GLOBAL RADIATION

The medians of differences between LCAS and VEIG22 are represented here with a contour plot. The global radiation values are on the X-axis and on the Y axis is the 2-meter wind speed value (2-minute average). Medians are used in all cases, providing that at least one data is available for both conditions on radiation and wind considered.

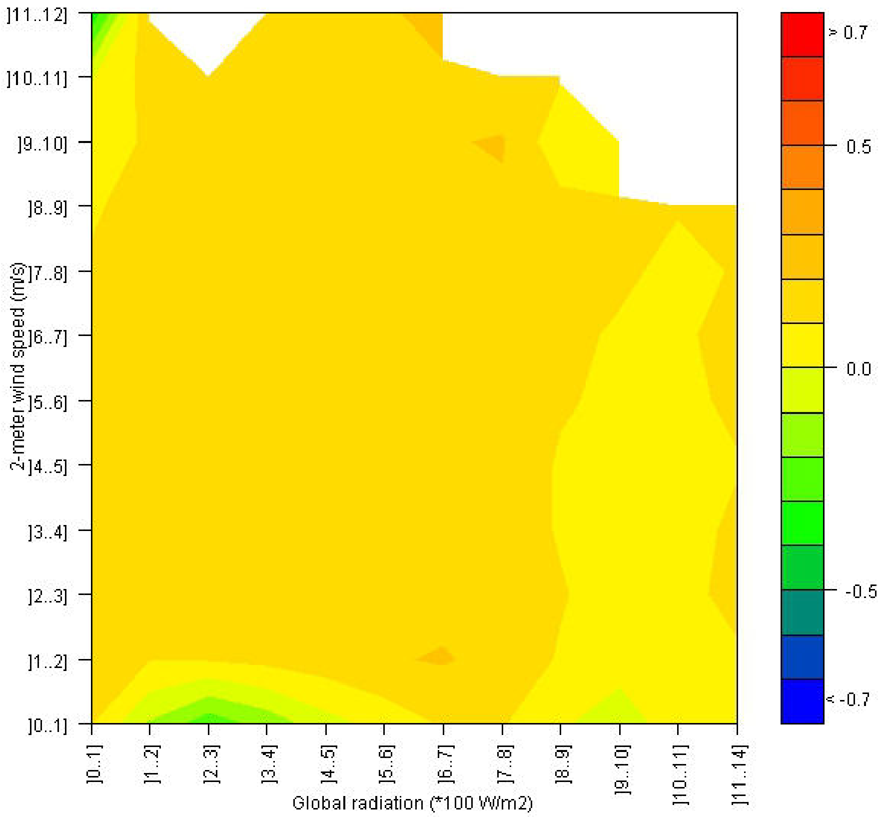


**Figure 10**

This plot shows LCAS screen is globally 0.1°C warmer than the reference. Specific behaviour for calm winds is visible: for global radiation values between 100 and 400 w/m$^2$, LCAS is colder than the reference.

## BEHAVIOUR DURING INCREASE/DECREASE OF TEMPERATURE

The distribution of differences between LCAS and the reference VEIG22 is plotted, using 1-minute quality checked data for the whole period of the intercomparison. Differences are classified according the temporal gradient of reference temperature over 1 minute. A screen faster (or slower, respectively) than the reference would be warmer (cooler) for positive gradient, cooler (warmer) for negative ones.

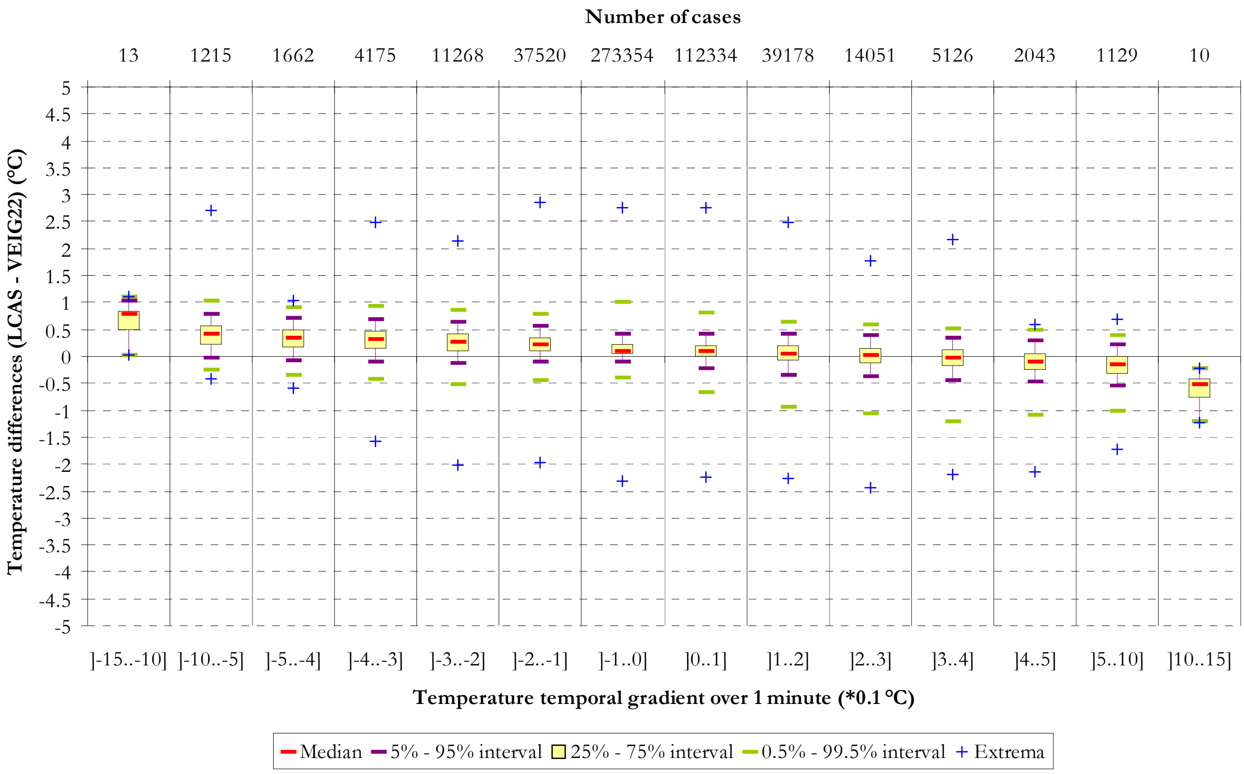


**Figure 11**

Differences are mainly positive for negative temperature gradients, and slightly negative for positive gradients: this shows a slight delay when temperature increases and a more sensitive delay when temperature decreases, maybe due to the thermal inertia of this screen (quite large dimensions, in wood).

## QUALITY CONTROL INFORMATION

### DATA AVAILABILITY

The intercomparison period extends from the 1st of November 2008 to the 1st of November 2009. The theoretical number of 1-minute data is 525600.

The next table sums up the total number of data for each possible QC flag.

**Table 3**

| **QC flag** | LCAS |
|---|---|
| 0 (good) | 503266 |
| 1 (inconsistent) | 0 |
| 2 (doubtful) | 0 |
| 3 (erroneous) | 0 |
| 7 (missing) | 22334 |

### MAINTENANCE

No action done during the intercomparison period.

# BM0 1195D0000 SOCRIMA
# – France –
# SSOC

## TECHNICAL SPECIFICATIONS (PROVIDED BY THE MANUFACTURER)

Dimensions: Length 20 cm x Width 20 cm x Height 50 cm

Weight: 2.5 kg

Material / Structure: ABS plastic, UV stabilized – Stainless Steel

Estimated radiation error: for 1000 W/$^2$ : 0.7 °C for wind < 1 m/s, 0.3 °C for wind > 5 m/s

Aspiration rate (in case of artificially ventilated screen/shield): naturally ventilated

Power supply: none

**Figure 1**

## OVERVIEW

Both screens give very close results. Screen #2 is about 0.1° warmer than screen #1. The differences between both screens do not depend on temperature.

Both screens are warmer than the reference, in more than 85% of the cases for screen #1, 95% for screen #2. Differences on daily maximum temperatures are larger than differences on daily minimum temperatures or differences on 1-minute values. Screen #2 has larger differences on maximum temperatures than screen #1.

These screens are slightly dependant on global radiation: when there is no radiation or low radiation (less than 100 /$m^2$), differences with the reference are close to 0. For higher values, differences are higher, around 0.4° for screen #1, 0.5° for screen #2. They are stable when radiation increases.

For both screens, differences are much higher during daytime than during night time. During daytime ,they reach the highest values for wind speeds between 1 and 4 m/s. In clear sky conditions, Socrima screens are around 0.1° warmer than in overcast conditions. Differences between these conditions are even higher for wind speeds between 1 and 5 m/s.

During night time, the cloudiness does not make a difference. Socrima screens may be slightly warmer in overcast conditions, for wind speeds around 4 to 5 m/s.

Differences for low sun elevation values are lower than for higher values.

Larger differences are obtained for low wind speeds and medium global radiation.

## CALIBRATION INFORMATION

The calibration of both probes was performed in Trappes.

**Table 1**

| Screen | Location | Pt100 probe serial number | Calibration date | Instrument bias (°C) | | | |
|---|---|---|---|---|---|---|---|
| | | | | -20°C | 0°C | 20°C | 40°C |
| SSOC1 | E3 | T44 | 30-Jan-2006 | 0.0160 | -0.0124 | -0.0319 | -0.0473 |
| SSOC2 | E6 | T45 | 9-Feb-2006 | 0.0337 | 0.0072 | -0.0113 | -0.0267 |

The result of calibration of reference VEIG22 is available in the main report of the intercomparison, section 5.4.1.

## COMPARISON OF BOTH SENSORS

The distribution of differences between screen 1 and screen 2 is plotted, using 1-minute quality checked data for the whole period of the intercomparison. Differences are classified according screen 1 temperature.

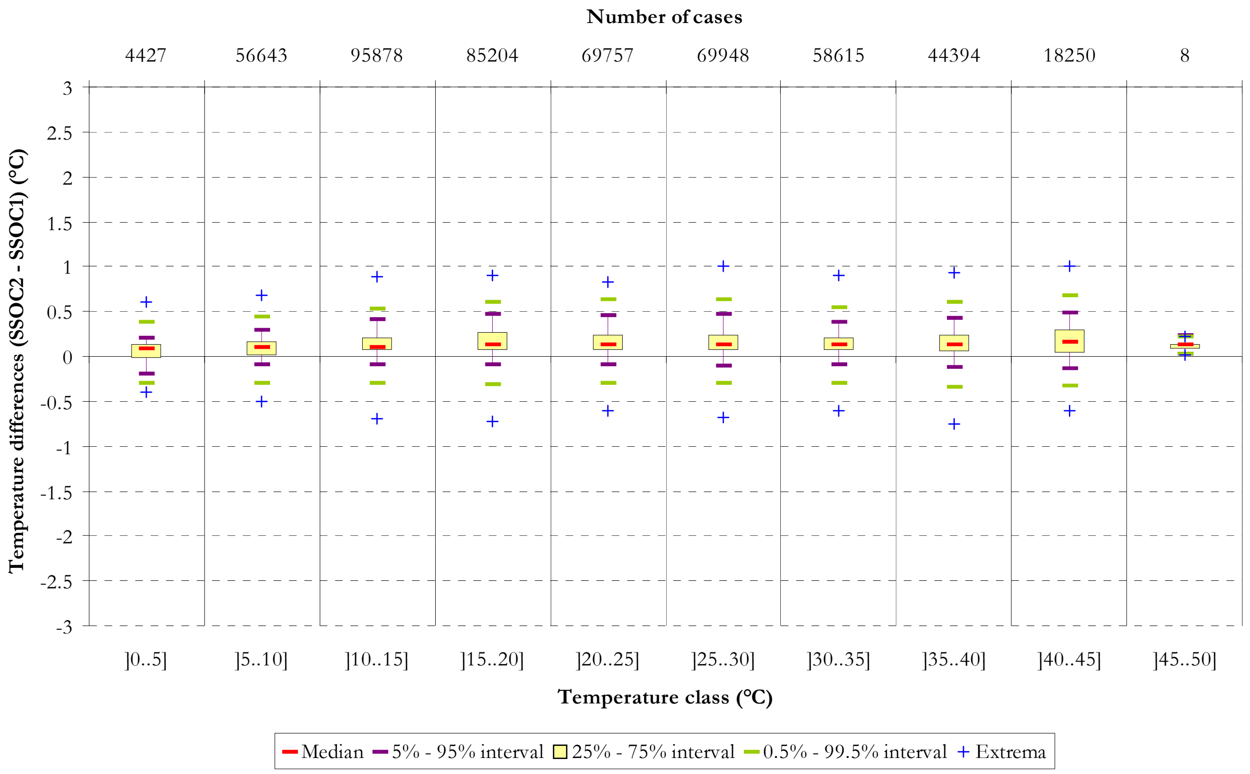


**Figure 2**

Both screens give very close results. Screen #2 is about 0.1° warmer than screen #1. The differences between both screens do not depend on temperature.

## COMPARISON WITH THE REFERENCE

### HISTOGRAM OF DIFFERENCES

The histogram of differences between SSOC and the reference VEIG22 is plotted, using 1-minute quality checked data for the whole period of the intercomparison. Differences are plotted by steps of 0.1K. The vertical axis is the frequency in percent for each class of differences.

Screen #1:

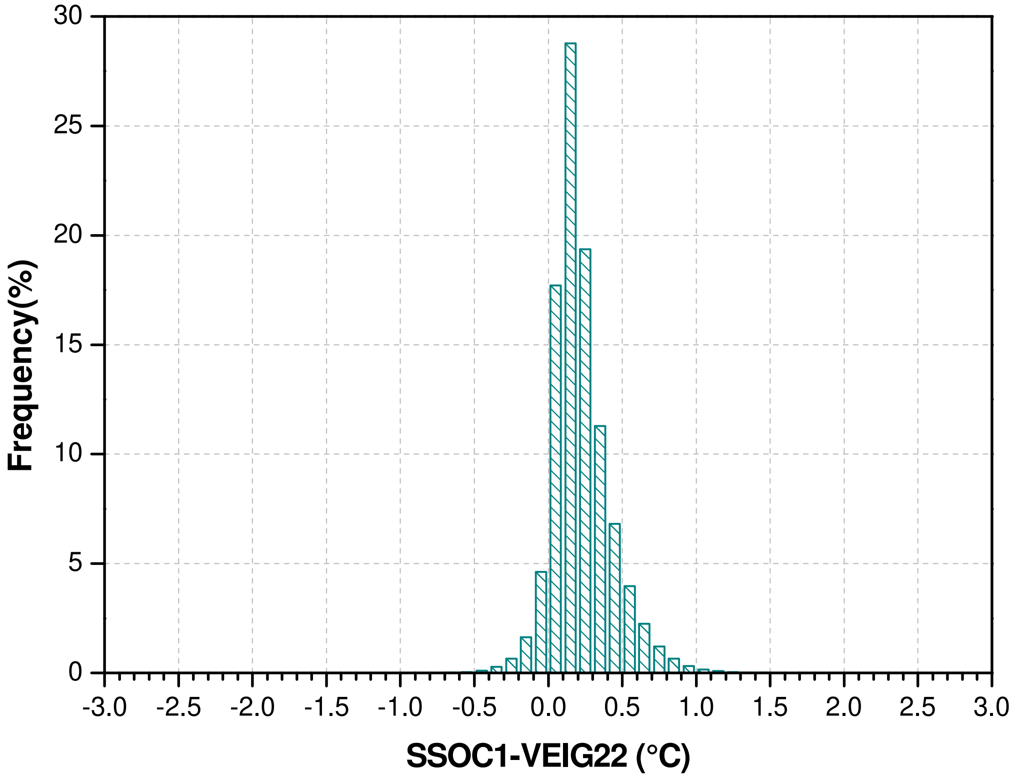


**Figure 3**

Screen #2:

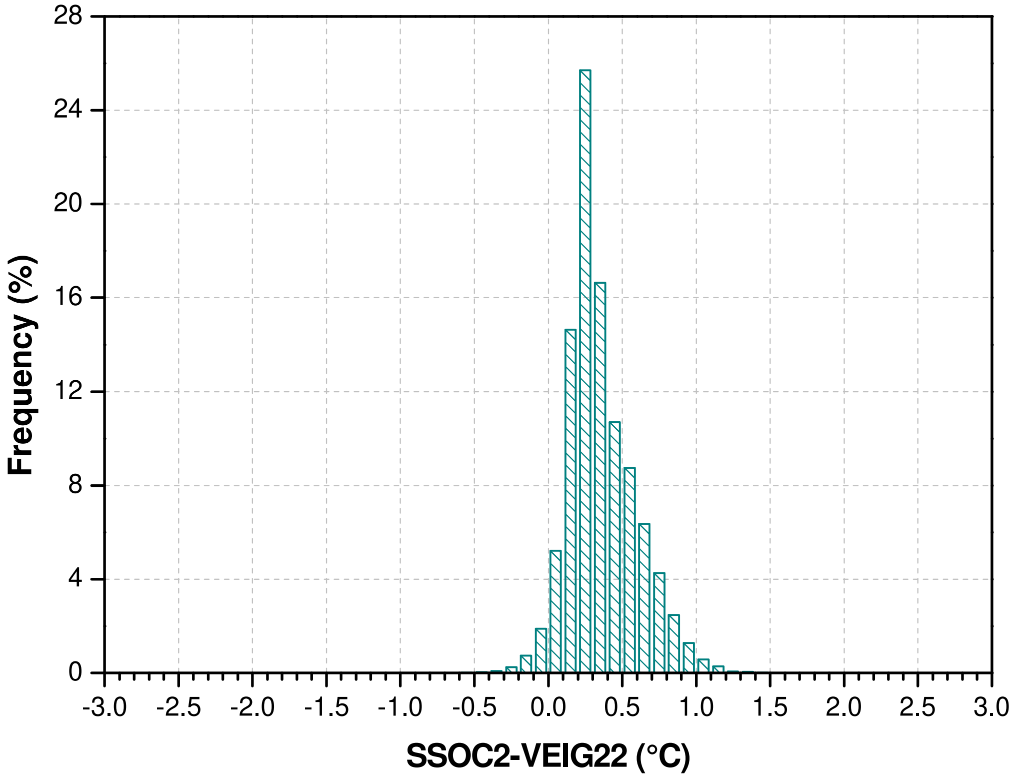


**Figure 4**

CUMULATIVE HISTOGRAMS OF DIFFERENCES OF DAILY EXTREME VALUES

The cumulative histograms of differences with the reference VEIG22 of T (1-minute quality checked data), Tn (daily minimum temperature) and Tx (daily maximum temperature) are plotted, for the whole period of the intercomparison. Differences are plotted by steps of 0.1K.

Screen #1:

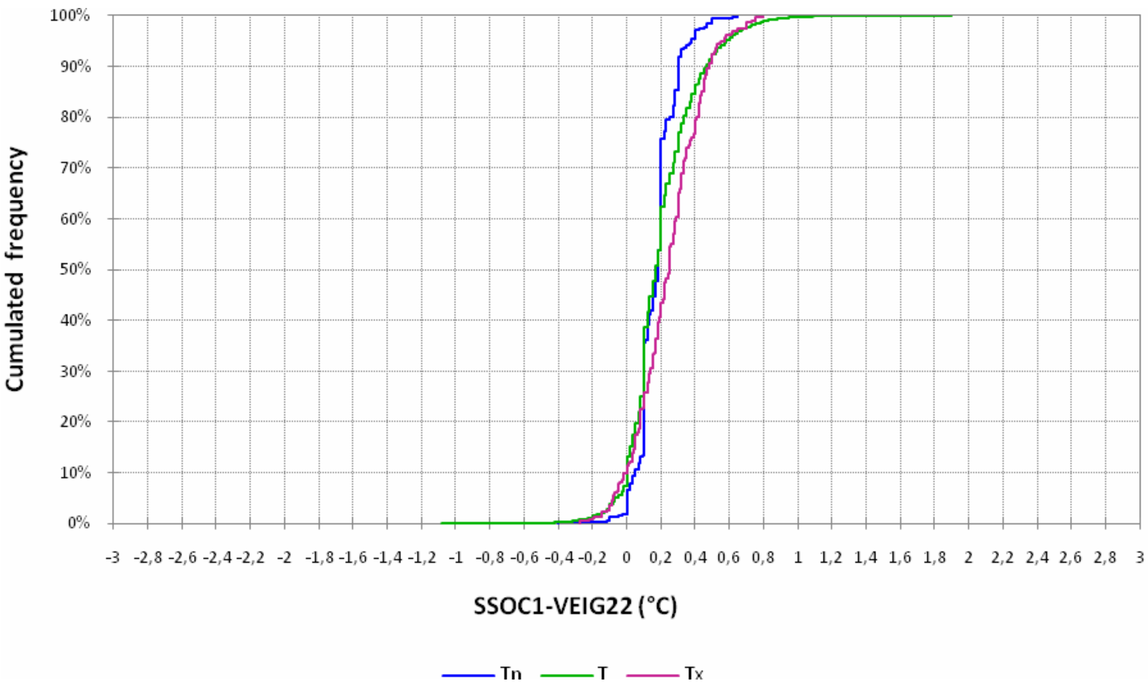


**Figure 5**

Screen #2:

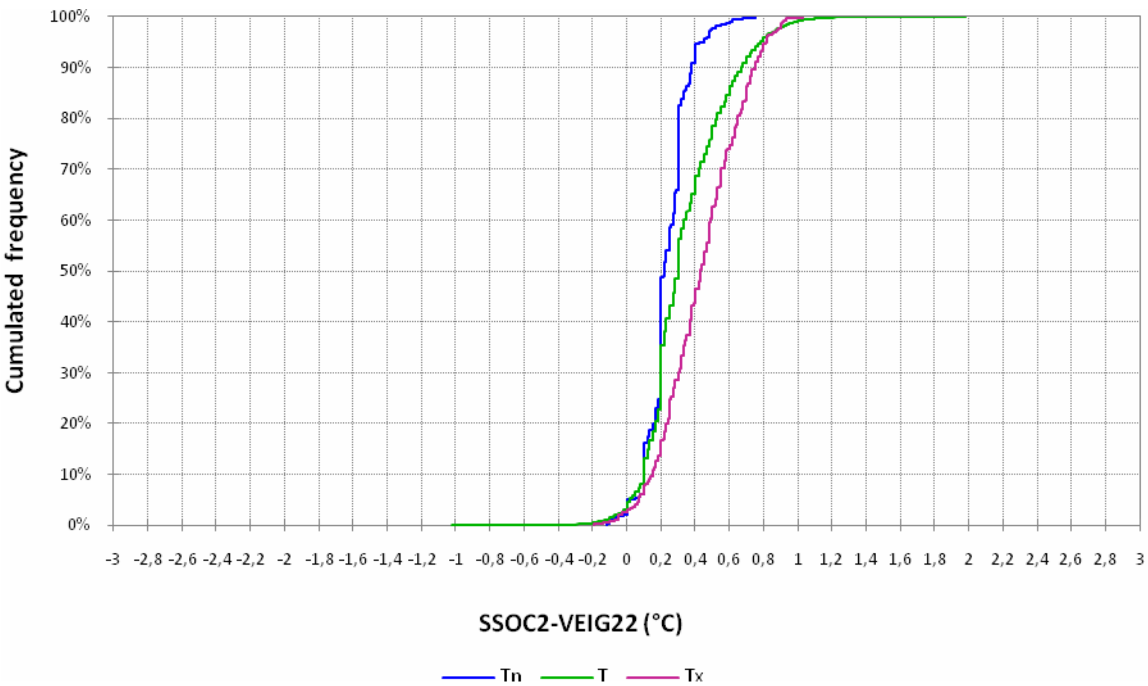


**Figure 6**

Both screens are warmer than the reference, in more than 85% of the cases for screen #1, 95% for screen #2. Differences on daily maximum temperatures are larger than differences on daily minimum temperatures or differences on 1-minute values. Screen #2 has larger differences on maximum temperatures than screen #1.

TABLE

The table 2 indicates the percentage of data that differ by less than 0.2°C (and 0.5°C) from the reference.

**Table 2**

| | | [-0.2°..0.2°] | [-0.5°..0.5°] |
|---|---|---|---|
| SSOC1 | T | 61.2 | 92.3 |
| | Tn | 71.4 | 99.4 |
| | Tx | 41.6 | 92.5 |
| SSOC2 | T | 35.0 | 78.4 |
| | Tn | 42.9 | 97.8 |
| | Tx | 15.2 | 62.6 |

## INFLUENCE OF GLOBAL RADIATION

The distribution of differences between SSOC and the reference VEIG22 is plotted, using 1-minute quality checked data for the whole period of the intercomparison. Differences are classified according global radiation.

Screen #1:

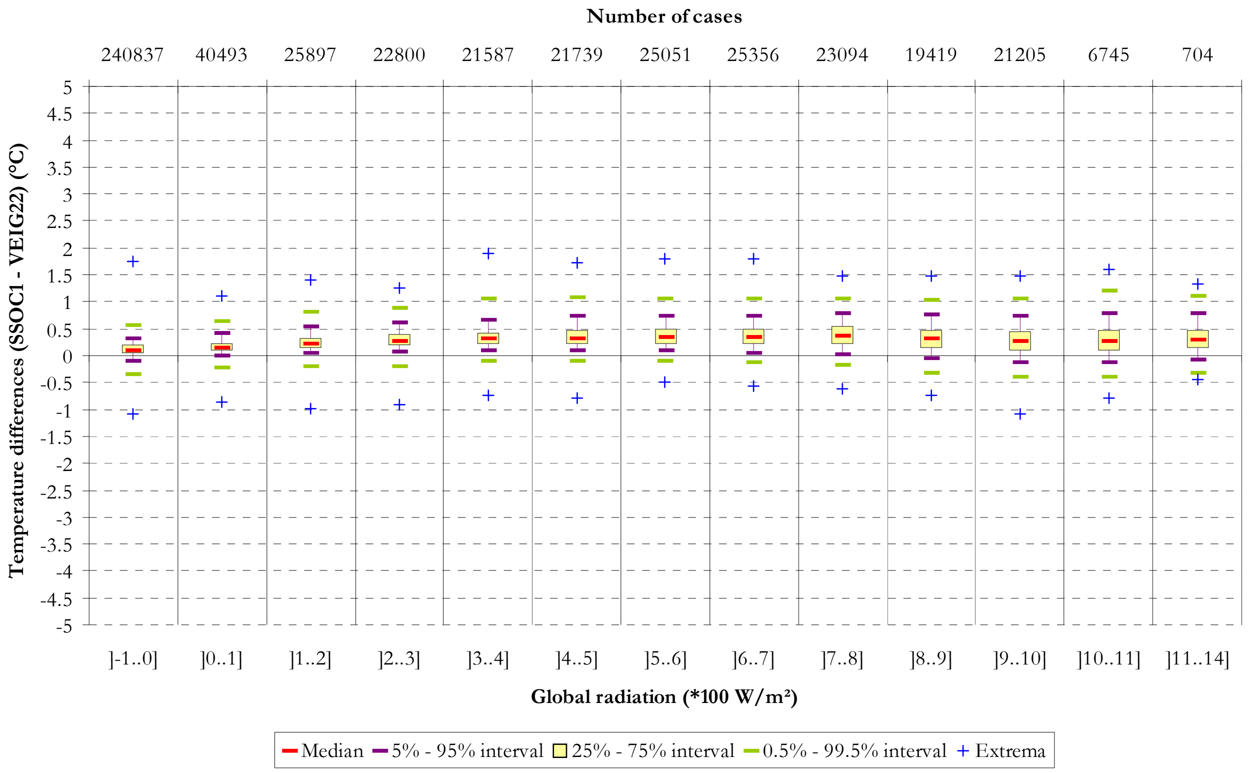


**Figure 7**

Screen #2:

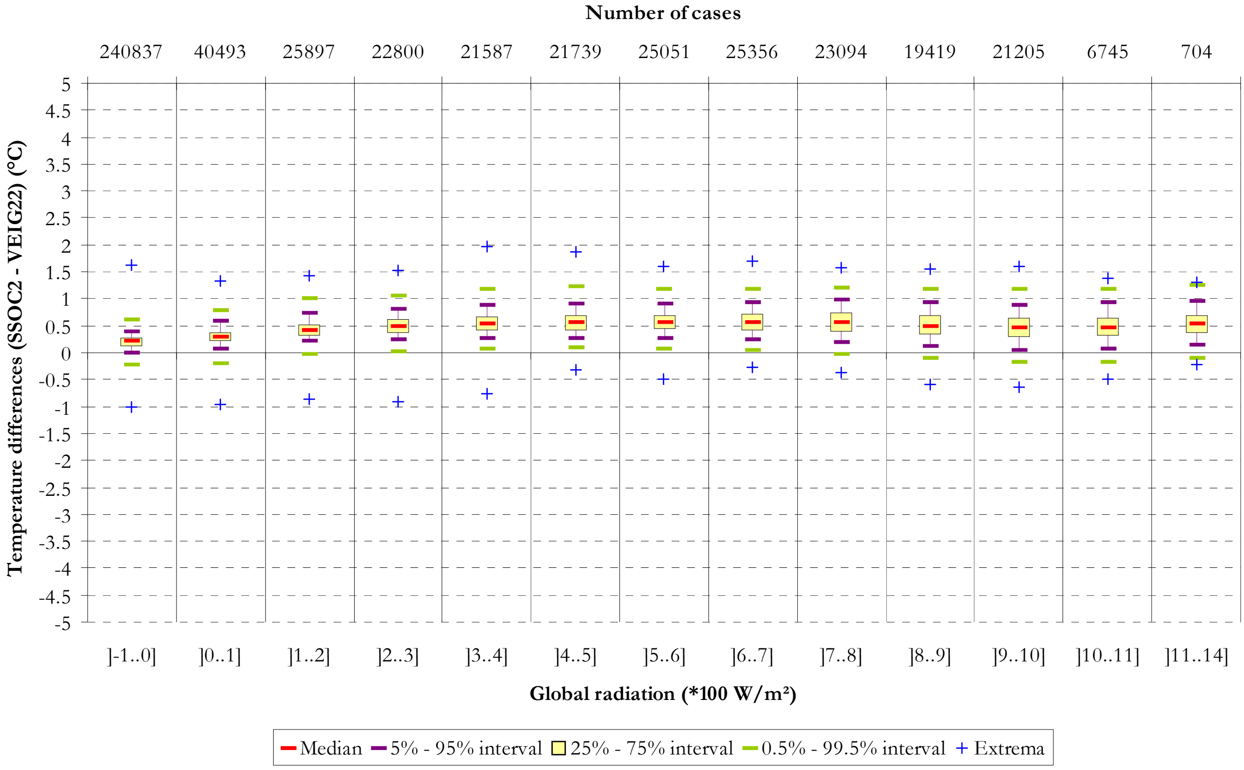


**Figure 8**

These screens are slightly dependant on global radiation: when there is no radiation or low radiation (less than 100 /m$^2$), differences with the reference are close to 0. For higher values, differences are higher, around 0.4° for screen #1, 0.5° for screen #2. They are stable when radiation increases.

## RADIATION EFFECT

### DIFFERENCES BETWEEN DAY AND NIGHT BEHAVIOUR

The median of differences between SSOC and VEIG22 is plotted, using 1-minute quality checked data for the whole period of the intercomparison. We filter data for which sun elevation is above -1° (day) or below -1° (night). Differences are classified according 2-meter wind speed (2-minute average).

Screen #1:

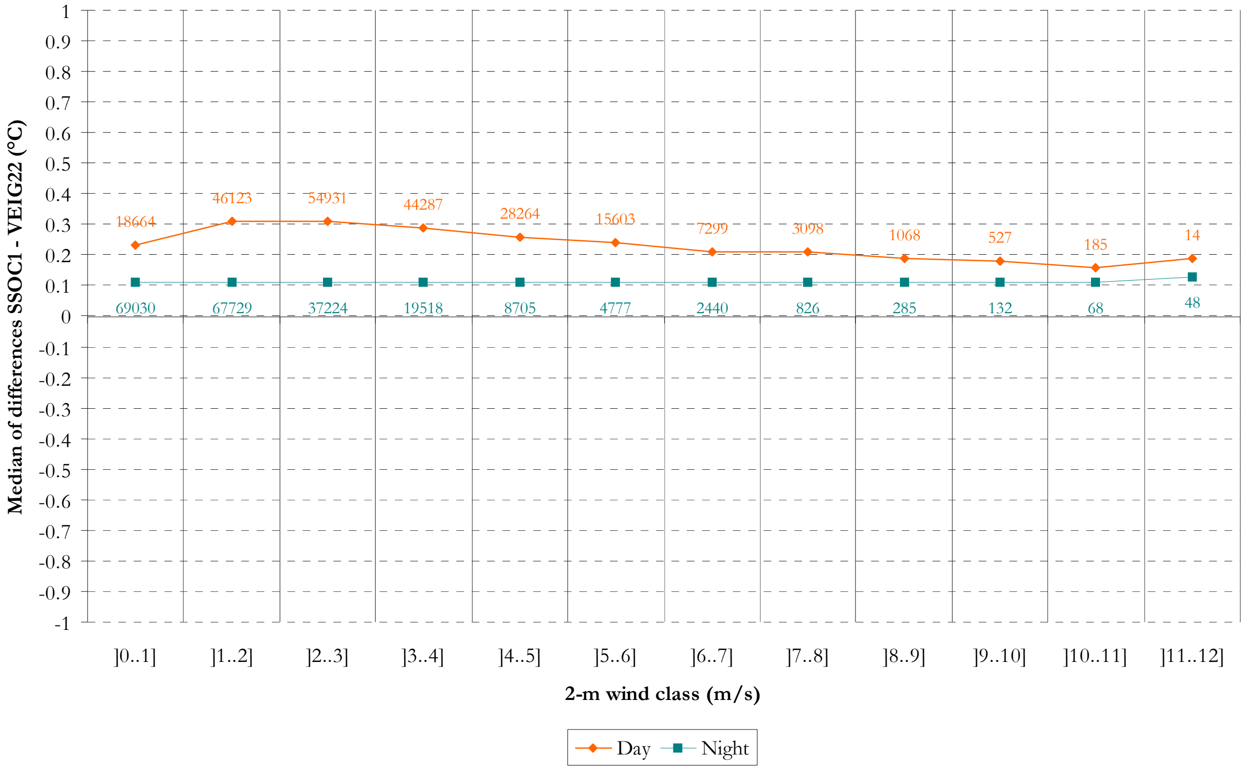


**Figure 9**

Screen #2:

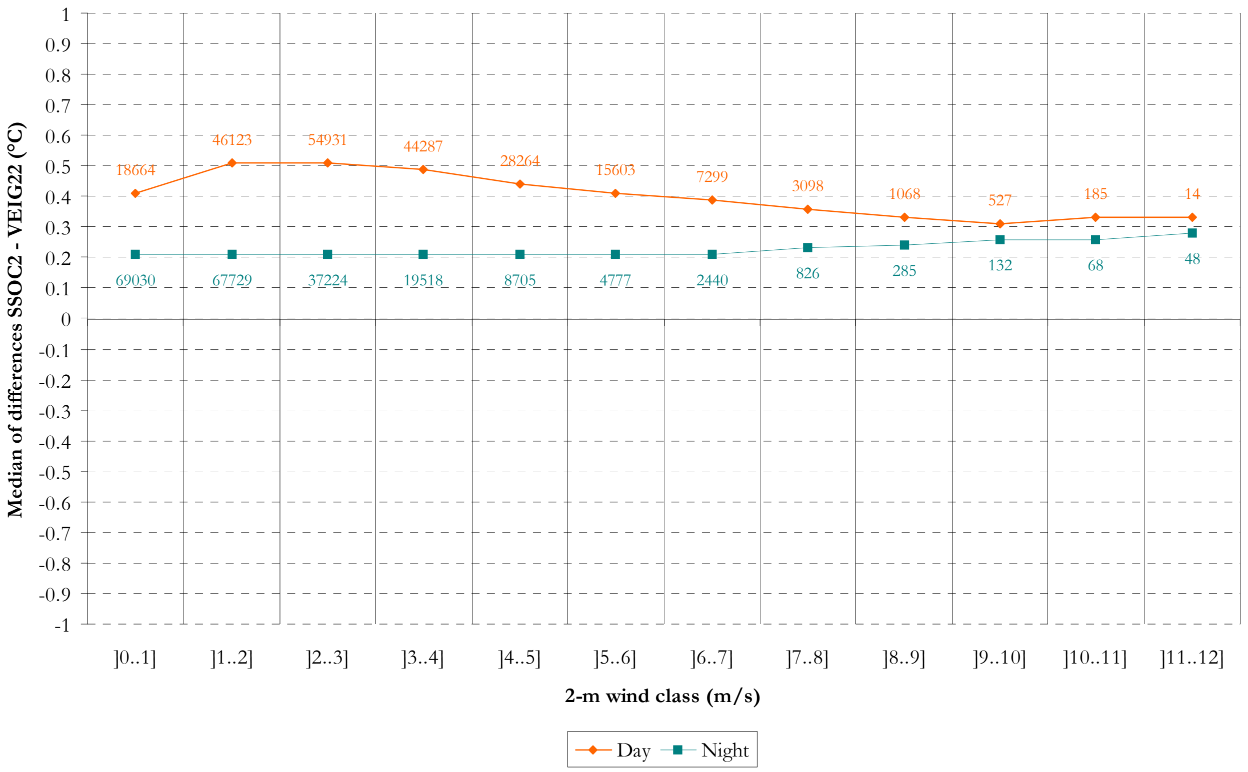


**Figure 10**

For both screens, differences are much higher during daytime than during night time. During daytime ,they reach the highest values for wind speeds between 1 and 4 m/s. During night time, differences do not depend on wind speeds for screen #1, they are stable around 0.1° value. For screen #2, they are stable around 0.2° for wind speeds below 7 m/s; above this value, differences increase slightly.

## DIFFERENCES BETWEEN CLEAR SKY AND OVERCAST SKY DURING DAYTIME

The median of differences between SSOC and VEIG22 is plotted, using 1-minute quality checked data. Here, we consider periods lasting six hours at least where cloudiness is less or equal to 1 (clear sky) or more or equal to 7 (overcast sky), during daytime (sun elevation above -1°). Differences are classified according 2-meter wind speed (2-minute average).

Screen #1:

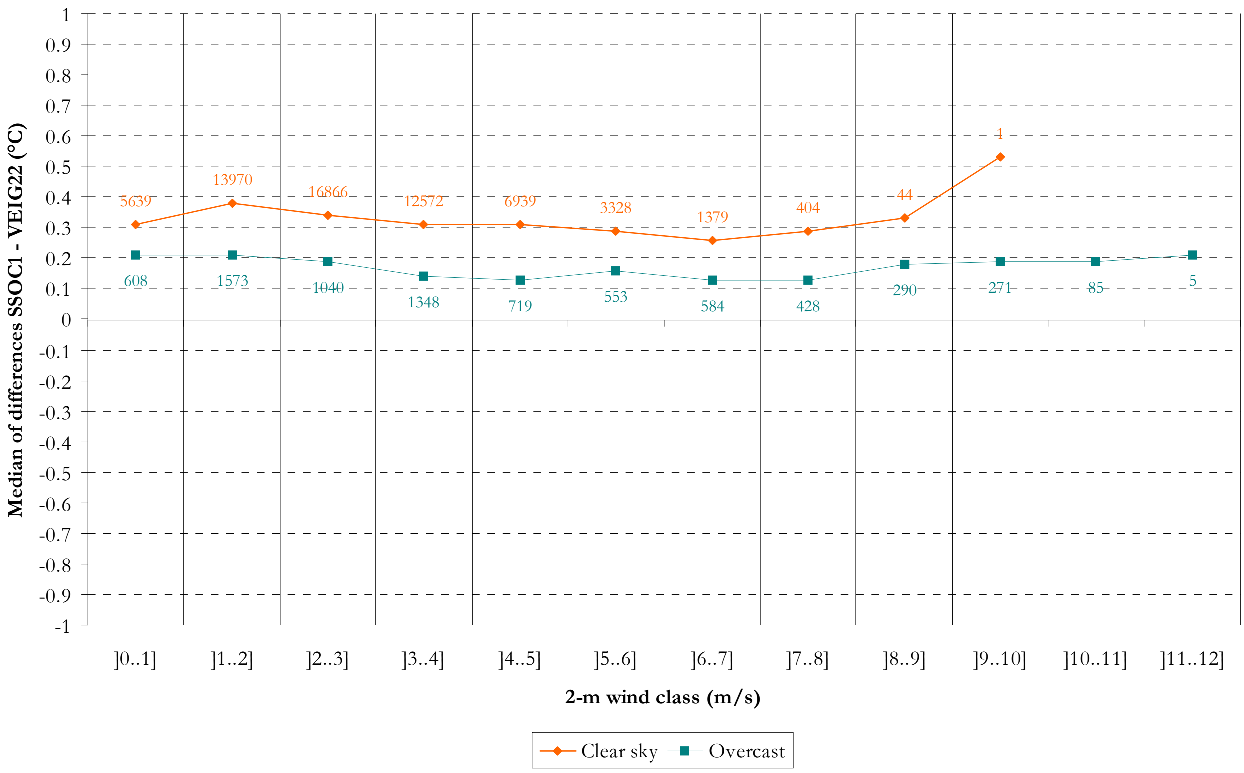


**Figure 11**

Screen #2:

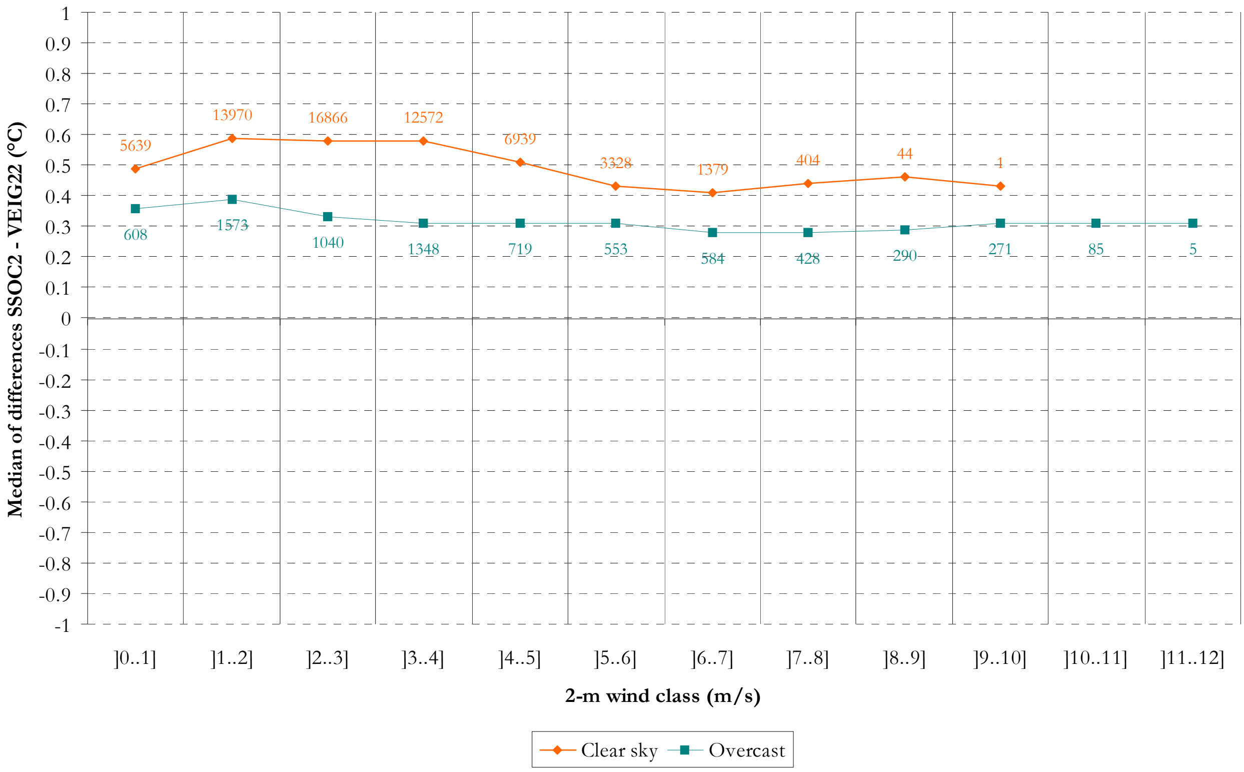


**Figure 12**

During daytime, in clear sky conditions, Socrima screens are around 0.1° warmer than in overcast conditions. Differences between these conditions are even higher for wind speeds between 1 and 5 m/s.

DIFFERENCES BETWEEN CLEAR SKY AND OVERCAST SKY DURING NIGHT TIME

The median of differences between SSOC and VEIG22 is plotted, using 1-minute quality checked data. Here, we consider periods lasting six hours at least where cloudiness is less or equal to 1 (clear sky) or more or equal to 7 (overcast sky), during night time (sun elevation below -1°). Differences are classified according 2-meter wind speed (2-minute average).

Screen #1:

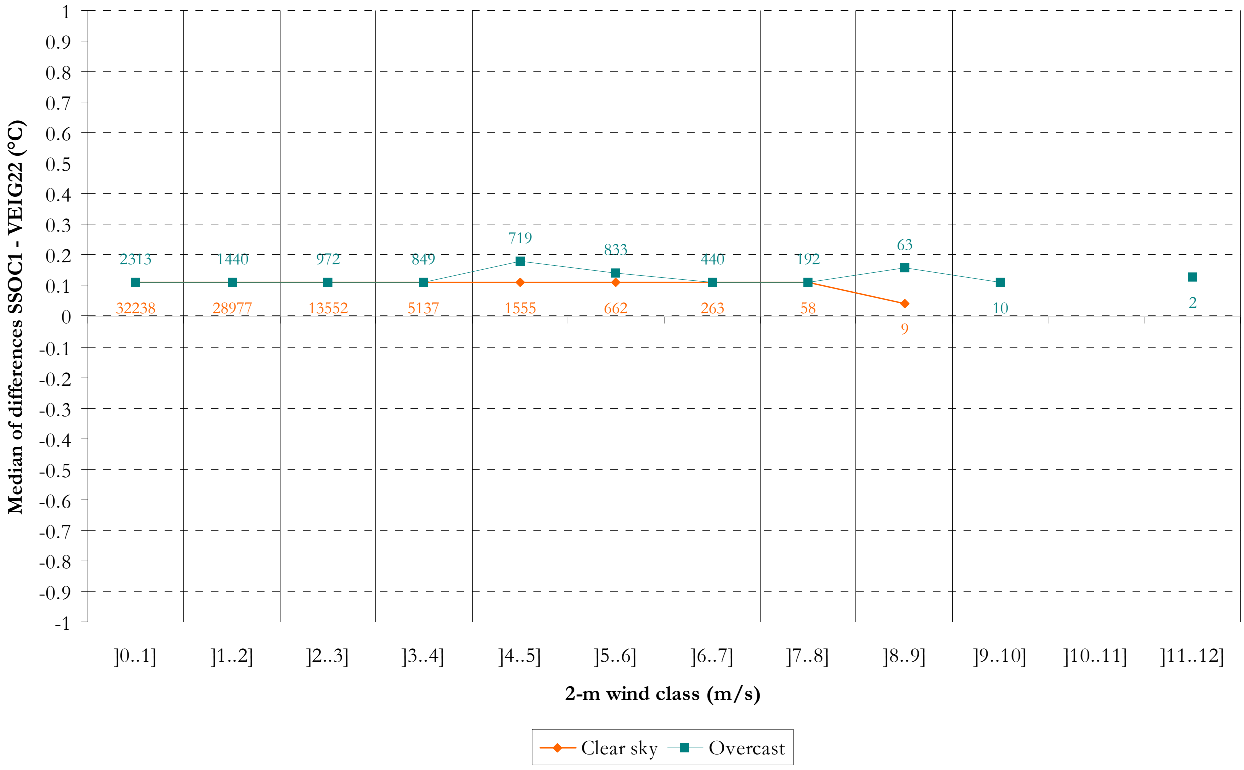


**Figure 13**

Screen #2:

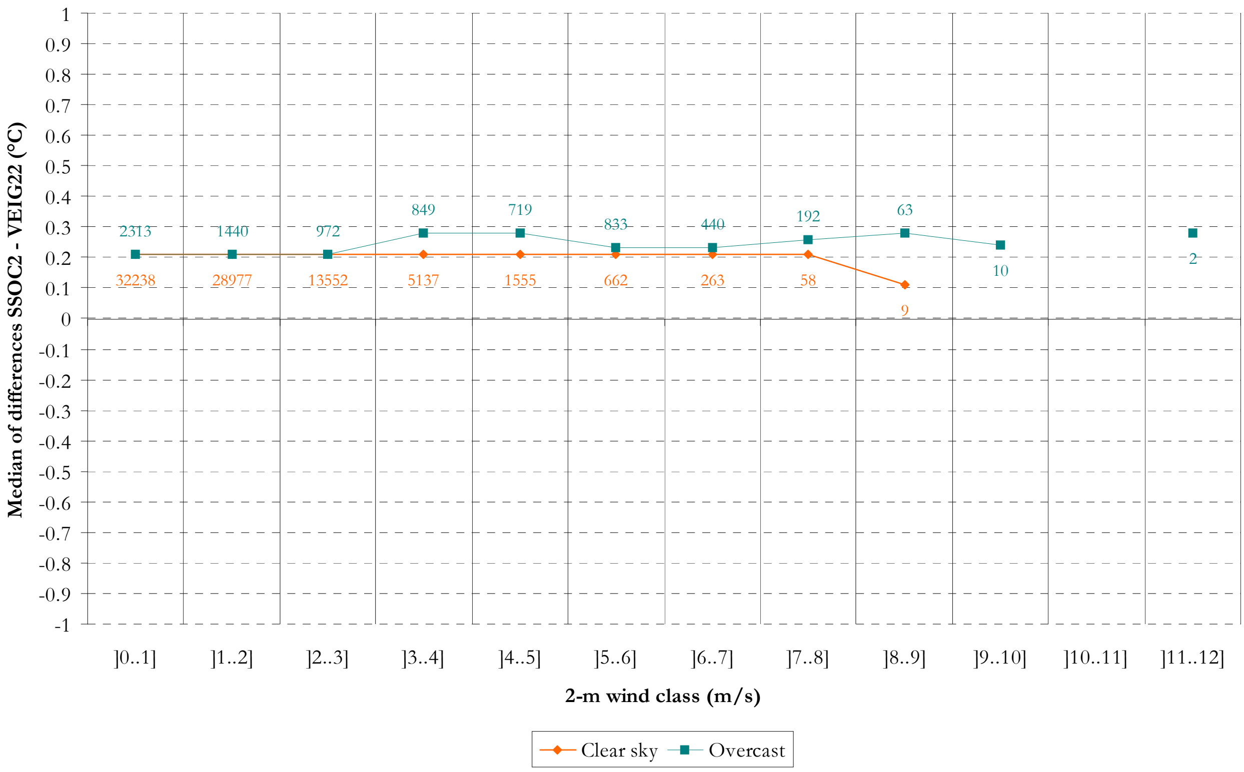


**Figure 14**

During night time, the cloudiness does not make a difference. Socrima screens may be slightly warmer in overcast conditions, for wind speeds around 4 to 5 m/s.

## EFFECT OF SUN ELEVATION

The median of differences between SSOC and VEIG22 is plotted, using 1-minute quality checked data. Here, we consider periods lasting six hours at least where cloudiness is less or equal to 1 (clear sky), during daytime (sun elevation above -1°). We filter data where sun elevation is low (below 10°), medium (between 10° and 45°) or high (above 45°). Differences are classified according 2-meter wind speed (2-minute average).

Screen #1:

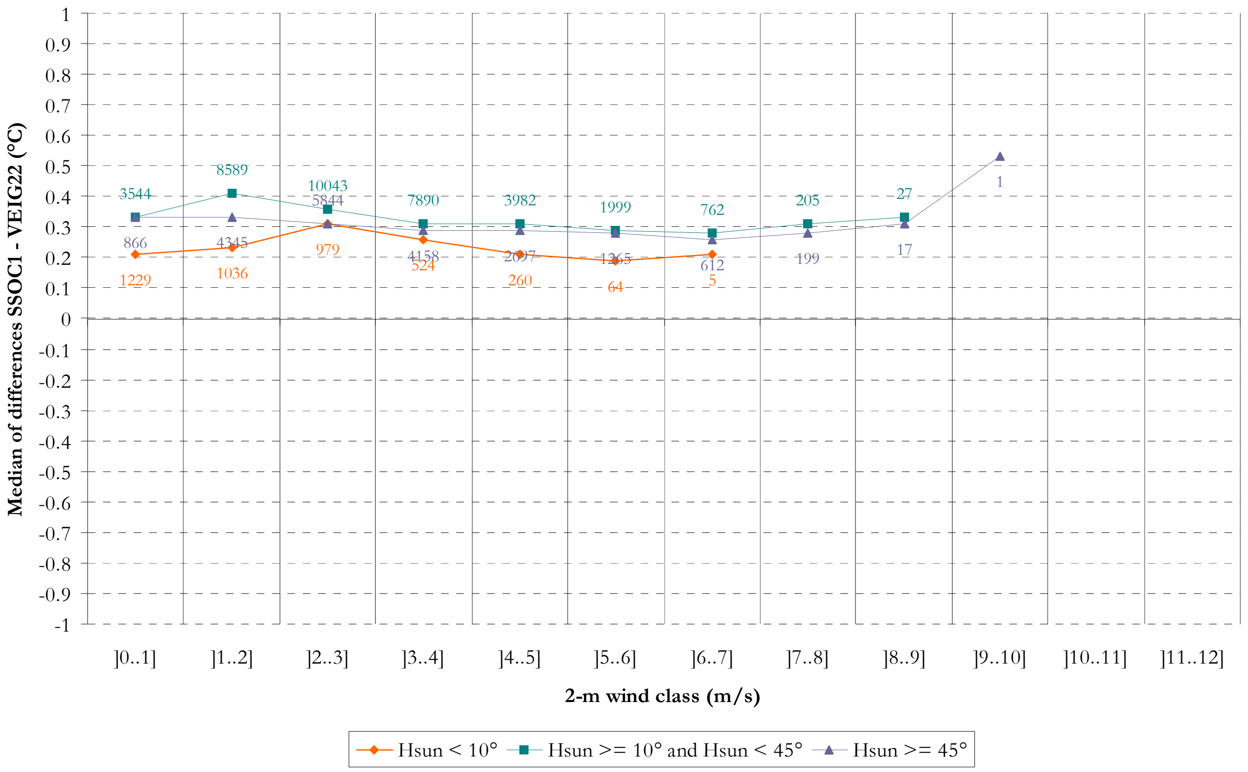


**Figure 15**

Screen #2:

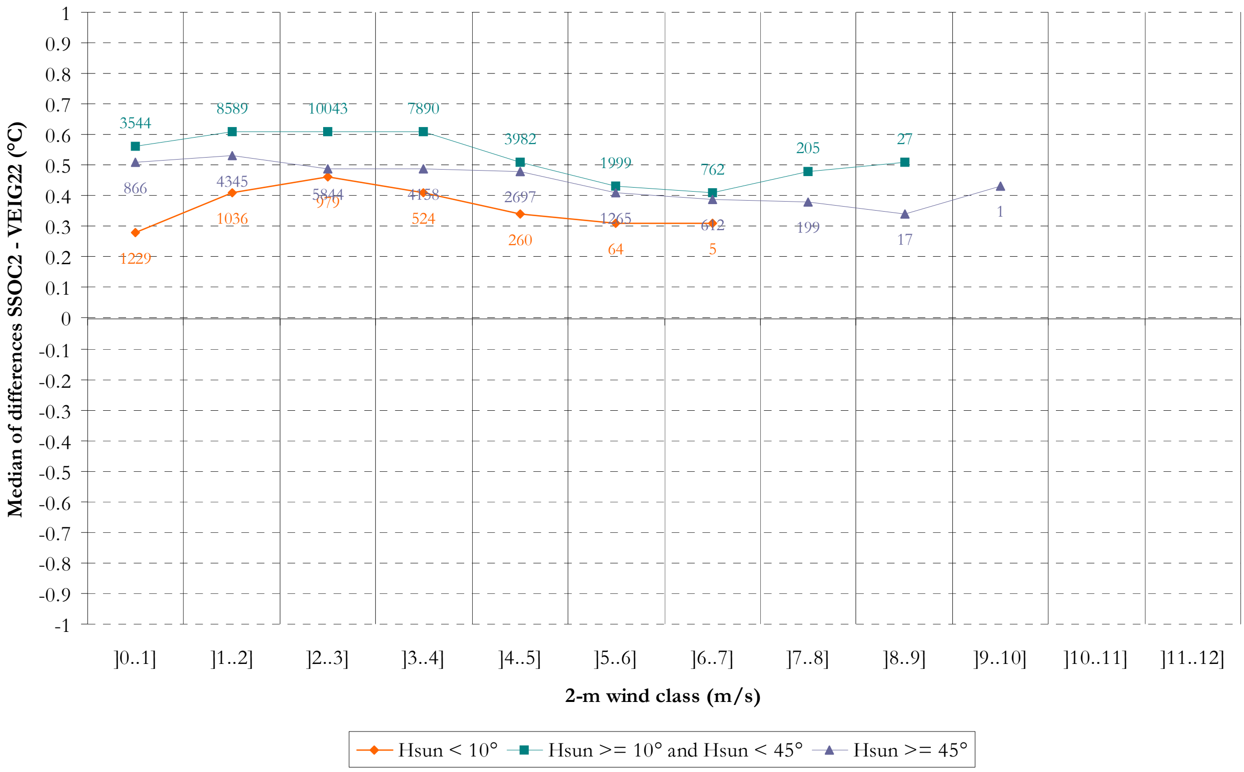


**Figure 16**

Differences for low sun elevation values are lower than for higher values.

## COMBINED EFFECT OF WIND AND GLOBAL RADIATION

The medians of differences between SSOC and VEIG22 are represented here with a contour plot. The global radiation values are on the X-axis and on the Y axis is the 2-meter wind speed value (2-minute average). Medians are used in all cases, providing that at least one data is available for both conditions on radiation and wind considered.

Screen #1:

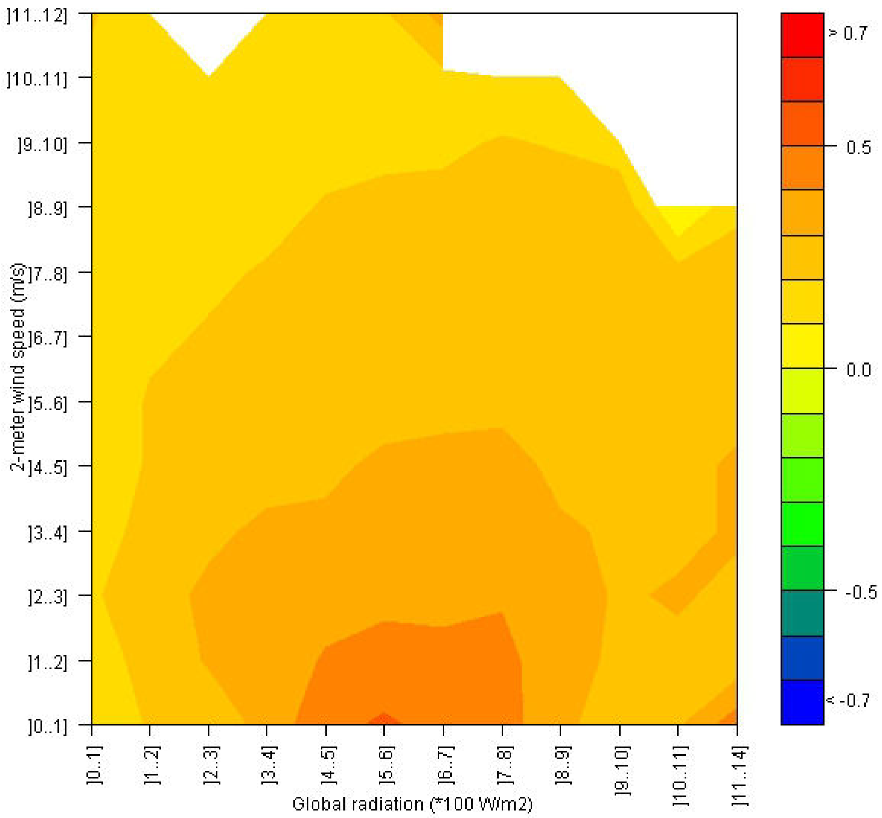


**Figure 17**

Screen #2:

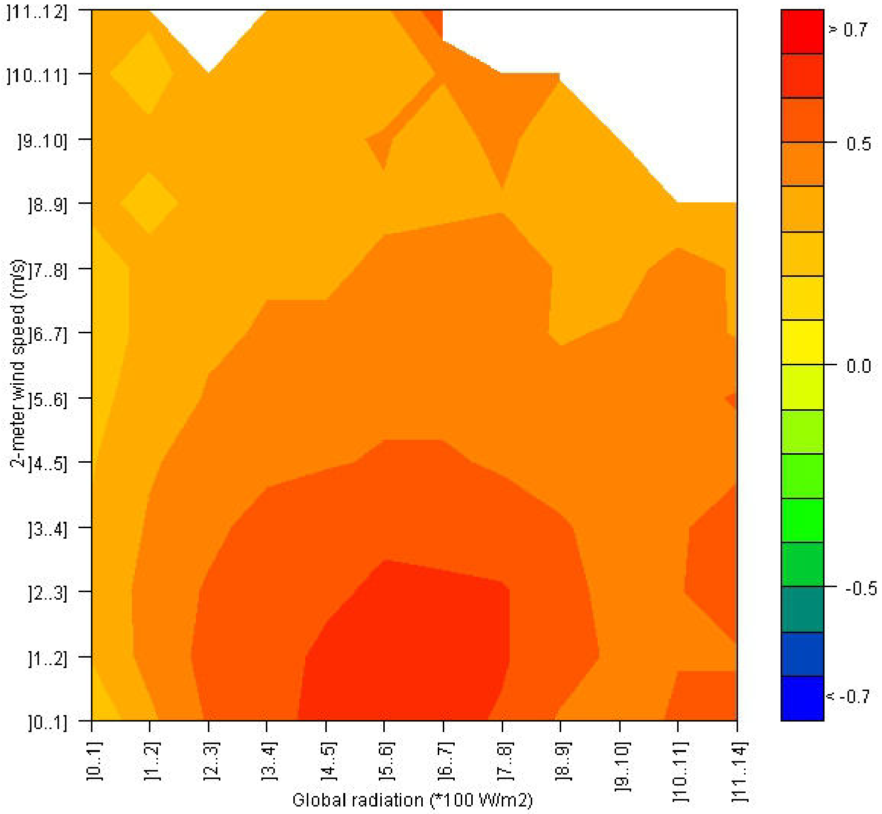


**Figure 18**

For both screens, larger differences are obtained for low wind speeds and medium global radiation.

## BEHAVIOUR DURING INCREASE/DECREASE OF TEMPERATURE

The distribution of differences between SSOC and the reference VEIG22 is plotted, using 1-minute quality checked data for the whole period of the intercomparison. Differences are classified according the temporal gradient of reference temperature over 1 minute. A screen faster (or slower, respectively) than the reference would be warmer (cooler) for positive gradient, cooler (warmer) for negative ones.

Screen #1:

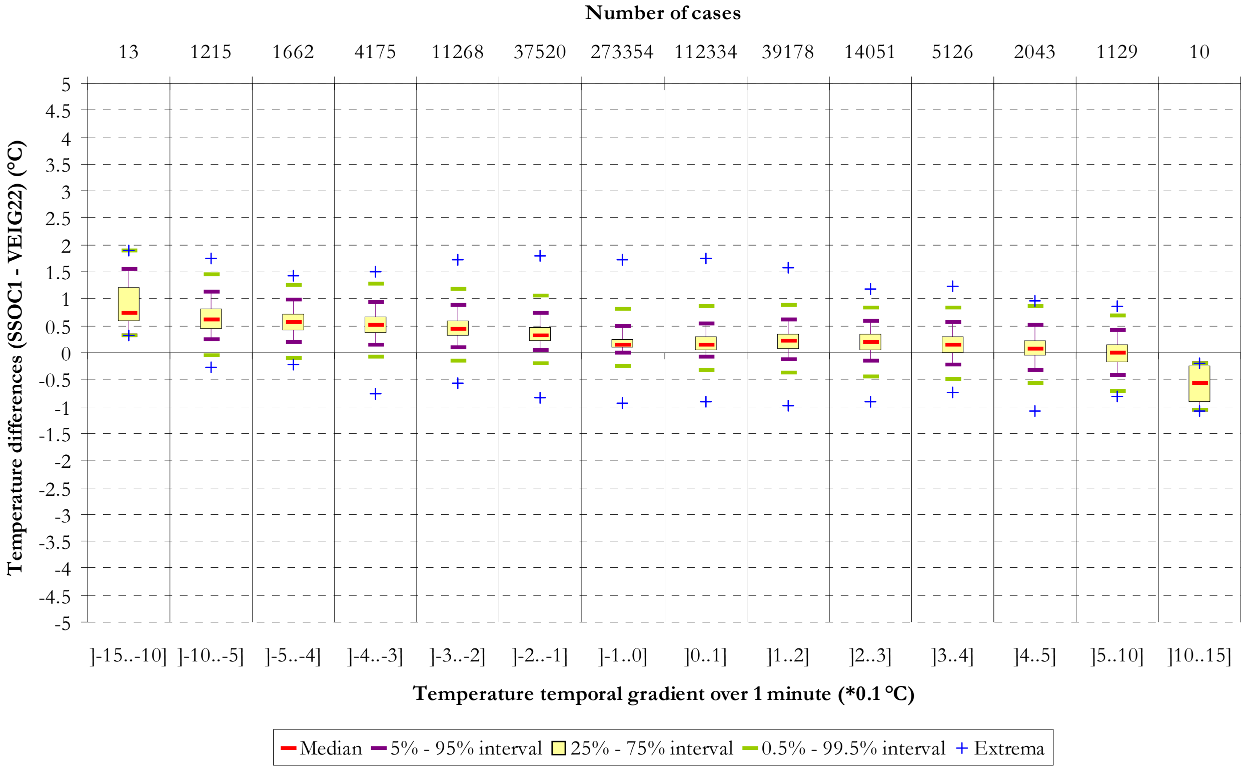


**Figure 19**

Screen #2:

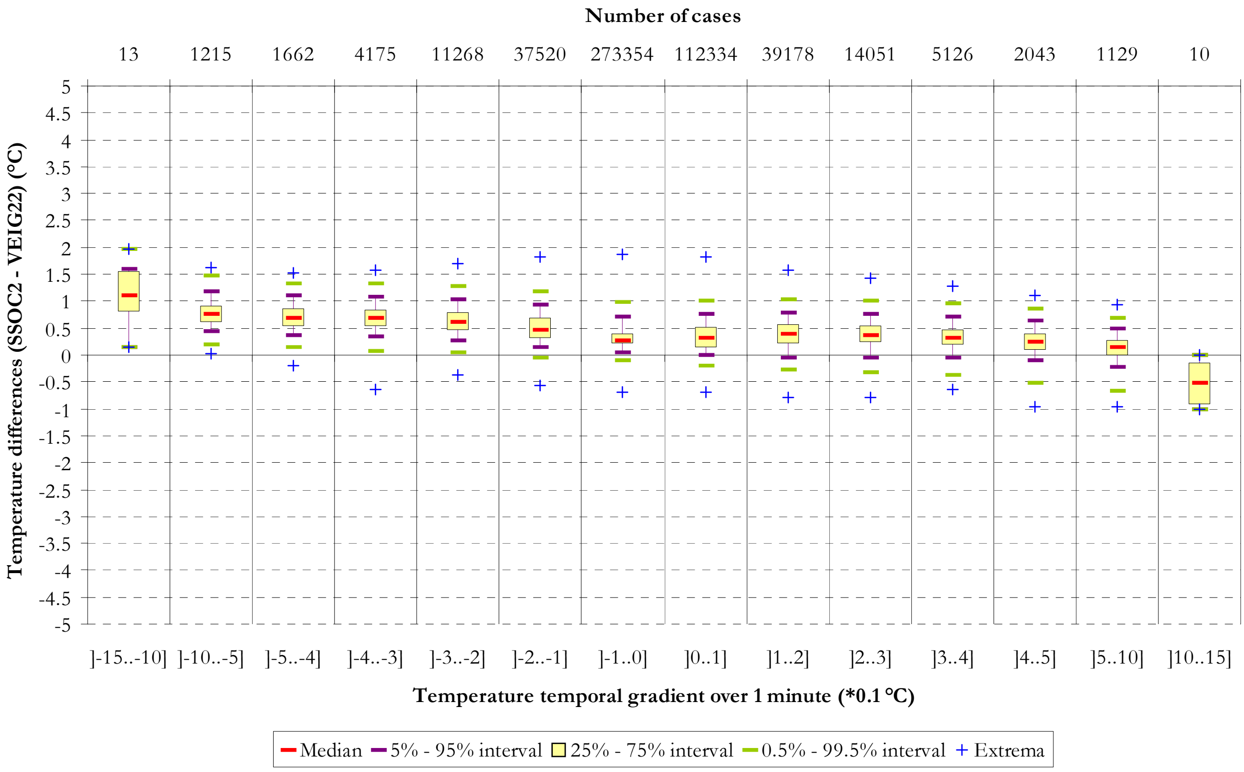


**Figure 20**

Both screens show some delay towards the reference: differences are slightly greater for negative temperature temporal gradient than for positive gradient.

## QUALITY CONTROL INFORMATION

### DATA AVAILABILITY

The intercomparison period extends from the 1st of November 2008 to the 1st of November 2009. The theoretical number of 1-minute data is 525600.

The next table sums up the total number of data for each screen and for each possible QC flag.

**Table 3**

| **QC flag** | SSOC1 | SSOC2 |
|---|---|---|
| 0 (good) | 503266 | 503266 |
| 1 (inconsistent) | 0 | 0 |
| 2 (doubtful) | 0 | 0 |
| 3 (erroneous) | 0 | 0 |
| 7 (missing) | 22334 | 22334 |

### MAINTENANCE

No action done during the intercomparison period.

# DTR13 VAISALA
# – Germany –
# SVAI

**TECHNICAL SPECIFICATIONS (PROVIDED BY THE MANUFACTURER)**

Dimensions: Length 7.7 cm x Width 18.3 cm x Height 11.9 cm

Weight: 1.6 kg

Material/Structure: Fiberglass filled polyester

Estimated radiation error:

Aspiration rate (in case of artificially ventilated screen/shield): naturally ventilated

Power supply: 230 VAC

This screen is installed in conjunction with HMT337 humidity and temperature transmitter and with HMT330MIK meteorological installation kit.

**Figure 1**

The temperature sensor was supplied by the manufacturer.

## OVERVIEW

This screen seems to have a lower radiation error than VEIG22 although it does not have an artificial ventilation. In low wind speed and high irradiance condition the difference amounts to -0.6 K.

Both SVAI screens are close to each other for all the temperature classes, with screen #2 slightly warmer than screen #1The differences between the two screens show a slight dependence on the variation in temperature.

Both SVAI screens agree with the reference within 0.5K for about 95% of valid data points, screen #1 being slightly colder than the reference and screen #2 being slightly warmer.

In terms of Tn, screen #1 is slightly warmer than the reference, while screen #2 is approximately equal to the reference. In terms of Tx, both screens are slightly colder than the reference.

Screen #1 shows a slight dependence on the global radiation, about 0.5°C, while screen #2 is essentially independent of the global radiation.

During the day time, overall, the two screens are colder than the reference for winds below 3m/s and similar or slightly warmer than the reference for higher wind speeds. Under clear-sky, the screens are colder than the reference, for wind speeds below 5m/s. For winds above 5m/s screen #1 is similar to the reference, while screen #2 is slightly warmer. The day-time overcast medians show a minimum dependence on wind speed, being similar to the reference for low wind conditions, and slightly warmer at wind speed of about 6 m/s.

The night-time behaviour of both screens is essentially independent of wind speed, consistently about 0.1°K warmer than the reference. The same results are noted under both clear-sky and overcast conditions.

For sun elevations of less than 10°, the SVAI screens are just marginally warmer than the reference for all the wind conditions.

In low wind conditions, the screens are colder when the sun elevations is above 10°, this effect is greater for sun elevation above 45°. As the wind increases, the medians of sun elevations greater than 10° get warmer (relative to the reference), and stabilize at about 0.1°C above or below the reference when the wind speed has increases above 4 m/s.

Both screens are colder than the reference for high global radiations and low wind speeds, and are warmer than the reference for low global radiations and high wind speeds. However, screen #1 is colder than the reference for almost all the wind conditions when the global radiation is above 600 W/m$^2$, whereas screen #2 is warmer than the reference for almost all global radiation values when the wind speed is greater than 6 m/s.

The data dispersion increases with the absolute value of the temperature temporal gradient, the two screens agree best with the reference when the temperature gradient is 0.1°.

When the temperature decreases, SVAI screen #1 is slightly colder, faster, than the reference, while SVAI screen #1 is symmetrical about the reference.

When the temperature increases, both screens are colder (slower) than the reference. For both screens, the dispersion increases as the temporal gradient increases in absolute value.

## CALIBRATION INFORMATION

Calibration was performed by manufacturer.

**Table 1**

| Screen | Location | Screen serial number | Calibration date | Instrument bias (°C) |
|---|---|---|---|---|
| | | | | -22°C |
| SVAI1 | B3 | B4940009 | 4-Jan-2007 | -0.04 |
| SVAI2 | B6 | B4940010 | 4-Jan-2007 | -0.04 |

The result of the calibration of the reference VEIG22 is available in the main report of the intercomparison, section 5.4.1.

## COMPARISON OF BOTH SENSORS

The distribution of differences between screen 1 and screen 2 is plotted, using 1-minute quality checked data for the whole period of the intercomparison. Differences are classified according screen 1 temperature.

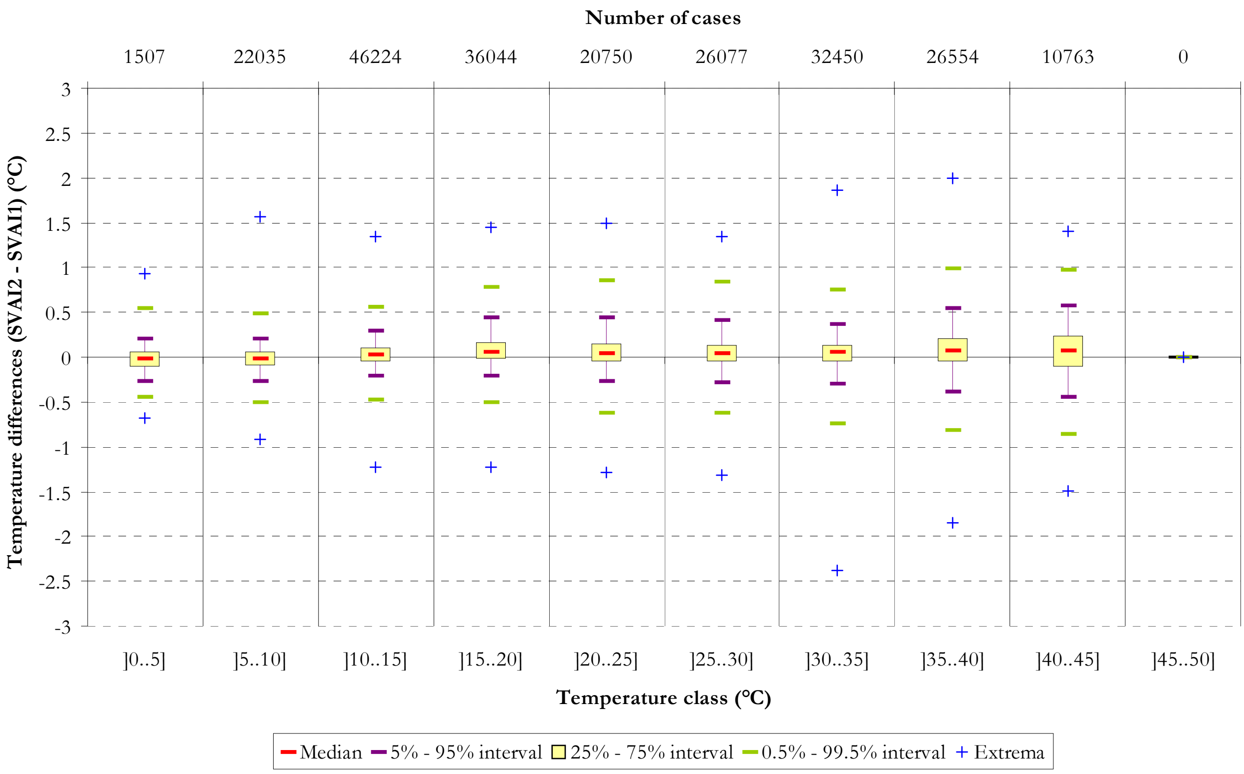


**Figure 2**

Both screens are very close to each other for all the temperature classes, with screen #2 slightly warmer than screen #1 with the median of the differences apparently less than 0.1°C. The differences between the two screens show a slight dependence on the variation in temperature.

## COMPARISON WITH THE REFERENCE

### HISTOGRAM OF DIFFERENCES

The histogram of differences between SVAI and the reference VEIG22 is plotted, using 1-minute quality checked data for the whole period of the intercomparison. Differences are plotted by steps of 0.1K. The vertical axis is the frequency in percent for each class of differences.

Screen #1:

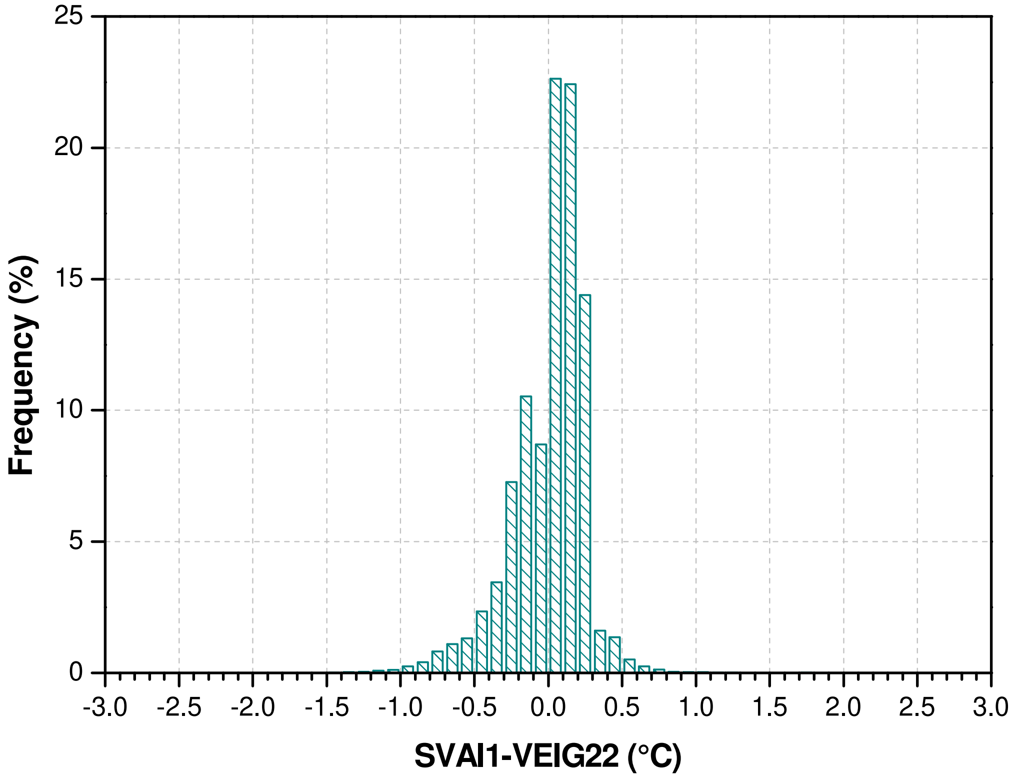


**Figure 3**

Screen #2:

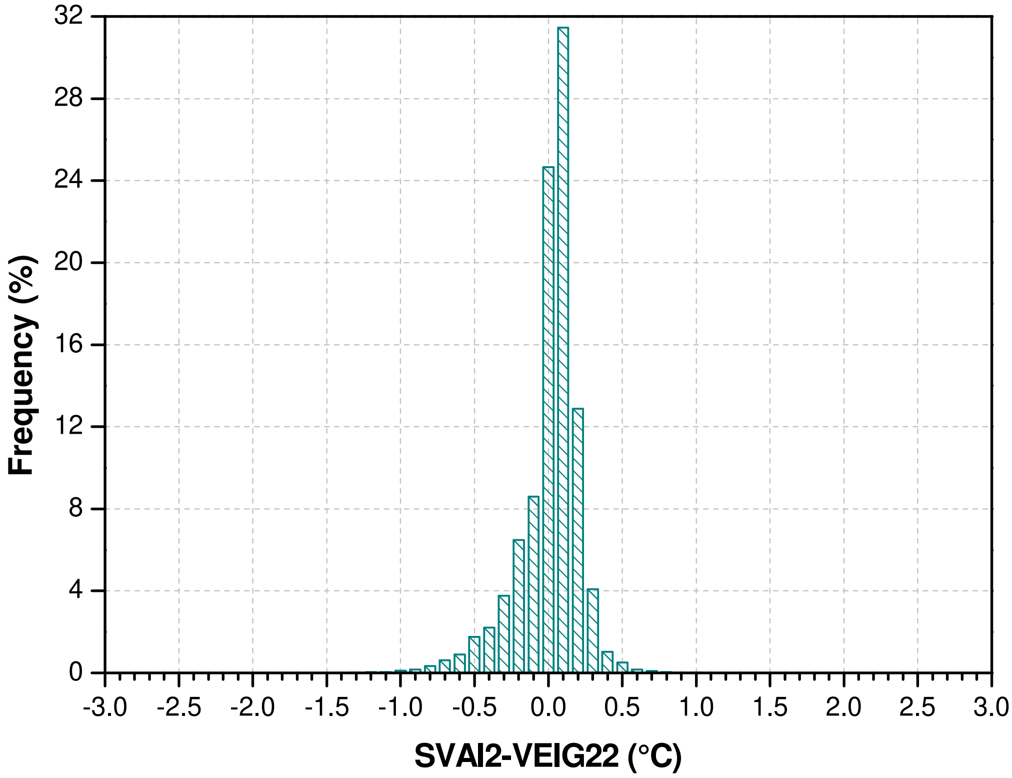


**Figure 4**

Screen #1 is slightly colder than the reference and screen #2 is slightly warmer.

CUMULATIVE HISTOGRAMS OF DIFFERENCES OF DAILY EXTREME VALUES

The cumulative histograms of differences with the reference VEIG22 of T (1-minute quality checked data), Tn (daily minimum temperature) and Tx (daily maximum temperature) are plotted, for the whole period of the intercomparison. Differences are plotted by steps of 0.1K.

Screen #1:

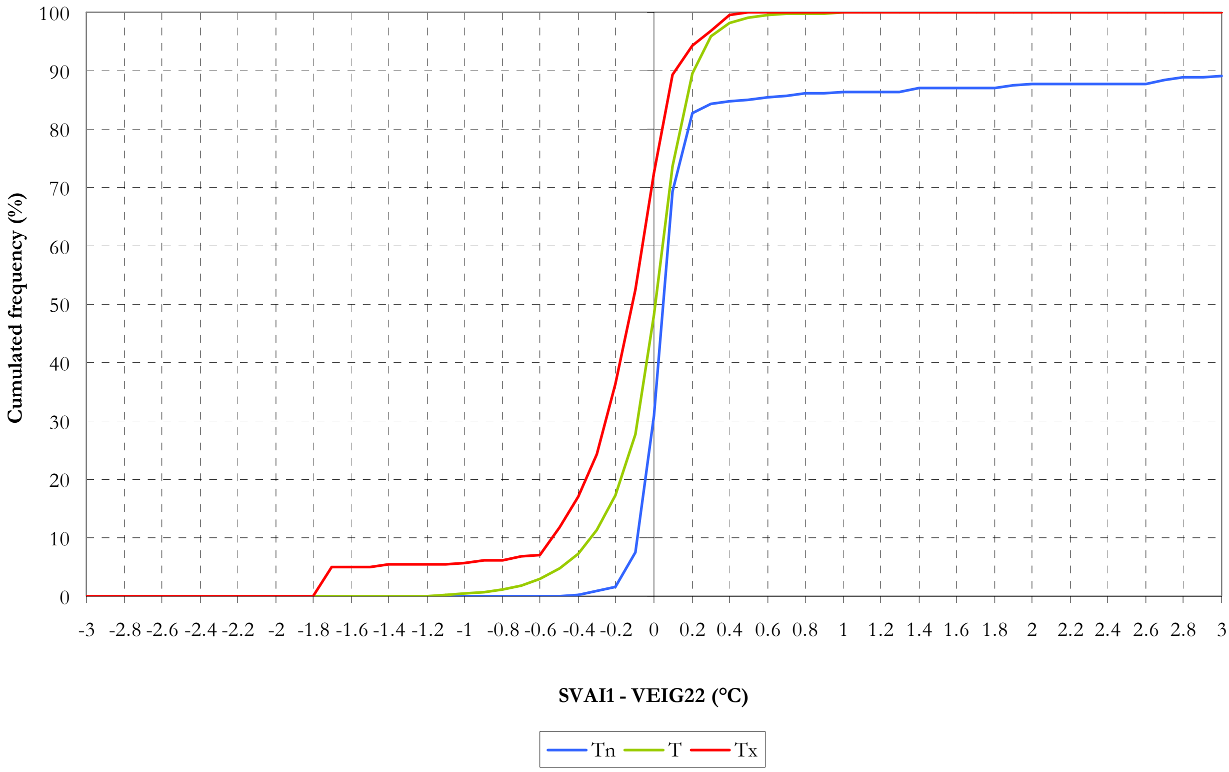


**Figure 5**

Screen #2:

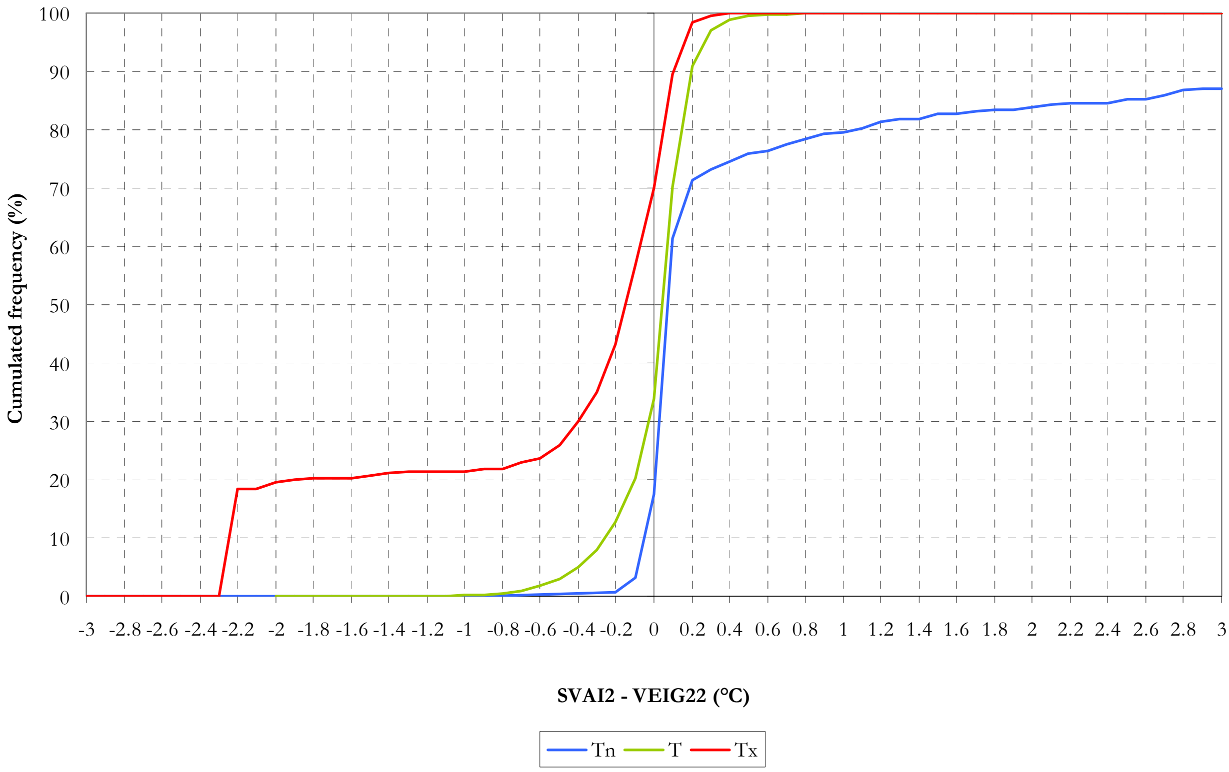


**Figure 6**

Screen #1symetrical about the reference, as the median of T between screen #1 and the reference is 0°C, i.e. 50% of positive differences and 50% of negative differences. In terms of Tn, screen #1 is slightly warmer than the reference with about 60% of positive differences, and in terms of Tx, screen #1 is slightly colder than the reference with more than 70% of negative differences.

Screen #2 is slightly warmer than the reference, in about 65% of the cases. In terms of Tn screen #2 is equal to the reference with roughly 50% positive differences and 50% of negative differences. In terms of Tx, screen #2 is slightly colder than the reference with more than 70% of negative differences.

TABLE

The table 2 indicates the percentage of data that differ by less than 0.2°C (and 0.5°C) from the reference.

**Table 2**

| | | [-0.2°..0.2°] | [-0.5°..0.5°] |
|---|---|---|---|
| SVAI1 | T | 72.1 | 94.4 |
| | Tn | 80.9 | 85.0 |
| | Tx | 57.9 | 88.2 |
| SVAI2 | T | 78.2 | 96.5 |
| | Tn | 70.6 | 76.0 |
| | Tx | 55.3 | 74.0 |

## INFLUENCE OF GLOBAL RADIATION

The distribution of differences between SVAI and the reference VEIG22 is plotted, using 1-minute quality checked data for the whole period of the intercomparison. Differences are classified according global radiation.

## Screen #1:

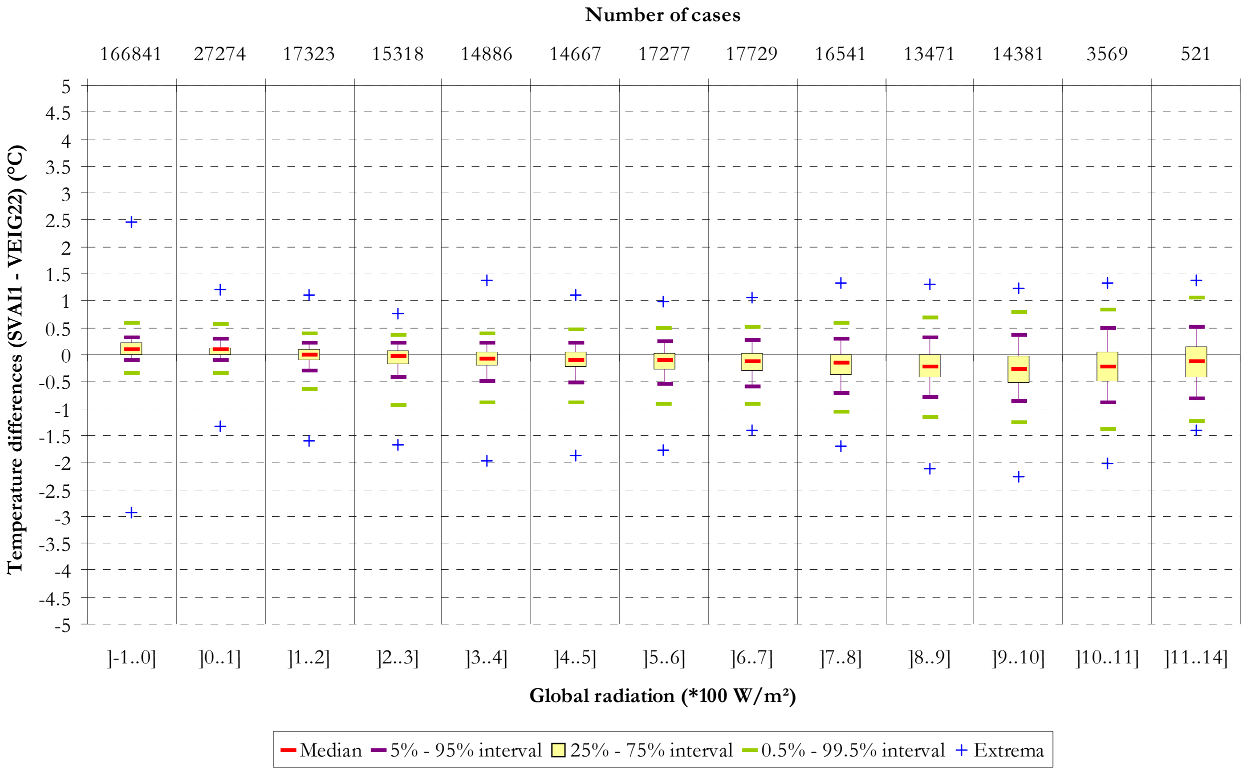


**Figure 7**

## Screen #2:

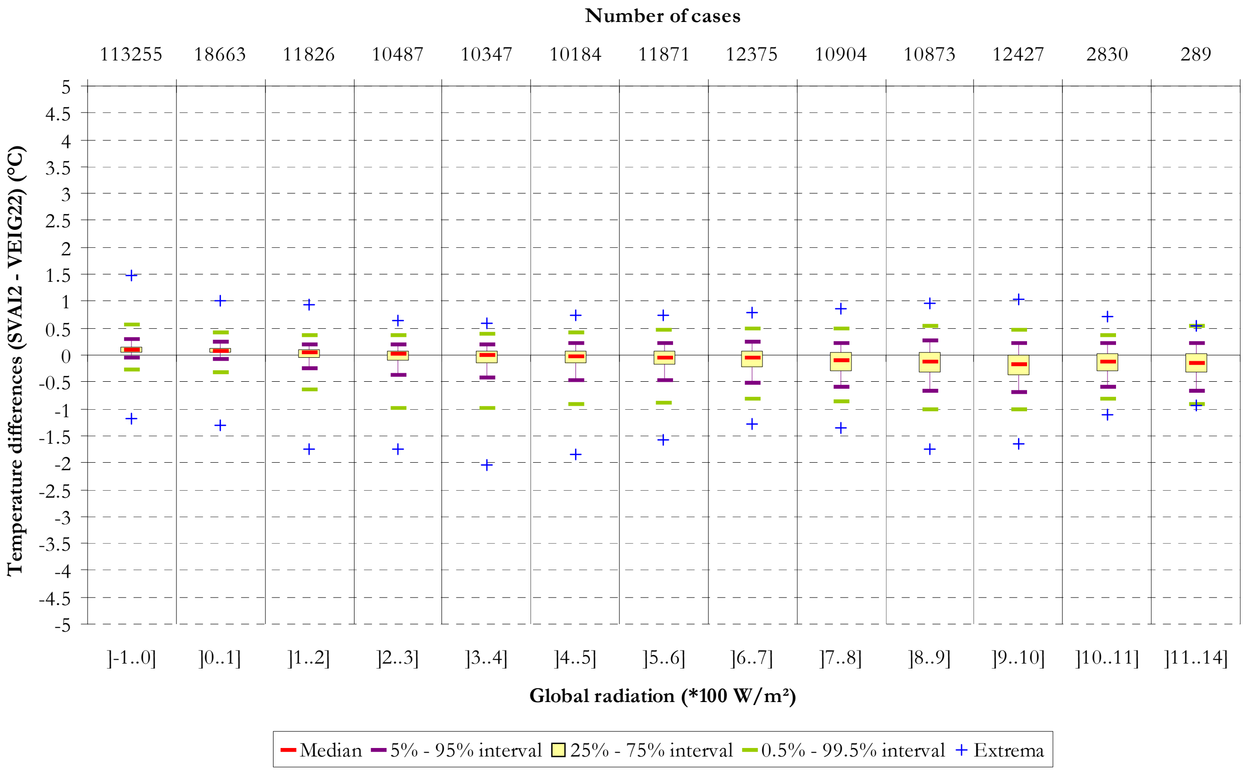


**Figure 8**

Screen #1 shows a slight dependence on the global radiation; 99% of the data from screen #1 is within 0.5°C of the reference for 0 W/m$^2$ global radiation and increases approximately linearly to within about 1°C for global radiation of 1000W/m$^2$, before decreasingly slightly.

Screen #2 is essentially independent of the global radiation, with the medians remaining close to the reference for all the radiation classes.

## RADIATION EFFECT

### DIFFERENCES BETWEEN DAY AND NIGHT BEHAVIOUR

The median of differences between SVAI and VEIG22 is plotted, using 1-minute quality checked data for the whole period of the intercomparison. We filter data for which sun elevation is above -1° (day) or below -1° (night). Differences are classified according 2-meter wind speed (2-minute average).

Screen #1:

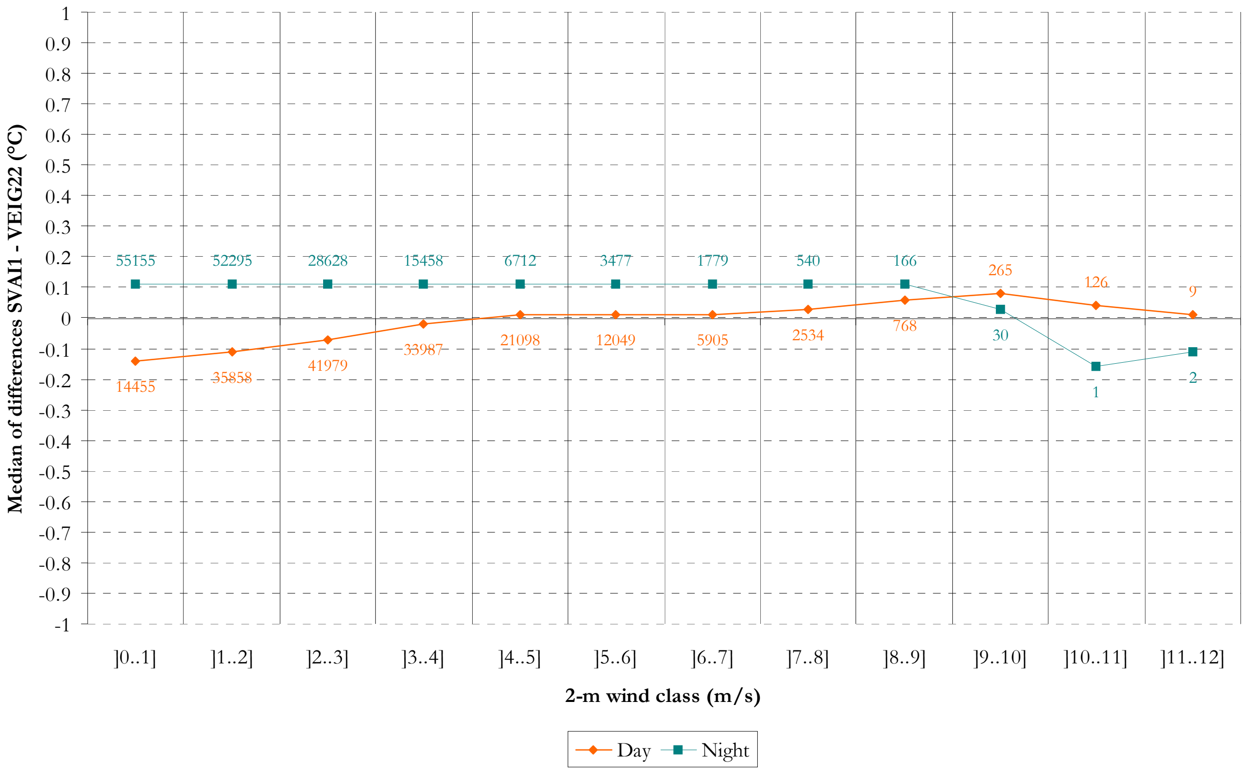


**Figure 9**

Screen #2:

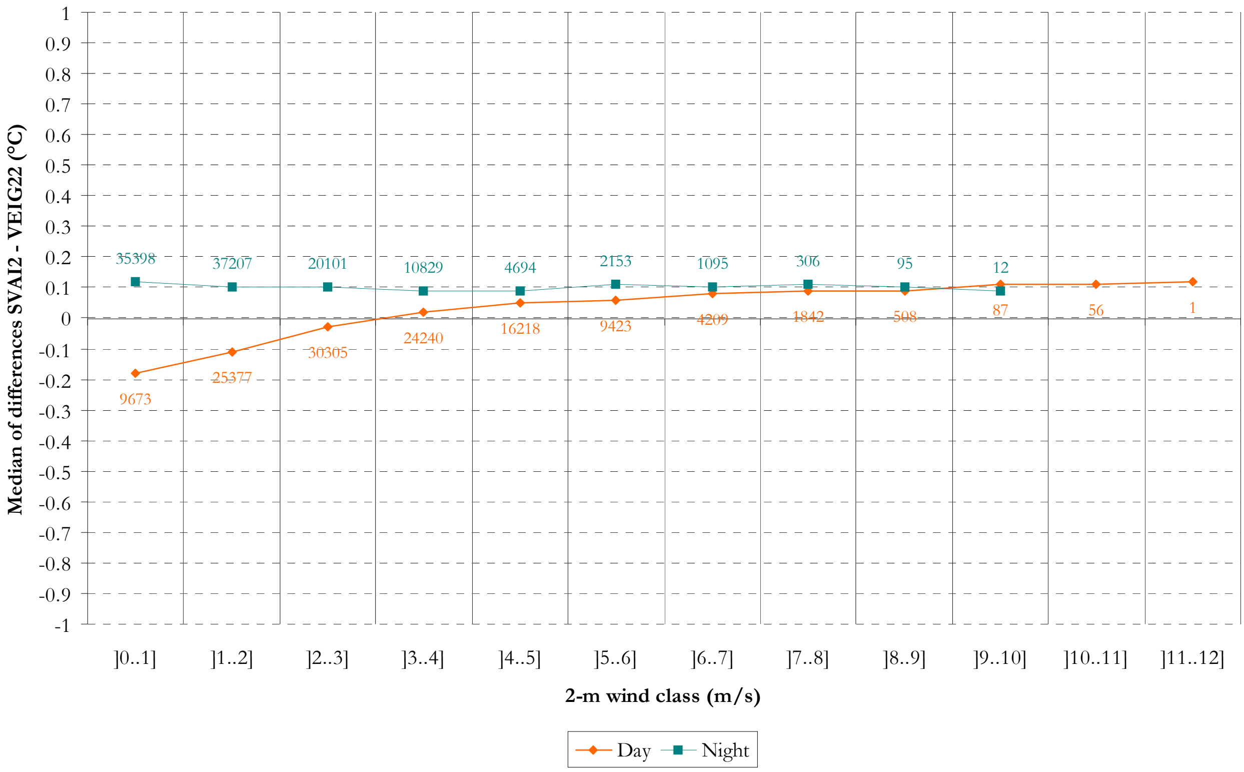


**Figure 10**

The night-time behaviour of both screens is essentially independent of wind speed, consistently about 0.1°C warmer than the reference.

During the day time, the two screens are colder than the reference for winds below 3m/s and similar or slightly warmer than the reference for higher wind speeds.

DIFFERENCES BETWEEN CLEAR SKY AND OVERCAST SKY DURING DAYTIME

The median of differences between SVAI and VEIG22 is plotted, using 1-minute quality checked data. Here, we consider periods lasting six hours at least where cloudiness is less or equal to 1 (clear sky) or more or equal to 7 (overcast sky), during daytime (sun elevation above -1°). Differences are classified according 2-meter wind speed (2-minute average).

Screen #1:

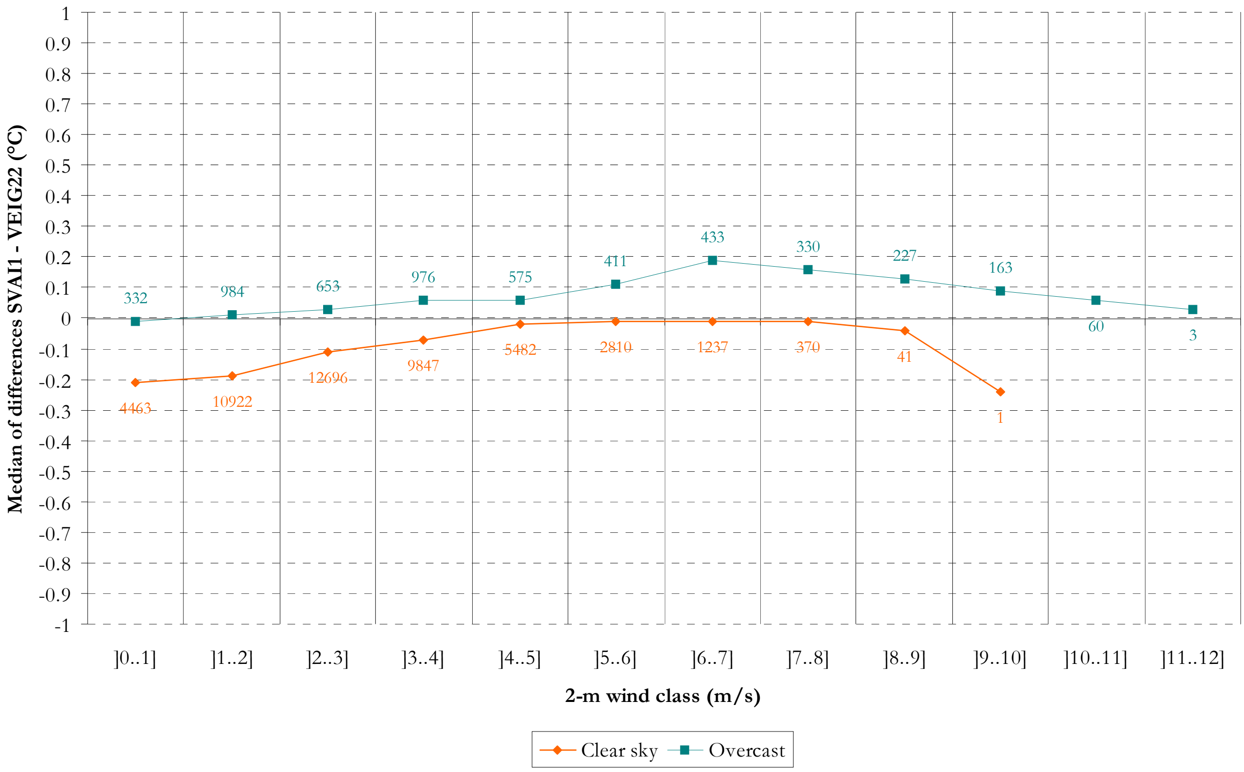


**Figure 11**

Screen #2:

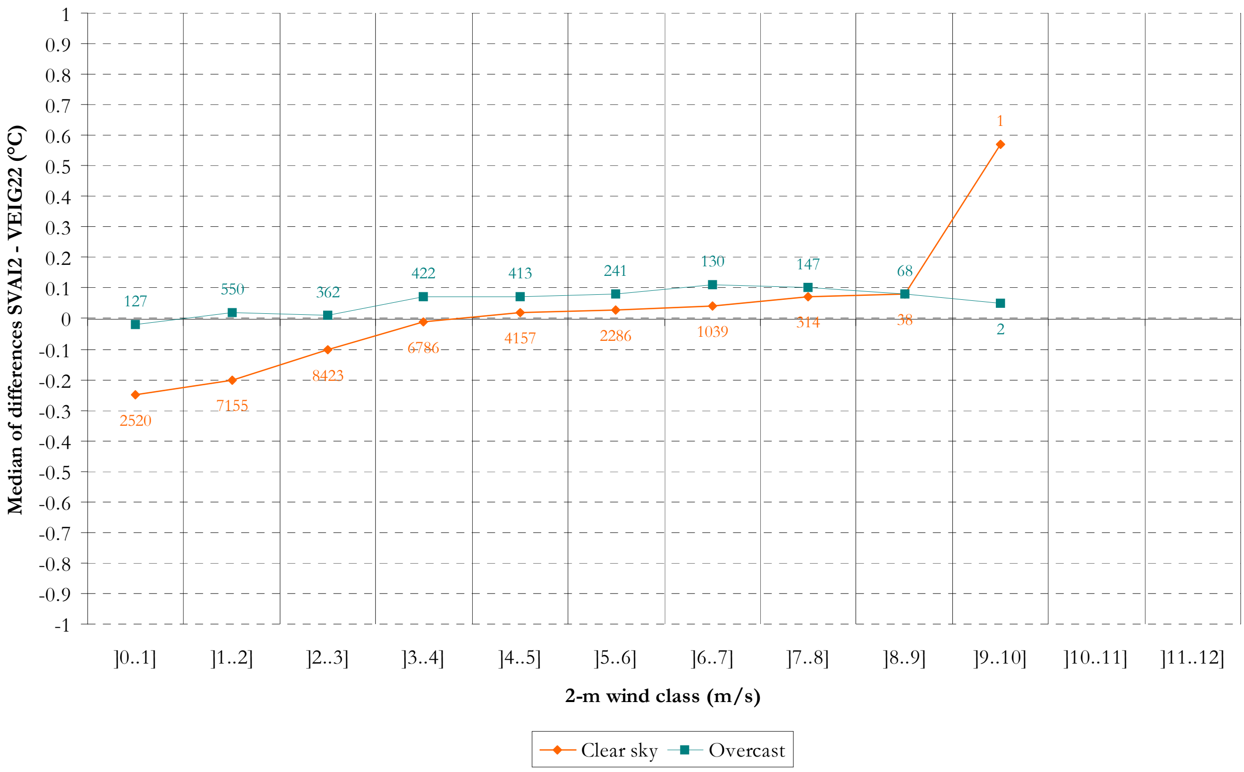


**Figure 12**

The clear-sky medians are negative for low wind conditions, screens are colder, and decrease in absolute value to about 0°C as the wind increases to about 5 m/s, and remain close to 0°C for screen #1(similar to the reference) and go slightly positive for screen #2 (slightly warmer).

The overcast medians show a minimum dependence on wind speed are similar to those of the reference for low wind conditions, and increase to a maximum of 0.2°C for screen #1 and of 0.1°C for screen at a wind speed of about 6 m/s.

DIFFERENCES BETWEEN CLEAR SKY AND OVERCAST SKY DURING NIGHT TIME

The median of differences between SVAI and VEIG22 is plotted, using 1-minute quality checked data. Here, we consider periods lasting six hours at least where cloudiness is less or equal to 1 (clear sky) or more or equal to 7 (overcast sky), during night time (sun elevation below -1°). Differences are classified according 2-meter wind speed (2-minute average).

Screen #1:

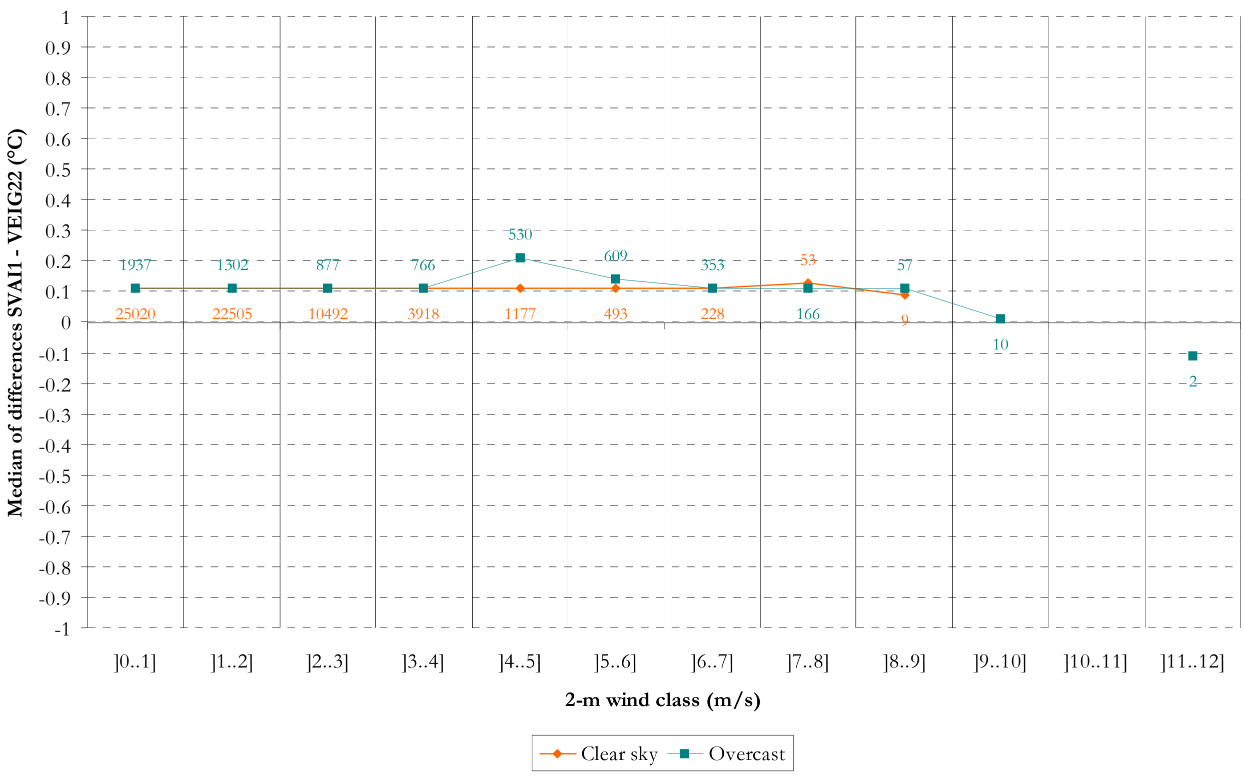


**Figure 13**

Screen #2:

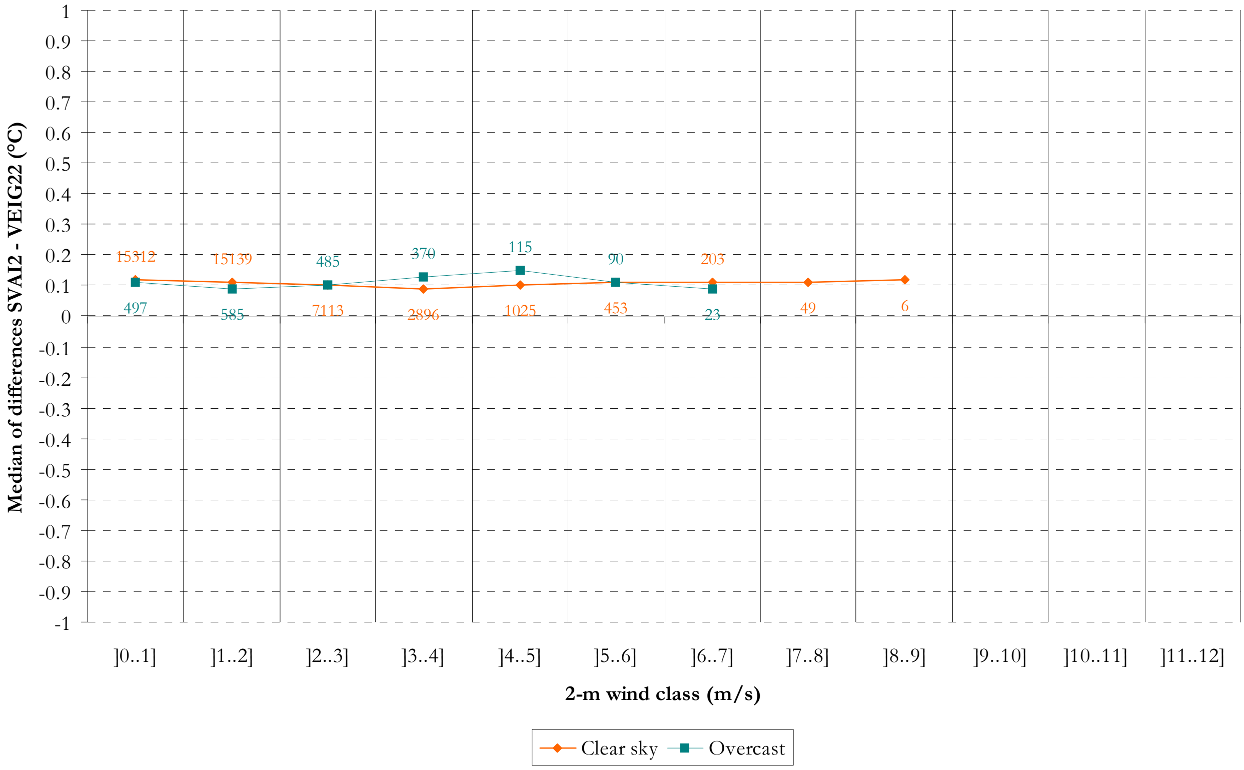


**Figure 14**

The night-time, clear-sky and overcast medians for both screens are essentially the same, about 0.1°C warmer than the reference for all the wind conditions.

EFFECT OF SUN ELEVATION

The median of differences between SVAI and VEIG22 is plotted, using 1-minute quality checked data. Here, we consider periods lasting six hours at least where cloudiness is less or equal to 1 (clear sky), during daytime (sun elevation above -1°). We filter data where sun elevation is low (below 10°), medium (between 10° and 45°) or high (above 45°). Differences are classified according 2-meter wind speed (2-minute average).

Screen #1:

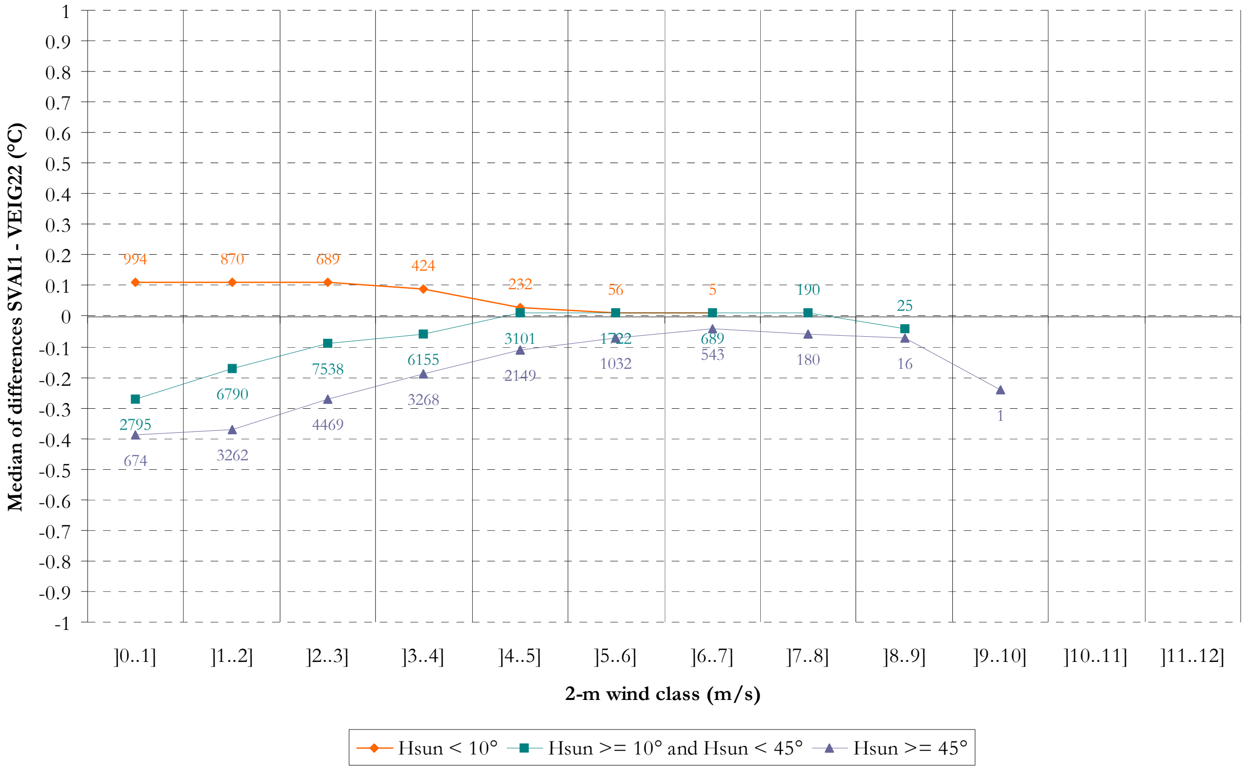


**Figure 15**

Screen #2:

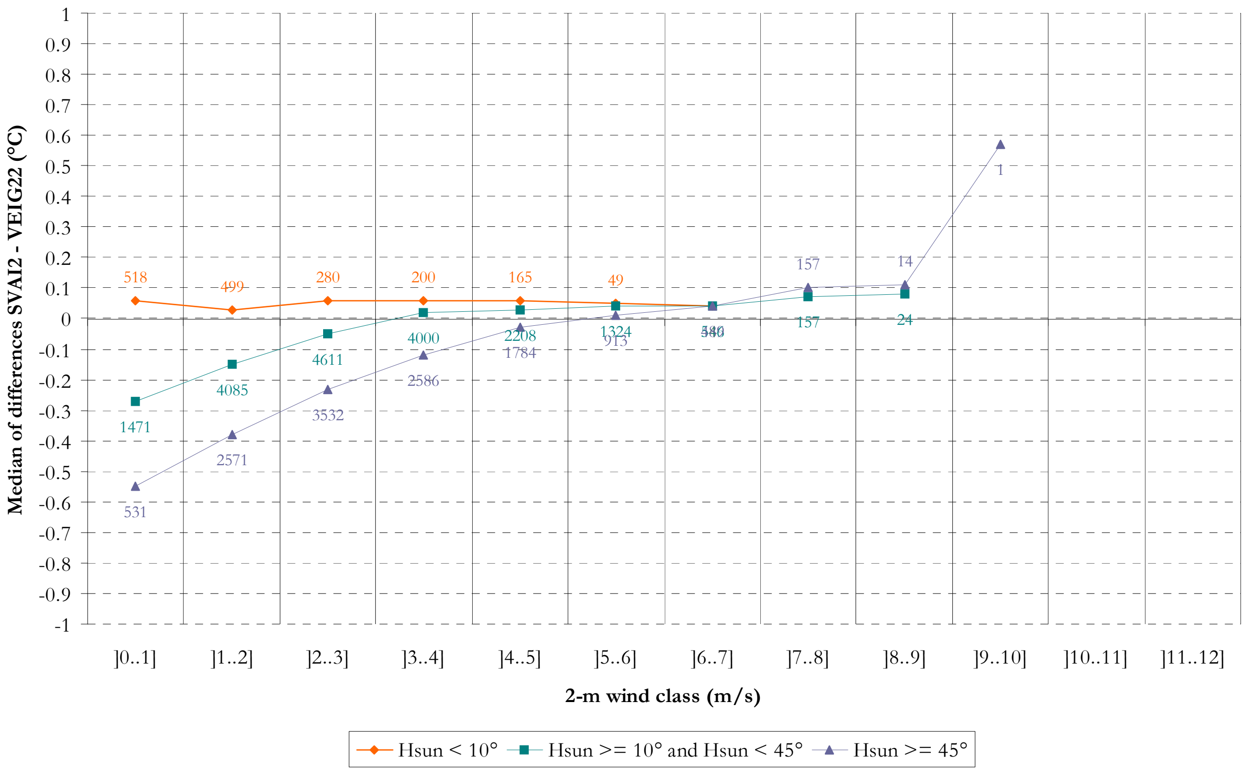


**Figure 16**

For sun elevations of less than 10°, the SVAI screens are just marginally warmer than the reference for all the wind conditions.

In low wind conditions, the medians of both screens are colder when the sun elevations is above 10°, this effect is greater for sun elevation above 45° As the wind increases, the medians of sun elevations greater than 10° get warmer (relative to the reference), and stabilize at about 0.1°C above or below the reference when the wind speed has increases above 4 m/s.

## COMBINED EFFECT OF WIND AND GLOBAL RADIATION

The medians of differences between SVAI and VEIG22 are represented here with a contour plot. The global radiation values are on the X-axis and on the Y axis is the 2-meter wind speed value (2-minute average). Medians are used in all cases, providing that at least one data is available for both conditions on radiation and wind considered.

<u>Screen #1:</u>

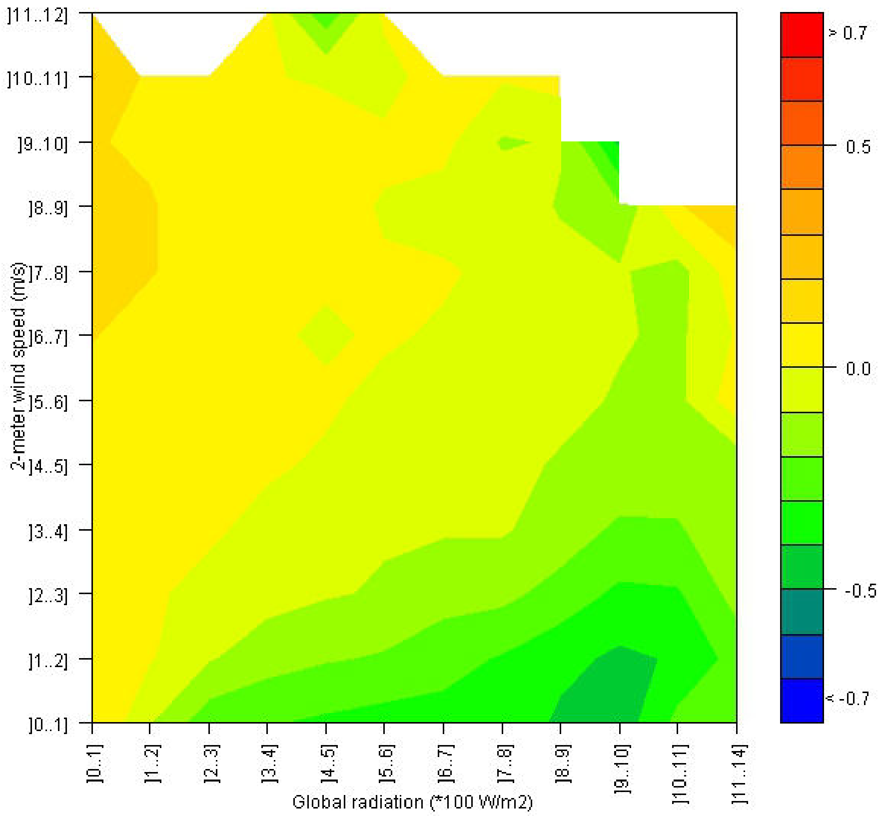


**Figure 17**

Screen #2:

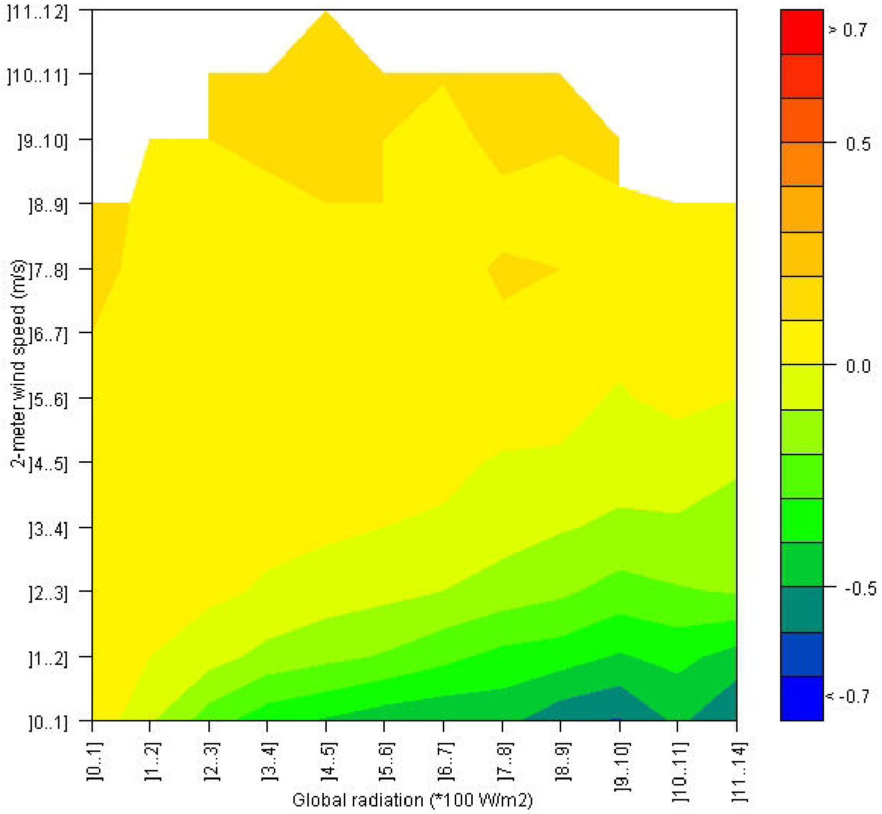


**Figure 18**

Both screens are colder than the reference for high global radiations and low wind speeds, and are warmer than the reference for low global radiations and high wind speeds. However, screen #1 is colder than the reference for almost all the wind conditions when the global radiation is above 600 W/m$^2$, whereas screen #2 is warmer than the reference for almost all global radiation values when the wind speed is greater than 6 m/s.

## BEHAVIOUR DURING INCREASE/DECREASE OF TEMPERATURE

The distribution of differences between SVAI and the reference VEIG22 is plotted, using 1-minute quality checked data for the whole period of the intercomparison. Differences are classified according the temporal gradient of reference temperature over 1 minute. A screen faster (or slower, respectively) than the reference would be warmer (cooler) for positive gradient, cooler (warmer) for negative ones.

## Screen #1:

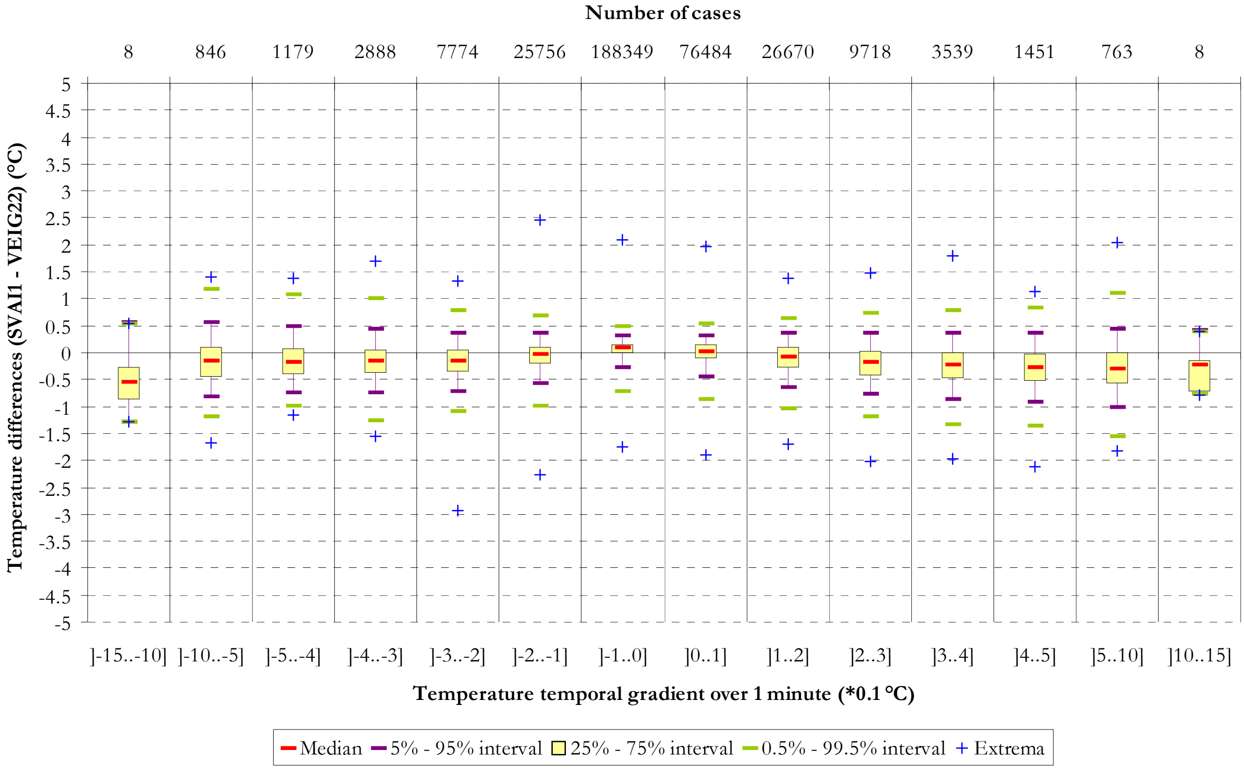


**Figure 19**

## Screen #2:

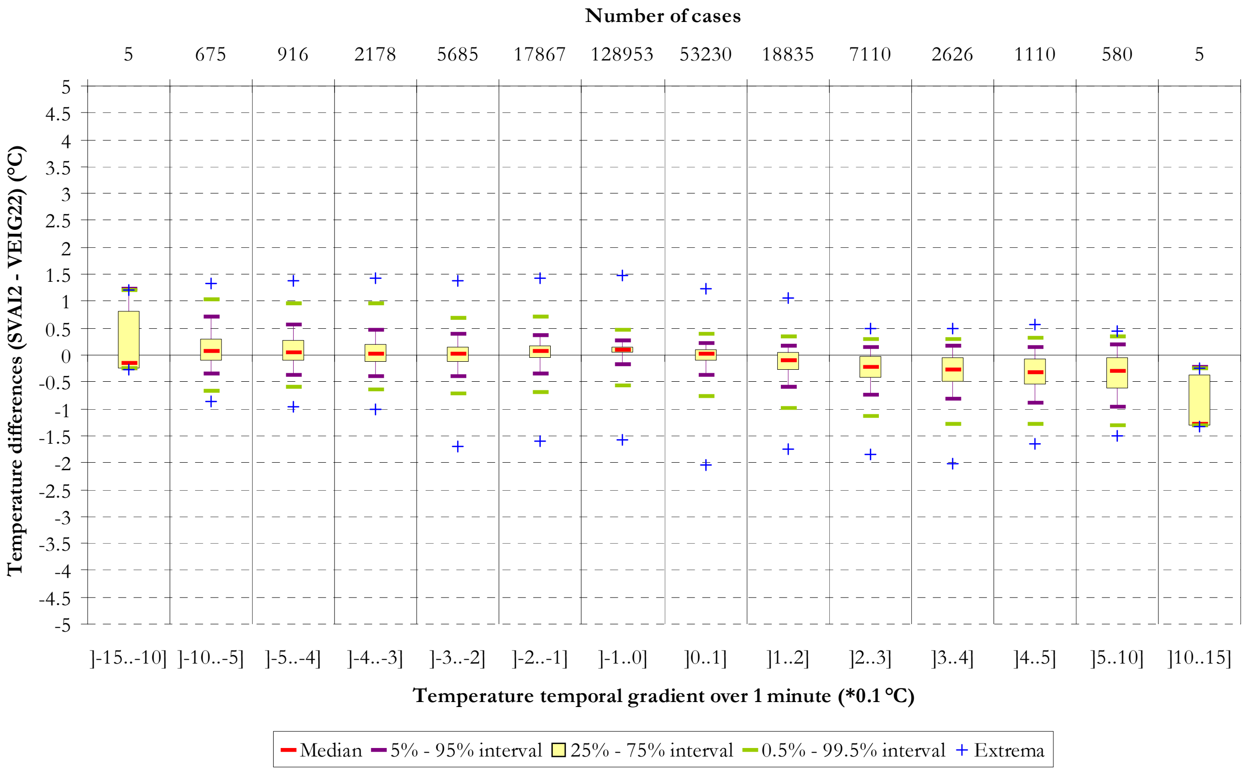


**Figure 20**

The data dispersion increases with the absolute value of the temperature temporal gradient, the two screens agree best with the reference when the temperature gradient is 0.1°.

When the temperature decreases, SVAI screen #1 is slightly colder, faster, than the reference, while SVAI screen #1 is symmetrical about the reference.

When the temperature increases, both screens are colder (slower) than the reference. Ignoring the temperature temporal gradients greater than 1.0°C, the medians of both screens are within 0.5°C of the origin. For both screens, the dispersion increases as the temporal gradient increases in absolute value.

## QUALITY CONTROL INFORMATION

### DATA AVAILABILITY

The intercomparison period extends from the 1st of November 2008 to the 1st of November 2009. The theoretical number of 1-minute data is 525600.

The next table sums up the total number of data for each screen and for each possible QC flag.

**Table 3**

| **QC flag** | SVAI1 | SVAI2 |
|---|---|---|
| 0 (good) | 354748 | 276366 |
| 1 (inconsistent) | 0 | 0 |
| 2 (doubtful) | 0 | 0 |
| 3 (erroneous) | 0 | 0 |
| 7 (missing) | 170852 | 249234 |

The main reason for missing data is frequent failures of the acquisition software, not problems of the sensors

### MAINTENANCE

No actions done during the intercomparison period

# T351-PX-D3 WINDSPEED
# – United Kingdom –
# SWIN

## TECHNICAL SPECIFICATIONS (PROVIDED BY THE MANUFACTURER)

Dimensions: Length 22.5 cm x Width 7.5 cm x Height 15 cm

Weight: 300 g

Material/Structure: ABS, Aluminium, Nylon

Estimated radiation error: 2.3°C/Kw/m$^2$

Aspiration rate (in case of artificially ventilated screen/shield): naturally ventilated

Power supply: none

**Figure 1**

## OVERVIEW

The two SWIN screens are very close to each other for all temperature classes, and their relative difference is only slightly variable with the temperature.

Overall, both SWIN screens are somewhat warmer than the reference, with the mode of the differences between 0°C and 0.2°C, and a symmetrical distribution about the mode. The minimum temperature reported from the two SWIN screens is symmetrically distributed around the reference for screen#2 and just slightly warmer than the reference for screen#1. The maximum temperatures reported from both SWIN screens are consistently higher than the reference, by up to 1.4°C.

The differences between the SWIN screens and the reference vary with the global radiation, being close to zero for very low irradiance and increasing with the increase in irradiance up to 600W/m$^2$, above which the differences are relatively constant.

Both screens were warmer during the day than during the night for the same wind speed, and warmer than the reference. The difference day versus night for the same wind conditions decreased with the increase in wind speed.

Both screens have similar behaviour during the day, under clear sky as well as under overcast conditions, both warmer than the reference, and each warmer under clear sky.

While under clear sky the median of the differences from the reference are relatively constant, decreasing slightly with the increase in wind speed, under overcast conditions for both screens, the median of differences approaches zero for winds around 7m/s, after which increase again up to 0.2°C.

During the night, both screens have similar behaviour under clear sky, as well as under overcast conditions.

The sun elevation only marginally influenced the behaviour of both SWIN screens.

Both SWIN screens were warmer than the reference under all combinations of wind speed and global radiation, becoming warmer for higher values of irradiance.

Both SWIN screens were slower than the reference for negative temperature temporal gradient and faster than the reference for positive temperature gradients.

## CALIBRATION INFORMATION

The calibration of both probes was performed in Trappes.

**Table 1**

| Screen | Location | Screen serial number | Calibration date | Instrument bias (°C) | | | |
|---|---|---|---|---|---|---|---|
| | | | | -20°C | 0°C | 20°C | 40°C |
| SWIN1 | E2 | 1398 | 14-Mar-2007 | 0.0145 | -0.0335 | -0.0727 | -0.1070 |
| SWIN2 | E5 | 1397 | 14-Mar-2007 | 0.0148 | -0.0381 | -0.0825 | -0.1232 |

The result of calibration of reference VEIG22 is available in the main report of the intercomparison, section 5.4.1.

## COMPARISON OF BOTH SENSORS

The distribution of differences between screen 1 and screen 2 is plotted, using 1-minute quality checked data for the whole period of the intercomparison. Differences are classified according screen 1 temperature.

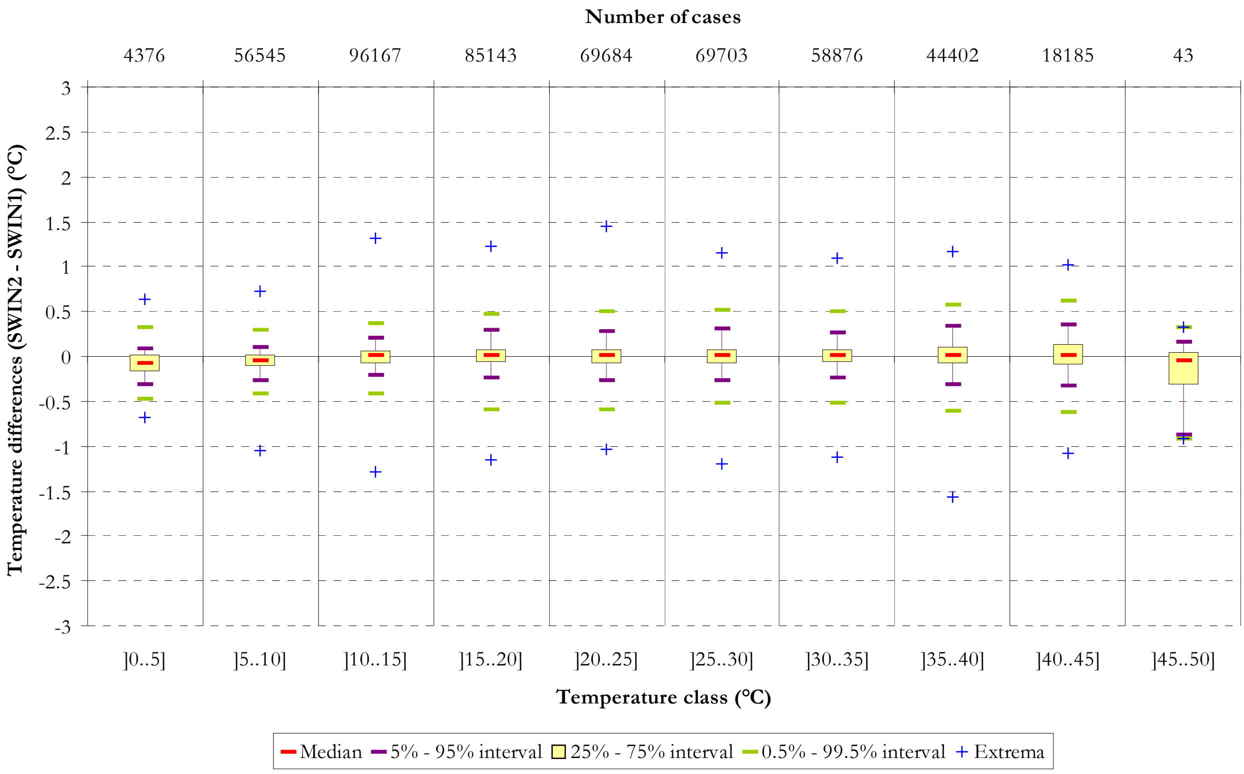


**Figure 2**

The two SWIN screen are very close to each other for all temperature classes, and their relative difference is only slightly variable with the temperature.

## COMPARISON WITH THE REFERENCE

### HISTOGRAM OF DIFFERENCES

The histogram of differences between SWIN and the reference VEIG22 is plotted, using 1-minute quality checked data for the whole period of the intercomparison. Differences are plotted by steps of 0.1K. The vertical axis is the frequency in percent for each class of differences.

Screen #1:

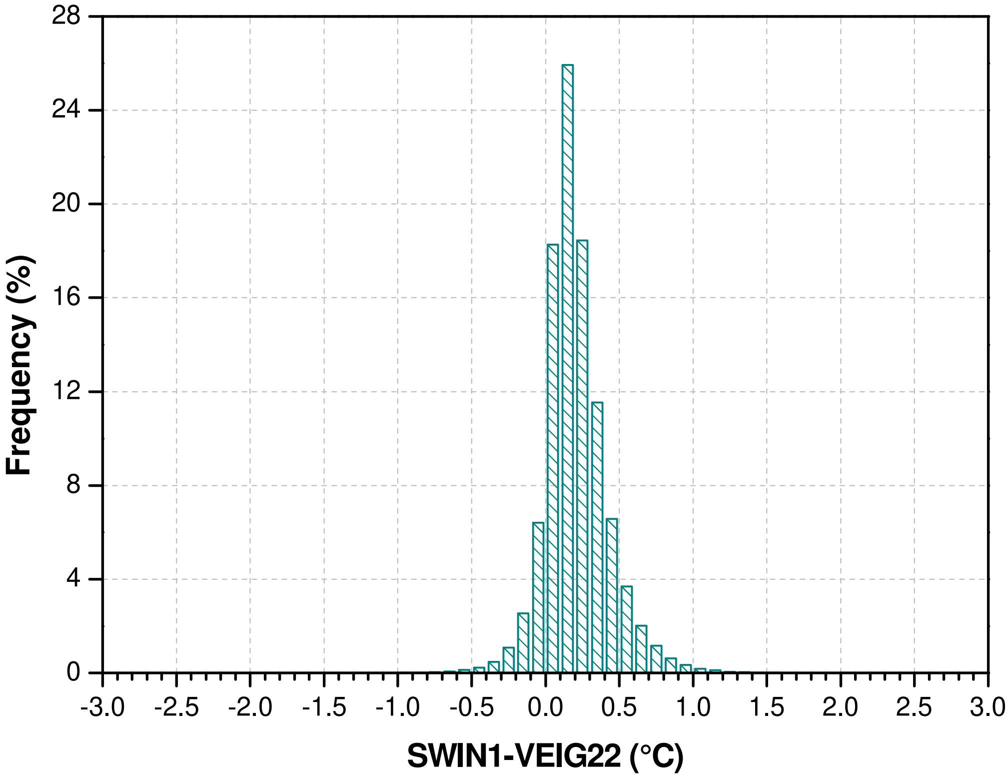


**Figure 3**

Screen #2:

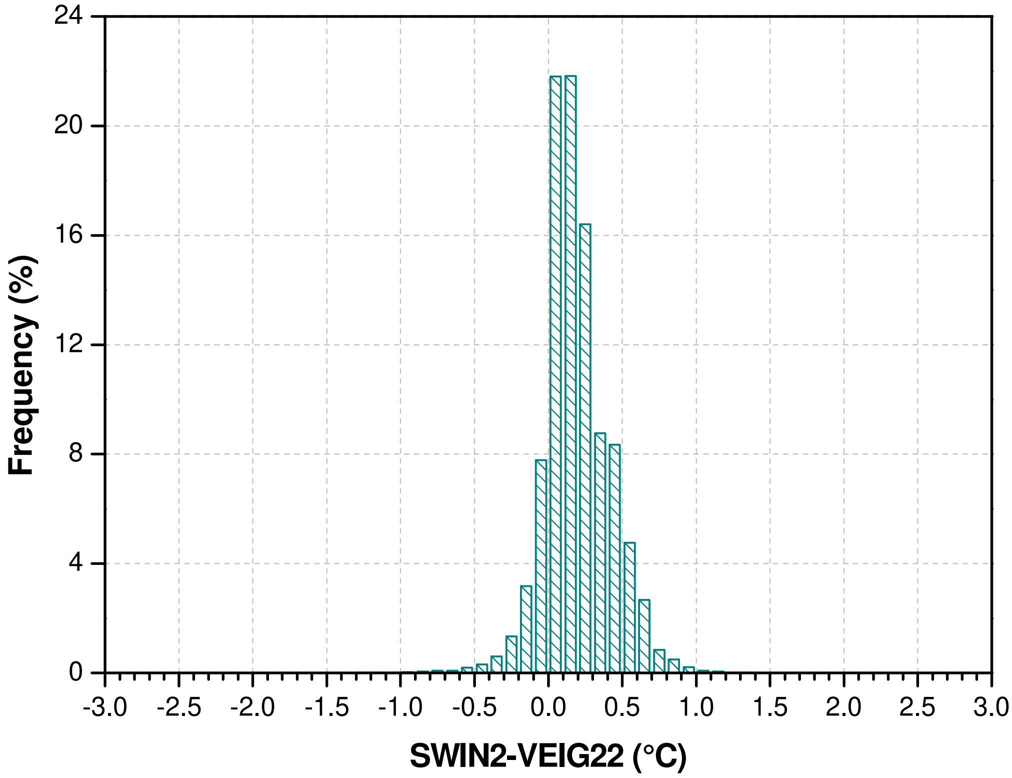


**Figure 4**

Overall, both SWIN screens are somewhat warmer than the reference, with the mode of the differences between 0°C and 0.2°C, and a symmetrical distribution about the mode.

CUMULATIVE HISTOGRAMS OF DIFFERENCES OF DAILY EXTREME VALUES

The cumulative histograms of differences with the reference VEIG22 of T (1-minute quality checked data), Tn (daily minimum temperature) and Tx (daily maximum temperature) are plotted, for the whole period of the intercomparison. Differences are plotted by steps of 0.1K.

Screen #1:

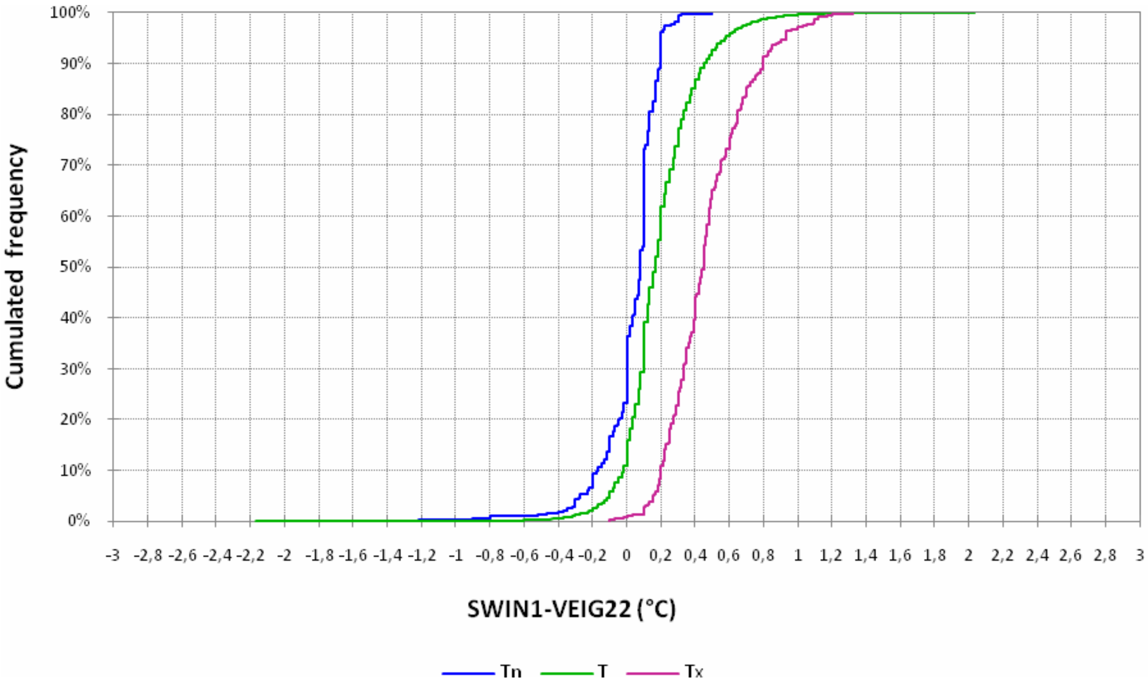


**Figure 5**

Screen #2:

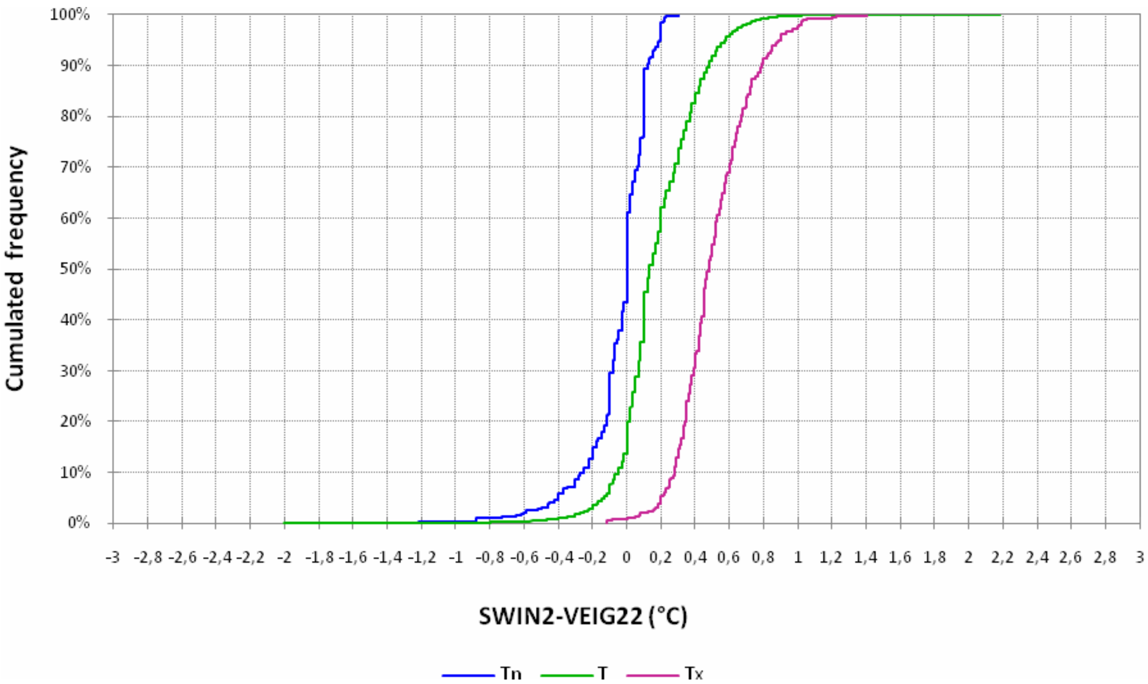


**Figure 6**

The minimum temperature reported from the two SWIN screens is symmetrically distributed around the reference for screen#2 and just slightly warmer than the reference for screen#1.

The maximum temperatures reported from both SWIN screens are consistently higher than the reference, by up to 1.4°C.

TABLE

The table 2 indicates the percentage of data that differ by less than 0.2°C (and 0.5°C) from the reference.

**Table 2**

| | | [-0.2°..0.2°] | [-0.5°..0.5°] |
|---|---|---|---|
| SWIN1 | T | 59.7 | 92.3 |
| | Tn | 87.9 | 98.8 |
| | Tx | 10.5 | 65.1 |
| SWIN2 | T | 59.3 | 91.5 |
| | Tn | 85.1 | 97.2 |
| | Tx | 5.0 | 54.9 |

## INFLUENCE OF GLOBAL RADIATION

The distribution of differences between SWIN and the reference VEIG22 is plotted, using 1-minute quality checked data for the whole period of the intercomparison. Differences are classified according global radiation.

Screen #1:

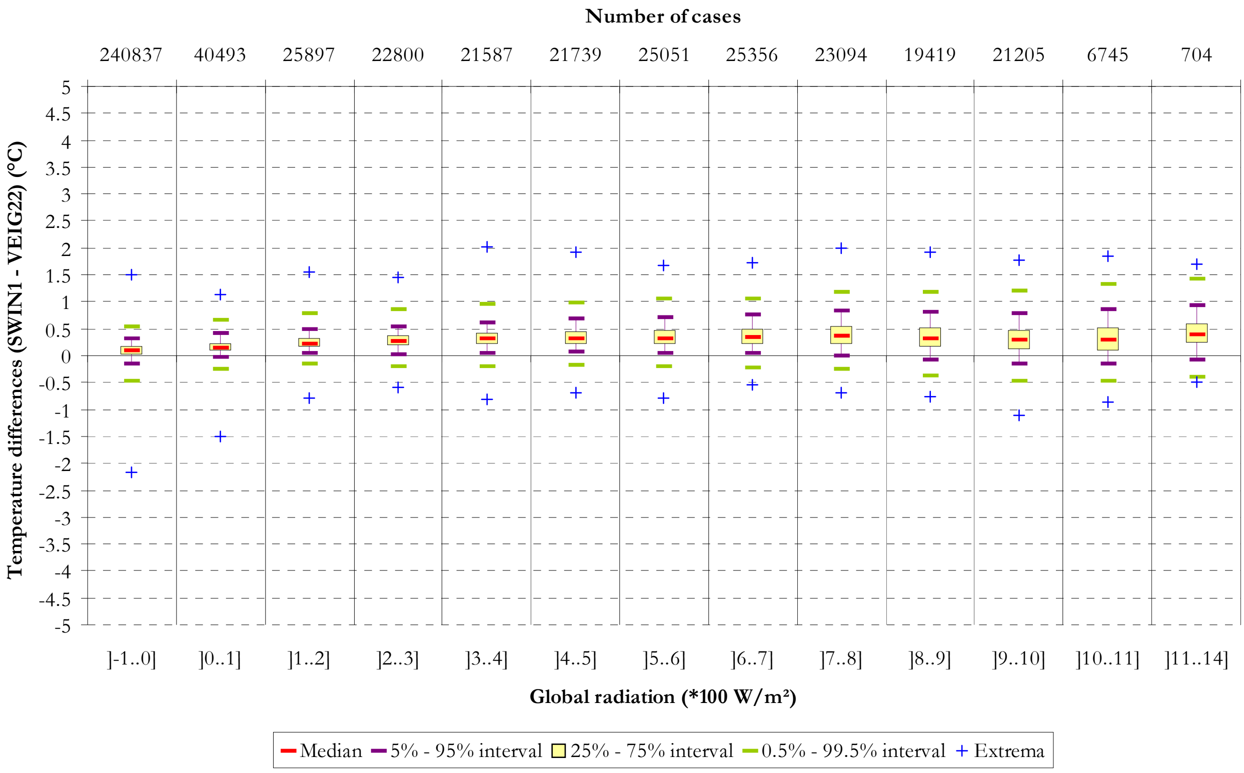


**Figure 7**

Screen #2:

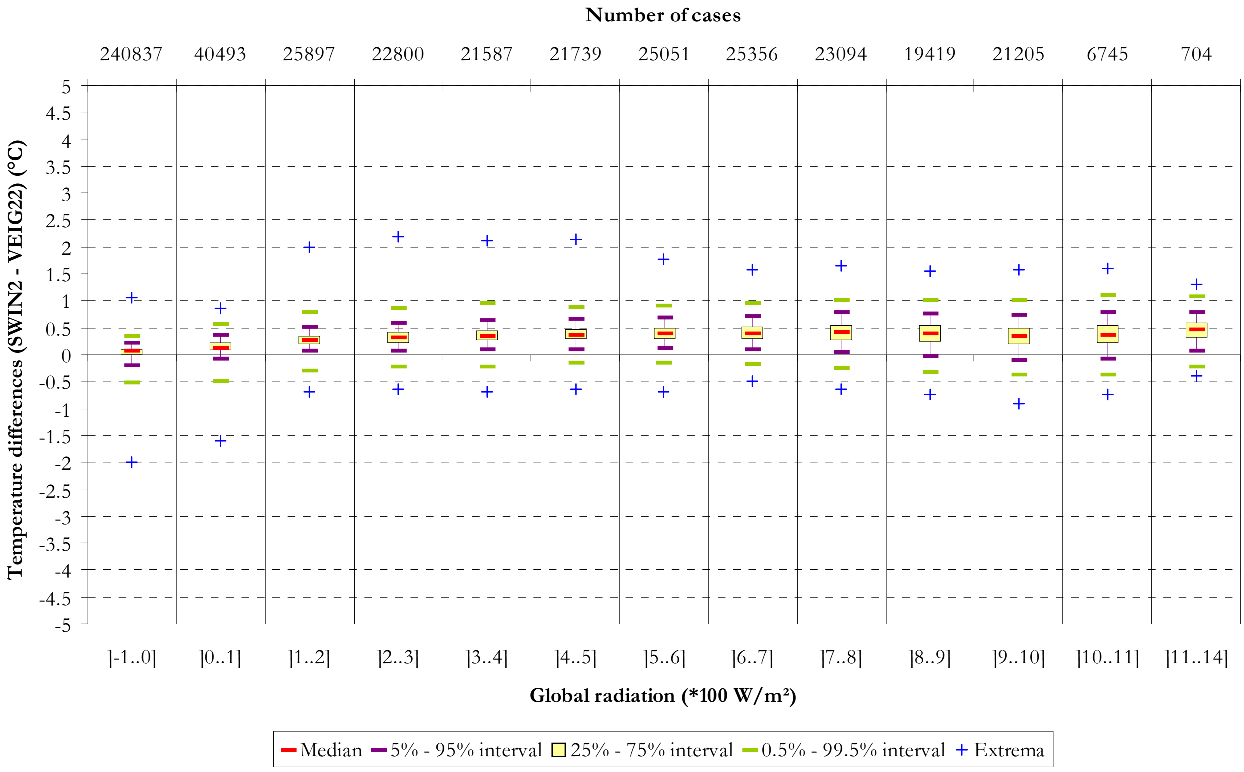


**Figure 8**

The differences between the SWIN screens and the reference vary with the global radiation, being close to zero for very low irradiance and increasing with the increase in irradiance up to 600W/m$^2$, above which the differences are relatively constant.

## RADIATION EFFECT

### DIFFERENCES BETWEEN DAY AND NIGHT BEHAVIOUR

The median of differences between SWIN and VEIG22 is plotted, using 1-minute quality checked data for the whole period of the intercomparison. We filter data for which sun elevation is above -1° (day) or below -1° (night). Differences are classified according 2-meter wind speed (2-minute average).

Screen #1:

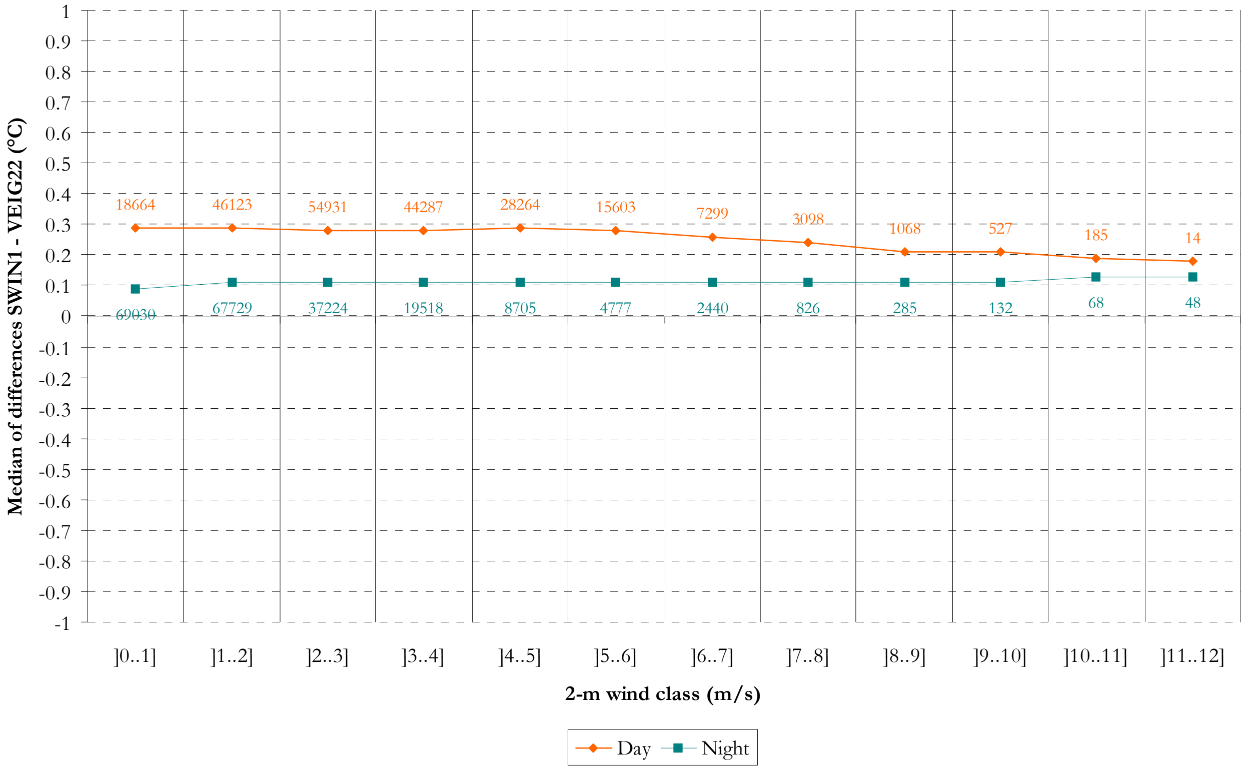


**Figure 9**

Screen #2:

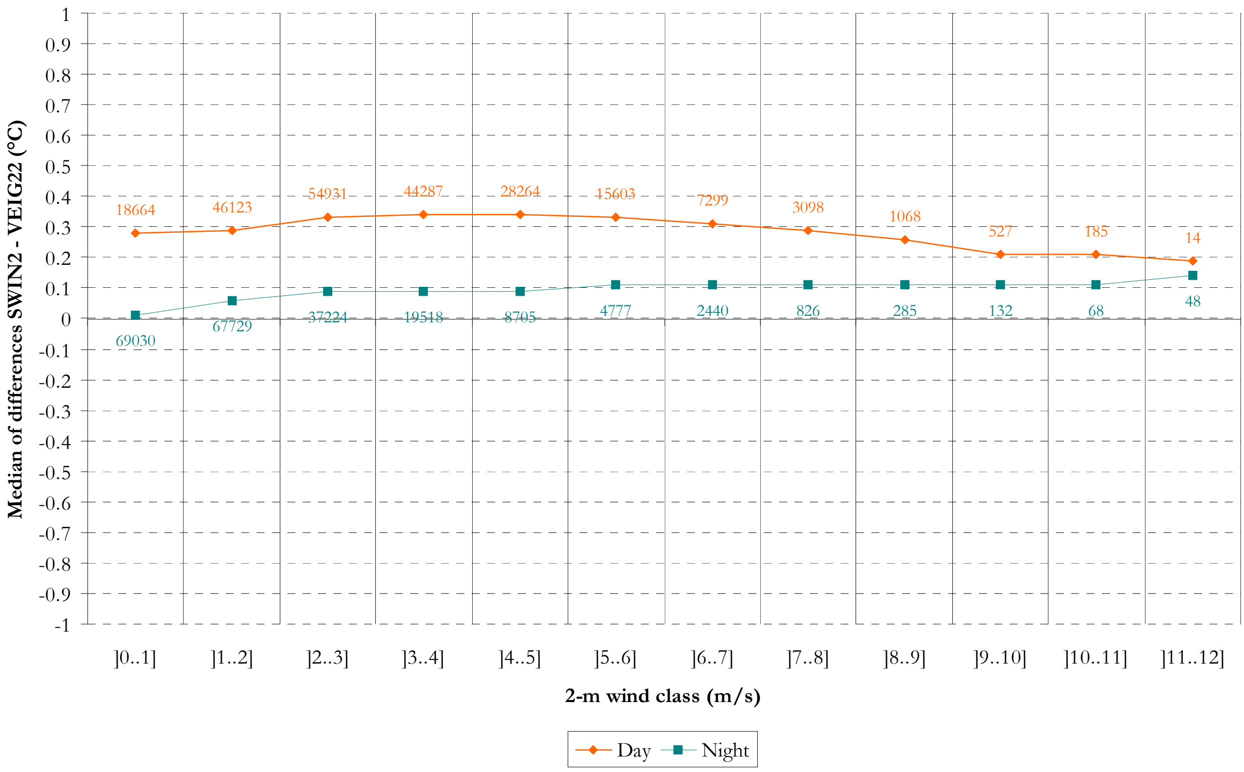


**Figure 10**

Both screens were warmer during the day than during the night for the same wind speed, and warmer than the reference.

The difference day versus night for the same wind conditions decreased with the increase in wind speed.

## DIFFERENCES BETWEEN CLEAR SKY AND OVERCAST SKY DURING DAYTIME

The median of differences between SWIN and VEIG22 is plotted, using 1-minute quality checked data. Here, we consider periods lasting six hours at least where cloudiness is less or equal to 1 (clear sky) or more or equal to 7 (overcast sky), during daytime (sun elevation above -1°). Differences are classified according 2-meter wind speed (2-minute average).

<u>Screen #1:</u>

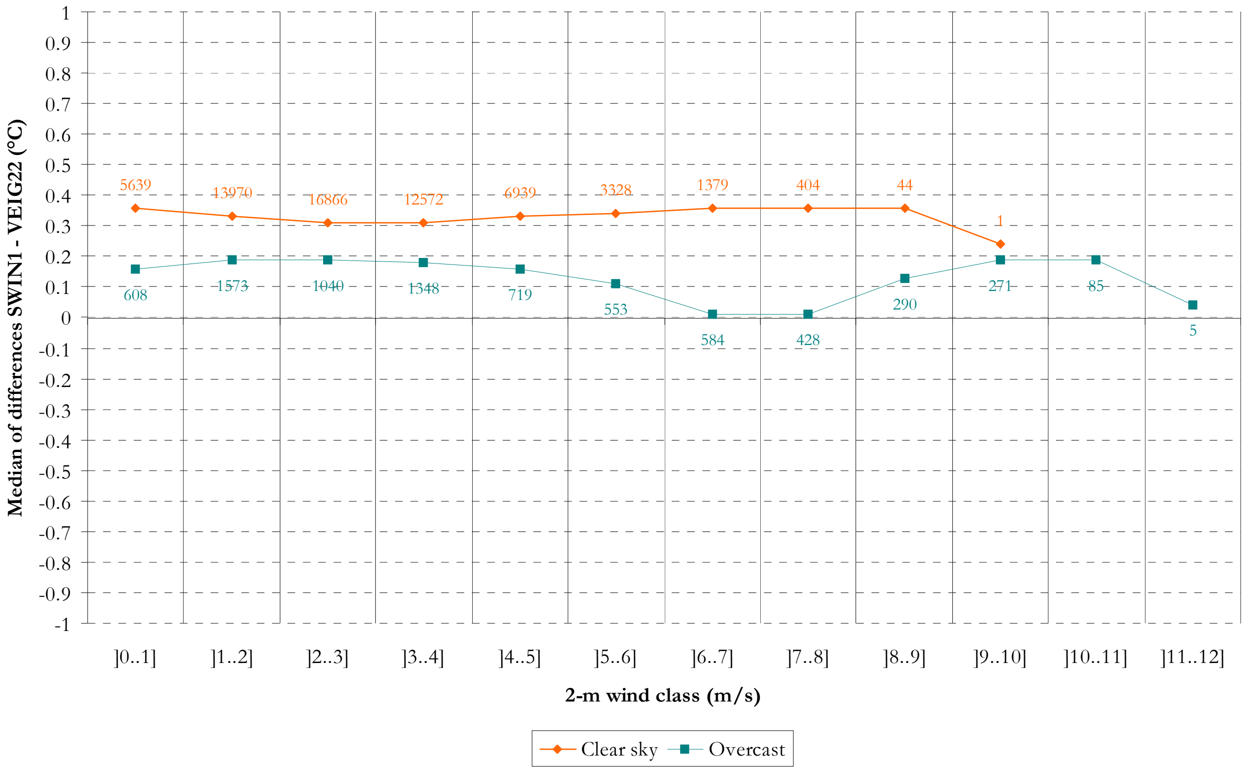


**Figure 11**

Screen #2:

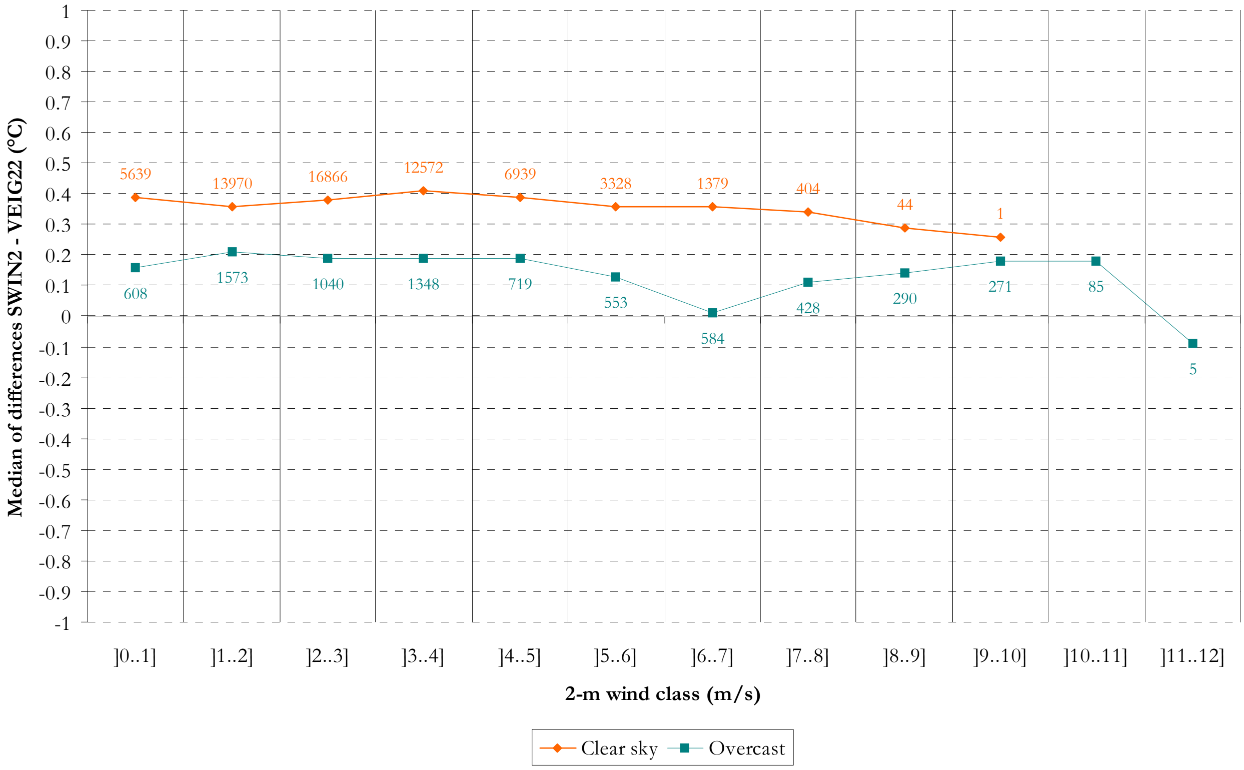


**Figure 12**

Both screens have similar behaviour during the day, under clear sky as well as under overcast conditions, both warmer than the reference, and each warmer under clear sky.

While under clear sky the median of the differences from the reference are relatively constant, decreasing slightly with the increase in wind speed, under overcast conditions for both screens, the median of differences approaches zero for winds around 7m/s, after which increase again up to 0.2°C.

## DIFFERENCES BETWEEN CLEAR SKY AND OVERCAST SKY DURING NIGHT TIME

The median of differences between SWIN and VEIG22 is plotted, using 1-minute quality checked data. Here, we consider periods lasting six hours at least where cloudiness is less or equal to 1 (clear sky) or more or equal to 7 (overcast sky), during night time (sun elevation below -1°). Differences are classified according 2-meter wind speed (2-minute average).

Screen #1:

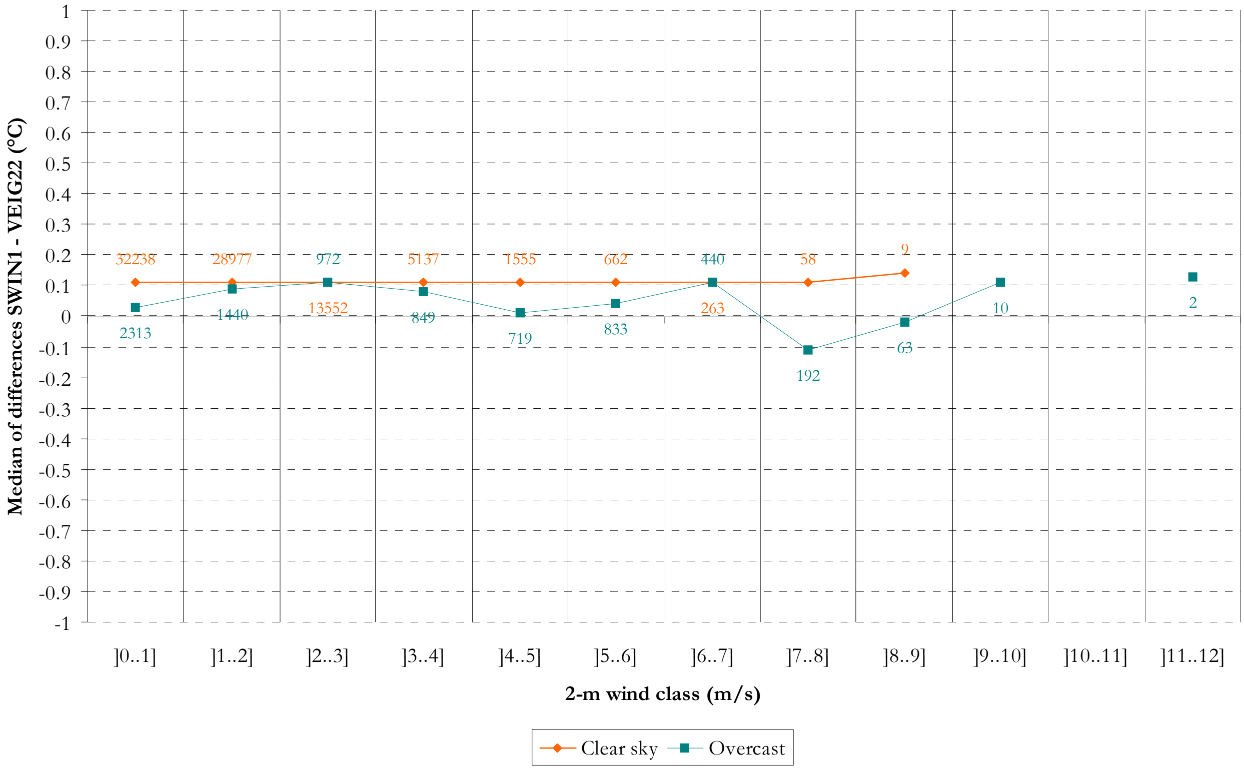


**Figure 13**

Screen #2:

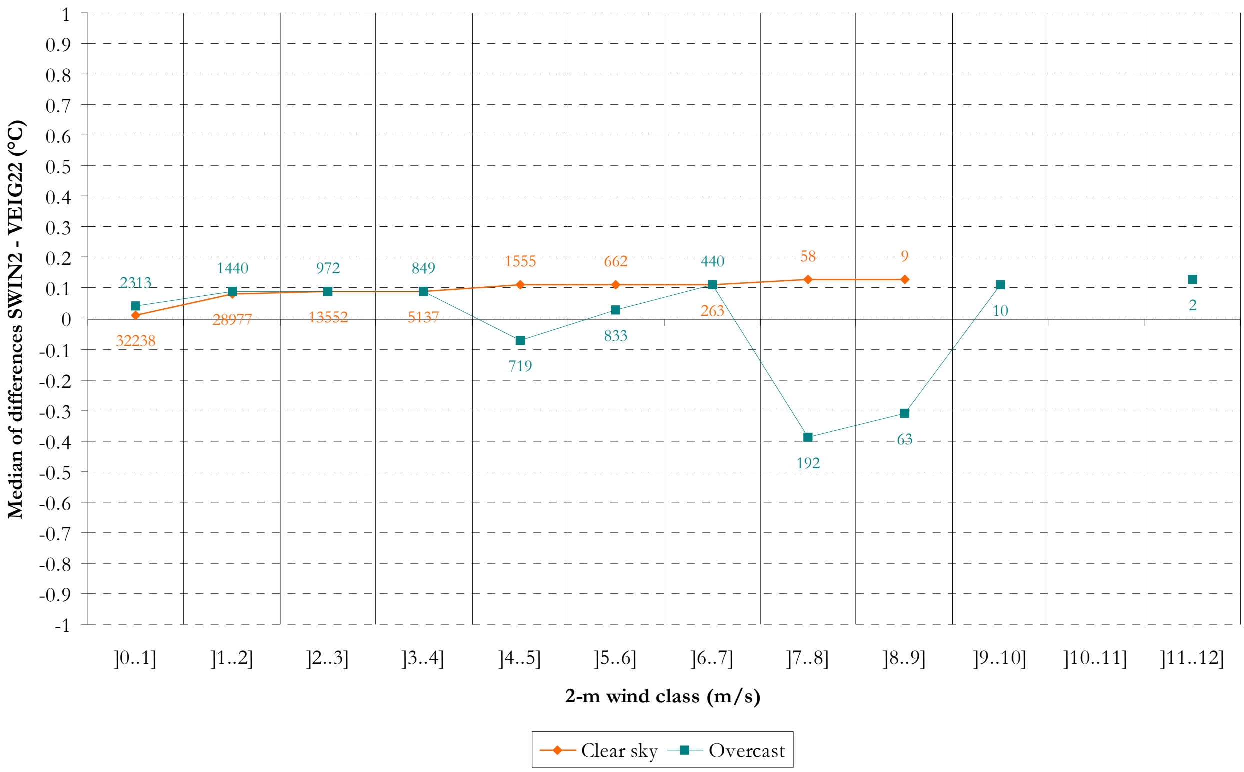


**Figure 14**

During the night, both screens have similar behaviour under clear sky, as well as under overcast conditions. Under clear sky both screens are slightly warmer than the reference by an approximately constant amount, less than 0.1°C.

Under overcast conditions, both screens displayed a variable behaviour, varying with the wind speed, with several peaks and lows.

## EFFECT OF SUN ELEVATION

The median of differences between SWIN and VEIG22 is plotted, using 1-minute quality checked data. Here, we consider periods lasting six hours at least where cloudiness is less or equal to 1 (clear sky), during daytime (sun elevation above -1°). We filter data where sun elevation is low (below 10°), medium (between 10° and 45°) or high (above 45°). Differences are classified according 2-meter wind speed (2-minute average).

Screen #1:

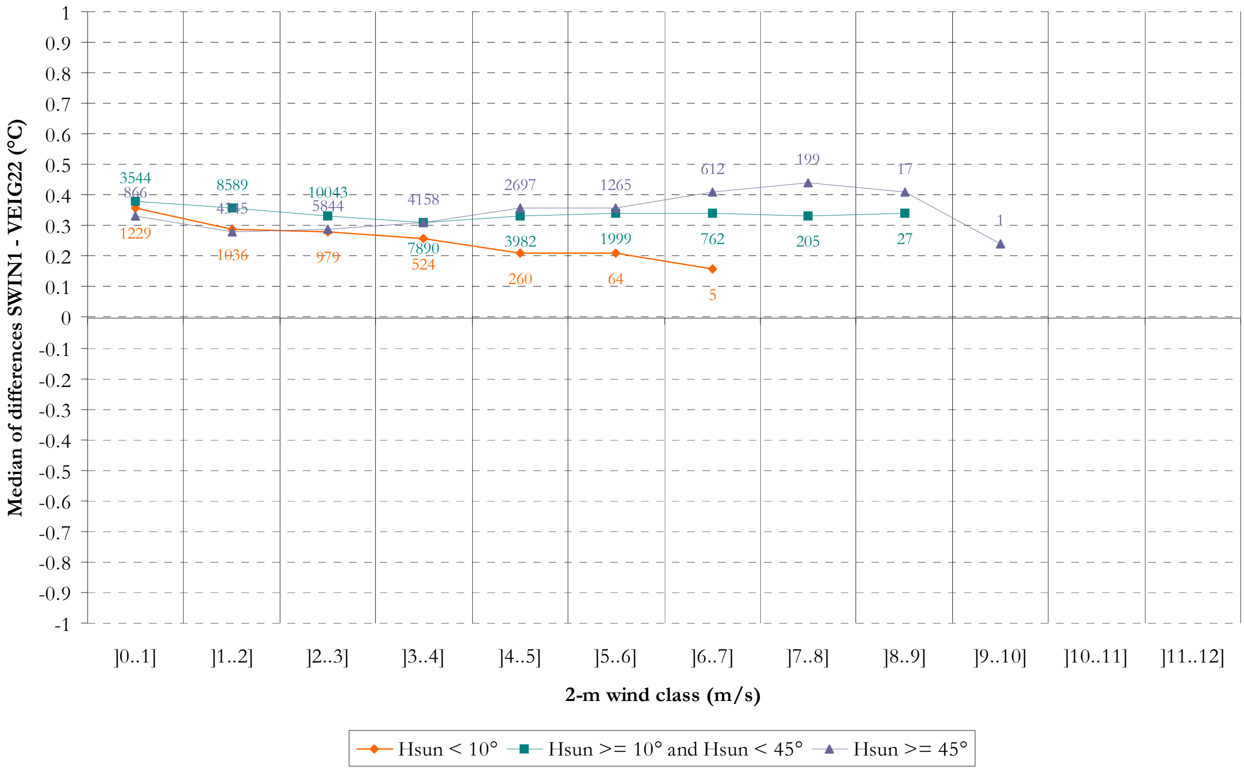


**Figure 15**

Screen #2:

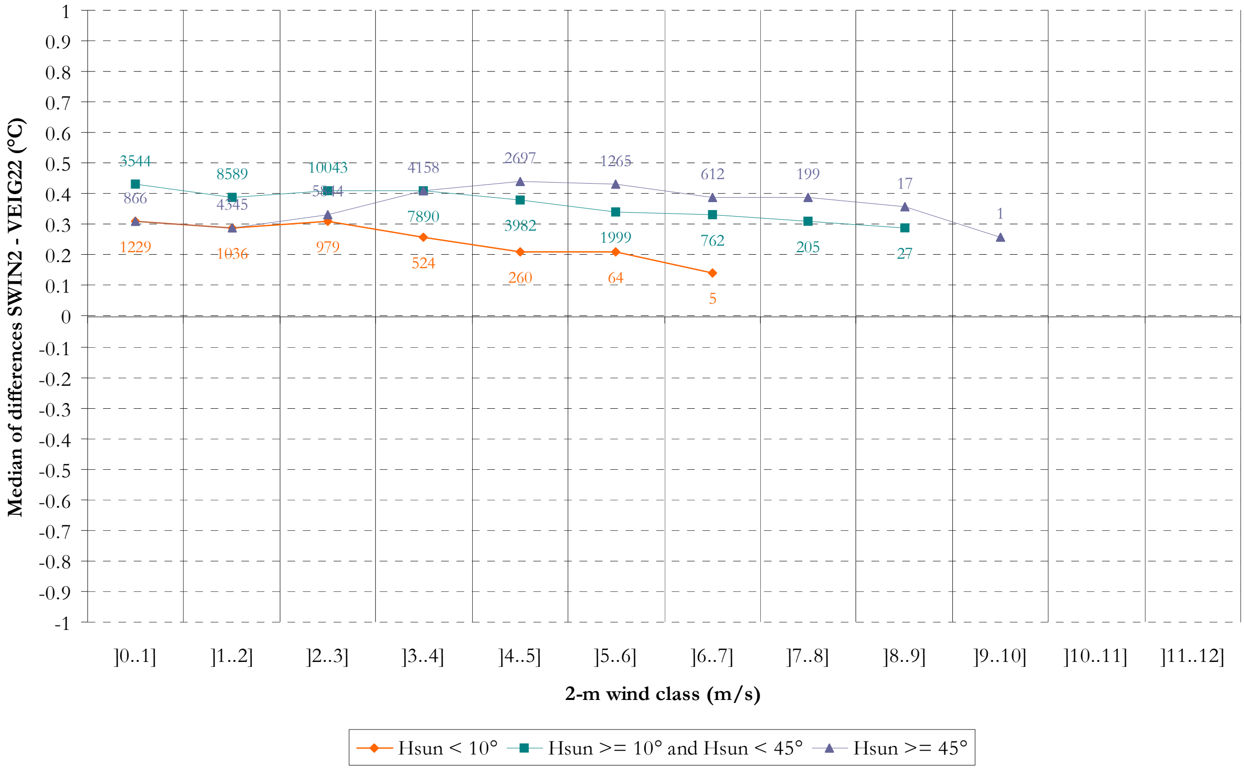


**Figure 16**

The sun elevation only marginally influenced the behaviour of both SWIN screens. The screens were warmer than the reference for all sun elevations, being the coldest for sun elevations below 10°. The medians of differences for each sun elevation class, for all classess of wind speed are within less than 0.3°C.

## COMBINED EFFECT OF WIND AND GLOBAL RADIATION

The medians of differences between SWIN and VEIG22 are represented here with a contour plot. The global radiation values are on the X-axis and on the Y axis is the 2-meter wind speed value (2-minute average). Medians are used in all cases, providing that at least one data is available for both conditions on radiation and wind considered.

Screen #1:

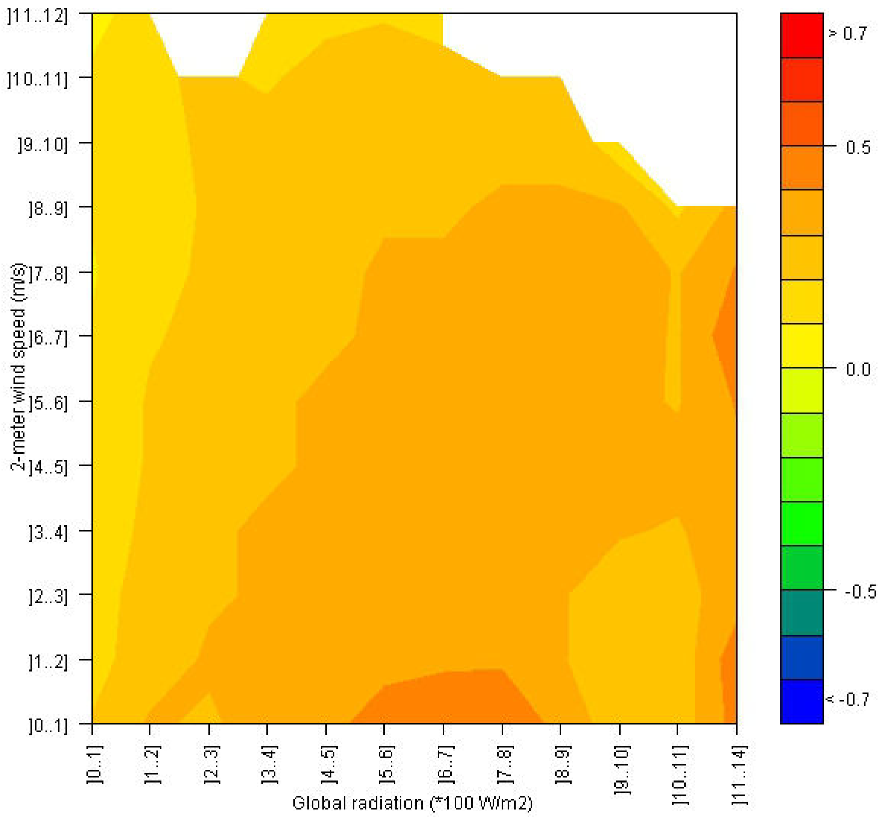


**Figure 17**

Screen #2:

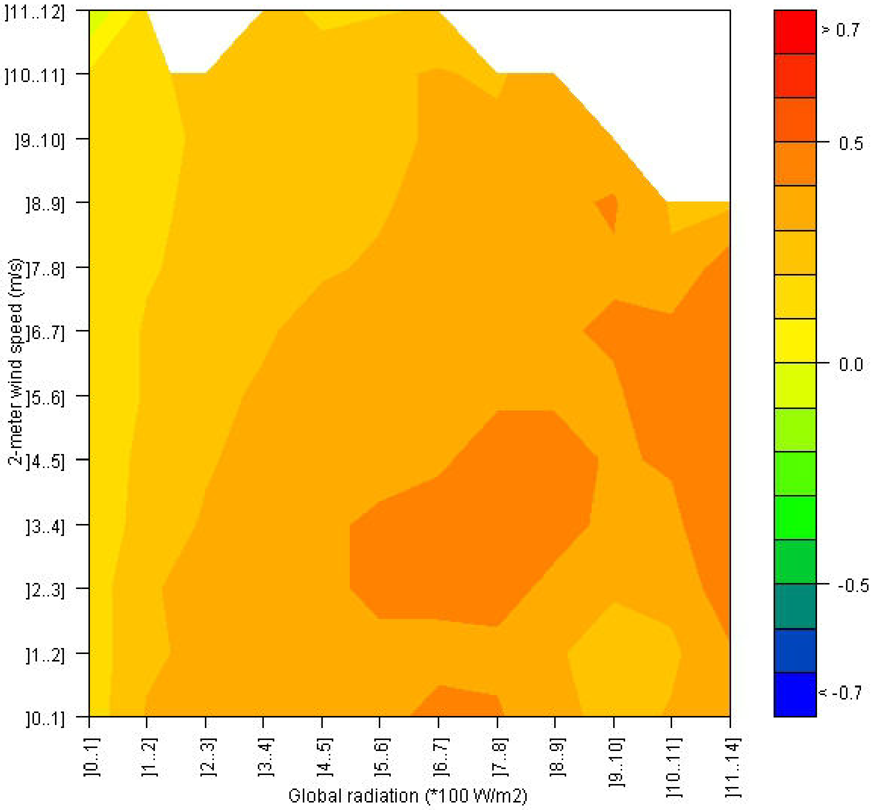


**Figure 18**

Both SWIN screens were warmer than the reference under all combinations of wind speed and global radiation, becoming warmer for higher values of irradiance.

## BEHAVIOUR DURING INCREASE/DECREASE OF TEMPERATURE

The distribution of differences between SWIN and the reference VEIG22 is plotted, using 1-minute quality checked data for the whole period of the intercomparison. Differences are classified according the temporal gradient of reference temperature over 1 minute. A screen faster (or slower, respectively) than the reference would be warmer (cooler) for positive gradient, cooler (warmer) for negative ones.

Screen #1:

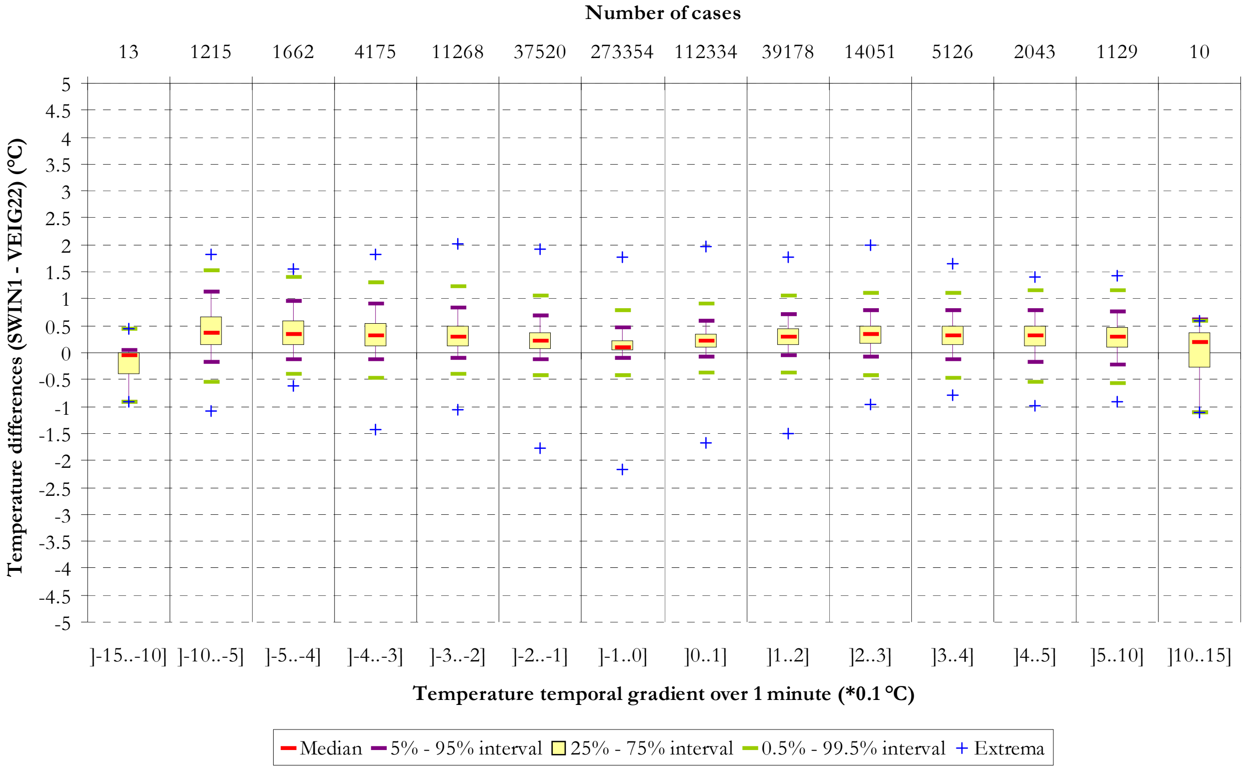


**Figure 19**

Screen #2:

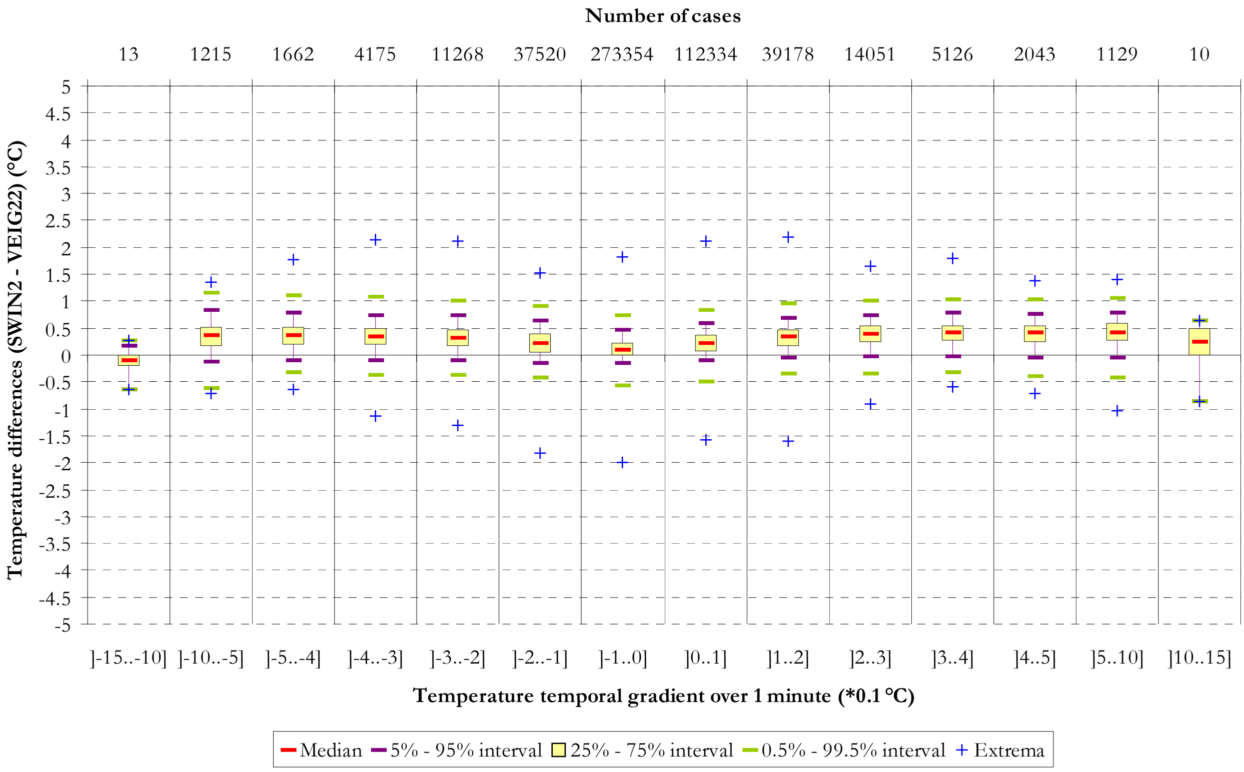


**Figure 20**

Both SWIN screens were slower than the reference for negative temperature temporal gradient and faster than the reference for positive temperature gradients.

## QUALITY CONTROL INFORMATION

### DATA AVAILABILITY

The intercomparison period extends from the 1st of November 2008 to the 1st of November 2009. The theoretical number of 1-minute data is 525600.

The next table sums up the total number of data for each screen and for each possible QC flag.

**Table 3**

| **QC flag** | SWIN1 | SWIN2 |
|---|---|---|
| 0 (good) | 503266 | 503266 |
| 1 (inconsistent) | 0 | 0 |
| 2 (doubtful) | 0 | 0 |
| 3 (erroneous) | 0 | 0 |
| 7 (missing) | 22334 | 22334 |

### MAINTENANCE

No action done during the intercomparison period.

# 07714 DAVIS
# – USA –
# SDAV

**TECHNICAL SPECIFICATIONS (PROVIDED BY THE MANUFACTURER)**

Dimensions: Length 21 cm x Width 18.5 cm x Height 14.5 cm

Weight: 1 kg

Material/Structure: plastic

Estimated radiation error: 2°C

Aspiration rate (in case of artificially ventilated screen/shield): naturally ventilated

Power supply: none

**Figure 1**

Temperature measurements are made with small glass Pt100 probes.

## OVERVIEW

The screens are naturally ventilated.

Over the duration of the intercomparison, the two screens demonstrated a consistent behaviour: the temperatures reported from the two screens remained within +/-0.4 °C of each other, and within +/-0.4 °C of the reference for screen 1, and +/-0.3 °C of the reference for screen 2, for 95% of data points and for all classes of temperature registered at the site.

For both screens the Tn, T, and Tx curves follow each other closely, and their relativity is similar, with Tn being the closest to the reference.

The two screens show different day and night behaviour, with respect to the reference and is a function of the wind speed, primarily for the daytime. During the daytime, the two screens are colder than the reference for wind speeds below 7 m/s for screen 1 and 4 m/s for screen 2.

Also, during the daytime, the two screens are consistently colder under clear sky than under an overcast sky, for the same wind conditions. The differences relative to the reference at low wind speeds are very close to those registered for high wind speeds.

At night, for the same wind conditions, there isn't a significant difference between clear sky and overcast sky behaviour for either of the two screens, over the entire range of wind speeds.

The two screens display similar behaviour function of sun elevation, being the coldest for sun elevations over $45^o$ and low wind speeds.

The intercomparison shows the general tendency of the two screens to be marginally colder than the reference for the entire range of wind speeds and global radiation reported at the site. The screens are the coldest at high global radiation, around $900 W/m^2$, and wind speeds below 2m/s.

The two screens are just marginally colder (slower) than the reference for the entire range of temperature gradients assessed.

## CALIBRATION INFORMATION

The calibration of both probes was performed in Trappes.

**Table 1**

| Screen | Location | Pt100 probe serial number | Calibration date | Instrument bias (°C) | | | |
|---|---|---|---|---|---|---|---|
| | | | | -20°C | 0°C | 20°C | 40°C |
| SDAV1 | A2 | UT68 | 3-May-2004 | 0.0850 | 0.0450 | 0.0160 | -0.0120 |
| SDAV2 | A5 | UT46 | 1-Apr-2004 | 0.0590 | 0.0200 | -0.0080 | -0.0380 |

The result of calibration of reference VEIG22 is available in the main report of the intercomparison, section 5.4.1.

## COMPARISON OF BOTH SENSORS

The distribution of differences between screen 1 and screen 2 is plotted, using 1-minute quality checked data for the whole period of the intercomparison. Differences are classified according screen 1 temperature.

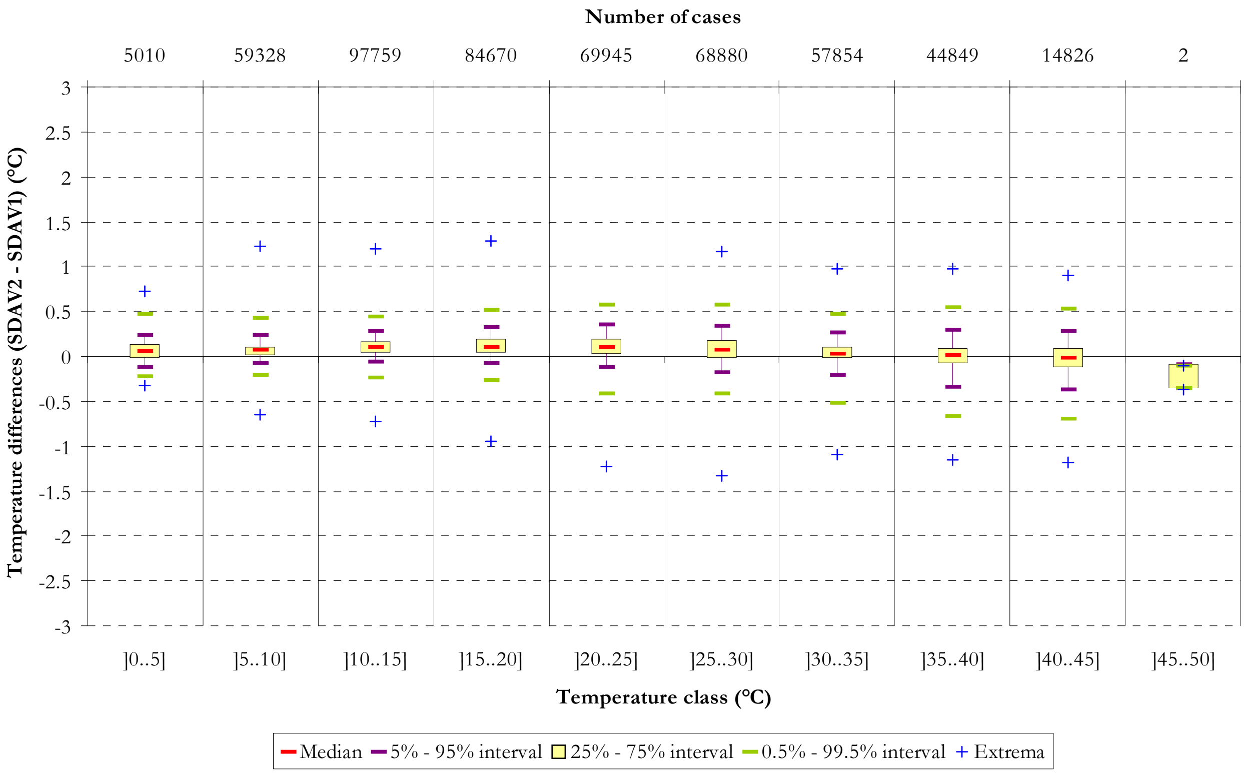


**Figure 2**

Over the duration of the intercomparison, the two screens demonstrated a consistent behaviour: the temperatures reported from the two screens remained within +/-0.4 °C of each other, for 95% of data points and for all classes of temperature registered at the site.

## COMPARISON WITH THE REFERENCE

### HISTOGRAM OF DIFFERENCES

The histogram of differences between SDAV and the reference VEIG22 is plotted, using 1-minute quality checked data for the whole period of the intercomparison. Differences are plotted by steps of 0.1K. The vertical axis is the frequency in percent for each class of differences.

Screen #1:

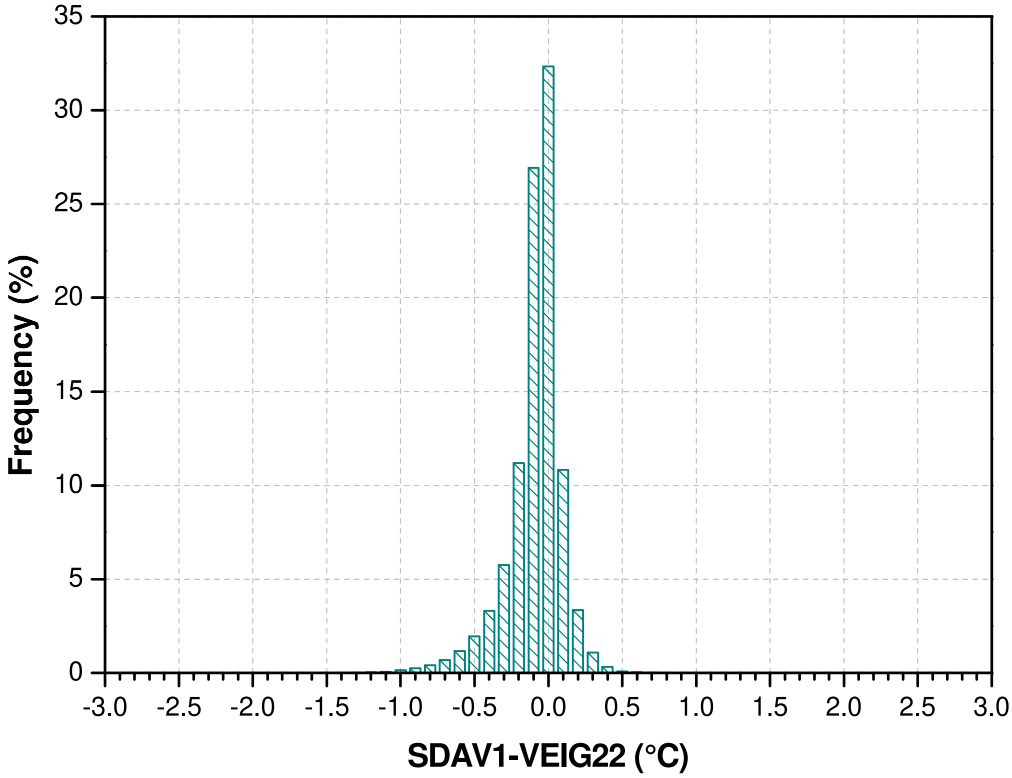


**Figure 3**

Screen #2:

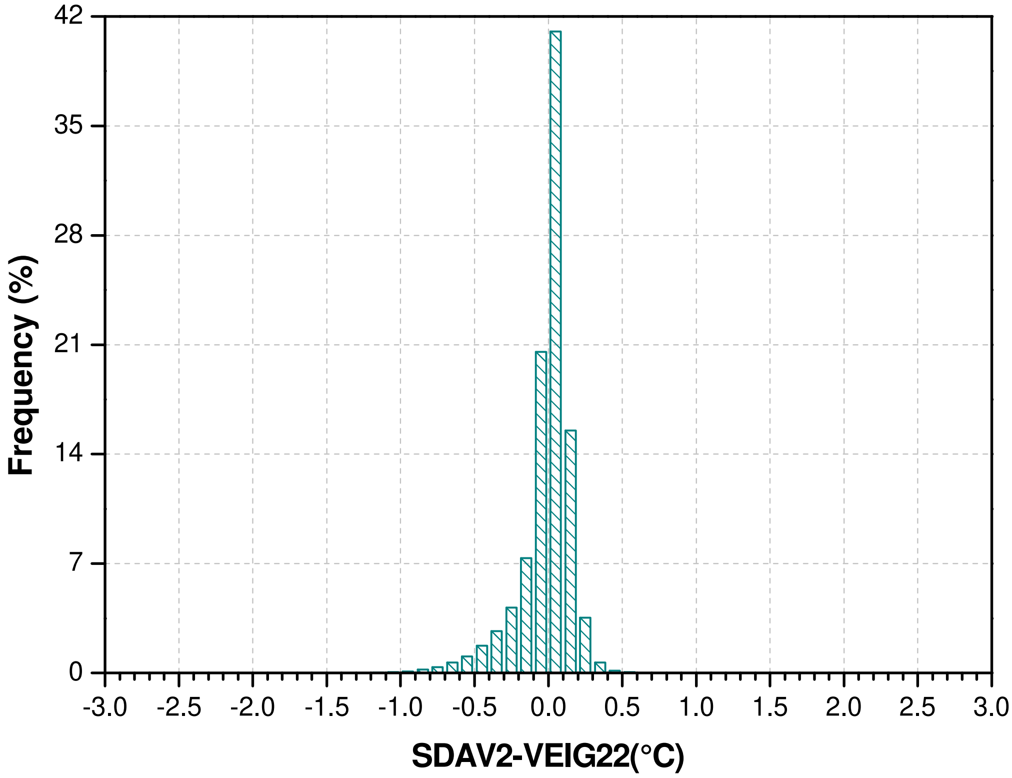


**Figure 4**

The temperatures reported from the two screens were within +/-0.4 °C of the reference for screen 1, and within +/-0.3 °C of the reference for screen 2, for 95% of the data points reported from each screen.

CUMULATIVE HISTOGRAMS OF DIFFERENCES OF DAILY EXTREME VALUES

The cumulative histograms of differences with the reference VEIG22 of T (1-minute quality checked data), Tn (daily minimum temperature) and Tx (daily maximum temperature) are plotted, for the whole period of the intercomparison. Differences are plotted by steps of 0.1K.

Screen #1:

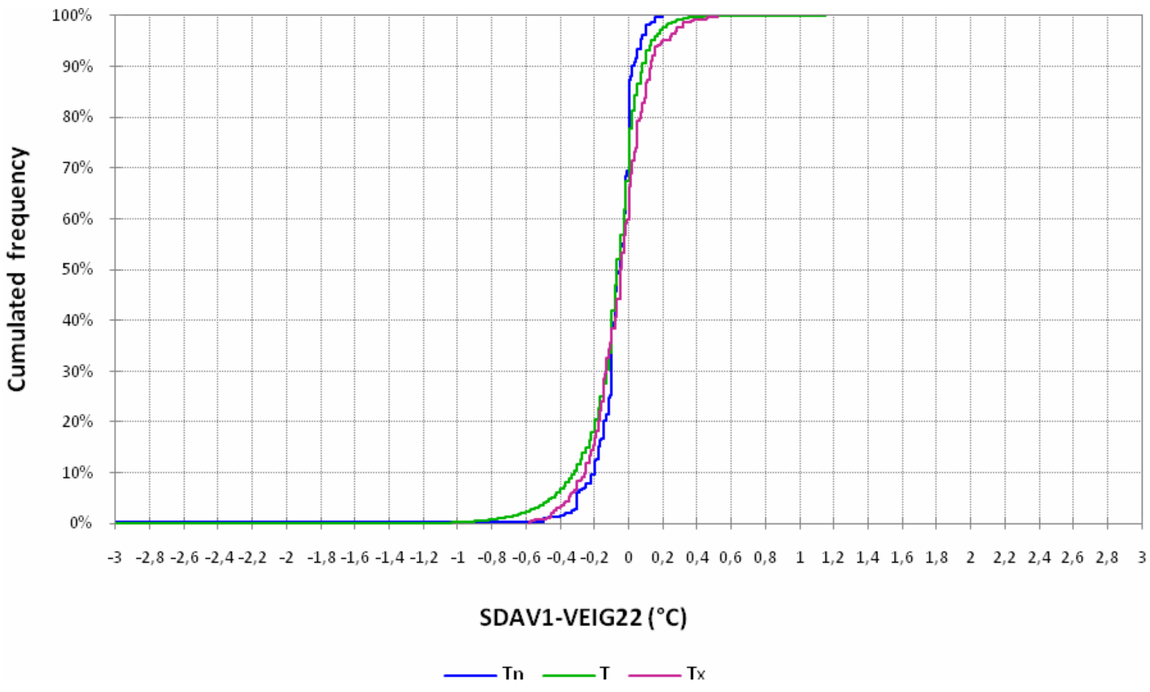


**Figure 5**

Screen #2:

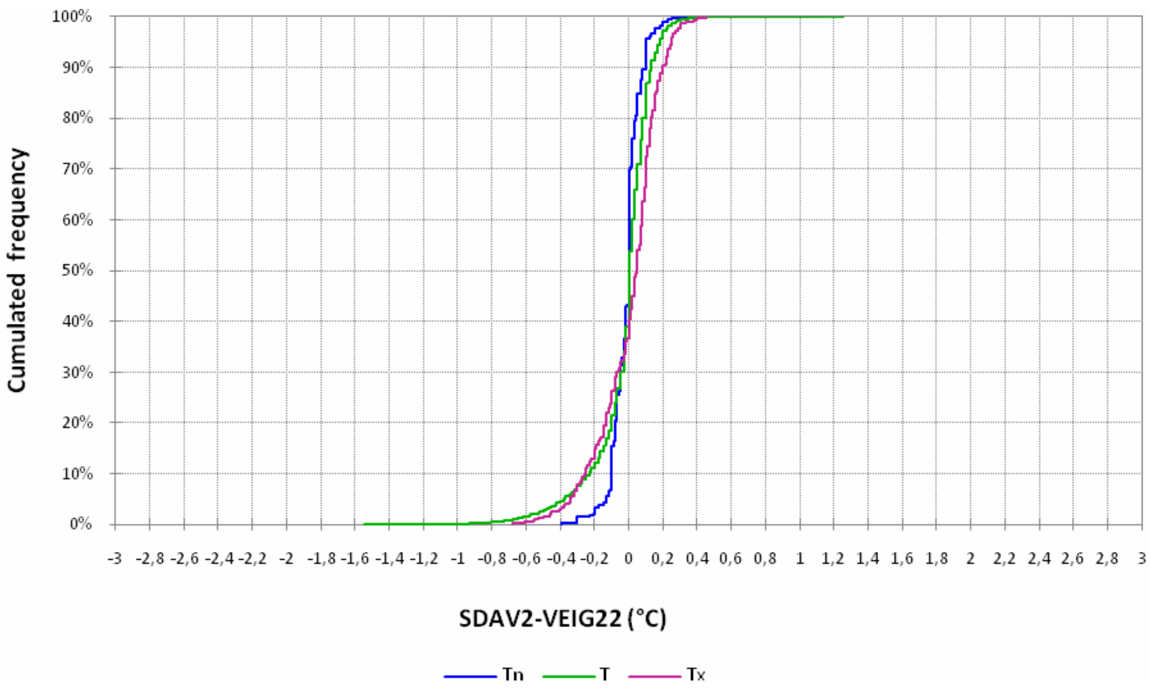


**Figure 6**

For approximately two thirds of the data points, the screen 1 is colder than the reference, while for approximately 40% of the data points, the screen 2 is colder that the reference.

For both screens the Tn, T, and Tx curves follow each other closely, and their relativity is similar, with Tn being the closest to the reference.

TABLE

The table 2 indicates the percentage of data that differ by less than 0.2°C (and 0.5°C) from the reference.

**Table 2**

| | | [-0.2°..0.2°] | [-0.5°..0.5°] |
|---|---|---|---|
| SDAV1 | T | 79.9 | 96.3 |
| | Tn | 89.4 | 99.7 |
| | Tx | 79.2 | 98.9 |
| SDAV2 | T | 86.1 | 97.4 |
| | Tn | 96.0 | 100.0 |
| | Tx | 76.2 | 98.6 |

## INFLUENCE OF GLOBAL RADIATION

The distribution of differences between SDAV and the reference VEIG22 is plotted, using 1-minute quality checked data for the whole period of the intercomparison. Differences are classified according global radiation.

Screen #1:

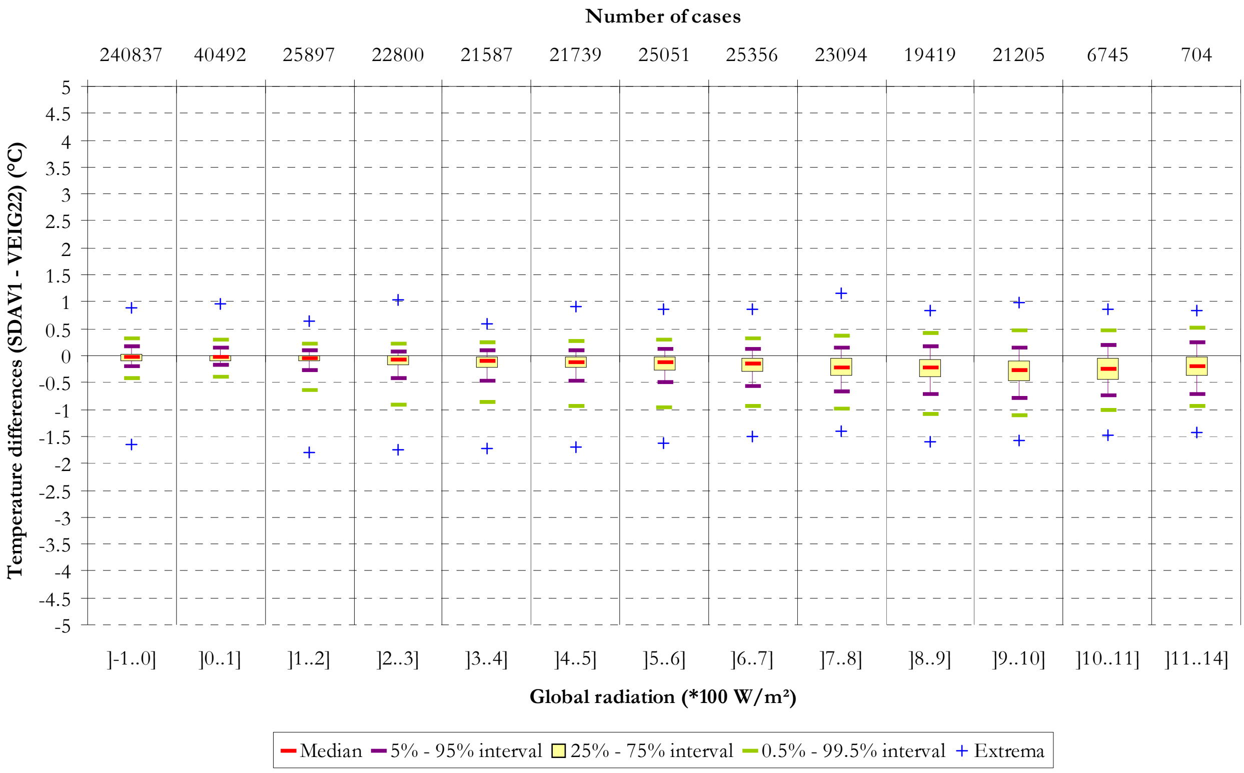


**Figure 7**

Screen #2:

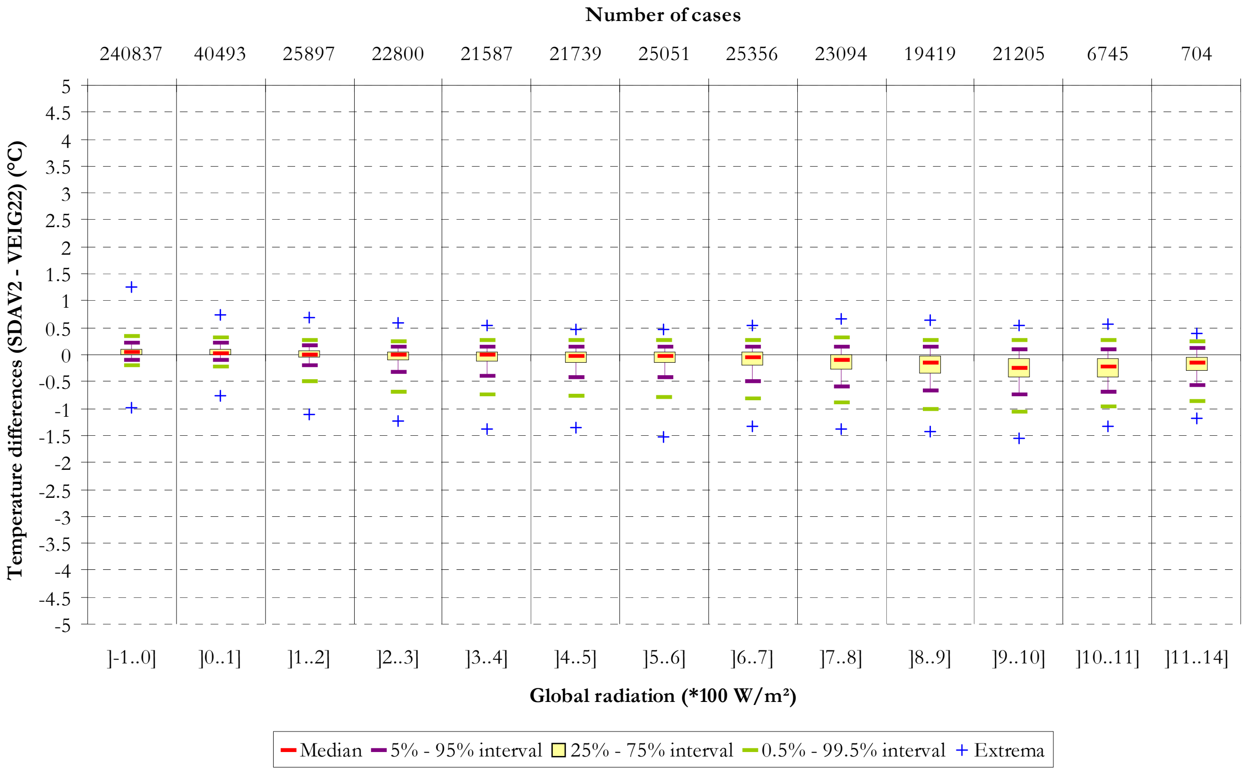


**Figure 8**

The two screens display similar behaviour, with respect to the variation of the global radiation. The global radiation only marginally influences the temperature reported from the two screens, with respect to the reference. Although minimal, the effect starts becoming more evident for over 600 W/m$^2$.

## RADIATION EFFECT

### DIFFERENCES BETWEEN DAY AND NIGHT BEHAVIOUR

The median of differences between SDAV and VEIG22 is plotted, using 1-minute quality checked data for the whole period of the intercomparison. We filter data for which sun elevation is above -1° (day) or below -1° (night). Differences are classified according 2-meter wind speed (2-minute average).

Screen #1:

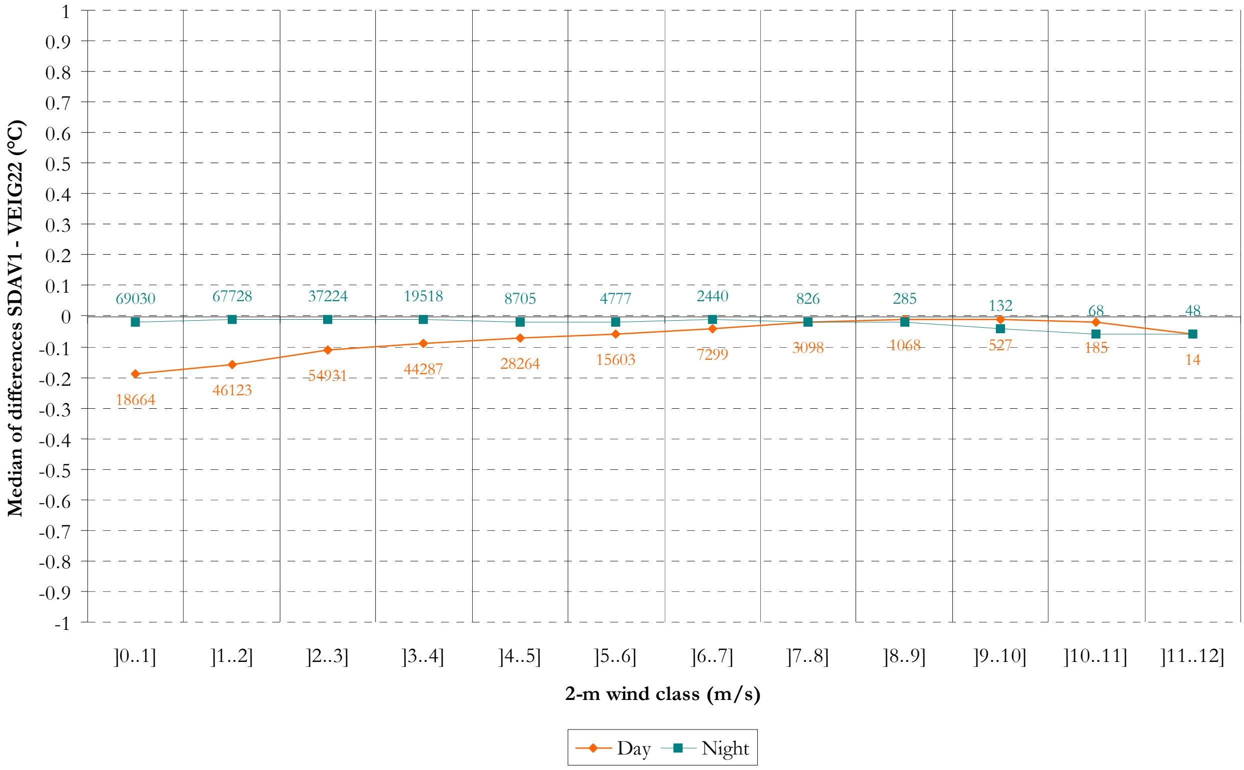


**Figure 9**

Screen #2:

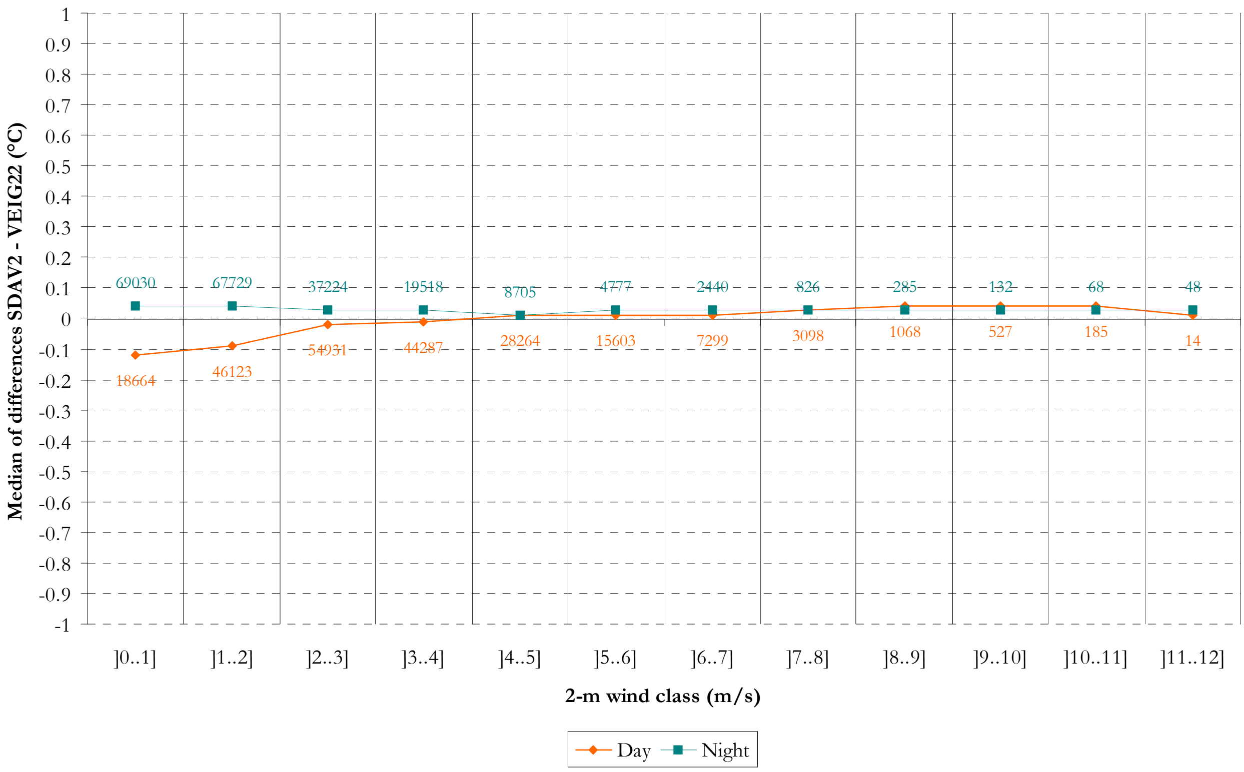


**Figure 10**

The two screens show different day and night behaviour and this is a function of the wind speed, primarily during the daytime. At night, the two screens behave similarly to the reference.

During the daytime, the two screens are colder than the reference for wind speeds below 7 m/s for screen 1, and below 4 m/s for screen 2. The largest temperature differential with respect to the reference is noted during calm conditions, about -0.2 deg C for screen 1 and -0.1 deg C for screen 2.

## DIFFERENCES BETWEEN CLEAR SKY AND OVERCAST SKY DURING DAYTIME

The median of differences between SDAV and VEIG22 is plotted, using 1-minute quality checked data. Here, we consider periods lasting six hours at least where cloudiness is less or equal to 1 (clear sky) or more or equal to 7 (overcast sky), during daytime (sun elevation above -1°). Differences are classified according 2-meter wind speed (2-minute average).

<u>Screen #1:</u>

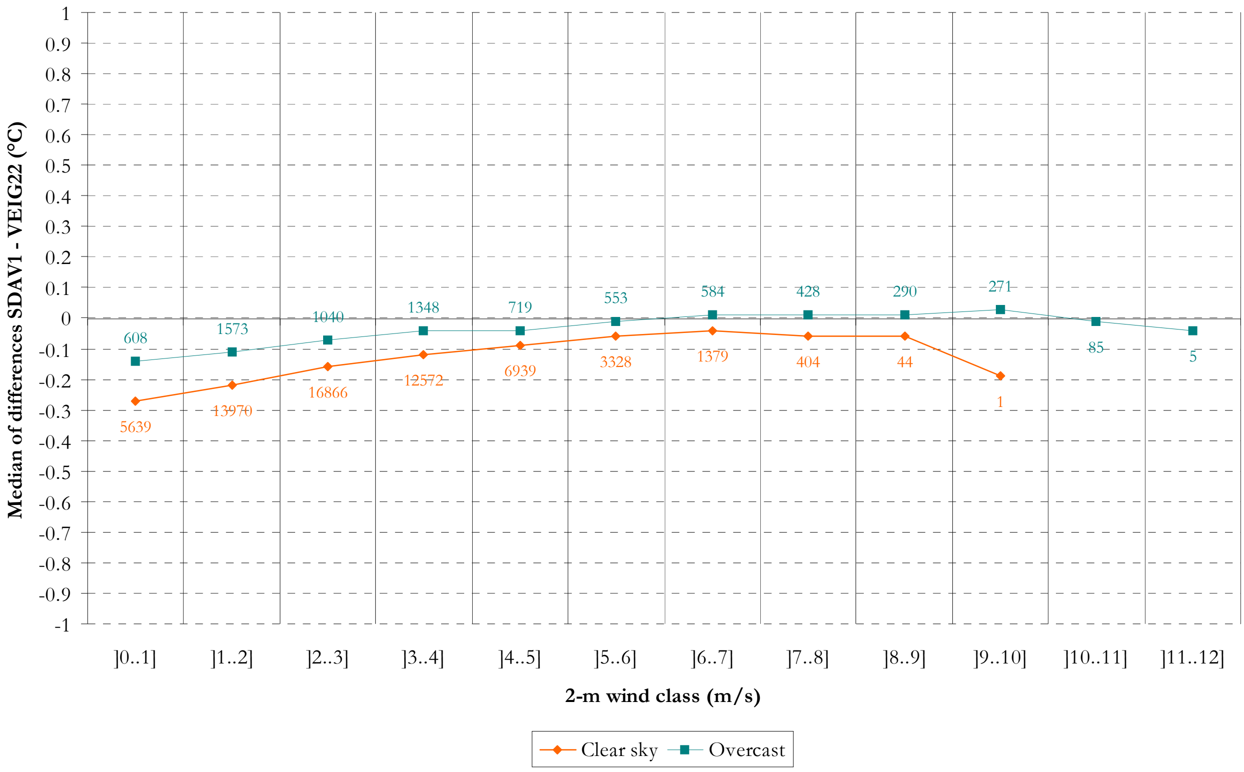


**Figure 11**

Screen #2:

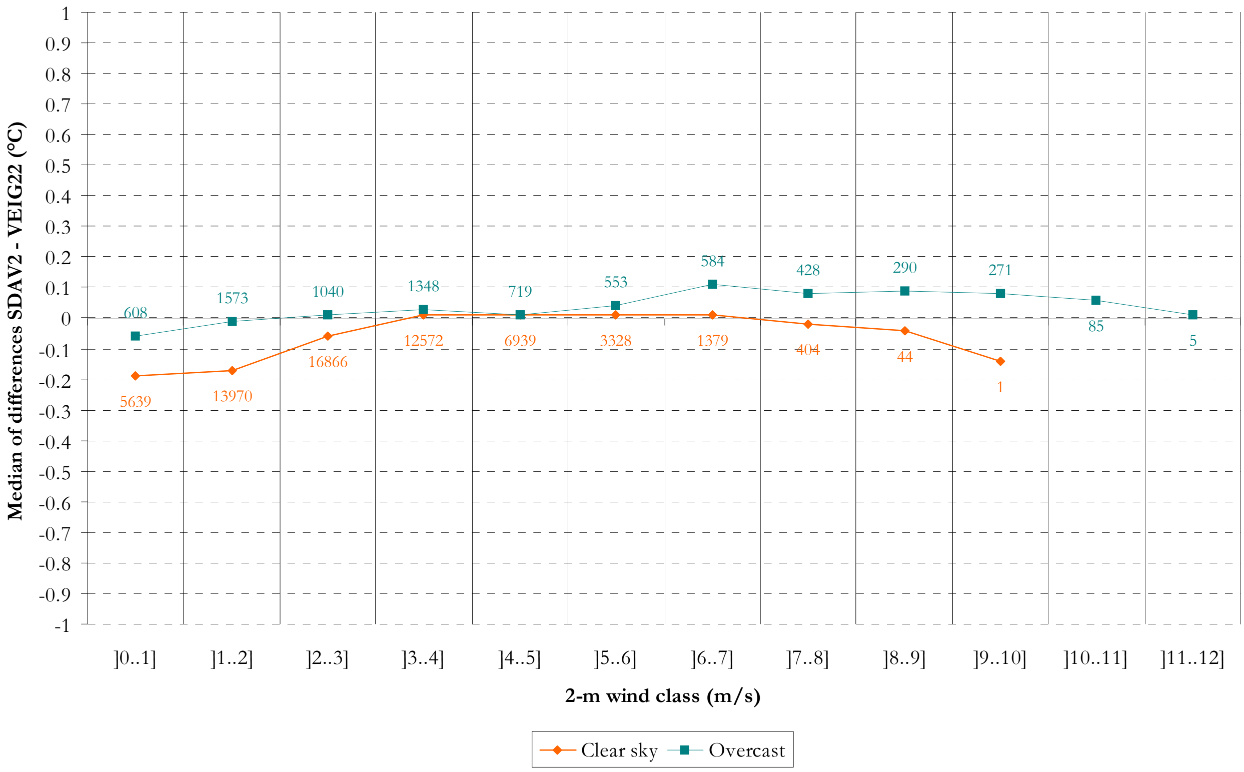


**Figure 12**

During the daytime, the two screens display similar behaviour; for the same wind conditions, they are consistently colder under clear sky than under an overcast sky. The differences relative to the reference at low wind speeds are very close to those at high wind speeds.

The two screens best emulate the reference at mid range wind speeds.

DIFFERENCES BETWEEN CLEAR SKY AND OVERCAST SKY DURING NIGHT TIME

The median of differences between SDAV and VEIG22 is plotted, using 1-minute quality checked data. Here, we consider periods lasting six hours at least where cloudiness is less or equal to 1 (clear sky) or more or equal to 7 (overcast sky), during night time (sun elevation below -1°). Differences are classified according 2-meter wind speed (2-minute average).

Screen #1:

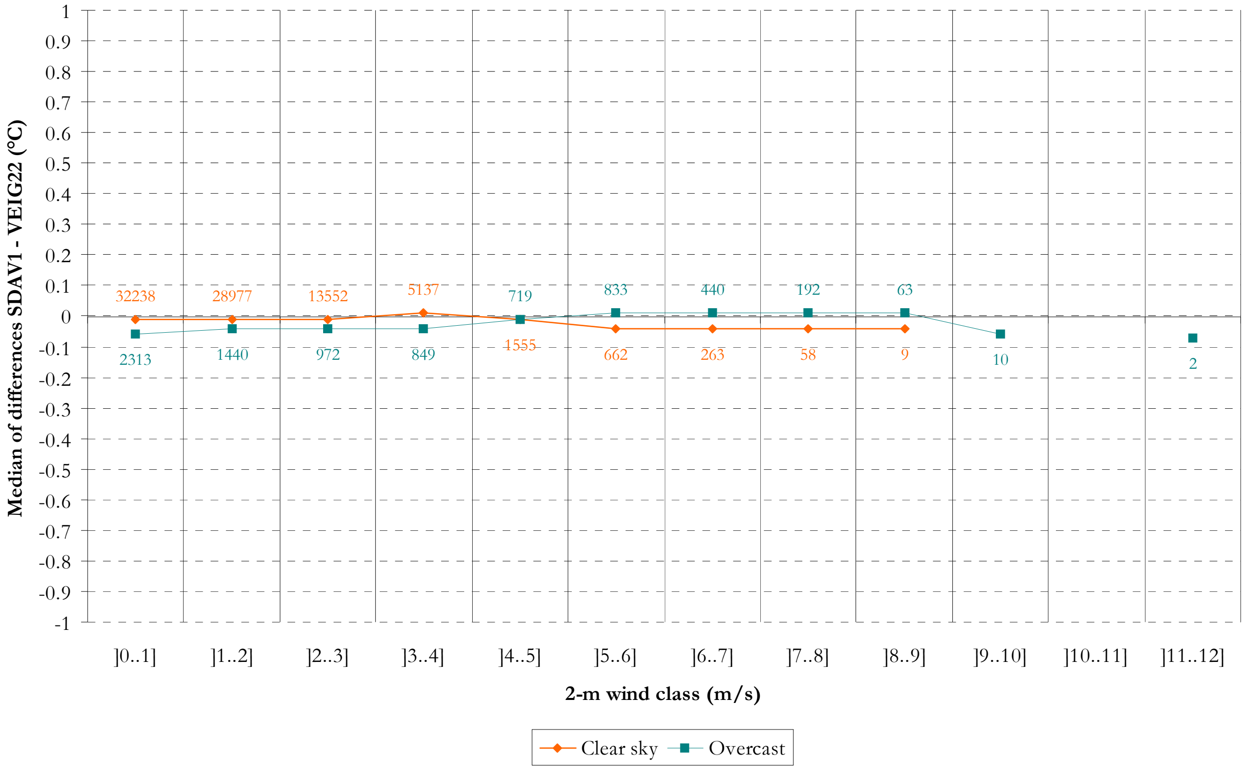


**Figure 13**

Screen #2:

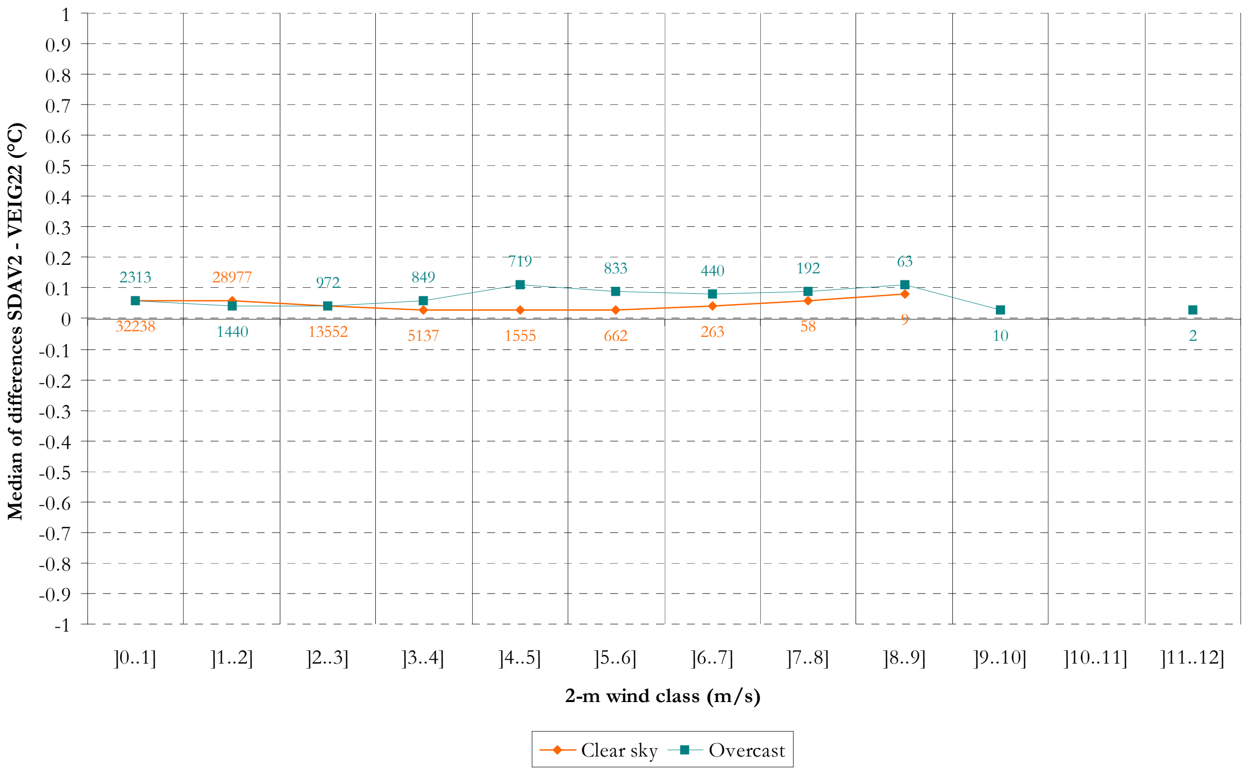


**Figure 14**

At night, the two screens display similar behaviour; for the same wind conditions, there isn't a significant difference between clear sky and overcast sky behavious for either of the two screens. The median of the differences relative to the reference is less than 0.1 deg C and is approximately constant for the entire range of wind speeds.

## EFFECT OF SUN ELEVATION

The median of differences between SDAV and VEIG22 is plotted, using 1-minute quality checked data. Here, we consider periods lasting six hours at least where cloudiness is less or equal to 1 (clear sky), during daytime (sun elevation above -1°). We filter data where sun elevation is low (below 10°), medium (between 10° and 45°) or high (above 45°). Differences are classified according 2-meter wind speed (2-minute average).

Screen #1:

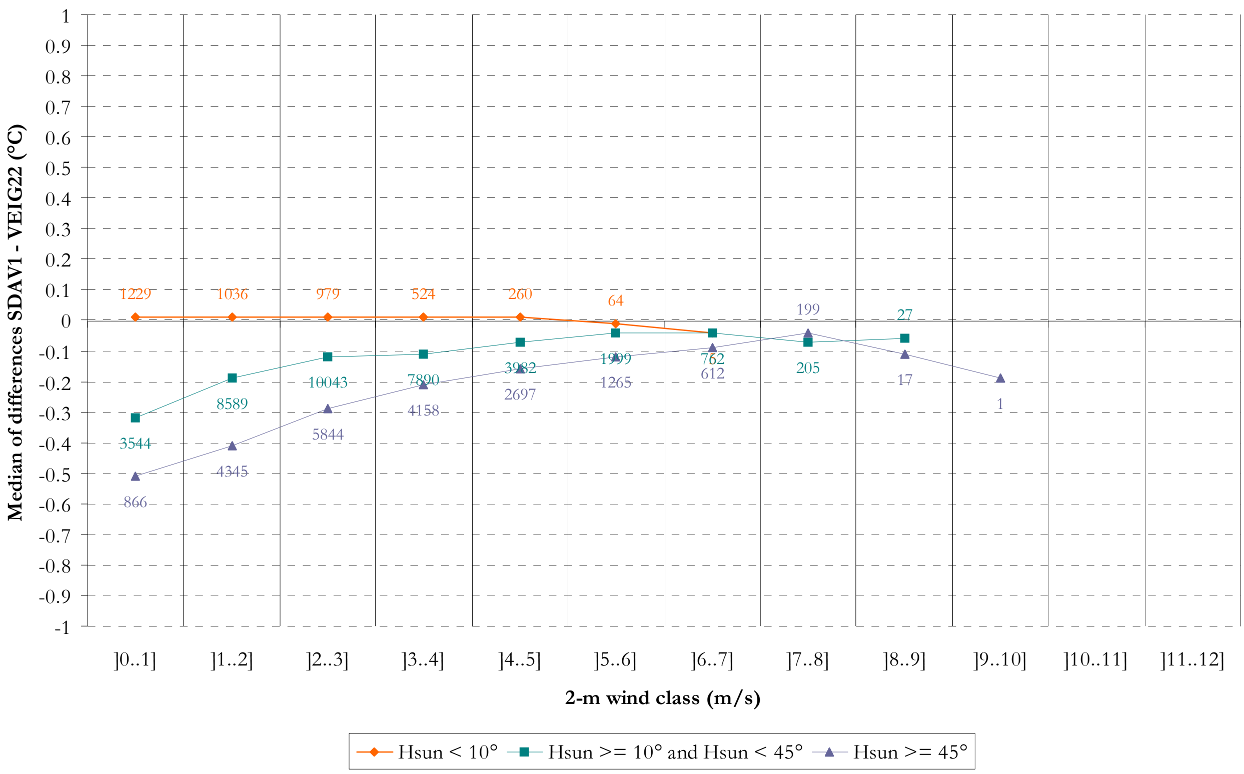


**Figure 15**

Screen #2:

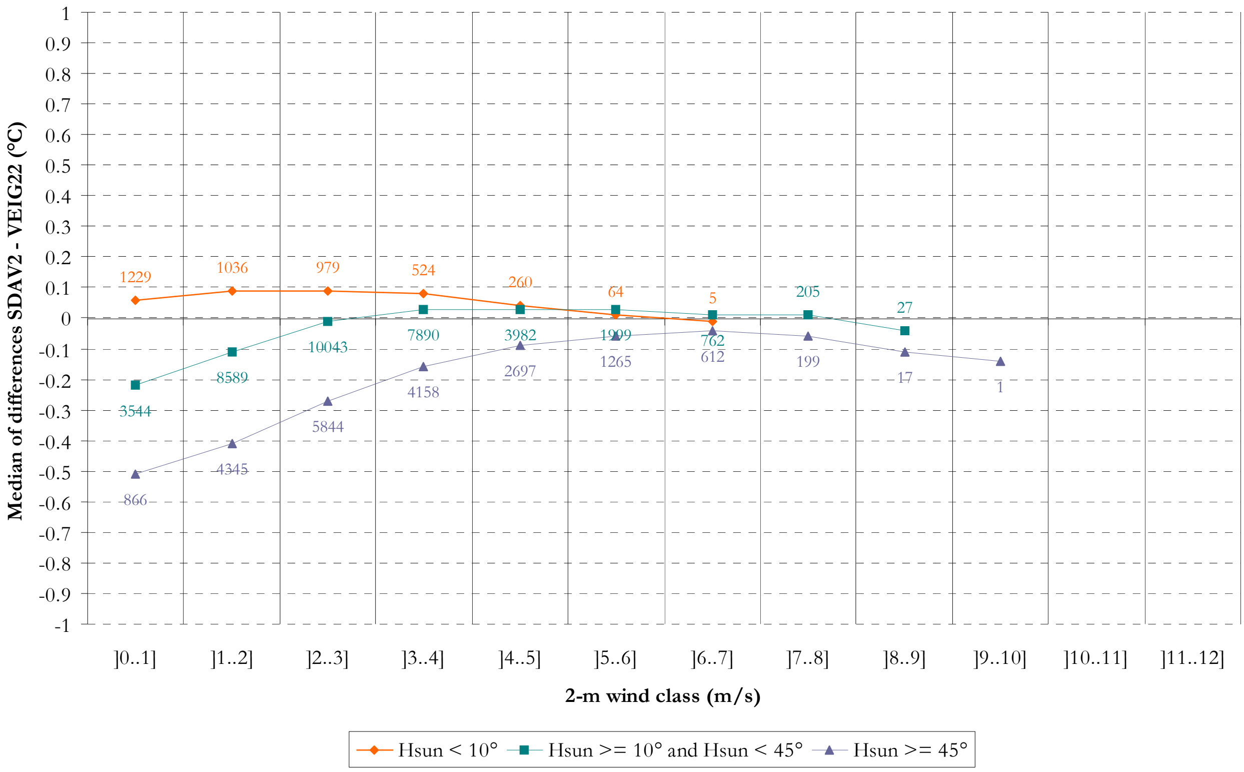


**Figure 16**

The two screens display similar behaviour function of sun elevation, being coldest for sun elevations over 45°.

For sun elevations below 10°, the differences between the temperature reported from each screen and that from the reference are only minimally influenced by sun, over the wind speed range measured. The sun elevation becomes a significant factor for elevations above 10°. For wind speeds below 5m/s the behaviour of the screens is greatly influenced by the sun elevation. At calm conditions, the spread of the median between sun below 10° and sun at over 45° approaches 0.6°C. Both screens are the coldest with respect to the reference, for calm conditions when the sun elevation is over 45°.

It's worth noting the tendency of both screens to be colder again when the wind speeds exceed 7m/s.

## COMBINED EFFECT OF WIND AND GLOBAL RADIATION

The medians of differences between SDAV and VEIG22 are represented here with a contour plot. The global radiation values are on the X-axis and on the Y axis is the 2-meter wind speed value (2-minute average). Medians are used in all cases, providing that at least one data is available for both conditions on radiation and wind considered.

Screen #1:

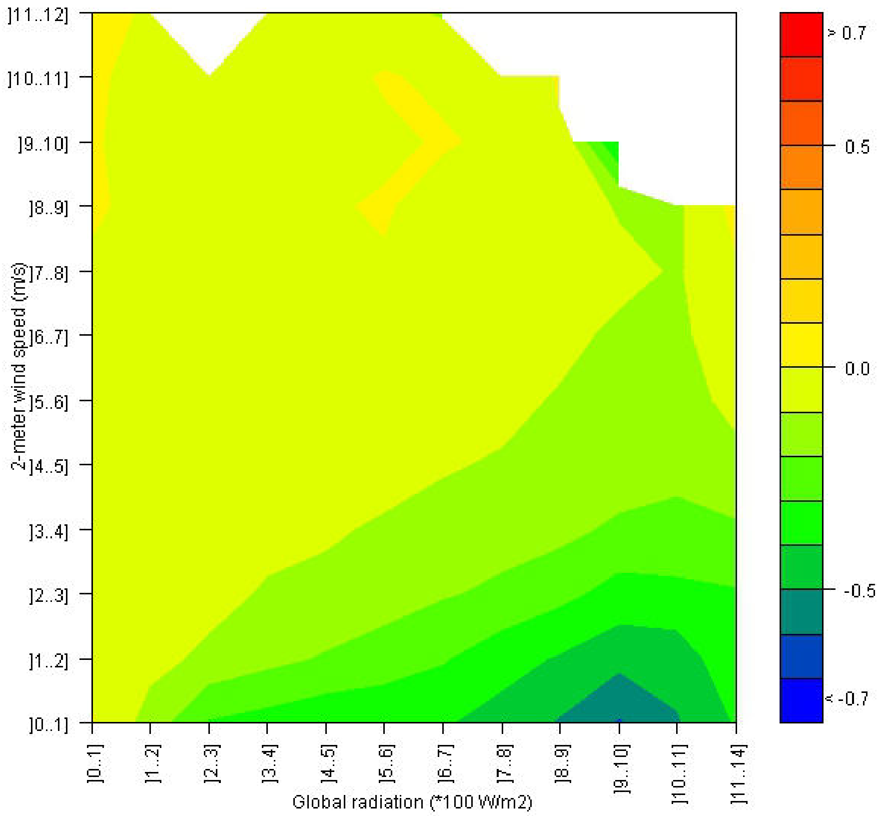


**Figure 17**

Screen #2:

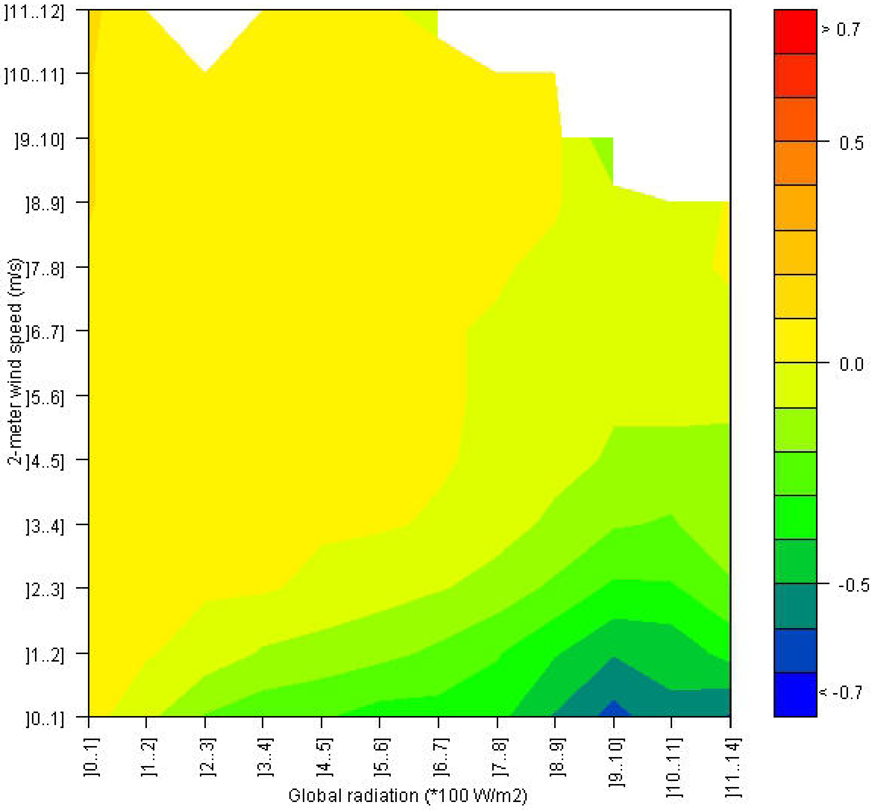


**Figure 18**

The graphs show the general tendency of the two screens to be marginally colder than the reference for the entire range of wind speeds and global radiation reported at the site during the intercomparison. The screens are the coldest at high global radiation, about 900 W/m$^2$, and wind speeds below 2m/s.

## BEHAVIOUR DURING INCREASE/DECREASE OF TEMPERATURE

The distribution of differences between SDAV and the reference VEIG22 is plotted, using 1-minute quality checked data for the whole period of the intercomparison. Differences are classified according the temporal gradient of reference temperature over 1 minute. A screen faster (or slower, respectively) than the reference would be warmer (cooler) for positive gradient, cooler (warmer) for negative ones.

Screen #1:

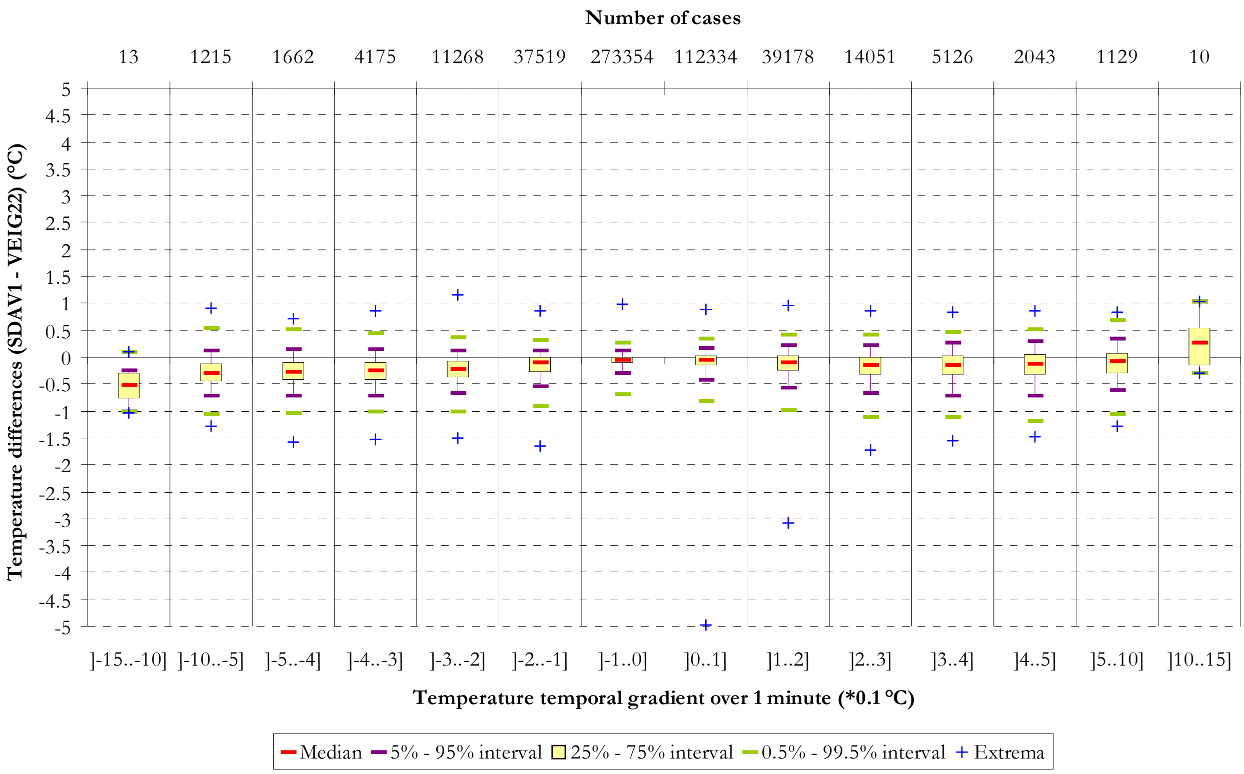


**Figure 19**

Screen #2:

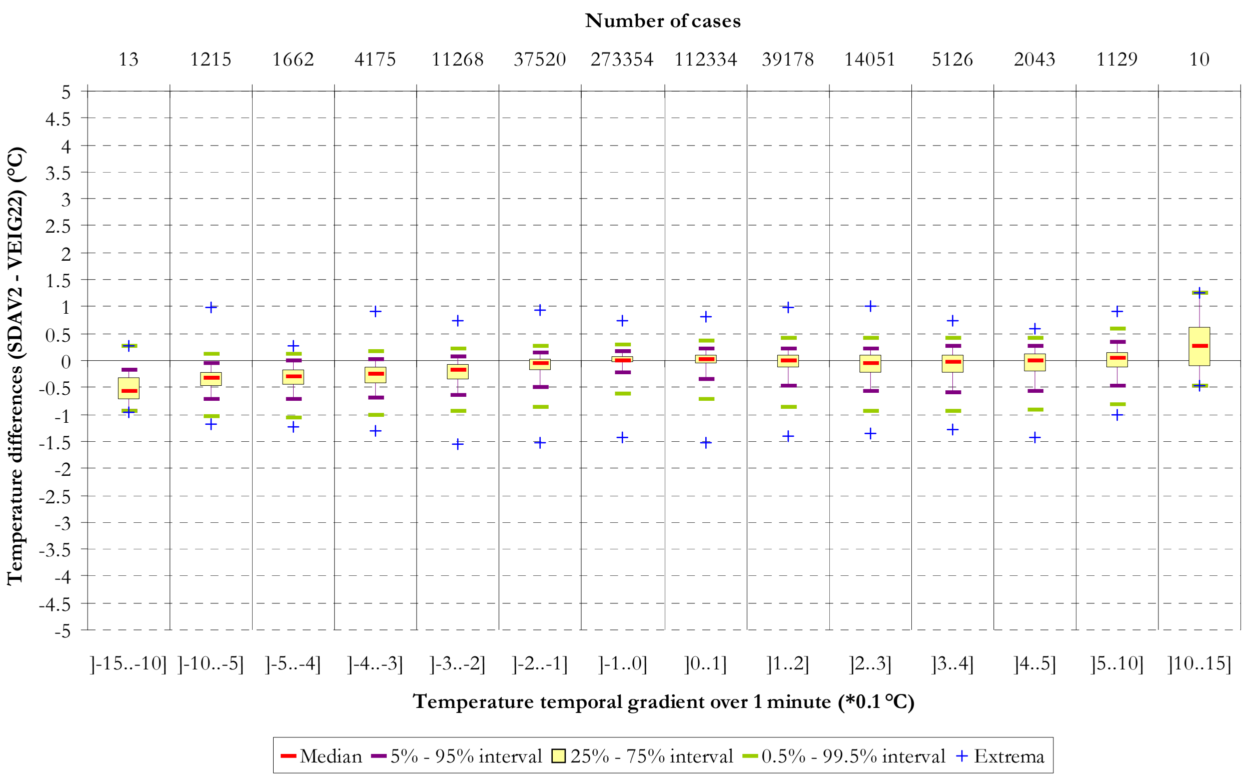


**Figure 20**

The two screens were just marginally colder (slower) than the reference for the entire range of temperature gradients assessed. The screens were slowest for a temperature gradient of -1.5°C. For a temperature gradient of +1.5°C, the two screens were slightly faster than the reference; however, given the reduced number of samples, this conclusion may be difficult to generalize.

## QUALITY CONTROL INFORMATION

DATA AVAILABILITY

The intercomparison period extends from the 1st of November 2008 to the 1st of November 2009. The theoretical number of 1-minute data is 525600.

The next table sums up the total number of data for each screen and for each possible QC flag.

**Table 3**

| **QC flag** | SDAV**1** | SDAV**2** |
|---|---|---|
| 0 (good) | 503265 | 503266 |
| 1 (inconsistent) | 0 | 0 |
| 2 (doubtful) | 1 | 0 |
| 3 (erroneous) | 0 | 0 |
| 7 (missing) | 22334 | 22334 |

MAINTENANCE

No action done during the intercomparison period.

# 41003 YOUNG
# – USA –
# SYOU

## TECHNICAL SPECIFICATIONS (PROVIDED BY THE MANUFACTURER)

Dimensions: Length 20 cm x Width 16 cm x Height 20 cm

Weight: 800 g

Material/Structure: Thermoplastic - Stainless steel - aluminium

Estimated radiation error: 0.4°C

Aspiration rate (in case of artificially ventilated screen/shield): naturally ventilated

Power supply: none

**Figure 1**

## OVERVIEW

The two SYOU screens are in close agreement with each other, over all classes of temperature. There is only a slight variation of the temperature difference between the two screens function of the class of temperature.

Relative to the reference, both screens are generally warmer. For both screens, the distribution of the differences is symmetrical around the highest frequency at 0.1°C-0.2°C.

Screen #1 shows a remarkable similarity in performance for Tn, T, and Tx, while screen #2 is cumulatively warmer for T than for Tn, and ever warmer for Tx. Both screens are generally warmer than the reference for Tn, T, and Tx.

The influence of global radiation is marginal for both screens. The screens are generally warmer than the reference for all classes of global radiation.

Both screens are warmer than the reference during the night and even warmer during the day, and their behaviour is minimally wind speed dependent.

During the day time, both screens are warmer than the reference under overcast conditions and even warmer under clear sky, being only marginally dependent on the wind conditions.

During the night time, both screens are warmer than the reference under clear sky conditions and just slightly warmer under overcast, being only marginally dependent on the wind conditions.

For sun elevation below 10°C, both screens become cooler as the wind speed increases. The overall temperature gradient is about 0.2°C. For sun elevations from 10° to 45°, both screens are becoming warmer, with an overall temperature gradient of less than 0.3°C. For sun elevations above 45°, both screens are minimally dependent of the wind speed, with a slight tendency to become cooler as the wind speed increases.

The two contour plots show the SYOU screens consistently warmer than the reference for most of the wind speed values and global radiation range, however the difference from the reference is minimum. The only exception is for the low winds and high radiation values, where the screens are slightly cooler or just about at the level of the reference.

The SYOU screens are warmer (slower) than the reference for the cases when the temperature decreases and approximately similar to the reference, when the temperature increases, with a small tendency to be faster warmer). Overall, the graphs indicate a minimum linearly decreasing dependency of the temperature differences with the temperature temporal gradient.

## CALIBRATION INFORMATION

The calibration of both probes was performed in Trappes.

**Table 1**

| Screen | Location | Pt100 probe serial number | Calibration date | Instrument bias (°C) | | | |
|---|---|---|---|---|---|---|---|
| | | | | -20°C | 0°C | 20°C | 40°C |
| SYOU1 | F2 | T53 | 3-Feb-2006 | 0.0246 | -0.0032 | 0.0216 | -0.0346 |
| SYOU2 | F5 | T51 | 7-Feb-2006 | 0.0304 | 0.0031 | -0.0131 | -0.0261 |

The result of the calibration of the reference VEIG22 is available in the main report of the intercomparison, section 5.4.1.

## COMPARISON OF BOTH SENSORS

The distribution of differences between screen 1 and screen 2 is plotted, using 1-minute quality checked data for the whole period of the intercomparison. Differences are classified according screen 1 temperature.

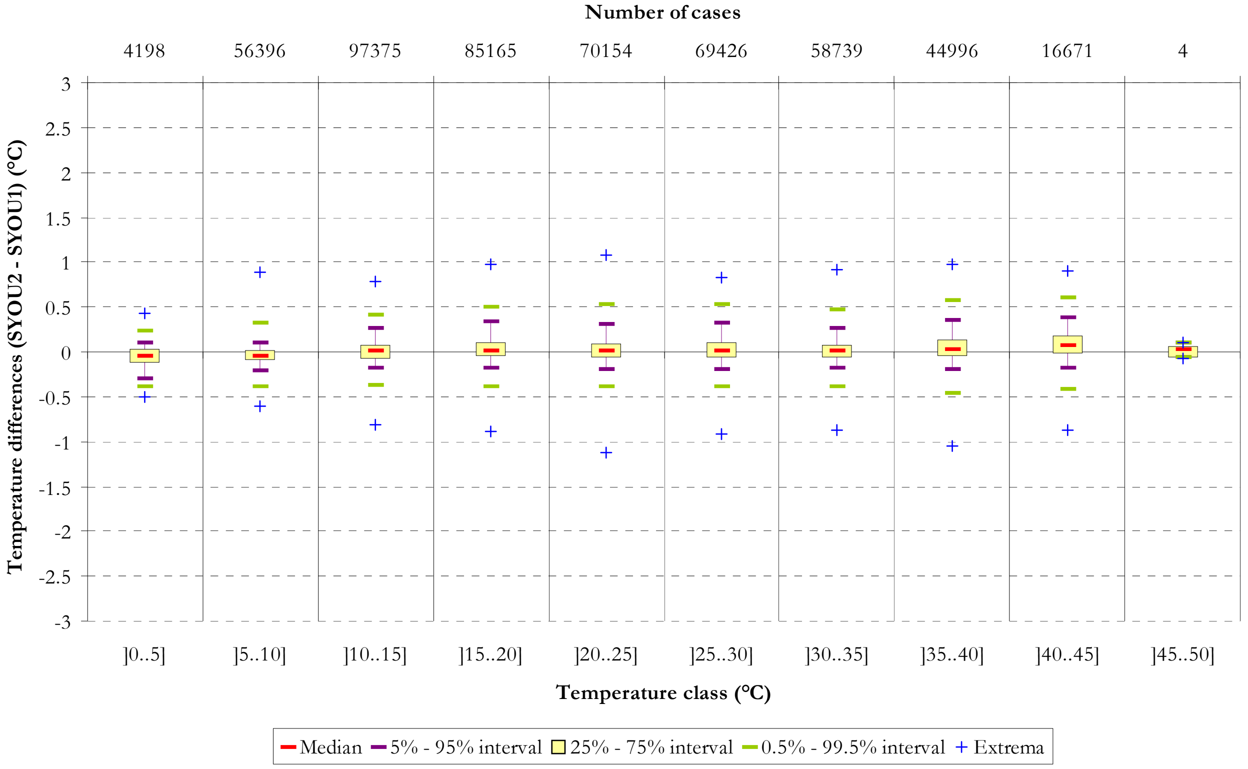


**Figure 2**

The two SYOU screens are in close agreement with each other, over all classes of temperature. There is only a slight variation of the temperature difference between the two screens function of the class of temperature.

## COMPARISON WITH THE REFERENCE

### HISTOGRAM OF DIFFERENCES

The histogram of differences between SYOU and the reference VEIG22 is plotted, using 1-minute quality checked data for the whole period of the intercomparison. Differences are plotted by steps of 0.1K. The vertical axis is the frequency in percent for each class of differences.

Screen #1:

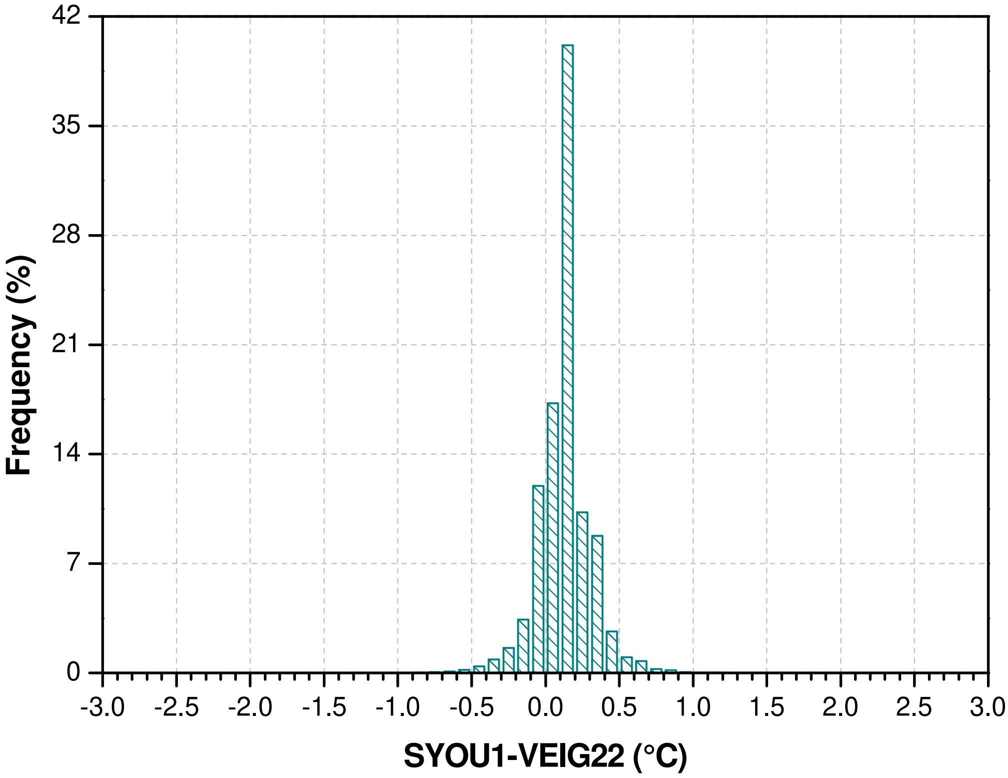


Figure 3

Screen #2:

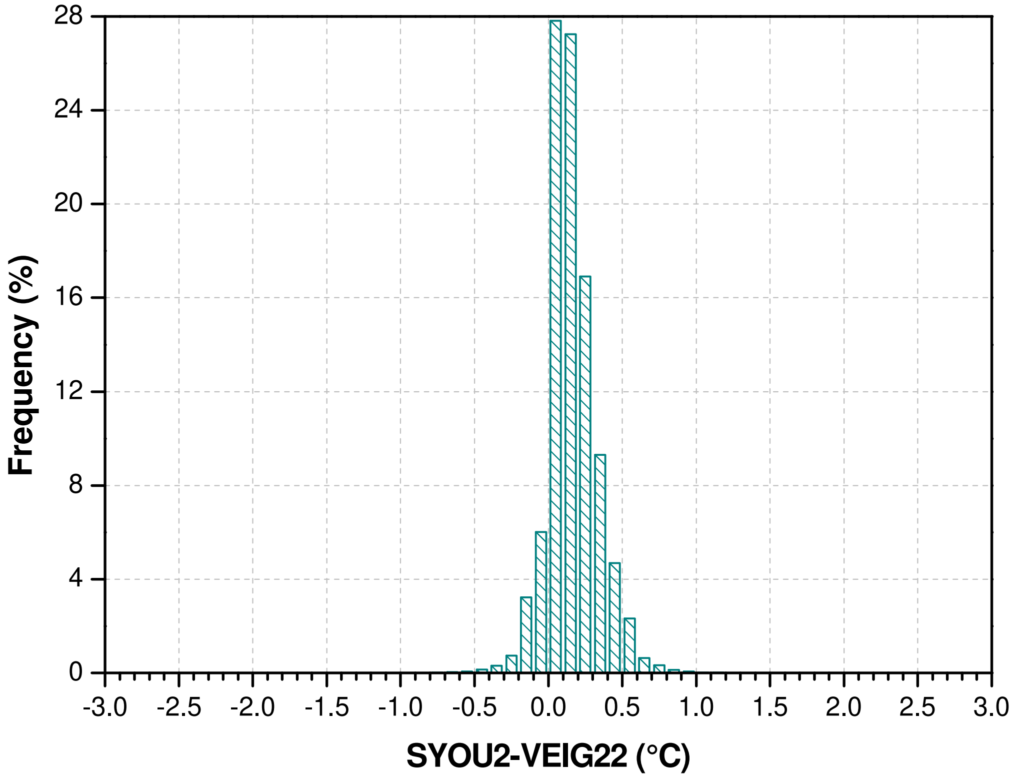


**Figure 4**

Relative to the reference, both screens are generally warmer, with approximately 50% of the data points within 0.2°C of the reference. For both screens, the distribution of the differences is symmetrical around the highest frequency at 0.1°C-0.2°C.

CUMULATIVE HISTOGRAMS OF DIFFERENCES OF DAILY EXTREME VALUES

The cumulative histograms of differences with the reference VEIG22 of T (1-minute quality checked data), Tn (daily minimum temperature) and Tx (daily maximum temperature) are plotted, for the whole period of the intercomparison. Differences are plotted by steps of 0.1K.

Screen #1:

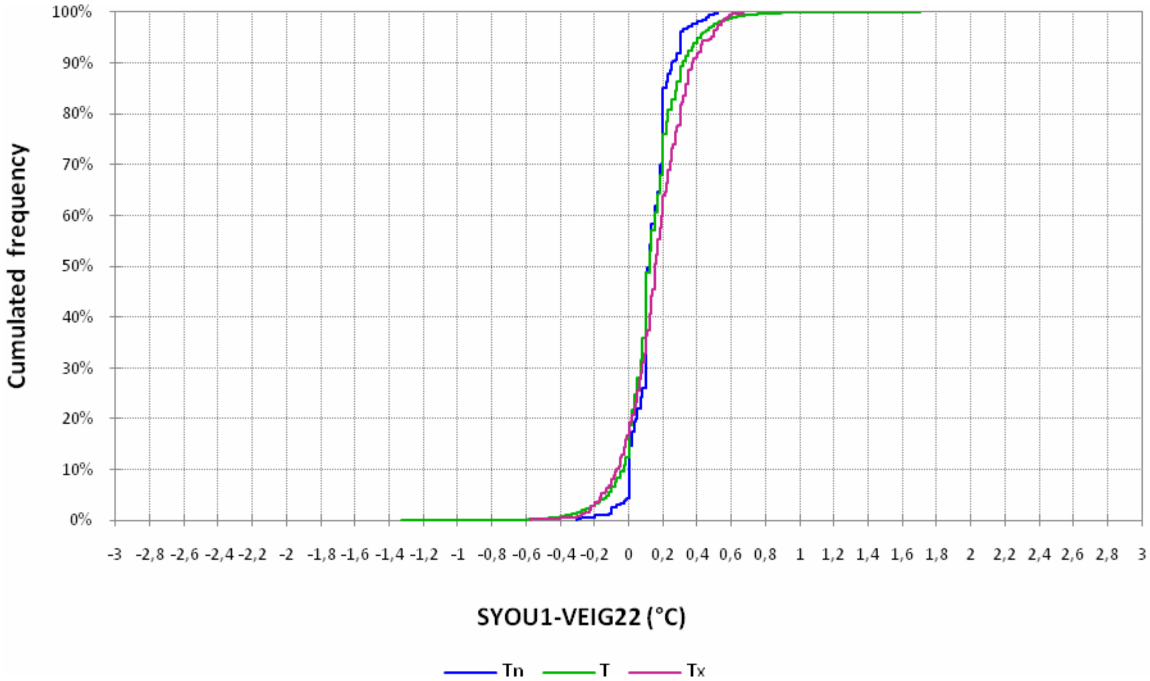


**Figure 5**

Screen #2:

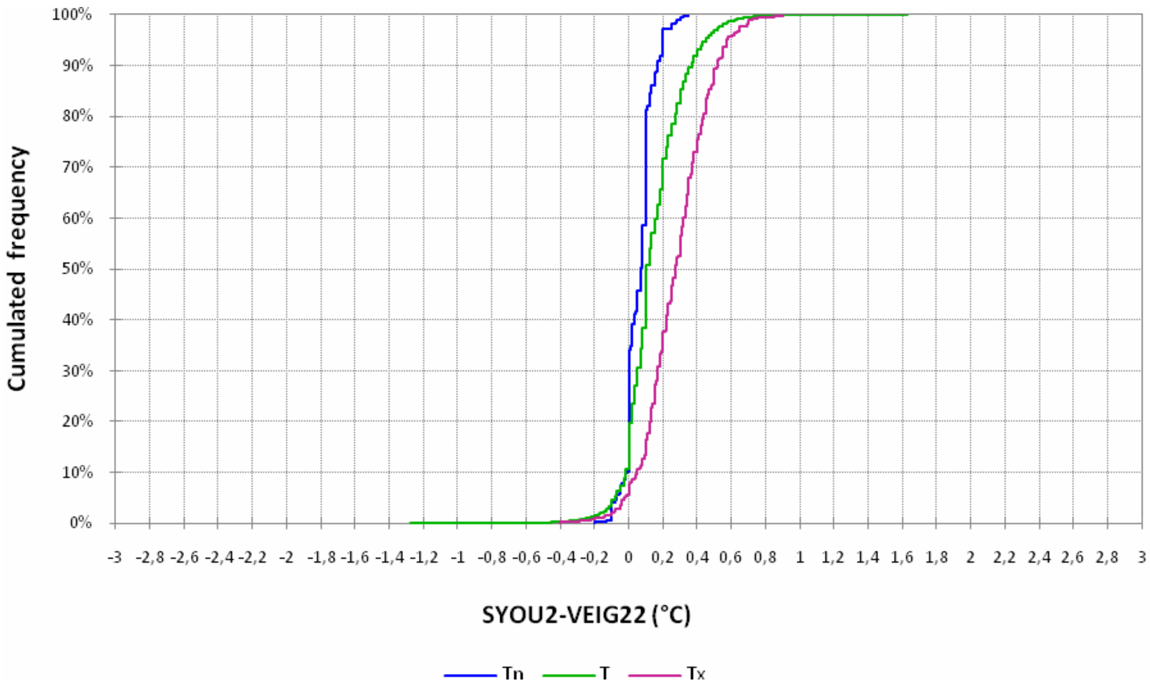


**Figure 6**

Screen #1 shows a remarkable similarity in performance for Tn, T, and Tx, while screen #2 is cumulatively warmer for T than for Tn, and ever warmer for Tx.

Both screens are generally warmer than the reference for Tn, T, and Tx.

TABLE

The table 2 indicates the percentage of data that differ by less than 0.2°C (and 0.5°C) from the reference.

**Table 2**

| | | [-0.2°..0.2°] | [-0.5°..0.5°] |
|---|---|---|---|
| SYOU1 | T | 73.2 | 97.4 |
| | Tn | 82.6 | 99.7 |
| | Tx | 58.7 | 96.1 |
| SYOU2 | T | 70.4 | 96.9 |
| | Tn | 96.3 | 100.0 |
| | Tx | 35.5 | 89.5 |

## INFLUENCE OF GLOBAL RADIATION

The distribution of differences between SYOU and the reference VEIG22 is plotted, using 1-minute quality checked data for the whole period of the intercomparison. Differences are classified according global radiation.

Screen #1:

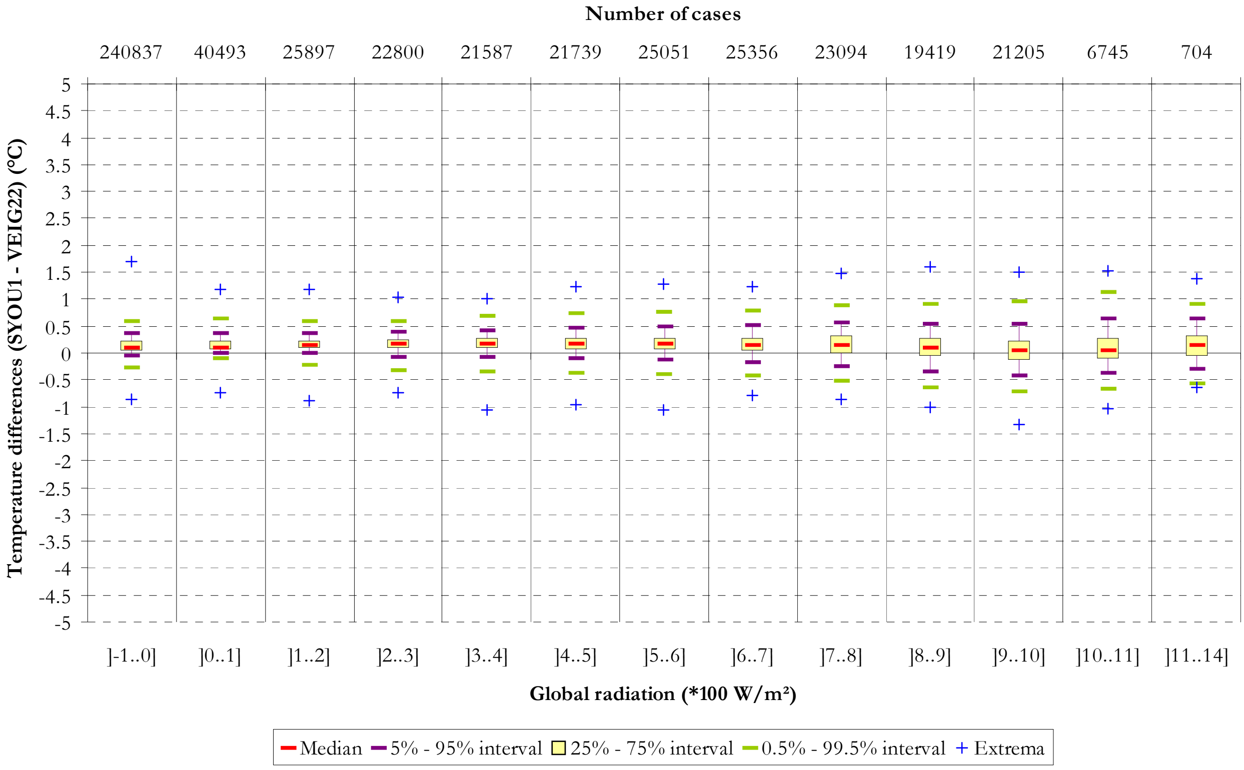


**Figure 7**

Screen #2:

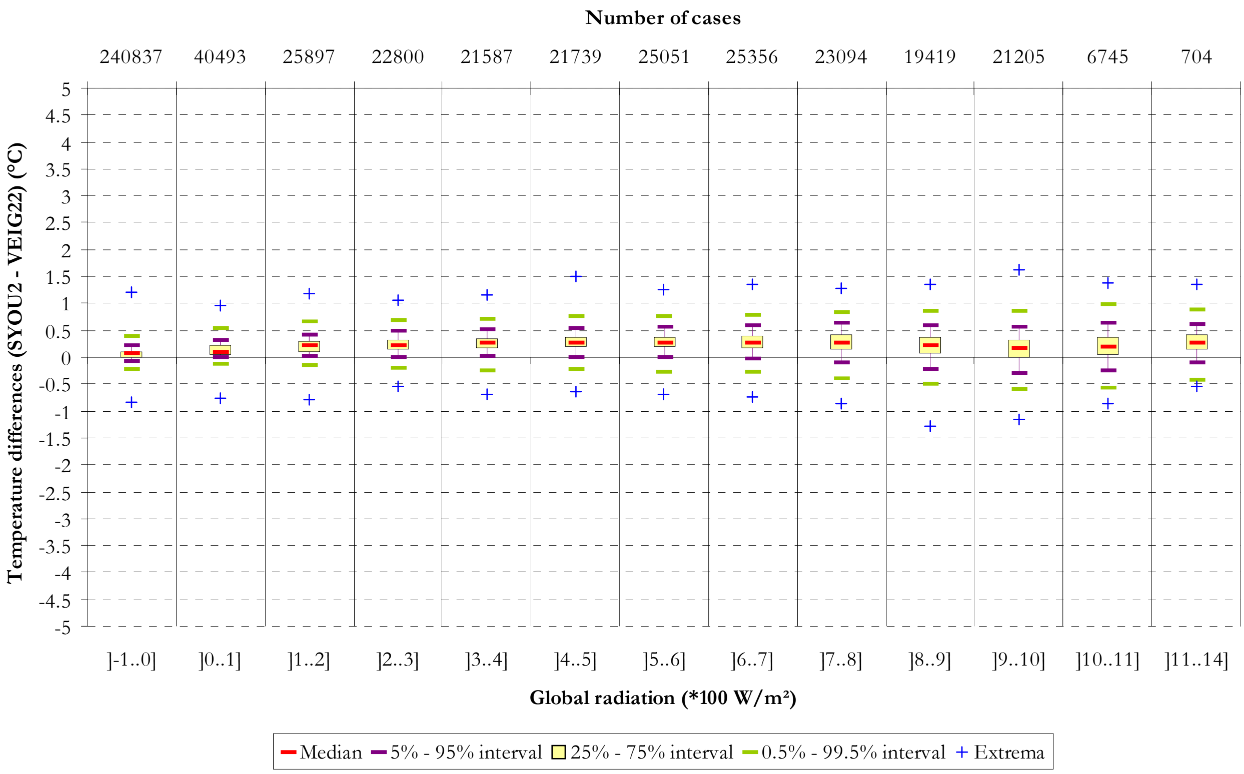


**Figure 8**

The influence of global radiation is marginal for both screens; the dispersion of temperature data from each screen, by classes of irradiance increases slightly with the increase in irradiance. The screens are generally warmer than the reference for all classes of global radiation.

## RADIATION EFFECT

### DIFFERENCES BETWEEN DAY AND NIGHT BEHAVIOUR

The median of differences between SYOU and VEIG22 is plotted, using 1-minute quality checked data for the whole period of the intercomparison. We filter data for which sun elevation is above -1° (day) or below -1° (night). Differences are classified according 2-meter wind speed (2-minute average).

Screen #1:

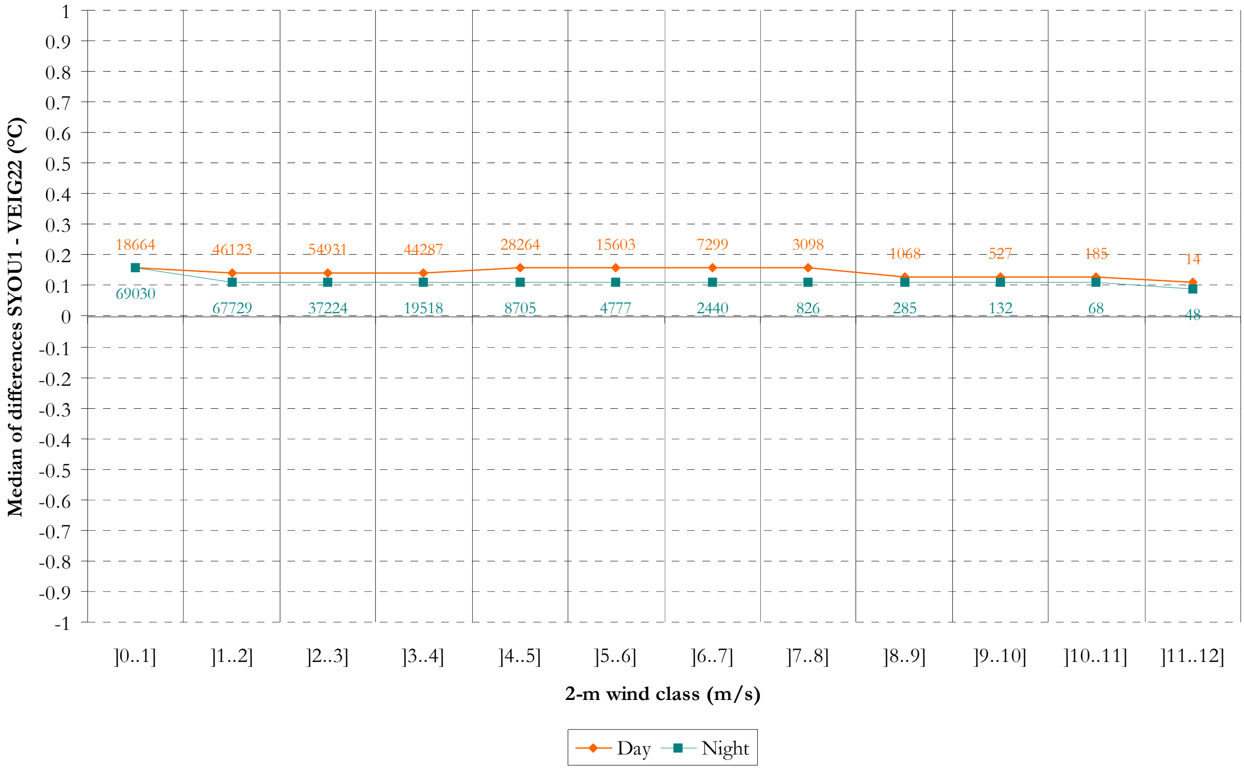


**Figure 9**

Screen #2:

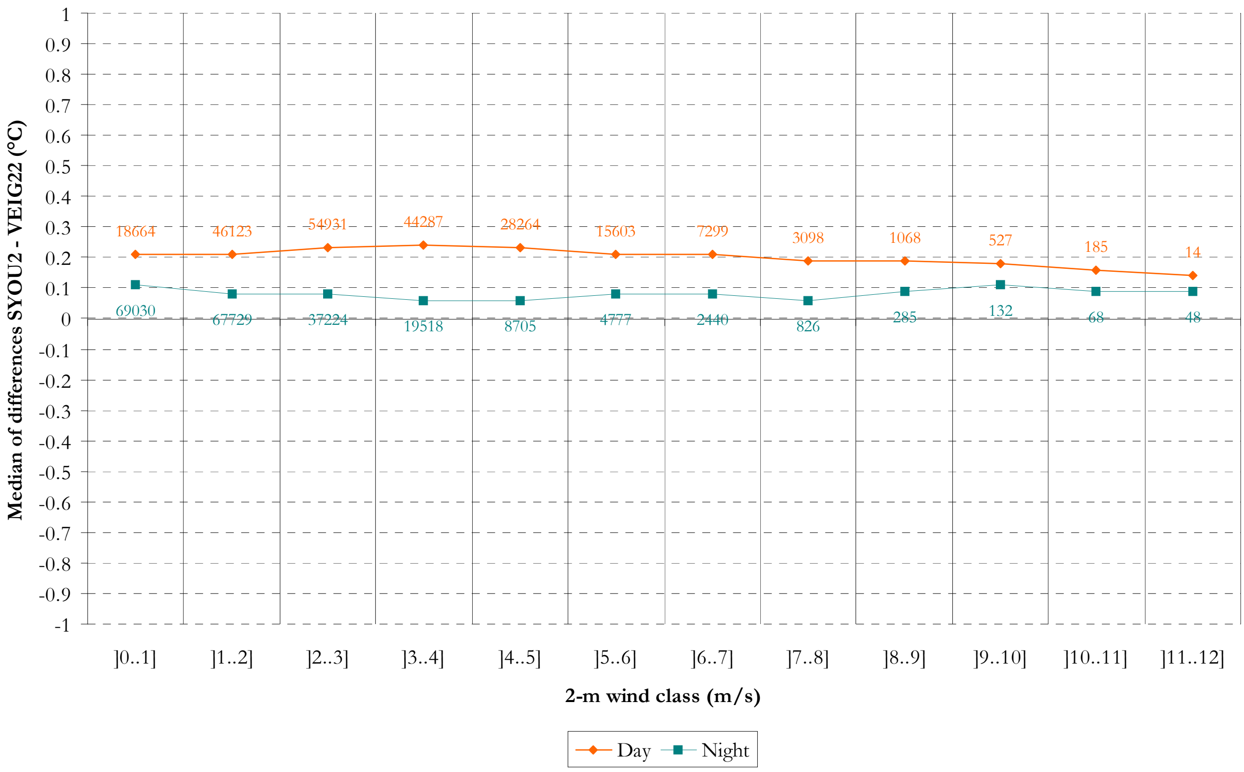


**Figure 10**

Both screens are warmer than the reference during the night and even warmer during the day, and their behaviour is minimally wind speed dependent.

Overall, the temperature gradient for the entire range of wind speeds is less than 0.1°C.

## DIFFERENCES BETWEEN CLEAR SKY AND OVERCAST SKY DURING DAYTIME

The median of differences between SYOU and VEIG22 is plotted, using 1-minute quality checked data. Here, we consider periods lasting six hours at least where cloudiness is less or equal to 1 (clear sky) or more or equal to 7 (overcast sky), during daytime (sun elevation above -1°). Differences are classified according 2-meter wind speed (2-minute average).

<u>Screen #1:</u>

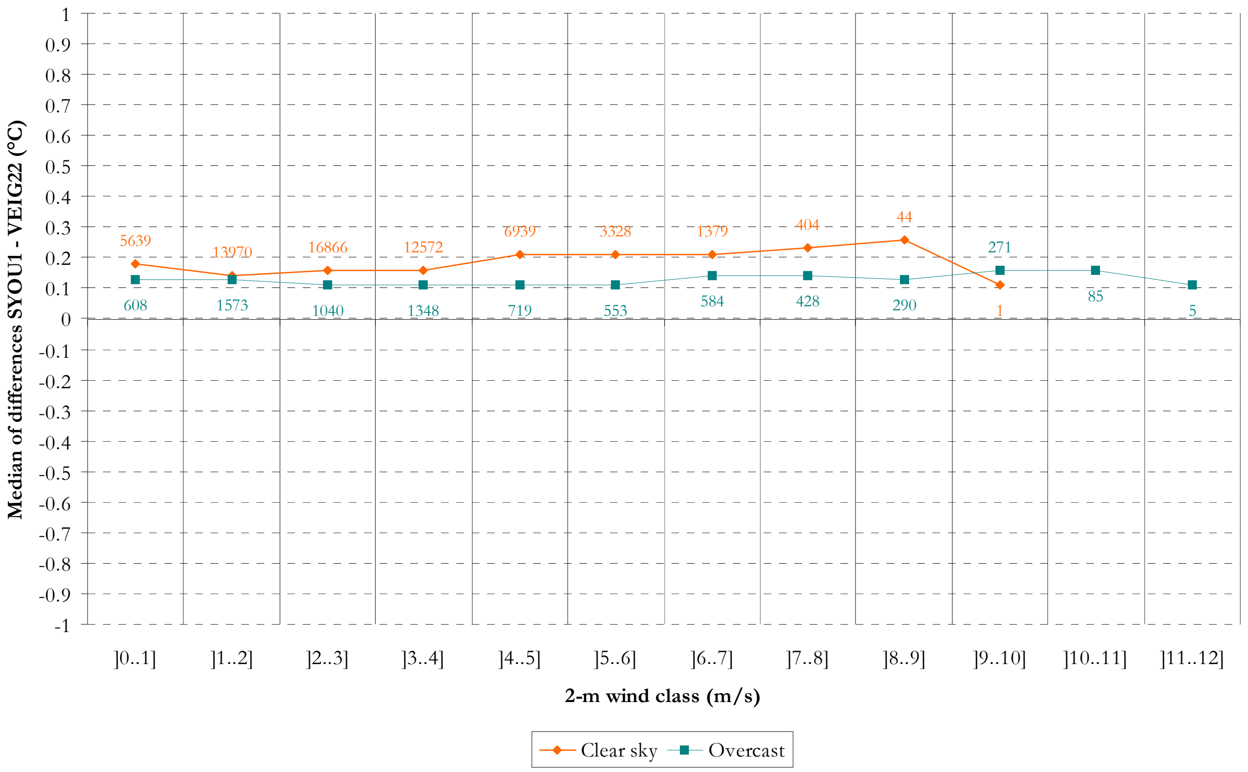


**Figure 11**

Screen #2:

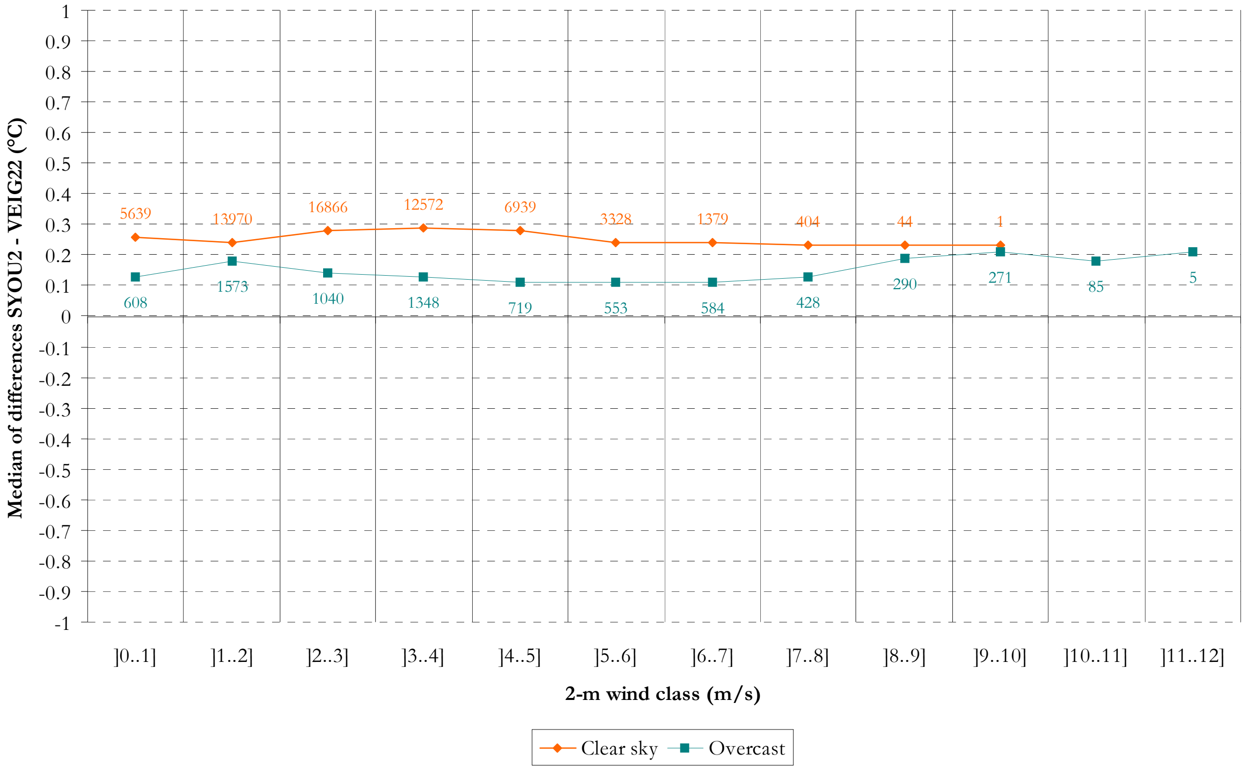


**Figure 12**

During the day time, both screens are warmer than the reference under overcast conditions and even warmer under clear sky, being only marginally dependent on the wind conditions.

Overall the temperature gradient is less than 0.1°C.

DIFFERENCES BETWEEN CLEAR SKY AND OVERCAST SKY DURING NIGHT TIME

The median of differences between SYOU and VEIG22 is plotted, using 1-minute quality checked data. Here, we consider periods lasting six hours at least where cloudiness is less or equal to 1 (clear sky) or more or equal to 7 (overcast sky), during night time (sun elevation below -1°). Differences are classified according 2-meter wind speed (2-minute average).

Screen #1:

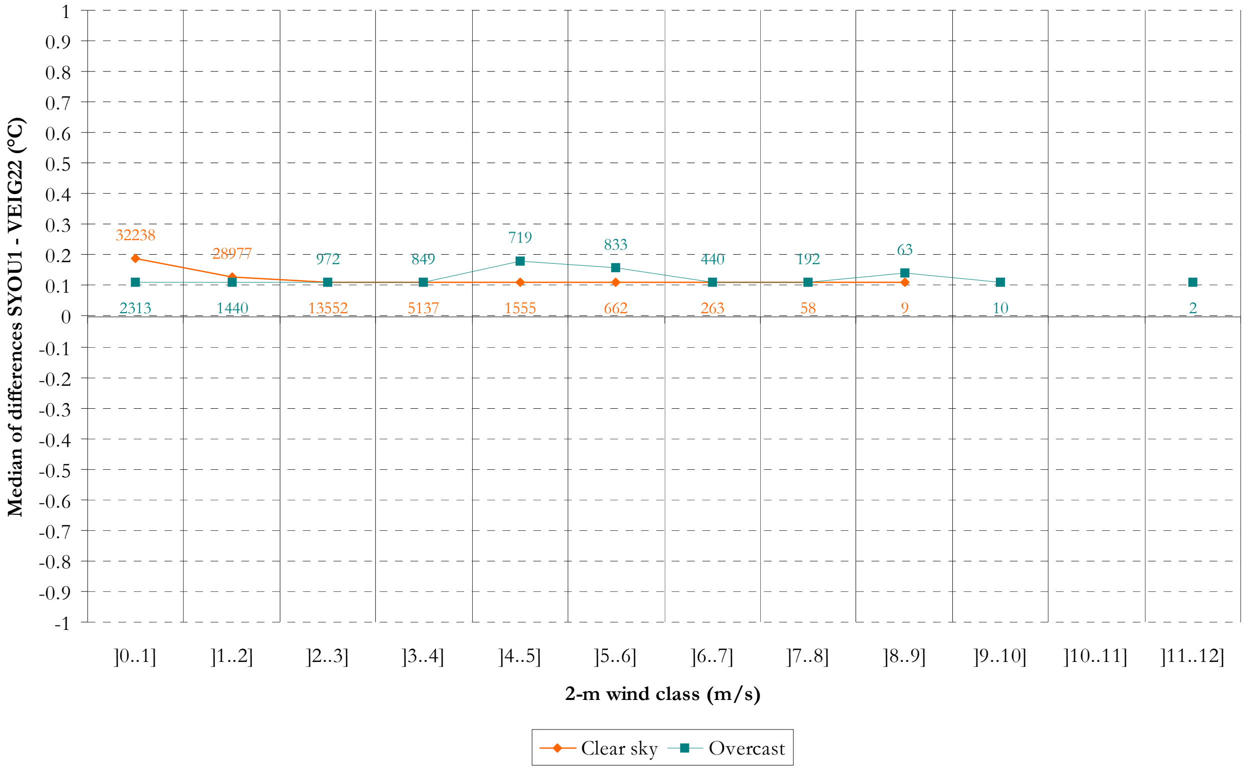


**Figure 13**

Screen #2:

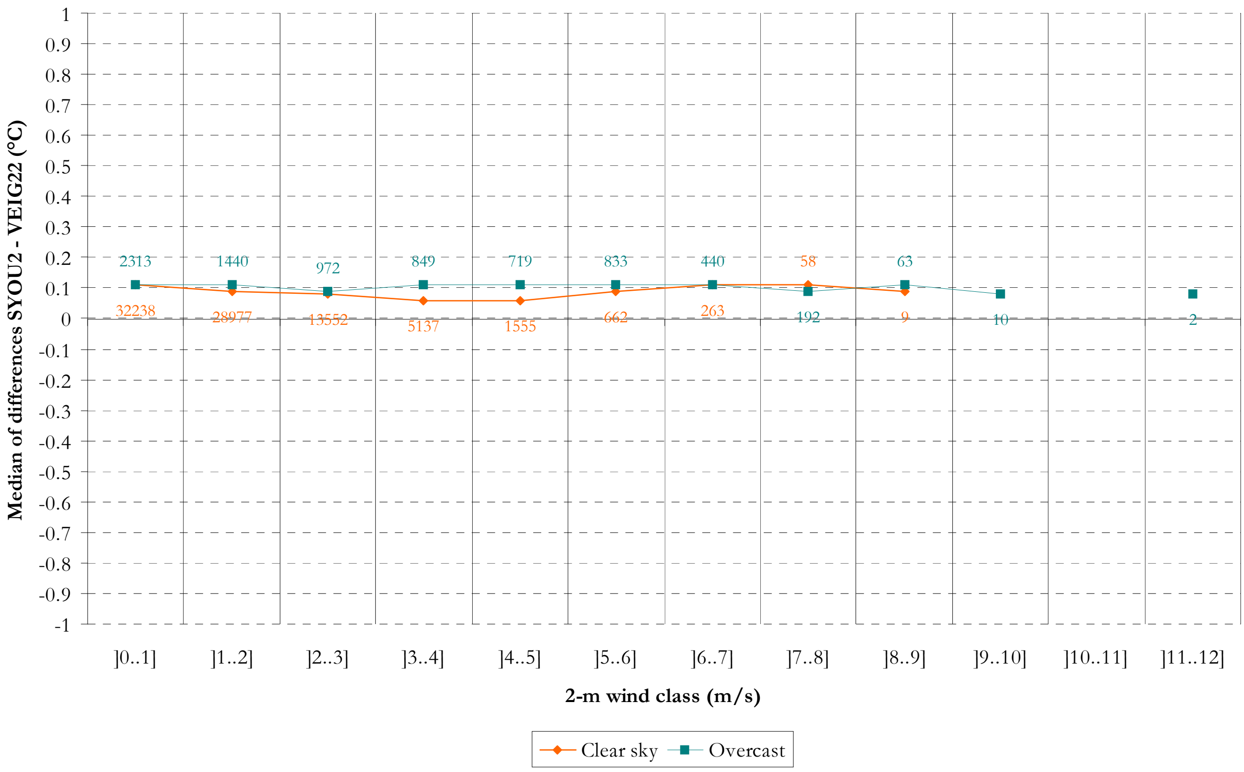


**Figure 14**

During the night time, both screens are warmer than the reference under clear sky conditions and just slightly warmer under overcast, being only marginally dependent on the wind conditions.

Overall the temperature gradient is less than 0.1°C.

## EFFECT OF SUN ELEVATION

The median of differences between SYOU and VEIG22 is plotted, using 1-minute quality checked data. Here, we consider periods lasting six hours at least where cloudiness is less or equal to 1 (clear sky), during daytime (sun elevation above -1°). We filter data where sun elevation is low (below 10°), medium (between 10° and 45°) or high (above 45°). Differences are classified according 2-meter wind speed (2-minute average).

Screen #1:

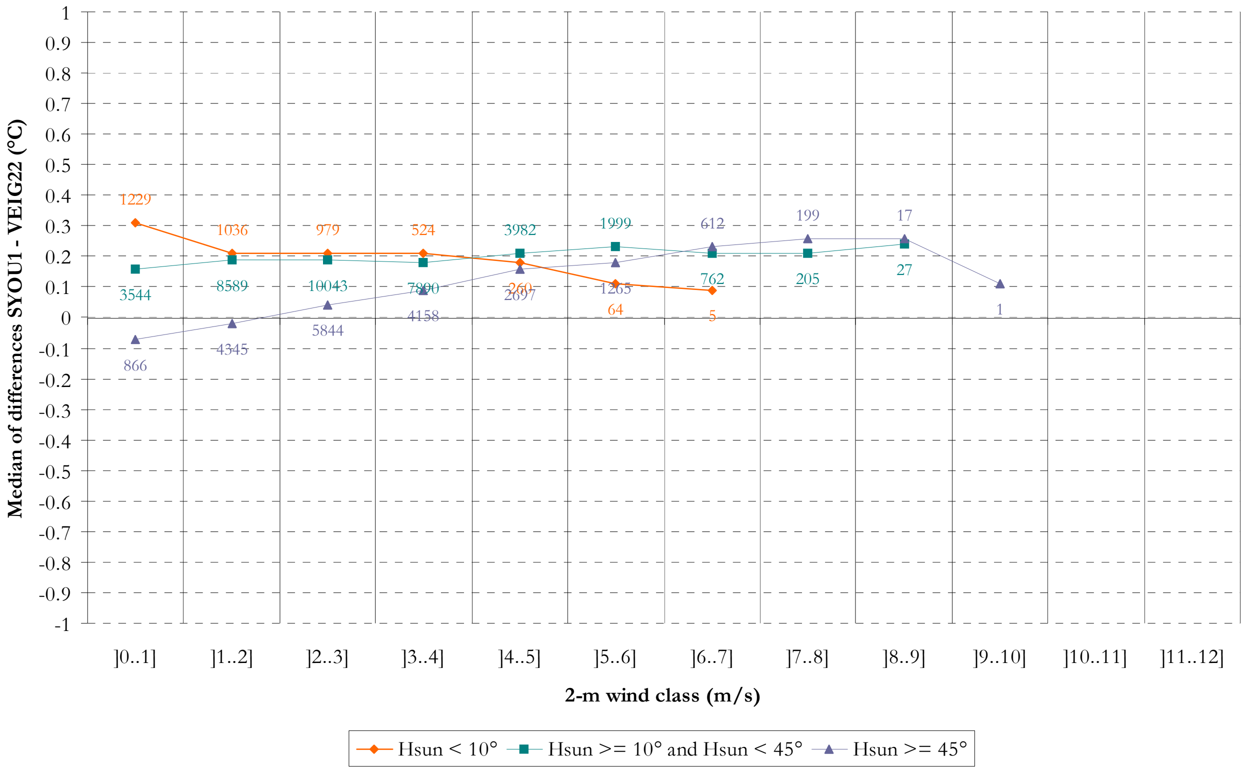


**Figure 15**

Screen #2:

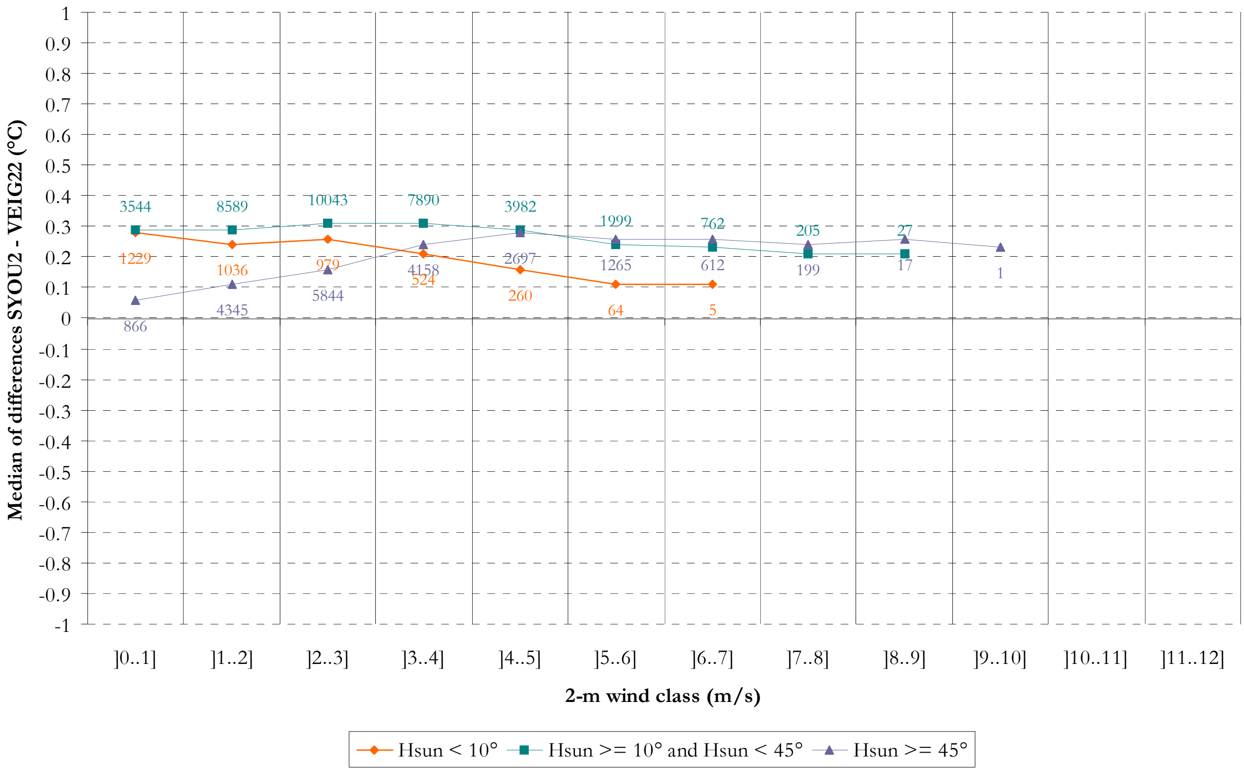


**Figure 16**

For sun elevation below 10$^{o}$C, both screens become cooler as the wind speed increases. The overall temperature gradient is about 0.2$^{o}$C.

For sun elevations from 10$^{o}$ to 45$^{o}$, both screens are becoming warmer, with an overall temperature gradient of less than 0.3$^{o}$C.

For sun elevations above 45$^{o}$, both screens are minimally dependent of the wind speed, with a slight tendency to become cooler as the wind speed increases.

Overall, for all sun elevations the screens are mostly warmer than the reference.

## COMBINED EFFECT OF WIND AND GLOBAL RADIATION

The medians of differences between SYOU and VEIG22 are represented here with a contour plot. The global radiation values are on the X-axis and on the Y axis is the 2-meter wind speed value (2-minute average). Medians are used in all cases, providing that at least one data is available for both conditions on radiation and wind considered.

Screen #1:

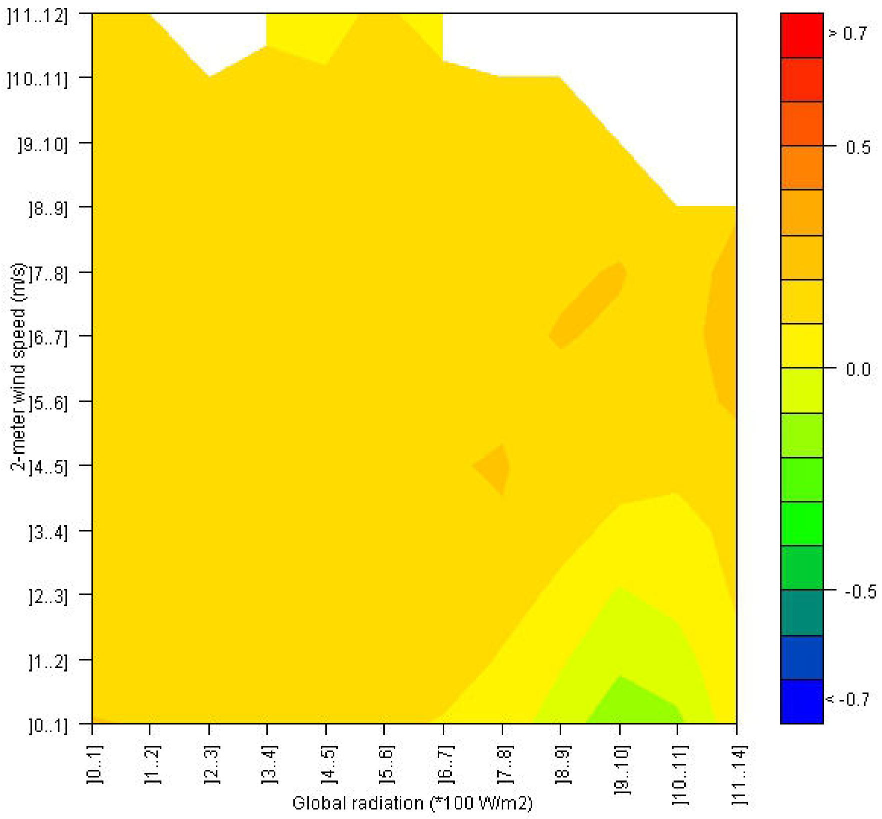


**Figure 17**

Screen #2:

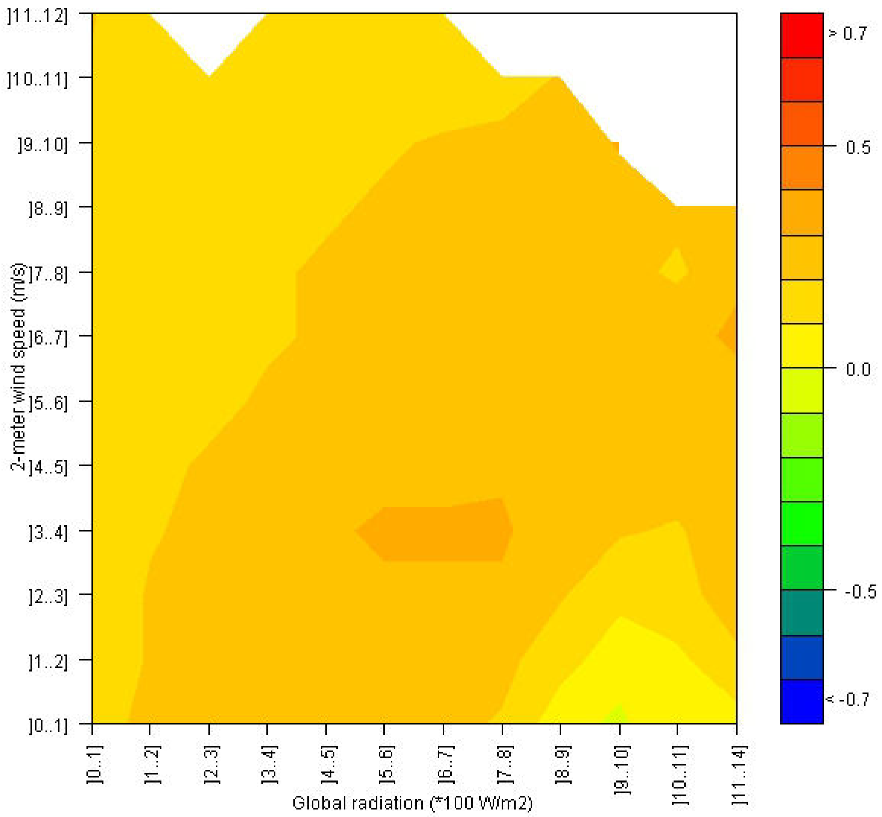


**Figure 18**

The two plots show the SYOU screens consistently warmer than the reference for most of the wind speed values and global radiation range, however the difference from the reference is minimum. The only exception is for the low winds and high radiation values, where the screens are slightly cooler or just about at the level of the reference.

## BEHAVIOUR DURING INCREASE/DECREASE OF TEMPERATURE

The distribution of differences between SYOU and the reference VEIG22 is plotted, using 1-minute quality checked data for the whole period of the intercomparison. Differences are classified according the temporal gradient of reference temperature over 1 minute. A screen faster (or slower, respectively) than the reference would be warmer (cooler) for positive gradient, cooler (warmer) for negative ones.

## Screen #1:

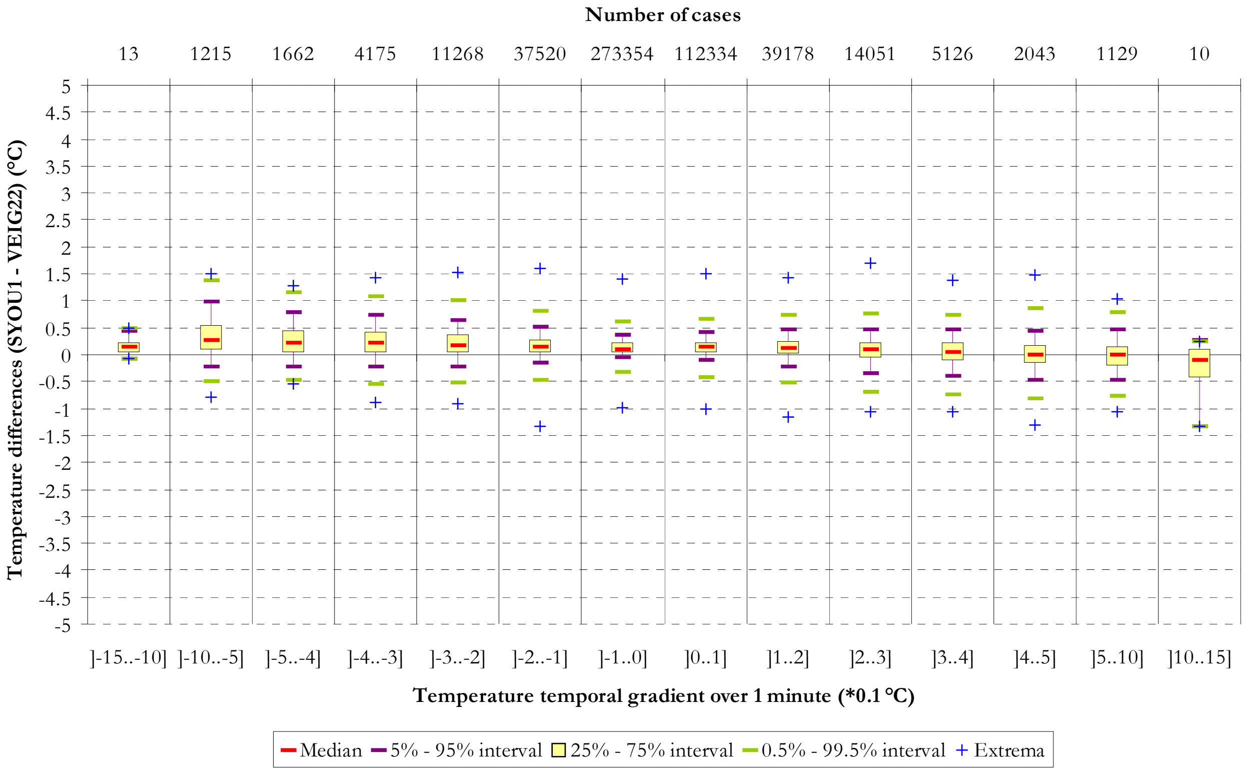


**Figure 19**

## Screen #2:

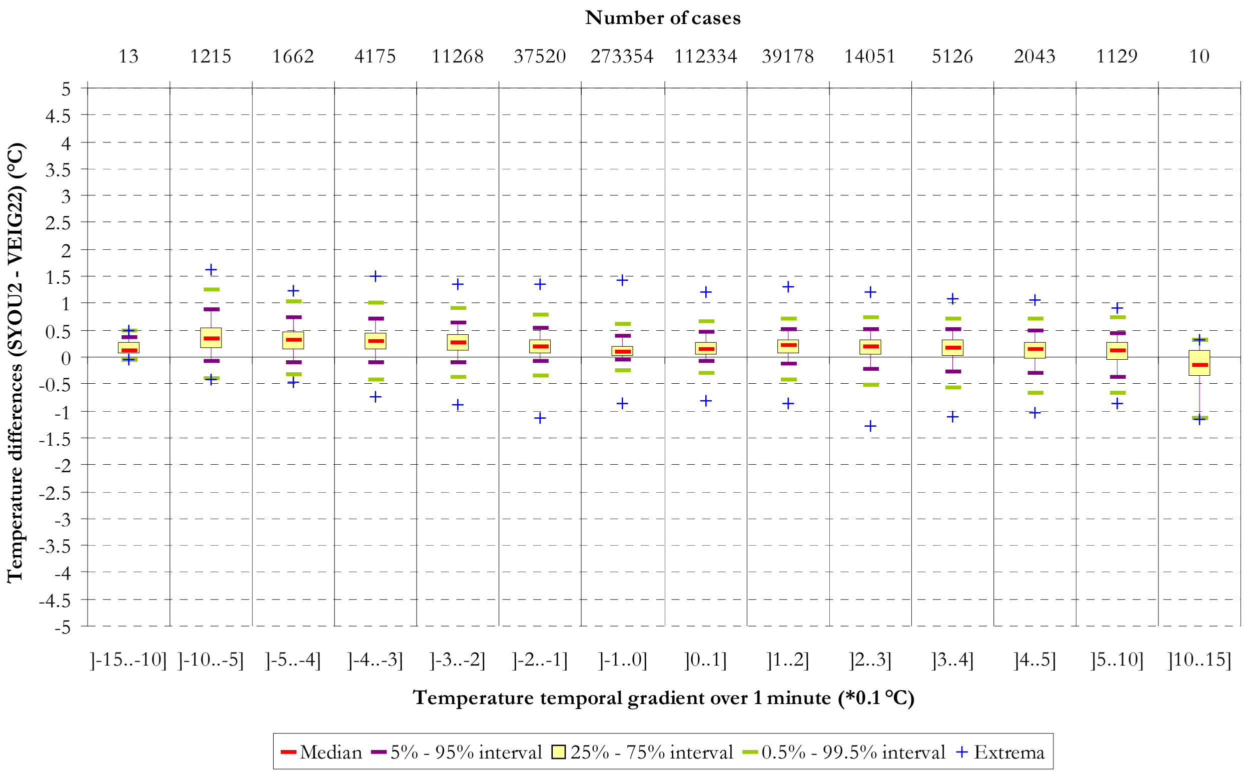


**Figure 20**

The SYOU screens are warmer (slower) than the reference for the cases when the temperature decreases and approximately similar to the reference, when the temperature increases, with a small tendency to be faster warmer).

Overall, the graphs indicate a minimum linearly decreasing dependency of the temperature differences with the temperature temporal gradient.

## QUALITY CONTROL INFORMATION

### DATA AVAILABILITY

The intercomparison period extends from the 1st of November 2008 to the 1st of November 2009. The theoretical number of 1-minute data is 525600.

The next table sums up the total number of data for each screen and for each possible QC flag.

**Table 3**

| **QC flag** | SYOU**1** | SYOU**2** |
|---|---|---|
| 0 (good) | 503266 | 503266 |
| 1 (inconsistent) | 0 | 0 |
| 2 (doubtful) | 0 | 0 |
| 3 (erroneous) | 0 | 0 |
| 7 (missing) | 22334 | 22334 |

### MAINTENANCE

No action done during the intercomparison period.

# 439102 FISCHER
# – Germany –
# VFIS

**TECHNICAL SPECIFICATIONS (PROVIDED BY THE MANUFACTURER)**

Dimensions: Length 18 cm x Diameter 16 cm

Weight: 1.6 kg

Material / Structure: White painted aluminium

Estimated radiation error:

Aspiration rate (in case of artificially ventilated screen/shield): 1.5 m/s

Power supply: 12 or 24 VDC

**Figure 1**

## OVERVIEW

The two VFIS screens agree well with each other for temperatures below 30°C. Above that the VFIS2 displayed a positive bias relative to VFIS1. For all temperature classes, the dispersion of the temperature differences is limited to less than 1°C.

The behaviour of the two VFIS screens was significantly different than that of the reference. While the mode of the temperature differences for both screens are around zero, both graphs are significantly skewed to the right, indicating that the two screens were consistently warmer than the reference, by a large margin. The daily minimum temperature was very closely to that reported from the reference, with one half of the data points just below the reference and the other half at or just above the level of the reference. The two VFIS screens significantly and consistently overestimated the daily maximum temperature by as much as 1.2°C-1.3°C.

The plots show very similar behaviour of the two VFIS screens as a function of the global radiation. The temperature differences vary with the irradiance.

The two plots show similar behaviour for the two VFIS screens during the day, as well as during the night. During the day the screens are significantly warmer than the reference for all wind conditions. During the night, the two VFIS screens are close to the reference. For wind speeds above 9m/s, the day-time and night-time behaviour are similar.

During daytime, the two VFIS screens had similar behaviour under clear sky, as well as under an overcast sky. Each screen was warmer during the day than during the night, for the same wind conditions.

Under clear sky, during the night, both VFIS screens were slightly colder than the reference for wind speeds below 3m/s and generally similar to the reference for winds above that. There is a minimum dependency of the median of the differences on the value of the wind speed. Under overcast conditions, the two VFIS screens were close to the reference for wind speeds up to 5m/s.

The sun elevation was a significant factor in the behaviour of VFIS screens for all classes of wind speeds. The screens were warmer than the reference for all sun elevations.

The two VFIS screens were significantly warmer than the reference for most of the wind and global radiation conditions. The exception was the case of very high wind speeds, above 9m/s and very low irradiance.

The two VFIS screens were notable slower than the reference when the temperature was decreasing.

## CALIBRATION INFORMATION

Calibration was performed by manufacturer.

**Table 1**

| Screen | Location | Screen serial number | Calibration date | Instrument bias (°C) |
|---|---|---|---|---|
| | | | | 20°C |
| VFIS1 | A4 | 188 | 19-Apr-2007 | 0.1 |
| VFIS2 | D4 | 189 | 19-Apr-2007 | 0.2 |

The result of calibration of reference VEIG22 is available in the main report of the intercomparison, section 5.4.1.

## COMPARISON OF BOTH SENSORS

The distribution of differences between screen 1 and screen 2 is plotted, using 1-minute quality checked data for the whole period of the intercomparison. Differences are classified according screen 1 temperature.

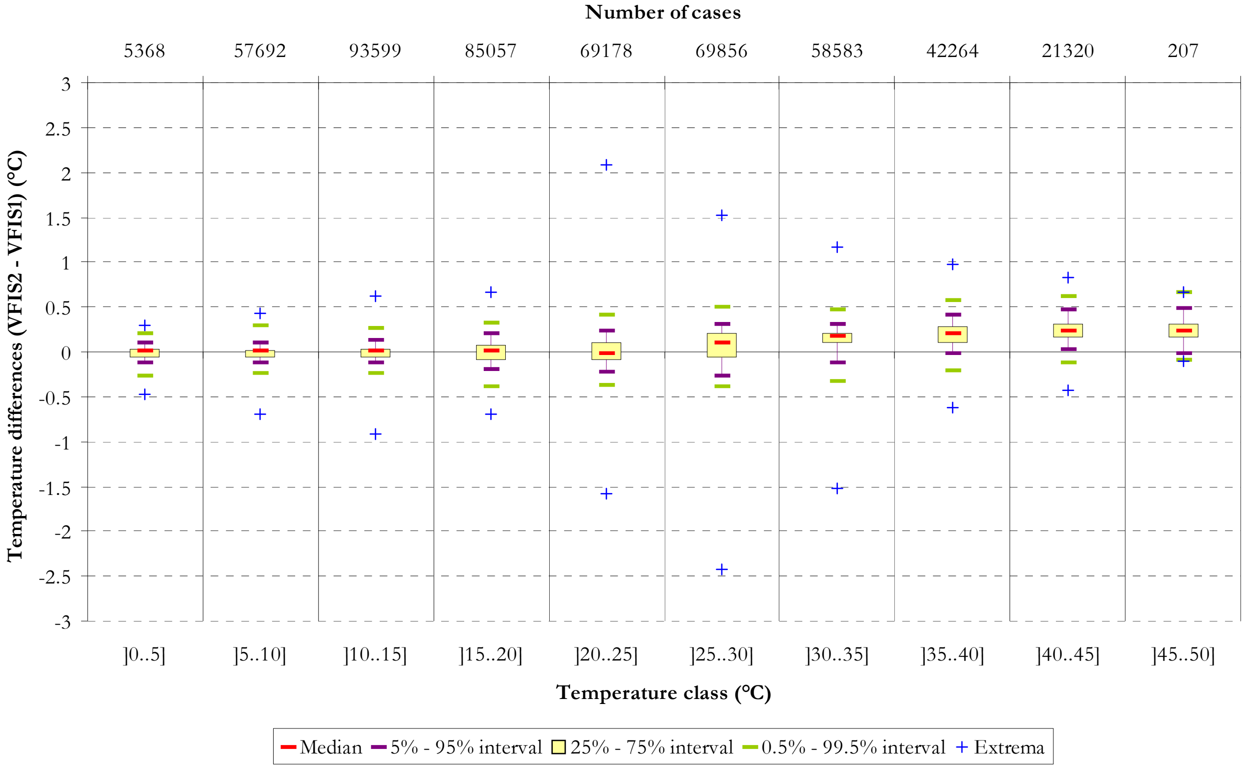


**Figure 2**

The two VFIS screens agree well with each other for temperatures below 30°C. Above that the VFIS2 displayed a positive bias relative to VFIS1. For all temperature classes, the dispersion of the temperature differences is limited to less than 1°C.

## COMPARISON WITH THE REFERENCE

### HISTOGRAM OF DIFFERENCES

The histogram of differences between VFIS and the reference VEIG22 is plotted, using 1-minute quality checked data for the whole period of the intercomparison. Differences are plotted by steps of 0.1K. The vertical axis is the frequency in percent for each class of differences.

Screen #1:

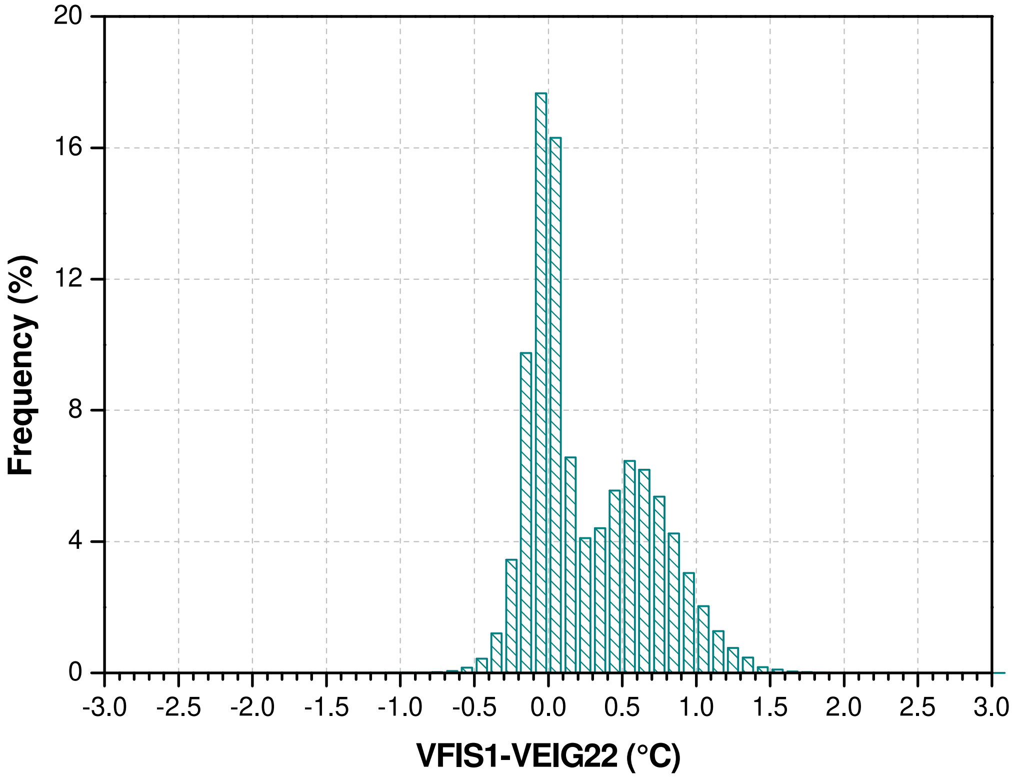


**Figure 3**

Screen #2:

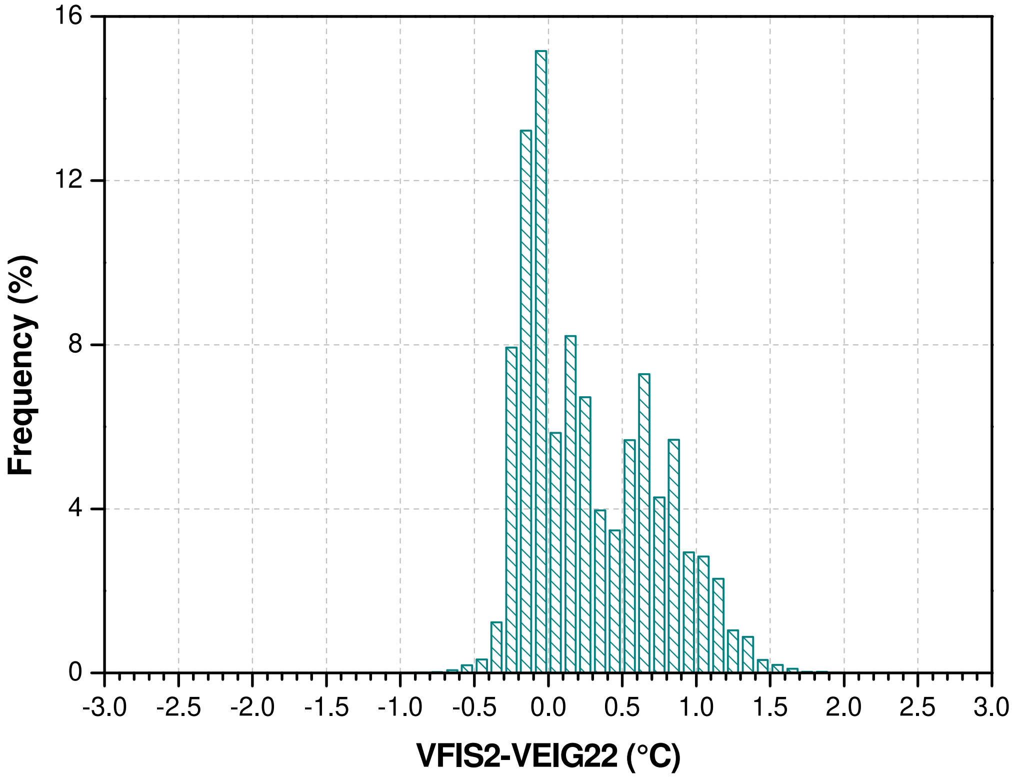


**Figure 4**

These two graphs show that the behaviour of the two VFIS screens was significantly different than that of the reference. While the mode of the temperature differences for both screens are around zero, both graphs are significantly skewed to the right, indicating that the two screens were consistently warmer than the reference, by a large margin.

CUMULATIVE HISTOGRAMS OF DIFFERENCES OF DAILY EXTREME VALUES

The cumulative histograms of differences with the reference VEIG22 of T (1-minute quality checked data), Tn (daily minimum temperature) and Tx (daily maximum temperature) are plotted, for the whole period of the intercomparison. Differences are plotted by steps of 0.1K.

Screen #1:

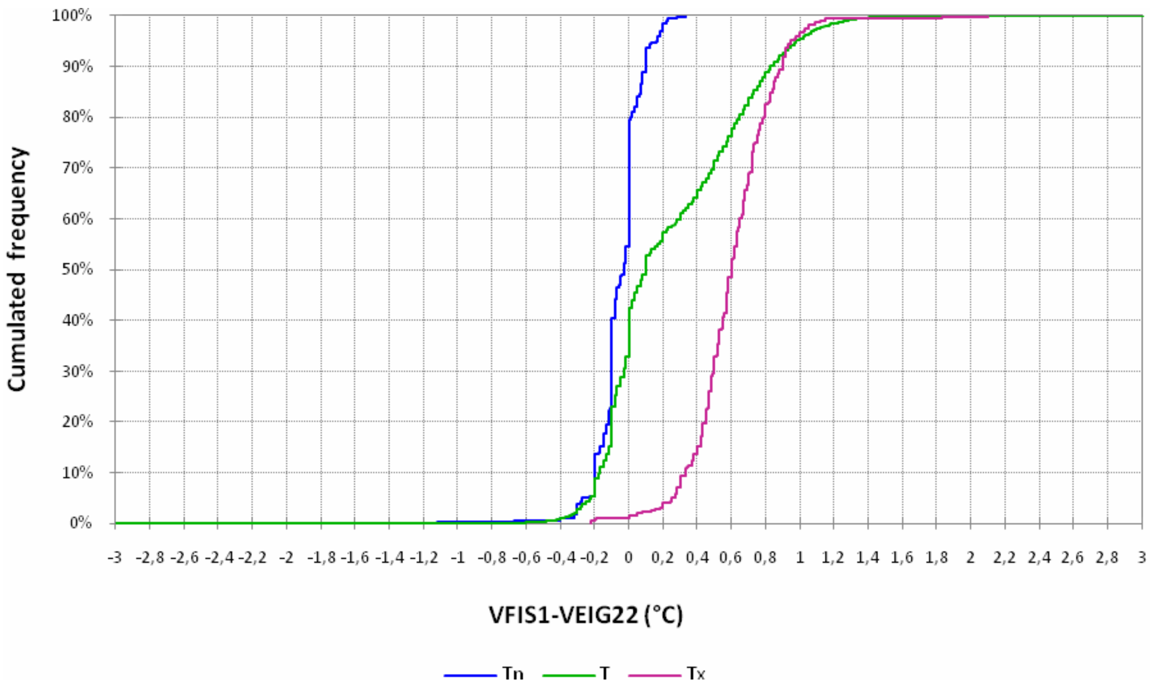


**Figure 5**

Screen #2:

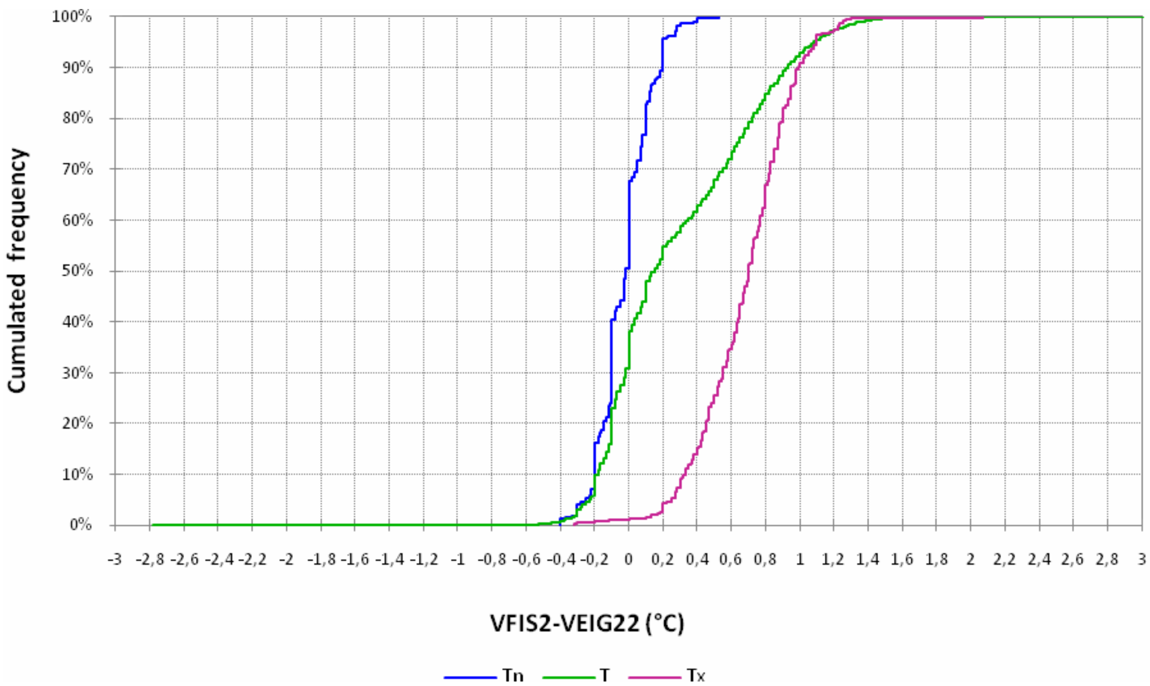


**Figure 6**

The cumulative histograms of differences of daily extreme values show that for both VFIS screens the daily minimum temperature was very closely to that reported from the reference, with 50% of the data points just below the reference and 50% at or just above the level of the reference.

The plots for the daily maximum temperature show that the two VFIS screens significantly and consistently overestimated it, by comparison to the reference. For virtually all data points, the Tx from the VFIS screen was higher than that from the reference screen by as much as 1.2°C-1.3°C.

The plots for the 1-minute data show that in about 40% of the cases, the VFIS screens were slightly colder than the reference, while in the balance of 60% of the cases were warmer than the reference, at times by a very large margin, about 1.4°C.

TABLE

The table 2 indicates the percentage of data that differ by less than 0.2°C (and 0.5°C) from the reference.

**Table 2**

| | | [-0.2°..0.2°] | [-0.5°..0.5°] |
|---|---|---|---|
| VFIS1 | T | 51.9 | 71.1 |
| | Tn | 91.0 | 99.4 |
| | Tx | 3.1 | 32.8 |
| VFIS2 | T | 49.1 | 67.7 |
| | Tn | 84.2 | 99.7 |
| | Tx | 3.6 | 25.5 |

## INFLUENCE OF GLOBAL RADIATION

The distribution of differences between VFIS and the reference VEIG22 is plotted, using 1-minute quality checked data for the whole period of the intercomparison. Differences are classified according global radiation.

Screen #1:

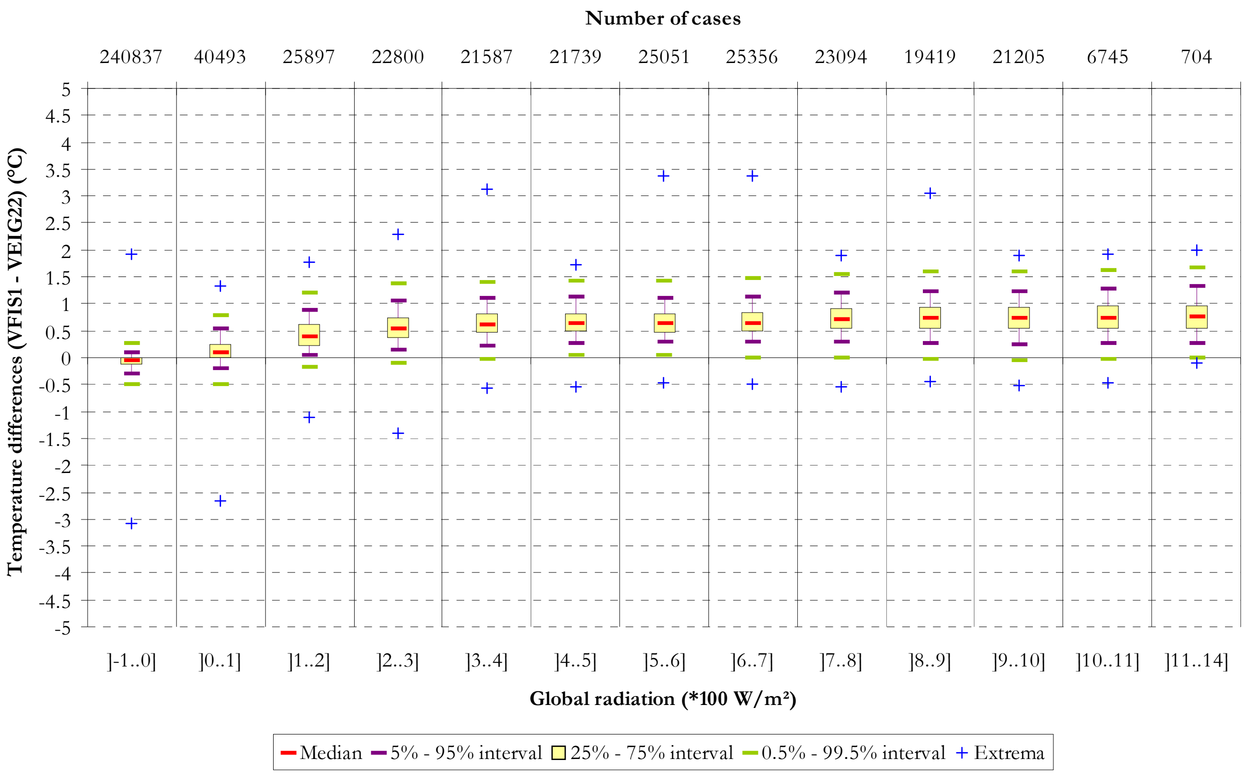


**Figure 7**

Screen #2:

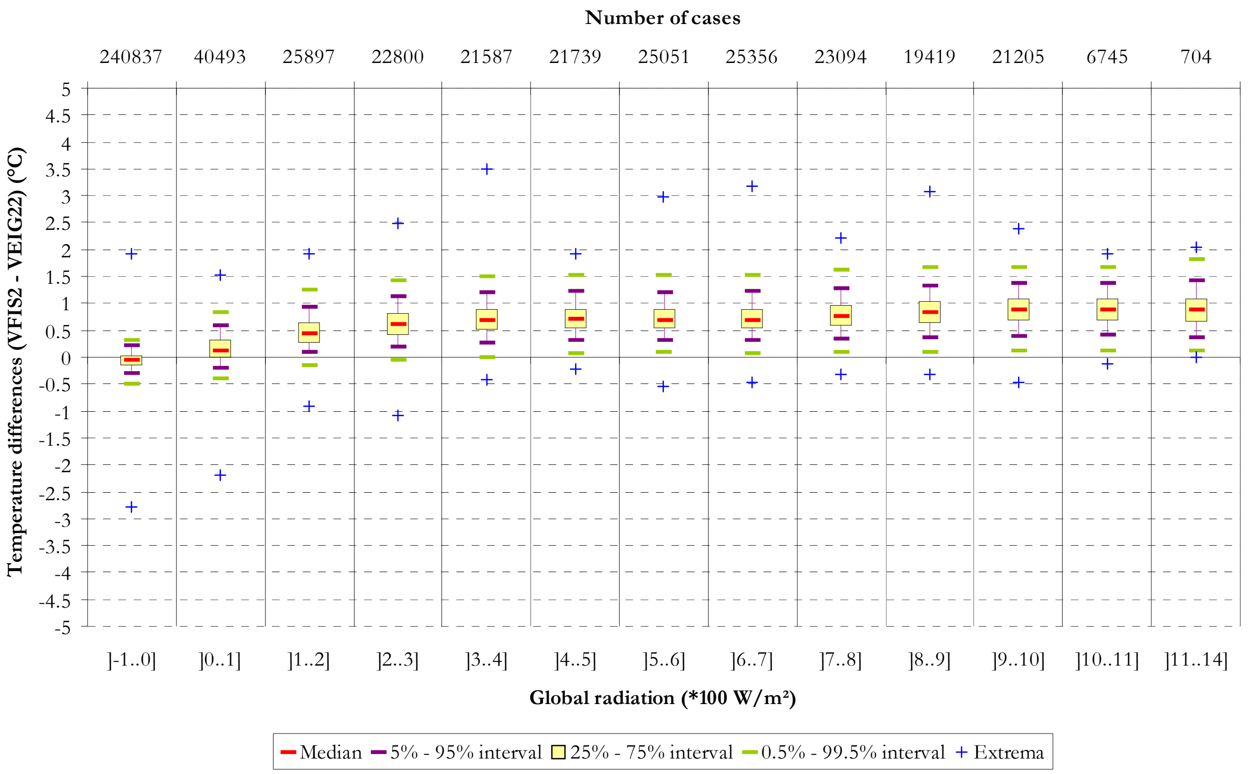


**Figure 8**

The plots show very similar behaviour of the two VFIS screens as a function of the global radiation. The temperature differences vary with the irradiance. The two screens were similar to the reference for low or zero irradiance, and became warmer when the irradiance increased. The median of differences remained relatively constant, below 1°C, for irradiance above 300W/m$^2$.

## RADIATION EFFECT

### DIFFERENCES BETWEEN DAY AND NIGHT BEHAVIOUR

The median of differences between VFIS and VEIG22 is plotted, using 1-minute quality checked data for the whole period of the intercomparison. We filter data for which sun elevation is above -1° (day) or below -1° (night). Differences are classified according 2-meter wind speed (2-minute average).

Screen #1:

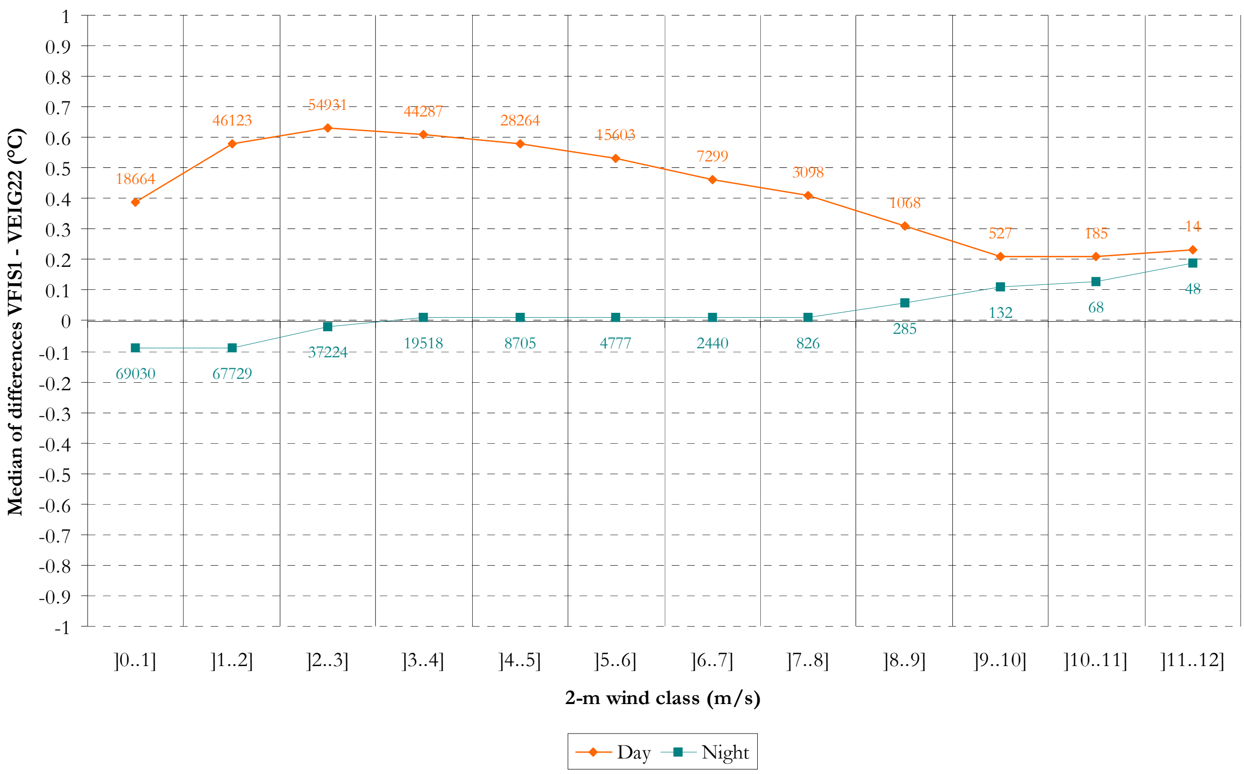


**Figure 9**

Screen #2:

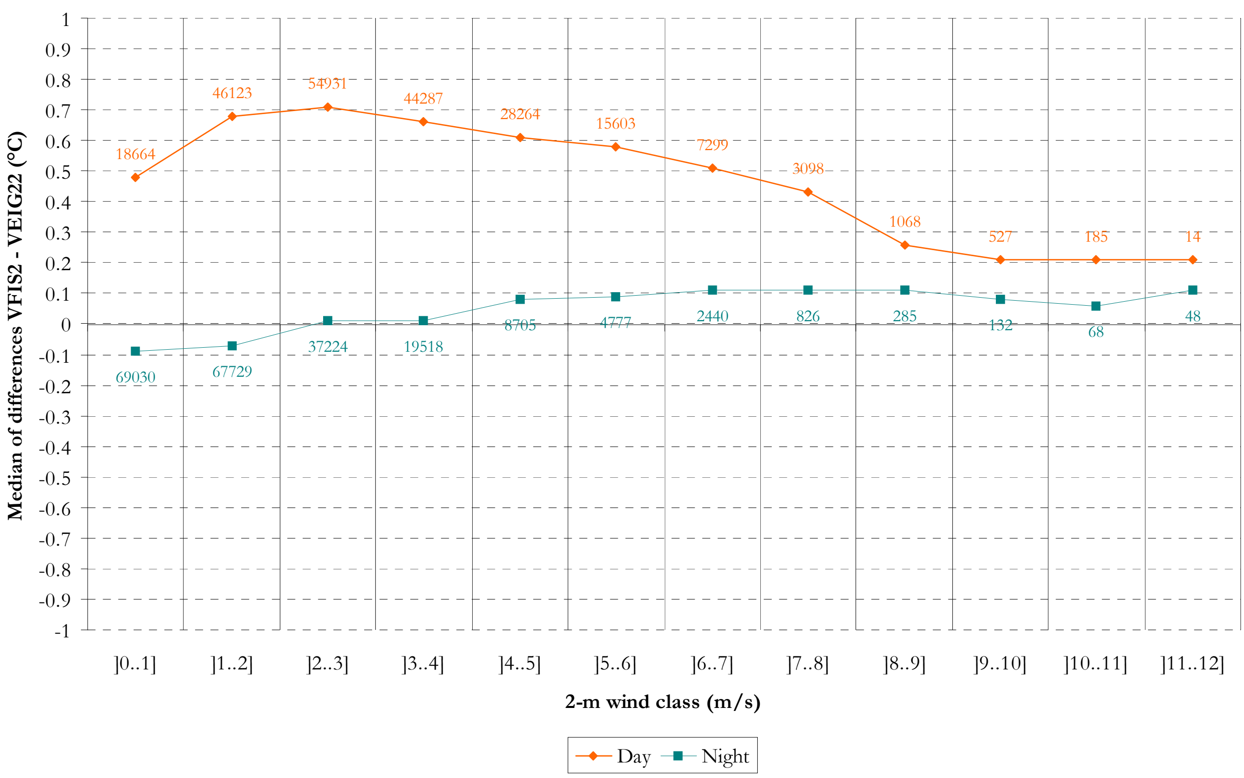


**Figure 10**

The two plots show similar behaviour for the two VFIS screens during the day, as well as during the night.

During the day the screens are significantly warmer than the reference for all wind conditions. The median of the differences reaches a peak of 0.7°C at wind speeds of 2-3m/s, then decreases approximately linearly for wind speeds up to 9m/s. Above that, the screens' behaviour is less dependent of the wind speeds.

During the night, the two VFIS screens are close to the reference, being slightly colder for wind speeds up to 2m/s and at similar to the reference of slightly warmer for wind speeds above 2m/s.

For wind speeds above 9m/s, the day-time and night-time behaviour are similar.

DIFFERENCES BETWEEN CLEAR SKY AND OVERCAST SKY DURING DAYTIME

The median of differences between VFIS and VEIG22 is plotted, using 1-minute quality checked data. Here, we consider periods lasting six hours at least where cloudiness is less or equal to 1 (clear sky) or more or equal to 7 (overcast sky), during daytime (sun elevation above -1°). Differences are classified according 2-meter wind speed (2-minute average).

Screen #1:

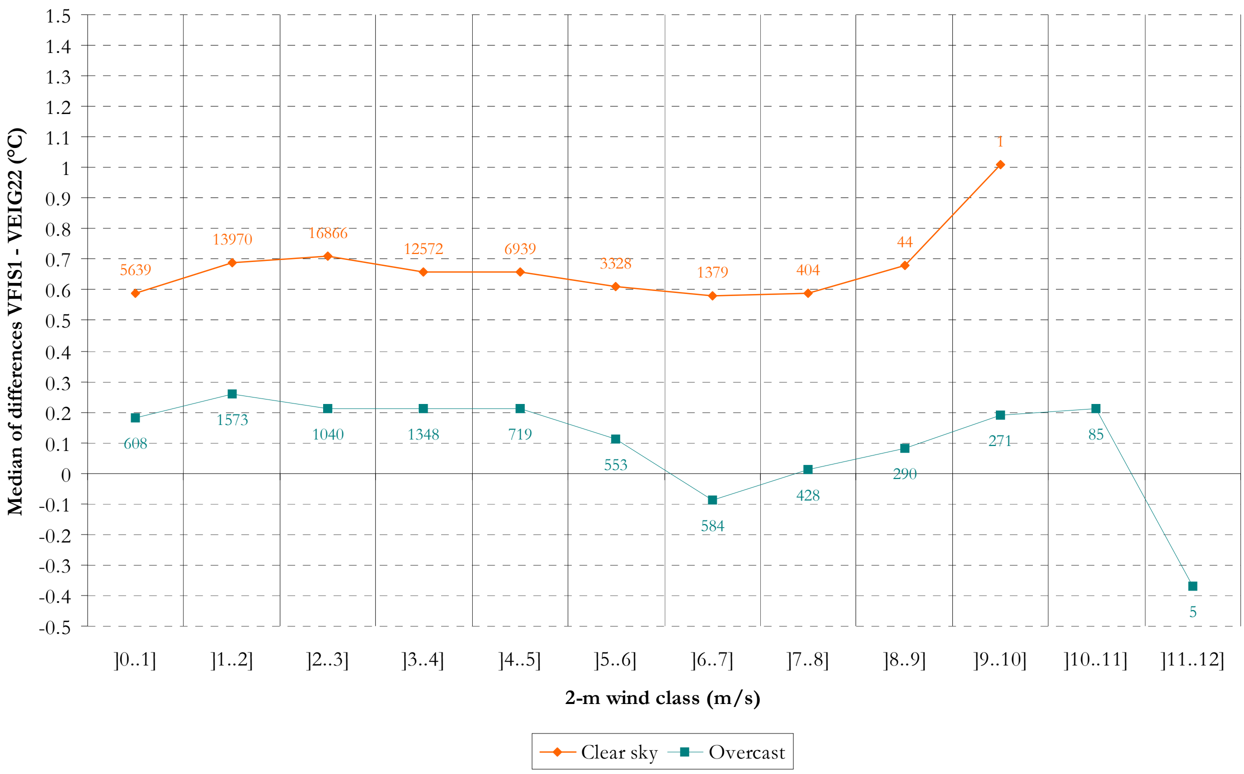


**Figure 11**

Screen #2:

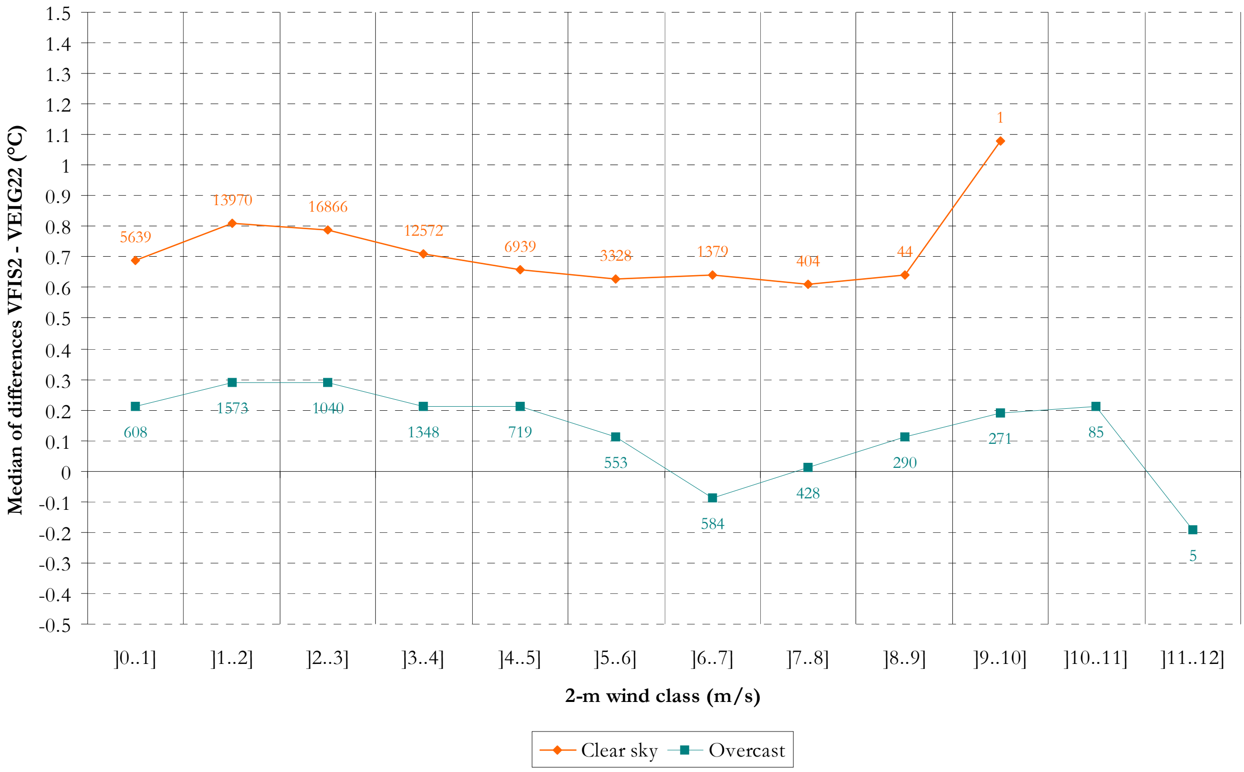


**Figure 12**

The plots indicate that the two VFIS screens had similar behaviour under clear sky, as well as under an overcast sky. Each screen was warmer during the day than during the night, for the same wind conditions.

Under clear sky, the two screens were significantly warmer than the reference, with a median of differences varying between 0.6°C and 0.8°C. The behaviour of the screen VFIS #2 was somewhat more susceptible to the increase in wind speed than the screen #1.

During the night, the two screens were consistently warmer than the reference for winds up to 4m/s, with a more notable dependency of wind speed for screen #2.

The wind speed between 4m/s and 6m/s had a cooling effect on both VFIS screens. For winds above 6m/s, the two screens became again warmer than the reference.

DIFFERENCES BETWEEN CLEAR SKY AND OVERCAST SKY DURING NIGHT TIME

The median of differences between VFIS and VEIG22 is plotted, using 1-minute quality checked data. Here, we consider periods lasting six hours at least where cloudiness is less or equal to 1 (clear sky) or more or equal to 7 (overcast sky), during night time (sun elevation below -1°). Differences are classified according 2-meter wind speed (2-minute average).

Screen #1:

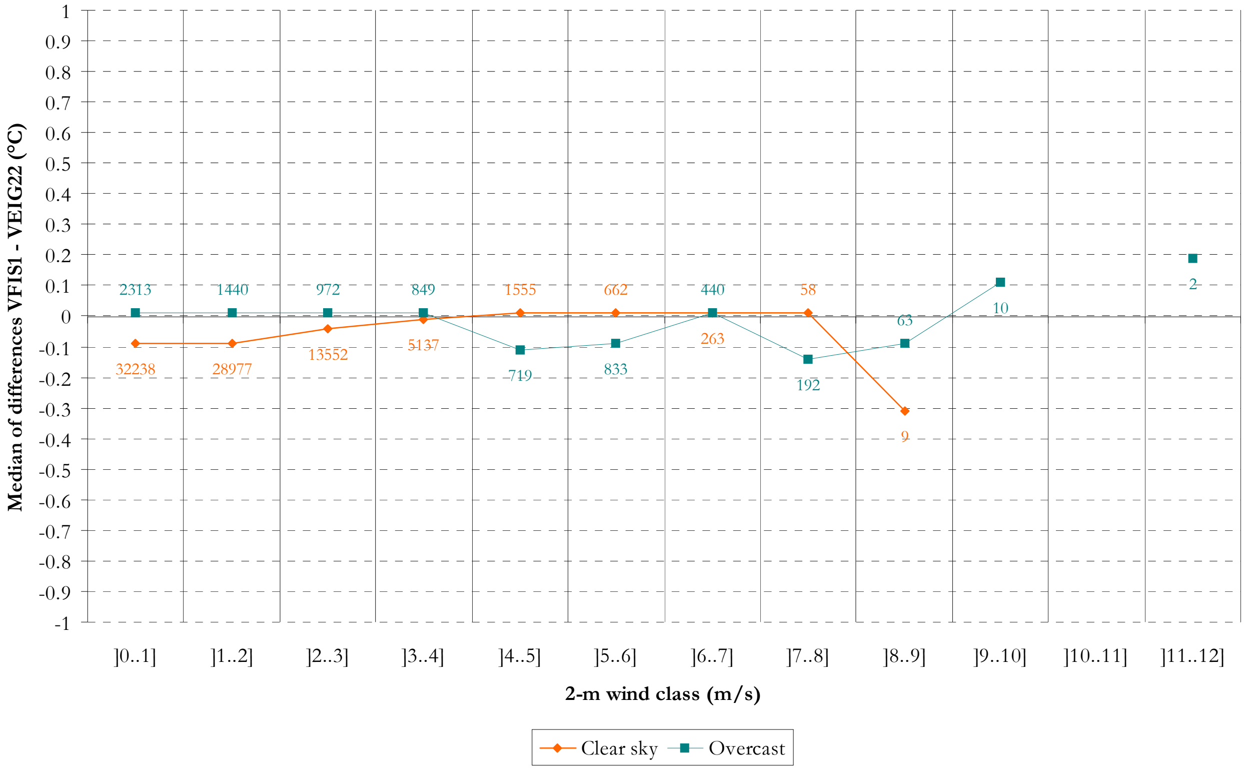


**Figure 13**

Screen #2:

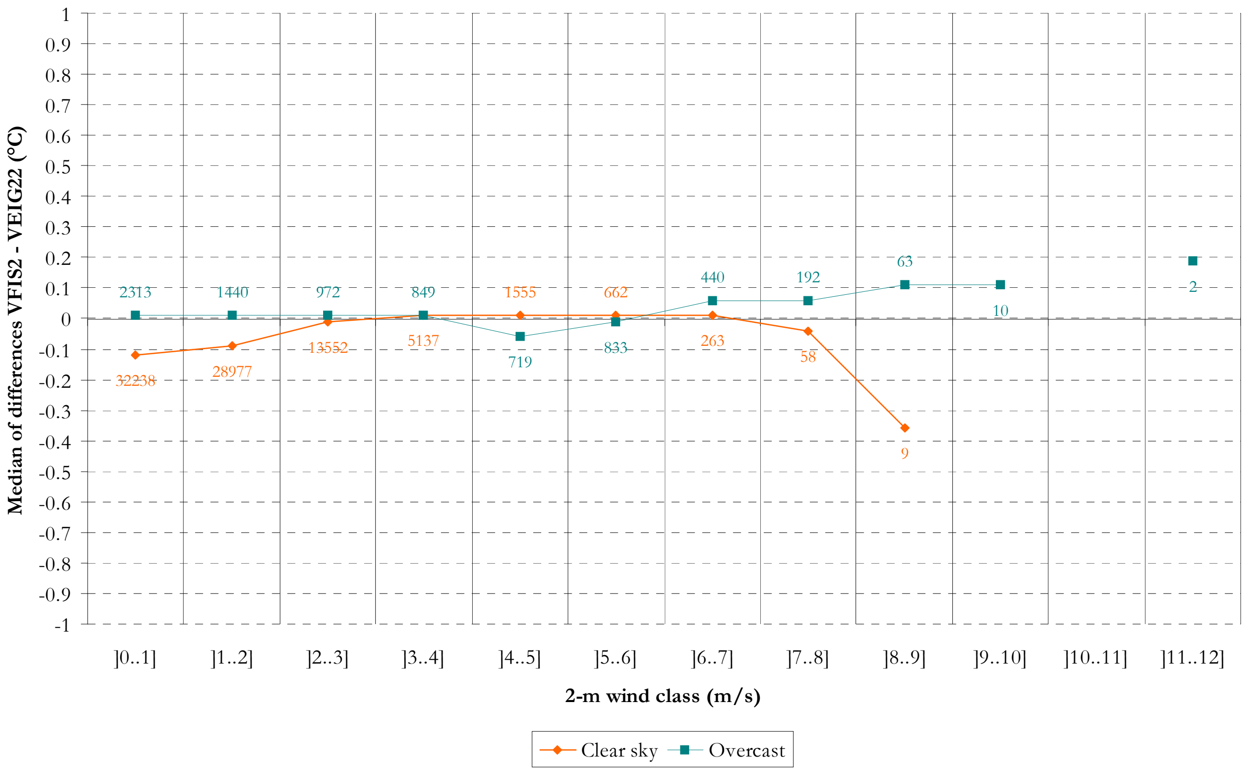


**Figure 14**

Under clear sky, during the night, both VFIS screens were slightly colder than the reference for wind speeds below 3m/s and generally similar to the reference for winds above that. There is a minimum dependency of the median of the differences on the value of the wind speed.

Under overcast conditions, the two VFIS screens were close to the reference for wind speeds up to 5m/s, and the median of the differences is minimally dependent on the wind speed p to that point. For wind speeds above 5m/s, the screen #1 became slightly colder than the reference, while the screen#2 became slightly warmer than the reference.

## EFFECT OF SUN ELEVATION

The median of differences between VFIS and VEIG22 is plotted, using 1-minute quality checked data. Here, we consider periods lasting six hours at least where cloudiness is less or equal to 1 (clear sky), during daytime (sun elevation above -1°). We filter data where sun elevation is low (below 10°), medium (between 10° and 45°) or high (above 45°). Differences are classified according 2-meter wind speed (2-minute average).

Screen #1:

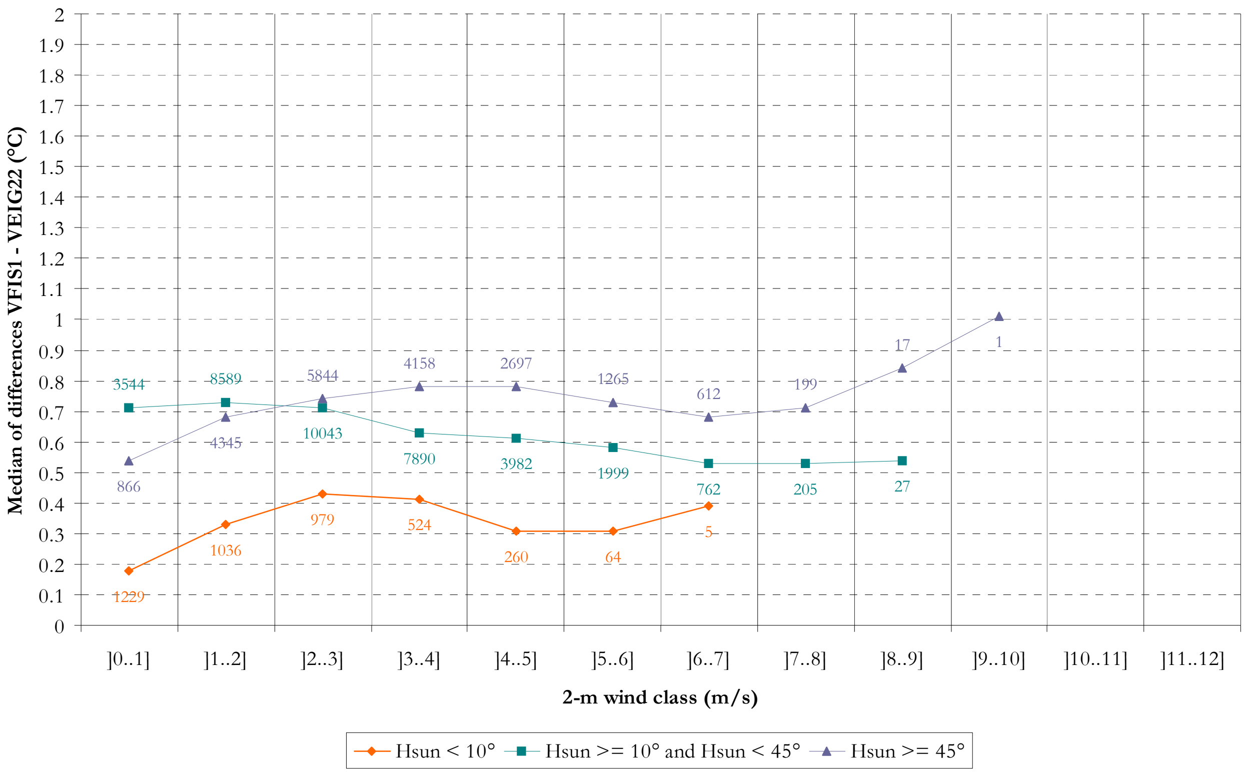


**Figure 15**

Screen #2:

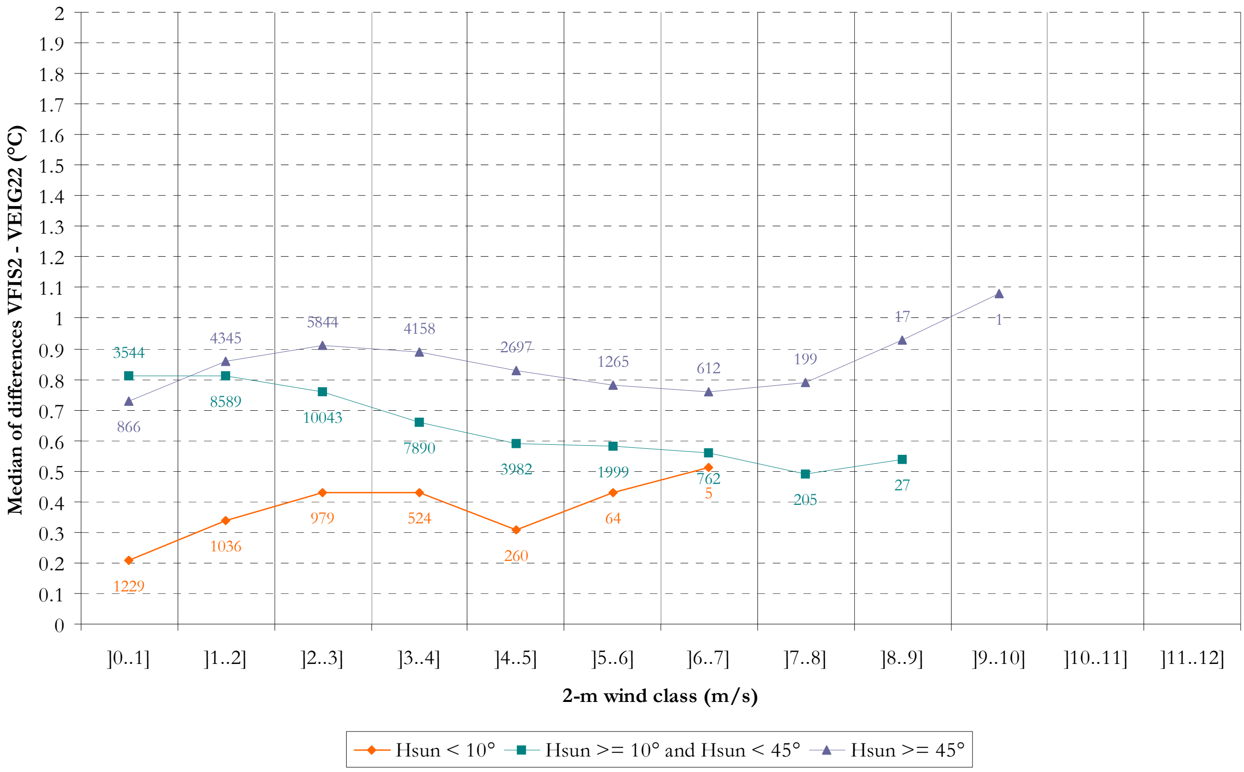


**Figure 16**

The two plots show that the sun elevation was a significant factor in the behaviour of VFIS screens for all classes of wind speeds. The screens were warmer than the reference for all sun elevations. The screens were closest to the reference for sun elevations below 10°, with a median of differences of 0.5°C or less, and warmest for sun elevations above 45°, the median of the differences varying from 0.7°C to 0.9°C .

For wind speeds up to 2m/s , the screens experience a slight warming effect when the sun is below 10° and above 45°. When the wind speed was above 2m/s the two screens become slightly cooler.

For sun elevations 10° to 45°, there was a cooling effect of the two screens with the increase in wind speed. For calm wind conditions,the screens were the warmest when the sun elevation was 10° to 45°.

## COMBINED EFFECT OF WIND AND GLOBAL RADIATION

The medians of differences between VFIS and VEIG22 are represented here with a contour plot. The global radiation values are on the X-axis and on the Y axis is the 2-meter wind speed value (2-minute average). Medians are used in all cases, providing that at least one data is available for both conditions on radiation and wind considered.

Screen #1:

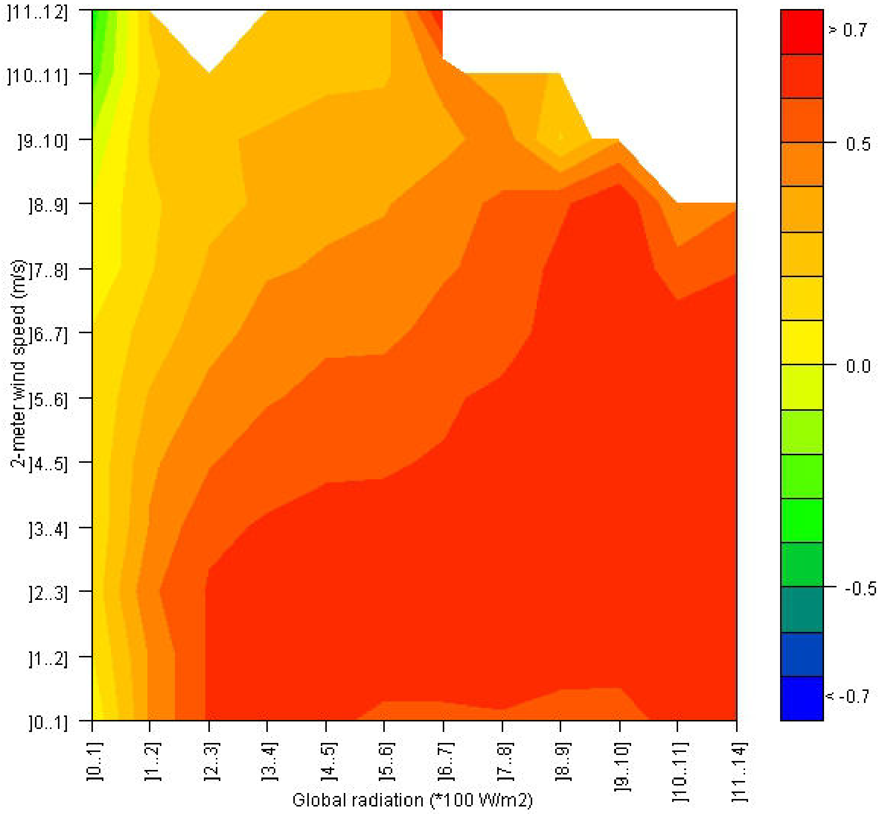


**Figure 17**

Screen #2:

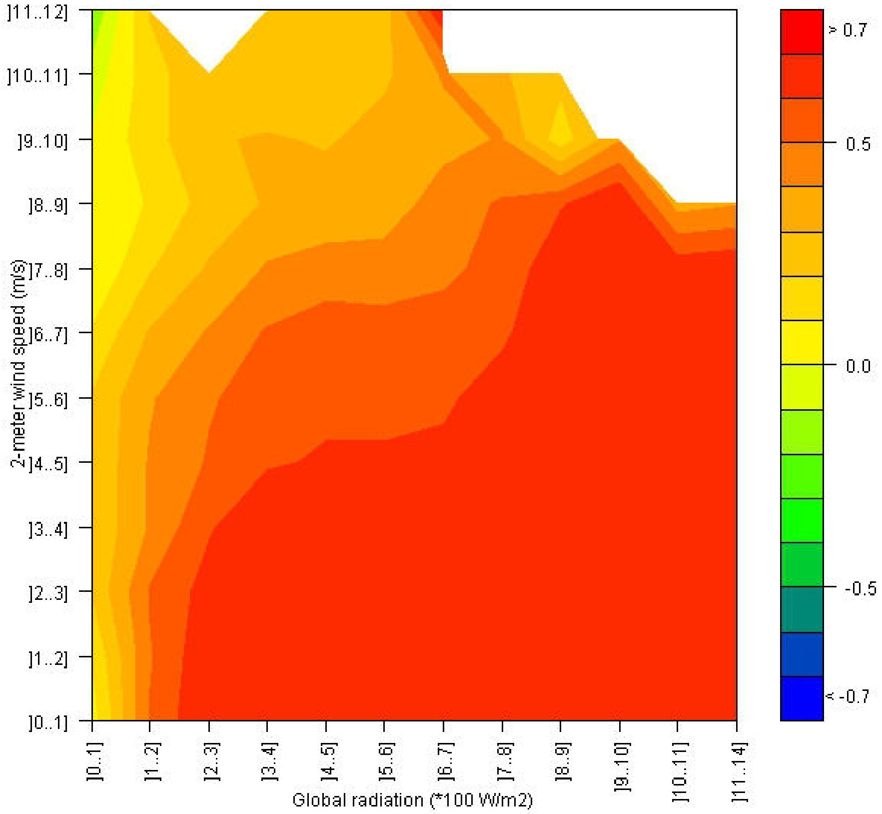


**Figure 18**

These two plots show that the two VFIS screens were significantly warmer than the reference for most of the wind and global radiation conditions. The exception was the case of very high wind speeds, above 9m/s and very low irradiance.

## BEHAVIOUR DURING INCREASE/DECREASE OF TEMPERATURE

The distribution of differences between VFIS and the reference VEIG22 is plotted, using 1-minute quality checked data for the whole period of the intercomparison. Differences are classified according the temporal gradient of reference temperature over 1 minute. A screen faster (or slower, respectively) than the reference would be warmer (cooler) for positive gradient, cooler (warmer) for negative ones.

Screen #1:

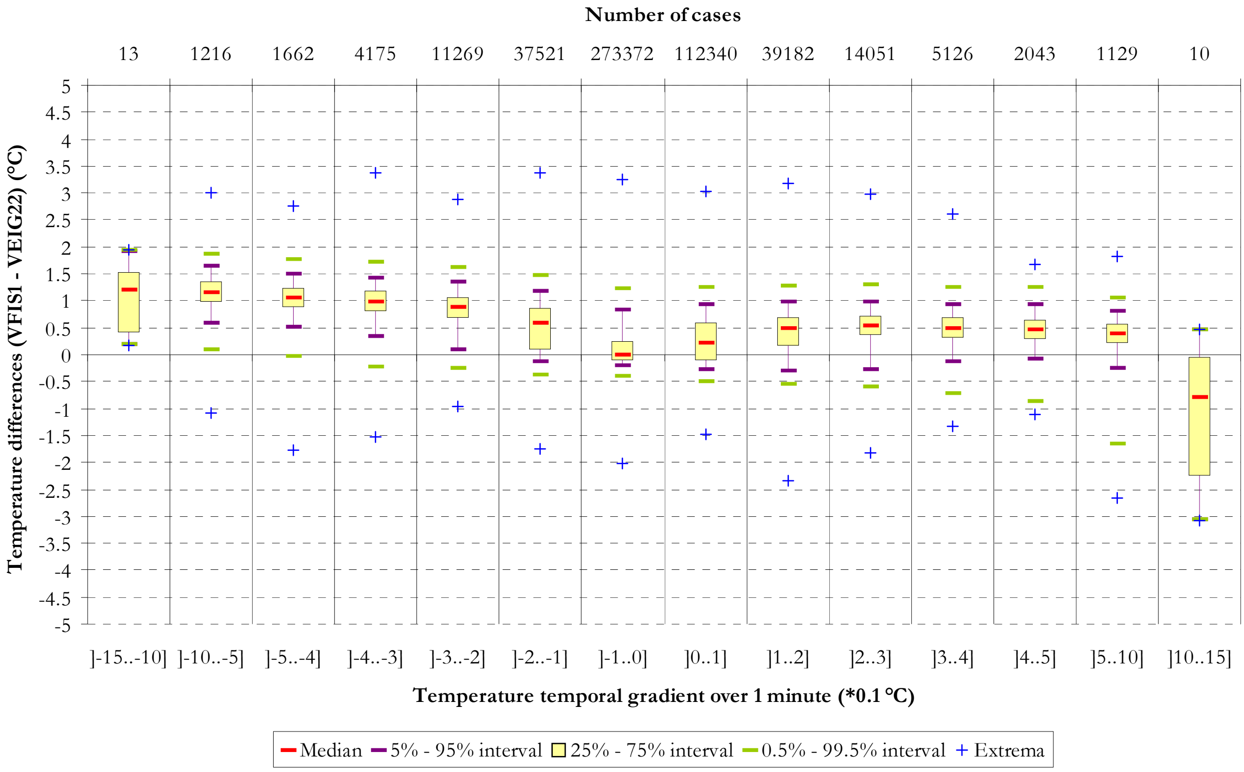


**Figure 19**

Screen #2:

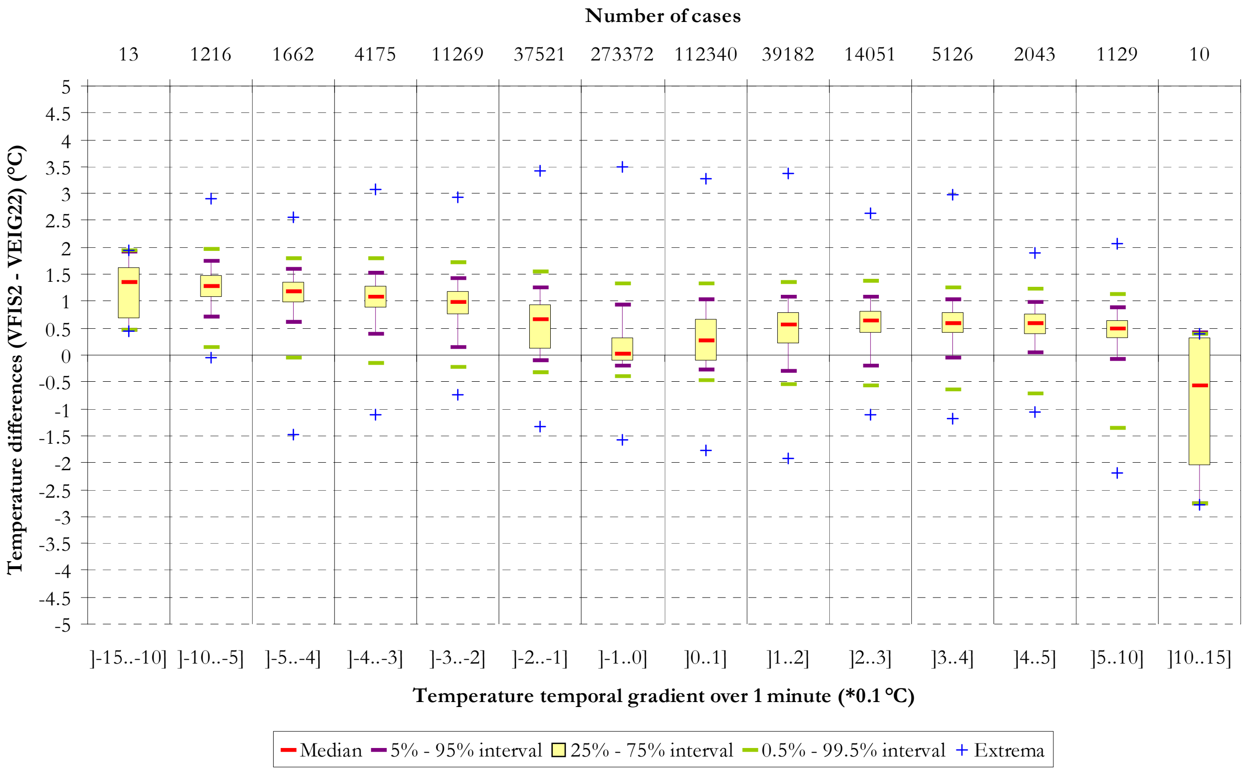


**Figure 20**

The two VFIS screens were notable slower than the reference when the temperature was decreasing. This effect was more evident for larger magnitudes of the temperature temporal gradient, 1°C or more.

For positive temperature temporal gradient, the VFIS screens were warmer but this was not a function of the value of the gradient.

## QUALITY CONTROL INFORMATION

### DATA AVAILABILITY

The intercomparison period extends from the 1st of November 2008 to the 1st of November 2009. The theoretical number of 1-minute data is 525600.

The next table sums up the total number of data for each screen and for each possible QC flag.

**Table 3**

| **QC flag** | VFIS1 | VFIS2 |
|---|---|---|
| 0 (good) | 503266 | 503266 |
| 1 (inconsistent) | 0 | 0 |
| 2 (doubtful) | 0 | 0 |
| 3 (erroneous) | 0 | 0 |
| 7 (missing) | 22334 | 22334 |

### MAINTENANCE

On the 29th of September, 2009, both sensors were removed and the fan was cleaned. Before the operation, the ventilation was good for VFIS1, medium for VFIS2. After the operation, it was better.

# LAM 630 EIGENBRODT
# – Germany –
# VEIG

**TECHNICAL SPECIFICATIONS (PROVIDED BY THE MANUFACTURER)**

Dimensions: Length 30 cm x Width 33 cm x Height 45 cm

Weight: 3.5 kg

Material/Structure: ABS Synthetic material, weather proof & gleaming white acryl glass

Estimated radiation error: + 0.8 K

Aspiration rate (in case of artificially ventilated screen/shield): approx 3500 rpm

Power supply: 12 V

**Figure 1**

Each screen includes two temperature probes and two relative humidity sensors.

## OVERVIEW

The four probes give very close results. There is no dependency with temperature.

The four probes give close results compared to the reference. No special effect on daily extreme temperatures is observed.

No effect of global radiation is observed.

For all sensors, the curves for day and night times are very close: there is less than 0.1°C between them. Both are stable with wind speed.

For all sensors, differences are less than 0.1°C between clear sky and overcast conditions, during daytime or night time conditions. They are stable when the wind speed increases.

The lines for different sun elevation values are very close one from another. They are very stable when wind speed increases.

For all probes, contour plots are very uniform around the 0 value.

No probe is in advance or late compared to the reference.

## CALIBRATION INFORMATION

The calibration of the four probes was performed in Trappes.

**Table 1**

| Sensor | Location | Pt100 probe serial number | Calibration date | Instrument bias (°C) | | | |
|---|---|---|---|---|---|---|---|
| | | | | -20°C | 0°C | 20°C | 40°C |
| VEIG11 | B2 | T49 | 9-Feb-2006 | 0.0273 | 0.0022 | 0.0230 | 0.0383 |
| VEIG12 | | T74 | 26-Jan-2006 | 0.0019 | 0.0247 | 0.0439 | 0.0598 |
| VEIG21 | B5 | T64 | 3-Feb-2006 | 0.0520 | 0.0201 | 0.0047 | 0.0268 |
| VEIG22 | | T73 | 26-Jan-2006 | 0.0230 | 0.0057 | 0.0297 | 0.0477 |

## COMPARISON OF BOTH SENSORS

The distribution of differences between screen 1 and screen 2 is plotted, using 1-minute quality checked data for the whole period of the intercomparison. Differences are classified according screen 1 temperature.

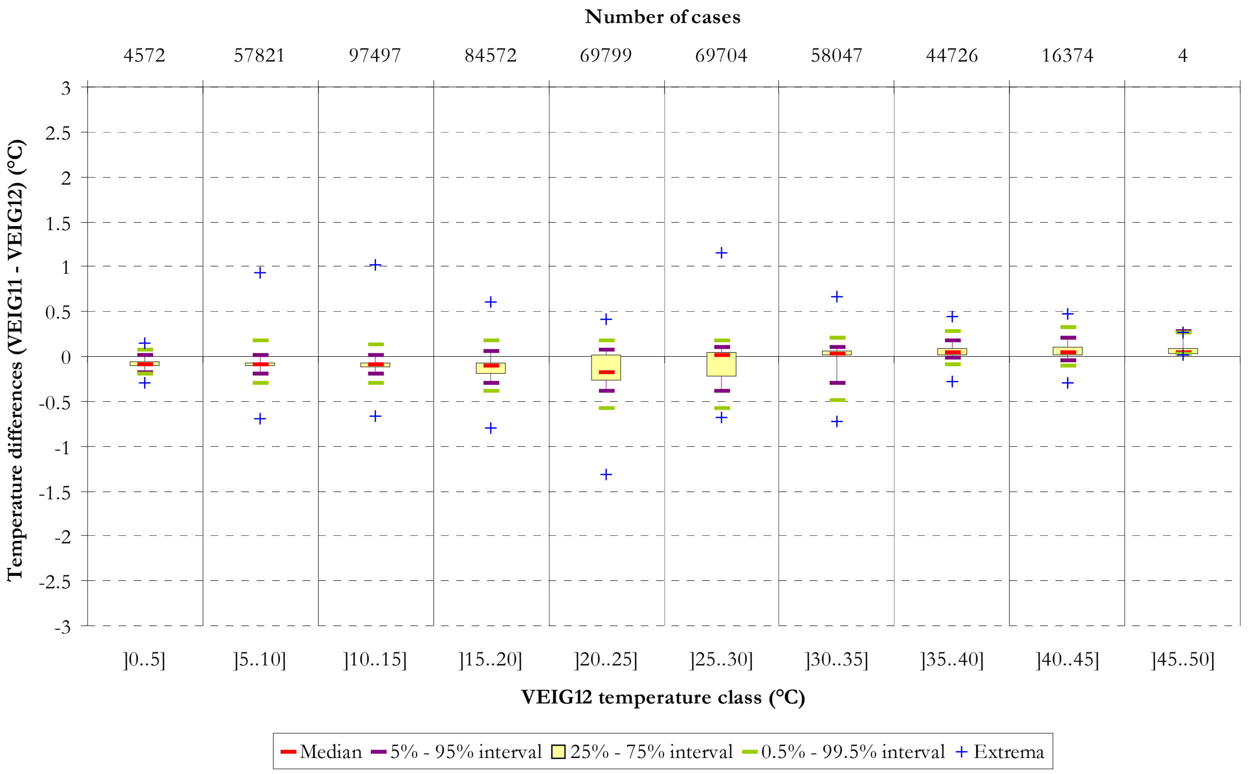


**Figure 2**

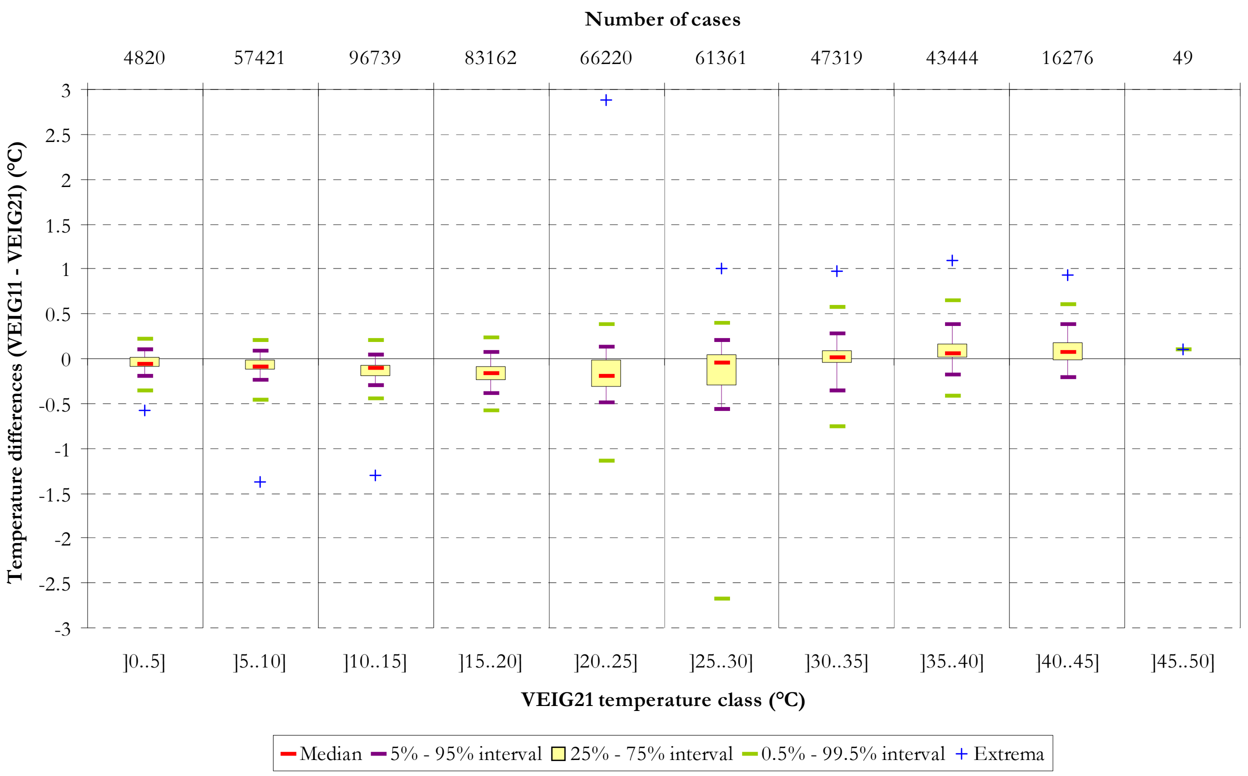


**Figure 3**

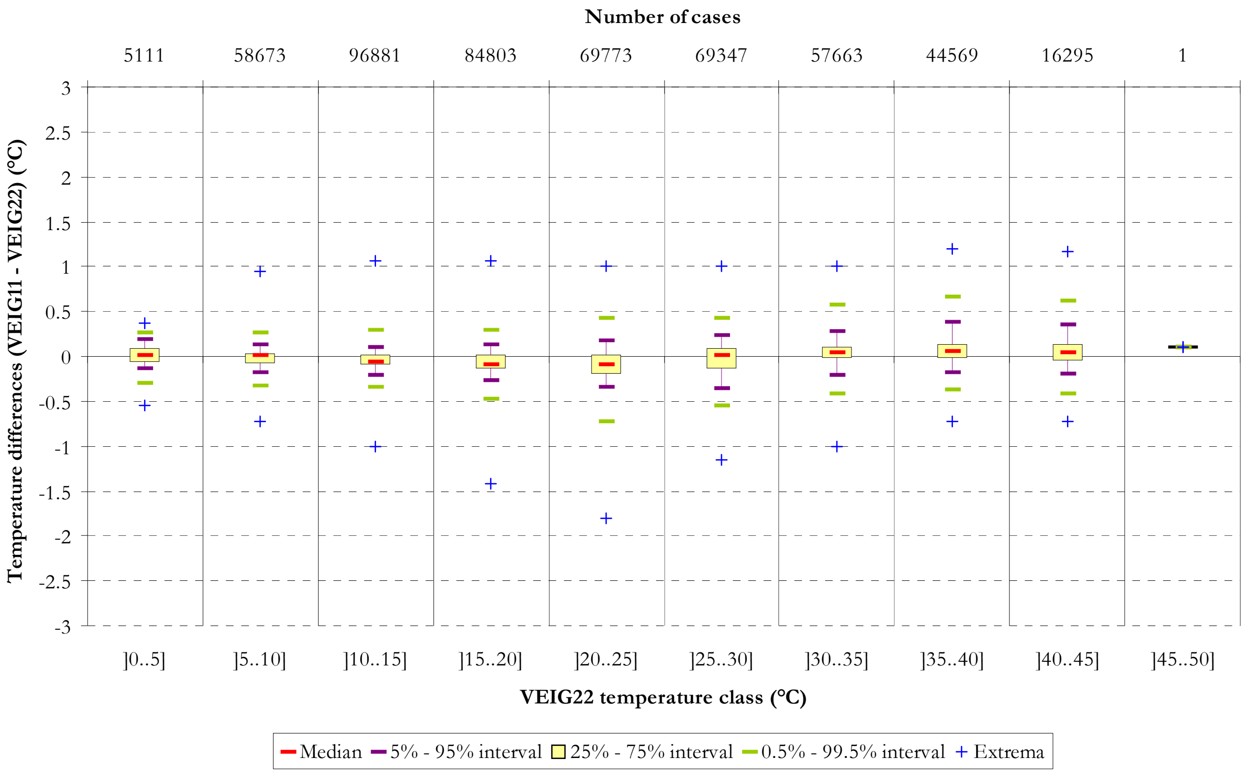


**Figure 4**

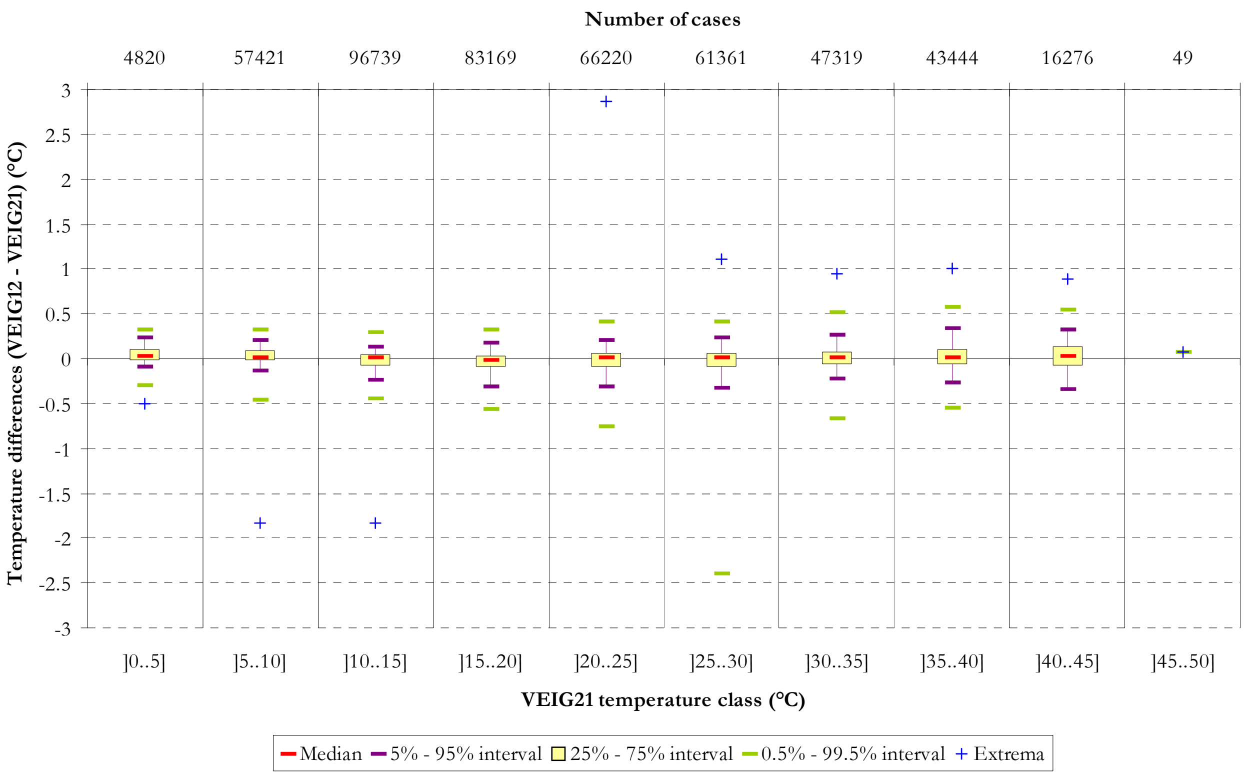


**Figure 5**

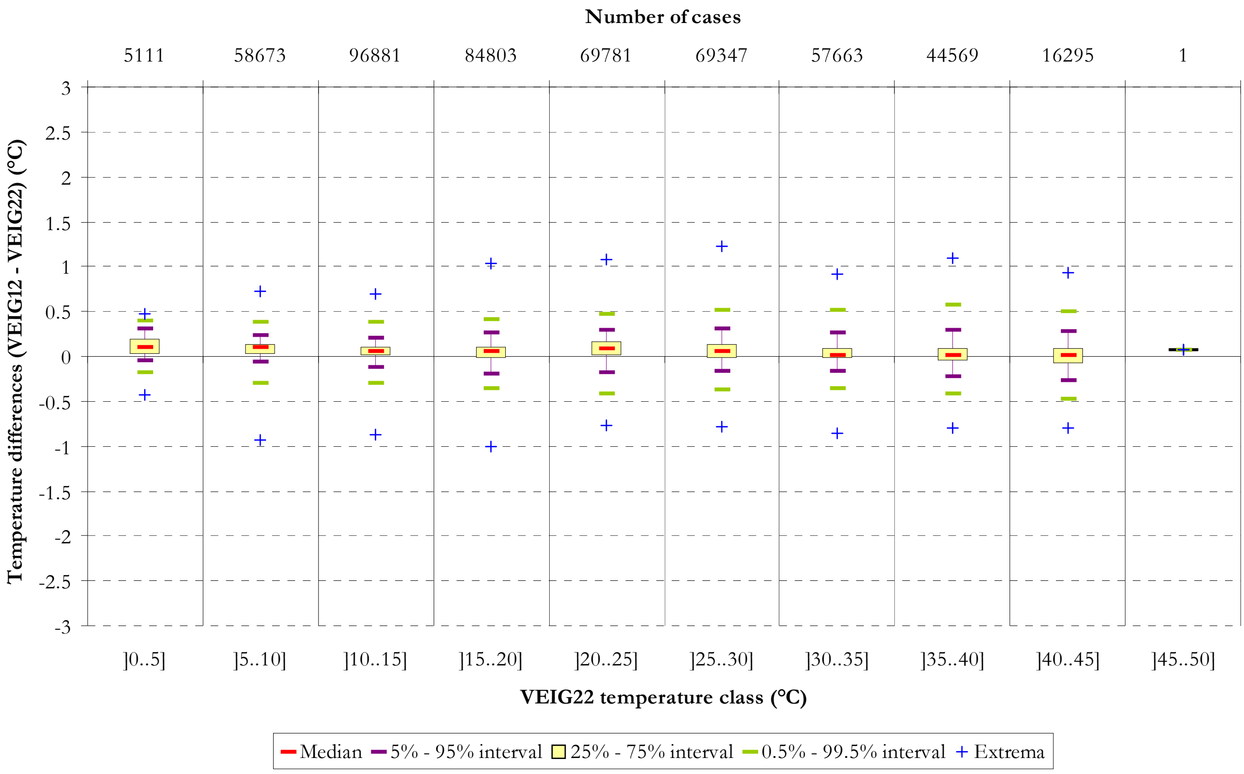


**Figure 6**

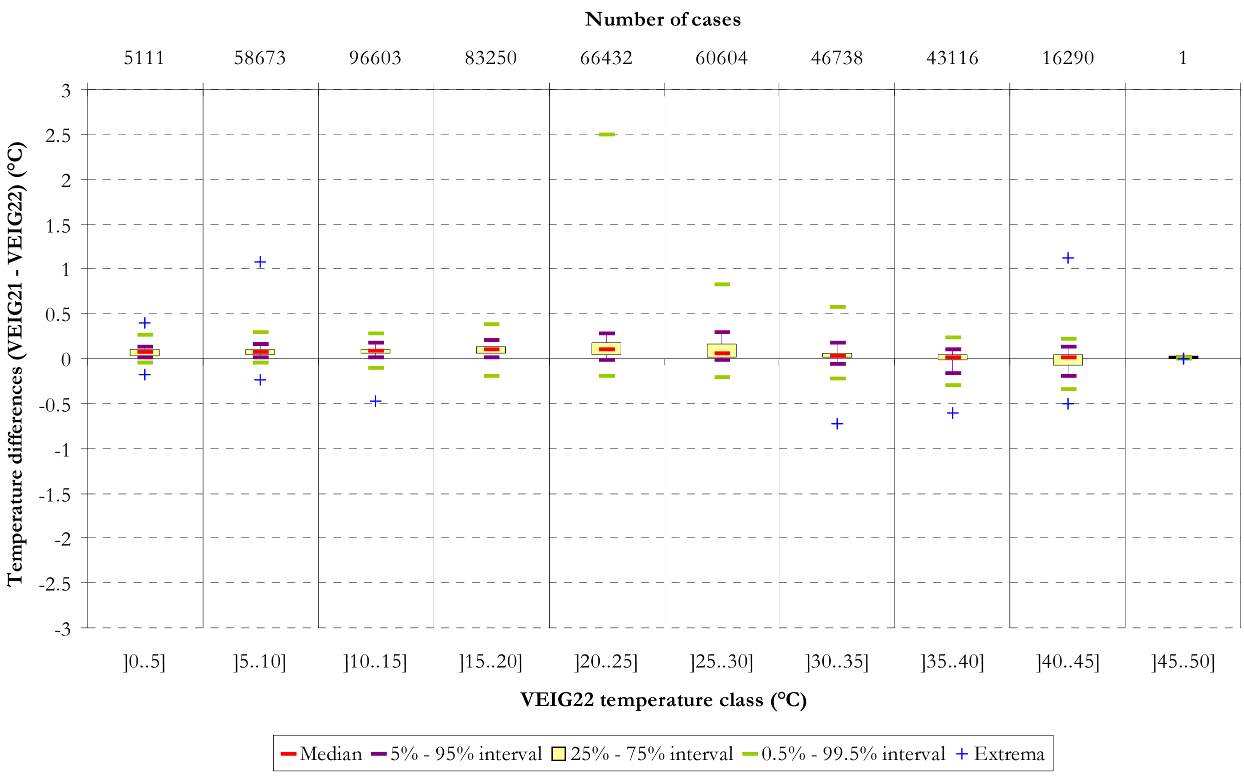


**Figure 7**

The four probes give very close results. There is no dependency with temperature.

## COMPARISON WITH THE REFERENCE

HISTOGRAM OF DIFFERENCES

The histogram of differences between VEIG and the reference VEIG22 is plotted, using 1-minute quality checked data for the whole period of the intercomparison. Differences are plotted by steps of 0.1K. The vertical axis is the frequency in percent for each class of differences.

Screen #1:

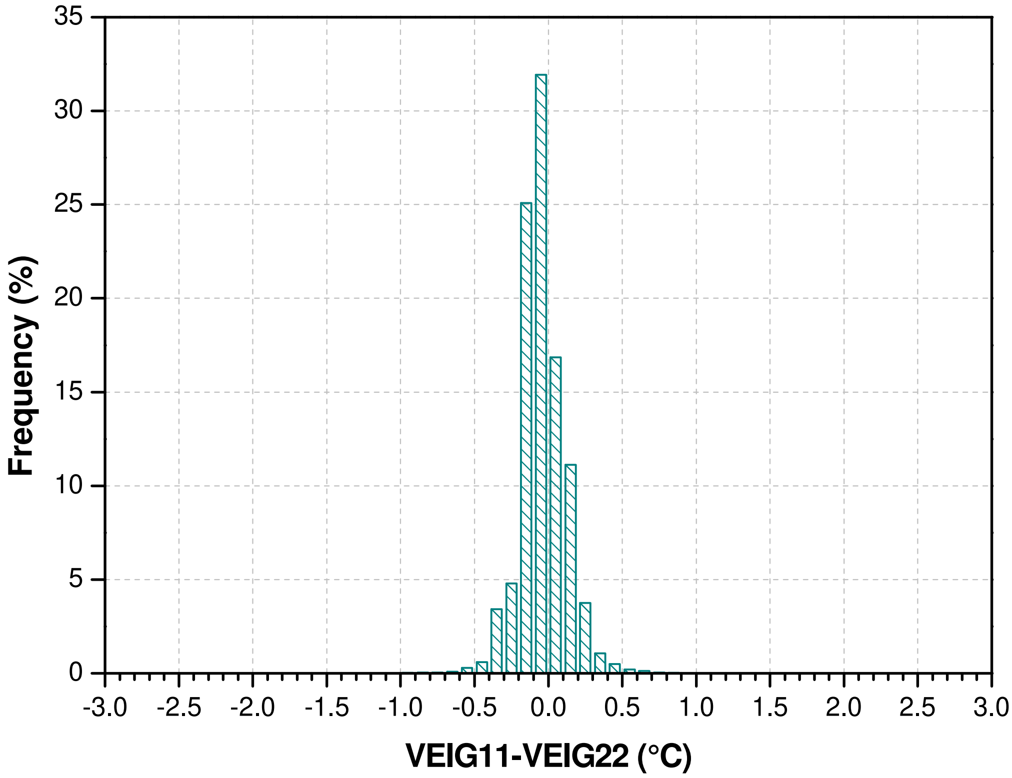


**Figure 8**

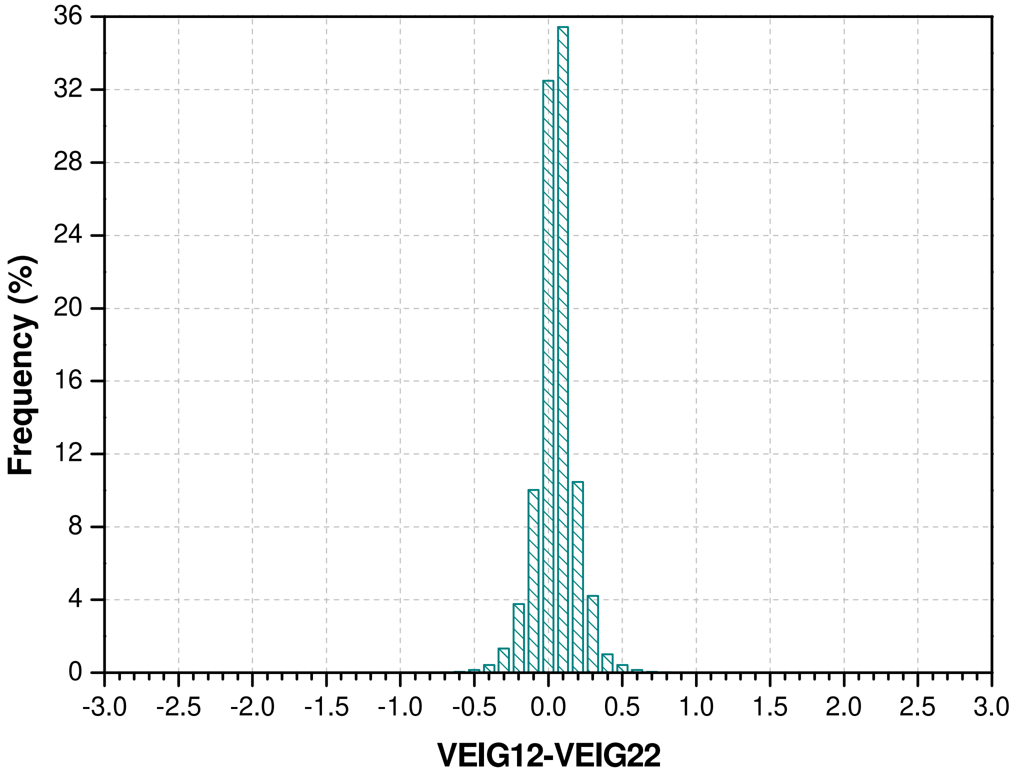
Frequency (%)
36
32
28
24
20
16
12
8
4
0
-3.0
-2.5
-2.0
-1.5
-1.0
-0.5
0.0
0.5
1.0
1.5
2.0
2.5
3.0
VEIG12-VEIG22

**Figure 9**

Screen #2:

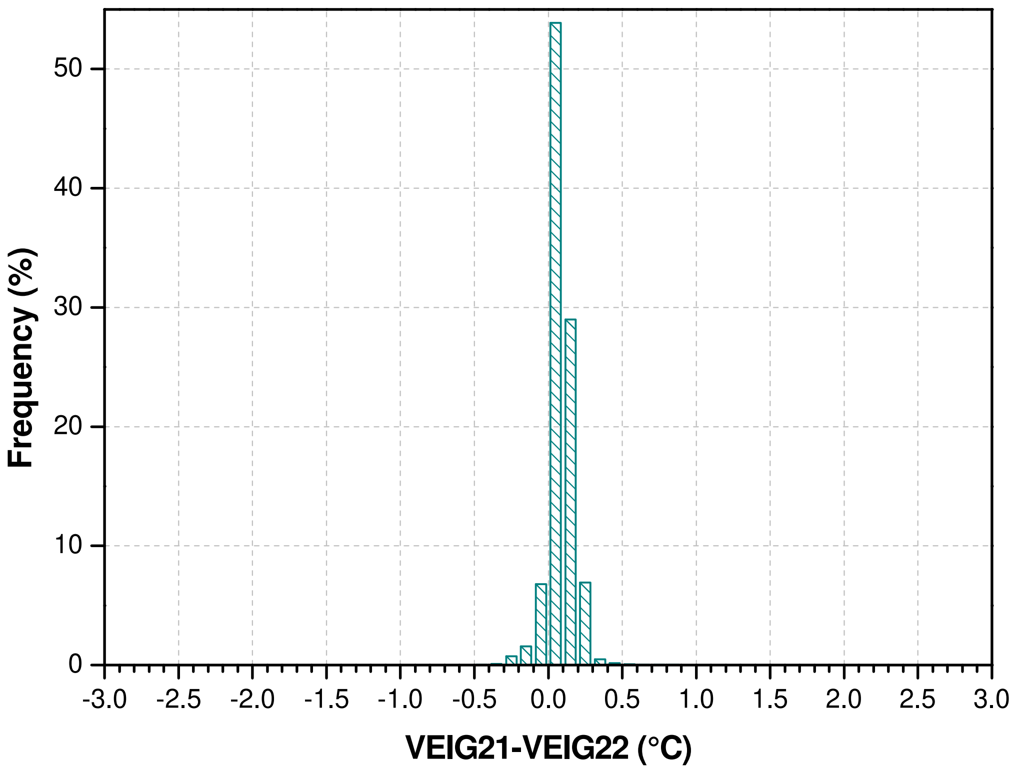


**Figure 10**

CUMULATIVE HISTOGRAMS OF DIFFERENCES OF DAILY EXTREME VALUES

The cumulative histograms of differences with the reference VEIG22 of T (1-minute quality checked data), Tn (daily minimum temperature) and Tx (daily maximum temperature) are plotted, for the whole period of the intercomparison. Differences are plotted by steps of 0.1K.

Screen #1:

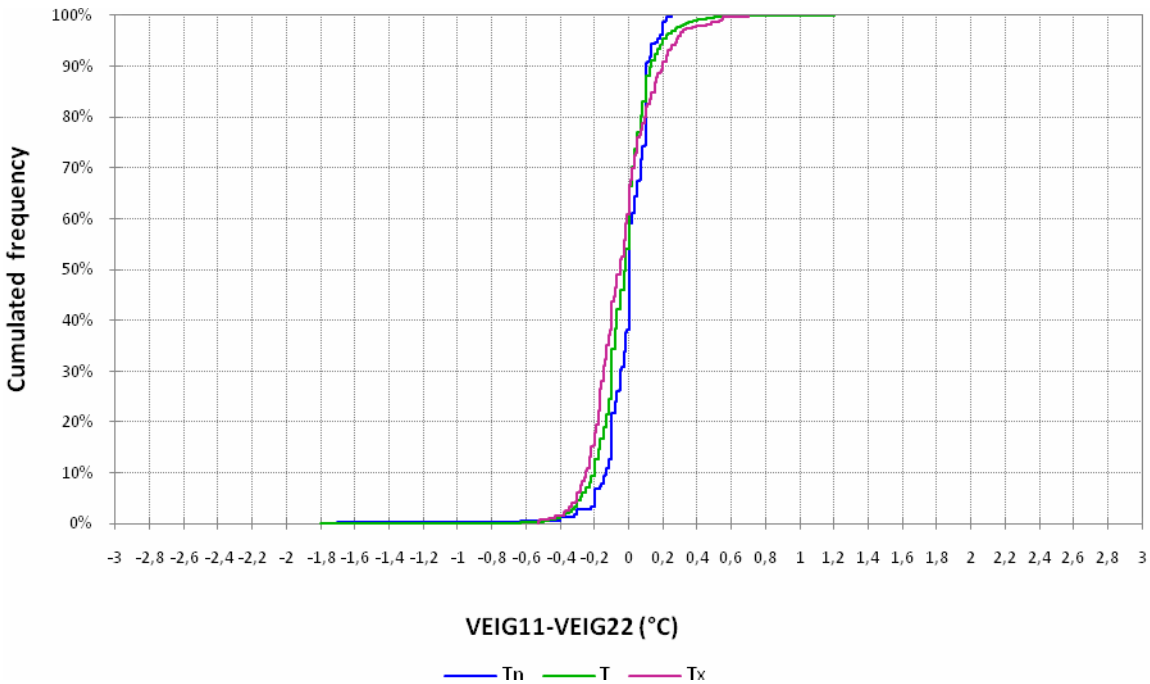


**Figure 11**

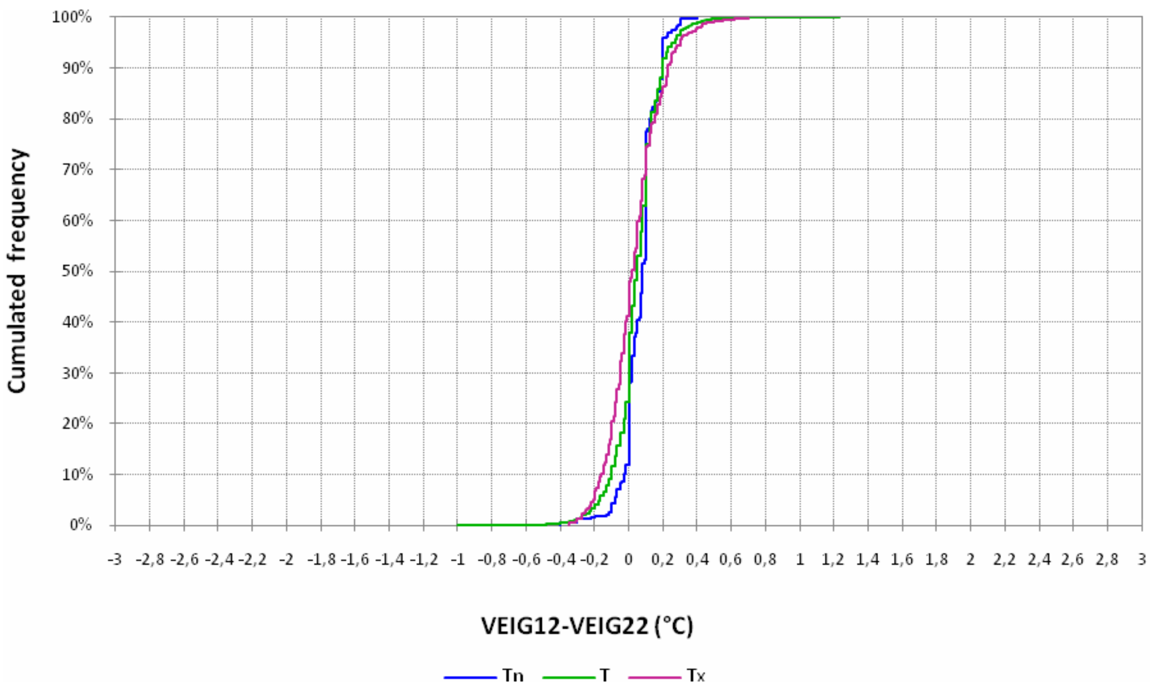


**Figure 12**

Screen #2:

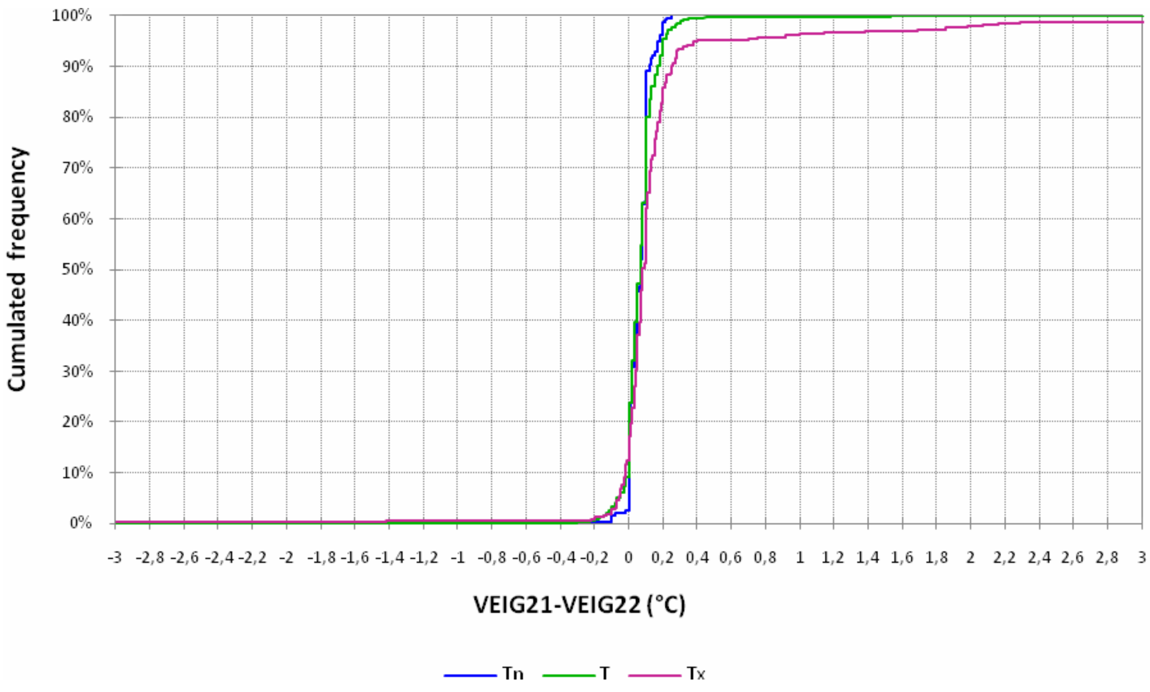


**Figure 13**

The four probes give close results compared to the reference. No special effect on daily extreme temperatures is observed.

TABLE

The table 2 indicates the percentage of data that differ by less than 0.2°C (and 0.5°C) from the reference.

**Table 2**

| | | [-0.2°..0.2°] | [-0.5°..0.5°] |
|---|---|---|---|
| VEIG11 | T | 86.2 | 99.2 |
| | Tn | 93.8 | 99.4 |
| | Tx | 72.8 | 97.8 |
| VEIG12 | T | 88.7 | 99.6 |
| | Tn | 6.2 | 100.0 |
| | Tx | 80.3 | 99.2 |
| VEIG21 | T | 94.8 | 99.6 |
| | Tn | 98.3 | 99.6 |
| | Tx | 83.3 | 93.8 |

## INFLUENCE OF GLOBAL RADIATION

The distribution of differences between VEIG and the reference VEIG22 is plotted, using 1-minute quality checked data for the whole period of the intercomparison. Differences are classified according global radiation.

## Screen #1:

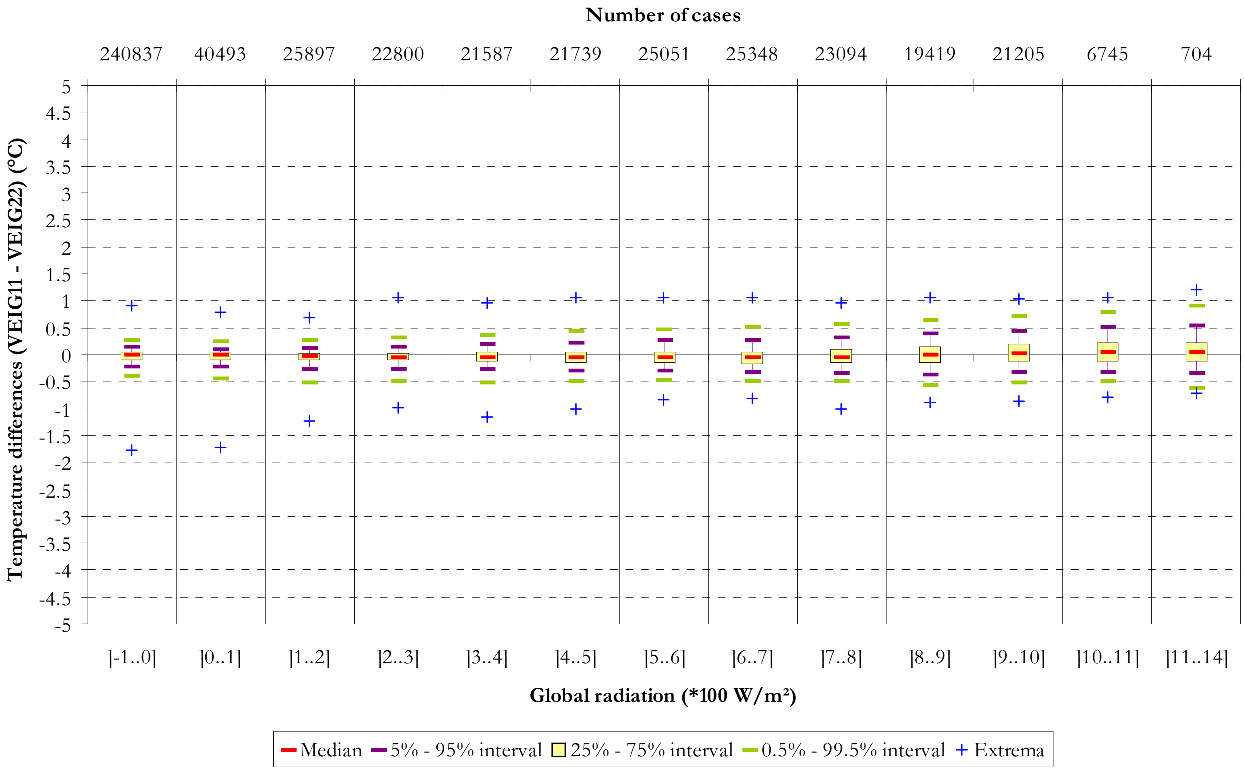


**Figure 14**

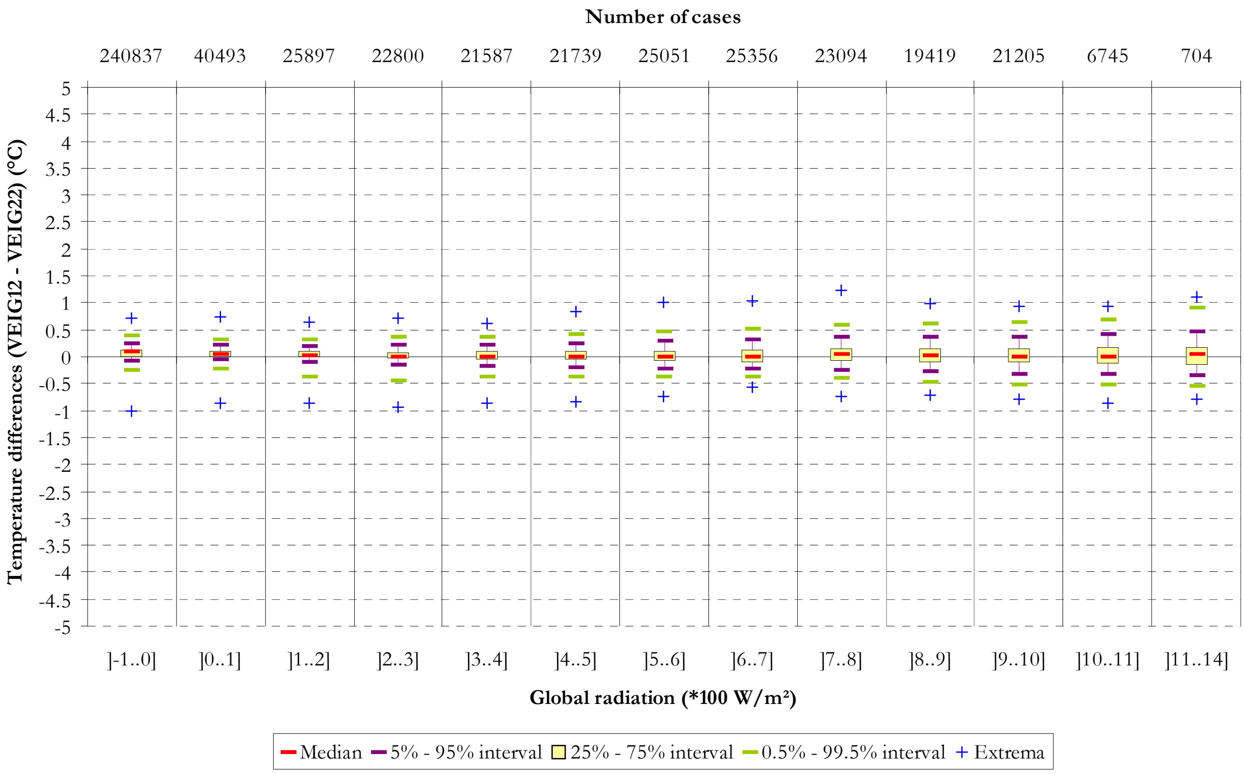


**Figure 15**

Screen #2:

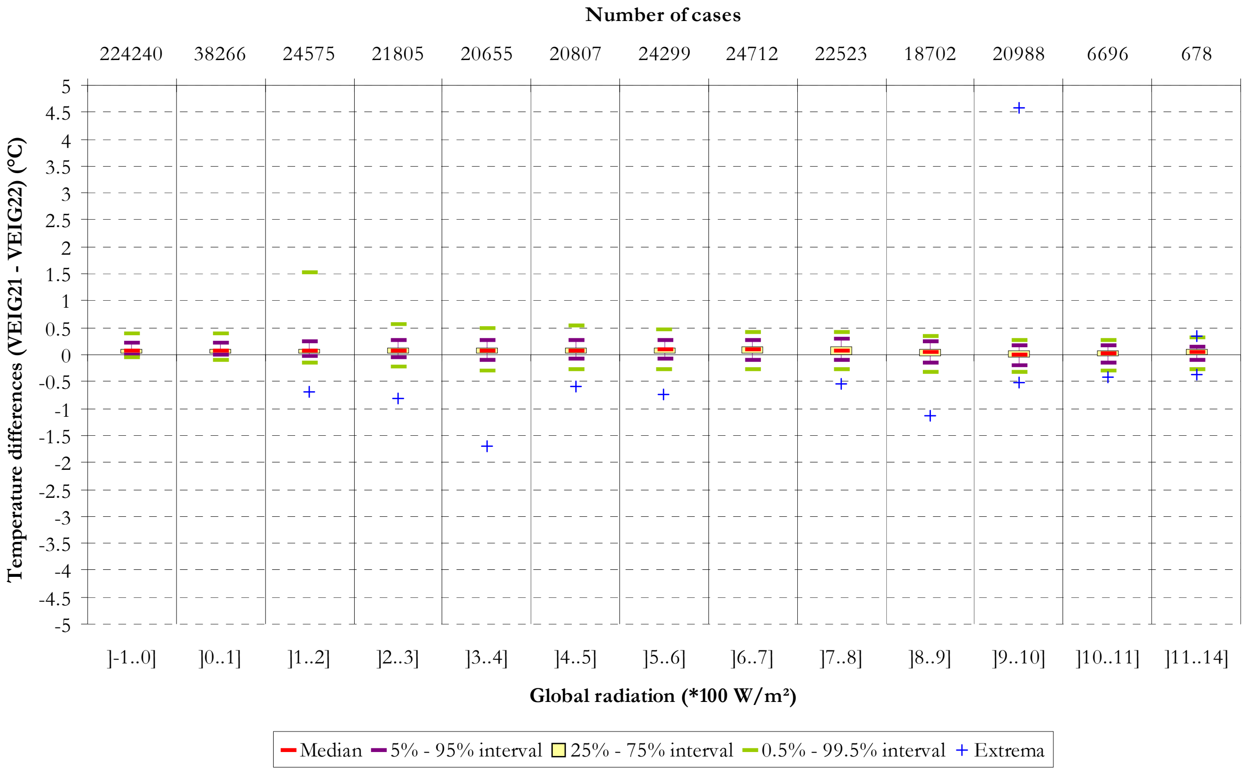


**Figure 16**

No effect of global radiation is observed.

## RADIATION EFFECT

### DIFFERENCES BETWEEN DAY AND NIGHT BEHAVIOUR

The median of differences between VEIG and VEIG22 is plotted, using 1-minute quality checked data for the whole period of the intercomparison. We filter data for which sun elevation is above -1° (day) or below -1° (night). Differences are classified according 2-meter wind speed (2-minute average).

Screen #1:

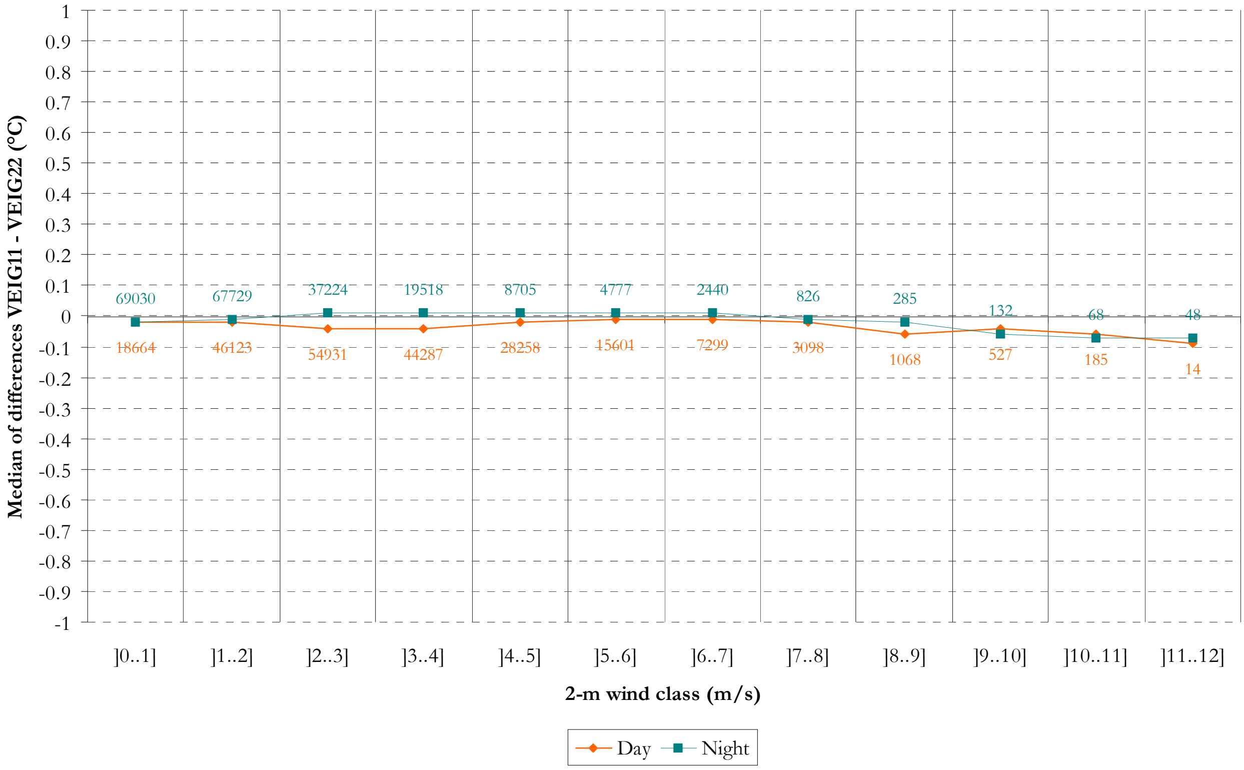


**Figure 17**

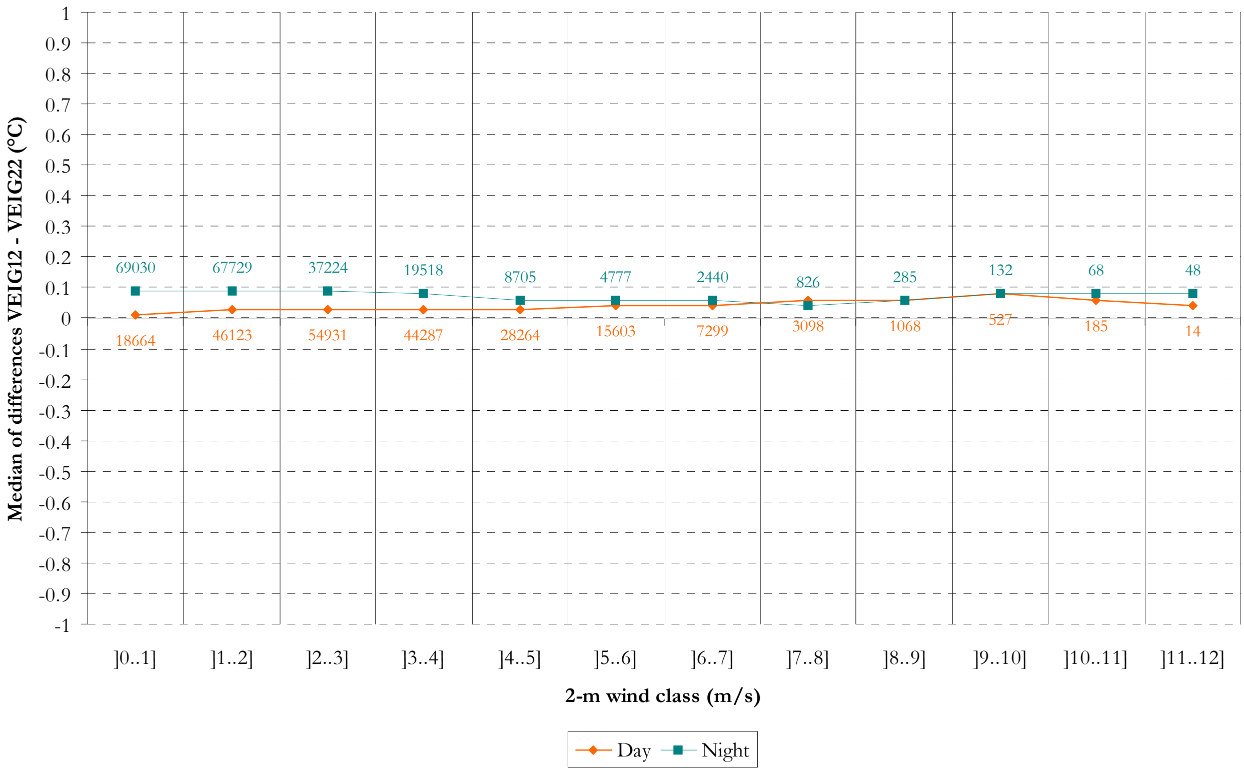


**Figure 18**

Screen #2:

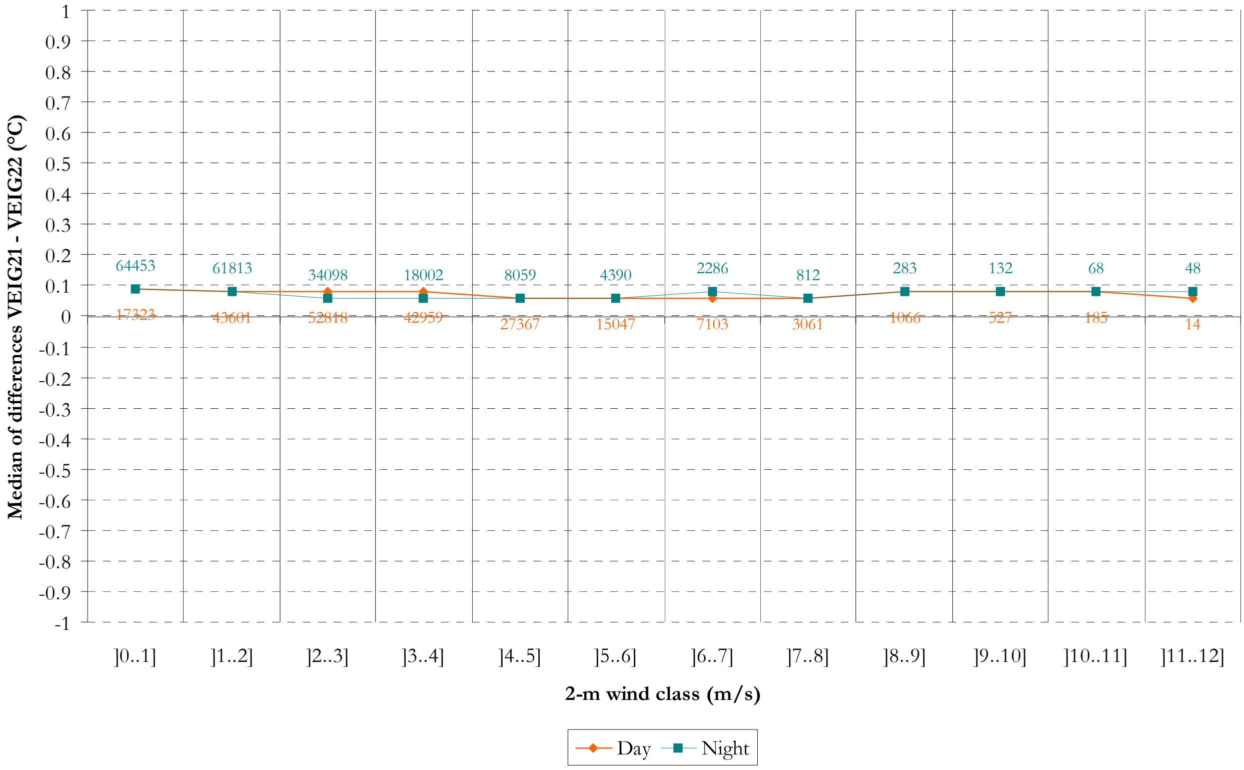


**Figure 19**

For all sensors, the curves for day and night times are very close: there is less than 0.1°C between them. Both are stable with wind speed.

DIFFERENCES BETWEEN CLEAR SKY AND OVERCAST SKY DURING DAYTIME

The median of differences between VEIG and VEIG22 is plotted, using 1-minute quality checked data. Here, we consider periods lasting six hours at least where cloudiness is less or equal to 1 (clear sky) or more or equal to 7 (overcast sky), during daytime (sun elevation above -1°). Differences are classified according 2-meter wind speed (2-minute average).

## Screen #1:

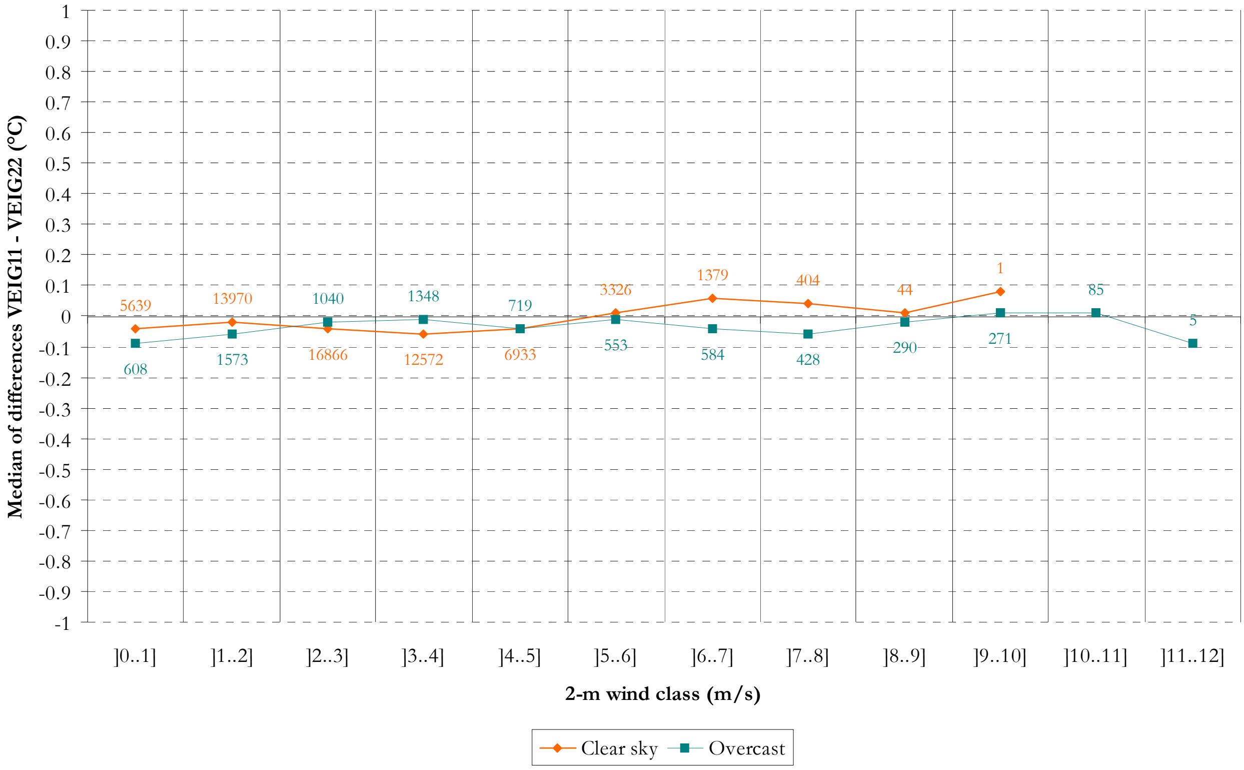


**Figure 20**

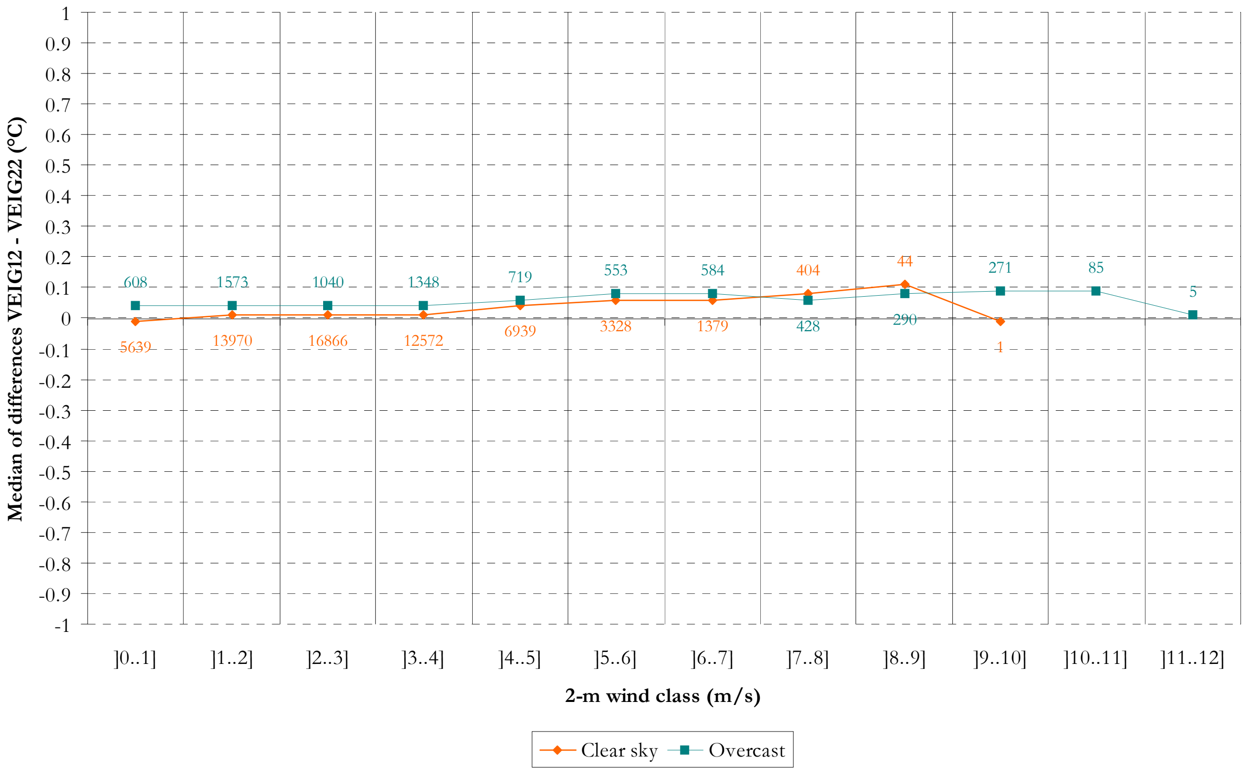


**Figure 21**

Screen #2:

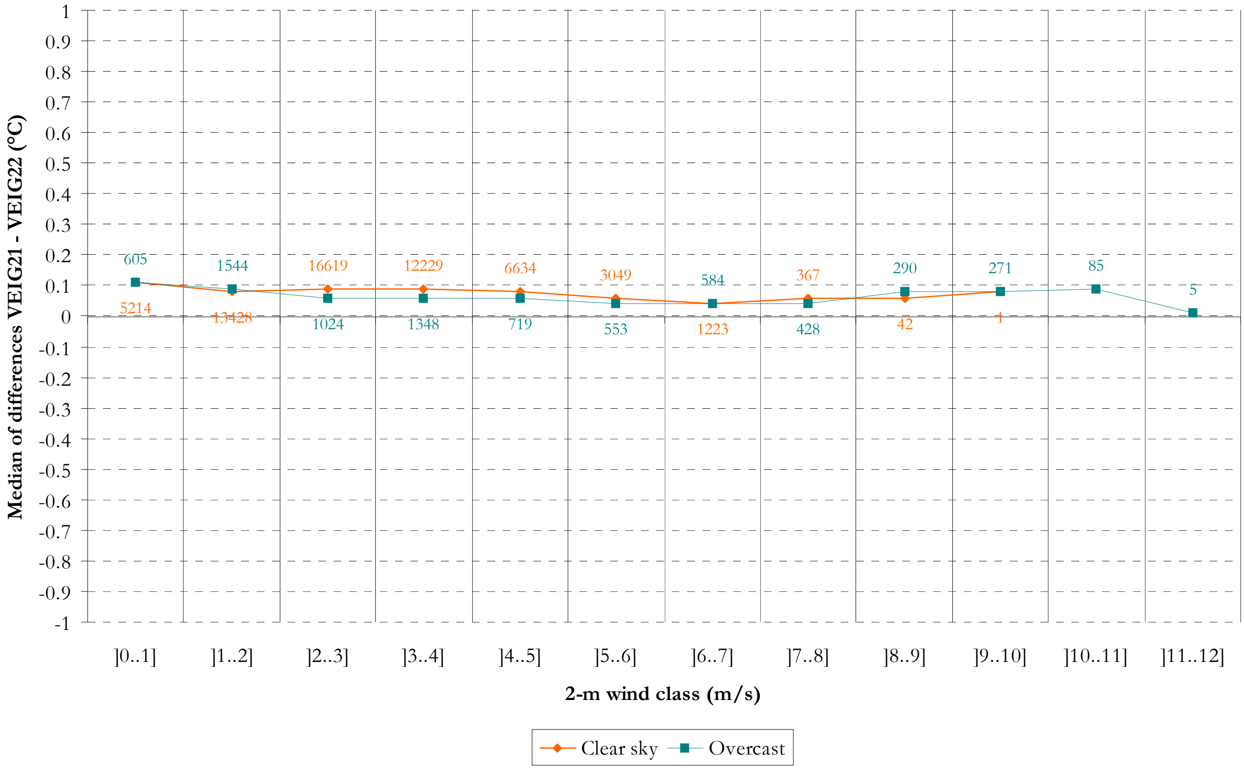


**Figure 22**

For all sensors, differences are less than 0.1°C between clear sky and overcast conditions. They are stable when the wind speed increases.

DIFFERENCES BETWEEN CLEAR SKY AND OVERCAST SKY DURING NIGHT TIME

The median of differences between VEIG and VEIG22 is plotted, using 1-minute quality checked data. Here, we consider periods lasting six hours at least where cloudiness is less or equal to 1 (clear sky) or more or equal to 7 (overcast sky), during night time (sun elevation below -1°). Differences are classified according 2-meter wind speed (2-minute average).

## Screen #1:

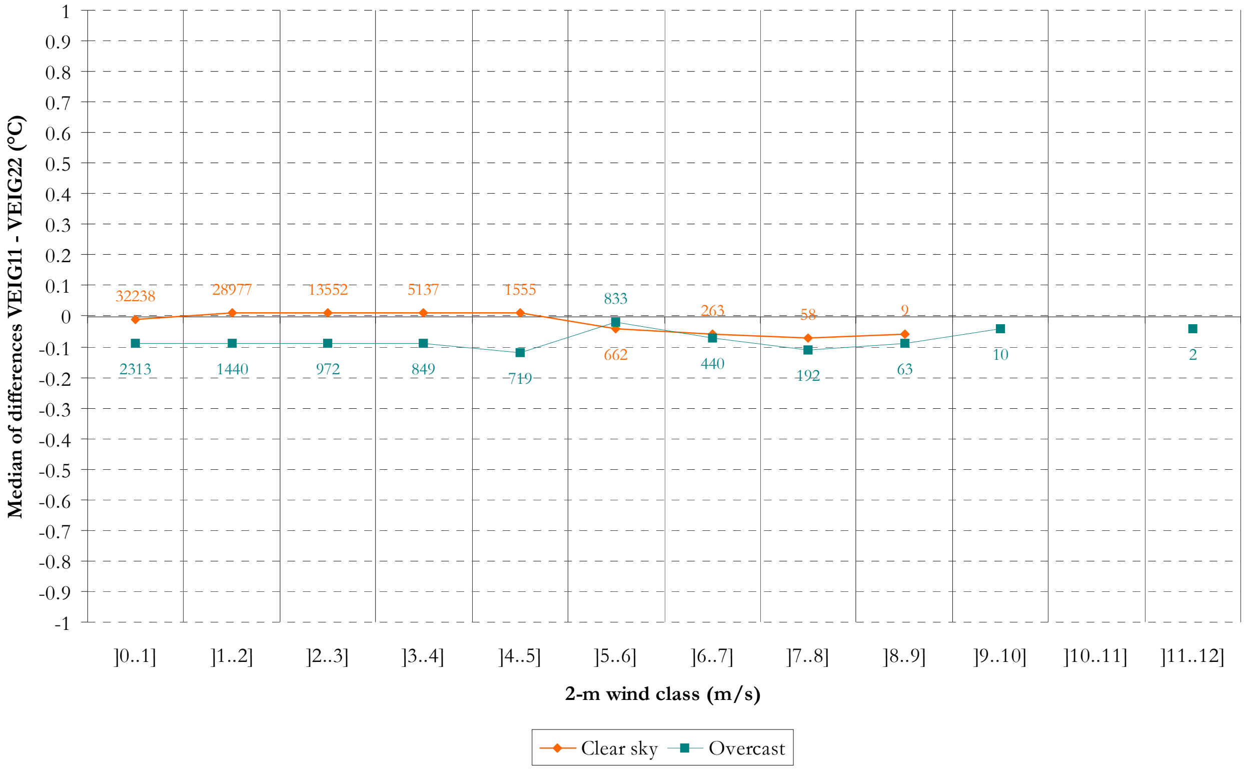


**Figure 23**

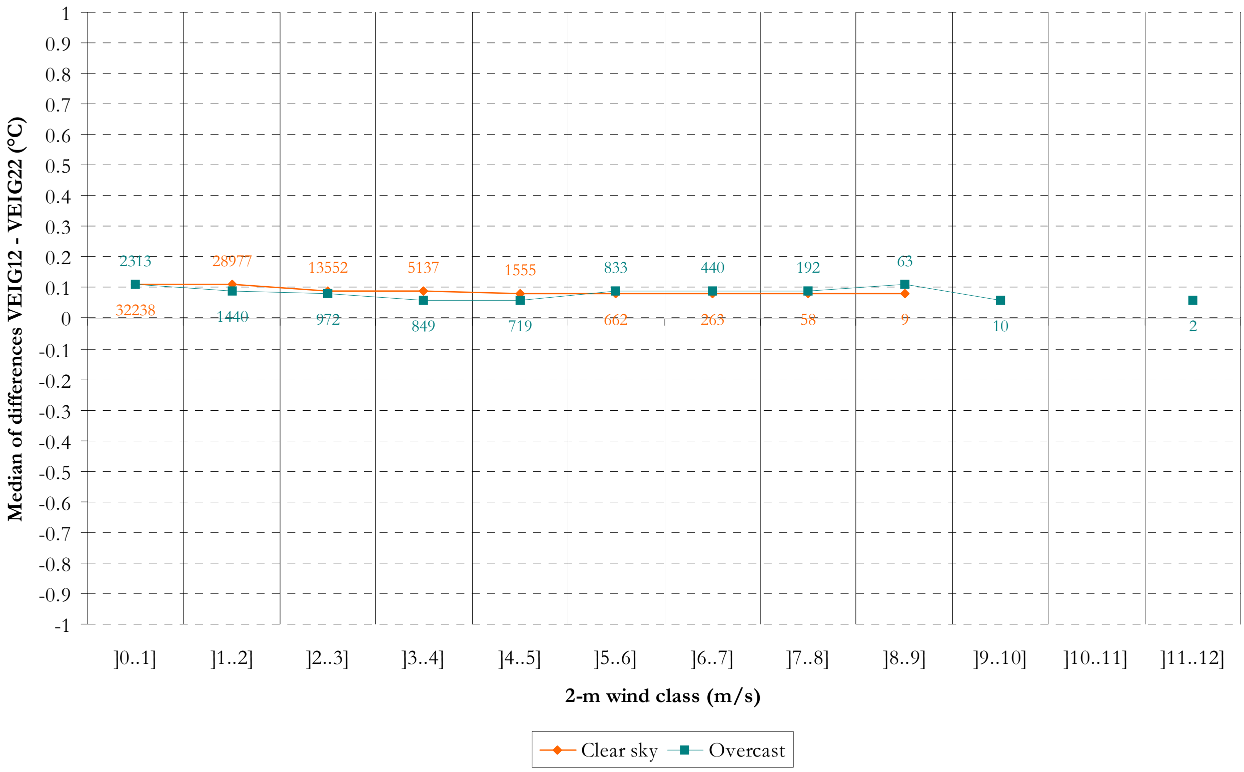


**Figure 24**

Screen #2:

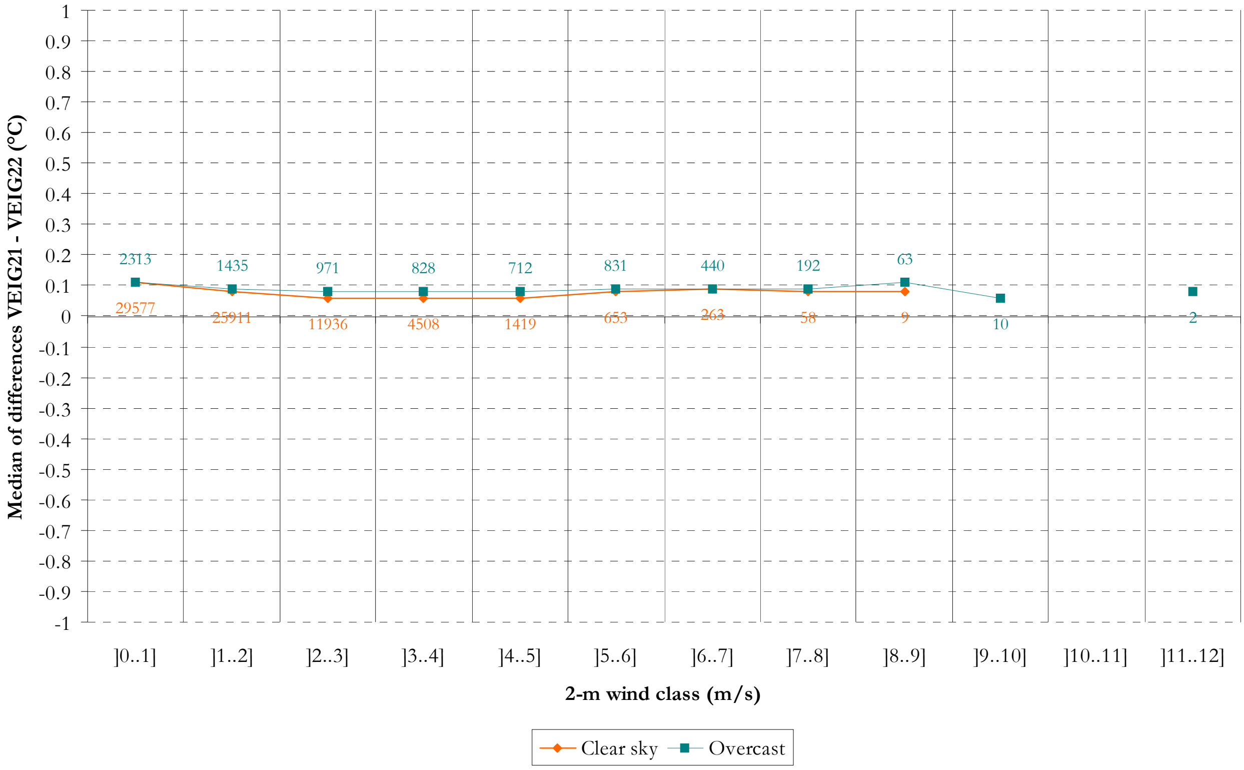


**Figure 25**

As for daytime condition, for all sensors, differences are less than 0.1°C between clear sky and overcast conditions. They are stable when the wind speed increases.

EFFECT OF SUN ELEVATION

The median of differences between VEIG and VEIG22 is plotted, using 1-minute quality checked data. Here, we consider periods lasting six hours at least where cloudiness is less or equal to 1 (clear sky), during daytime (sun elevation above -1°). We filter data where sun elevation is low (below 10°), medium (between 10° and 45°) or high (above 45°). Differences are classified according 2-meter wind speed (2-minute average).

## Screen #1:

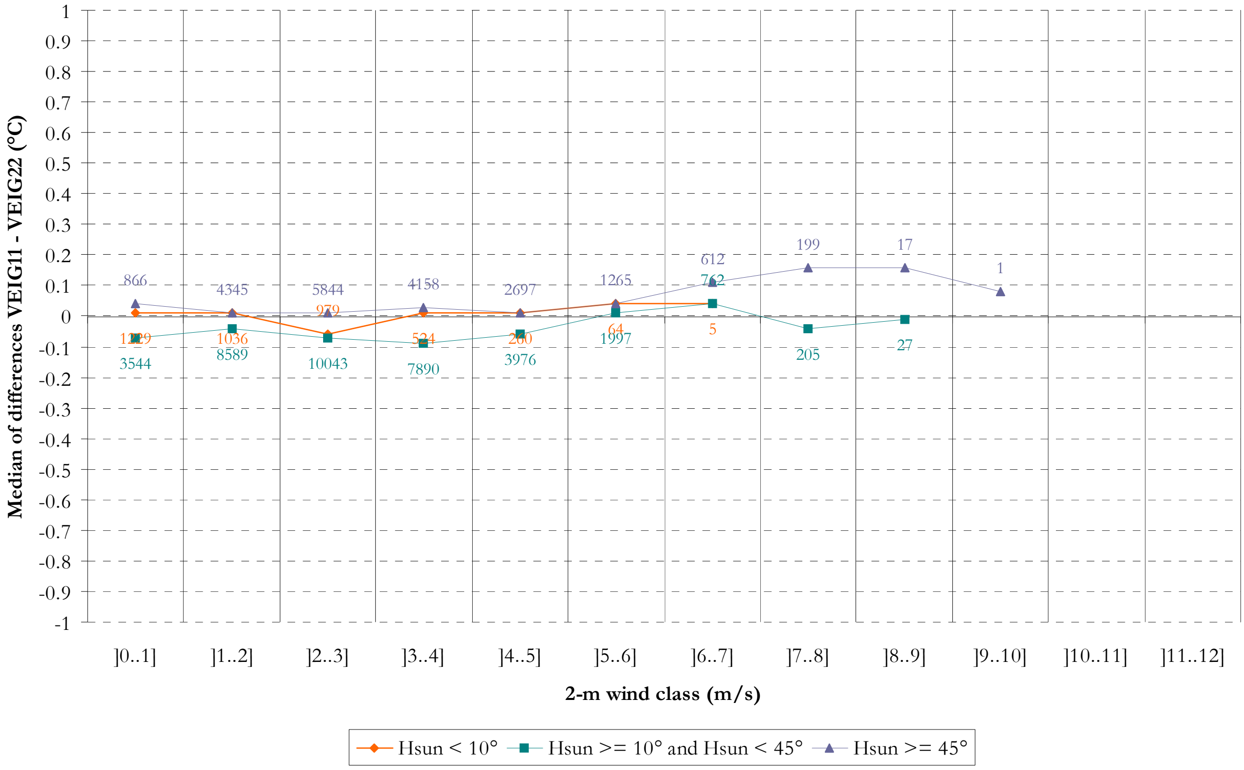


**Figure 26**

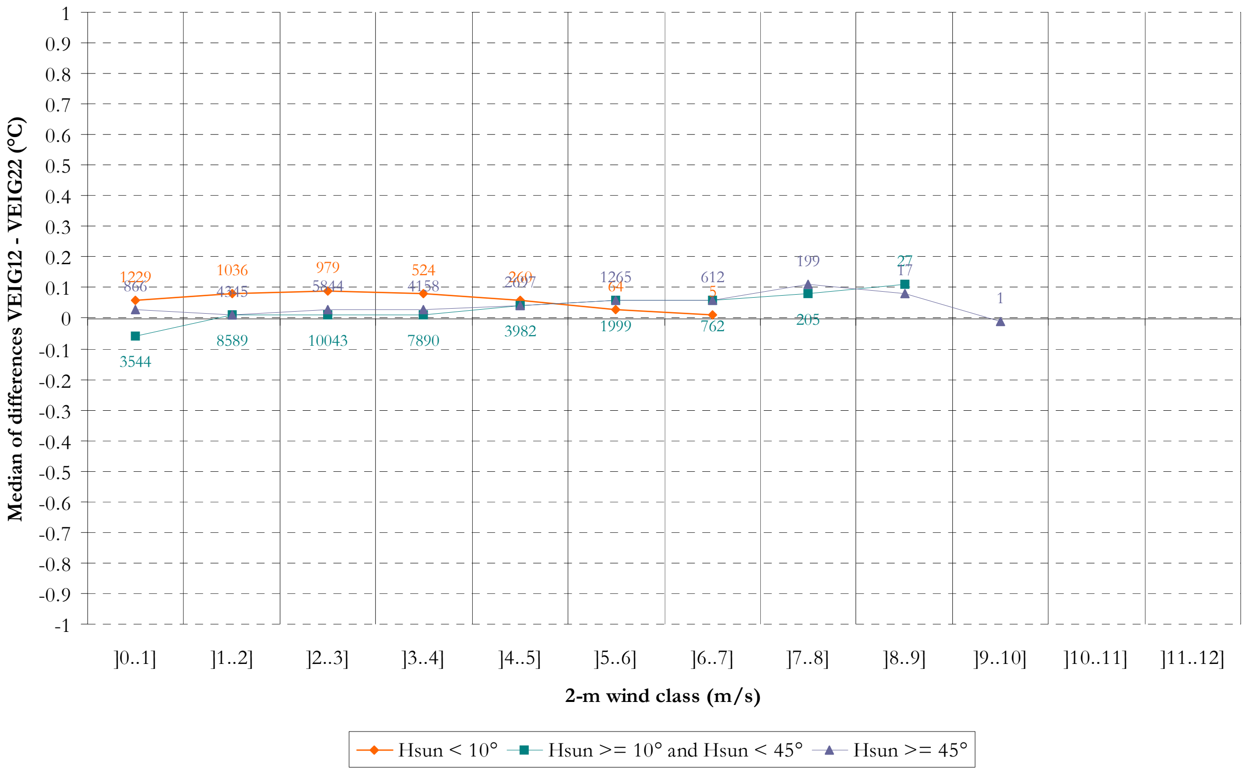


**Figure 27**

Screen #2:

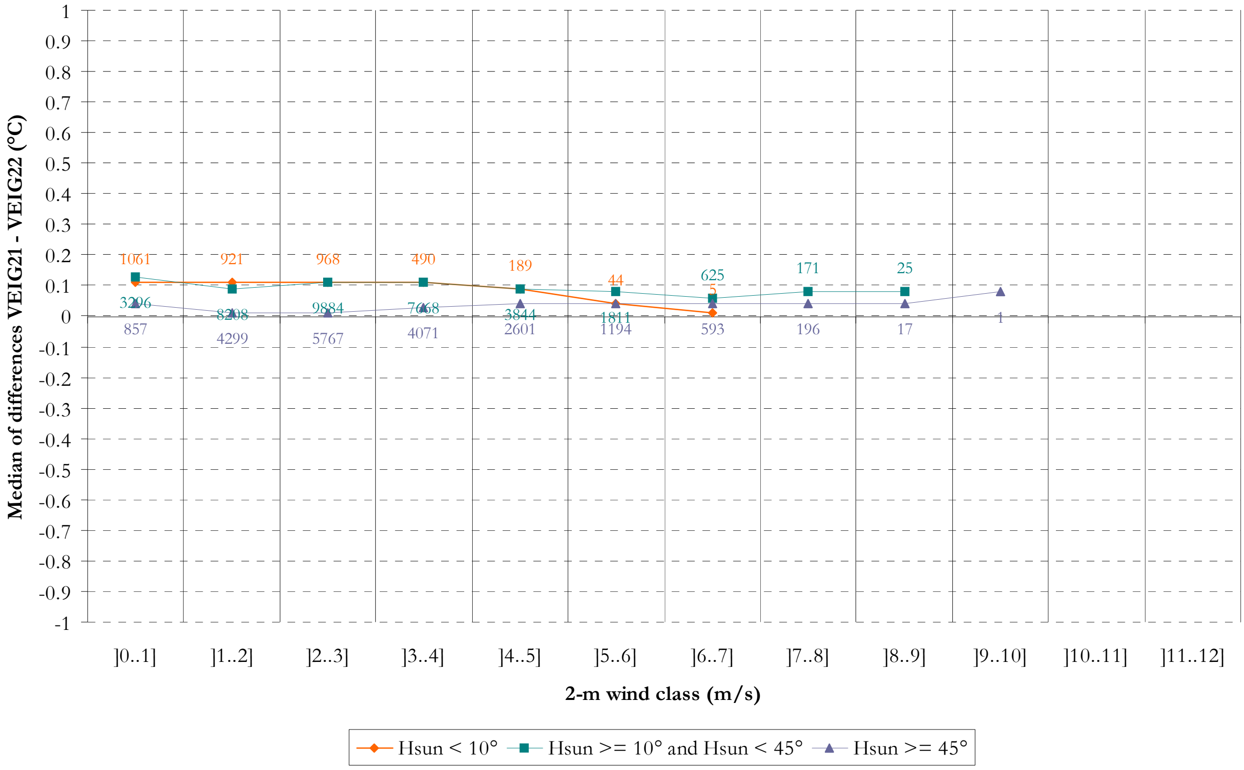


**Figure 28**

The lines for different sun elevation values are very close one from another. They are very stable when wind speed increases.

## COMBINED EFFECT OF WIND AND GLOBAL RADIATION

The medians of differences between VEIG and VEIG22 are represented here with a contour plot. The global radiation values are on the X-axis and on the Y axis is the 2-meter wind speed value (2-minute average). Medians are used in all cases, providing that at least one data is available for both conditions on radiation and wind considered.

Screen #1:

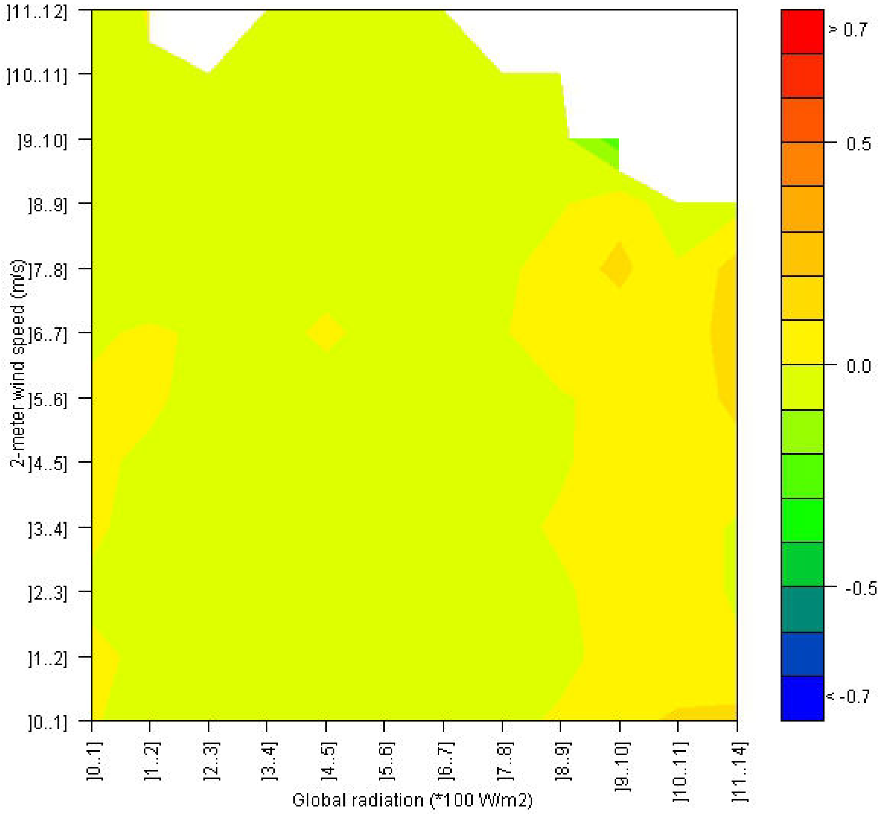


**Figure 29**

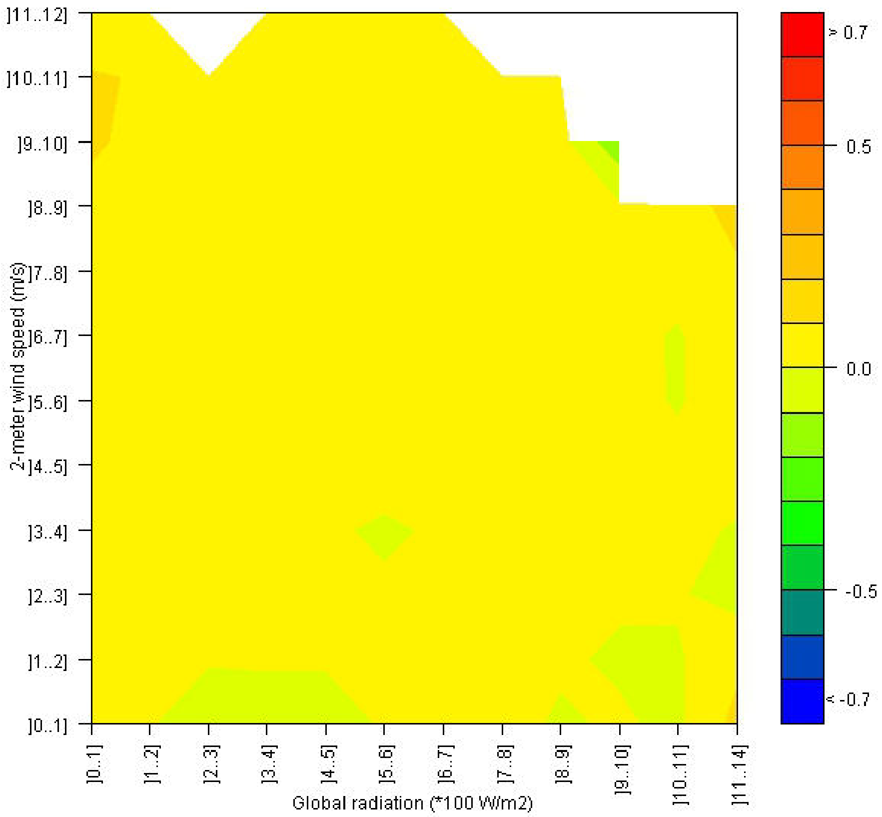

]11..12]
]10..11]
]9..10]
]8..9]
]7..8]
]6..7]
]5..6]
]4..5]
]3..4]
]2..3]
]1..2]
]0..1]
2-meter wind speed (m/s)
]0..1]
]1..2]
]2..3]
]3..4]
]4..5]
]5..6]
]6..7]
]7..8]
]8..9]
]9..10]
]10..11]
]11..14]
Global radiation (*100 W/m2)
> 0.7
0.5
0.0
-0.5
< -0.7


**Figure 30**

Screen #2:

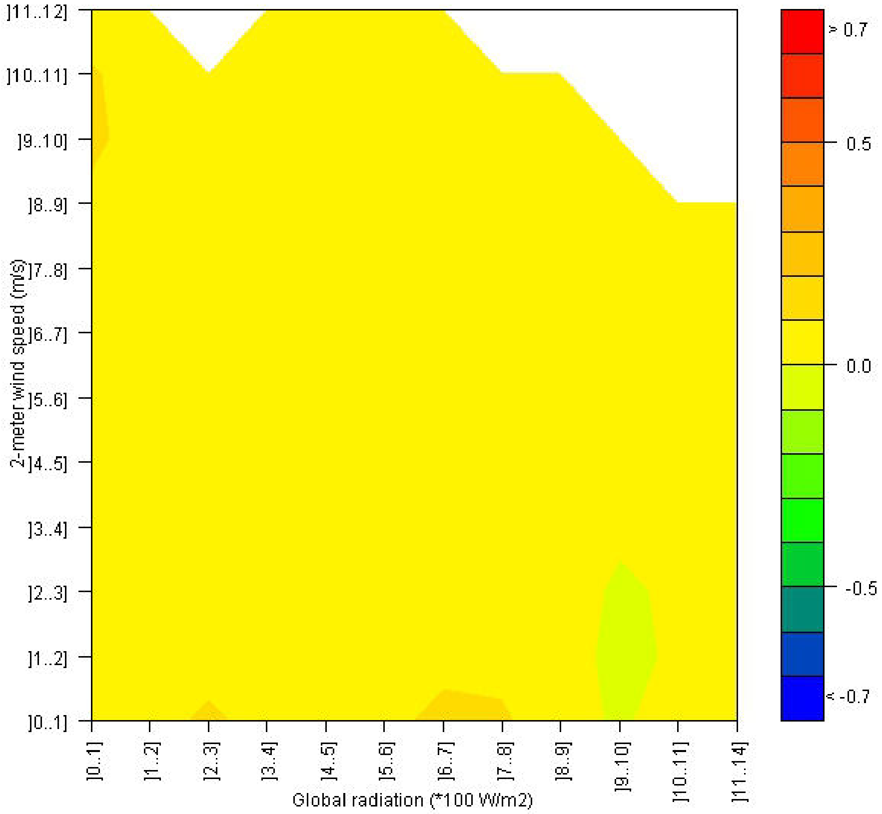


**Figure 31**

For all probes, contour plots are very uniform around the 0 value.

## BEHAVIOUR DURING INCREASE/DECREASE OF TEMPERATURE

The distribution of differences between VEIG and the reference VEIG22 is plotted, using 1-minute quality checked data for the whole period of the intercomparison. Differences are classified according the temporal gradient of reference temperature over 1 minute. A screen faster (or slower, respectively) than the reference would be warmer (cooler) for positive gradient, cooler (warmer) for negative ones.

Screen #1:

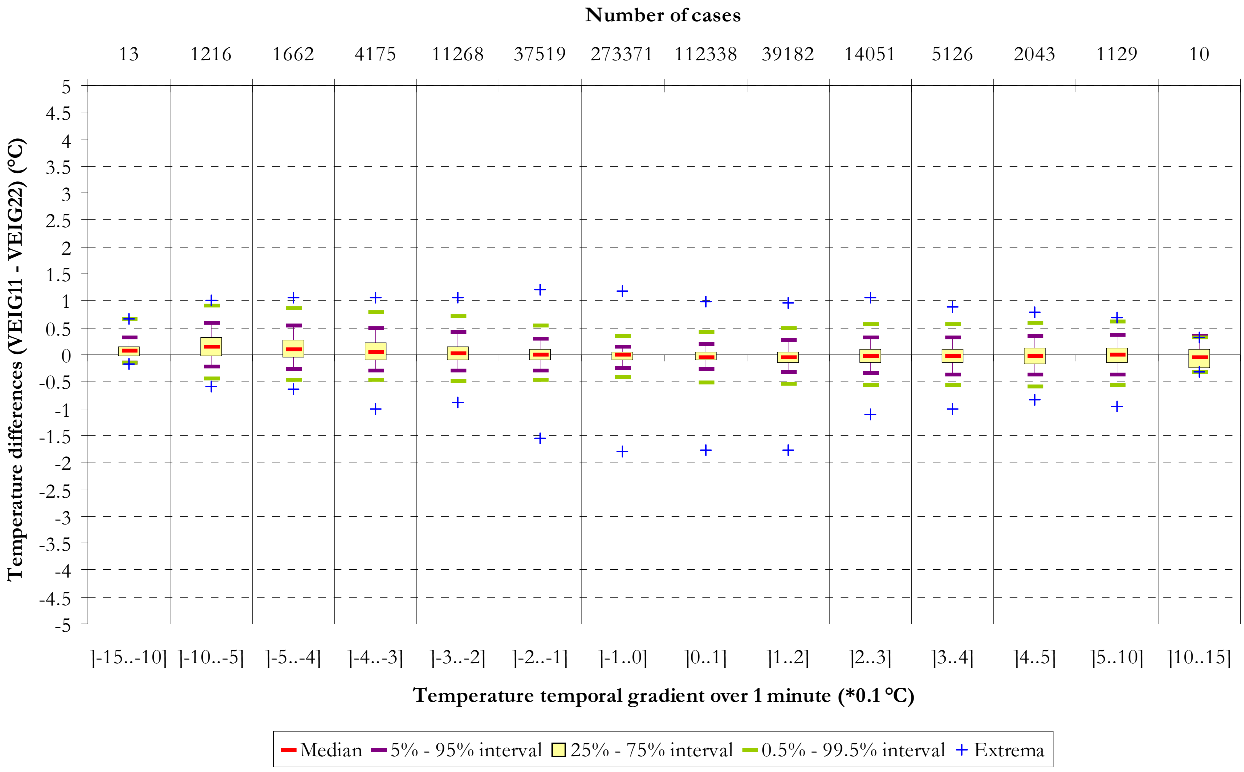


**Figure 32**

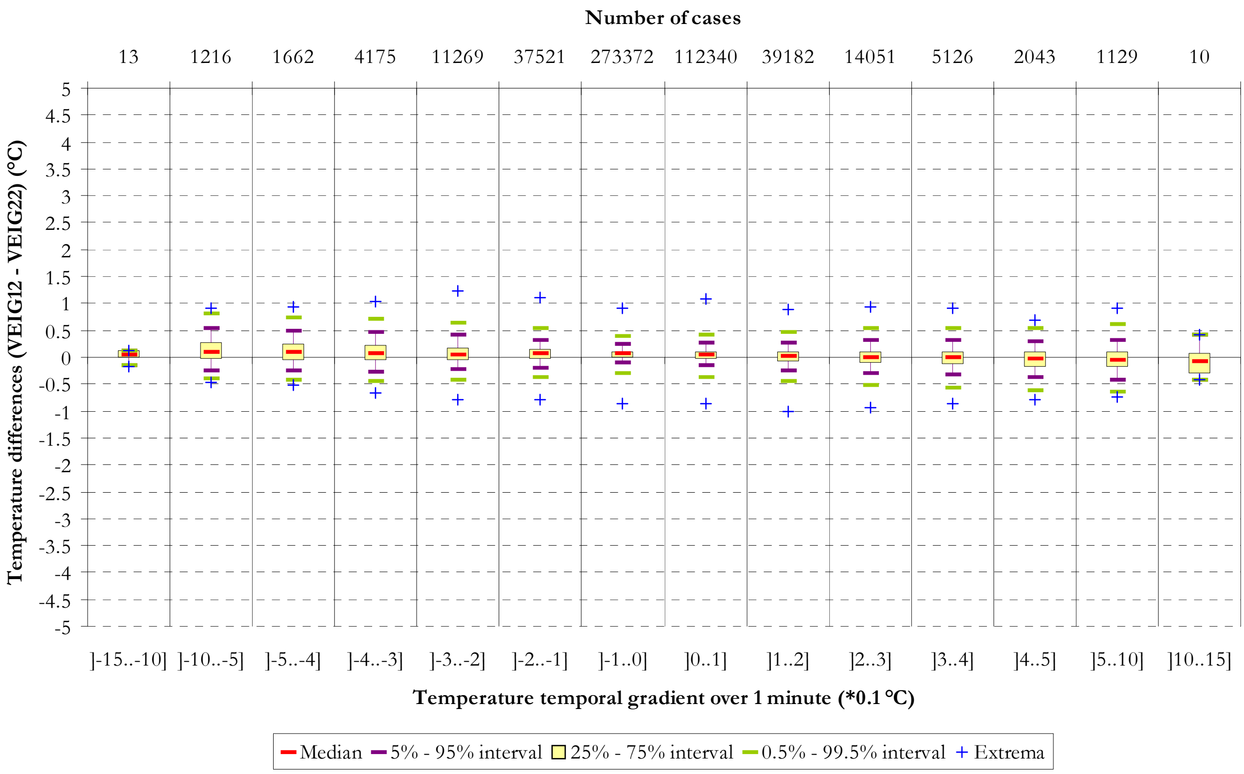


**Figure 33**

Screen #2:

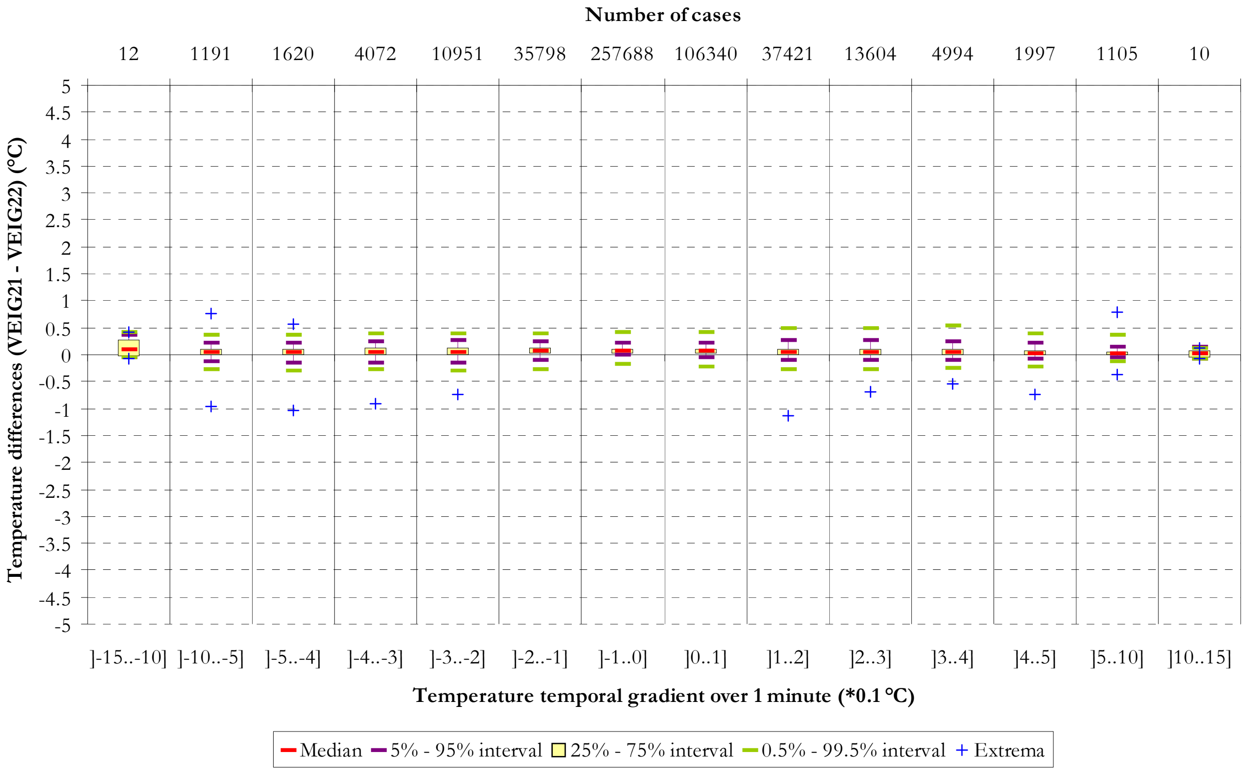


**Figure 34**

All distributions are very close to zero value. No probe is in advance or late compared to the reference.

## QUALITY CONTROL INFORMATION

### DATA AVAILABILITY

The intercomparison period extends from the 1st of November 2008 to the 1st of November 2009. The theoretical number of 1-minute data is 525600.

The next table sums up the total number of data for each screen and for each possible QC flag.

**Table 3**

| QC flag | VEIG11 | VEIG12 | VEIG21 | VEIG22 |
|---|---|---|---|---|
| 0 (good) | 503256 | 503266 | 477521 | 503266 |
| 1 (inconsistent) | 0 | 0 | 0 | 0 |
| 2 (doubtful) | 0 | 0 | 193 | 0 |
| 3 (erroneous) | 10 | 0 | 6939 | 0 |
| 7 (missing) | 22334 | 22334 | 40947 | 22334 |

### MAINTENANCE

On the 30th of September, 2009, both sensors were removed and the fan was cleaned. Before the operation, the ventilation was good. After the operation, it was even better.

# THYGAN VTP37 METEOLABOR AG
# – Switzerland –
# VTHY

**TECHNICAL SPECIFICATIONS (PROVIDED BY THE MANUFACTURER)**

Dimensions: Length 28.8 cm x Width 22.3 cm x Height 35.7 cm

Weight: 9.5 kg

Material/Structure: Aluminium

Estimated radiation error: zero

Aspiration rate (in case of artificially ventilated screen/shield): 3.5 m/s

Power supply: 12 VDC / 48VAC


**Figure 1**

## OVERVIEW

Sensor #1 gave no data after the 2nd of March, 2009 at 7:00.

Sensor #2 gave no data after the 2nd of May, 2009 at 17:40.

When the sensors were functioning, the status in the messages did not show any trouble in the ventilation.

Both sensors are in good agreement. Sensor #1 is slightly warmer than sensor #2. Both sensors show very dispersed histograms for T and consequently, for Tn and Tx. Daily maximum temperatures are particularly affected.

Thygan sensors overestimate the temperature during day and underestimate it during night. Basically, the ventilation of these sensors is not efficient enough.

With the exception of very low numbers of data, the higher the global radiation, the warmer the Thygan sensors are. The medians of differences with the reference reach more than 2°C for global radiation values greater than 700W/m$^2$.

These sensors are much warmer than the reference during day. Overheating is moderate for calm winds. When the wind speed increases, the differences with the reference are reduced.

During night, the cooling is moderate. When the wind speed increases, the cooling is reduced: for winds above 5m/s, Thygan sensors give measurements close to the reference.

During daytime, when the sky is clear, differences with the reference are lower for calm winds (0 to 1m/s) than for low values of wind speed (1 to 2m/s). Then, when the wind speed increases, differences decrease.

During night time, when the sky is clear, Thygan sensors are cooler than the reference. As wind speed increases, they get closer to the reference.

For medium values of sun elevation, overheating of Thygan sensors is reduced when the wind is stronger.

Differences with the reference are mainly positive for all temperature gradients. These plots do not show a delay or an advance of these sensors compared to the reference.

## CALIBRATION INFORMATION

The calibration was performed by manufacturer in June 2005.

**Table 1**

| Screen | Location | Screen serial number | Instrument bias (°C) |
|---|---|---|---|
| | | | 22°C |
| VTHY1 | C3 | 338 | -0.03 |
| VTHY2 | C4 | 339 | -0.05 |

The result of calibration of reference VEIG22 is available in the main report of the intercomparison, section 5.4.1.

## COMPARISON OF BOTH SENSORS

The distribution of differences between screen 1 and screen 2 is plotted, using 1-minute quality checked data for the whole period of the intercomparison. Differences are classified according screen 1 temperature.

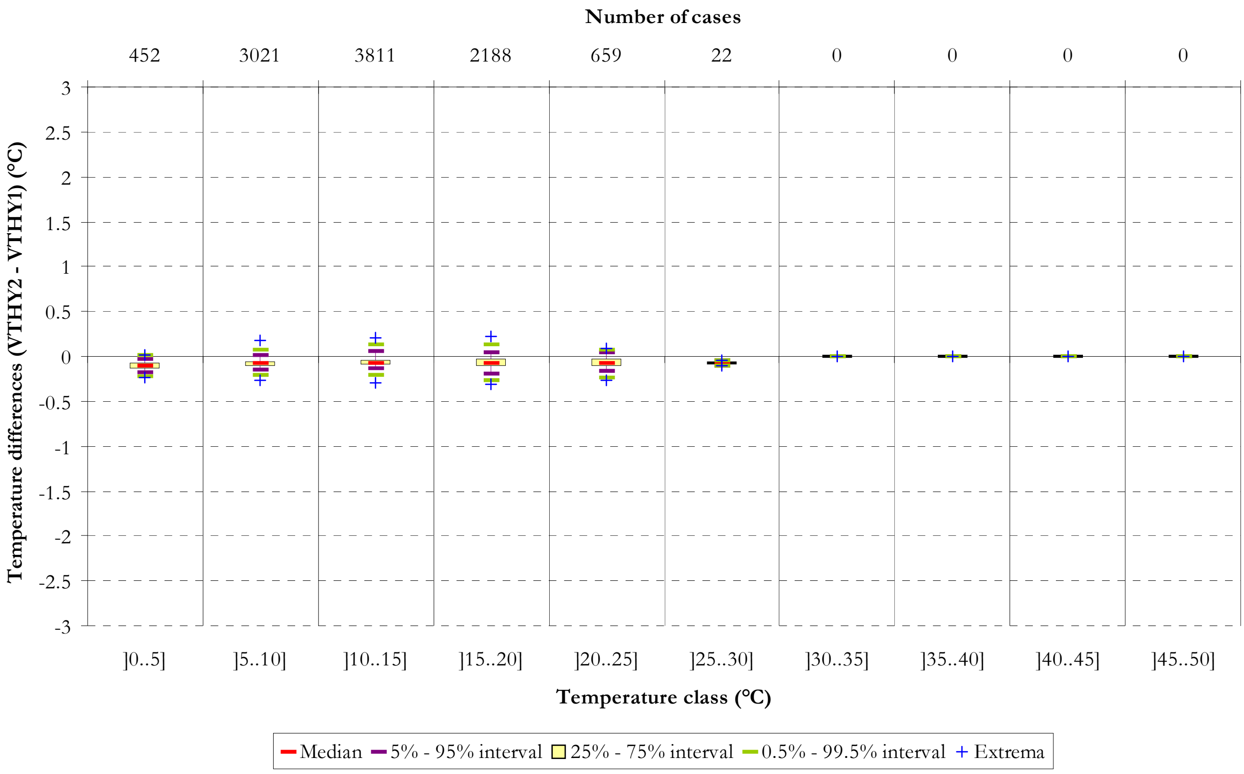


**Figure 2**

Both sensors are in good agreement. Sensor #1 is slightly warmer than sensor #2.

## COMPARISON WITH THE REFERENCE

### HISTOGRAM OF DIFFERENCES

The histogram of differences between VTHY and the reference VEIG22 is plotted, using 1-minute quality checked data for the whole period of the intercomparison. Differences are plotted by steps of 0.1K. The vertical axis is the frequency in percent for each class of differences.

Screen #1:

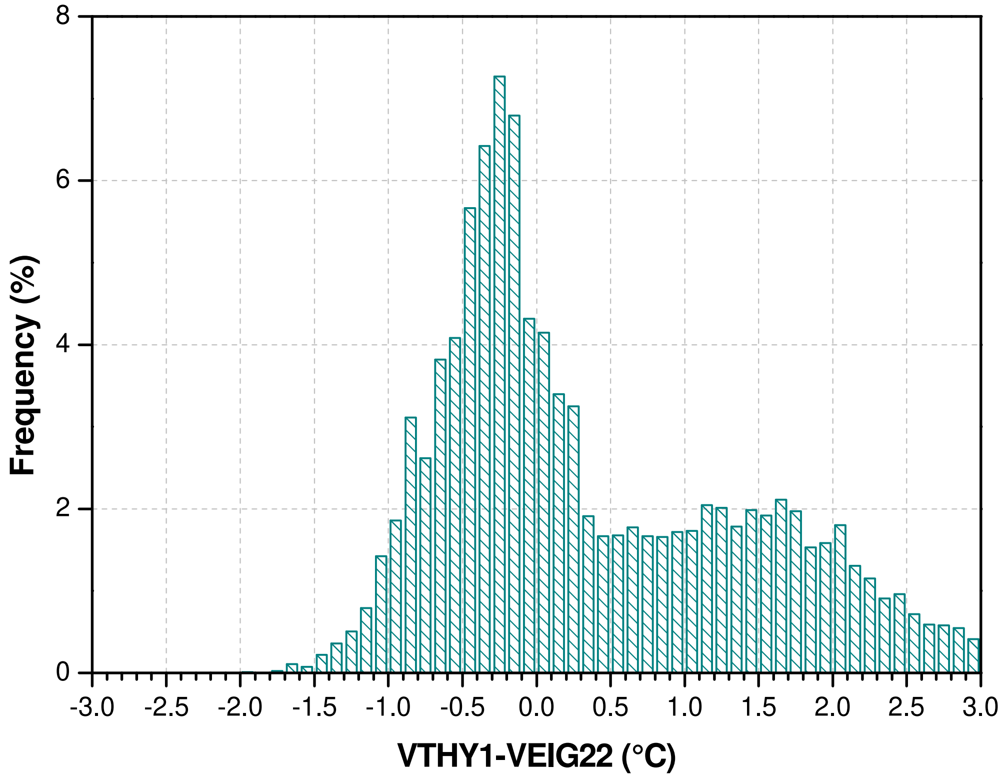


**Figure 3**

Screen #2:

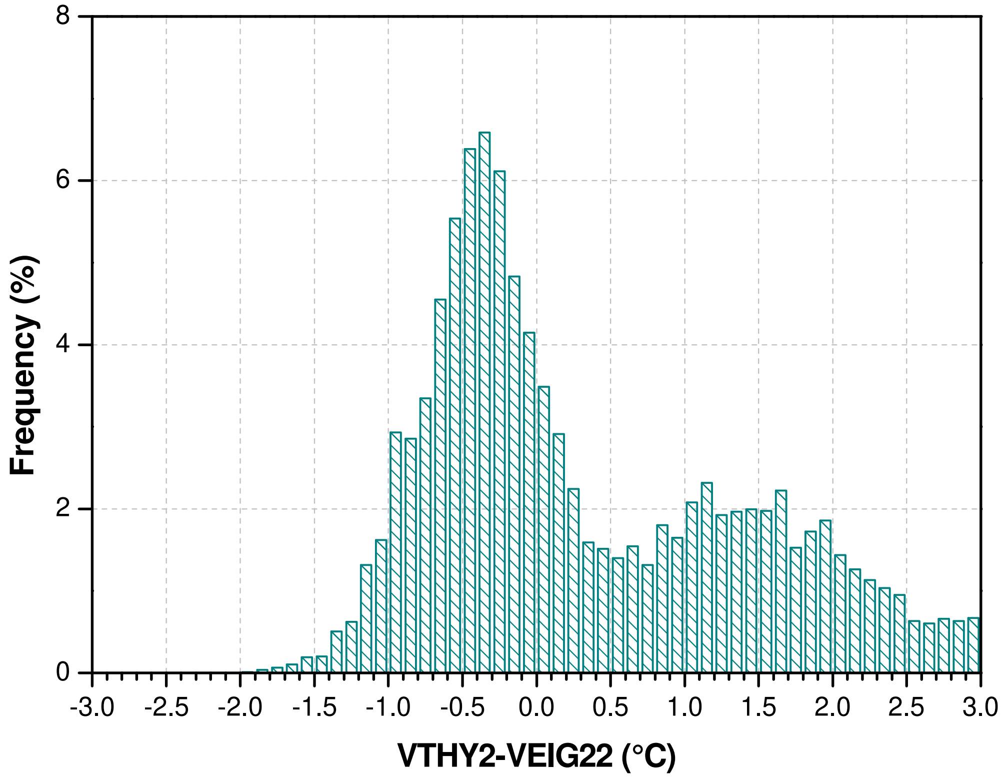


**Figure 4**

For both sensors the histograms are very dispersed. The figure 5 shows on the top the temporal variation of both Thygan sensors and the reference during 4 days: 7th to 10th to of November, 2008. In the middle is the global radiation. The 2-meter wind speed (2-minute average) is the bottom plot. These are 10-minute values.

Thygan sensors overestimate the temperature during day and underestimate it during night. Basically, the ventilation of these sensors is not efficient enough.

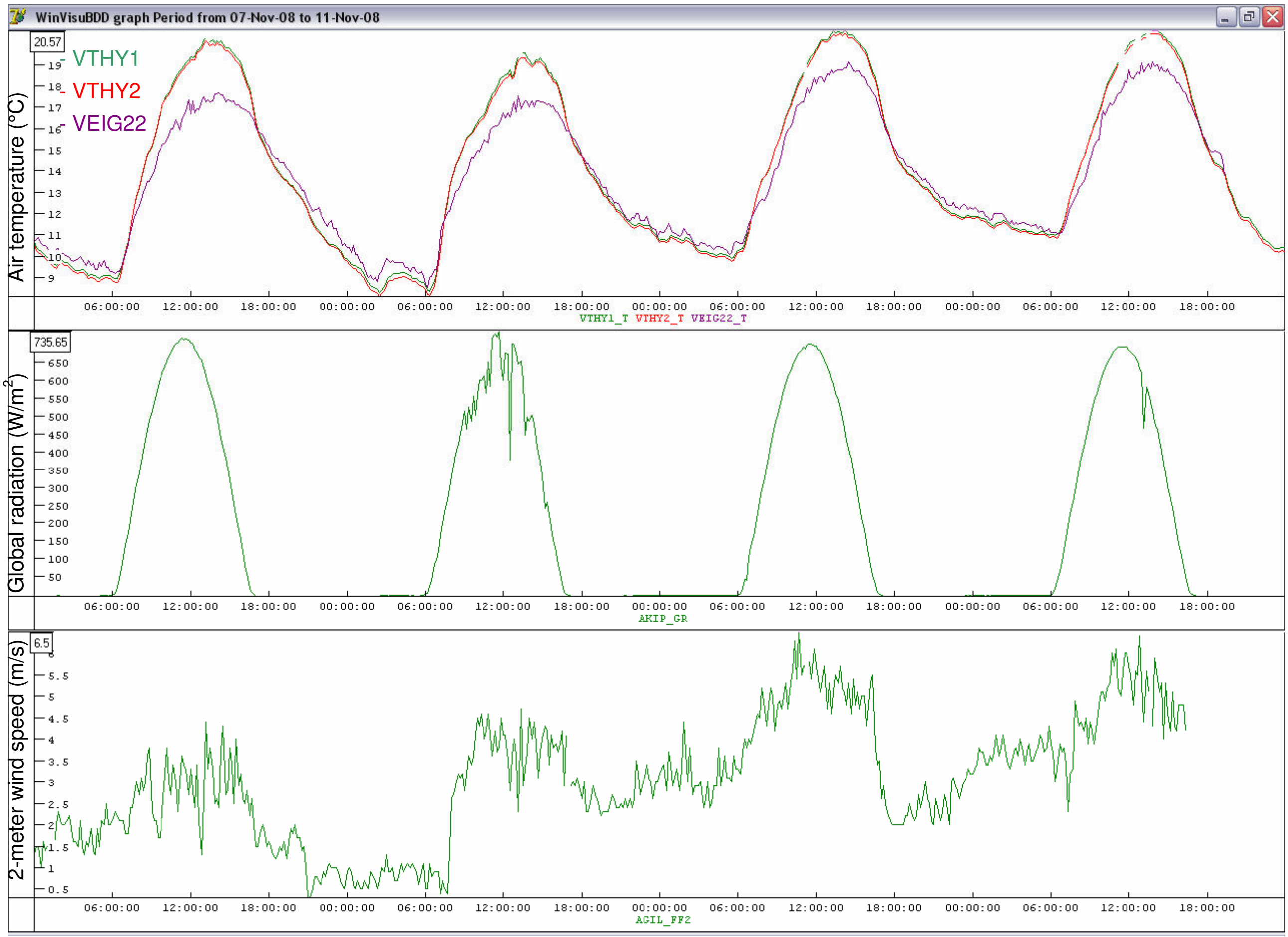


**Figure 5**

CUMULATIVE HISTOGRAMS OF DIFFERENCES OF DAILY EXTREME VALUES

The cumulative histograms of differences with the reference VEIG22 of T (1-minute quality checked data), Tn (daily minimum temperature) and Tx (daily maximum temperature) are plotted, for the whole period of the intercomparison. Differences are plotted by steps of 0.1K.

Screen #1:

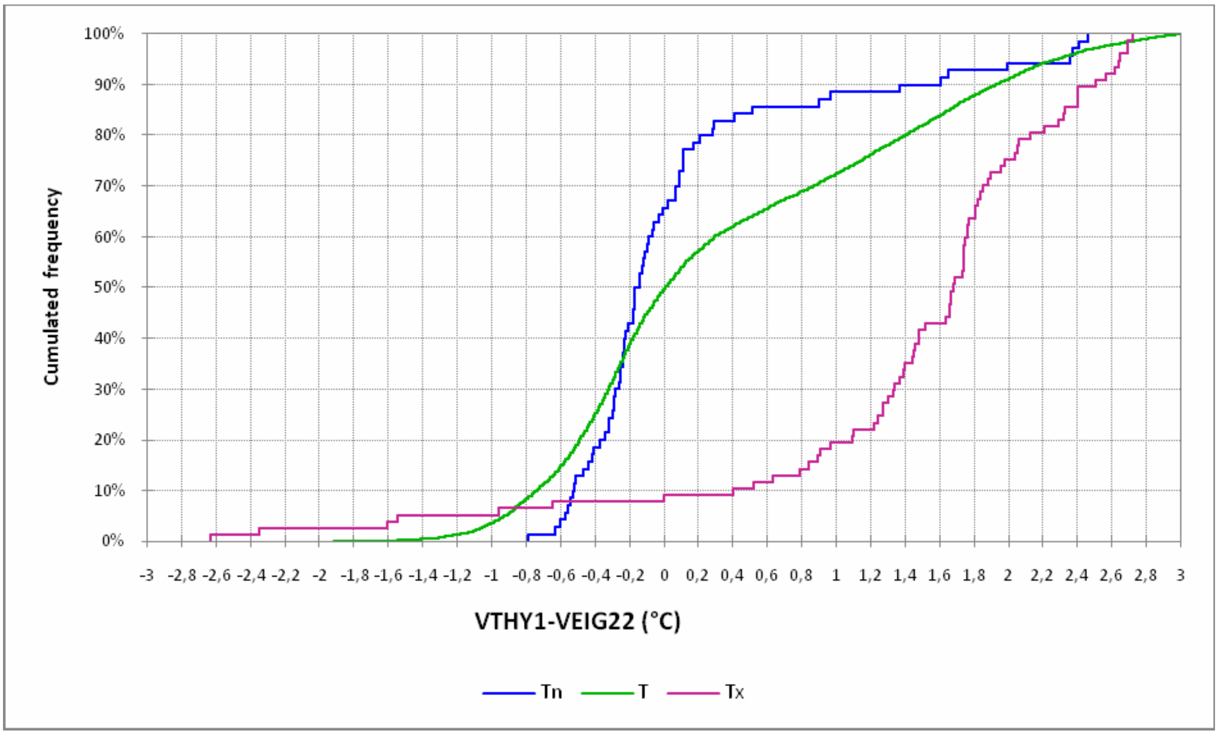


**Figure 6**

Screen #2:

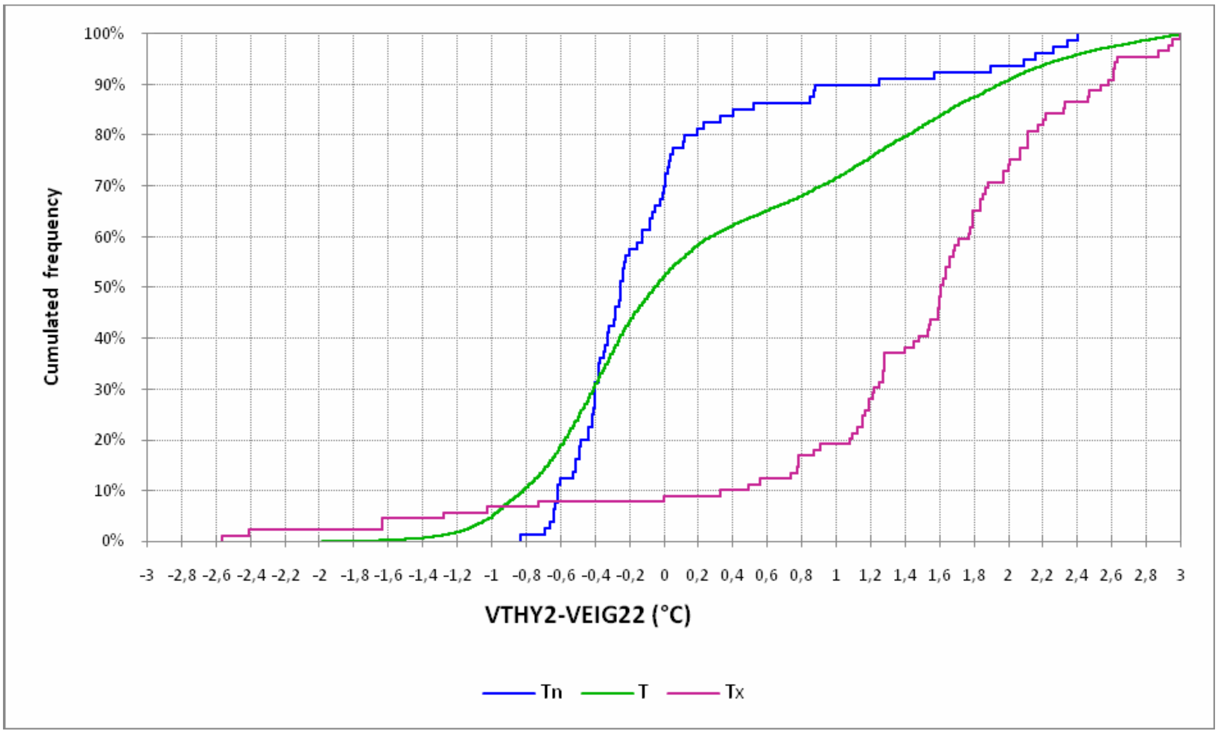


**Figure 7**

Both sensors show very dispersed histograms for T and consequently, for Tn and Tx. Daily maximum temperatures are particularly affected.

TABLE

The table 2 indicates the percentage of data that differ by less than 0.2°C (and 0.5°C) from the reference.

**Table 2**

| | | [-0.2°..0.2°] | [-0.5°..0.5°] |
|---|---|---|---|
| VTHY1 | T | 18.5 | 44.2 |
| | Tn | 33.8 | 67.6 |
| | Tx | 1.1 | 2.2 |
| VTHY2 | T | 15.3 | 39.0 |
| | Tn | 21.8 | 63.2 |
| | Tx | 0.9 | 2.8 |

## INFLUENCE OF GLOBAL RADIATION

The distribution of differences between VTHY and the reference VEIG22 is plotted, using 1-minute quality checked data for the whole period of the intercomparison. Differences are classified according global radiation.

Screen #1:

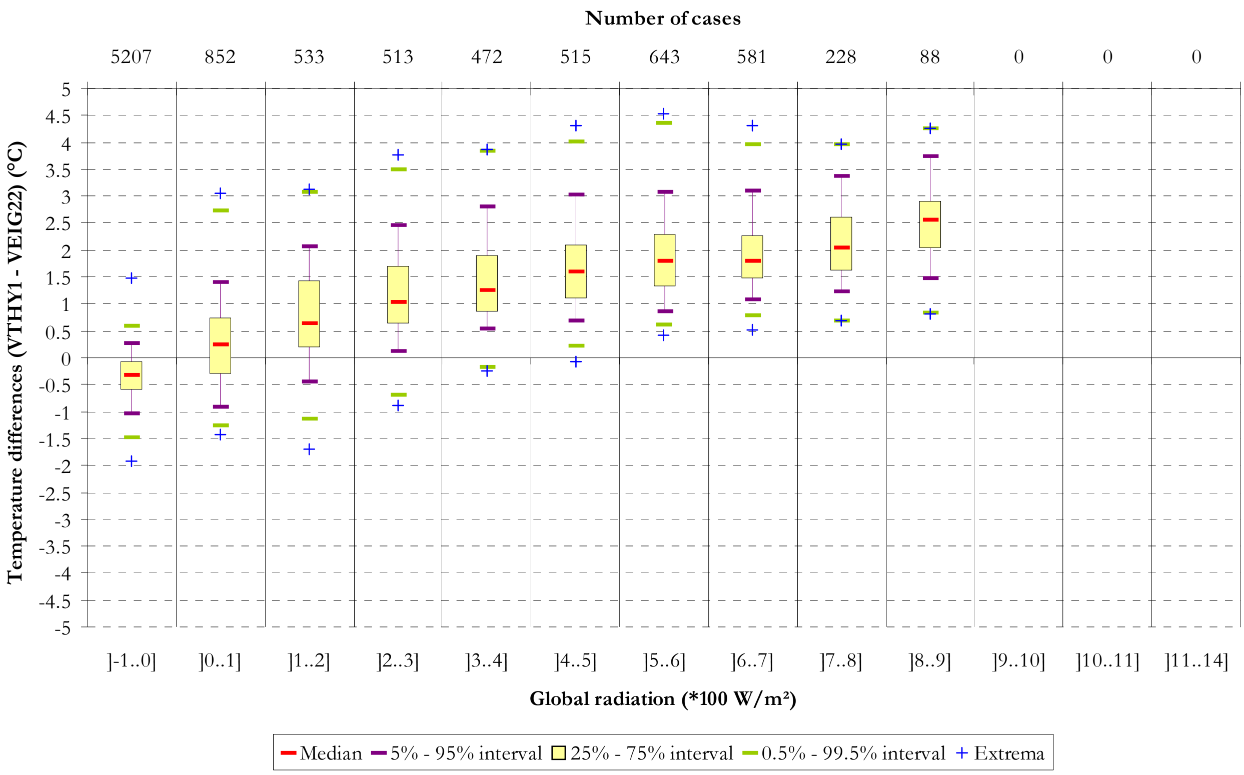


**Figure 8**

Screen #2:

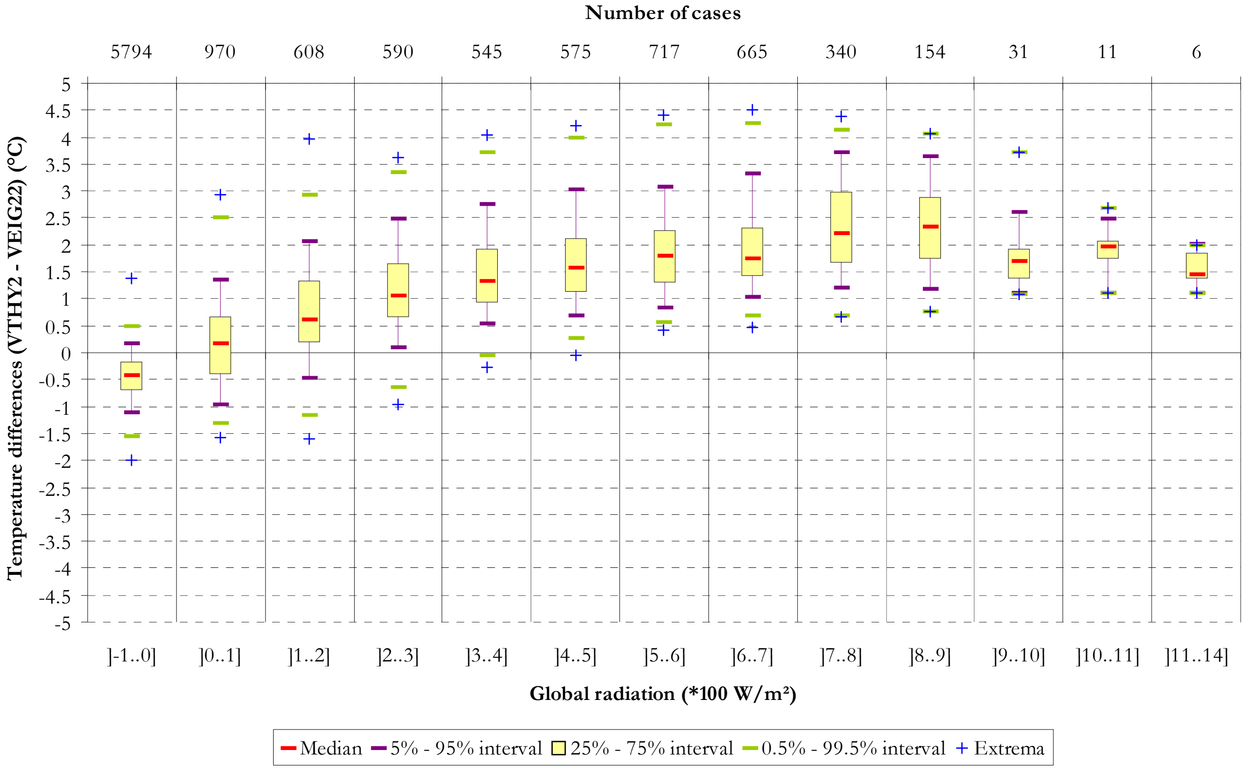


**Figure 9**

With the exception of very low numbers of data, the higher the global radiation, the warmer the Thygan sensors are. The medians of differences with the reference reach more than 2°C for global radiation values greater than 700W/$m^2$.

## RADIATION EFFECT

### DIFFERENCES BETWEEN DAY AND NIGHT BEHAVIOUR

The median of differences between VTHY and VEIG22 is plotted, using 1-minute quality checked data for the whole period of the intercomparison. We filter data for which sun elevation is above -1° (day) or below -1° (night). Differences are classified according 2-meter wind speed (2-minute average).

Screen #1:

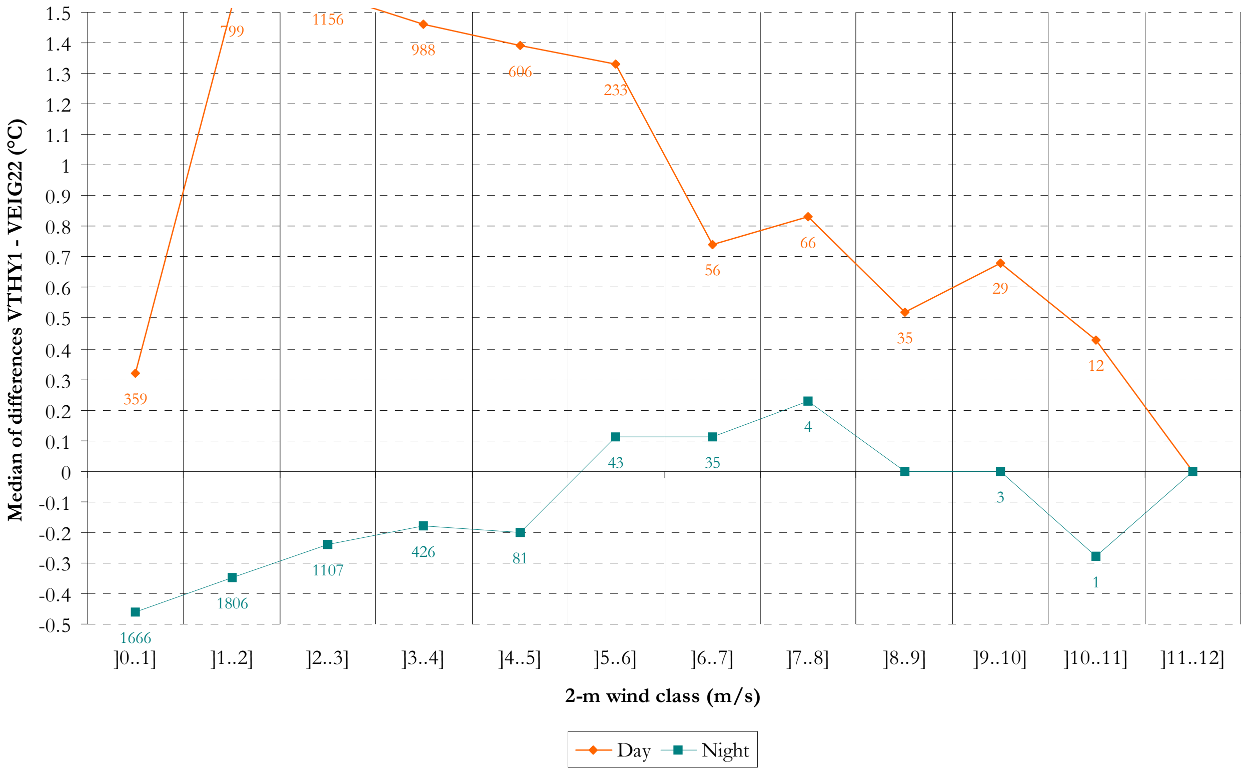


**Figure 10**

Screen #2:

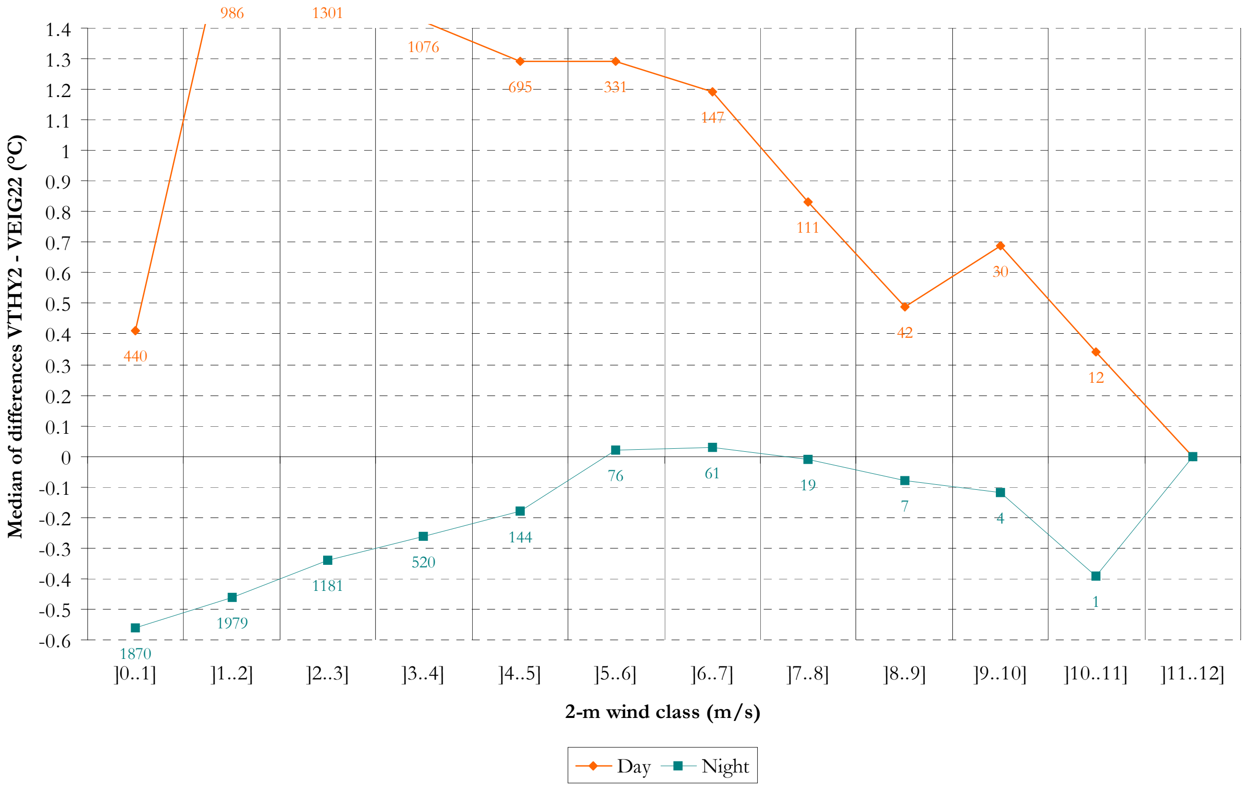


**Figure 11**

These sensors are much warmer than the reference during day. Overheating is moderate for calm winds. When the wind speed increases, the differences with the reference are reduced.

During night, the cooling is moderate. When the wind speed increases, the cooling is reduced: for winds above 5m/s, Thygan sensors give measurements close to the reference.

DIFFERENCES BETWEEN CLEAR SKY AND OVERCAST SKY DURING DAYTIME

The median of differences between VTHY and VEIG22 is plotted, using 1-minute quality checked data. Here, we consider periods lasting six hours at least where cloudiness is less or equal to 1 (clear sky) or more or equal to 7 (overcast sky), during daytime (sun elevation above -1°). Differences are classified according 2-meter wind speed (2-minute average).

Screen #1:

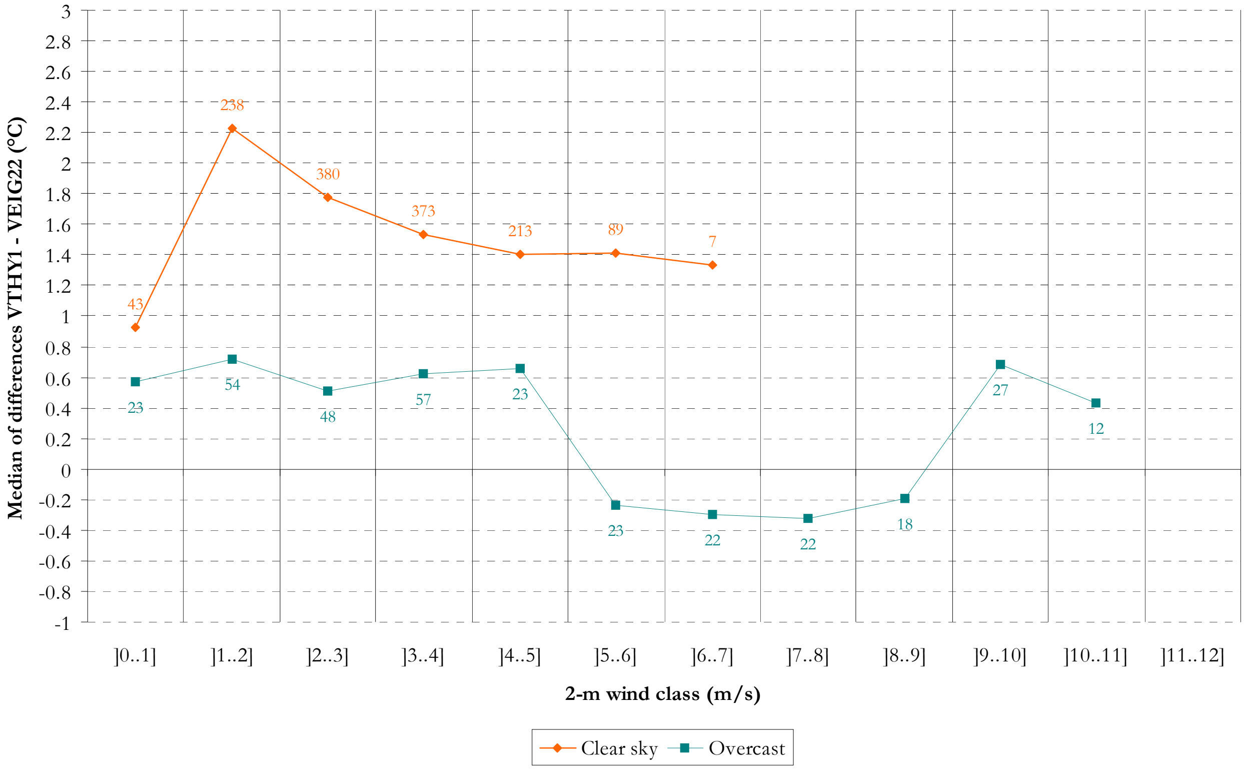


**Figure 12**

Screen #2:

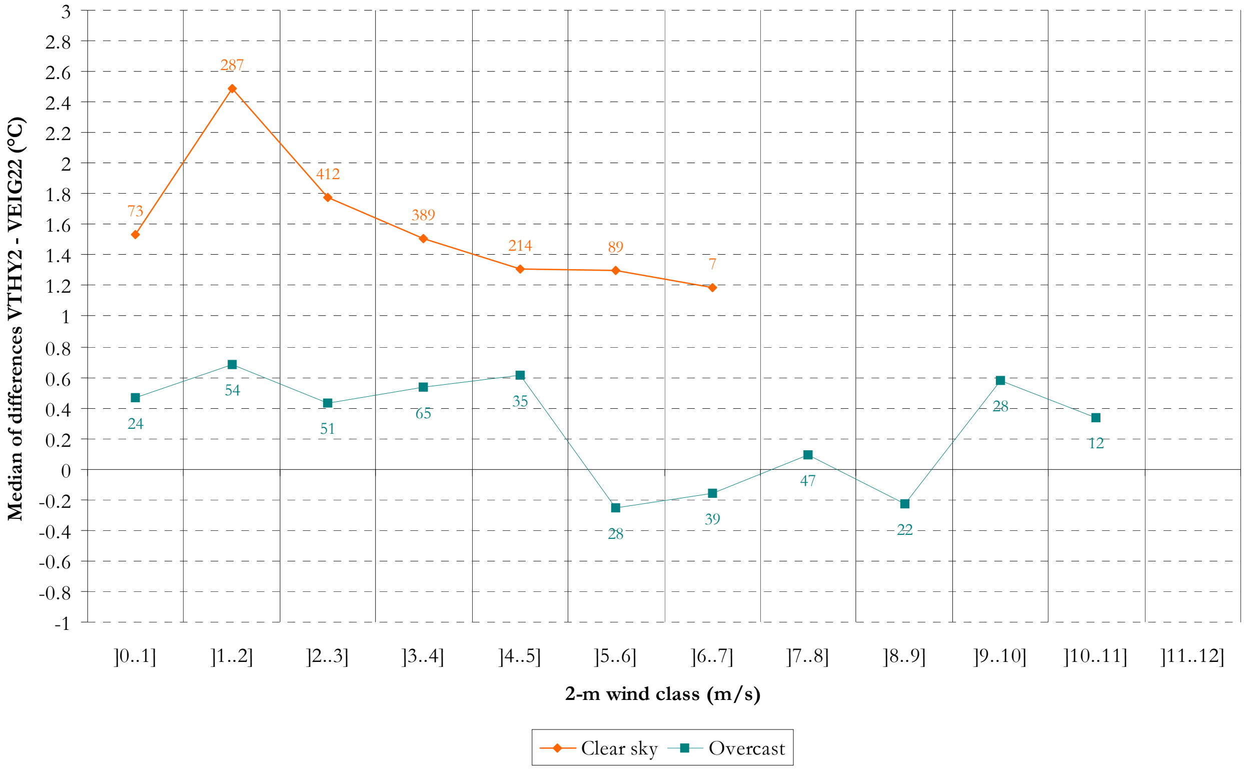


**Figure 13**

It may be not relevant to conclude for overcast conditions, since the numbers of data are very low here.

During daytime, when the sky is clear, differences with the reference are lower for calm winds (0 to 1m/s) than for low values of wind speed (1 to 2m/s). Then, when the wind speed increases, differences decrease.

DIFFERENCES BETWEEN CLEAR SKY AND OVERCAST SKY DURING NIGHT TIME

The median of differences between VTHY and VEIG22 is plotted, using 1-minute quality checked data. Here, we consider periods lasting six hours at least where cloudiness is less or equal to 1 (clear sky) or more or equal to 7 (overcast sky), during night time (sun elevation below -1°). Differences are classified according 2-meter wind speed (2-minute average).

Screen #1:

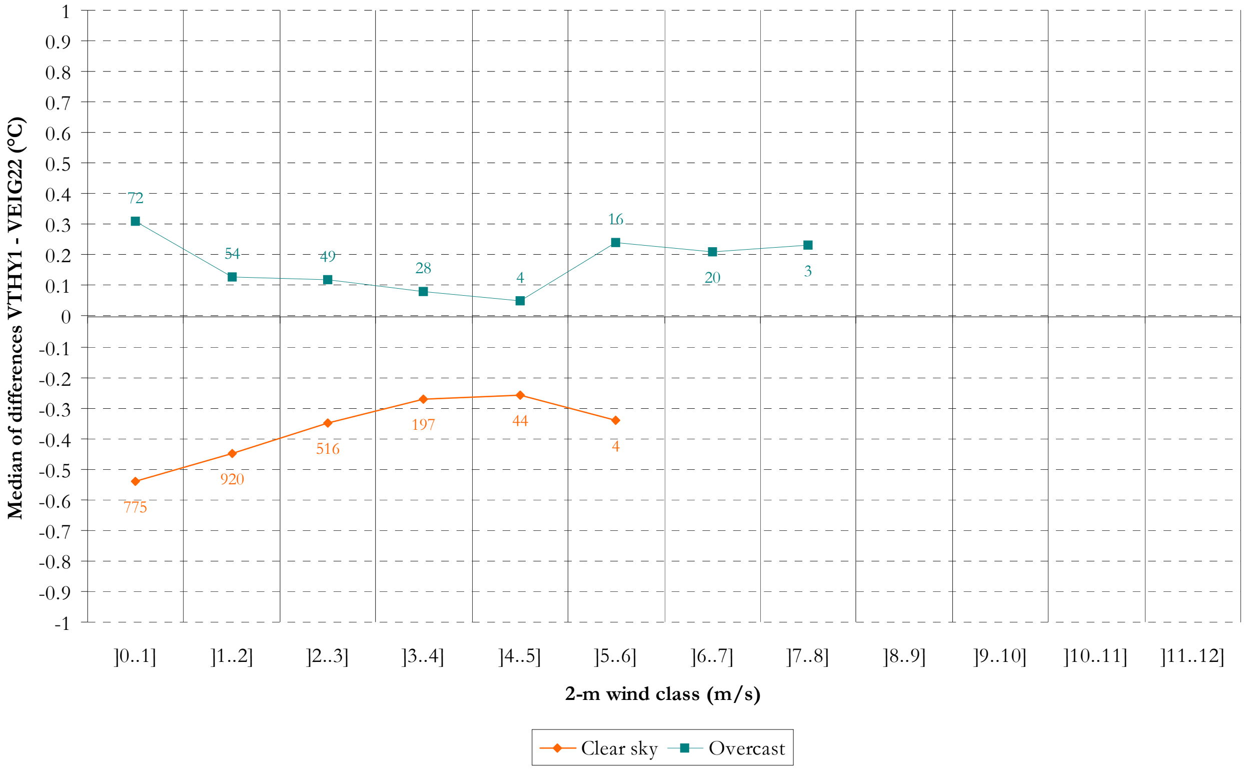


**Figure 14**

Screen #2:

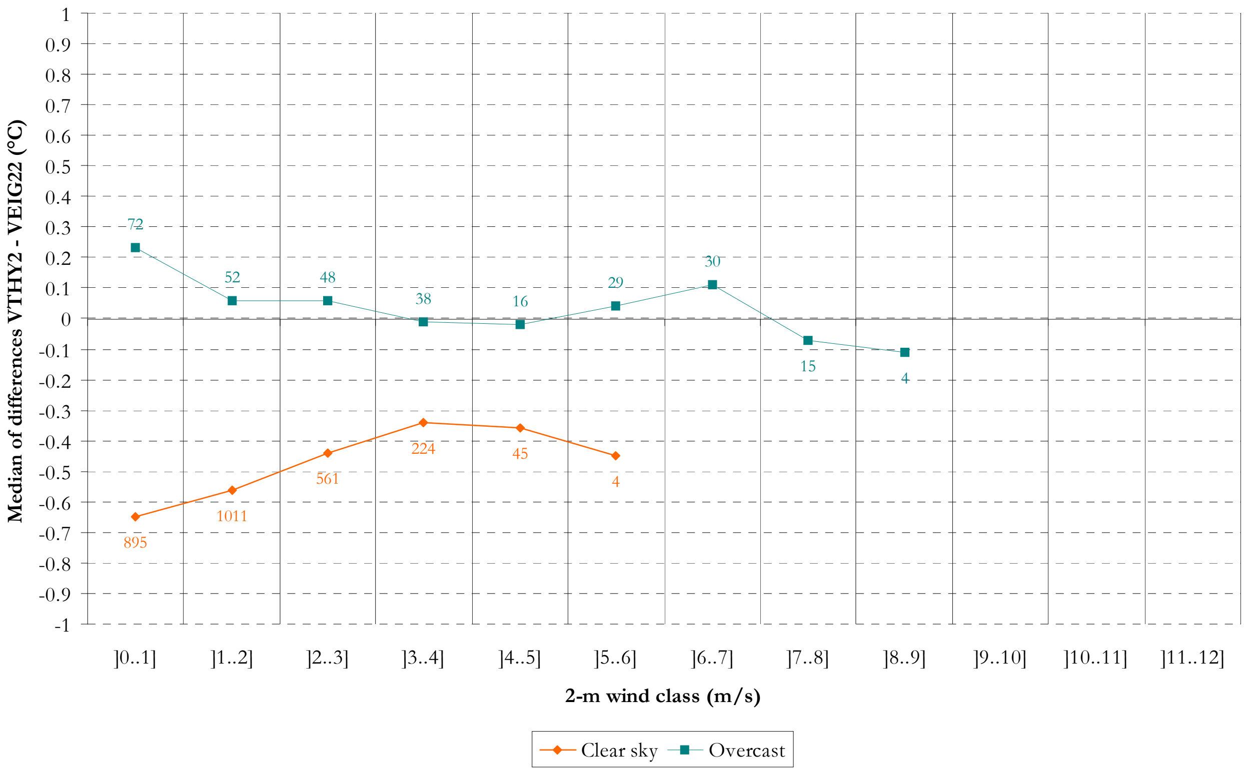


**Figure 15**

It may be not relevant to conclude for overcast conditions, since the numbers of data are very low here.

During night time, when the sky is clear, Thygan sensors are cooler than the reference. As wind speed increases, they get closer to the reference.

## EFFECT OF SUN ELEVATION

The median of differences between VTHY and VEIG22 is plotted, using 1-minute quality checked data. Here, we consider periods lasting six hours at least where cloudiness is less or equal to 1 (clear sky), during daytime (sun elevation above -1°). We filter data where sun elevation is low (below 10°), medium (between 10° and 45°) or high (above 45°). Differences are classified according 2-meter wind speed (2-minute average).

Screen #1:

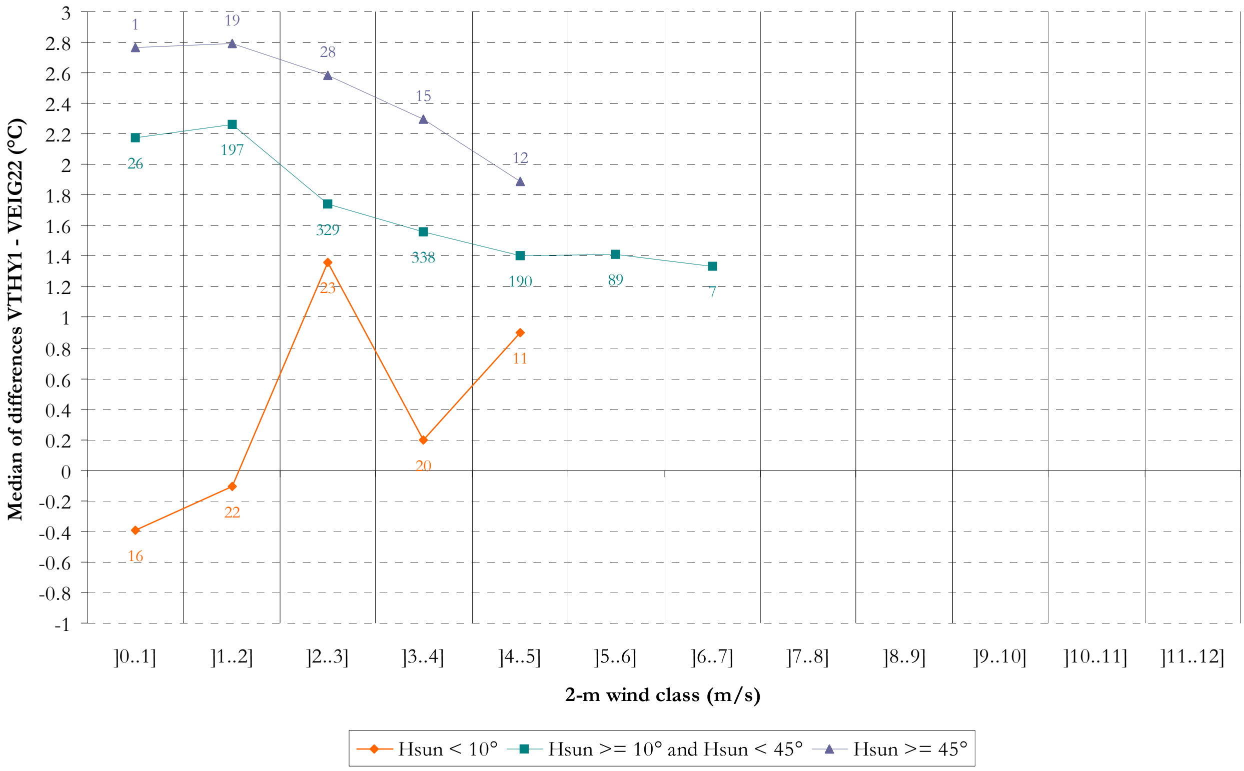


**Figure 16**

Screen #2:

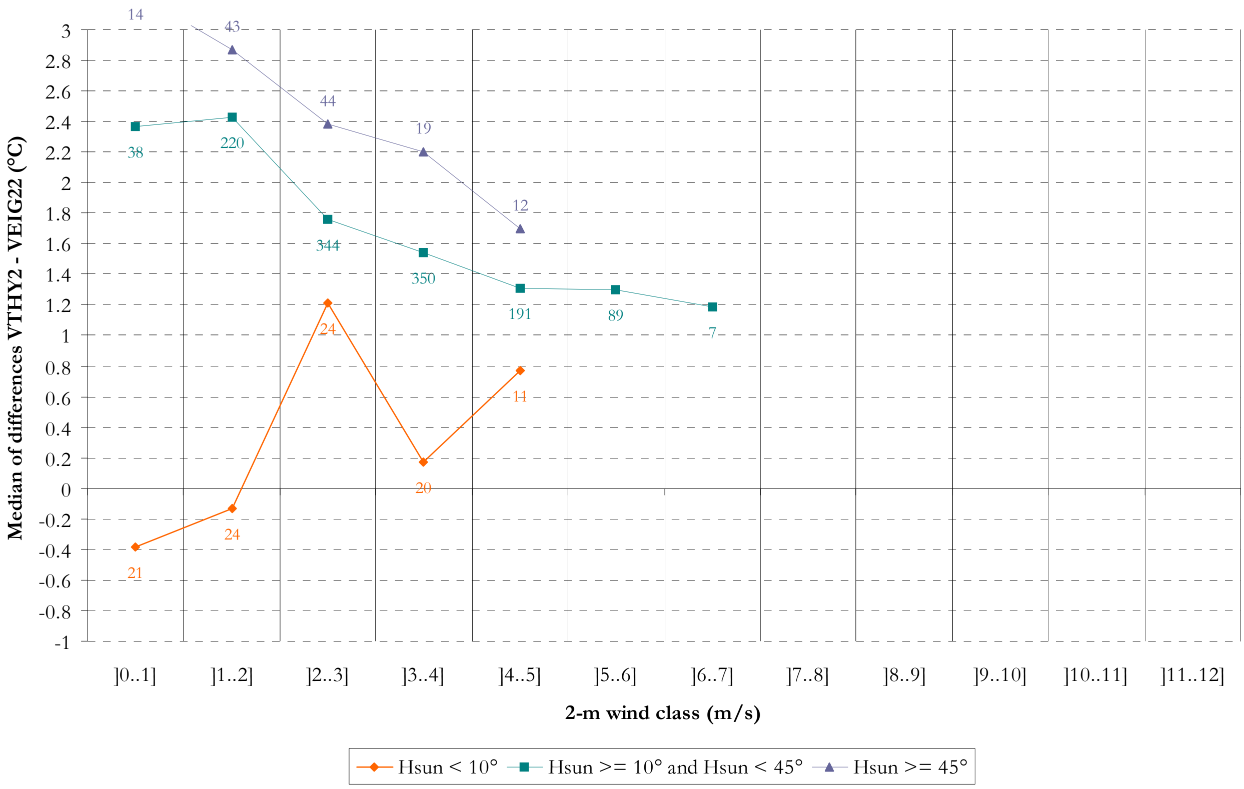


**Figure 17**

It may be not relevant to conclude for low and high values of sun elevation, since the numbers of data are very low here.

For medium values of sun elevation, overheating of Thygan sensors is reduced when the wind is stronger.

## COMBINED EFFECT OF WIND AND GLOBAL RADIATION

The medians of differences between VTHY and VEIG22 are represented here with a contour plot. The global radiation values are on the X-axis and on the Y axis is the 2-meter wind speed value (2-minute average). Medians are used in all cases, providing that at least one data is available for both conditions on radiation and wind considered.

Screen #1:

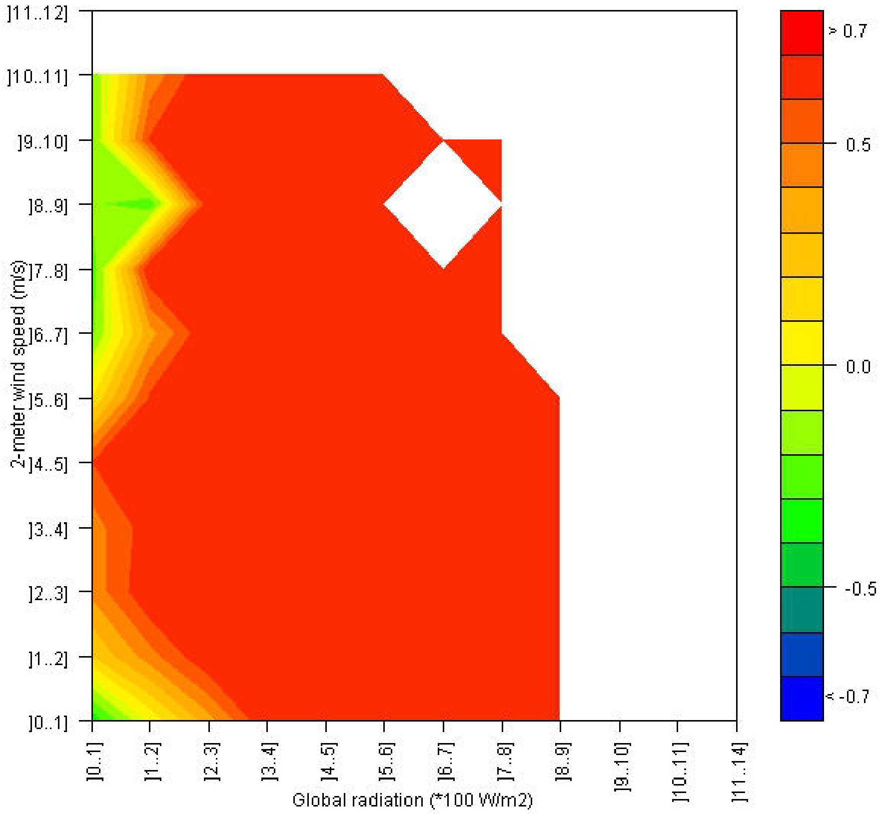


**Figure 18**

Screen #2:

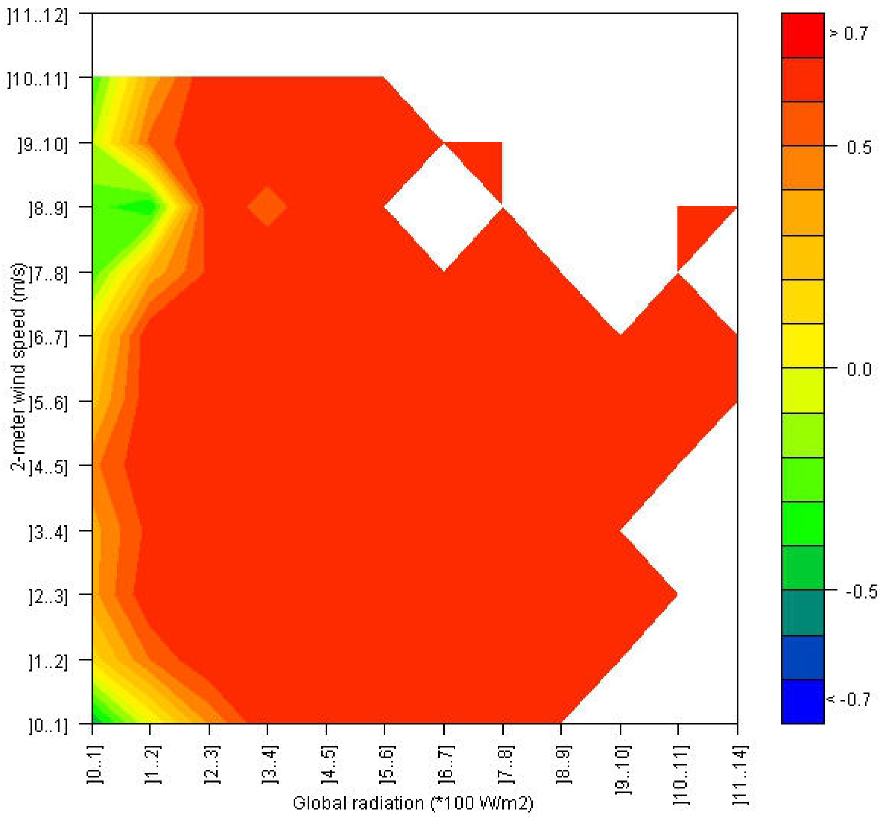


**Figure 19**

These plots show the overestimation of the temperature by Thygan sensors in most of the conditions. Only for calm winds, they are close to the reference and sometimes colder.

## BEHAVIOUR DURING INCREASE/DECREASE OF TEMPERATURE

The distribution of differences between VTHY and the reference VEIG22 is plotted, using 1-minute quality checked data for the whole period of the intercomparison. Differences are classified according the temporal gradient of reference temperature over 1 minute. A screen faster (or slower, respectively) than the reference would be warmer (cooler) for positive gradient, cooler (warmer) for negative ones.

## Screen #1:

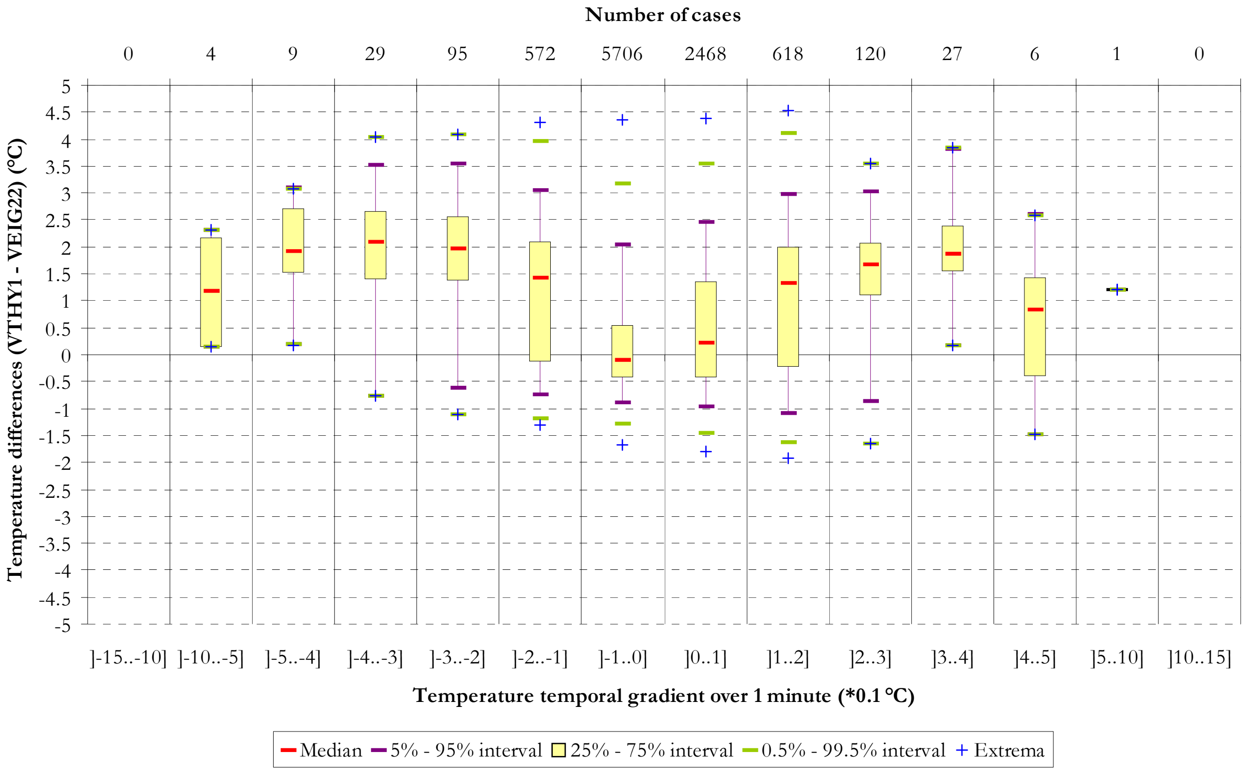


**Figure 20**

## Screen #2:

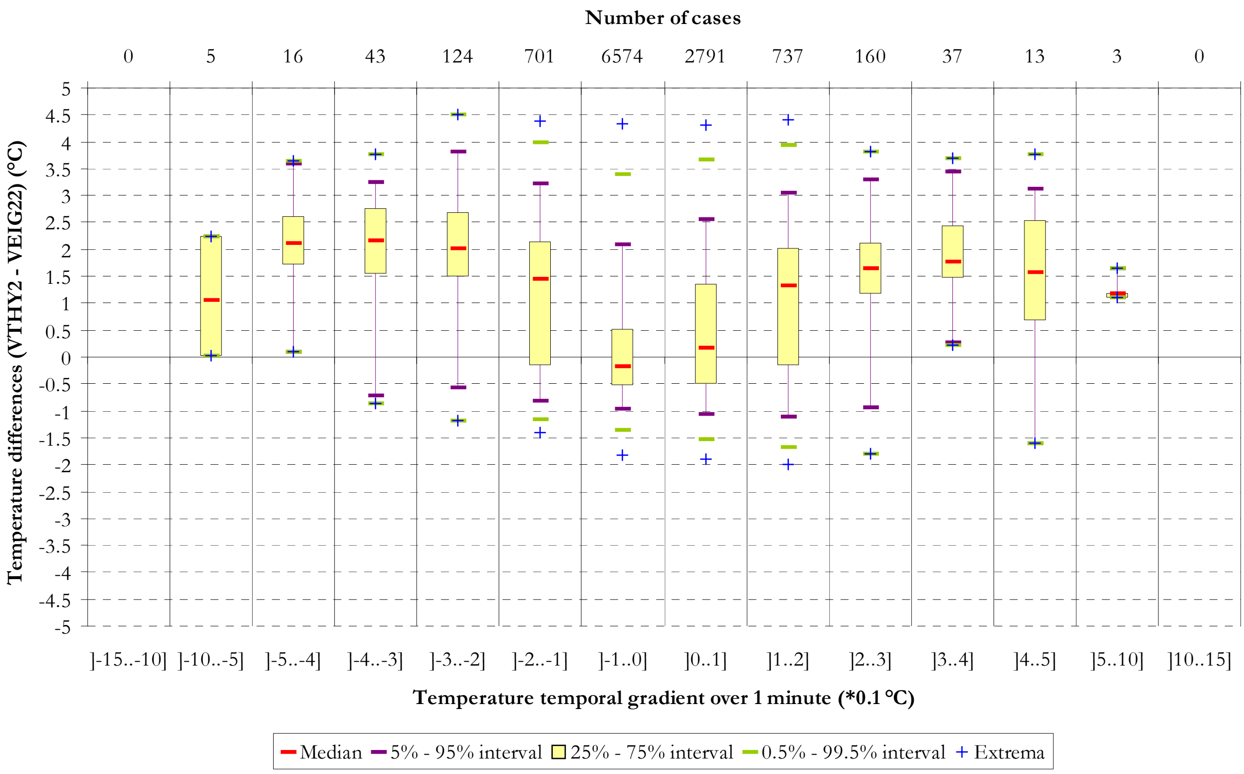


**Figure 21**

Differences with the reference are mainly positive for all temperature gradients. These plots do not show a delay or an advance of these sensors compared to the reference.

## QUALITY CONTROL INFORMATION

### DATA AVAILABILITY

The intercomparison period extends from the 1st of November 2008 to the 1st of November 2009. The theoretical number of 1-minute data is 525600.

The next table sums up the total number of data for each screen and for each possible QC flag.

**Table 3**

| **QC flag** | VTHY1 | VTHY2 |
|---|---|---|
| 0 (good) | 11693 | 11821 |
| 1 (inconsistent) | 0 | 0 |
| 2 (doubtful) | 0 | 0 |
| 3 (erroneous) | 0 | 0 |
| 7 (missing) | 513907 | 513779 |

The reasons for missing data are frequent failures of the acquisition software and the stop of transmission from Thygan sensors from May 2009

### MAINTENANCE

The acquisition software ordered for time synchronization and cleaning the mirror once per day.

Sensor #1 gave no data after the 2nd of March, 2009 at 7:00.

Sensor #2 gave no data after the 2nd of March, 2009 at 17:40.

An interface device common to the two sensors had a failure this day.

# RS12T ROTRONIC
# – Switzerland –
# VROT

**TECHNICAL SPECIFICATIONS (PROVIDED BY THE MANUFACTURER)**

Dimensions: Length 54 cm x Width 20cm x Height 17 cm

Weight: 3 kg

Material/Structure: Double shell Aluminium

Estimated radiation error:

Aspiration rate (in case of artificially ventilated screen/shield): 3.5 m/s

Power supply: 12 V

**Figure 1**

## OVERVIEW

Screen #2 had large percentage of erroneous data, in addition to missing and doubtful data. It gave a signal that obviously was not a temperature, so it was not considered for the analysis.

Screen #1 was warmer than the reference for most of the data points. The graph shows a symmetrical distribution of the differences around the mode, which is 0.3°C. Screen #1 was also warmer than the reference, most of the times, for Tn and Tx, with the Tn being the closest to that reported from the reference.

The graph indicates that the performance of the VROT screen #1 was slightly influenced by the magnitude of solar radiation. When the irradiance increases, the screen became predominantly warmer and the dispersion of the temperature differences increased relatively linearly, but not exceeding 1.5°C.

The graph indicates that the VROT screen #1 became warmer with the increase of the wind speed, both, during the day and during the night. During the day, the change in wind speed had a more significant influence up to about 8m/s, above which the warming effect became stable. During the night, for wind speeds up to about 8m/s, the screen maintained a constant performance, and became increasingly warmer for wind speeds above that.

During the day, the effect of warming is more pronounced under clear sky, which increases linearly with the wind speeds. Under overcast conditions, the screen became warmer with the wind speeds, for up to 8m/s, above which it became more stabile relative to the reference. For calm conditions, the screen was just colder than the reference under clear sky. For the same wind conditions, the screen was colder under clear sky than under overcast sky, for winds up to about 3m/s, above which the performance reversed.

At night time, the screen was warmer than the reference under both, clear sky and overcast conditions. Under overcast sky, the screen was consistently warmer than under clear sky.

For all sun elevations and all wind conditions the screen was warmer than the reference, with the exception when the sun was above 10° and the wind was calm.

For calm winds the screen was slightly colder than the reference, independent of the value of irradiance.

The VROT screen #1 was warmer than the reference for all temperature gradients. The median of the differences was closest to zero for temperature gradients of -0.1°C and above, essentially remaining constant for positive gradients. For negative gradients, the median of the temperature differences increased in value with the increase of the absolute gradient, indicating that the screen #1 was slower than the reference when the temperature was decreasing. The dispersion of the temperature differences increases with the increase of the absolute temperature temporal gradient, 90% of the data covering an interval of less than 1.5°C.

## CALIBRATION INFORMATION

The calibration of both probes was performed by manufacturer.

**Table 1**

| Screen | Location | Screen serial number | Instrument bias (°C) | | | |
|---|---|---|---|---|---|---|
| | | | -20°C | 0°C | 20°C | 40°C |
| VROT1 | B1 | 47090001 | | | | |
| VROT2 | B4 | 47090002 | | | | |

The result of calibration of reference VEIG22 is available in the main report of the intercomparison, section 5.4.1.

## COMPARISON WITH THE REFERENCE

### HISTOGRAM OF DIFFERENCES

The histogram of differences between VROT1 and the reference VEIG22 is plotted, using 1-minute quality checked data for the whole period of the intercomparison. Differences are plotted by steps of 0.1K. The vertical axis is the frequency in percent for each class of differences.

Screen #1:

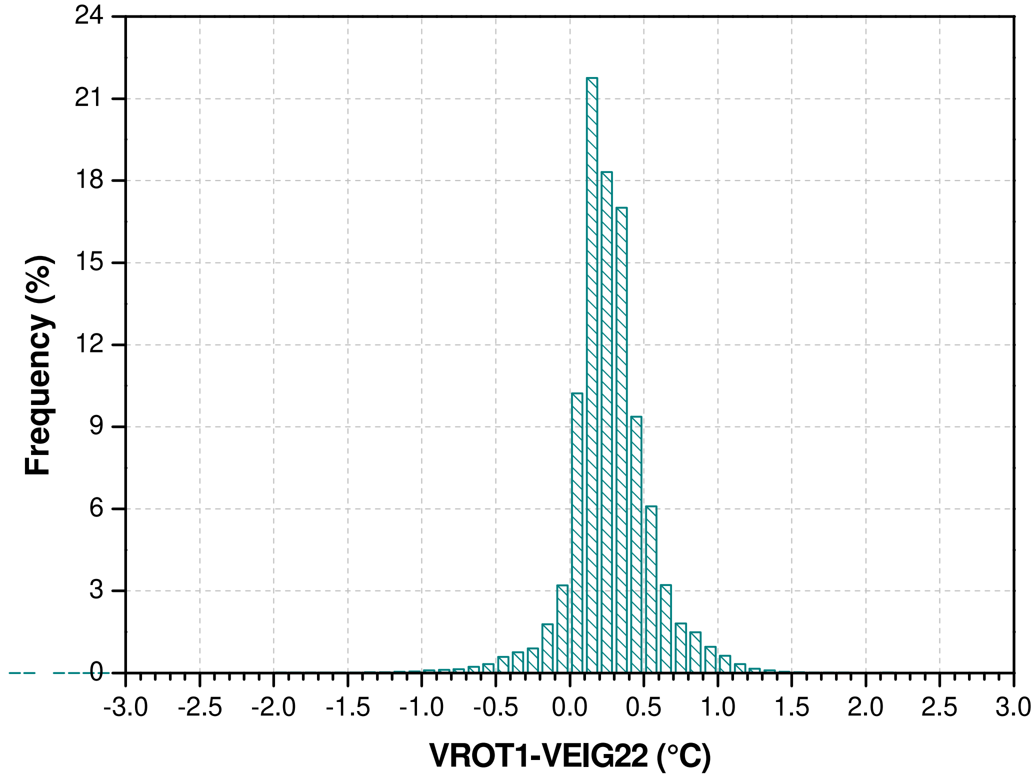


**Figure 2**

Screen #1 was warmer than the reference for most of the data points. The graph shows a symmetrical distribution of the differences around the mode, which is 0.3°C.

### CUMULATIVE HISTOGRAMS OF DIFFERENCES OF DAILY EXTREME VALUES

The cumulative histograms of differences with the reference VEIG22 of T (1-minute quality checked data), Tn (daily minimum temperature) and Tx (daily maximum temperature) are plotted, for the whole period of the intercomparison. Differences are plotted by steps of 0.1K.

Screen #1:

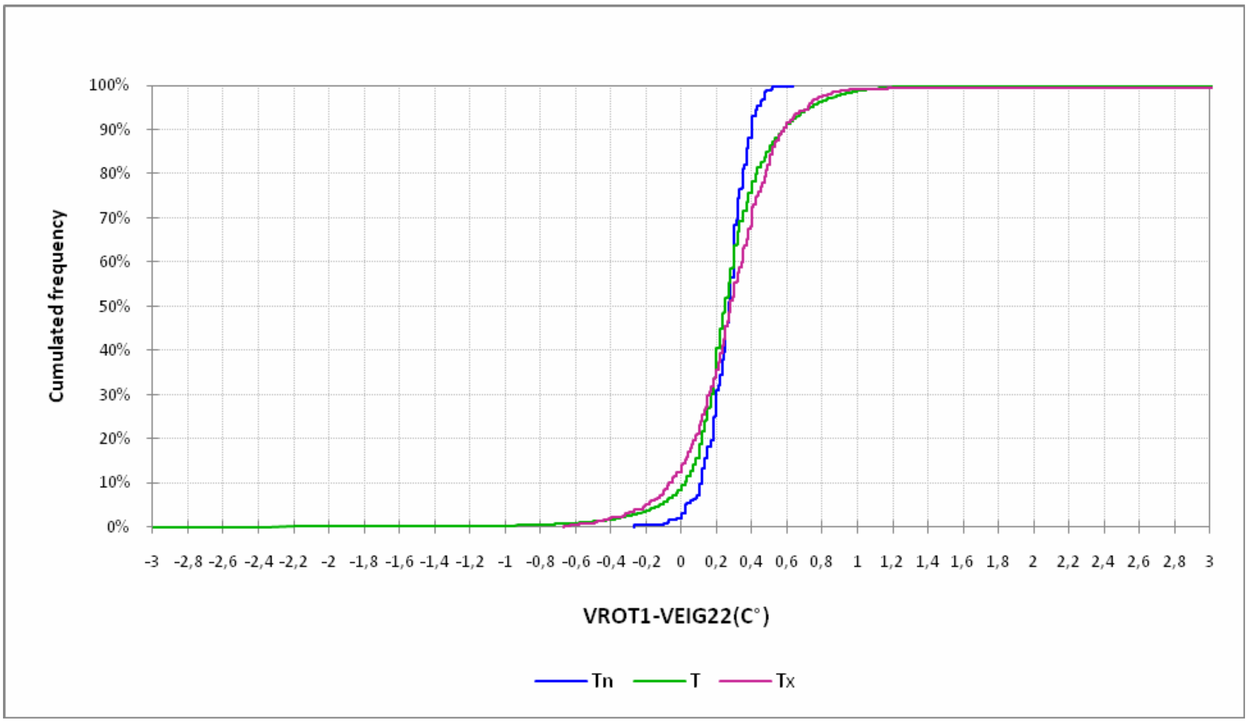


**Figure 3**

Screen #1 was warmer than the reference, most of the times, for Tn, T, and Tx, with the Tn being the closest to that reported from the reference. The graph also indicates that, relative to the reference, the screen maintained a consistent performance for the minimum, maximum, and for the 1-minute temperature.

TABLE

The table 2 indicates the percentage of data that differ by less than 0.2°C (and 0.5°C) from the reference.

**Table 2**

| | | [-0.2°..0.2°] | [-0.5°..0.5°] |
|---|---|---|---|
| VROT1 | T | 37.0 | 85.2 |
| | Tn | 29.6 | 96.7 |
| | Tx | 30.4 | 84.7 |

## INFLUENCE OF GLOBAL RADIATION

The distribution of differences between VROT1 and the reference VEIG22 is plotted, using 1-minute quality checked data for the whole period of the intercomparison. Differences are classified according global radiation.

Screen #1:

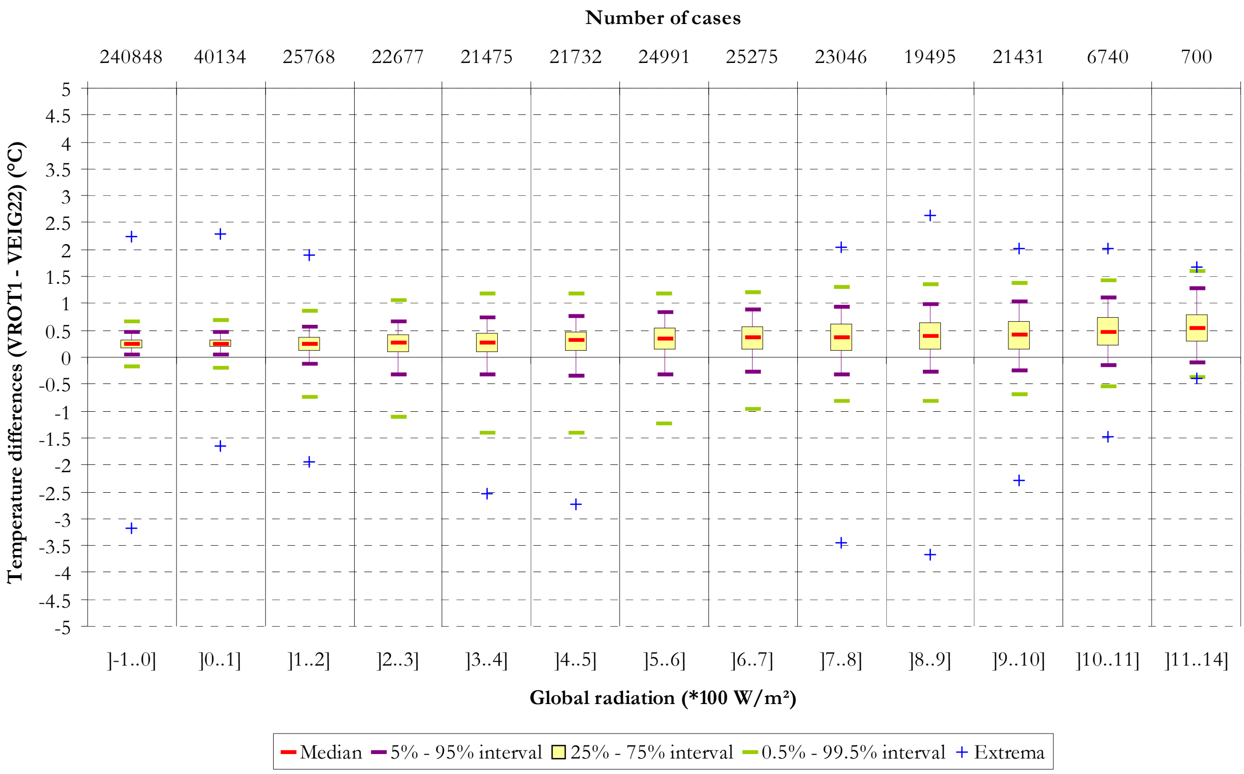


**Figure 4**

The graph indicates that the performance of the VROT screen #1 was slightly influenced by the magnitude of solar radiation. When the irradiance increases, the screen became predominantly warmer and the dispersion of the temperature differences increased relatively linearly, but not exceeding 1.5°C.

## RADIATION EFFECT

### DIFFERENCES BETWEEN DAY AND NIGHT BEHAVIOUR

The median of differences between VROT1 and VEIG22 is plotted, using 1-minute quality checked data for the whole period of the intercomparison. We filter data for which sun elevation is above -1° (day) or below -1° (night). Differences are classified according 2-meter wind speed (2-minute average).

Screen #1:

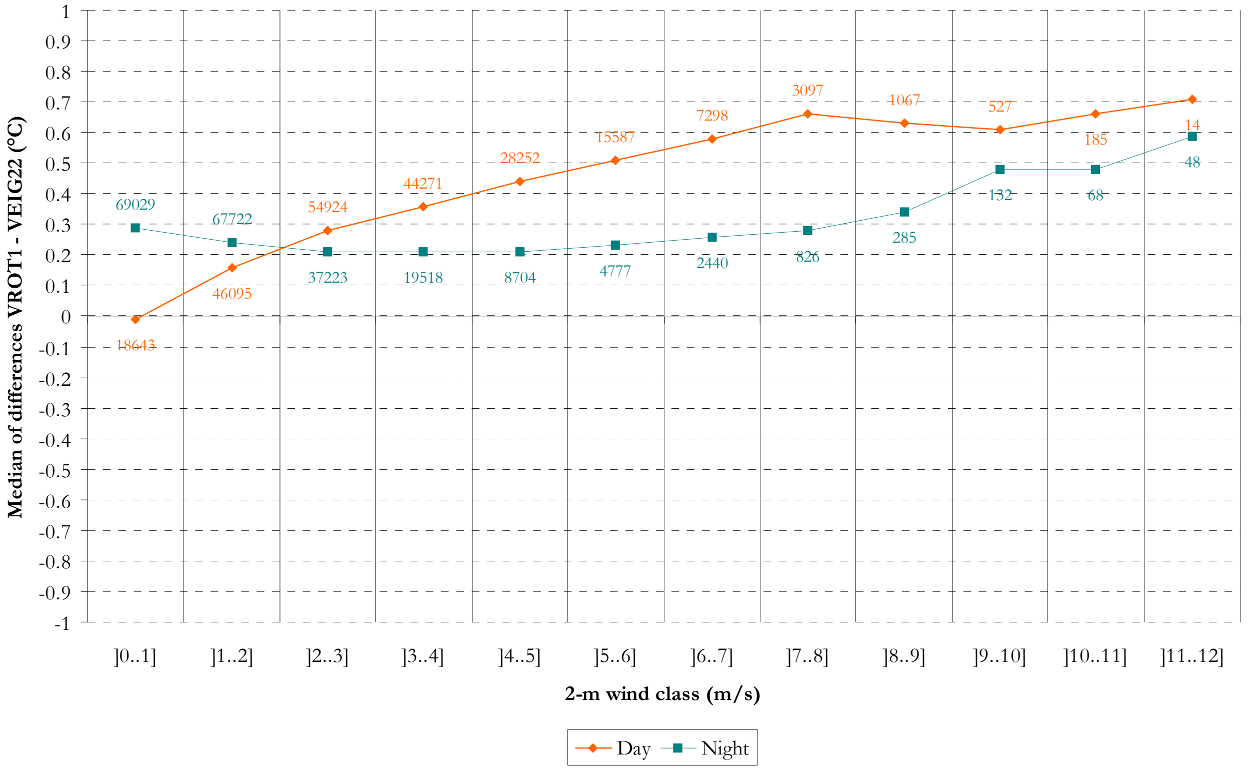


**Figure 5**

The graph indicates that the VROT screen #1 became warmer with the increase of the wind speed, both, during the day and during the night.

During the day, the change in wind speed had a more significant influence up to about 8m/s, above which the warming effect became stable.

During the night, for wind speeds up to about 8m/s, the screen maintained a constant performance, and became increasingly warmer for wind speeds above that.

DIFFERENCES BETWEEN CLEAR SKY AND OVERCAST SKY DURING DAYTIME

The median of differences between VROT1 and VEIG22 is plotted, using 1-minute quality checked data. Here, we consider periods lasting six hours at least where cloudiness is less or equal to 1 (clear sky) or more or equal to 7 (overcast sky), during daytime (sun elevation above -1°). Differences are classified according 2-meter wind speed (2-minute average).

## Screen #1:

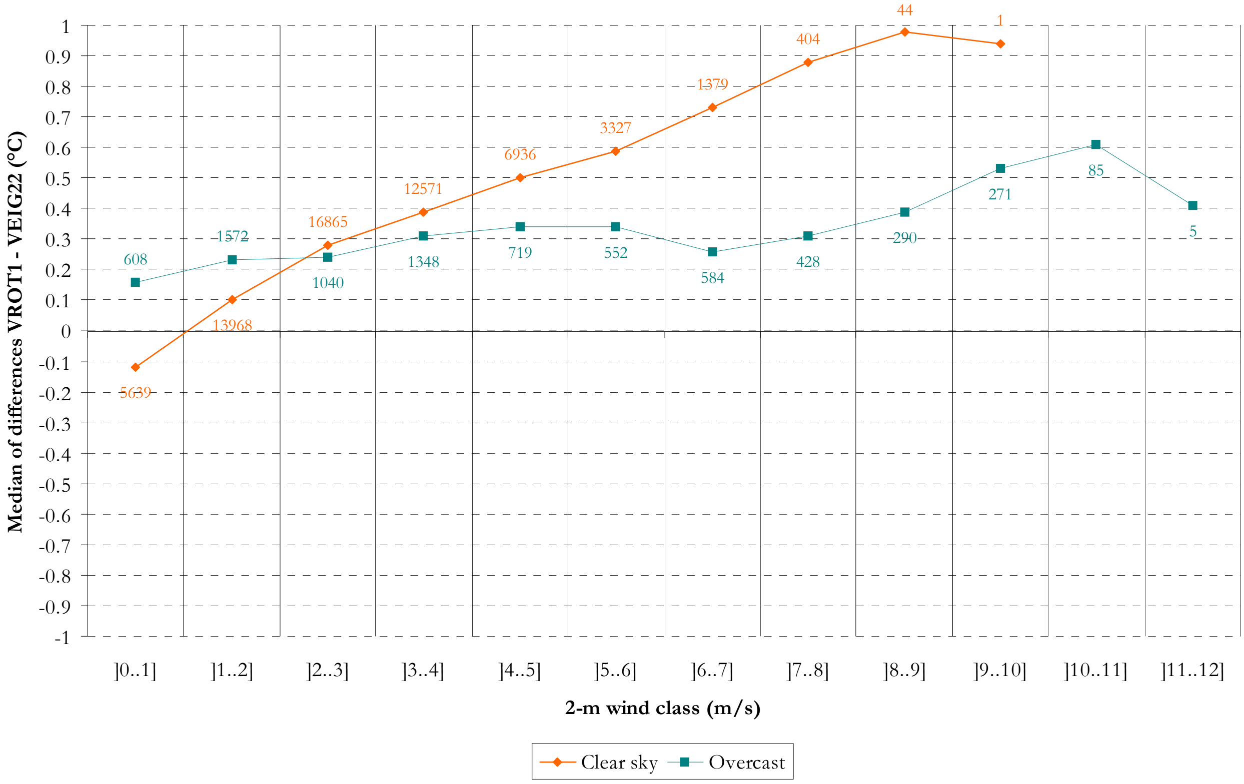


**Figure 6**

During the day, the increase in wind speeds has similar effect on the performance of the screen, under both, clear sky and overcast conditions. The effect of warming is more pronounced under clear sky, which increases linearly with the wind speeds. Under overcast conditions, the screen became warmer with the wind speeds, for up to 8m/s, above which it became more stabile relative to the reference.

For calm conditions, the screen was just colder than the reference under clear sky.

For the same wind conditions, the screen was colder under clear sky than under overcast sky, for winds up to about 3m/s, above which the performance reversed.

### DIFFERENCES BETWEEN CLEAR SKY AND OVERCAST SKY DURING NIGHT TIME

The median of differences between VROT1 and VEIG22 is plotted, using 1-minute quality checked data. Here, we consider periods lasting six hours at least where cloudiness is less or equal to 1 (clear sky) or more or equal to 7 (overcast sky), during night time (sun elevation below -1°). Differences are classified according 2-meter wind speed (2-minute average).

Screen #1:

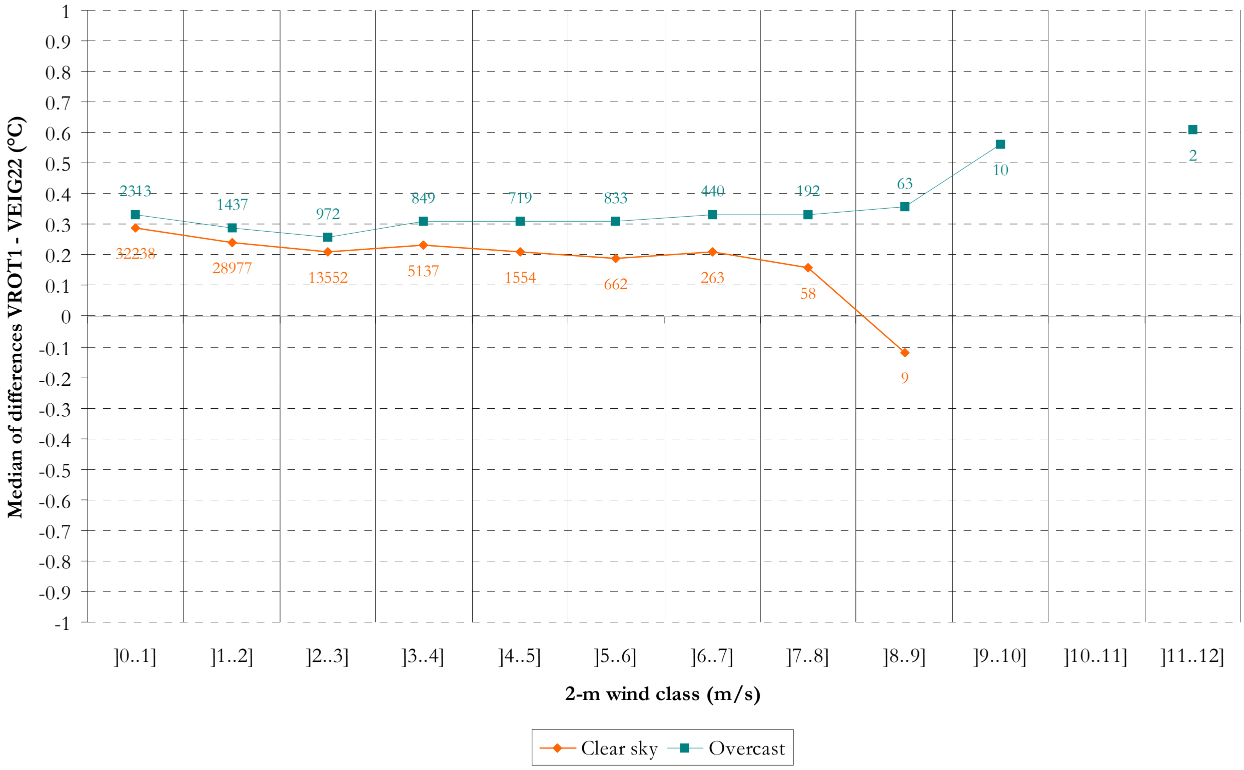


**Figure 7**

Without taking into consideration the classes with a small number of data points, is can be concluded that at night time, the screen was warmer than the reference under both, clear sky and overcast conditions. The screen maintained a relative constant performance with respect to the reference. Under overcast sky, the screen was consistently warmer than under clear sky.

## EFFECT OF SUN ELEVATION

The median of differences between VROT1 and VEIG22 is plotted, using 1-minute quality checked data. Here, we consider periods lasting six hours at least where cloudiness is less or equal to 1 (clear sky), during daytime (sun elevation above -1°). We filter data where sun elevation is low (below 10°), medium (between 10° and 45°) or high (above 45°). Differences are classified according 2-meter wind speed (2-minute average).

Screen #1:

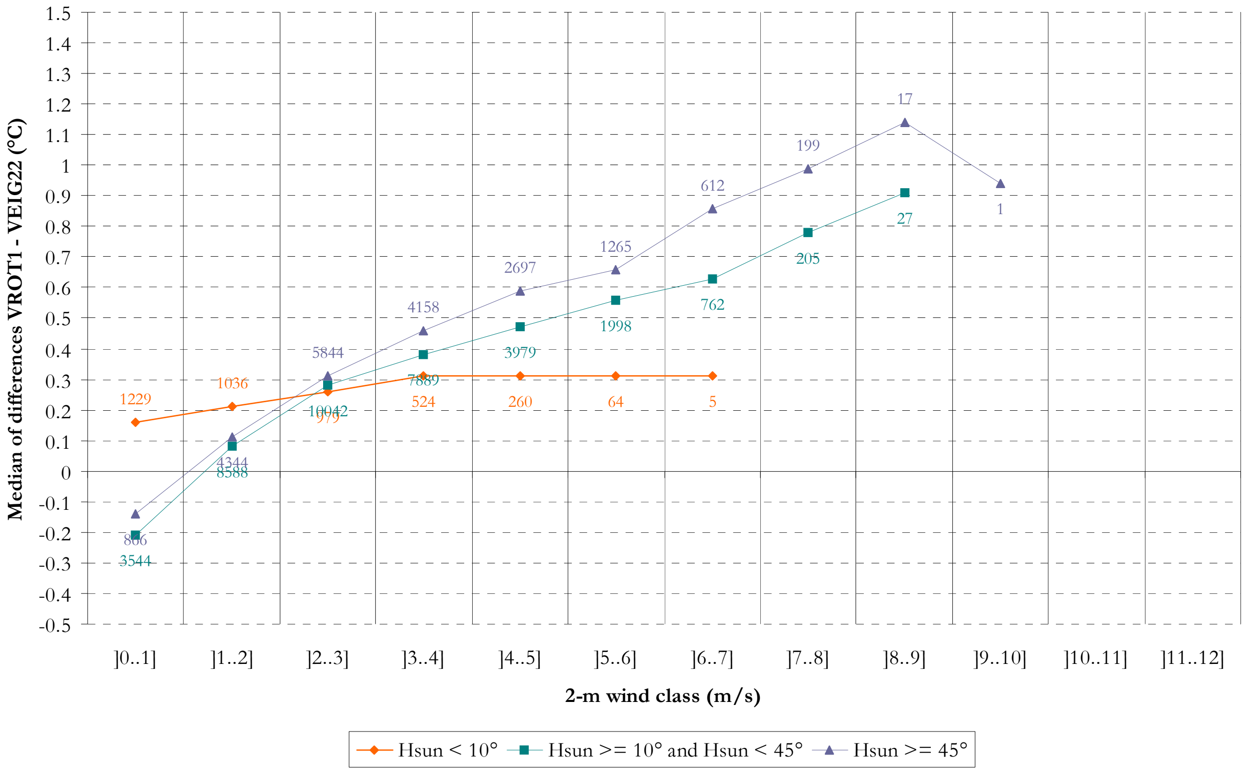


**Figure 8**

For all sun elevations and all wind conditions the screen was warmer than the reference, with the exception when the sun was above 10° and the wind was calm.

For sun elevations below 10°, the VROT screen #1was warmer than the reference by a relative constant amount, that displayed a slight tendency of increasing, followed by a slight decrease, when the wind speed increased.

For sun elevations between 10° and 45°, the screen became significantly warmer with the increase in wind speed, the median of references relative to the reference, reaching over 1.1°C, for wind speeds of 9m/s.

For sun elevations above 45°, the screen became progressively warmer with the increase in wind speed, but the warming gradient was at or below that for sun elevations between 10° and 45°.

## COMBINED EFFECT OF WIND AND GLOBAL RADIATION

The medians of differences between VROT1 and VEIG22 are represented here with a contour plot. The global radiation values are on the X-axis and on the Y axis is the 2-meter wind speed value (2-minute average). Medians are used in all cases, providing that at least one data is available for both conditions on radiation and wind considered.

Screen #1:

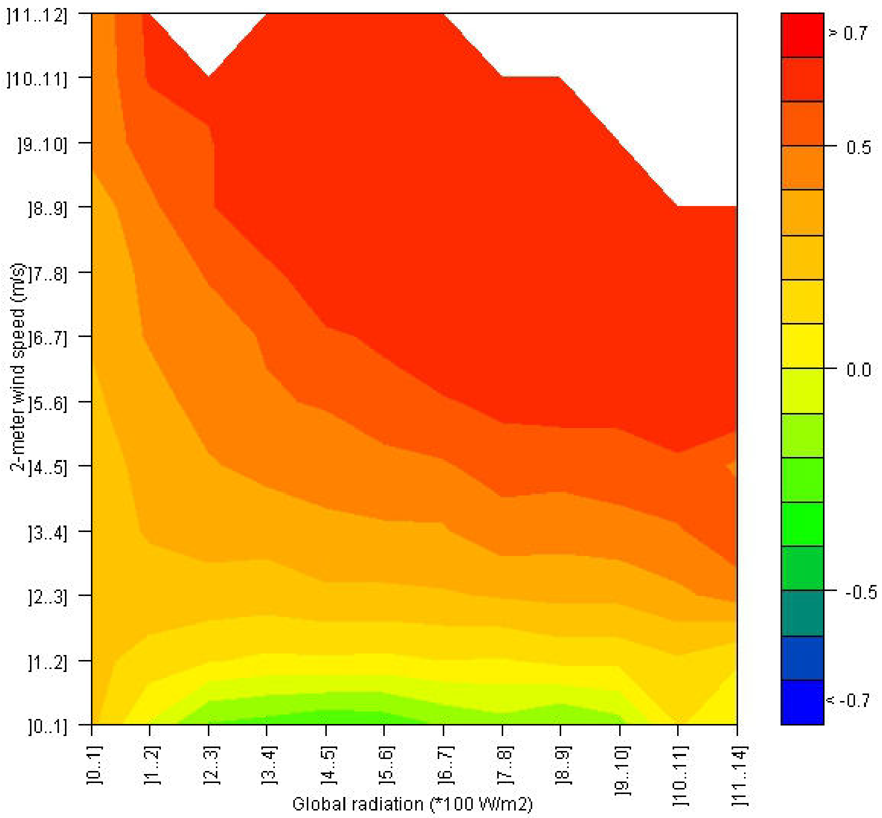


**Figure 9**

The graph indicates that the screen VROT #1 was increasingly warmer than the reference when the wind speed increased, for all values of global radiation.

For calm winds the screen was slightly colder than the reference, independent of the value of irradiance.

## BEHAVIOUR DURING INCREASE/DECREASE OF TEMPERATURE

The distribution of differences between VROT1 and the reference VEIG22 is plotted, using 1-minute quality checked data for the whole period of the intercomparison. Differences are classified according the temporal gradient of reference temperature over 1 minute. A screen faster (or slower, respectively) than the reference would be warmer (cooler) for positive gradient, cooler (warmer) for negative ones.

Screen #1:

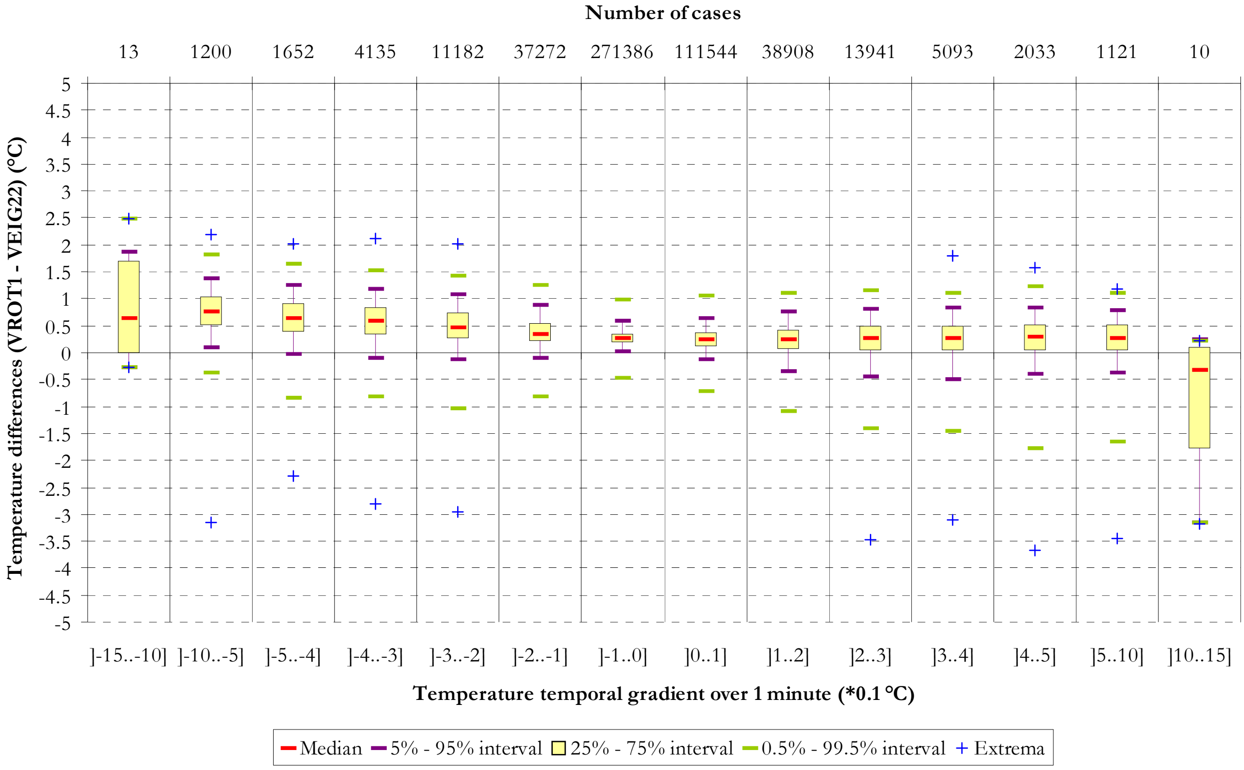


**Figure 10**

The VROT screen #1 was warmer than the reference for all temperature gradients. The median of the differences was closest to zero for temperature gradients of -0.1°C and above, essentially remaining constant for positive gradients.

For negative gradients, the median of the temperature differences increased in value with the increase of the absolute gradient, indicating that the screen #1 was slower than the reference when the temperature was decreasing.

The dispersion of the temperature differences increases with the increase of the absolute temperature temporal gradient, 90% of the data covering an interval of less than 1.5°C.

For temperature temporal gradient of +/-1.5°C, the number of data points is insufficient to draw an overarching conclusion.

## QUALITY CONTROL INFORMATION

### DATA AVAILABILITY

The intercomparison period extends from the 1st of November 2008 to the 1st of November 2009. The theoretical number of 1-minute data is 525600.

The next table sums up the total number of data for each screen and for each possible QC flag.

**Table 3**

| **QC flag** | VROT**1** | VROT**2** |
|---|---|---|
| 0 (good) | 500386 | 237862 |
| 1 (inconsistent) | 0 | 0 |
| 2 (doubtful) | 5 | 4547 |
| 3 (erroneous) | 3579 | 259082 |
| 7 (missing) | 21630 | 24109 |

### MAINTENANCE

On the 29th of September, 2009, both sensors were removed and the fan was cleaned. Before the operation, the ventilation was good for VROT1, medium for VROT2. After the operation, it was better.

# 07755 DAVIS
# – USA –
# VDAV

## TECHNICAL SPECIFICATIONS (PROVIDED BY THE MANUFACTURER)

Dimensions: Length 24 cm x Width 22 cm x Height 23 cm

Weight: 2 kg

Material/Structure: plastic

Estimated radiation error: 1°C

Aspiration rate (in case of artificially ventilated screen/shield): 1.2 m/s

Power supply: Solar power

**Figure 1**

## OVERVIEW

Both screens are very close to each other for all temperature classes, and the differences between the screens do not appear to depend on the variation in temperature.

The plots show similar a behaviour for both screens, slightly skewed to the right (warmer than the reference), with the highest frequency of differences (about 25%) just below the reference values.

The two screens behave relatively similar in terms of cumulated frequency of T, but differently in terms of Tn and Tx. In terms of Tn, screen #1 appears to be colder than the reference, well equilibrated for T and warmer than the reference for Tx for about 70% of data points. Screen #2 is colder than the reference for Tn, in about 85% of cases and for T, in about 75% of cases. For Tx, it is warmer than the reference in close to 90% of cases. The reporting of T and Tx is relatively similar from screen #1, but warmer than the reference to a larger degree for Tx than the T, from screen #2.

Both screens are affected by the variation in global radiation. As global radiation increases, both screens get warmer than the reference, with as much as 0.5°C for screen #1 and 0.7°C for screen #2. The dispersions of both screens also increase as the global radiation increases.

During the day-time, the screens are colder than the reference and than during the nigh-time, for calm wind conditions, but warmer for winds above that. Under clear sky, the screens become warmer than during overcast conditions, as the wind speed increases. The exception is the performance at low wind speeds when the screens are colder during clear sky than during overcast conditions, as well as colder than the reference.

During the night-time, clear-sky and overcast medians of both screens are relatively un-affected by the variation in wind speed. The general behaviour shows a slightly colder screen under clear sky conditions.

Both screens display a similar performance under overcast conditions, during the day-time as well as at night, while the clear sky behaviour is significantly dependent on the wind conditions during the day time, as opposed to the night time.

Overall, the two screens are colder than the reference for winds below 2m/s, for all sun elevations and warmer above that, being the warmest for sun elevations from 10° to 45°.

The contour plots show that the increase of wind and of the irradiance causes the screens to become increasingly warmer than the reference.

Both screens are warmer (slower) than the reference for the cases when the temperature decreases and warmer (faster) than the reference when the temperature raises. The dependency on the temperature gradient is more significant for negative temperature gradients.

## CALIBRATION INFORMATION

The calibration of both probes was performed in Trappes.

**Table 1**

| Screen | Location | Pt100 probe serial number | Calibration date | Instrument bias (°C) | | | |
|---|---|---|---|---|---|---|---|
| | | | | -20°C | 0°C | 20°C | 40°C |
| VDAV1 | D6 | 772 | 6-Jan-2006 | 0.0827 | 0.0544 | 0.0299 | 0.0087 |
| VDAV2 | F3 | 728 | 10-Jan-2006 | 0.1022 | 0.0756 | 0.0522 | 0.0216 |

The result of the calibration of the reference VEIG22 is available in the main report of the intercomparison, section 5.4.1.

## COMPARISON OF BOTH SENSORS

The distribution of differences between screen 1 and screen 2 is plotted, using 1-minute quality checked data for the whole period of the intercomparison. Differences are classified according screen 1 temperature.

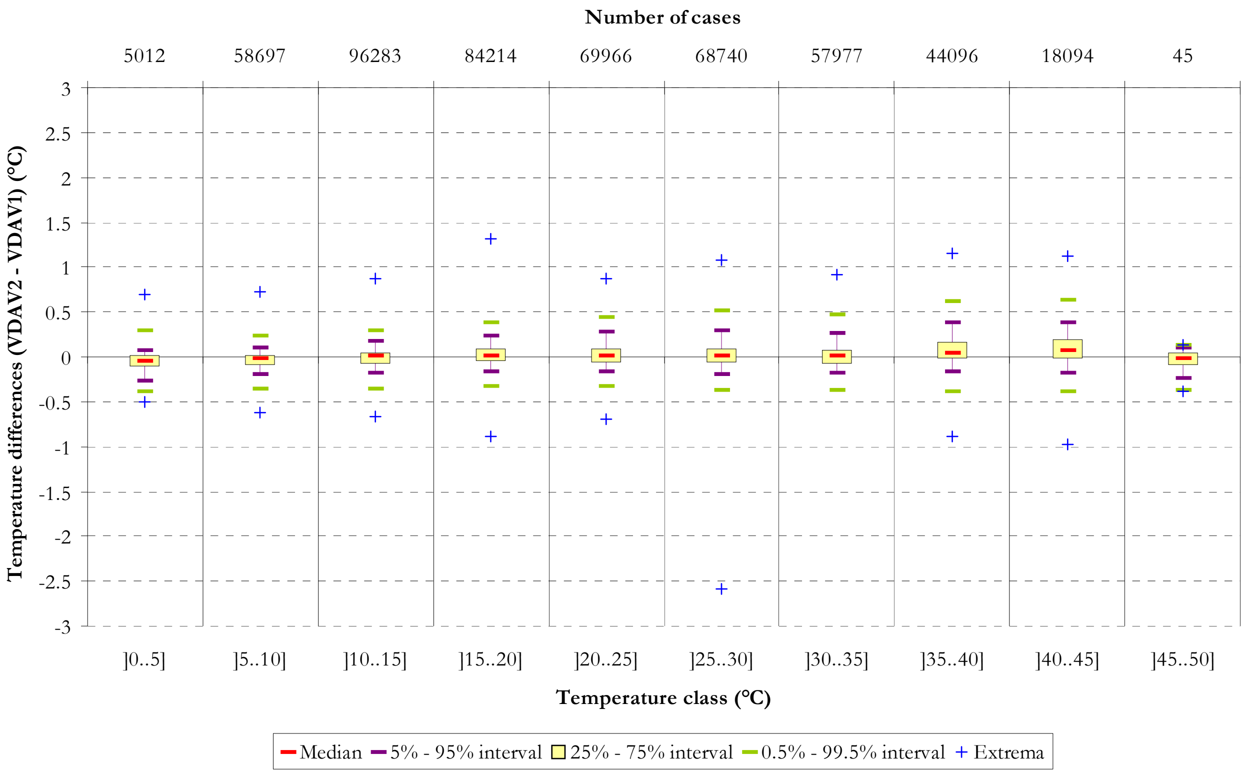


**Figure 2**

Both screens are very close to each other for all temperature classes, and the differences between the screens do not appear to depend on the variation in temperature.

## COMPARISON WITH THE REFERENCE

### HISTOGRAM OF DIFFERENCES

The histogram of differences between VDAV and the reference VEIG22 is plotted, using 1-minute quality checked data for the whole period of the intercomparison. Differences are plotted by steps of 0.1K. The vertical axis is the frequency in percent for each class of differences.

Screen #1:

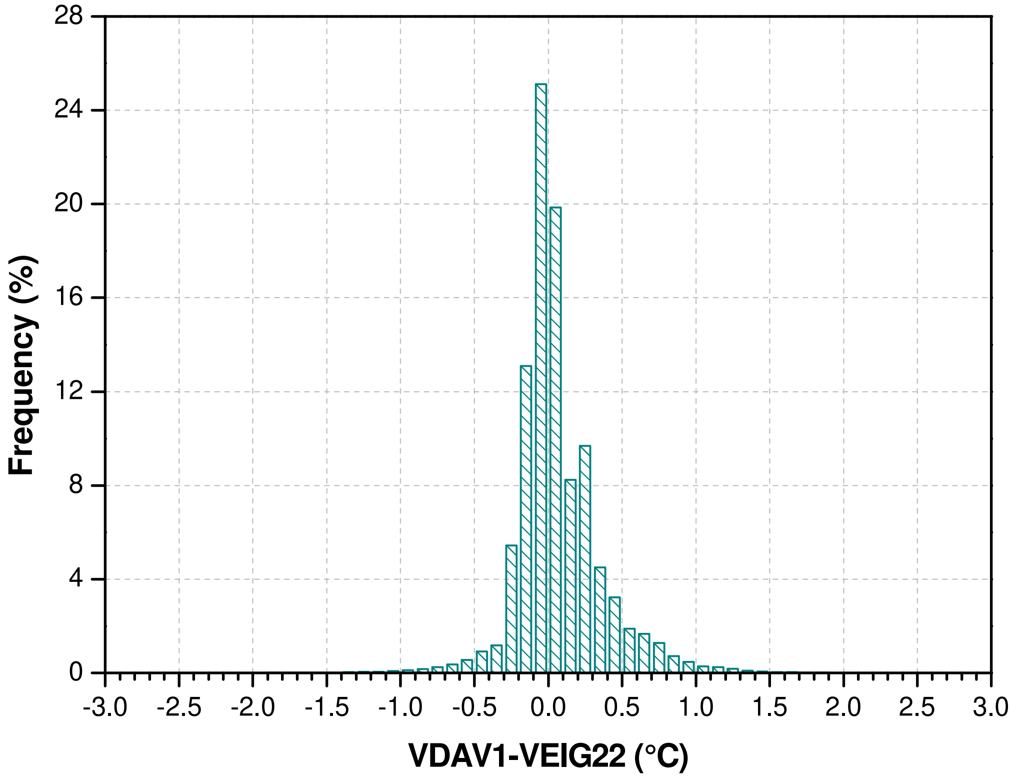


**Figure 3**

Screen #2:

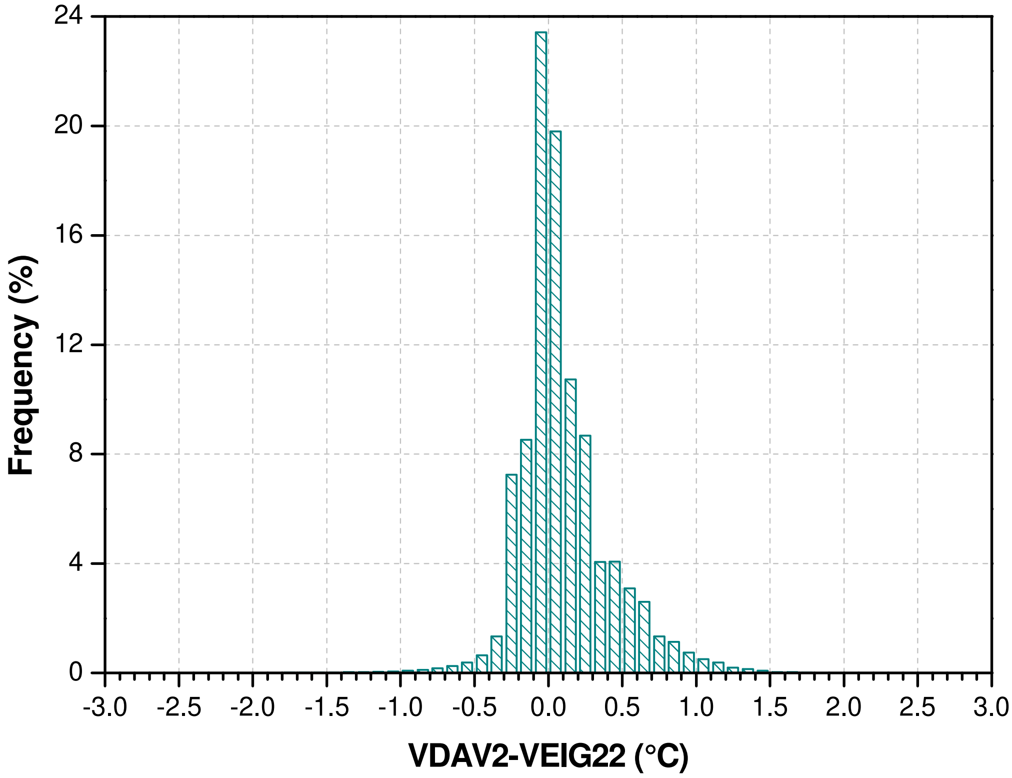


**Figure 4**

The plots show similar a behaviour for both screens, slightly skewed to the right (warmer than the reference), with the highest frequency of differences (about 25%) just below the reference values.

CUMULATIVE HISTOGRAMS OF DIFFERENCES OF DAILY EXTREME VALUES

The cumulative histograms of differences with the reference VEIG22 of T (1-minute quality checked data), Tn (daily minimum temperature) and Tx (daily maximum temperature) are plotted, for the whole period of the intercomparison. Differences are plotted by steps of 0.1K.

Screen #1:

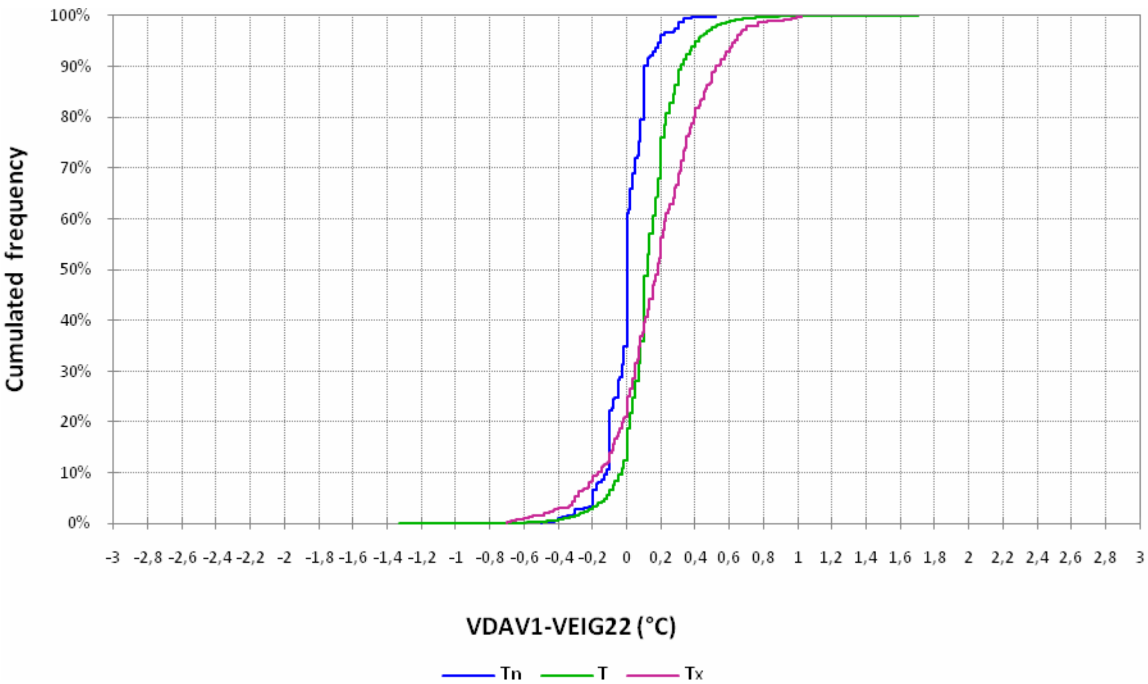


**Figure 5**

Screen #2 :

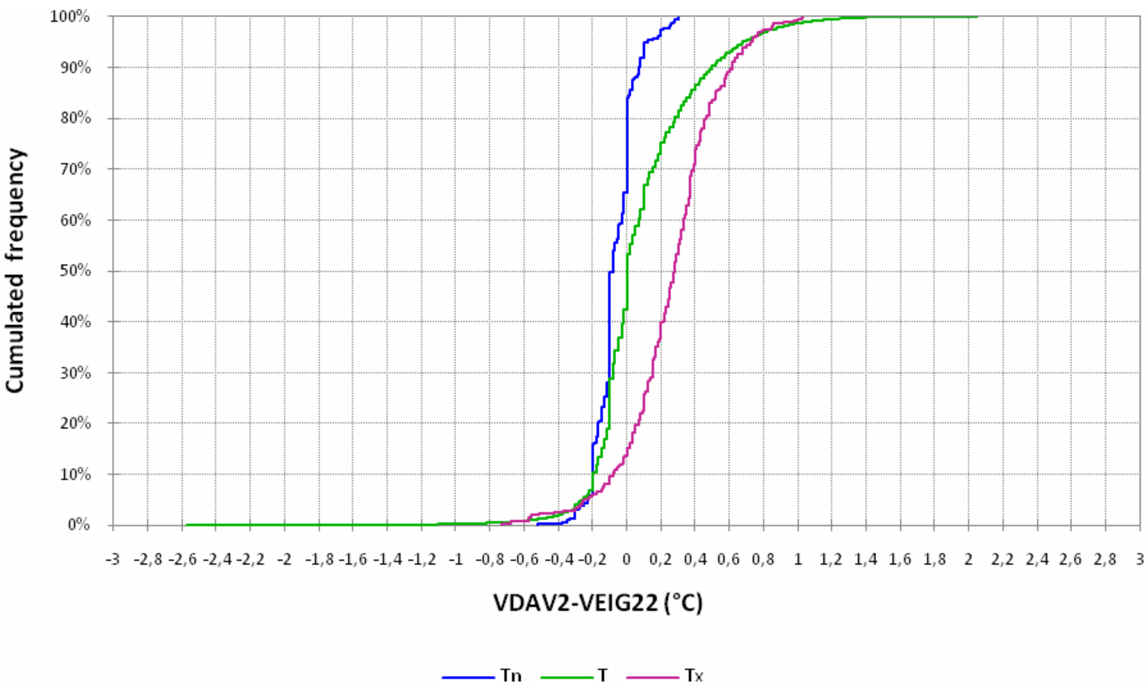


**Figure 6**

The two screens behave relatively similar in terms of cumulated frequency of T, but differently in terms of Tn and Tx.

In terms of Tn, screen #1 appears to be colder than the reference, well equilibrated for T and warmer than the reference for Tx for about 70% of data points.

Screen #2 is colder than the reference for Tn, in about 85% of cases and for T, in about 75% of cases. For Tx, it is warmer than the reference in close to 90% of cases. The reporting of T and Tx is relatively similar from screen #1, but warmer than the reference to a larger degree for Tx than the T, from screen #2.

TABLE

The table 2 indicates the percentage of data that differ by less than 0.2°C (and 0.5°C) from the reference.

**Table 2**

| | | [-0.2°..0.2°] | [-0.5°..0.5°] |
|---|---|---|---|
| VDAV1 | T | 71.5 | 91.4 |
| | Tn | 91.9 | 0.3 |
| | Tx | 46.3 | 87.3 |
| VDAV2 | T | 68.4 | 89.2 |
| | Tn | 89.4 | 99.7 |
| | Tx | 32.8 | 81.4 |

## INFLUENCE OF GLOBAL RADIATION

The distribution of differences between VDAV and the reference VEIG22 is plotted, using 1-minute quality checked data for the whole period of the intercomparison. Differences are classified according global radiation.

<u>Screen #1:</u>

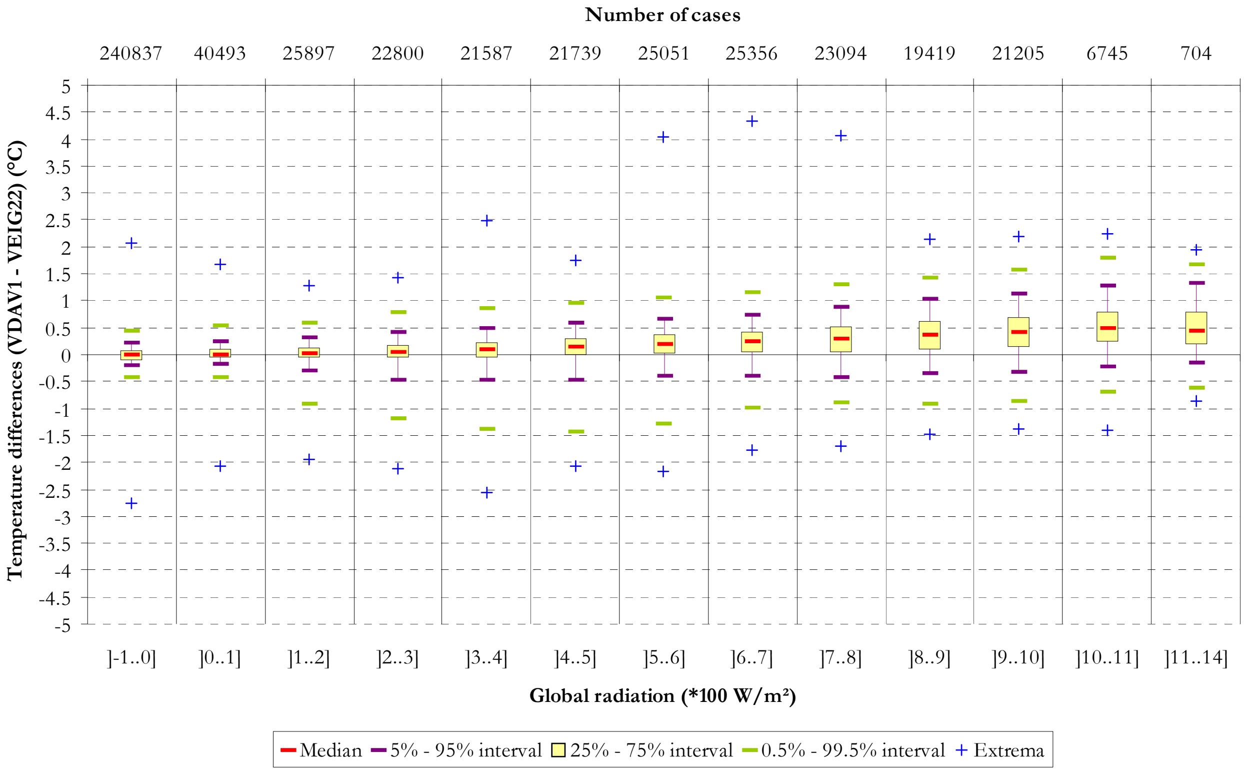


**Figure 7**

Screen #2:

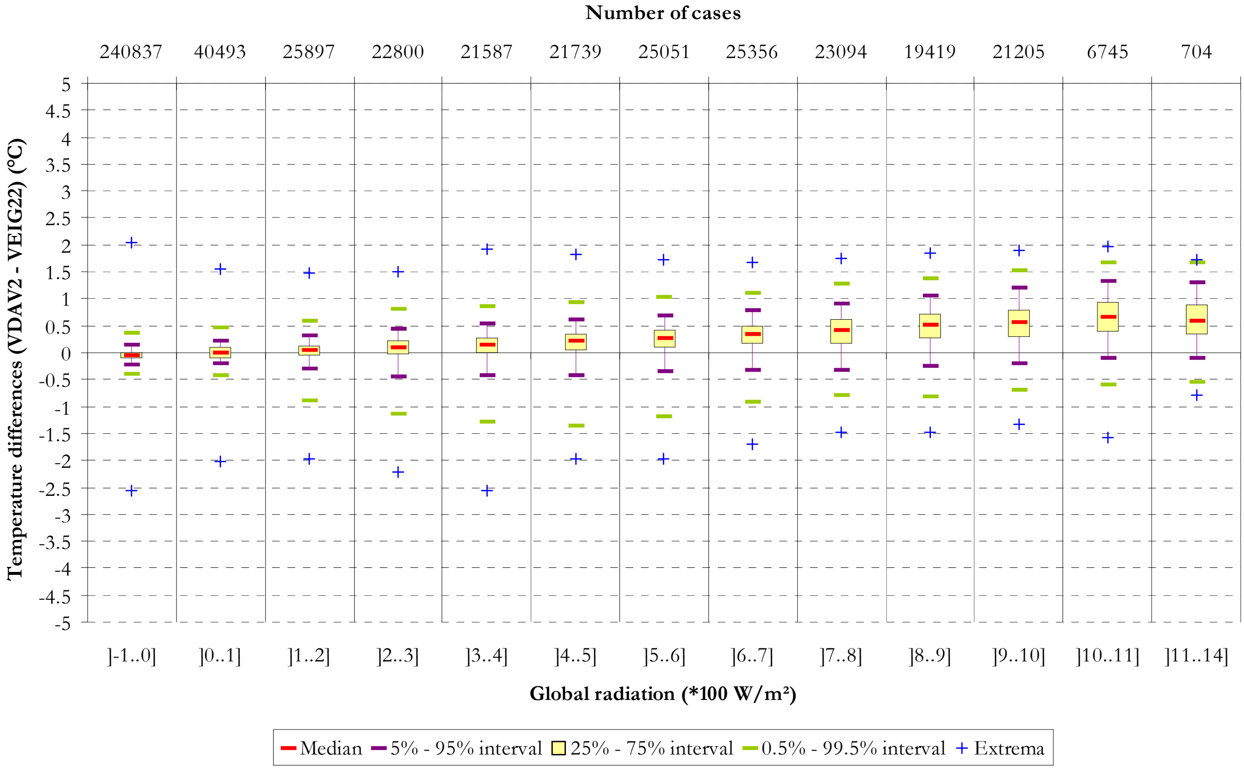


**Figure 8**

Both screens are affected by the variation in global radiation. As global radiation increases, both screens get warmer than the reference, with as much as 0.5°C for screen #1 and 0.7°C for screen #2. The dispersions of both screens also increase as the global radiation increases.

## RADIATION EFFECT

### DIFFERENCES BETWEEN DAY AND NIGHT BEHAVIOUR

The median of differences between VDAV and VEIG22 is plotted, using 1-minute quality checked data for the whole period of the intercomparison. We filter data for which sun elevation is above -1° (day) or below -1° (night). Differences are classified according 2-meter wind speed (2-minute average).

Screen #1:

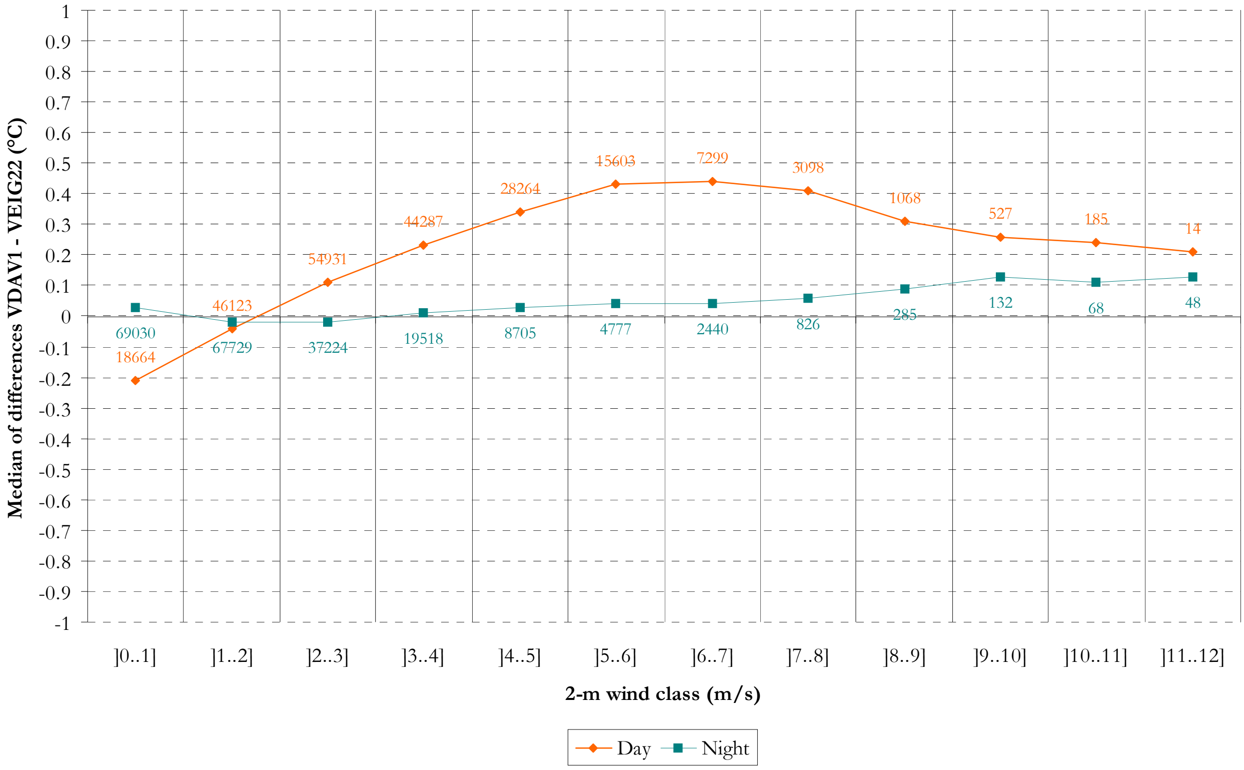


**Figure 9**

Screen #2:

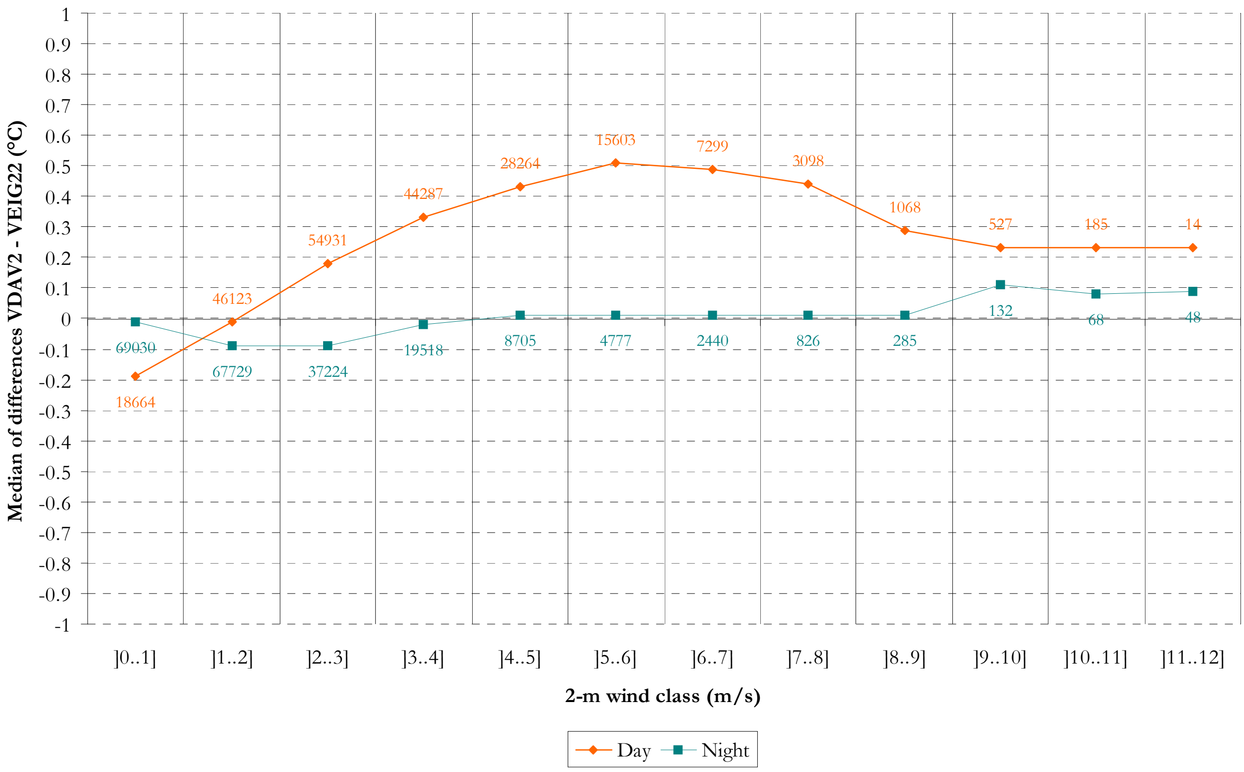


**Figure 10**

The night-time medians of the differences of both screens vary slightly with the wind speed, but stay within ±0.1°C of the origin. The general tendency is for both VDAV screens to become warmer as the wind speed increases.

The daytime medians of both screens are significant different from those of night-time; they can be as much as 0.5°C. At low wind speed, the medians of both screens are about -0.2°C. As the wind speed increases, the medians of both screens reach a peak of about 0.5°C at wind speed about 6 m/s, and then decrease and level off to about 0.2°C for wind speeds above that.

Overall, during the day-time, the screens are colder than the reference and than during the nigh-time, for calm wind conditions, but warmer for winds above that.

## DIFFERENCES BETWEEN CLEAR SKY AND OVERCAST SKY DURING DAYTIME

The median of differences between VDAV and VEIG22 is plotted, using 1-minute quality checked data. Here, we consider periods lasting six hours at least where cloudiness is less or equal to 1 (clear sky) or more or equal to 7 (overcast sky), during daytime (sun elevation above -1°). Differences are classified according 2-meter wind speed (2-minute average).

<u>Screen #1:</u>

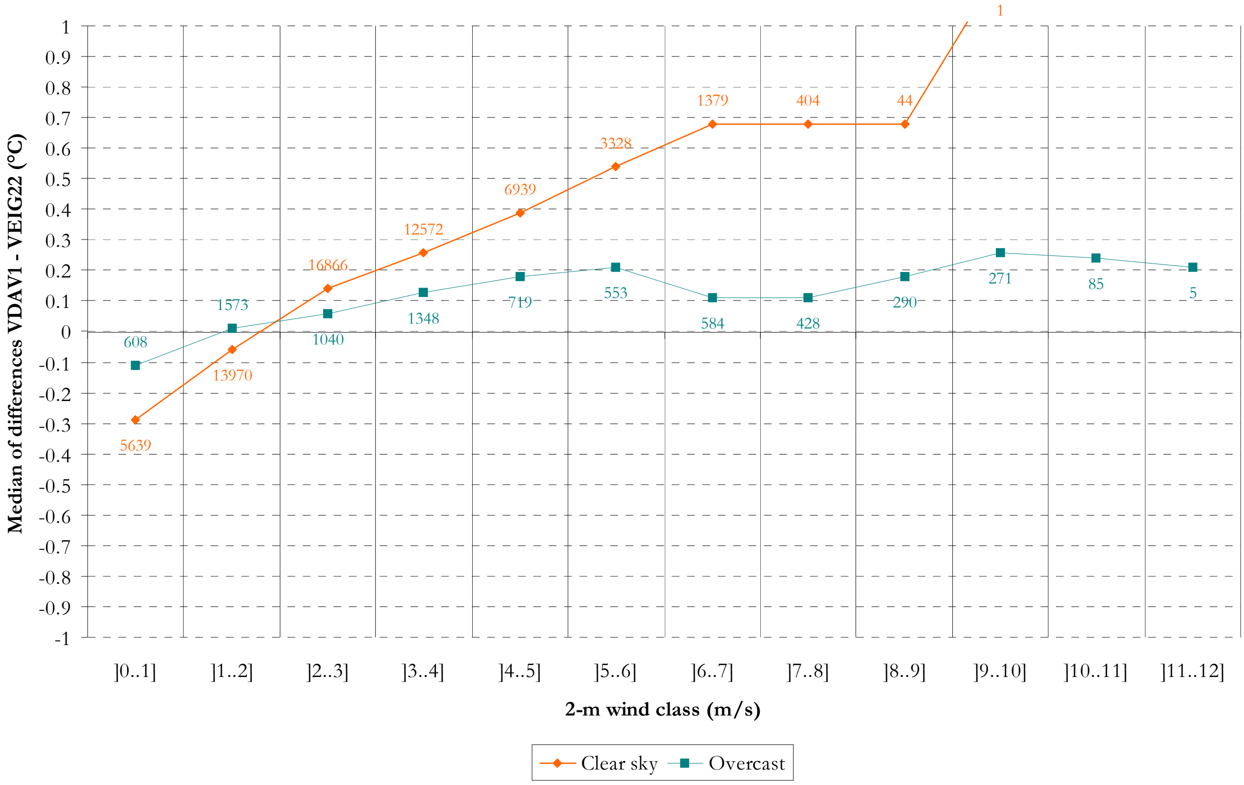


**Figure 11**

Screen #2:

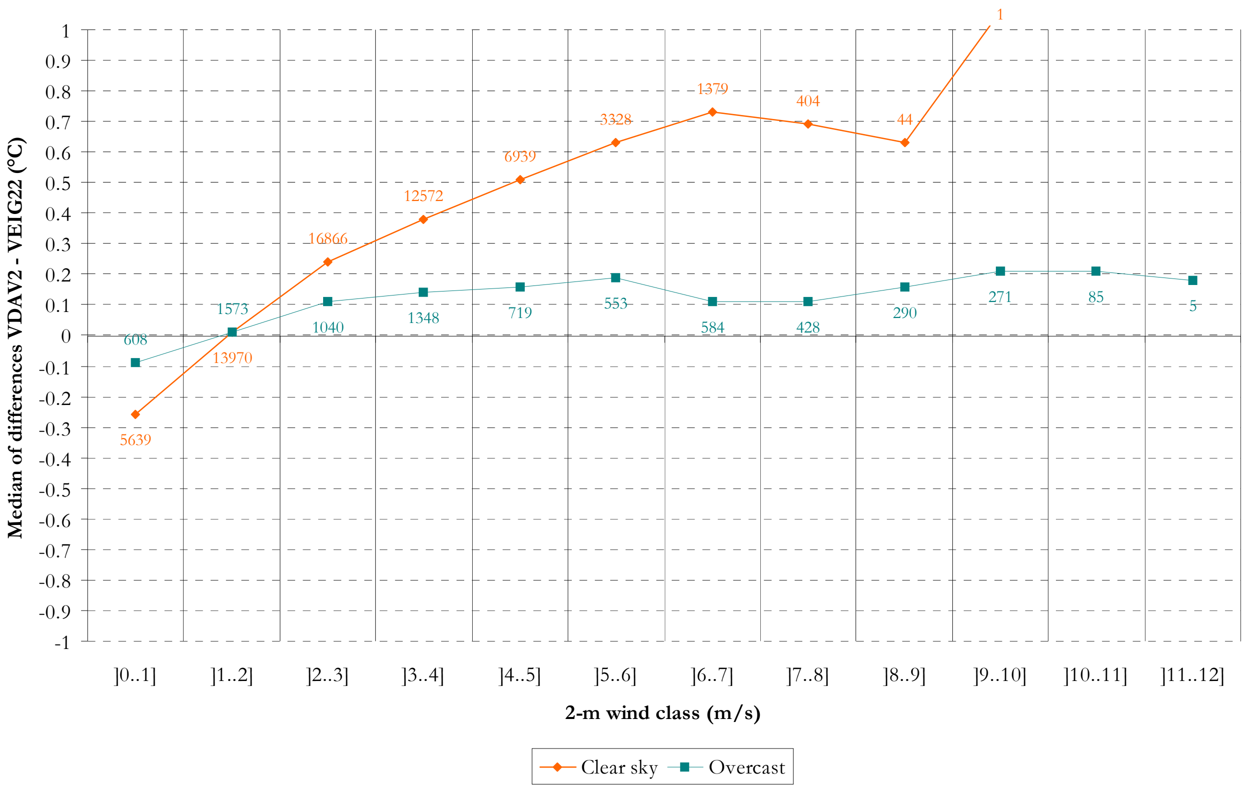


**Figure 12**

The overcast medians of both screens stay within about 0.2°C of the reference, and they increase slightly and then level off as the wind speed increases. On the other hand, the clear-sky medians of both screens increase more rapidly, to a maximum of about 0.7°C, as the wind increases.

Overall, under clear sky, the screens become warmer than during overcast conditions, as the wind speed increases. The exception is the performance at low wind speeds when the screens are colder during clear sky than during overcast conditions, as well as colder than the reference.

## DIFFERENCES BETWEEN CLEAR SKY AND OVERCAST SKY DURING NIGHT TIME

The median of differences between VDAV and VEIG22 is plotted, using 1-minute quality checked data. Here, we consider periods lasting six hours at least where cloudiness is less or equal to 1 (clear sky) or more or equal to 7 (overcast sky), during night time (sun elevation below -1°). Differences are classified according 2-meter wind speed (2-minute average).

Screen #1:

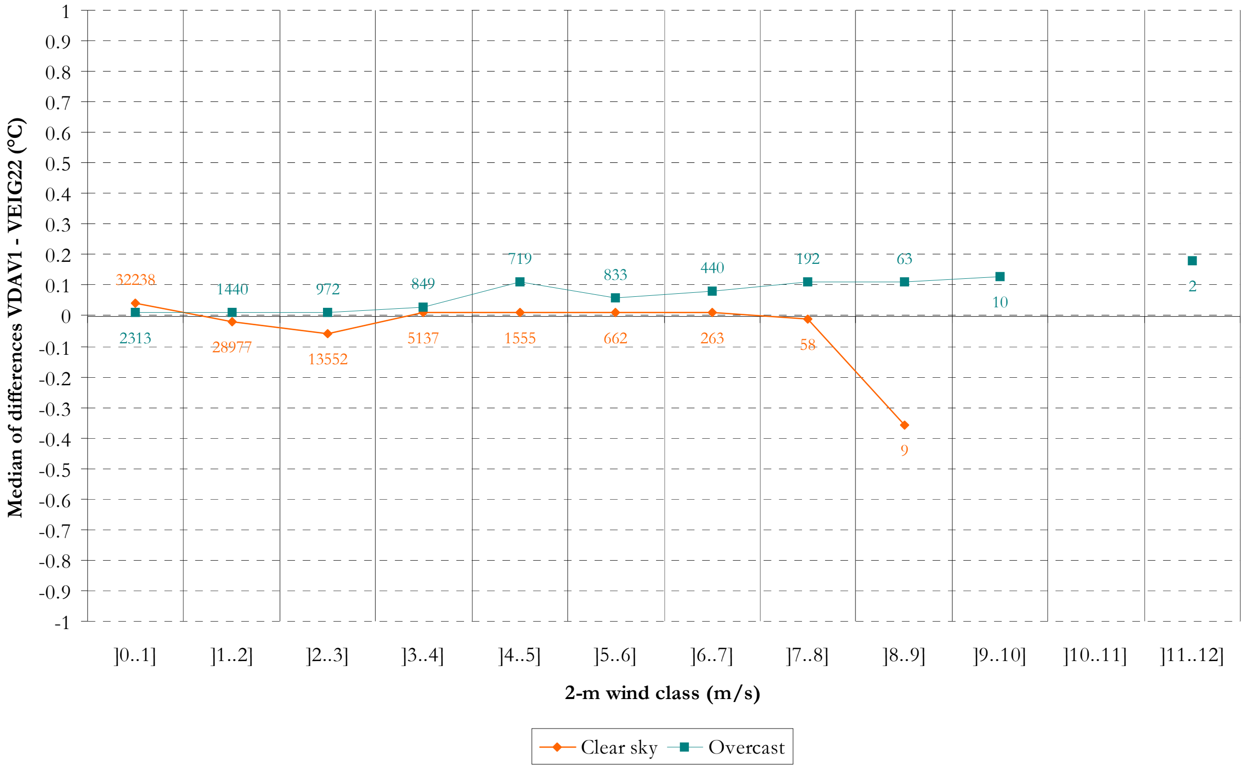


**Figure 13**

Screen #2:

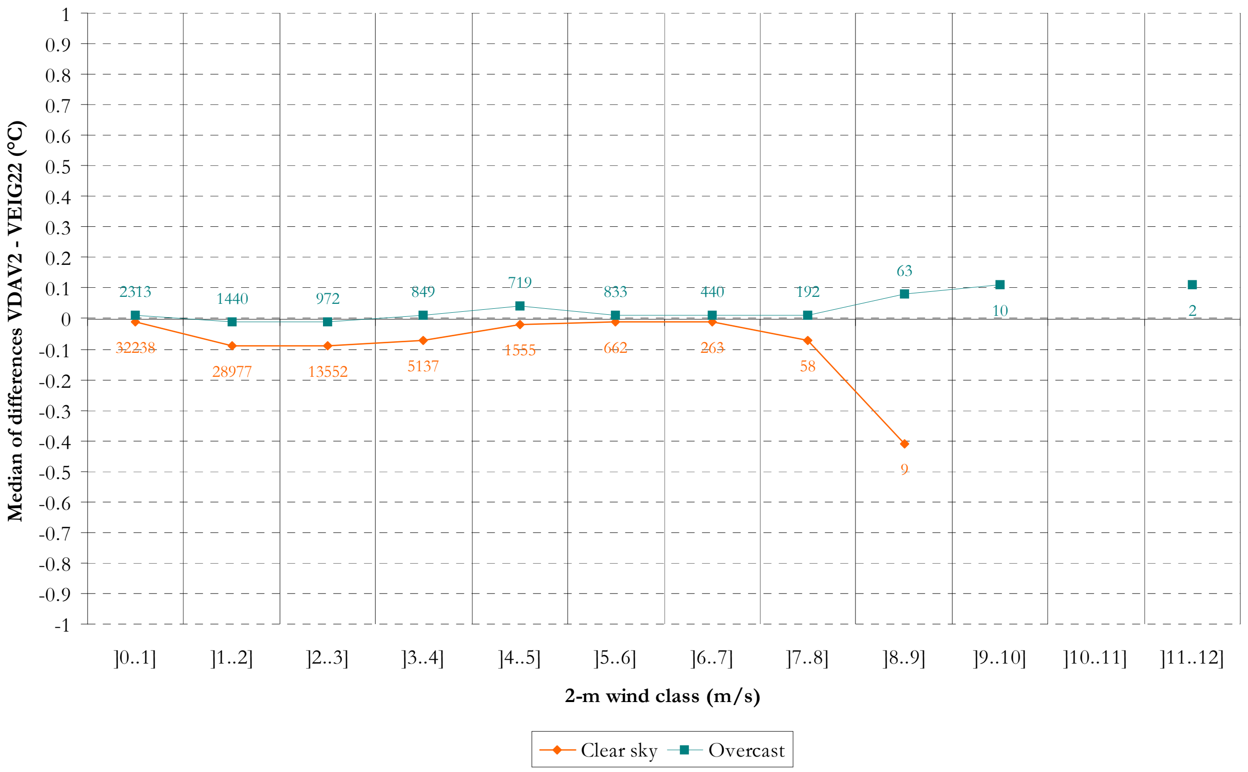


**Figure 14**

Ignoring classes with small number of data points, the night-time, clear-sky and overcast medians of both screens stay with 0.1°C of the origin, and are relatively un-affected by the variation in wind speed. The general behaviour shows a slightly colder screen under clear sky conditions.

Both screens display a similar performance under overcast conditions, during the day-time as well as at night, while the clear sky behaviour is significantly dependent on the wind conditions during the day time, as opposed to the night time.

## EFFECT OF SUN ELEVATION

The median of differences between VDAV and VEIG22 is plotted, using 1-minute quality checked data. Here, we consider periods lasting six hours at least where cloudiness is less or equal to 1 (clear sky), during daytime (sun elevation above -1°). We filter data where sun elevation is low (below 10°), medium (between 10° and 45°) or high (above 45°). Differences are classified according 2-meter wind speed (2-minute average).

Screen #1:

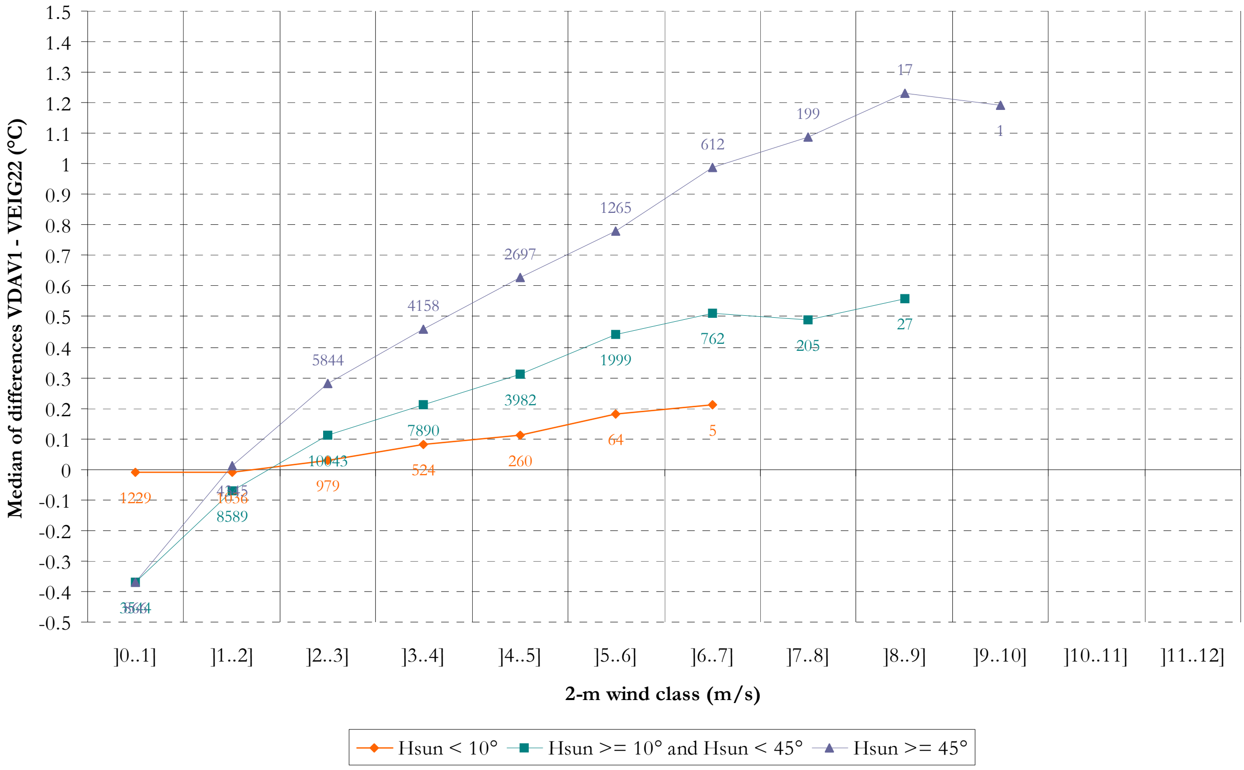


**Figure 15**

Screen #2:

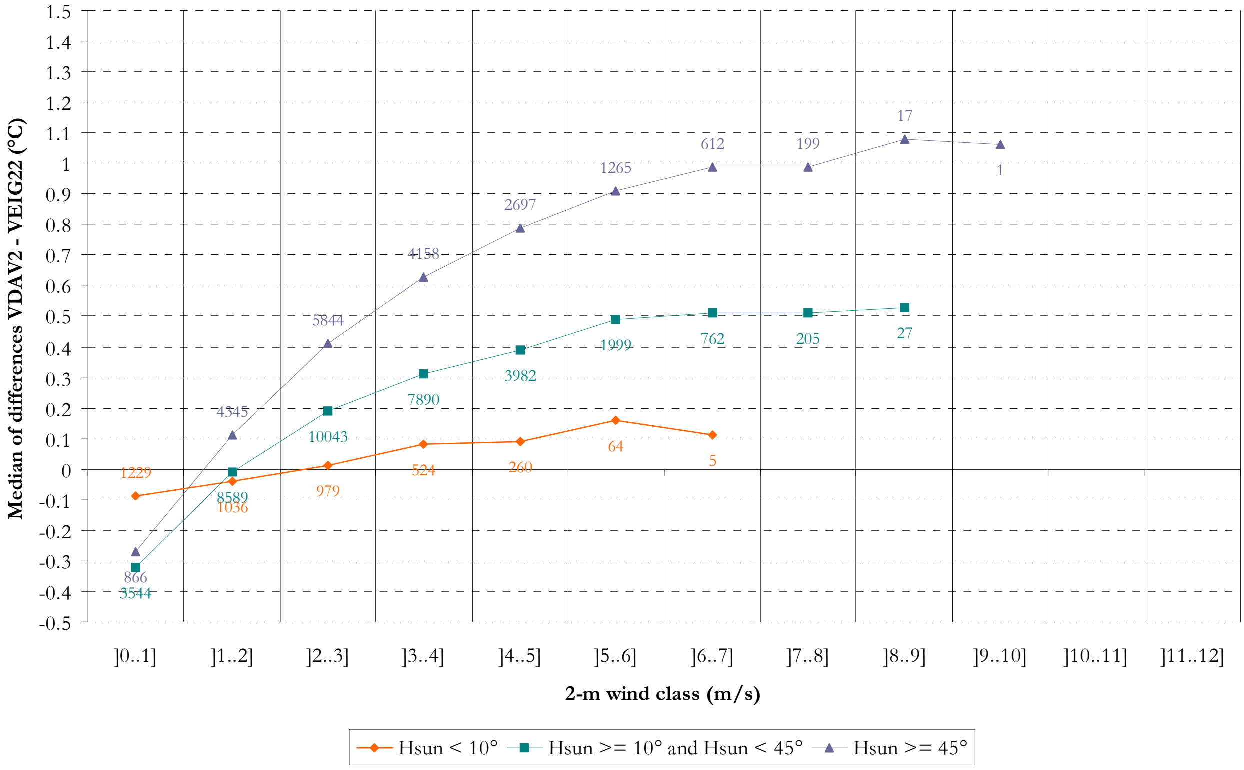


**Figure 16**

The medians of both screens with sun elevation less than 10° are within 0.1°C of the origin at low wind speed. As the wind speed increases, the medians of both screens increase to as much as 0.2°C.

The medians of both screens with sun elevation between 10° and 45°, and greater than 45° are all about -0.3°C to -0.4°C at low wind speed. They also increase as the wind speed increases, but at more rapid rates than the medians with sun elevation less than 10°, and with medians with sun elevation greater than 45° increasing most rapidly. The medians level off at high wind, approximately 8 m/s, to about 0.5°C for sun elevation between 10° and 45°, and to about 1.2°C for elevation greater than 45°.

Overall, the two screens are colder than the reference for winds below 2m/s, for all sun elevations and warmer above that, being the warmest for sun elevations from 10o to 45o.

## COMBINED EFFECT OF WIND AND GLOBAL RADIATION

The medians of differences between VDAV and VEIG22 are represented here with a contour plot. The global radiation values are on the X-axis and on the Y axis is the 2-meter wind speed value (2-minute average). Medians are used in all cases, providing that at least one data is available for both conditions on radiation and wind considered.

Screen #1:

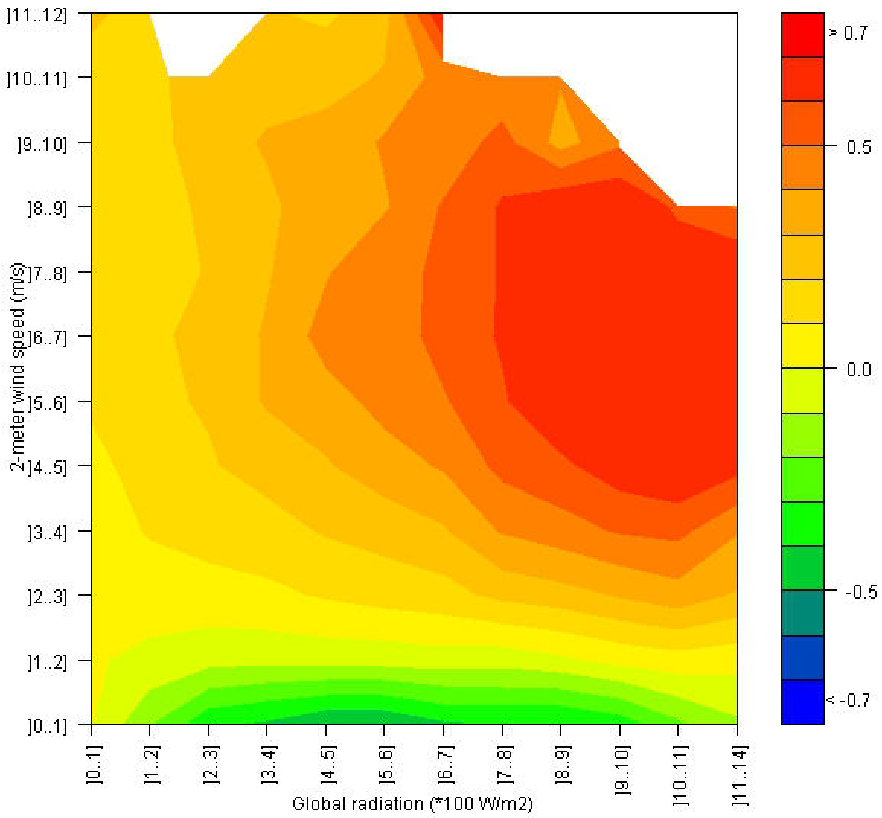


**Figure 17**

Screen #2:

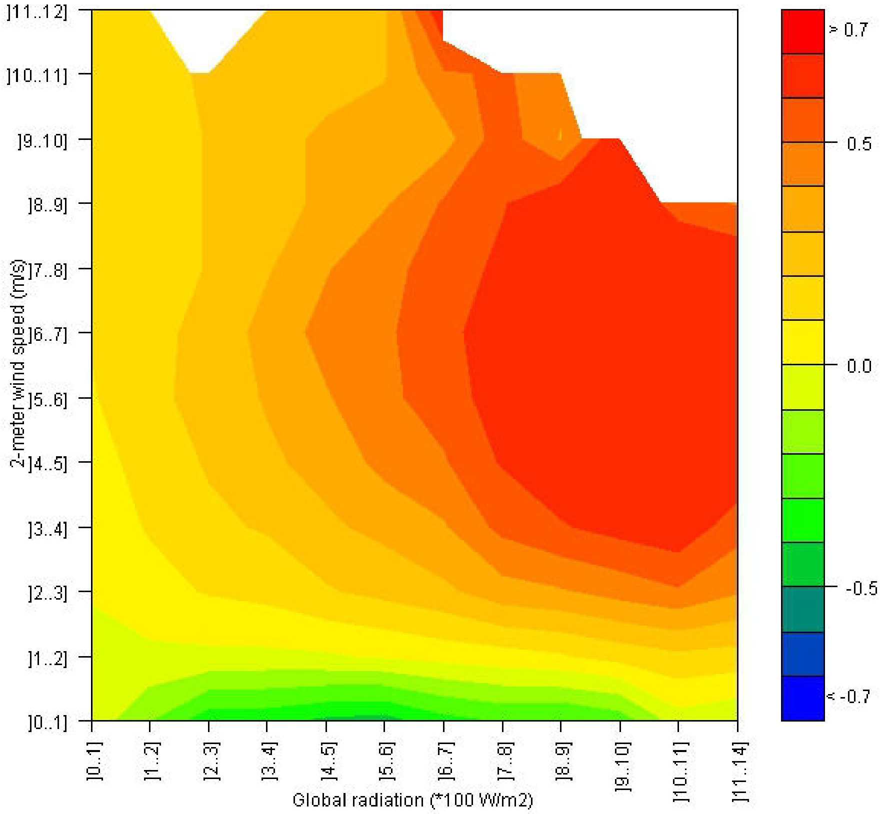


**Figure 18**

The contour plots of both screens are similar, with maximum (median of difference greater than 0.7°C) at high global radiations (greater than 800 W/m$^2$) and medium wind speeds (between about 4 m/s and 8 m/s), and with minimum (median of difference about -0.3°C to -0.4°C) at low wind speed (less than 1 m/s) and medium global radiation (between about 400W/m$^2$ and 700W/m$^2$).

Overall, the increase of wind and of the irradiance causes the screens to become increasingly warmer than the reference.

## BEHAVIOUR DURING INCREASE/DECREASE OF TEMPERATURE

The distribution of differences between VDAV and the reference VEIG22 is plotted, using 1-minute quality checked data for the whole period of the intercomparison. Differences are classified according the temporal gradient of reference temperature over 1 minute. A screen faster (or slower, respectively) than the reference would be warmer (cooler) for positive gradient, cooler (warmer) for negative ones.

Screen #1:

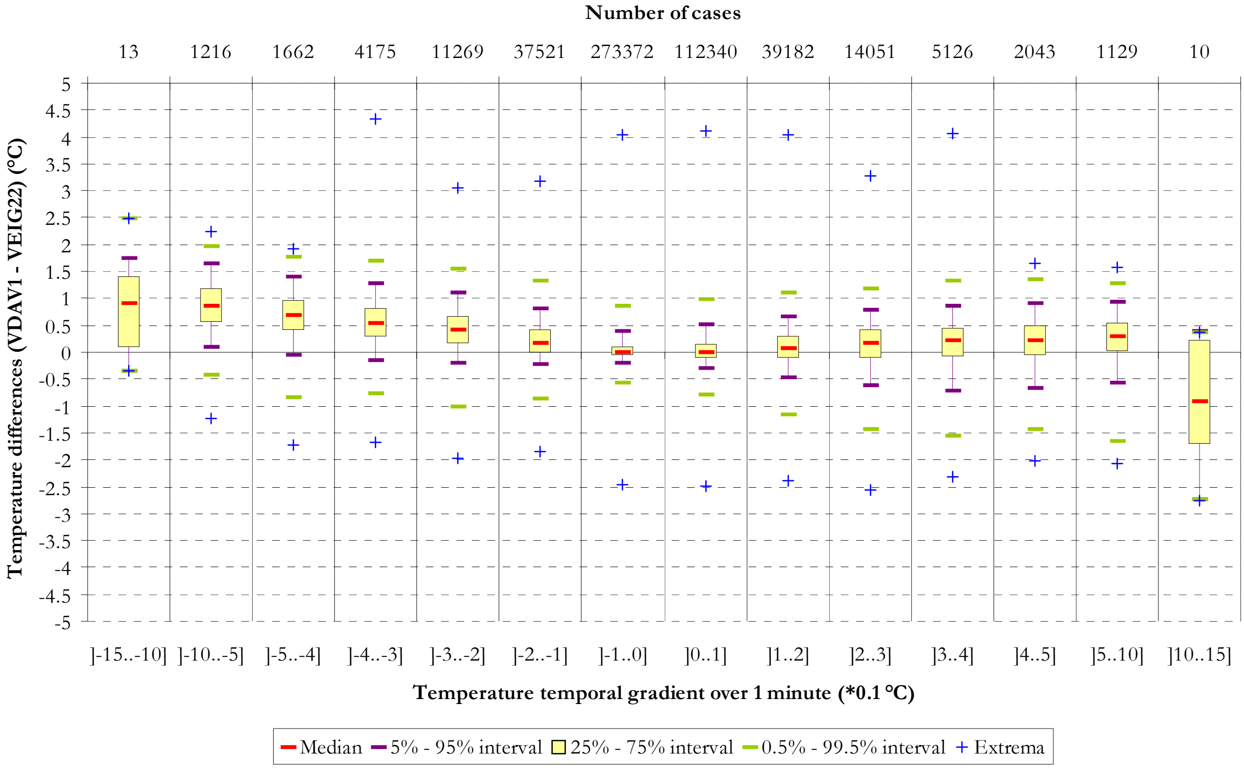


**Figure 19**

Screen #2:

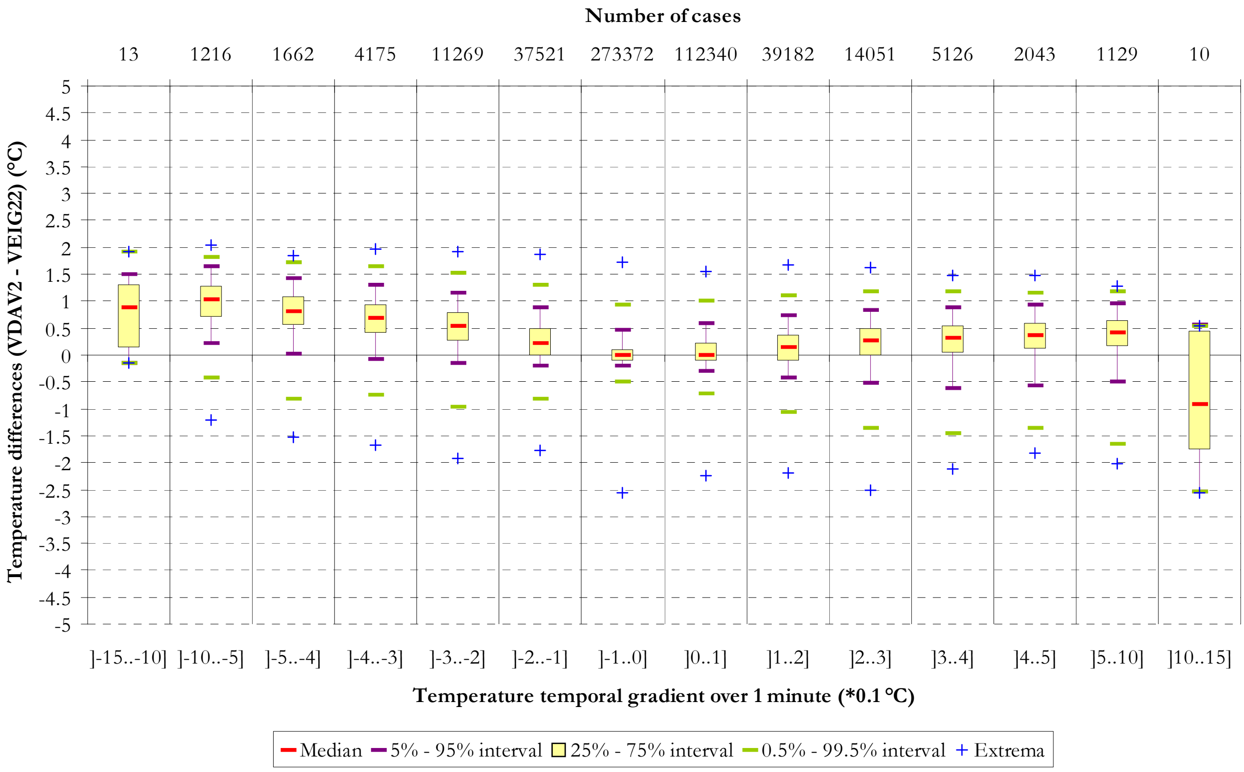


**Figure 20**

Ignoring the gradient classes with about 10 data points the medians of both screens increase, as the absolute gradients increase, and they are 0°C when the gradients are zero. The dispersions of both screens also increase as the absolute gradients increase.

Both screens are warmer (slower) than the reference for the cases when the temperature decreases and warmer (faster) than the reference when the temperature raises. The dependency on the temperature gradient is more significant for negative temperature gradients.

## QUALITY CONTROL INFORMATION

DATA AVAILABILITY

The intercomparison period extends from the 1st of November 2008 to the 1st of November 2009. The theoretical number of 1-minute data is 525600.

The next table sums up the total number of data for each screen and for each possible QC flag.

**Table 3**

| **QC flag** | VDAV1 | VDAV2 |
|---|---|---|
| 0 (good) | 503266 | 503266 |
| 1 (inconsistent) | 0 | 0 |
| 2 (doubtful) | 0 | 0 |
| 3 (erroneous) | 0 | 0 |
| 7 (missing) | 22334 | 22334 |

MAINTENANCE

Solar panels were cleaned once per month.

On the 30th of September, 2009, both sensors were removed and the fan was cleaned. Before the operation, the ventilation was good. After the operation, it was even better.

# 43502 YOUNG COMPANY
# – USA –
# VYOU

## TECHNICAL SPECIFICATIONS (PROVIDED BY THE MANUFACTURER)

Dimensions: Length 34 cm x Width 20 cm x Height 35 cm

Weight: 1.2 kg

Material/Structure: Thermoplastic - Stainless steel - aluminium

Estimated radiation error: 0.2°C

Aspiration rate (in case of artificially ventilated screen/shield): 6.8 to 9.2 m/s

Power supply: 12 V

**Figure 1**

## OVERVIEW

These screens had their artificial ventilation shut off during the intercomparison period. It was repaired at the end of September, 2009. So only one month of valid data is available for the analysis: October, 2009. As no period occurred with overcast conditions (day or night), it was not possible to analyse the effect of cloudiness on this screen.

The two screens demonstrated very similar performance for all temperature classes where data are available. The median of the differences between the temperatures reported by the two VYOU screens is zero or close to zero for all temperature classes.

They also indicate a medium dispersion of the differences between each of the two VYOU screens and the reference, from about -1 °C to above +0.8 °C. The mode of the differences for each of the screens is at about +0.3 °C, with a frequency of more than 24%. The histograms of differences for both screens are skewed to the left. The daily extreme values were reported similarly from both screens. Both for daily minimum and maximum temperature, both screens were warmer than the reference.

The median of the temperature difference is stable, slightly positive for all radiation classes.

Both VYOU screens display similar behaviour during the day and during the night, for all classes of wind speeds. During the day, the screens were colder than the reference for winds below 2m/s. For winds above 2m/s, VYOU screens are warmer than the reference. During the night, the median of the differences from the reference slightly decrease for increasing wind speeds.

For sun elevations below 10°, the screens display a minimum dependency on the wind speed, being 0.1°C to 0.2°C warmer than the reference. For sun elevations above 10°, the screens experienced a warming effect with the increase in wind speed. For wind speeds above 2m/s, the screens were significantly warmer than the reference, and there is a notable dependency of the median of the differences with the wind speed.

Both VYOU screens are influenced significantly by the wind speed for all solar radiation classes. For calm wind conditions and high irradiance the screens are significantly colder than the reference. For all other conditions, the screens are slightly warmer than the reference, and the predominant factor seems to be the wind speed.

For negative temperature temporal gradient, the VYOU screens were slower than the reference. The median of the differences is about 0.5°C and is minimally dependent on the magnitude of the temperature gradient. For constant temperature, or a temperature temporal gradient of magnitude less than 0.1°C, the median of the temperature differences approaches 0.2°C. For positive temperature temporal gradient, the two VYOU screens are as fast as the reference. The median of the temperature differences is around 0.

## CALIBRATION INFORMATION

The calibration of both probes was performed in Trappes.

**Table 1**

| Screen | Location | Pt100 probe serial number | Calibration date | Instrument bias (°C) | | | |
|---|---|---|---|---|---|---|---|
| | | | | -20°C | 0°C | 20°C | 40°C |
| VYOU1 | E1 | T54 | 7-Feb-2006 | 0.0241 | -0.0030 | -0.0189 | -0.0307 |
| VYOU2 | E4 | T55 | 1-Feb-2006 | 0.0157 | -0.0128 | -0.0294 | -0.0435 |

The result of calibration of reference VEIG22 is available in the main report of the intercomparison, section 5.4.1.

## COMPARISON OF BOTH SENSORS

The distribution of differences between screen 1 and screen 2 is plotted, using 1-minute quality checked data for the whole period of the intercomparison. Differences are classified according screen 1 temperature.

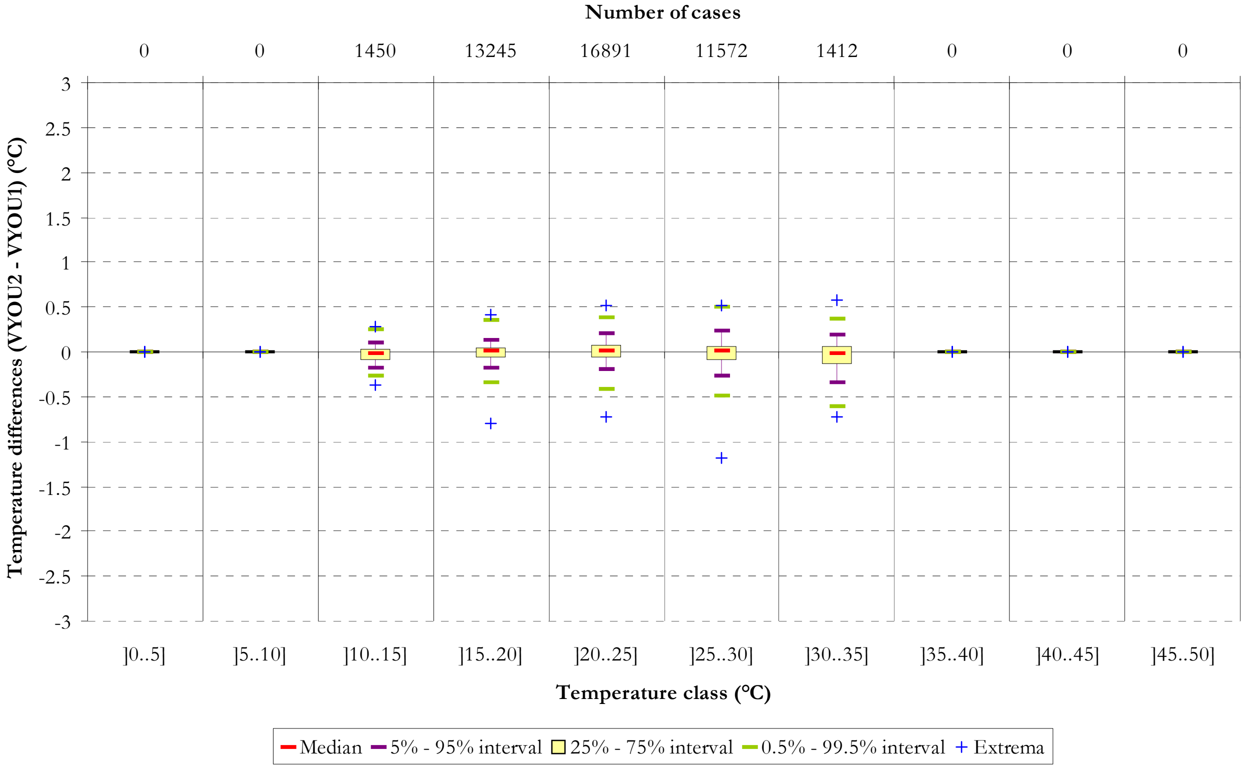


**Figure 2**

The two screens demonstrated very similar performance for all temperature classes where data are available.

The median of the differences between the temperatures reported by the two VYOU screens is zero or close to zero for all temperature classes.

## COMPARISON WITH THE REFERENCE

### HISTOGRAM OF DIFFERENCES

The histogram of differences between VYOU and the reference VEIG22 is plotted, using 1-minute quality checked data for the whole period of the intercomparison. Differences are plotted by steps of 0.1K. The vertical axis is the frequency in percent for each class of differences.

Screen #1:

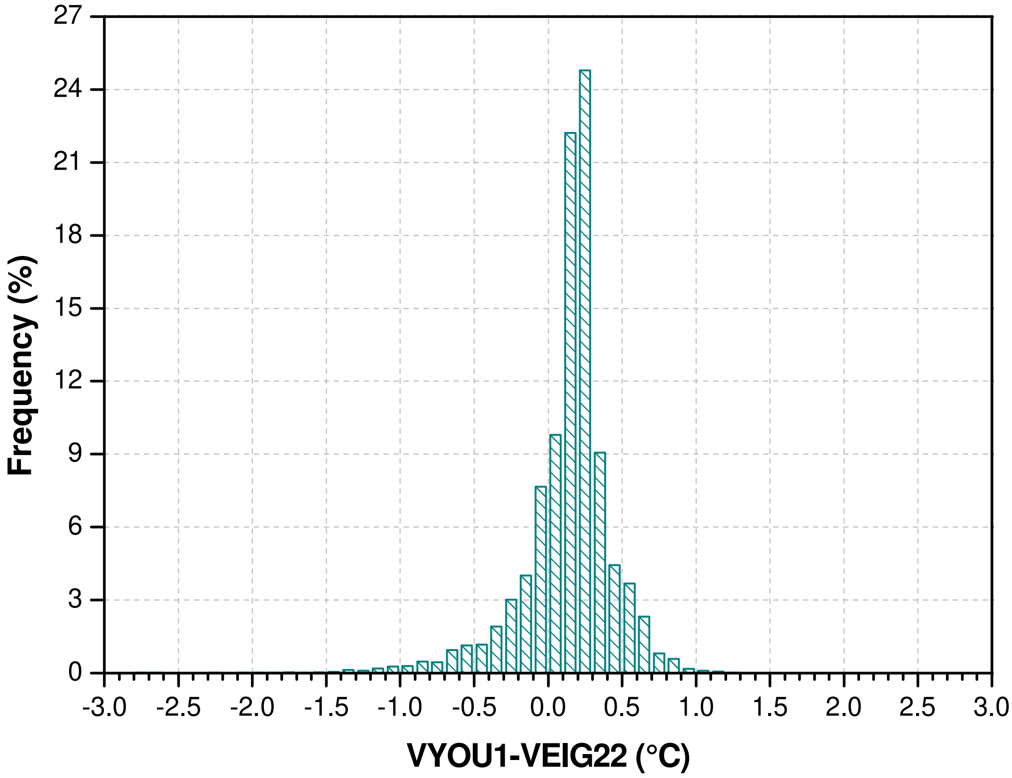


Figure 3

Screen #2 :

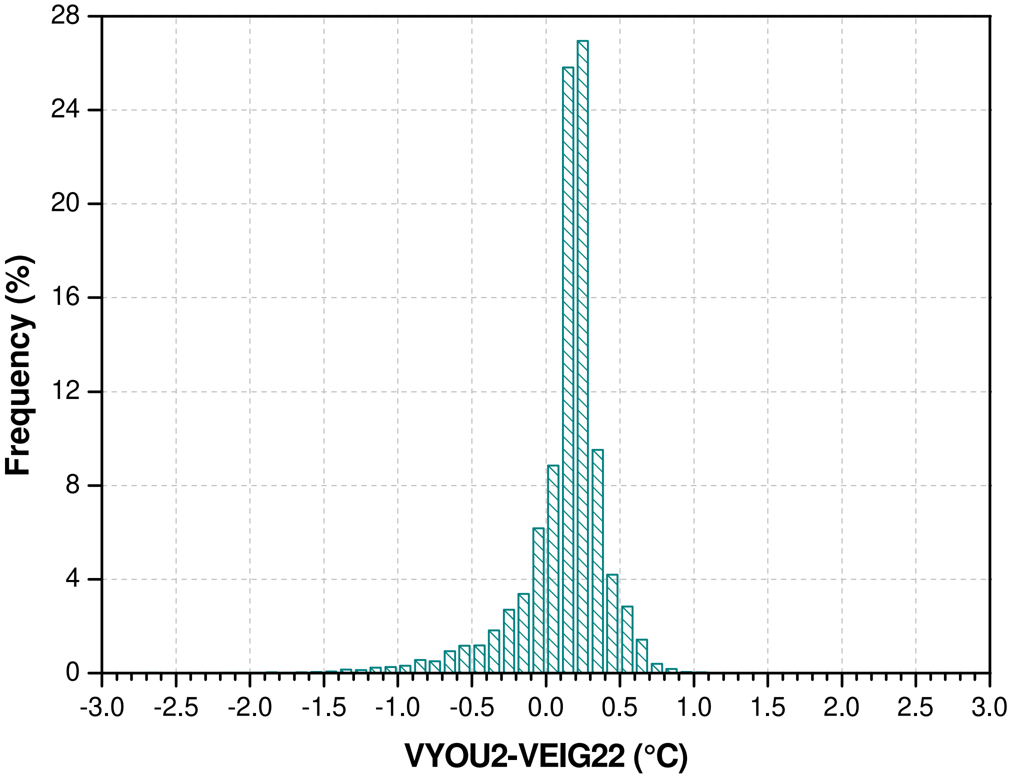


**Figure 4**

The graphs show that the two screens had very similar behaviour relative to the reference. They also indicate a medium dispersion of the differences between each of the two VYOU screens and the reference, from about -1 $^{o}$C to above +0.8 $^{o}$C. The mode of the differences for each of the screens is at about +0.3 $^{o}$C, with a frequency of more than 24%. The histograms of differences for both screens are skewed to the left.

CUMULATIVE HISTOGRAMS OF DIFFERENCES OF DAILY EXTREME VALUES

The cumulative histograms of differences with the reference VEIG22 of T (1-minute quality checked data), Tn (daily minimum temperature) and Tx (daily maximum temperature) are plotted, for the whole period of the intercomparison. Differences are plotted by steps of 0.1K.

Screen #1:

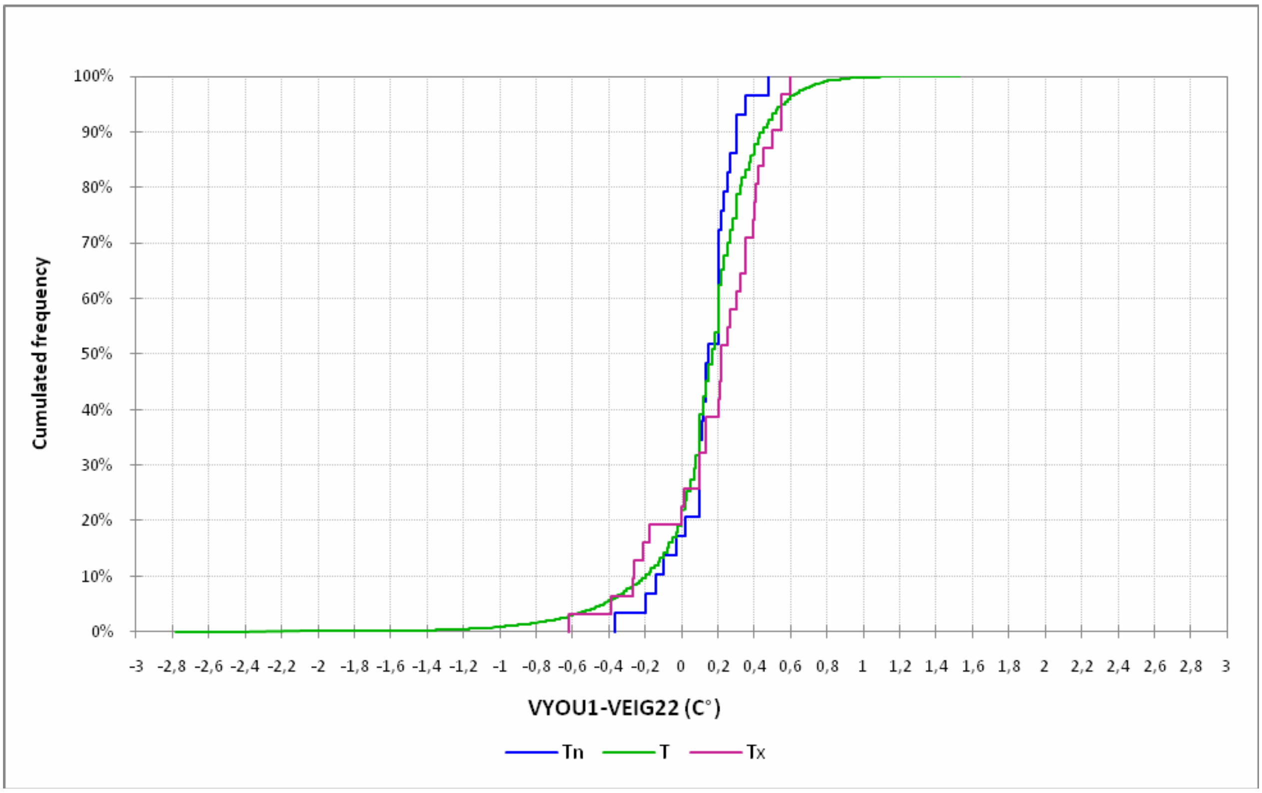


**Figure 5**

Screen #2:

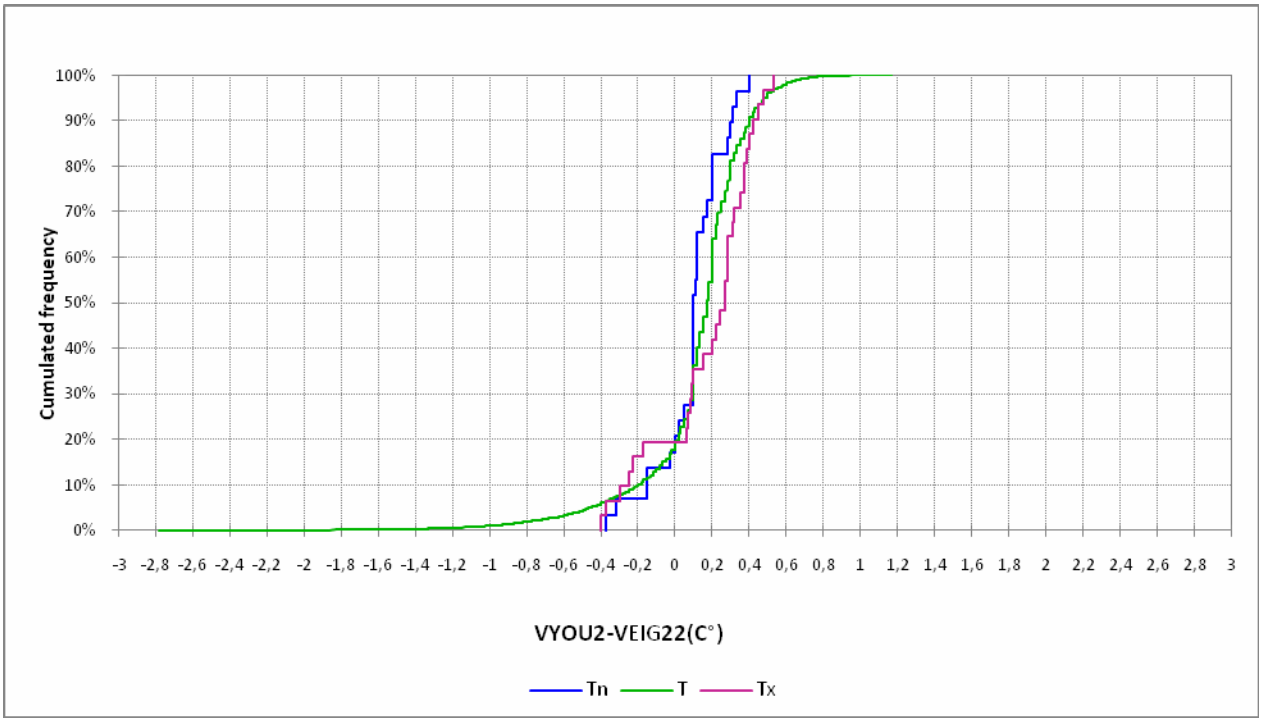


**Figure 6**

The cumulative histograms of differences show that the daily extreme values were reported similarly from both screens.

Both for daily minimum and maximum temperature, both screens were warmer than the reference for about 80% of the data points.

TABLE

The table 2 indicates the percentage of data that differ by less than 0.2°C (and 0.5°C) from the reference.

**Table 2**

| | | [-0.2°..0.2°] | [-0.5°..0.5°] |
|---|---|---|---|
| VYOU1 | T | 52.9 | 89.5 |
| | Tn | 64.5 | 100.0 |
| | Tx | 26.7 | 86.6 |
| VYOU2 | T | 54.5 | 91.9 |
| | Tn | 74.2 | 100.0 |
| | Tx | 23.3 | 96.6 |

## INFLUENCE OF GLOBAL RADIATION

The distribution of differences between VYOU1 and the reference VEIG22 is plotted, using 1-minute quality checked data for the whole period of the intercomparison. Differences are classified according global radiation.

Screen #1:

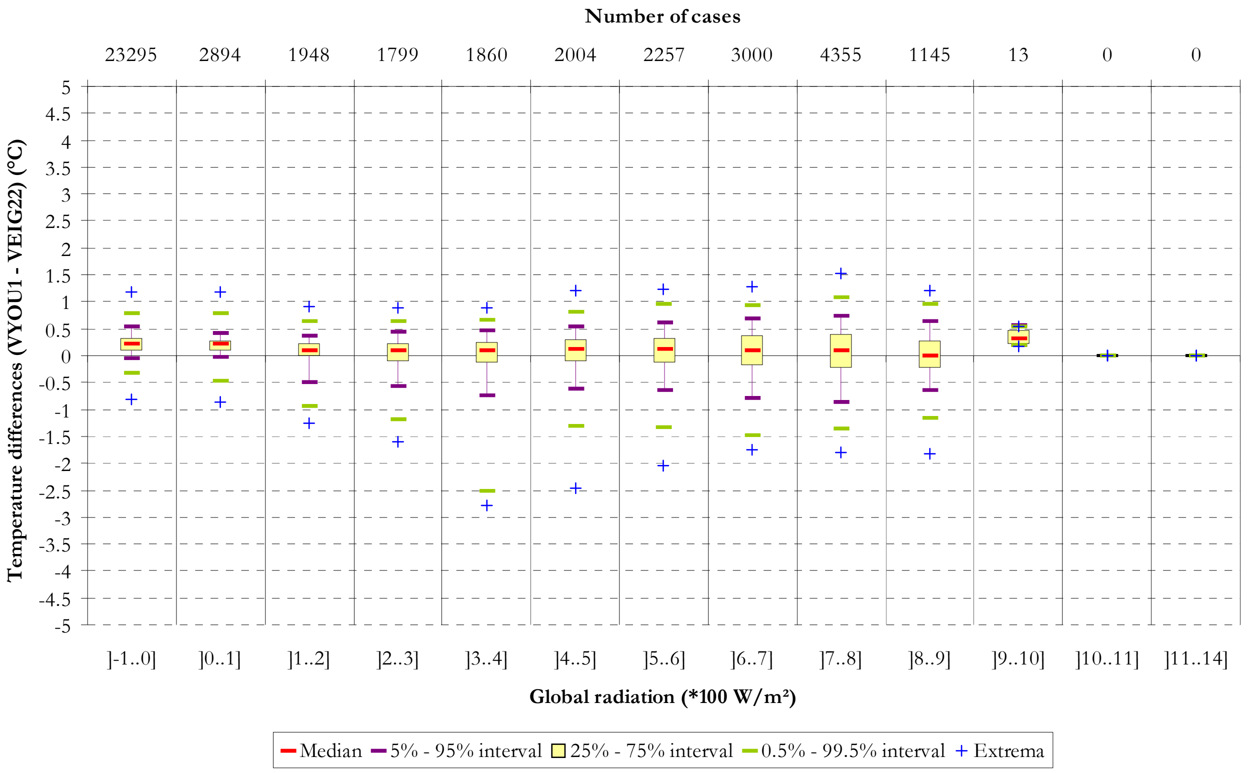


**Figure 7**

Screen #2:

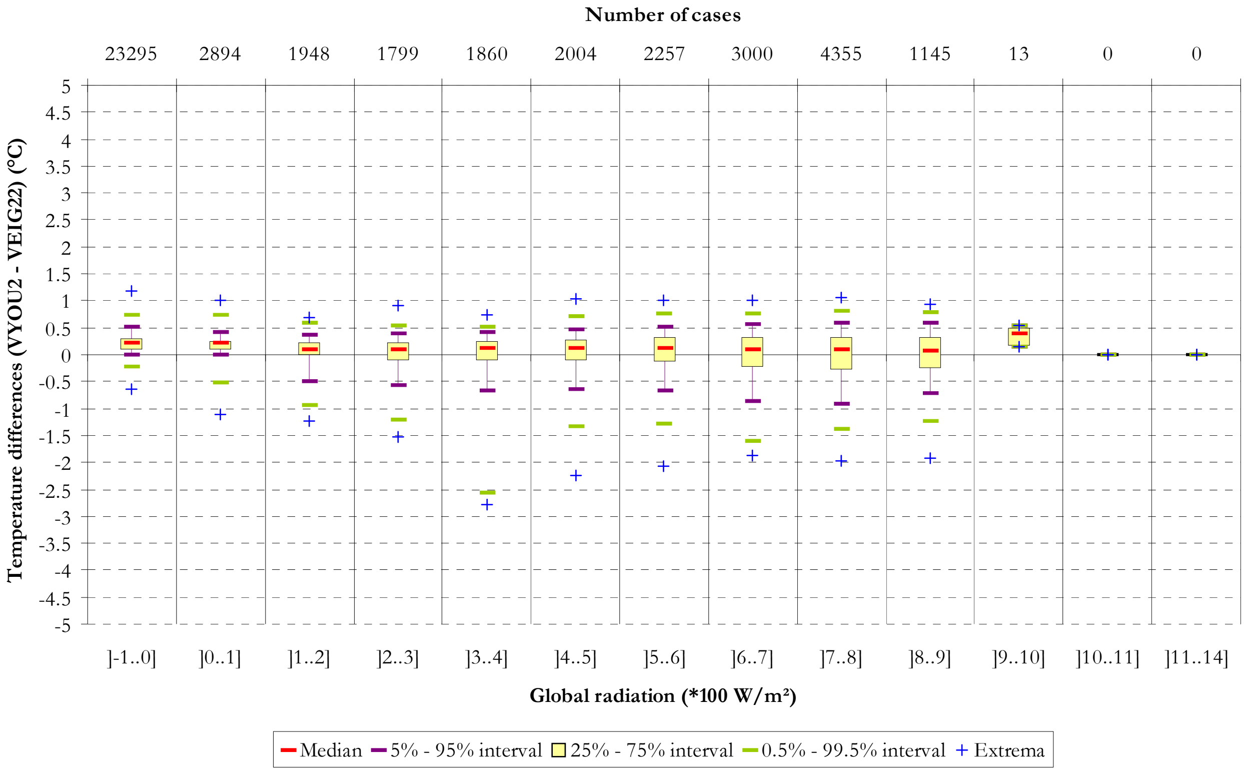


**Figure 8**

These two graphs indicate a very similar behaviour for the two VYOU screens during the intercomparison. Overall, the median of the temperature difference is stable, slightly positive for all radiation classes.

## RADIATION EFFECT

### DIFFERENCES BETWEEN DAY AND NIGHT BEHAVIOUR

The median of differences between VYOU and VEIG22 is plotted, using 1-minute quality checked data for the whole period of the intercomparison. We filter data for which sun elevation is above -1° (day) or below -1° (night). Differences are classified according 2-meter wind speed (2-minute average).

Screen #1:

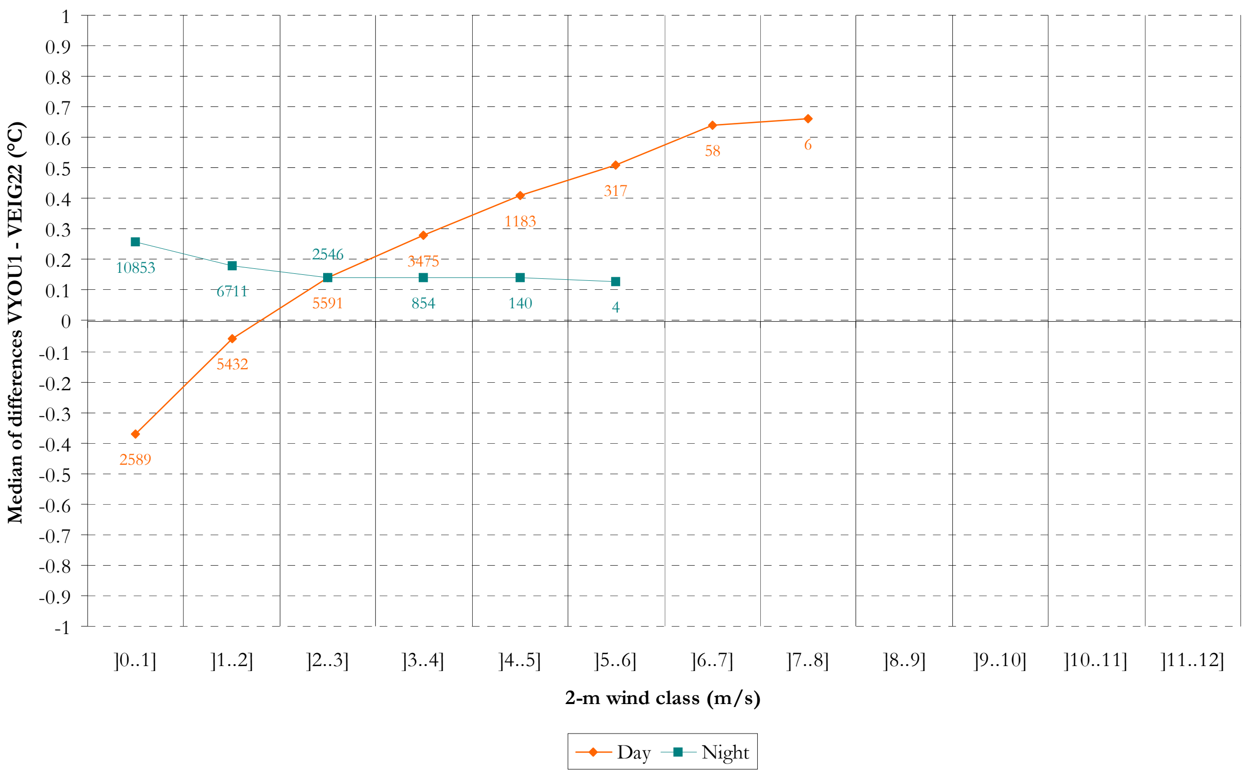


**Figure 9**

Screen #2:

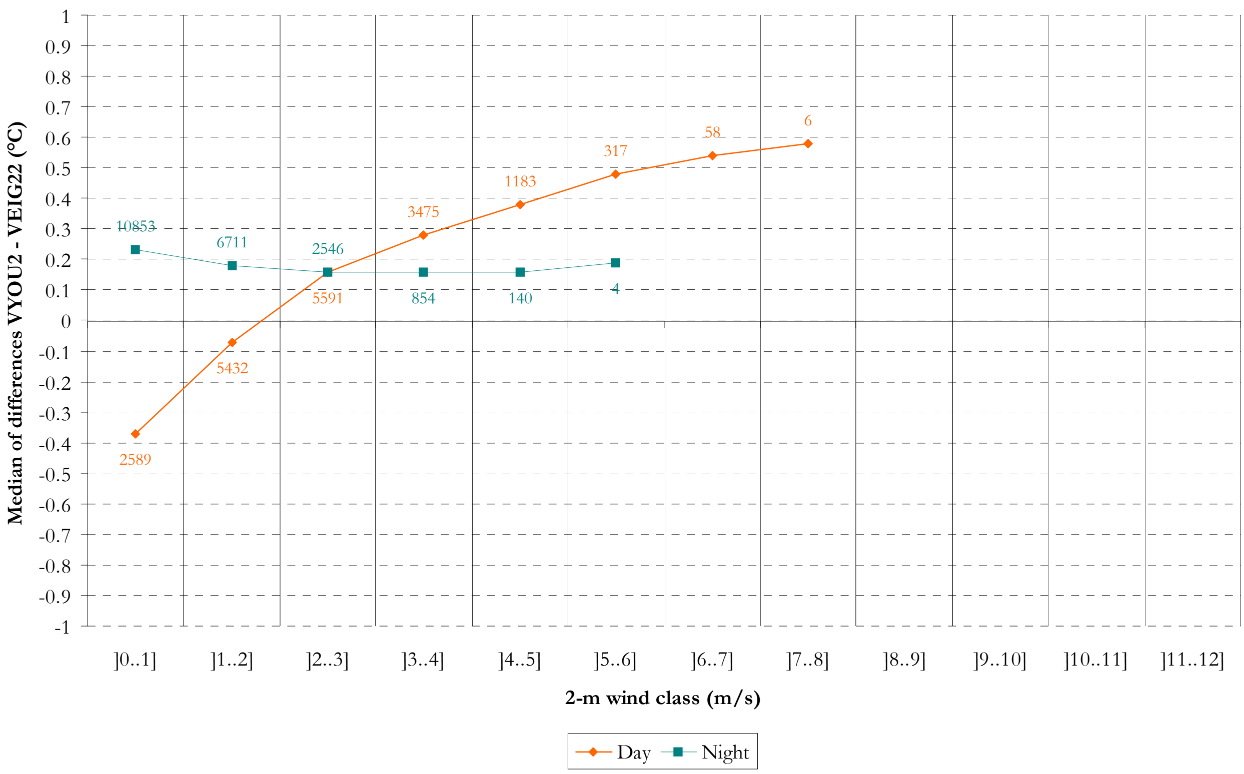


**Figure 10**

Both VYOU screens display similar behaviour during the day and during the night, for all classes of wind speeds.

During the day, the screens were colder than the reference for winds below 2m/s. For winds above 2m/s, VYOU screens are warmer than the reference. The medians of the differences increases when the wind speed increases.

During the night, the median of the differences from the reference slightly decrease for increasing wind speeds. VYOU screens are 0.2°C warmer than the reference during night time.

## EFFECT OF SUN ELEVATION

The median of differences between VYOU and VEIG22 is plotted, using 1-minute quality checked data. Here, we consider periods lasting six hours at least where cloudiness is less or equal to 1 (clear sky), during daytime (sun elevation above -1°). We filter data where sun elevation is low (below 10°), medium (between 10° and 45°) or high (above 45°). Differences are classified according 2-meter wind speed (2-minute average).

Screen #1:

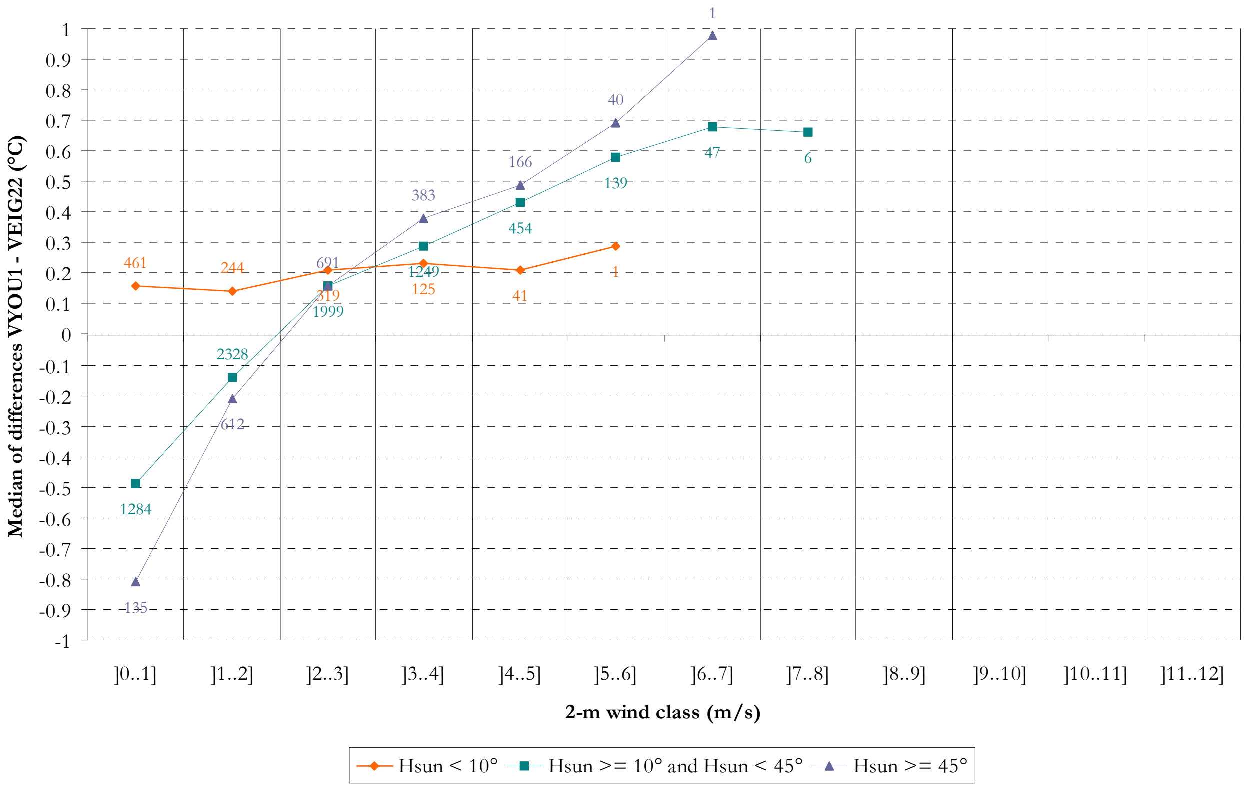


**Figure 11**

Screen #2:

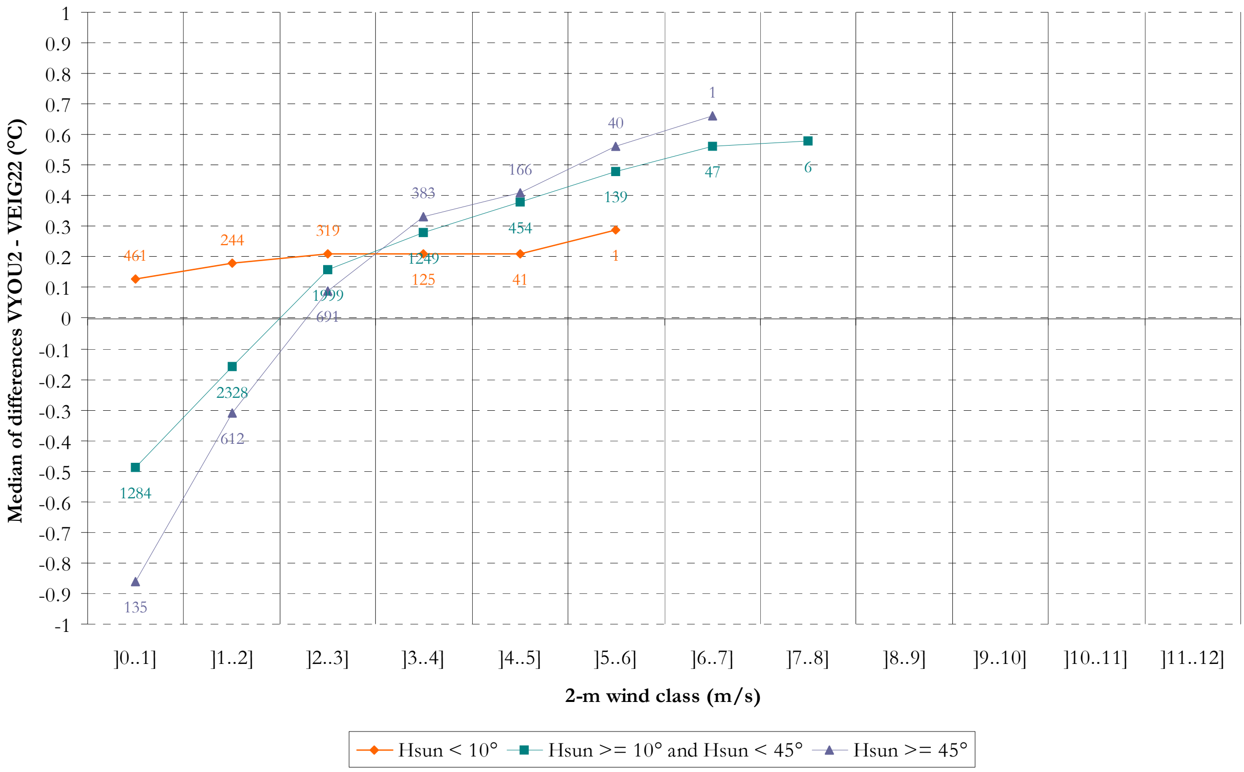


**Figure 12**

The two screens display similar behaviour for the three classes of sun elevation. The two graphs show a significant effect of solar radiation, in particular for sun elevations above 10°.

For sun elevations below 10°, the screens display a minimum dependency on the wind speed, being 0.1°C to 0.2°C warmer than the reference.

For sun elevations above 10°, the screens experienced a warming effect with the increase in wind speed. For wind speeds above 2m/s, the screens were significantly warmer than the reference, and there is a notable dependency of the median of the differences with the wind speed.

## COMBINED EFFECT OF WIND AND GLOBAL RADIATION

The medians of differences between VYOU and VEIG22 are represented here with a contour plot. The global radiation values are on the X-axis and on the Y axis is the 2-meter wind speed value (2-minute average). Medians are used in all cases, providing that at least one data is available for both conditions on radiation and wind considered.

Screen #1:

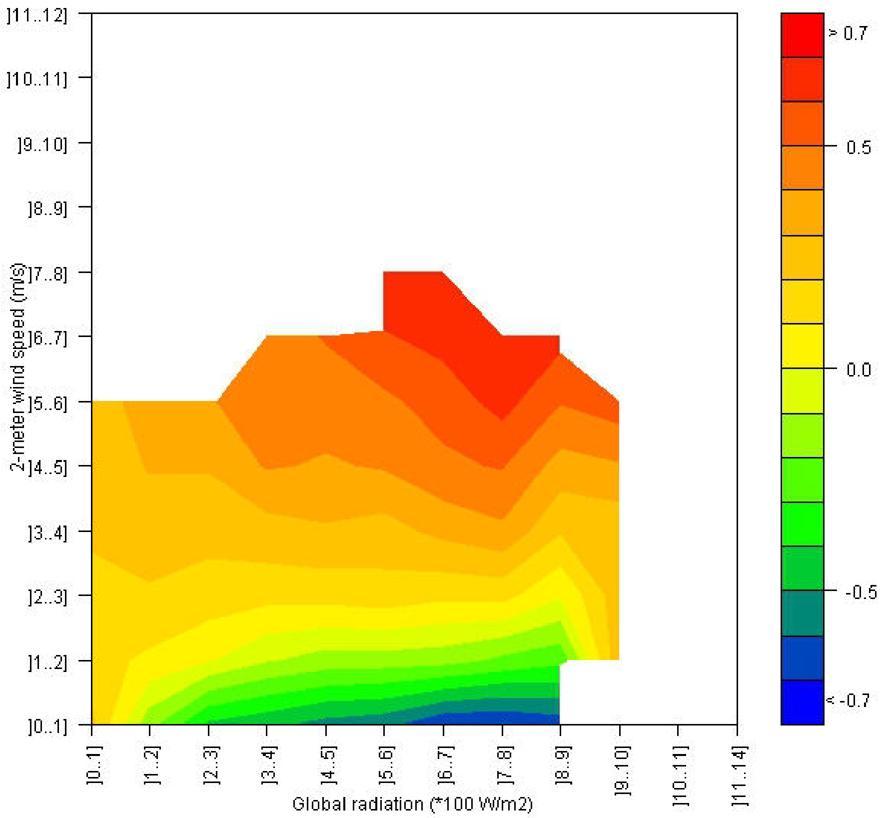


**Figure 13**

Screen #2:

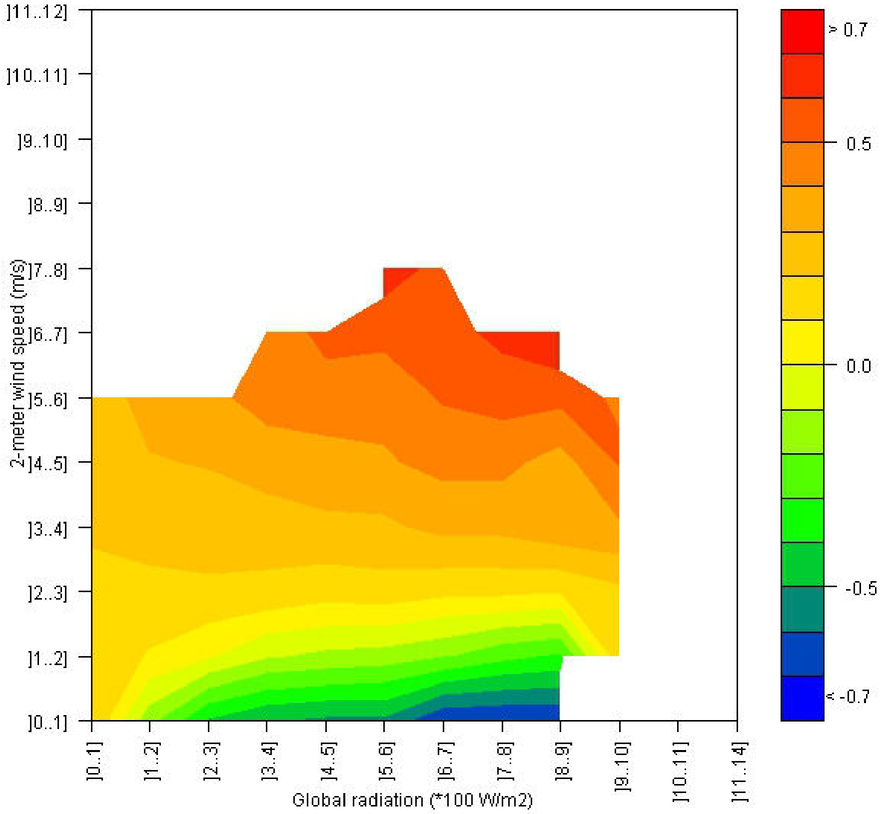


**Figure 14**

The two plots above show that both VYOU screens are influenced significantly by the wind speed for all solar radiation classes. For calm wind conditions and high irradiance the screens are significantly colder than the reference. For all other conditions, the screens are slightly warmer than the reference, and the predominant factor seems to be the wind speed.

## BEHAVIOUR DURING INCREASE/DECREASE OF TEMPERATURE

The distribution of differences between VYOU and the reference VEIG22 is plotted, using 1-minute quality checked data for the whole period of the intercomparison. Differences are classified according the temporal gradient of reference temperature over 1 minute. A screen faster (or slower, respectively) than the reference would be warmer (cooler) for positive gradient, cooler (warmer) for negative ones.

Screen #1:

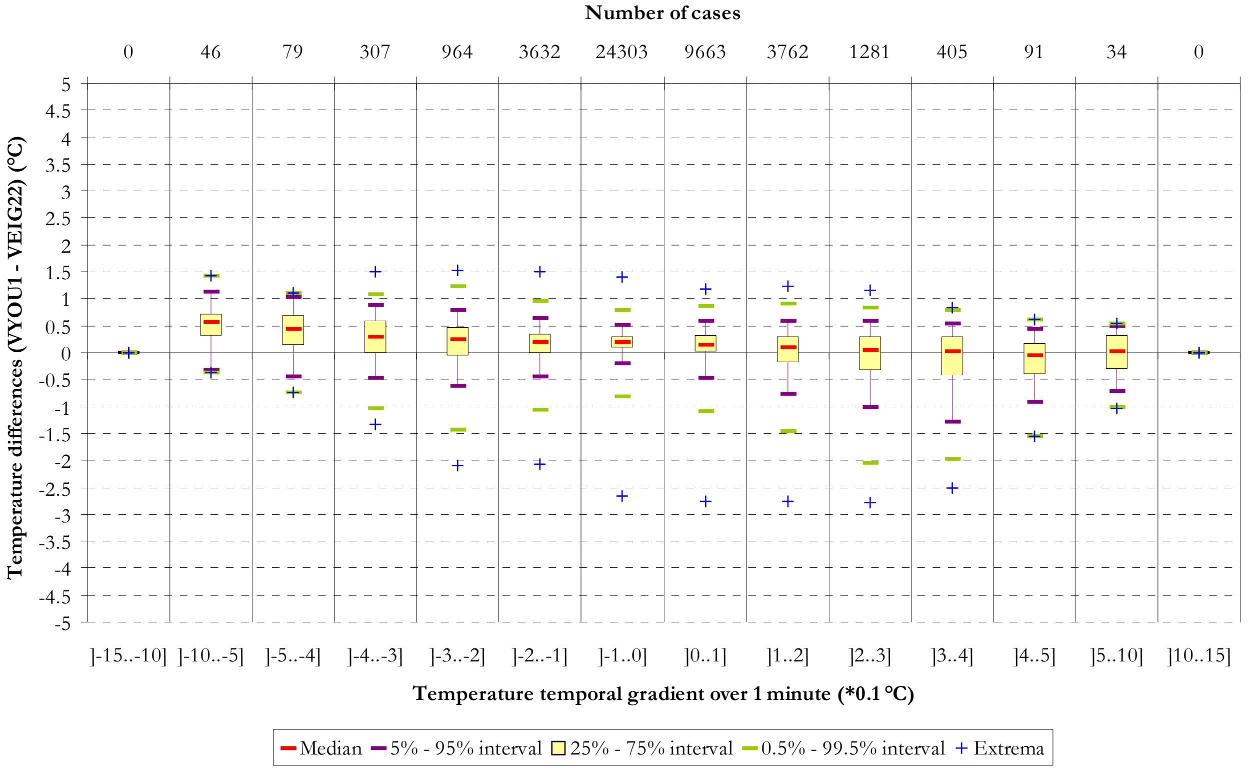


**Figure 15**

Screen #2:

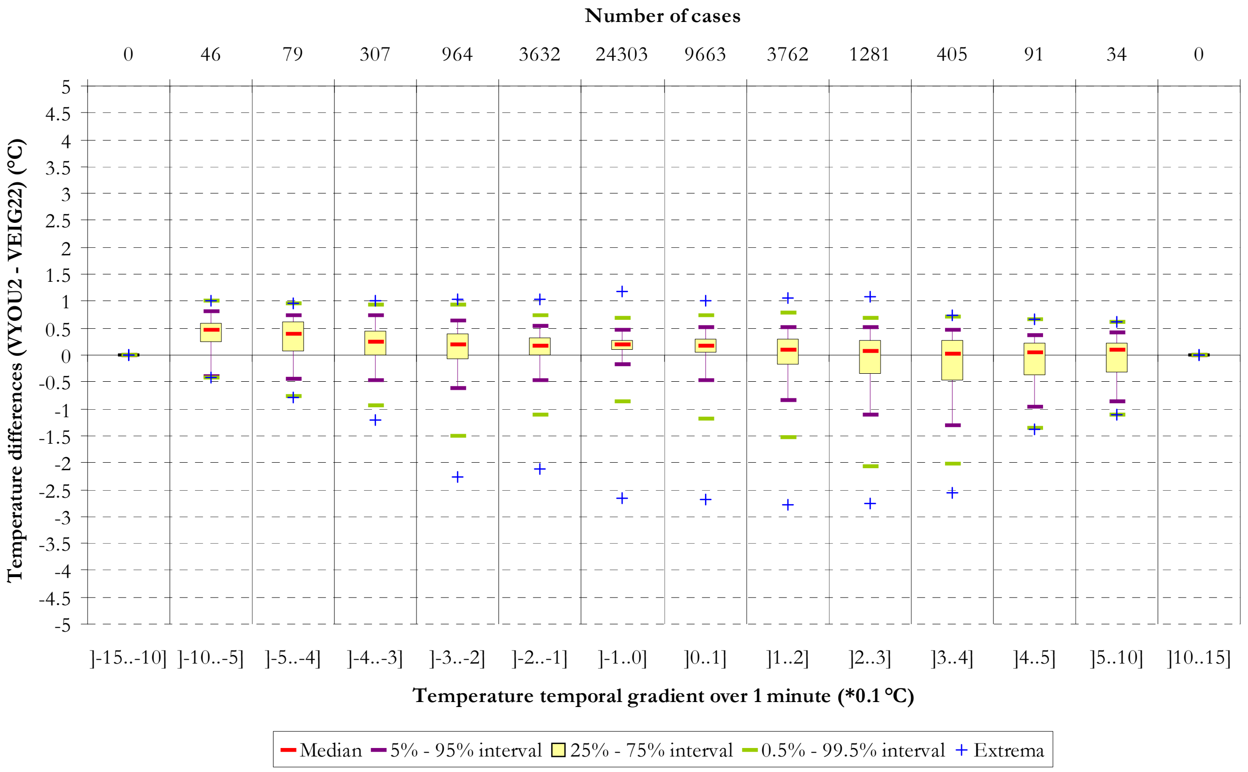


**Figure 16**

For negative temperature temporal gradient, the VYOU screens were slower than the reference. The median of the differences is about 0.5°C and is minimally dependent on the magnitude of the temperature gradient.

For constant temperature, or a temperature temporal gradient of magnitude less than 0.1°C, the median of the temperature differences approaches 0.2°C.

For positive temperature temporal gradient, the two VYOU screens are as fast as the reference. The median of the temperature differences is around 0.

## QUALITY CONTROL INFORMATION

### DATA AVAILABILITY

The intercomparison period extends from the 1st of November 2008 to the 1st of November 2009. The theoretical number of 1-minute data is 525600.

The next table sums up the total number of data for each screen and for each possible QC flag.

**Table 3**

| **QC flag** | VYOU1 | VYOU2 |
|---|---|---|
| 0 (good) | 503266 | 503266 |
| 1 (inconsistent) | 0 | 0 |
| 2 (doubtful) | 0 | 0 |
| 3 (erroneous) | 0 | 0 |
| 7 (missing) | 22334 | 22334 |

### MAINTENANCE

On the 30th of September, 2009, both screens were controlled. The ventilation was not working: the power supply was out of order, since the beginning of the intercomparison. It was replaced and the fan was cleaned.

After the operation, the ventilation was very good.

# Ultrasonic anemometer 2D THIES CLIMA – Germany – ATHI

**TECHNICAL SPECIFICATIONS (PROVIDED BY THE MANUFACTURER)**

Dimensions: Length 42 cm x Diameter 28 cm

Weight: 2.5 kg

Material / Structure: V4A Stainless steel

Estimated radiation error: up to ± 2°K

Power supply: none

This sensor measures acoustic-virtual temperature. Real air temperature is processed using humidity and pressure data.

**Figure 1**

## OVERVIEW

Both sensors give close results. Sensor #2 is about 0.5°C colder than sensor #1. The differences between both sensors decrease when temperature increases.

Sensor #1 is well equilibrated with the reference for 1-minute values: 50% of positive differences, 50% negative ones. The differences on daily extrema are larger: the median value is about –0.3° for maxima and +0.2°C for minima. Sensor #2 is colder: the median value for 1-minute temperature data is about –0.5°C.

Differences between Thies sensors and the reference decrease when global radiation increases: a priori the Thies sensor is not affected by solar radiation, so it may be an effect of radiation on the reference itself.

The medians of differences are not the same for day or night conditions. During daytime, there is a clear effect of the wind speed: when the wind speed increases, absolute differences decrease. There is a strong effect of cloudiness on the differences, for all classes of wind speed. In clear sky conditions, absolute differences are at least 0.5°C colder than for overcast conditions. They are higher for low wind speed values.

During night time, both sensors indicate a decrease of differences when wind speeds increases from 0 to 5 m/s. Above 5 m/s, differences increase and then decrease, reaching a maximum for the ]6..7m/s] wind class. During night time, cloudiness does not affect much the differences between Thies sensors and the reference.

For both sensors, when the sun elevation is above 10°, absolute differences decrease for increasing wind speeds. When the sun is very low, absolute differences increase when the wind speed increases.

Both sensors show globally the same tendency: the highest differences with the reference are obtained for large global radiation values and low wind speeds.

## CALIBRATION INFORMATION

The calibration of both sensors was performed by manufacturer.

**Table 1**

| Sensor | Location | Serial number | Calibration date | Instrument bias °C |
|---|---|---|---|---|
| ATHI1 | C1 | 0407100 | 18 Apr 2007 | ± 1°C |
| ATHI2 | C6 | 0407099 | 18 Apr 2007 | ± 1°C |

The result calibration of reference VEIG22 is available in the main report of the intercomparison, section 5.4.1.of

## COMPARISON OF BOTH SENSORS

The distribution of differences between screen 1 and screen 2 is plotted, using 1-minute quality checked data for the whole period of the intercomparison. Differences are classified according screen 1 temperature.

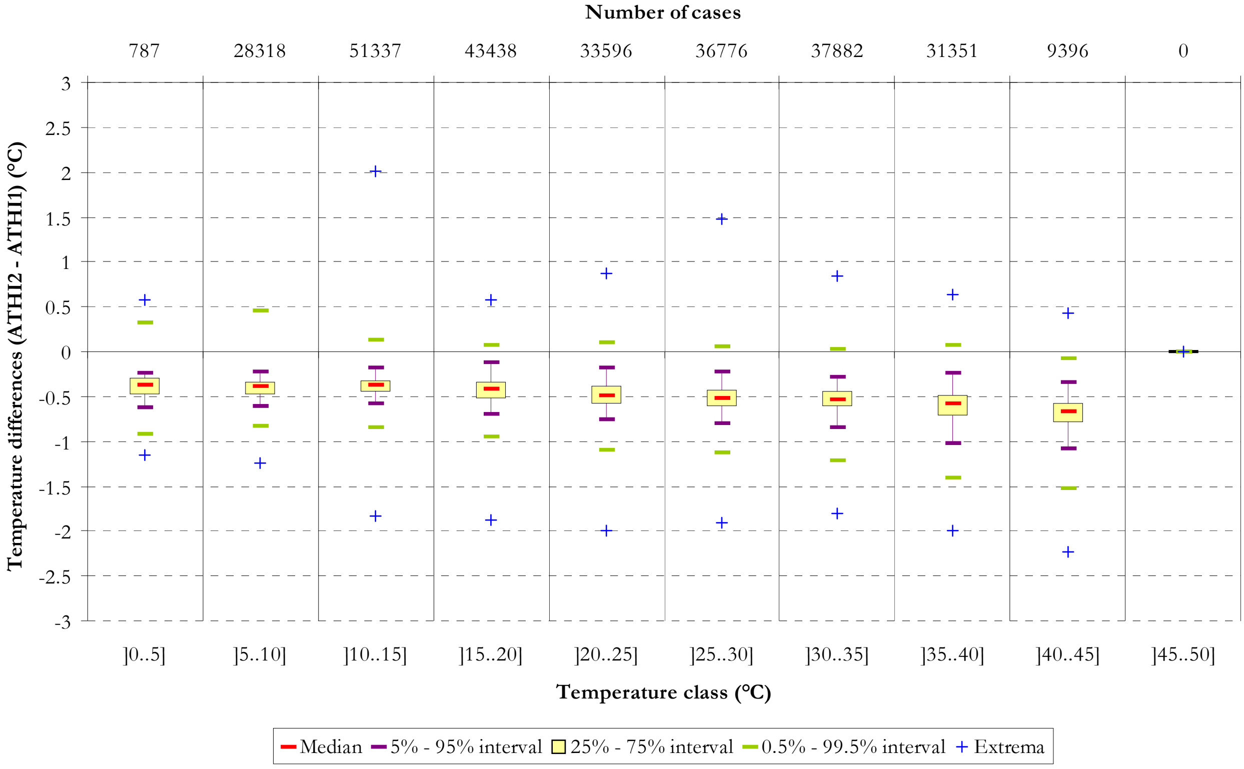


**Figure 2**

Both sensors give close results. Sensor #2 is about 0.5°C colder than sensor #1. The differences between both sensors decrease when temperature increases.

## COMPARISON WITH THE REFERENCE

### HISTOGRAM OF DIFFERENCES

The histogram of differences between ATHI and the reference VEIG22 is plotted, using 1-minute quality checked data for the whole period of the intercomparison. Differences are plotted by steps of 0.1K. The vertical axis is the frequency in percent for each class of differences.

Screen #1:

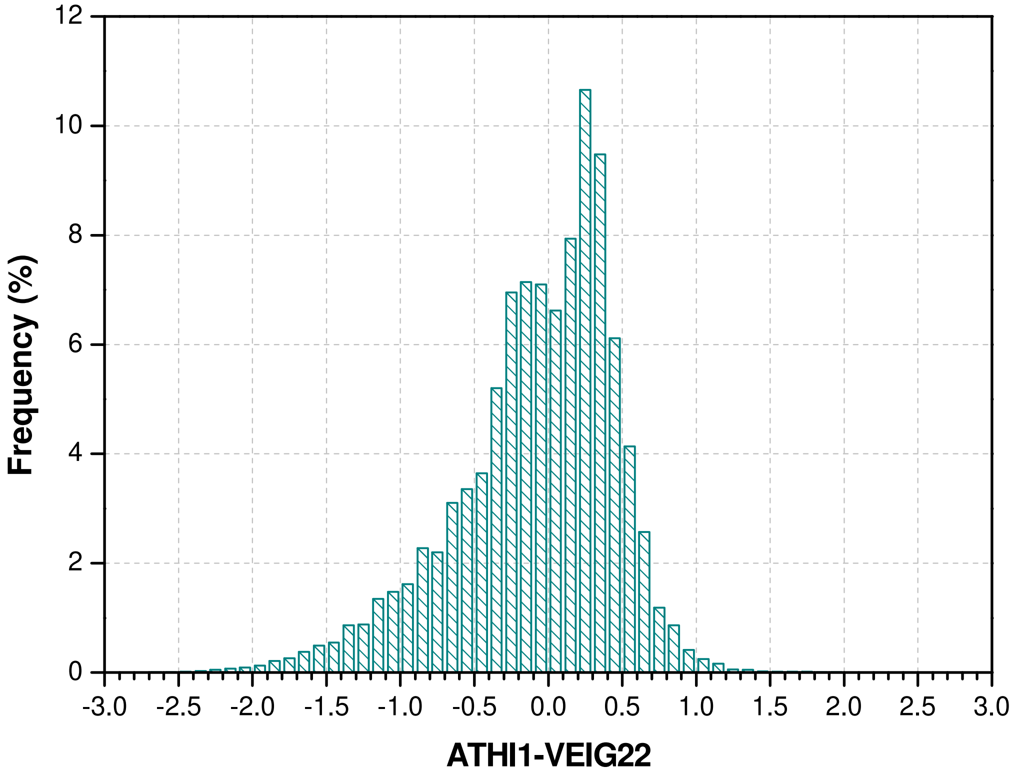


**Figure 3**

Screen #2:

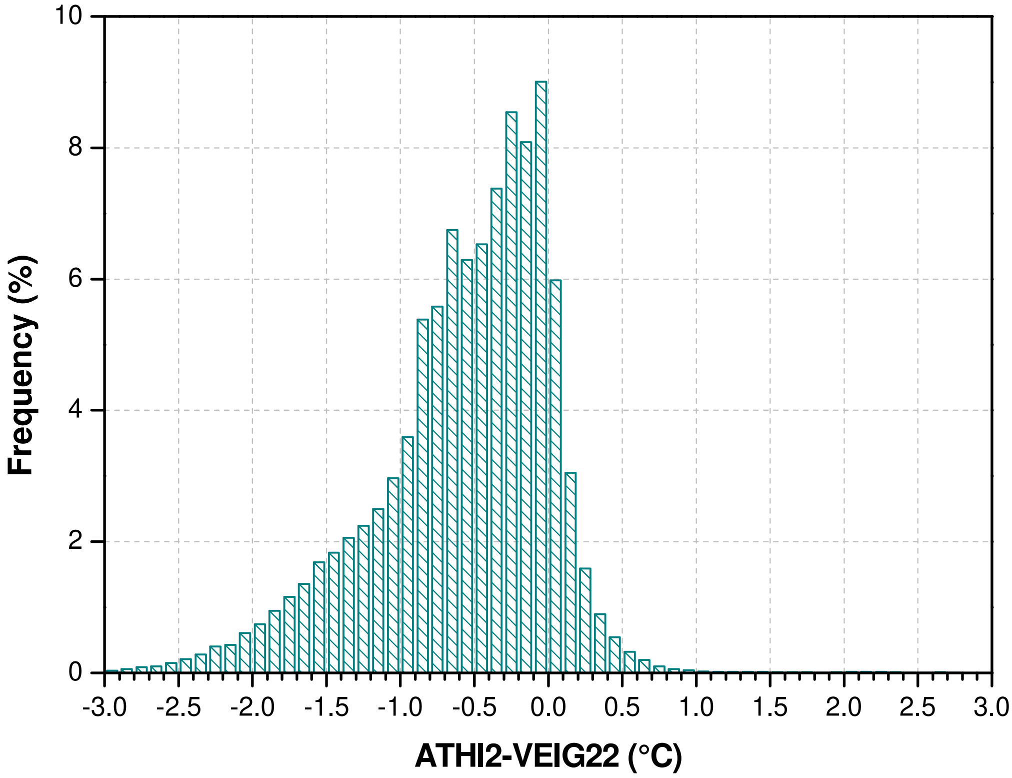


**Figure 4**

CUMULATIVE HISTOGRAMS OF DIFFERENCES OF DAILY EXTREME VALUES

The cumulative histograms of differences with the reference VEIG22 of T (1-minute quality checked data), Tn (daily minimum temperature) and Tx (daily maximum temperature) are plotted, for the whole period of the intercomparison. Differences are plotted by steps of 0.1K.

Screen #1:

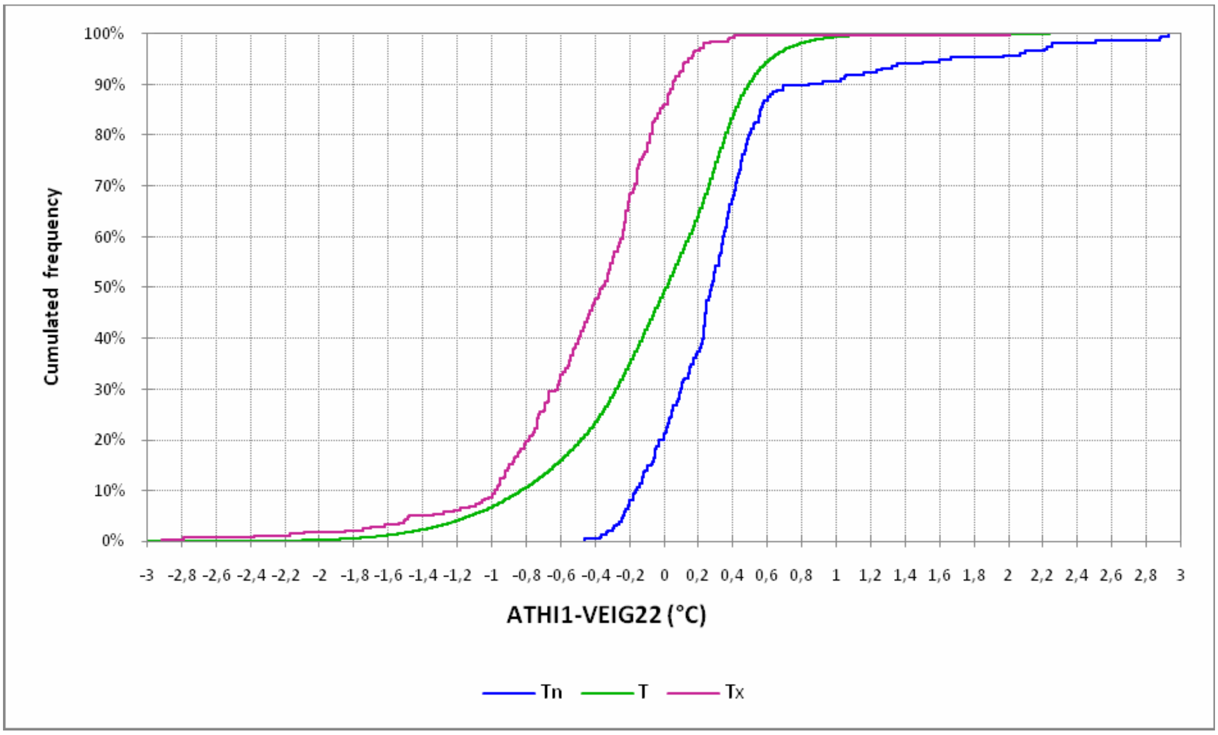


**Figure 5**

Screen #2:

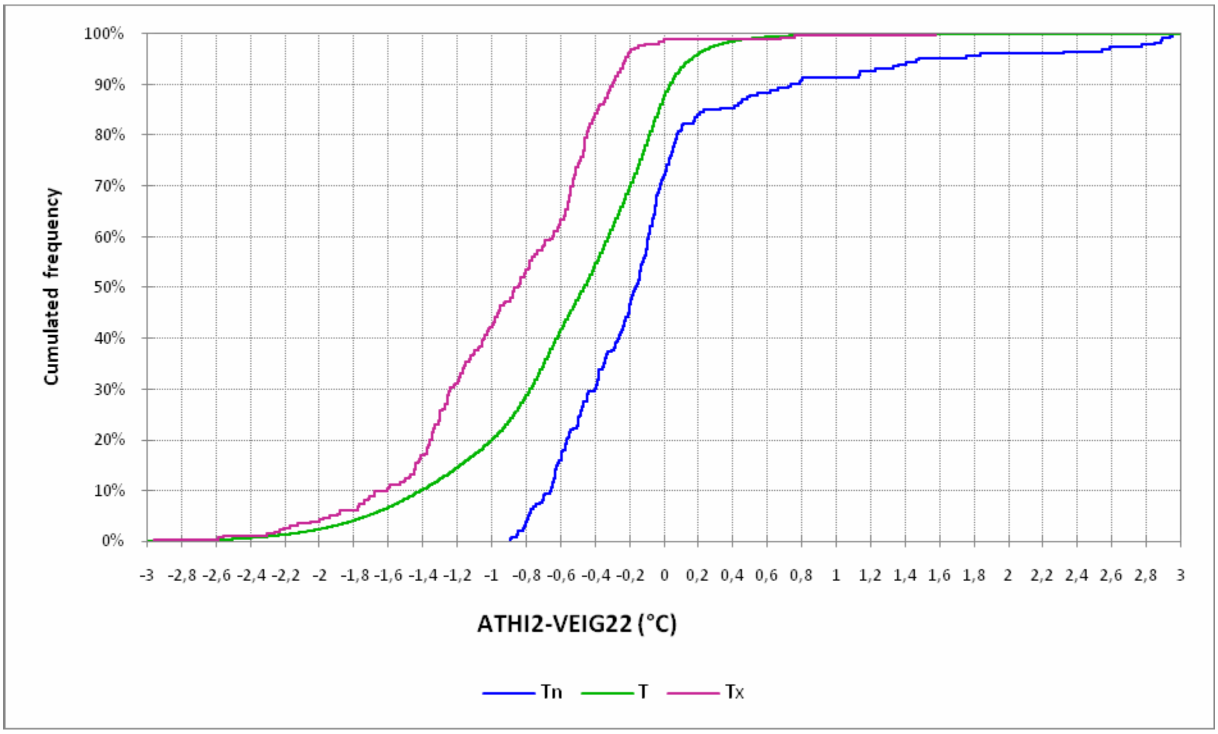


**Figure 6**

Sensor #1 is well equilibrated with the reference for 1-minute values: 50% of positive differences, 50% negative ones. The differences on daily extrema are larger: the median value is about -0.3° for maxima and +0.3°C for minima for sensor #1. Sensor #2 is colder: the median value for 1-minute temperature data is about -0.5°C.

TABLE

The table 2 indicates the percentage of data that differ by less than 0.2°C (and 0.5°C) from the reference.

**Table 2**

| | | [-0.2°..0.2°] | [-0.5°..0.5°] |
|---|---|---|---|
| ATHI1 | T | 30.4 | 71.7 |
| | Tn | 27.0 | 74.2 |
| | Tx | 28.5 | 59.4 |
| ATHI2 | T | 27.1 | 51.5 |
| | Tn | 34.9 | 59.6 |
| | Tx | 2.6 | 23.7 |

## INFLUENCE OF GLOBAL RADIATION

The distribution of differences between ATHI and the reference VEIG22 is plotted, using 1-minute quality checked data for the whole period of the intercomparison. Differences are classified according global radiation.

Screen #1:

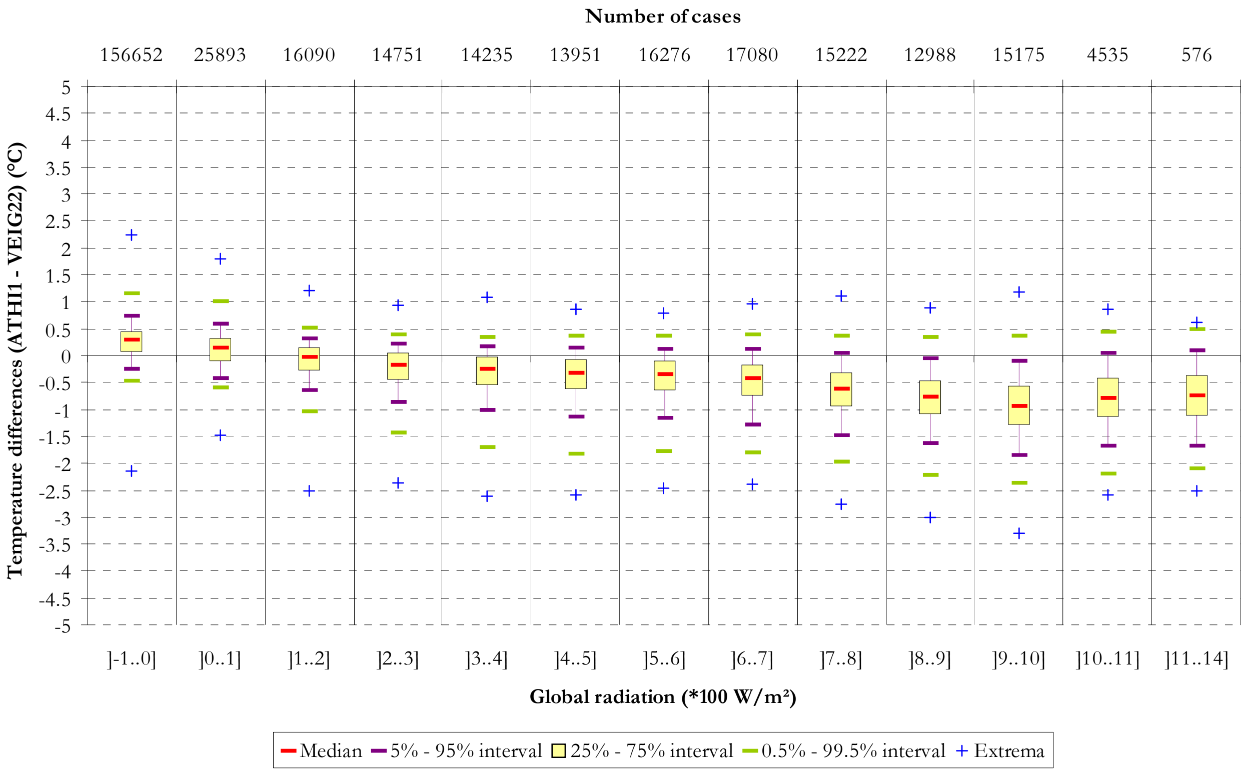


**Figure 7**

Screen #2:

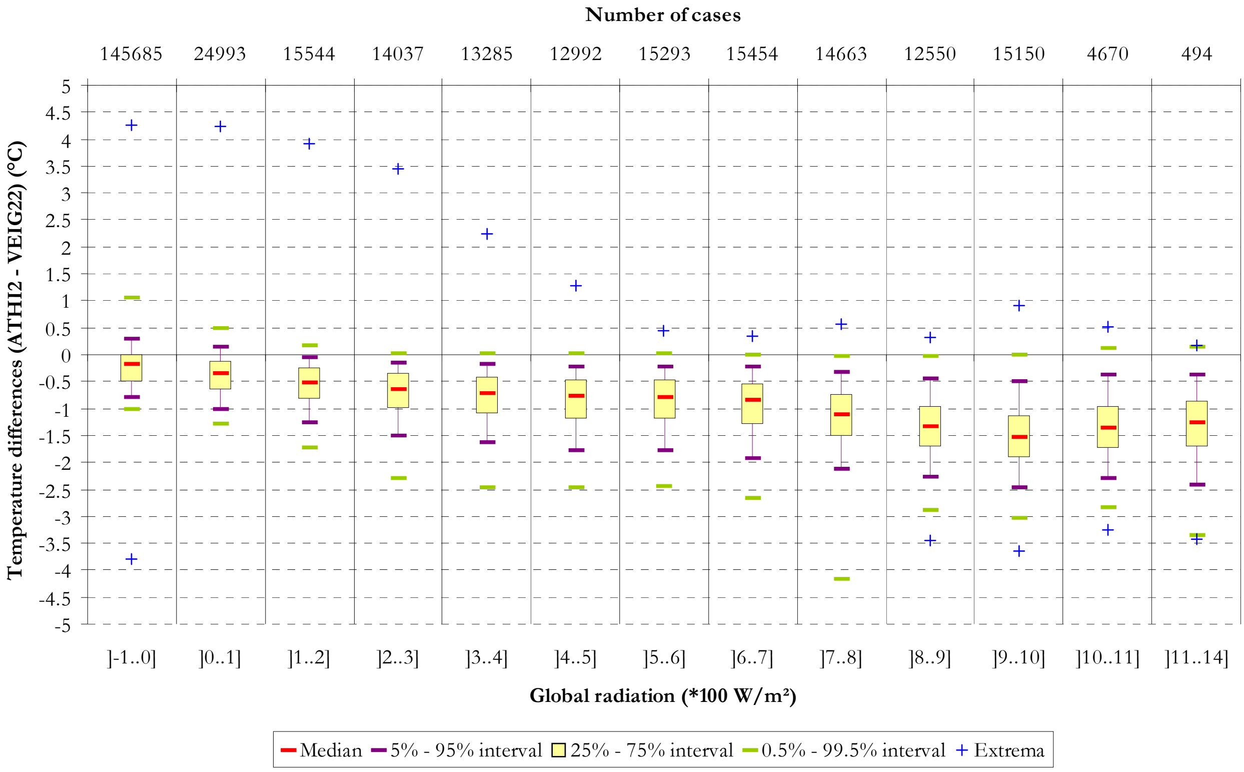


**Figure 8**

Differences between Thies sensors and the reference decrease when global radiation increases: a priori the Thies sensor is not affected by solar radiation, so it may be an effect of radiation on the reference itself.

## RADIATION EFFECT

### DIFFERENCES BETWEEN DAY AND NIGHT BEHAVIOUR

The median of differences between ATHI and VEIG22 is plotted, using 1-minute quality checked data for the whole period of the intercomparison. We filter data for which sun elevation is above -1° (day) or below -1° (night). Differences are classified according 2-meter wind speed (2-minute average).

Screen #1:

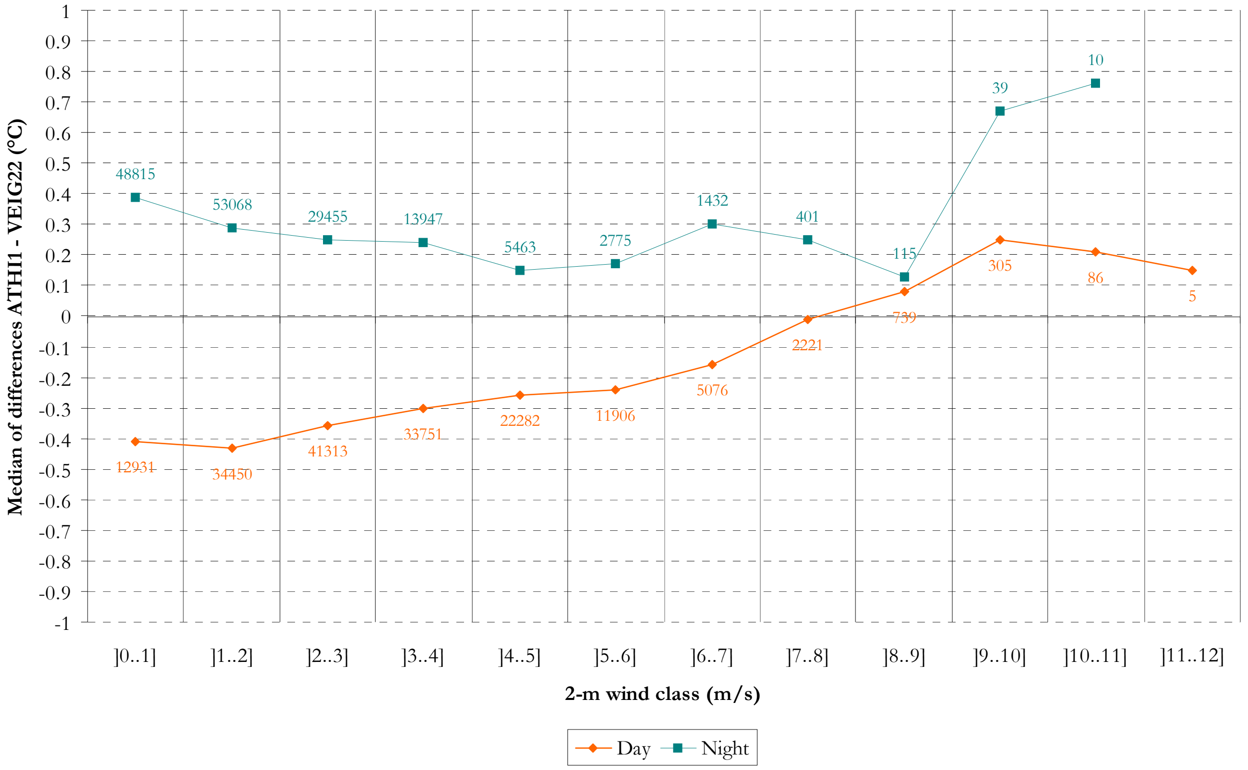


**Figure 9**

Screen #2:

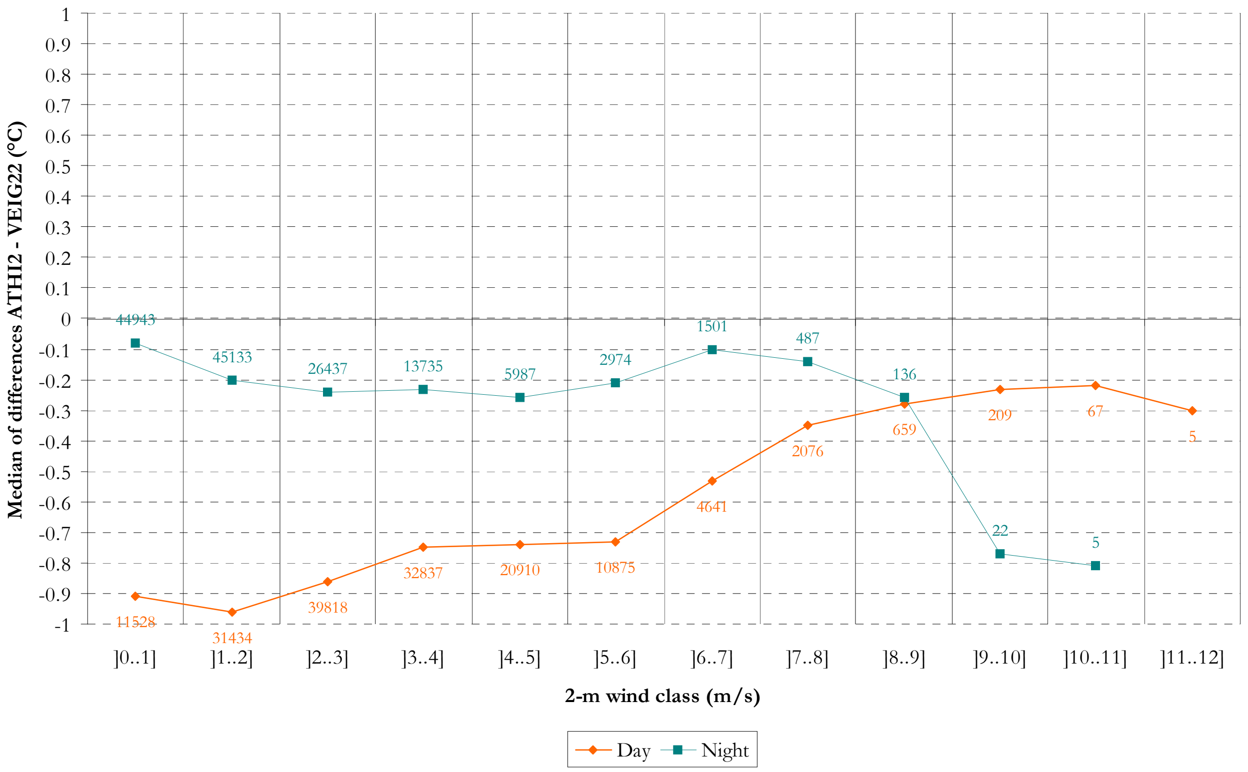


**Figure 10**

The medians of differences are not the same for day or night conditions. During daytime, there is a clear effect of the wind speed: when the wind speed increases, absolute differences decrease. During night time, both sensors indicate a decrease of differences when wind speeds increases from 0 to 5 m/s. Above 5 m/s, differences increase and then decrease, reaching a maximum for the ]6..7m/s] wind class.

## DIFFERENCES BETWEEN CLEAR SKY AND OVERCAST SKY DURING DAYTIME

The median of differences between ATHI and VEIG22 is plotted, using 1-minute quality checked data. Here, we consider periods lasting six hours at least where cloudiness is less or equal to 1 (clear sky) or more or equal to 7 (overcast sky), during daytime (sun elevation above -1°). Differences are classified according 2-meter wind speed (2-minute average).

Screen #1:

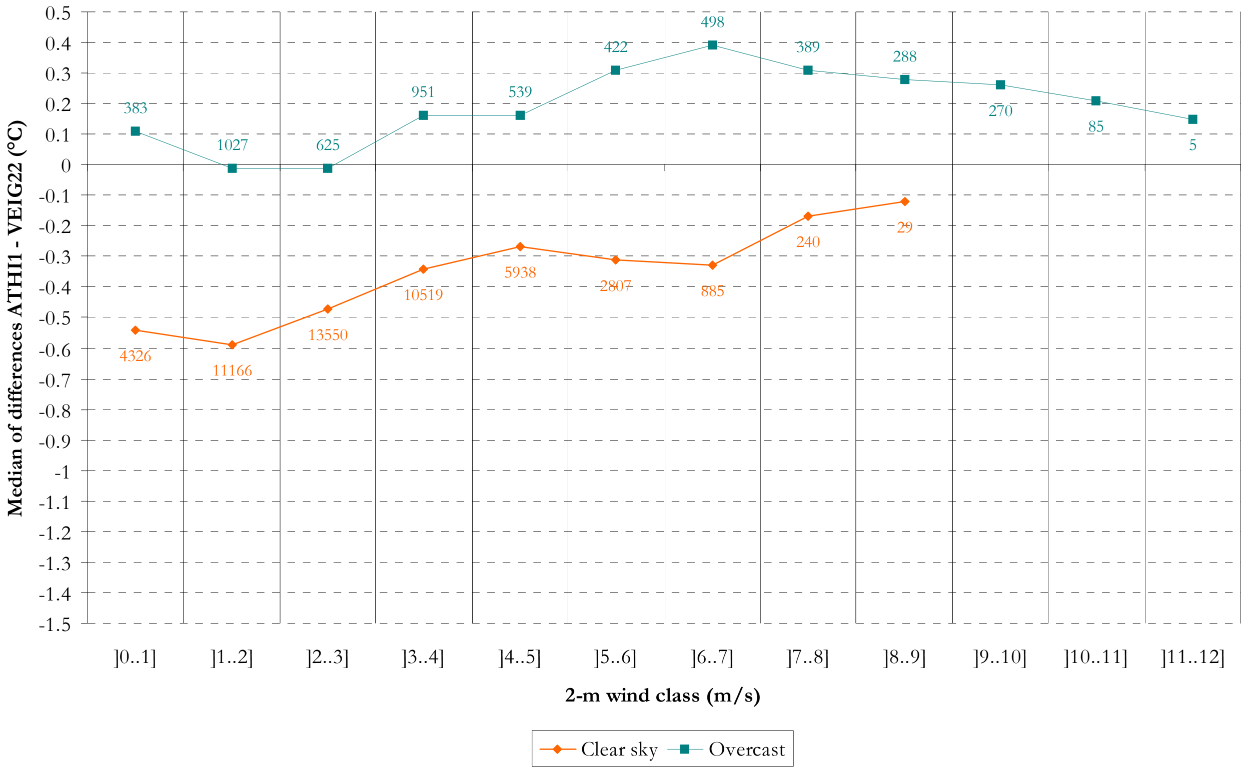


**Figure 11**

Screen #2:

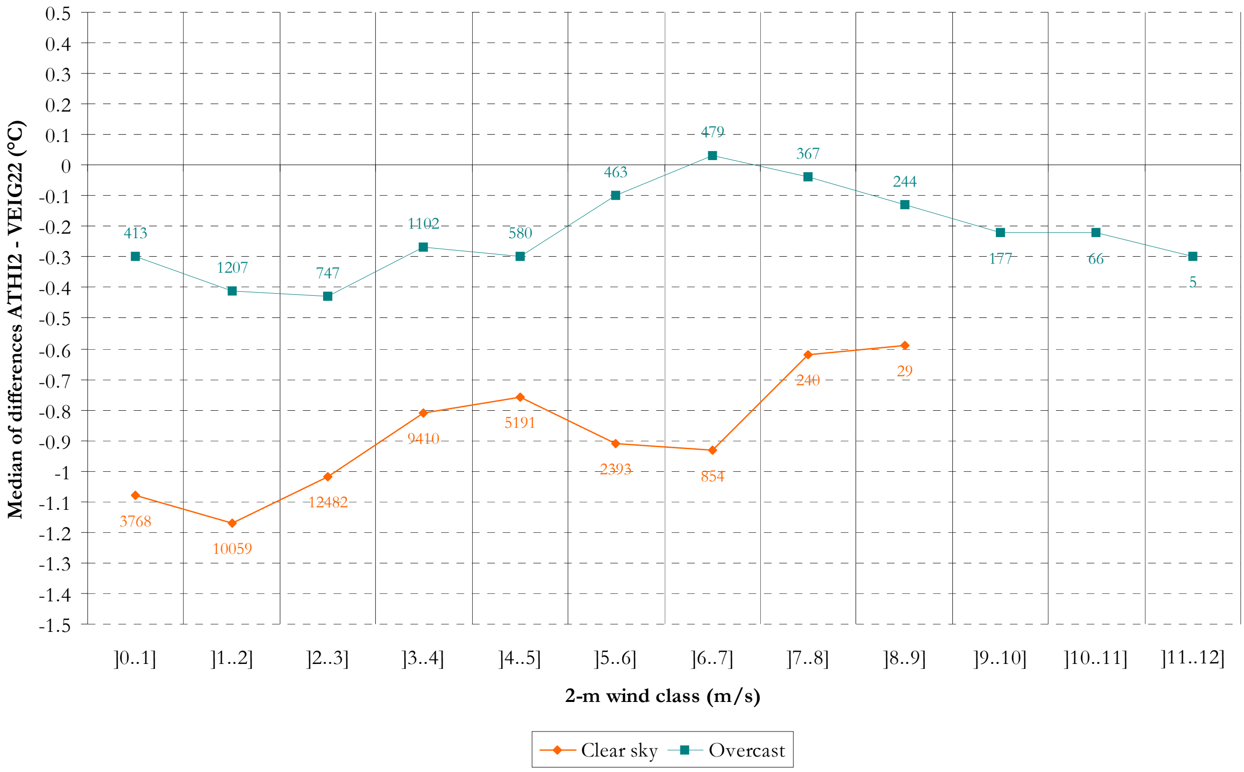


**Figure 12**

During daytime, there is a strong effect of cloudiness on the differences, for all classes of wind speed. In clear sky conditions, absolute differences are at least 0.5°C colder than for overcast conditions. They are higher for low wind speed values.

DIFFERENCES BETWEEN CLEAR SKY AND OVERCAST SKY DURING NIGHT TIME

The median of differences between ATHI and VEIG22 is plotted, using 1-minute quality checked data. Here, we consider periods lasting six hours at least where cloudiness is less or equal to 1 (clear sky) or more or equal to 7 (overcast sky), during night time (sun elevation below -1°). Differences are classified according 2-meter wind speed (2-minute average).

Screen #1:

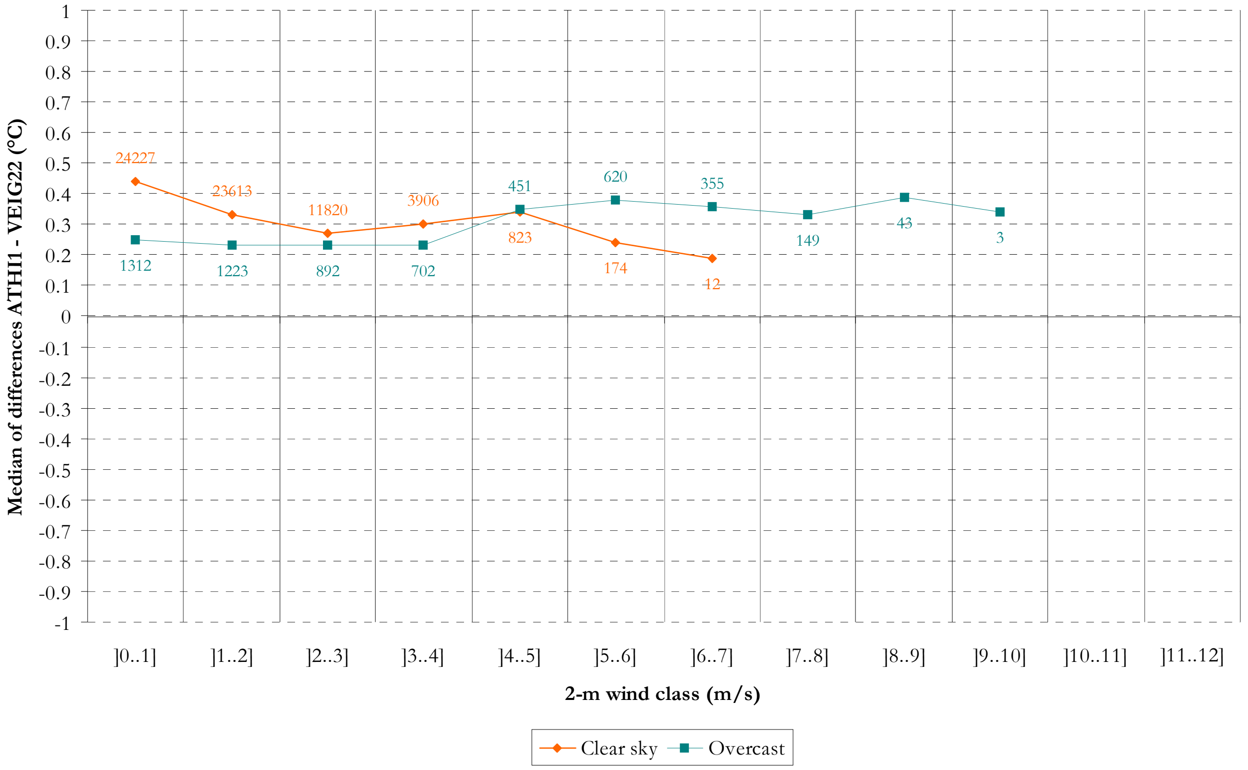


**Figure 13**

Screen #2:

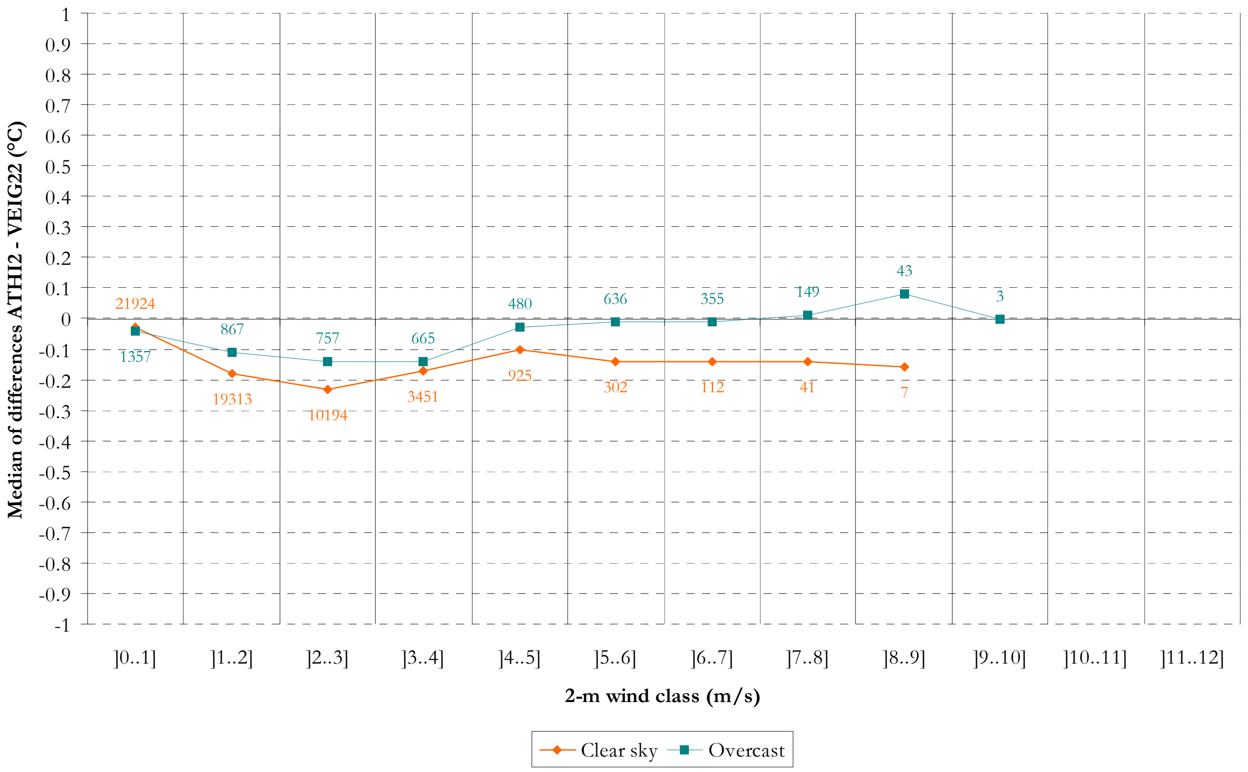


**Figure 14**

During night time, cloudiness does not affect much the differences between Thies sensors and the reference.

## EFFECT OF SUN ELEVATION

The median of differences between ATHI and VEIG22 is plotted, using 1-minute quality checked data. Here, we consider periods lasting six hours at least where cloudiness is less or equal to 1 (clear sky), during daytime (sun elevation above -1°). We filter data where sun elevation is low (below 10°), medium (between 10° and 45°) or high (above 45°). Differences are classified according 2-meter wind speed (2-minute average).

<u>Screen #1:</u>

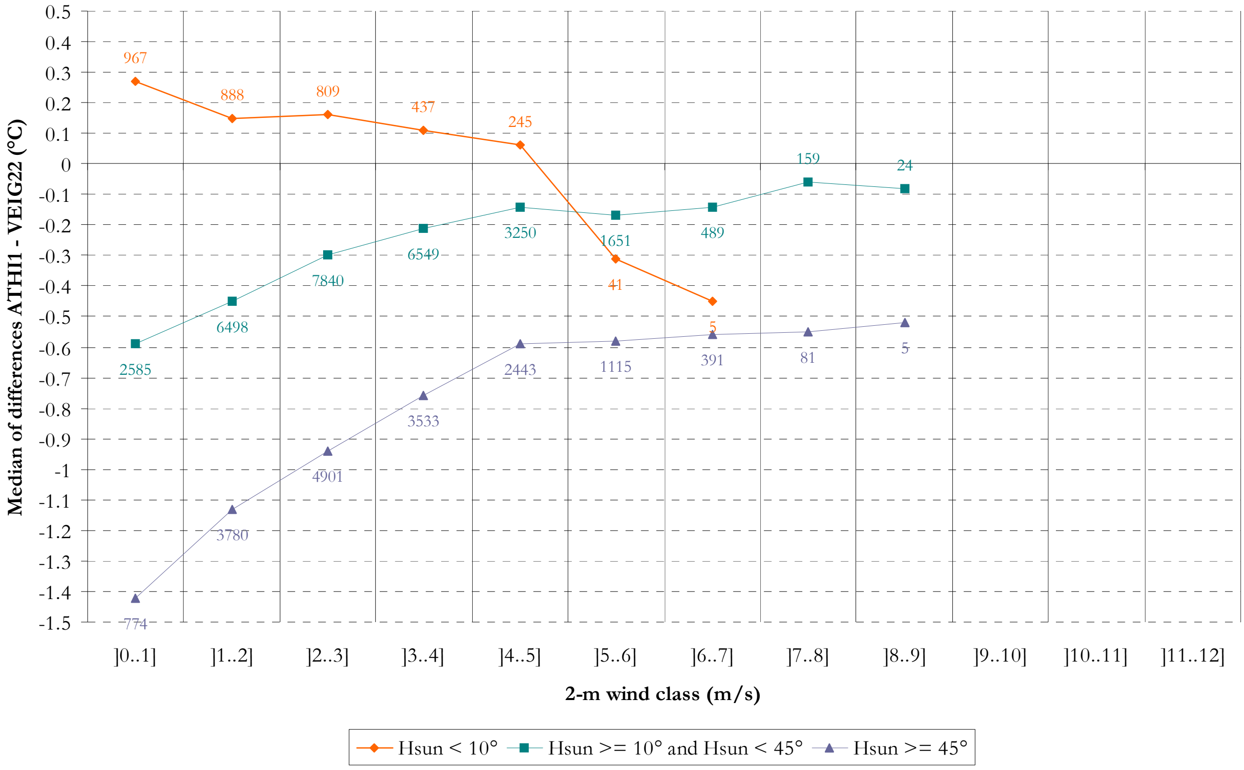


**Figure 15**

Screen #2:

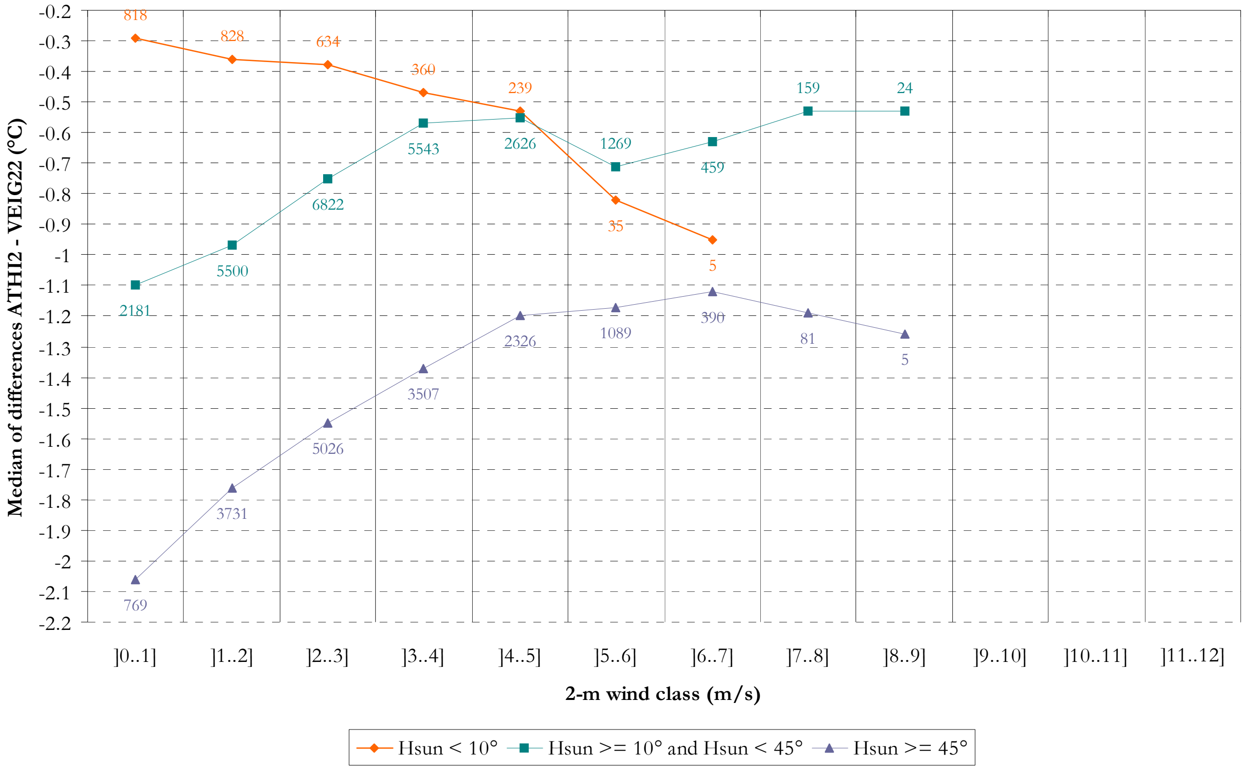


**Figure 16**

For both sensors, when the sun elevation is above 10°, absolute differences decrease for increasing wind speeds. When the sun is very low, absolute differences increase when the wind speed increases.

## COMBINED EFFECT OF WIND AND GLOBAL RADIATION

The medians of differences between ATHI and VEIG22 are represented here with a contour plot. The global radiation values are on the X-axis and on the Y axis is the 2-meter wind speed value (2-minute average). Medians are used in all cases, providing that at least one data is available for both conditions on radiation and wind considered.

Screen #1:

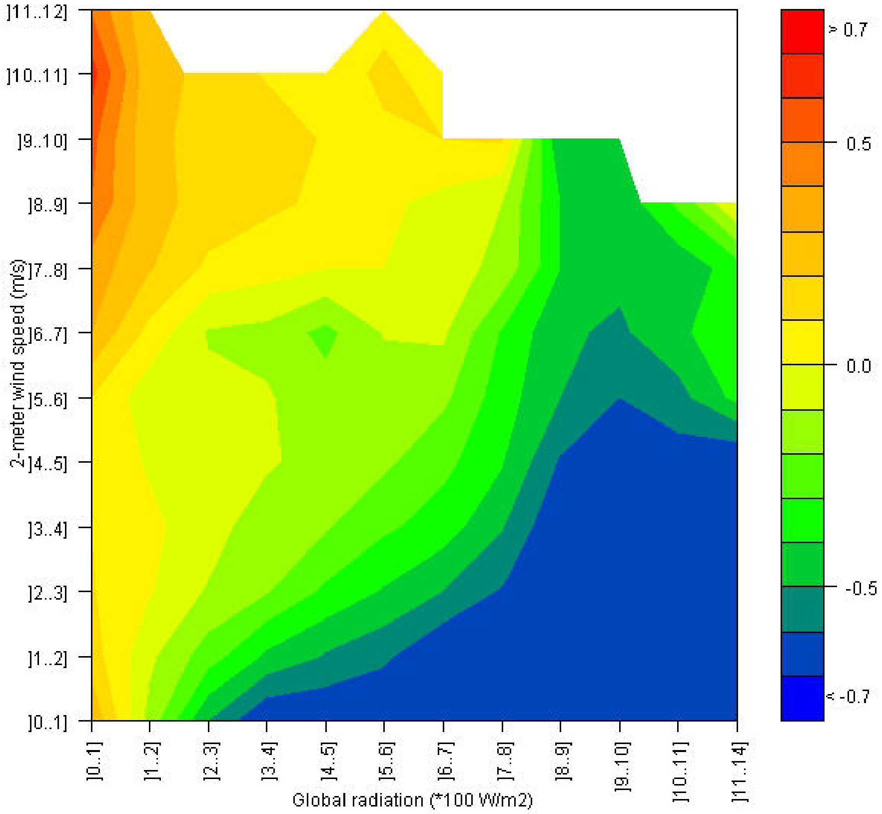


**Figure 17**

Screen #2:

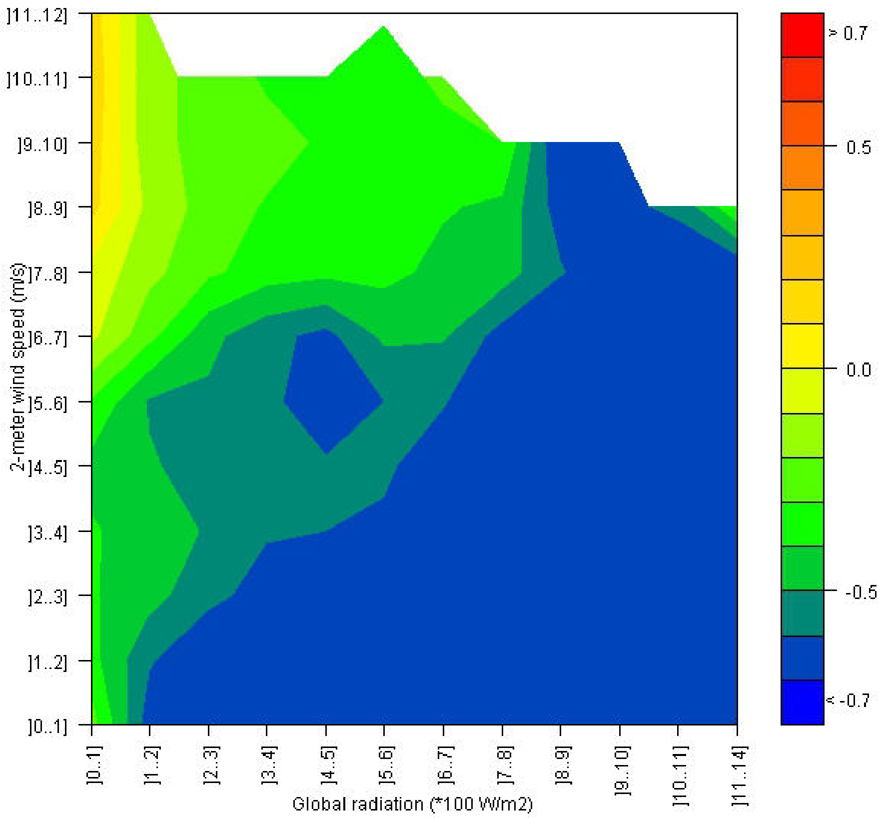


**Figure 18**

Both sensors show globally the same tendency: the highest differences with the reference are obtained for large global radiation values and low wind speeds.

## BEHAVIOUR DURING INCREASE/DECREASE OF TEMPERATURE

The distribution of differences between ATHI and the reference VEIG22 is plotted, using 1-minute quality checked data for the whole period of the intercomparison. Differences are classified according the temporal gradient of reference temperature over 1 minute. A screen faster (or slower, respectively) than the reference would be warmer (cooler) for positive gradient, cooler (warmer) for negative ones.

Screen #1:

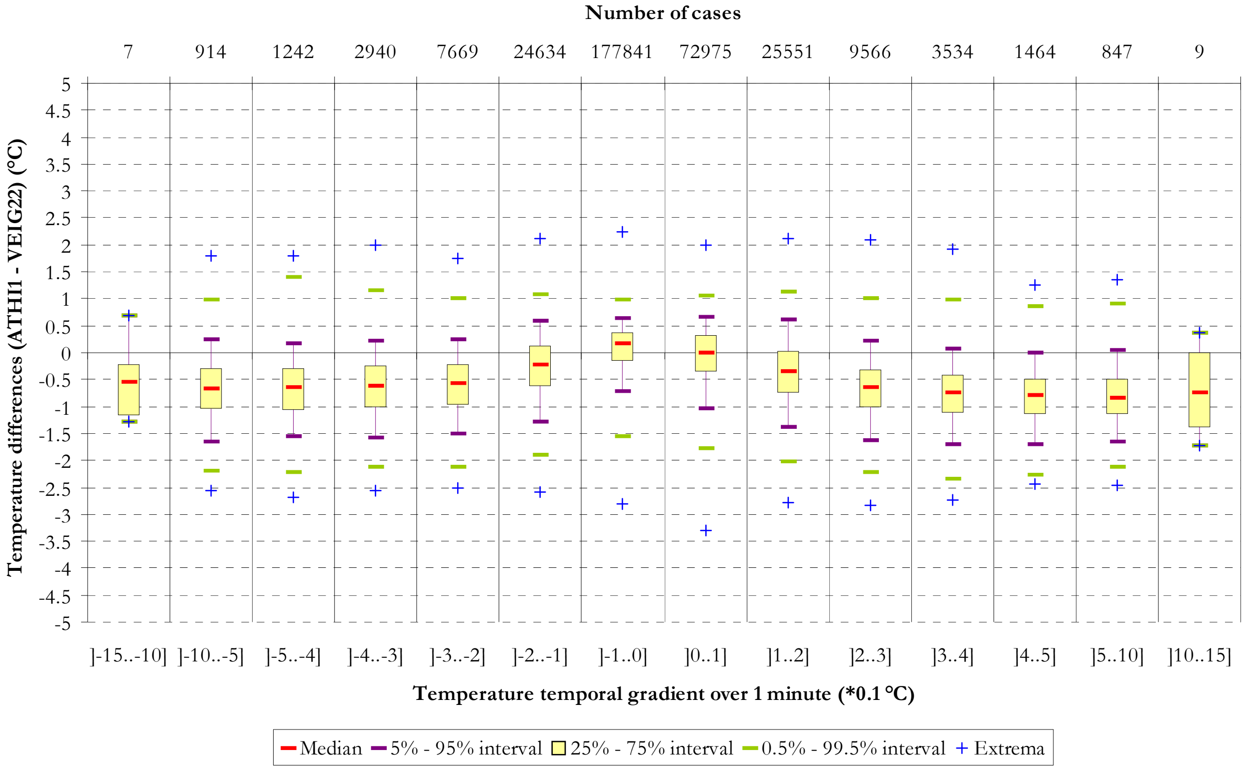


**Figure 19**

Screen #2:

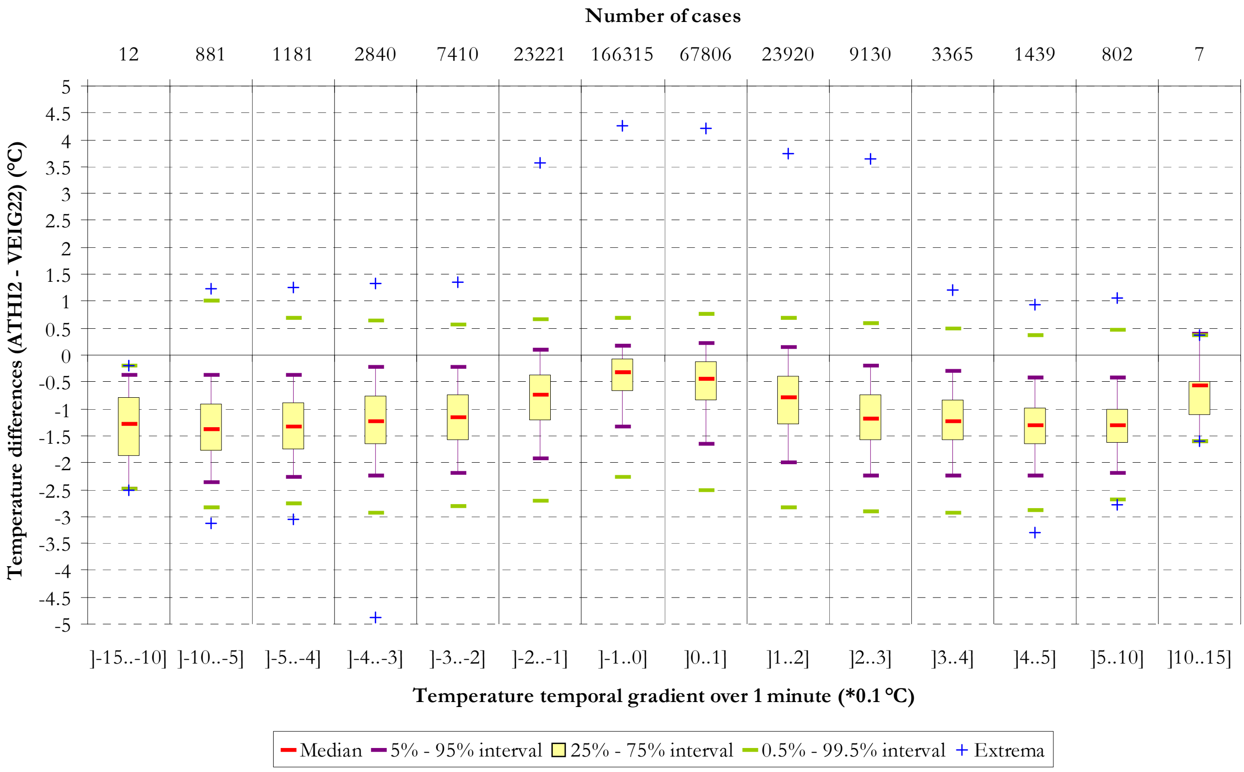


**Figure 20**

It seems that differences are reduced when temperature is stable. They are more important when temperature changes, increasing or decreasing. Thies sensors are colder than the reference.

## QUALITY CONTROL INFORMATION

### DATA AVAILABILITY

The intercomparison period extends from the 1st of November 2008 to the 1st of November 2009. The theoretical number of 1-minute data is 525600.

The next table sums up the total number of data for each screen and for each possible QC flag.

**Table 3**

| **QC flag** | ATHI1 | ATHI2 |
|---|---|---|
| 0 (good) | 339844 | 321186 |
| 1 (inconsistent) | 0 | 0 |
| 2 (doubtful) | 0 | 0 |
| 3 (erroneous) | 0 | 0 |
| 7 (missing) | 185756 | 204414 |

The main reason for missing data is frequent failures of the acquisition software, not problems of the sensors

### MAINTENANCE

No actions done during the intercomparison period

# TU 20 AS CAE
# – Italy –
# SCAE

**TECHNICAL SPECIFICATIONS (PROVIDED BY THE MANUFACTURER)**

Dimensions: Length 28 cm x Width 28 cm x Height 27 cm

Weight: 1.2 kg

Material/Structure: painted duralinium

Estimated radiation error: < 0.2°C

Aspiration rate (in case of artificially ventilated screen/shield): naturally ventilated

Power supply: 12 V


**Figure 1**

## OVERVIEW

This screen has a double shield to protect the sensors against the radiation. To improve the natural ventilation, the external shield is partly opened in one direction and must be oriented towards north (in northern hemisphere), to avoid any direct solar radiation on the internal shield.

Though this constraint was indicated in the documentation, the two sensors were mistakenly oriented towards south and the results obtained are not significant at all for the temperature measurements.

Therefore, it was decided in agreement with the manufacturer to skip any data from these screens and the results, non significant at all of this equipment, are excluded from this report, both for temperature and relative humidity.

# APPENDIX 2

## Humidity Measuring Instruments

LBOM

VFIS

SVAI

UHMP

UTES

VTHY

VROT

SCAE

*This page left intentionally blank.*

# HMP45DB VAISALA
# – Australia –
# LBOM

## TECHNICAL SPECIFICATIONS (PROVIDED BY THE MANUFACTURER)

Dimensions: Length 30 cm x Diameter 4 cm
Principle of operation: Humicap 180 capacitive sensor
Accuracy: ± 2 % RH (10..90% RH) at 20°C
Power supply: 7..30 VDC
Outputs: 0..1 V

**Figure 1**

This sensor was installed in LBOM screen:

**Figure 2**

## OVERVIEW

98% of the measurements were found within ±3% of the Thygan reference.

Medians of differences with UHMP2 reference show small variations. Differences are positive in most of the cases. Higher values are obtained for low values of relative humidity. Dispersion seems to increase with increasing values of UHMP2 relative humidity, except the higher class (maybe less reliable because of the small number of data). Differences with VTHY2 reference are greater and show large variations. The dispersion is also higher. But numbers of data are quite small for each class.

Medians of differences with UHMP2 increase with higher temperatures. At the same time, dispersion decreases.

The highest differences are obtained for temperatures above 25°C and humidity values lower than 50%. The HMP45BD sensor in screen LBOM gives relative humidity values higher (nearly 1 percentage point more) than the reference.

Variations along the intercomparison period are quite low. No drift versus the reference is detected.

## CALIBRATION INFORMATION

The sensor was received calibrated by Australia in 2007. No further calibration was performed.

## COMPARISON WITH THE REFERENCE

Thygan sensor #2 was first chosen as the reference for humidity measurements. But it was not available after April 2009. That is why a second reference was selected, which is the average of two HMP45D probes from Vaisala, when the difference between both values is lower than 1 percentage point of relative humidity.

For more details about the choice of references for humidity measurement, please refer to part 5.5.1 of the final report.

### HISTOGRAM OF DIFFERENCES

The histograms of differences between LBOM and the references are plotted, using 1-minute quality checked data for the whole period of the intercomparison. Differences are plotted by steps of 1 %. The vertical axis is the frequency in percent for each class of differences.

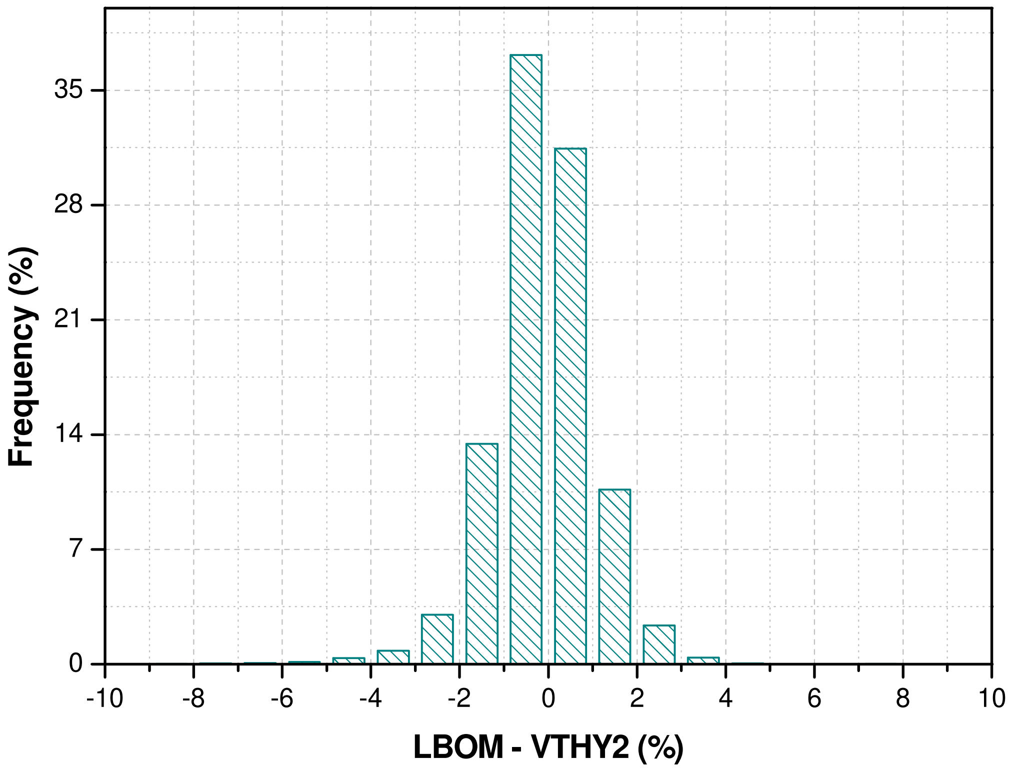


**Figure 3**

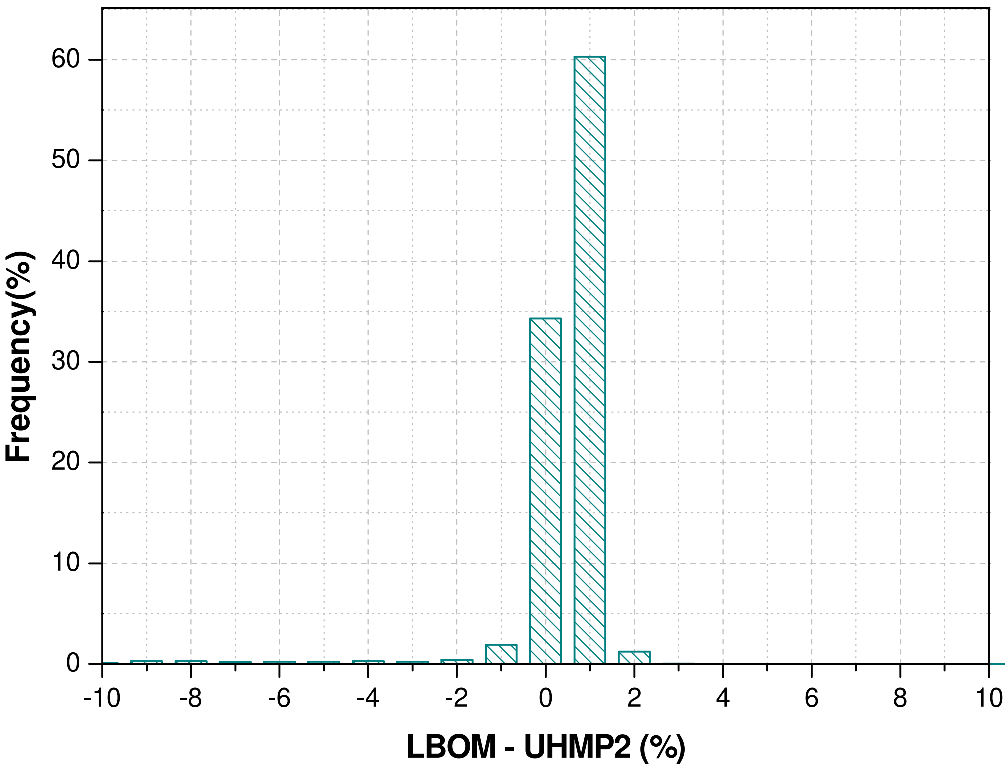


**Figure 4**

TABLE

The table 1 indicates the percentage of data that differ by less than 3 (and 6) % from the reference considered (VTHY2 or UHMP2).

**Table 1**

| | VTHY2 | | UHMP2 | |
|---|---|---|---|---|
| | [-3..3] | [-6..6] | [-3..3] | [-6..6] |
| LBOM | 98.0 | 99.8 | 99.7 | 99.8 |

## INFLUENCE OF HUMIDITY

The distributions of differences between LBOM and the references are plotted, using 1-minute quality checked data for the whole period of the intercomparison. Differences are classified according the reference relative humidity.

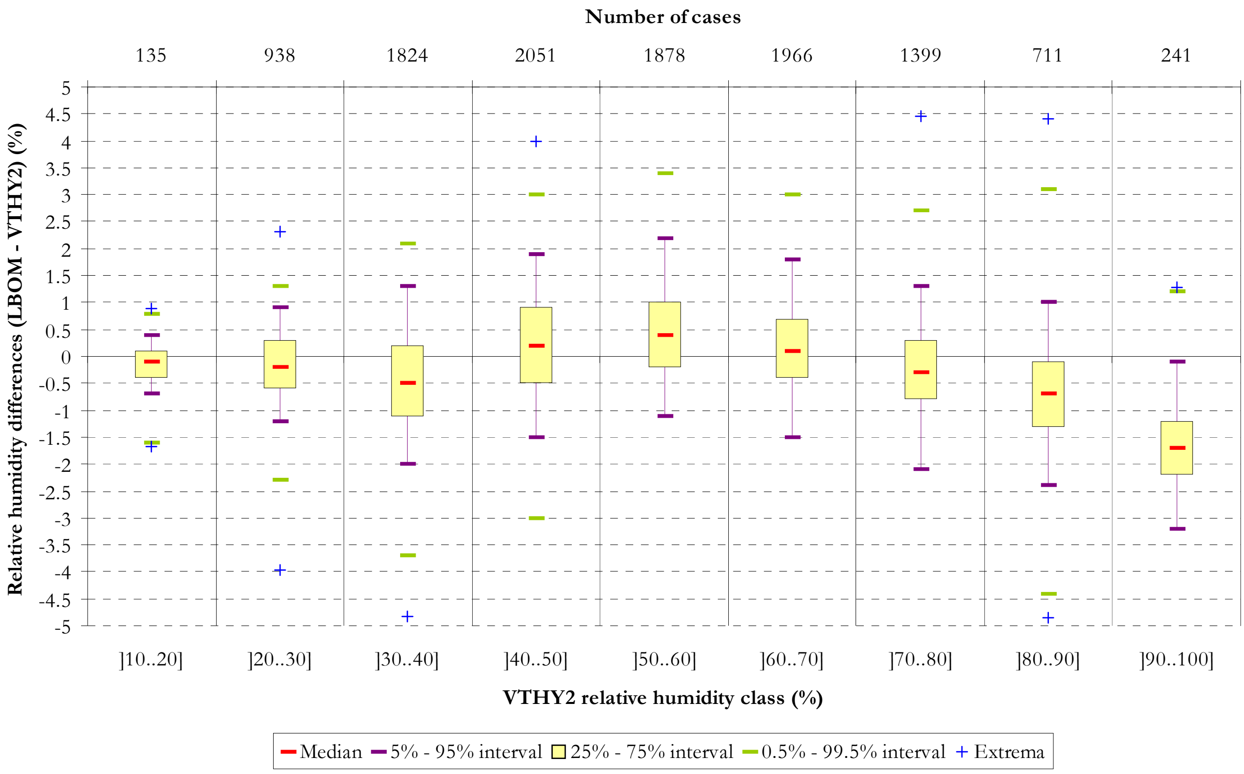


**Figure 5**

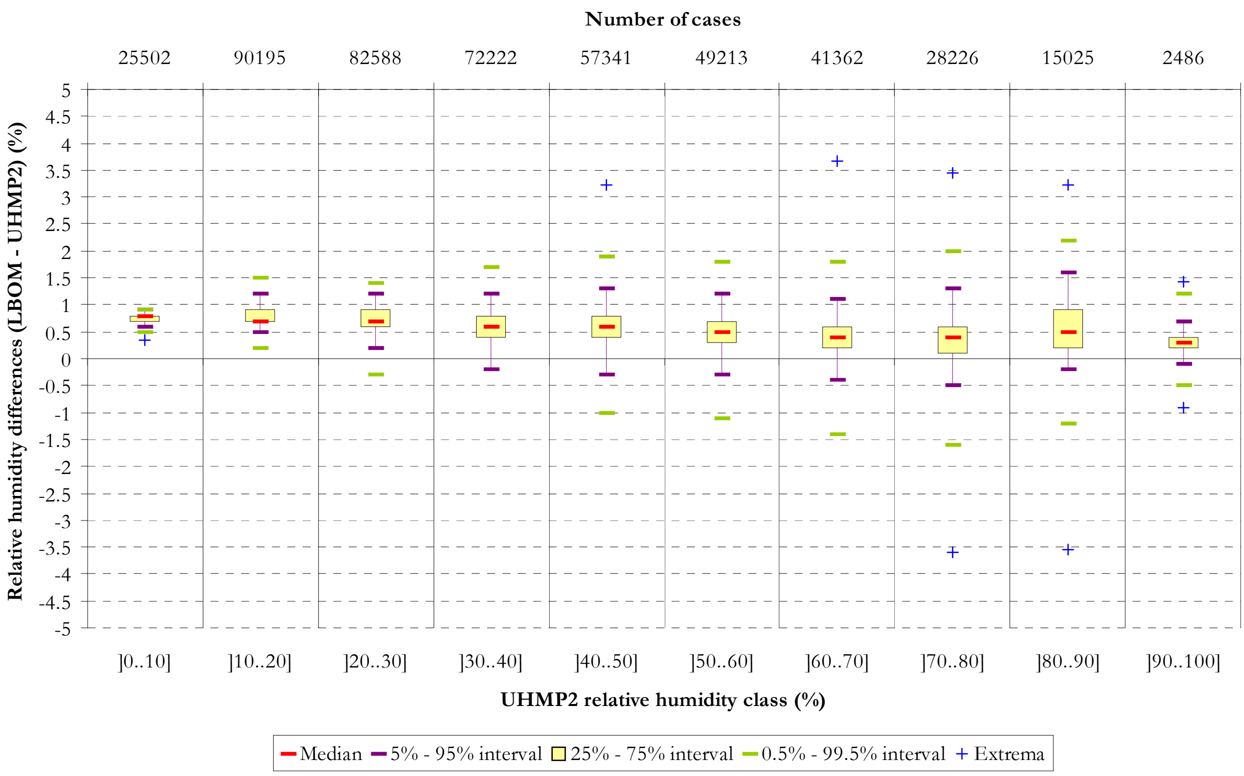


**Figure 6**

Medians of differences with UHMP2 reference show small variations. Differences are positive in most of the cases. Higher values are obtained for low values of relative humidity. Dispersion seems to increase with increasing values of UHMP2 relative humidity, except for class 90-100 (maybe less reliable because of the small number of data).

Differences with VTHY2 reference are greater and show large variations. The dispersion is also higher. But numbers of data are quite small for each class.

## INFLUENCE OF TEMPERATURE

The distributions of differences between LBOM and the references are plotted, using 1-minute quality checked data for the whole period of the intercomparison. Differences are classified according VEIG22 temperature.

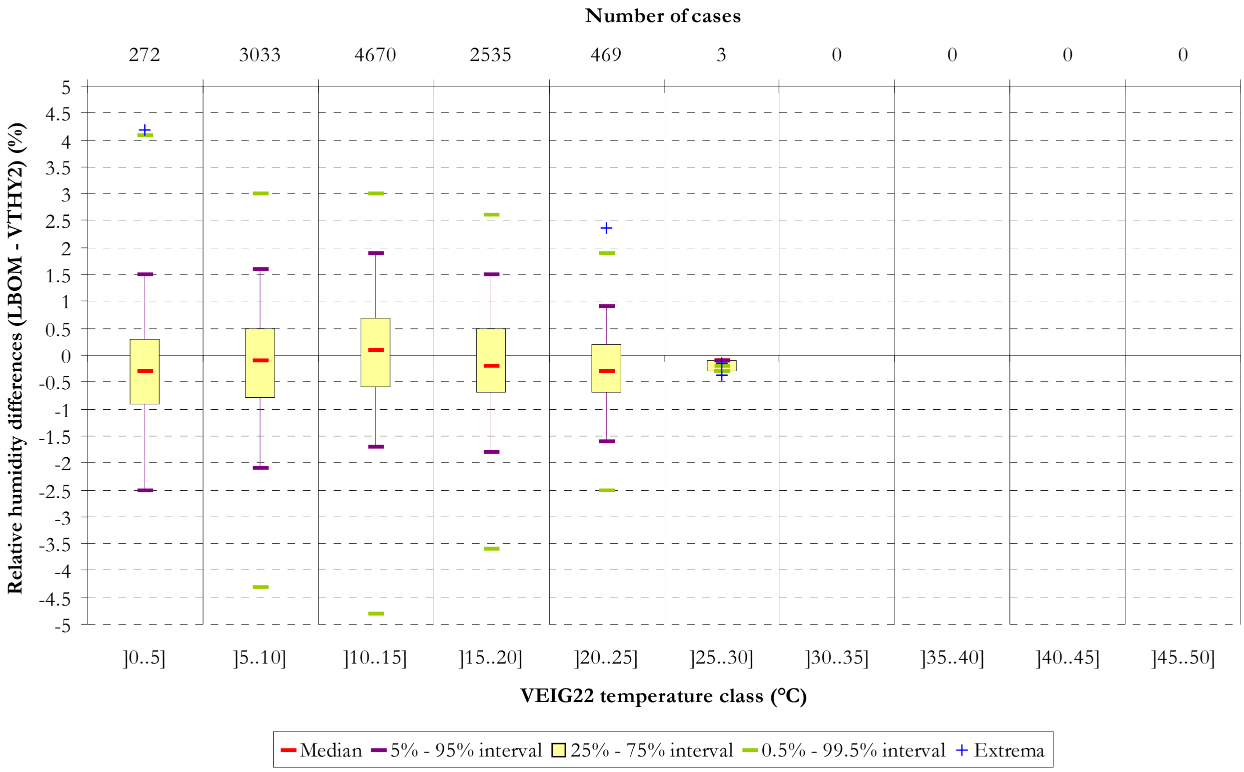


**Figure 7**

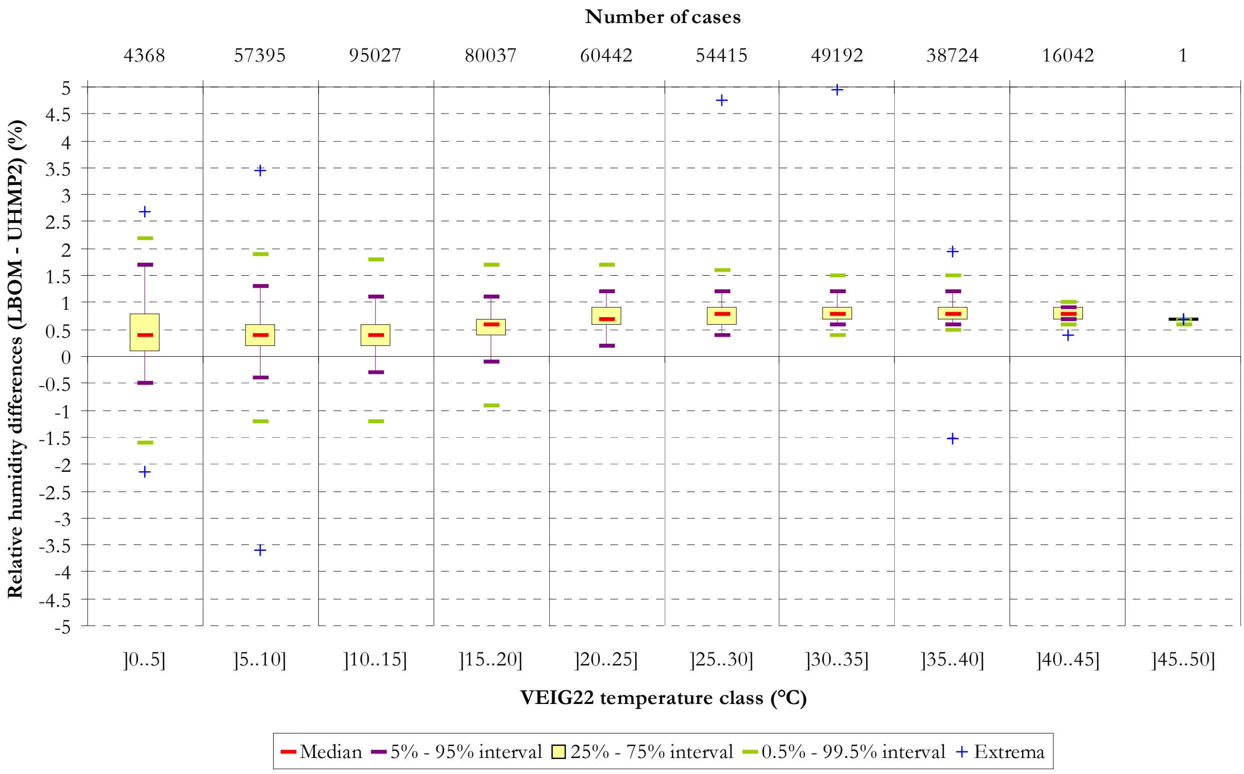


**Figure 8**

Medians of differences with UHMP2 slightly increase with higher temperatures. At the same time, dispersion decreases.

## COMBINED INFLUENCE OF TEMPERATURE AND RELATIVE HUMIDITY

The medians of differences between LBOM and UHMP2 reference are represented here with a contour plot. The VEIG22 temperature is on the X-axis and the reference relative humidity is on the Y-axis. Medians are used in all cases, provided that at least one data is available for both conditions of temperature and humidity considered.

The scale was chosen so as to be the same for all relative humidity sensors.

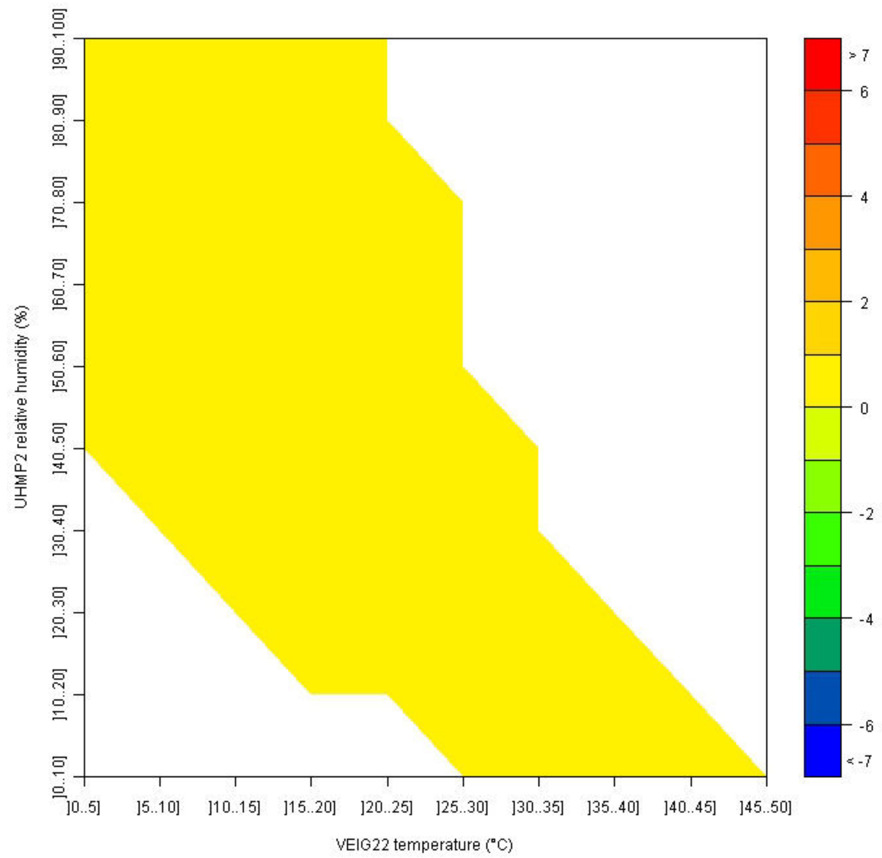


**Figure 9**

All contour plots are very uniform around the 0 value. No combined effect of temperature and humidity can be seen.

## TIME DRIFT

The distributions of differences between LBOM and the references are plotted, using 1-minute quality checked data for the whole period of the intercomparison, by step of one month. Reference relative humidity between 20% and 50% are only considered here: this is the common range in order to have data every month, without introducing influence of humidity itself.

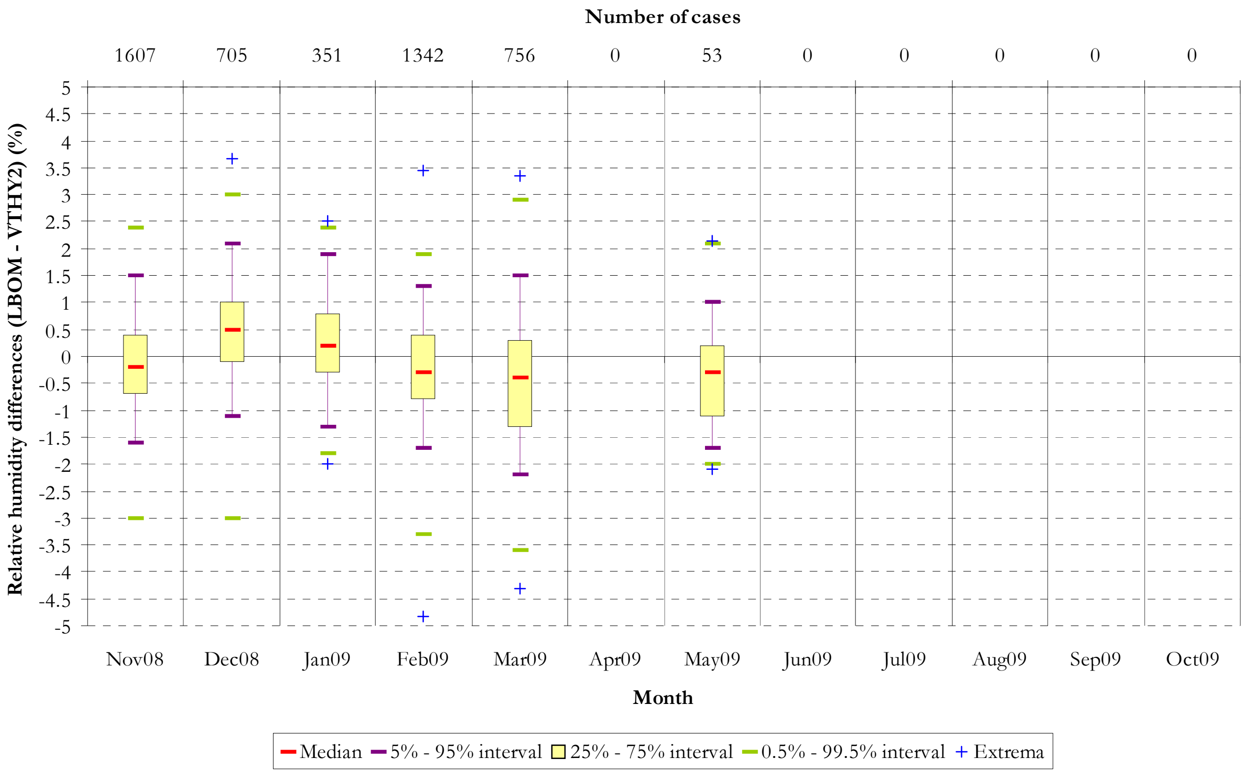


**Figure 10**

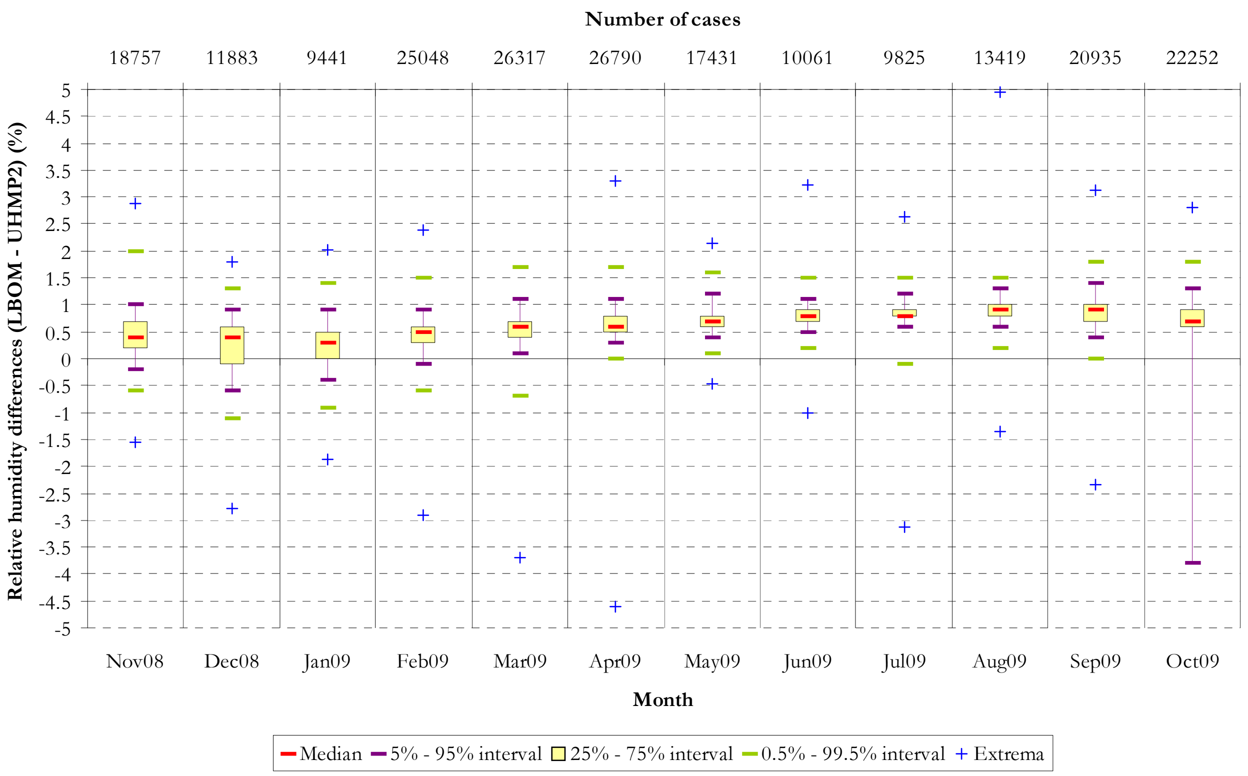


**Figure 11**

Variations along the intercomparison period are quite low. The difference between the medians of October 2009 and November 2008 is less than 0.5 percentage point. The dispersion has not much changed, so no drift versus the reference is detected.

## QUALITY CONTROL INFORMATION

### DATA AVAILABILITY

The intercomparison period extends from the 1st of November 2008 to the 1st of November 2009. The theoretical number of 1-minute data is 525600.

The table 2 sums up the total number of data for each sensor and for each possible QC flag.

**Table 2**

| QC flag | LBOM |
|---|---|
| 0 (good) | 503133 |
| 1 (inconsistent) | 0 |
| 2 (doubtful) | 7 |
| 3 (erroneous) | 3665 |
| 7 (missing) | 18795 |

### MAINTENANCE

No action done during the intercomparison period.

# 431401 FISCHER
# – Germany –
# VFIS

## TECHNICAL SPECIFICATIONS (PROVIDED BY THE MANUFACTURER)

Dimensions: 115x60x40mm; Sensing element holder: 148 mm x Ø12 mm

Principle of operation: capacitive humidity sensor. Temperature measurement: Pt100 with 4-wire connection

Accuracy: Humidity: ± 2 % (25°C, 5 ... 95 %). Temperature: ± 0.3 K (-30...70 °C)

Power supply: 8..28 VDC

Outputs: 1 output 0..1V


**Figure 1**

These sensors were installed in VFIS screen, provided by same manufacturer:

**Figure 2**

## OVERVIEW

Both sensors have the same behavior globally.

Sensor #2 gives higher values than sensor #1, around 2% more. This can not be explained by calibration, performed in April 2007, more than 18 months before the beginning of intercomparison. Moreover, the higher the humidity, the higher the dispersion (25%-50% interval) between both sensors.

For sensor #1, about 80 % of the measurements were found within ±3% of the reference.
For sensor #2, about 96 % of the measurements were found within ±3% of the reference.

The medians of differences are stabilized for relative humidity below 50%. Above this value, medians of differences increase with humidity.

Medians of differences decrease when temperature increases, for temperatures below 15°C. Above this temperature, medians level off.

Medians of differences were quite constant during the intercomparison period, around -2% for VFIS1, around 0% for VFIS2 (within more or less 0.5%), except in February and March 2009. Dispersion of differences remains quite stable all year long.

## CALIBRATION INFORMATION

Calibration by manufacturer (19 April 2007):

**Table 1**

| Sensor | Serial number | 23°C | | |
|---|---|---|---|---|
| | | 33% | 75% | 90% |
| VFIS1 | 188 | 0.3 | 0.8 | -1.5 |
| VFIS2 | 189 | 0.0 | -0.1 | -1.8 |

## COMPARISON OF BOTH SENSORS

The distribution of differences between VFIS1 and VFIS2 is plotted, using 1-minute quality checked data for the whole period of the intercomparison. Differences are classified according VFIS1 relative humidity.

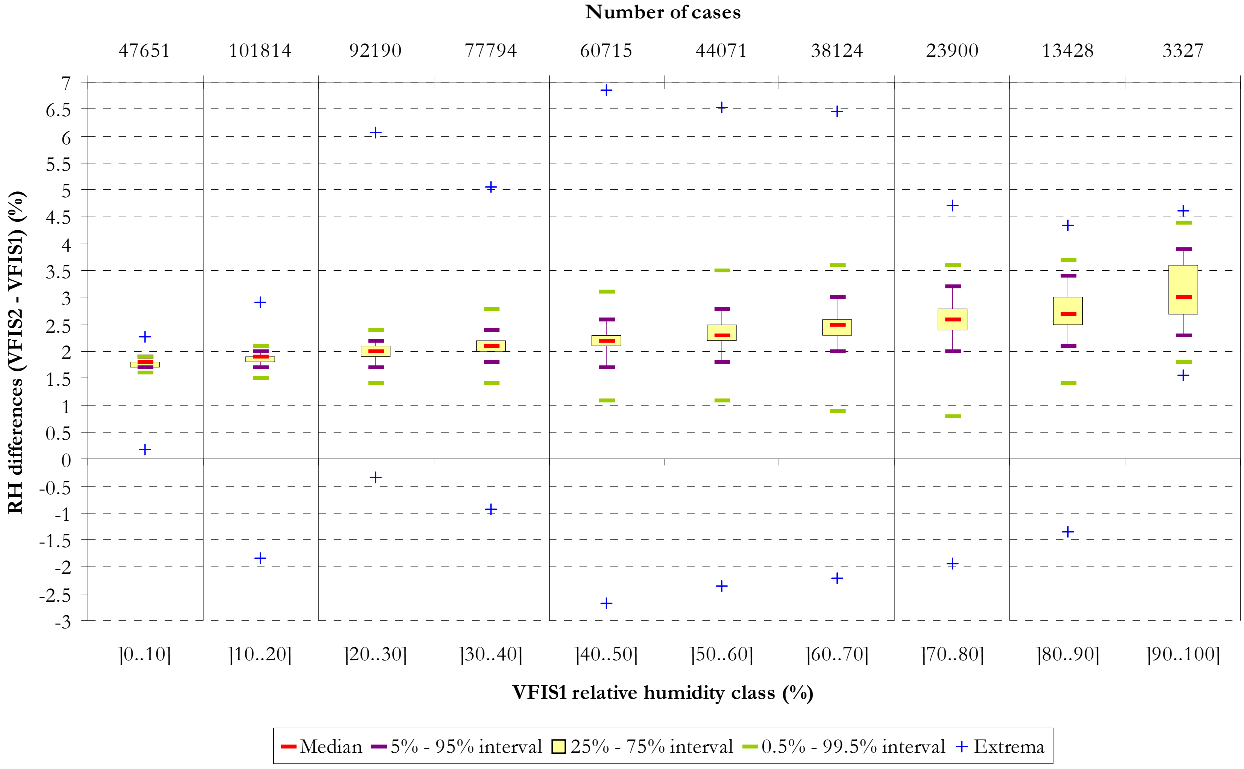


**Figure 3**

Sensor #2 gives higher values than sensor #1, around 2% more. Moreover, the higher the humidity, the higher the dispersion (25%-50% interval) between both sensors.

## COMPARISON WITH THE REFERENCE

Thygan sensor #2 was first chosen as the reference for humidity measurements. But it was not available after April 2009. That is why a second reference was selected, which is the average of two HMP45D probes from Vaisala, when the difference between both values is lower than 1 percentage point of relative humidity.

For more details about the choice of references for humidity measurement, please refer to part 5.5.1 of the final report.

### HISTOGRAM OF DIFFERENCES

The histograms of differences between VFIS and the references are plotted, using 1-minute quality checked data for the whole period of the intercomparison. Differences are plotted by steps of 1 %. The vertical axis is the frequency in percent for each class of differences.

Sensor #1:

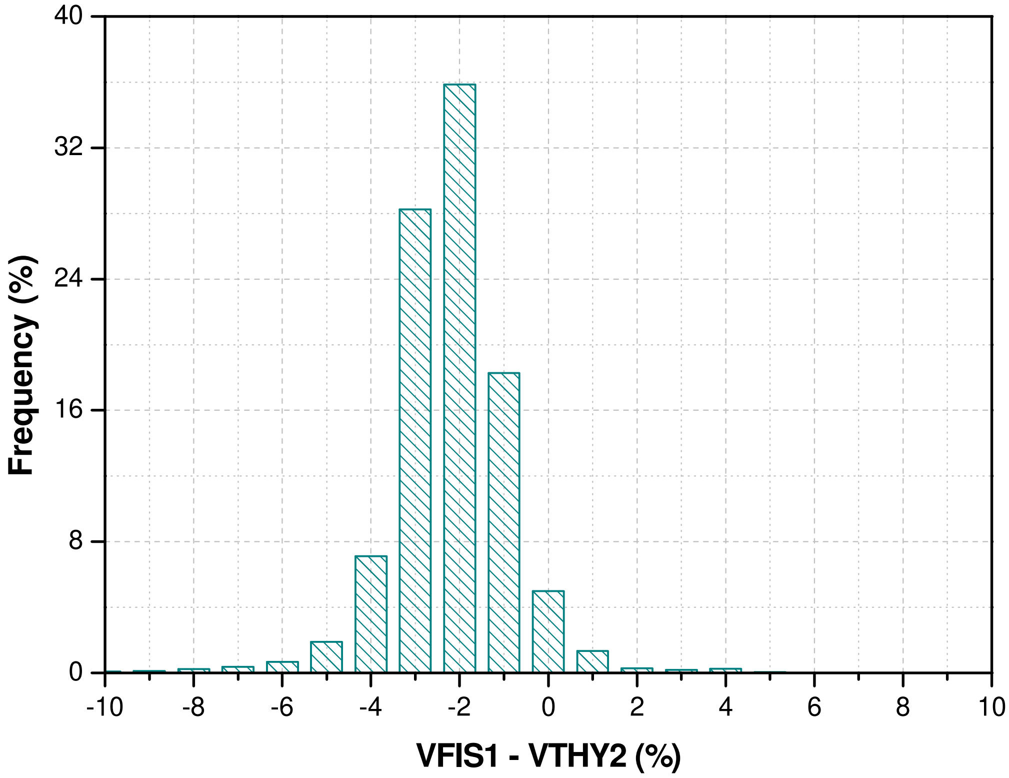


**Figure 4**

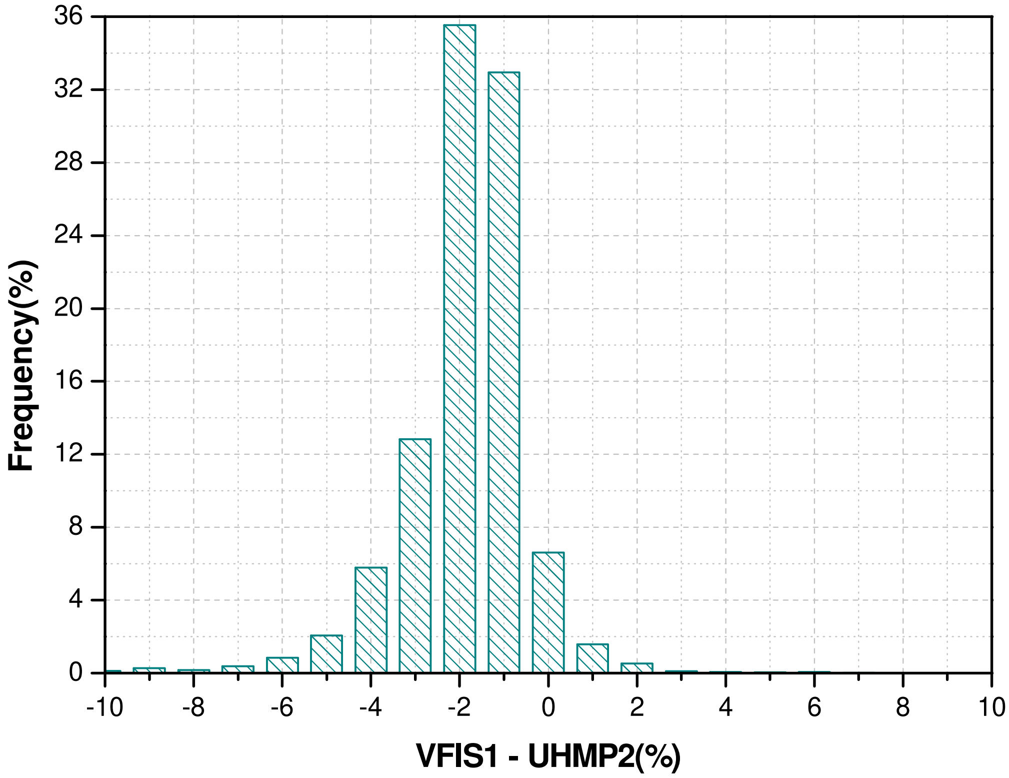


**Figure 5**

Sensor #2:

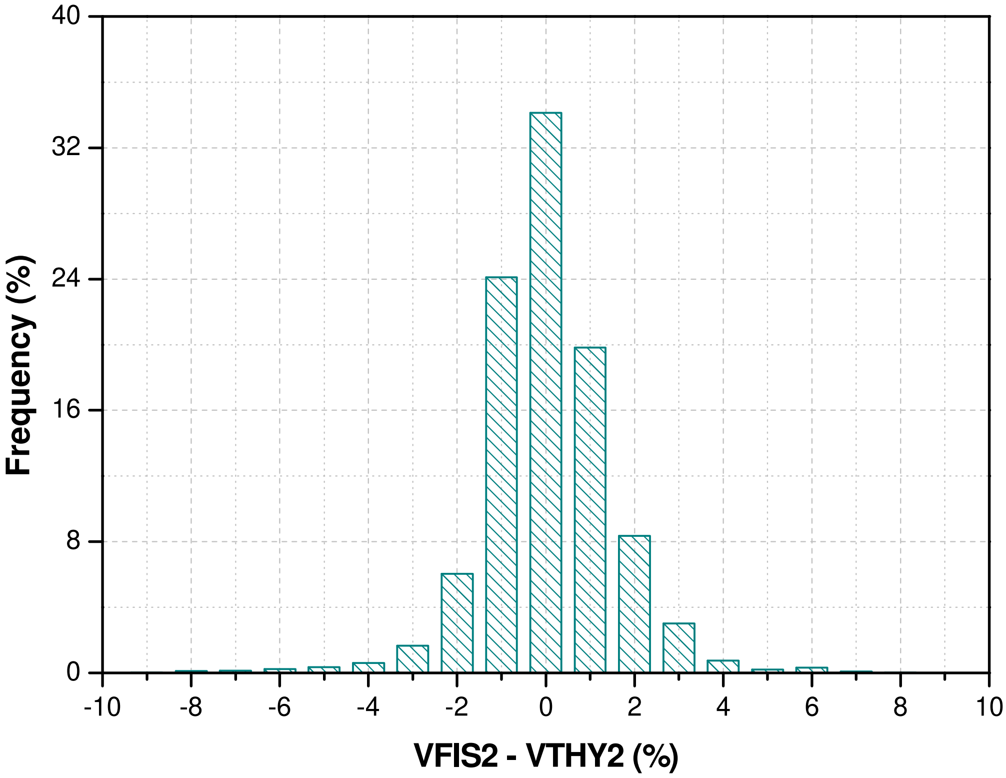


**Figure 6**

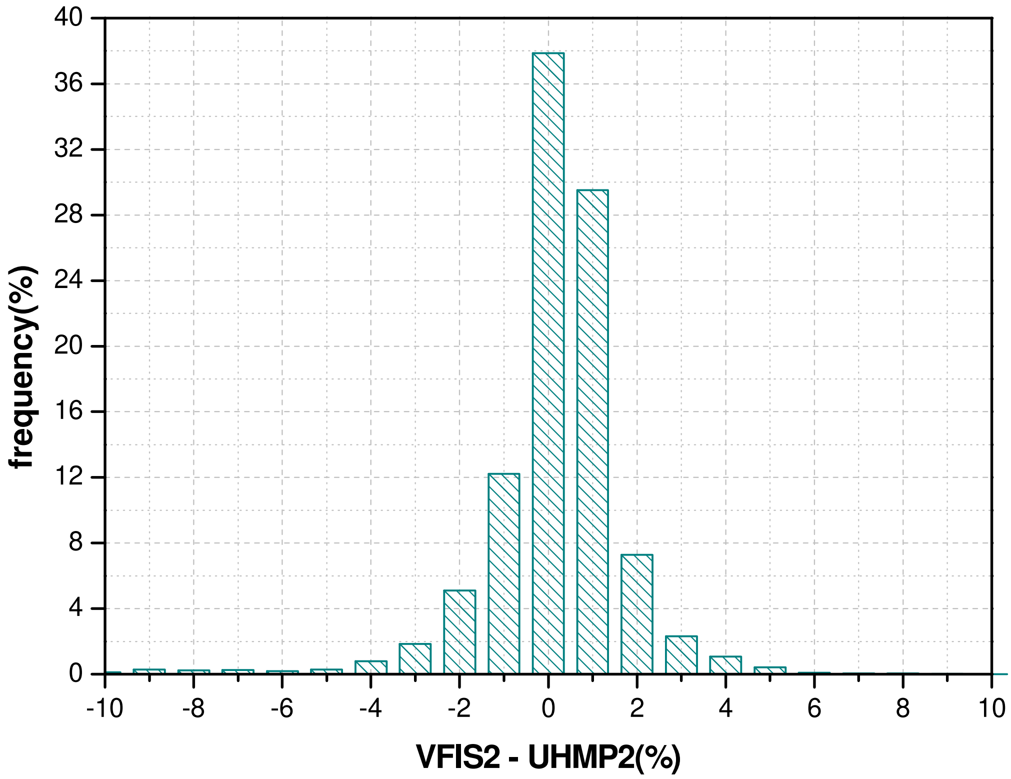


**Figure 7**

TABLE

The table 2 indicates the percentage of data that differ by less than 3% (and 6%) from the reference considered (VTHY2 or UHMP2).

**Table 2**

| | VTHY2 | | UHMP2 | |
|---|---|---|---|---|
| | [-3..3] | [-6..6] | [-3..3] | [-6..6] |
| VFIS1 | 73.9 | 98.8 | 85.3 | 99.3 |
| VFIS2 | 95.7 | 99.3 | 96.0 | 99.6 |

## INFLUENCE OF HUMIDITY

The distributions of differences between VFIS and the references are plotted, using 1-minute quality checked data for the whole period of the intercomparison. Differences are classified according the reference relative humidity.

## Sensor #1:

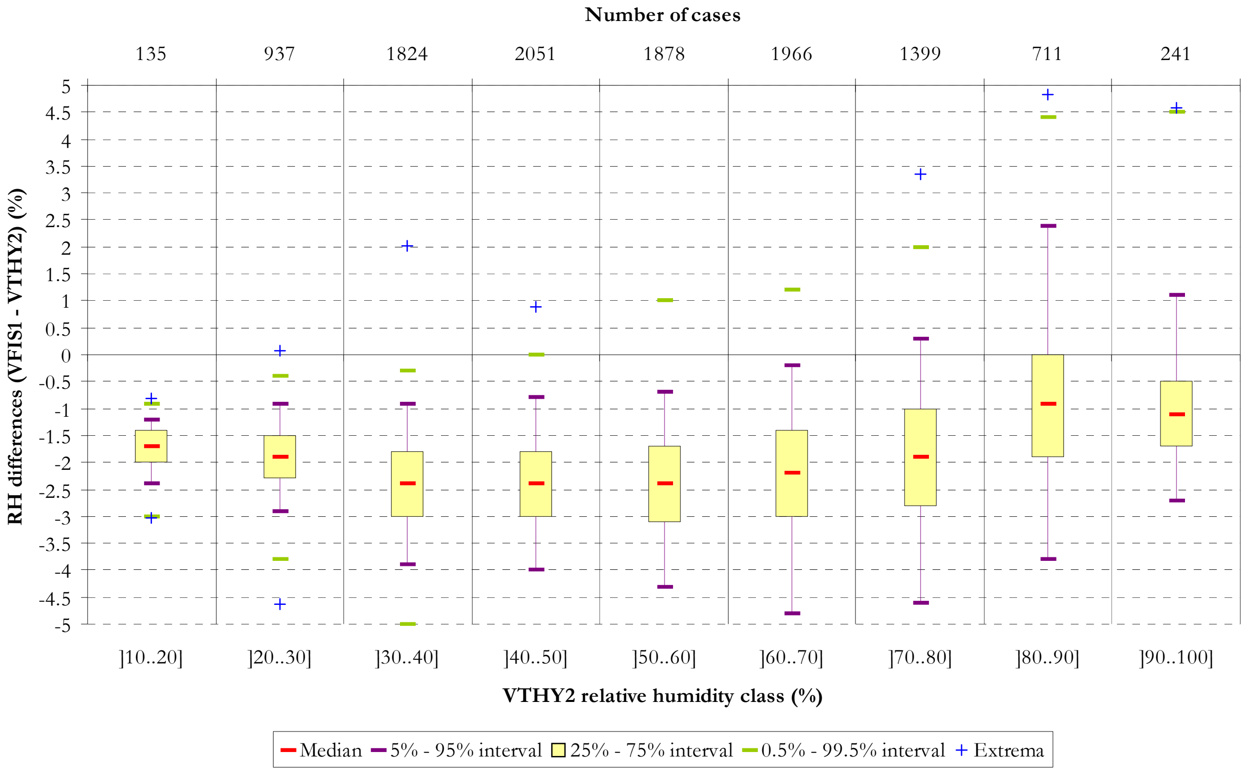


**Figure 8**

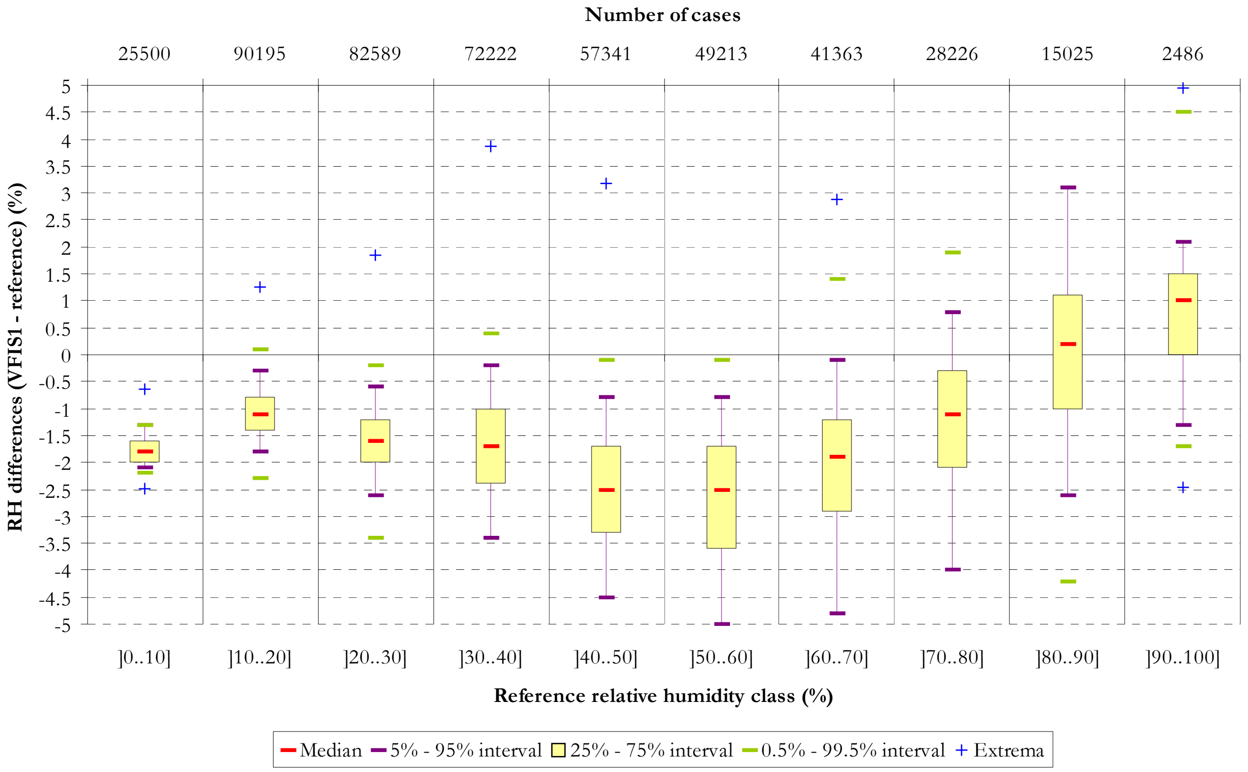


**Figure 9**

Sensor #2:

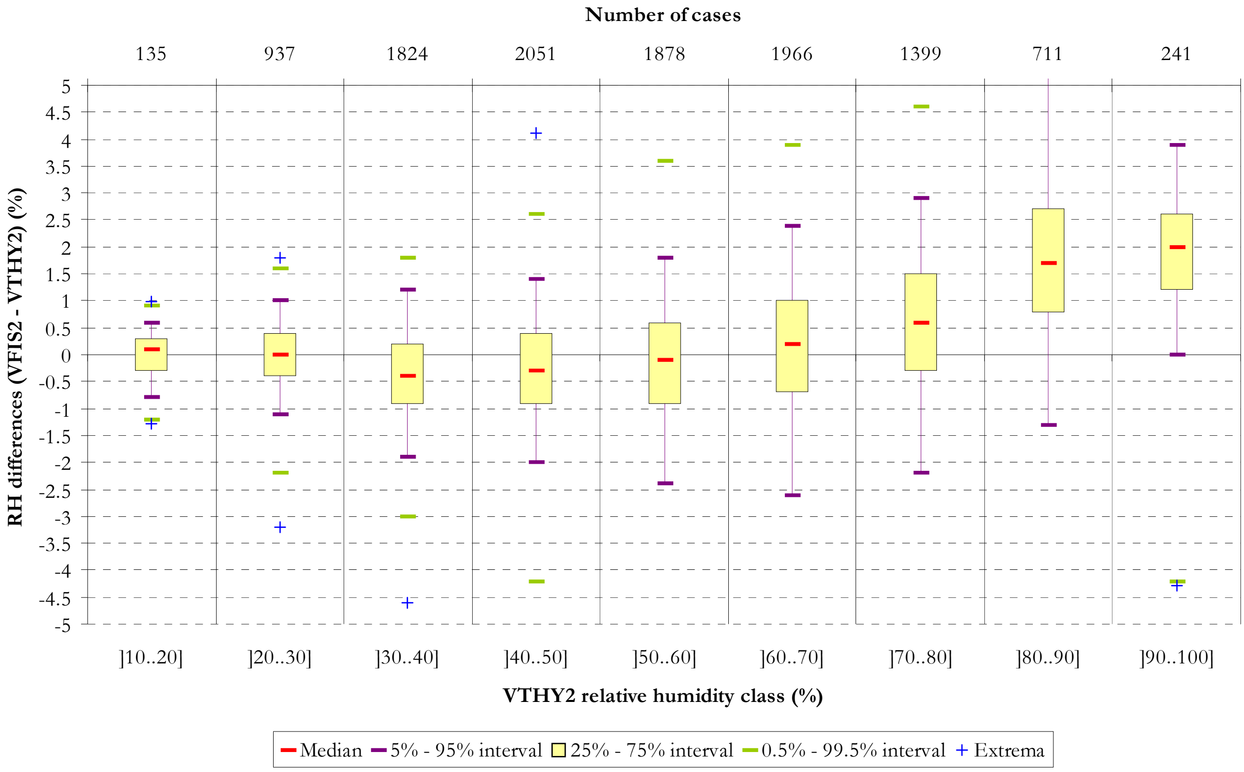


**Figure 10**

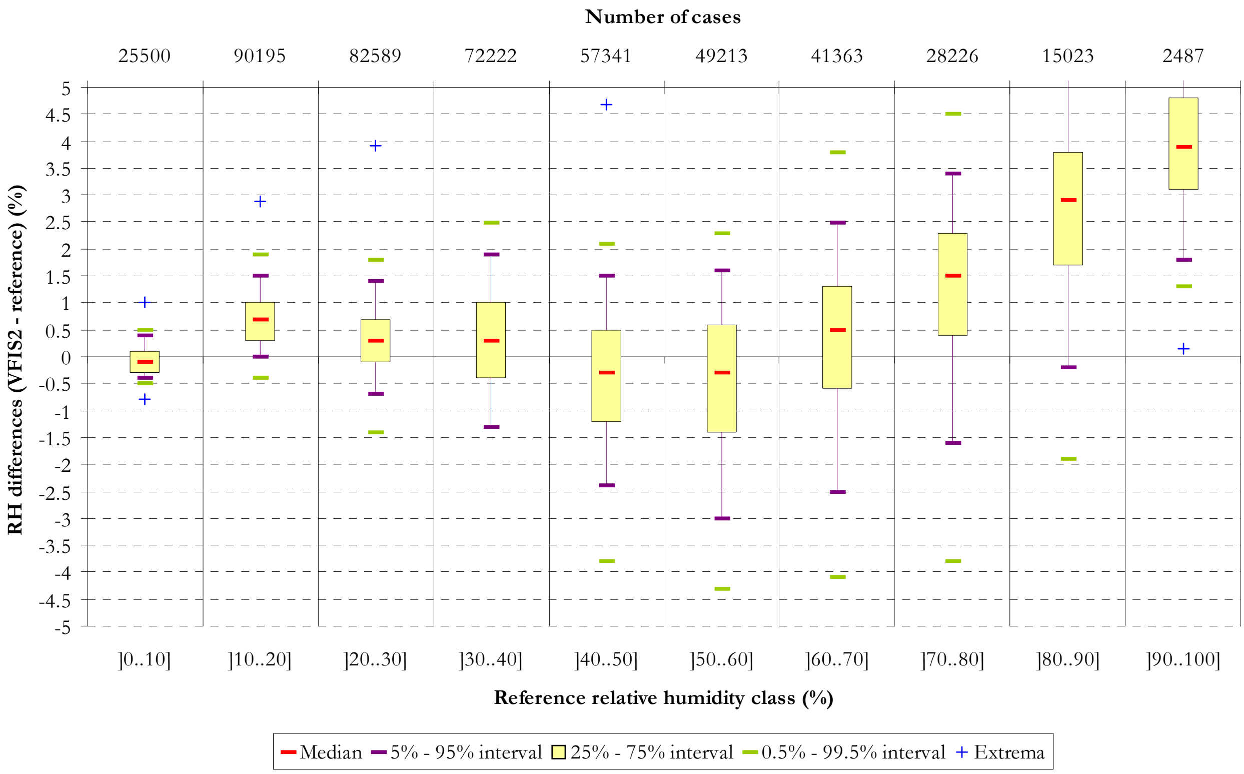


**Figure 11**

Both sensors have the same behavior globally. The medians of differences are stabilized for relative humidity below 50%. Above this value, medians of differences increase with humidity. VFIS2 shows values 2%higher than VFIS1.

The dispersion of differences is quite low for humidity values below 30% (the 25-75% interval width is less than 1 percentage point). Above 30%, the 25-75% interval width increases. It reaches 2.1% for the ]80..90%] class, for both sensors compared to UHMP reference.

## INFLUENCE OF TEMPERATURE

The distributions of differences between VFIS and the references are plotted, using 1-minute quality checked data for the whole period of the intercomparison. Differences are classified according VEIG22 temperature.

Sensor #1:

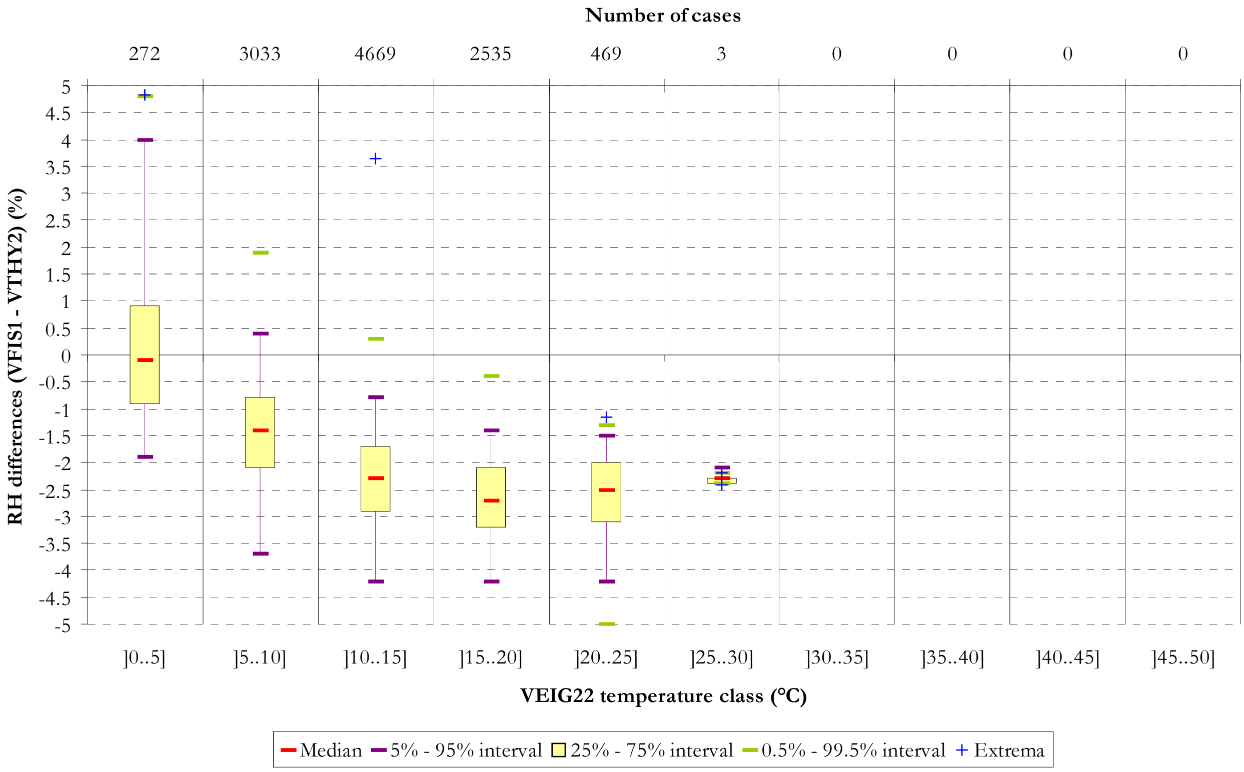


**Figure 12**

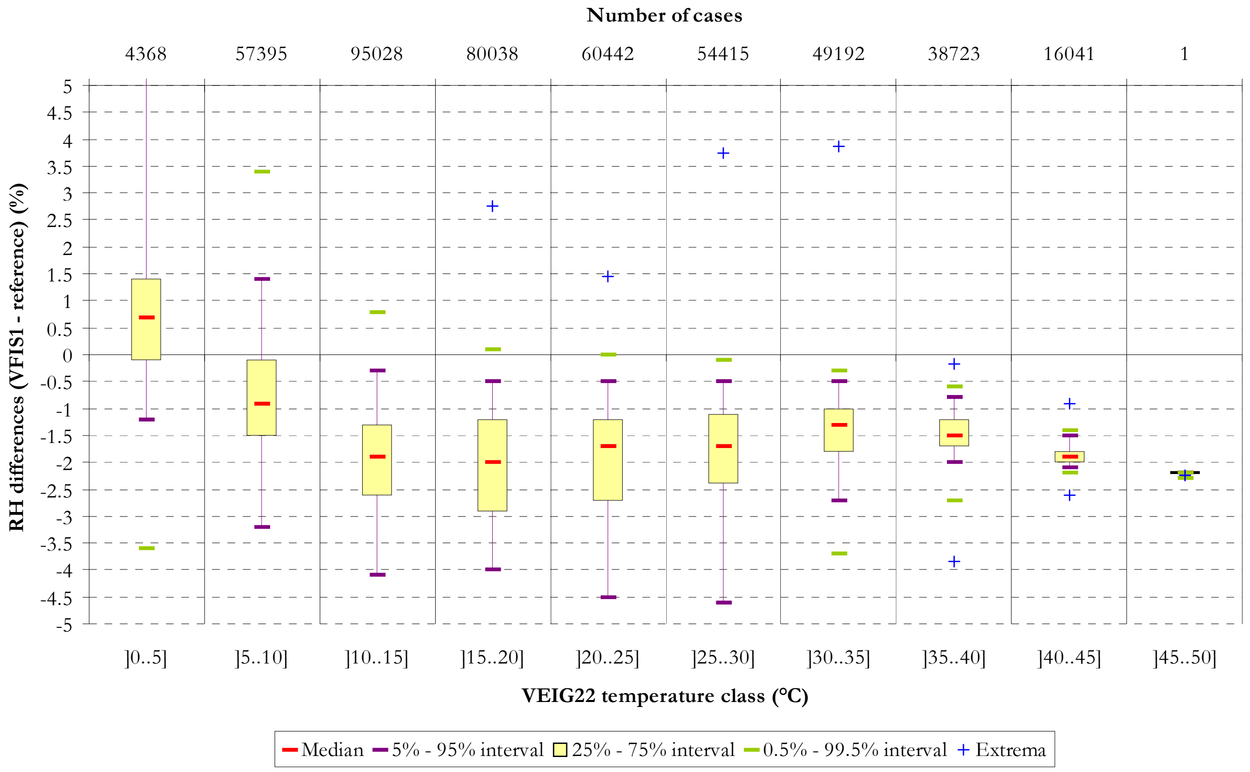


**Figure 13**

## Sensor #2:

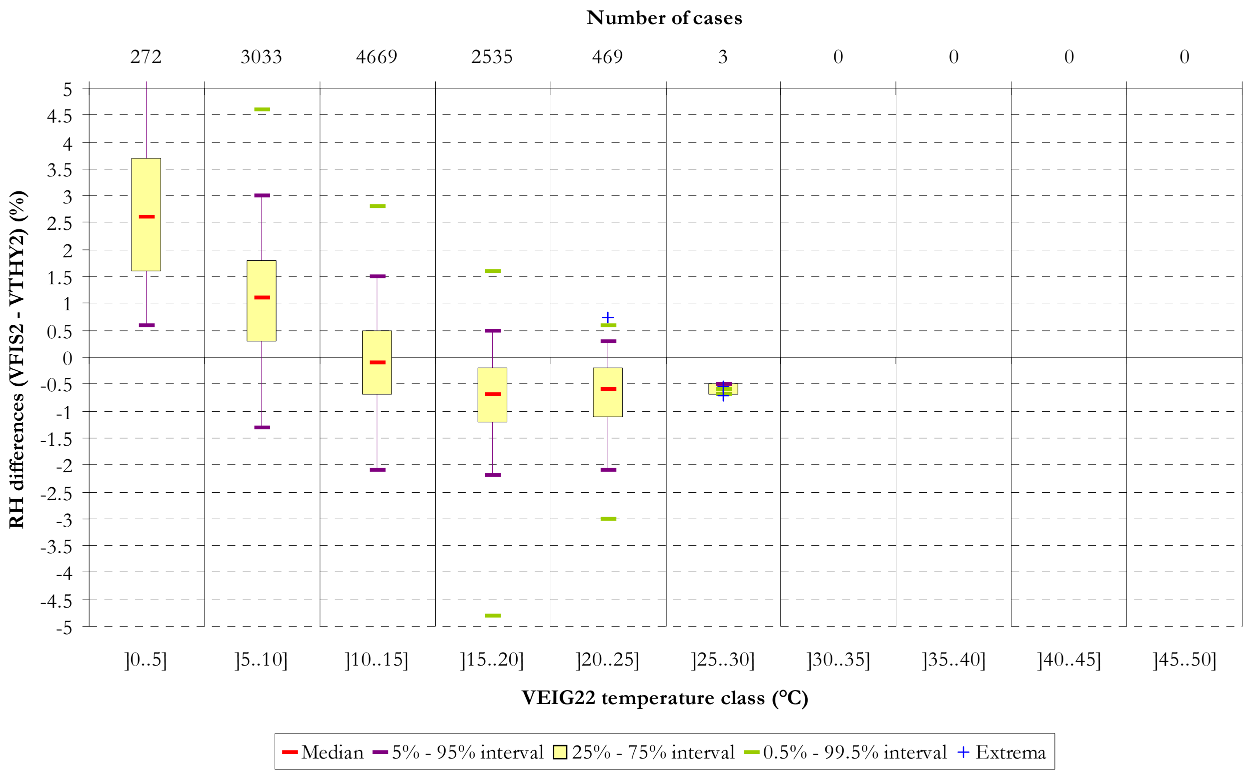


**Figure 14**

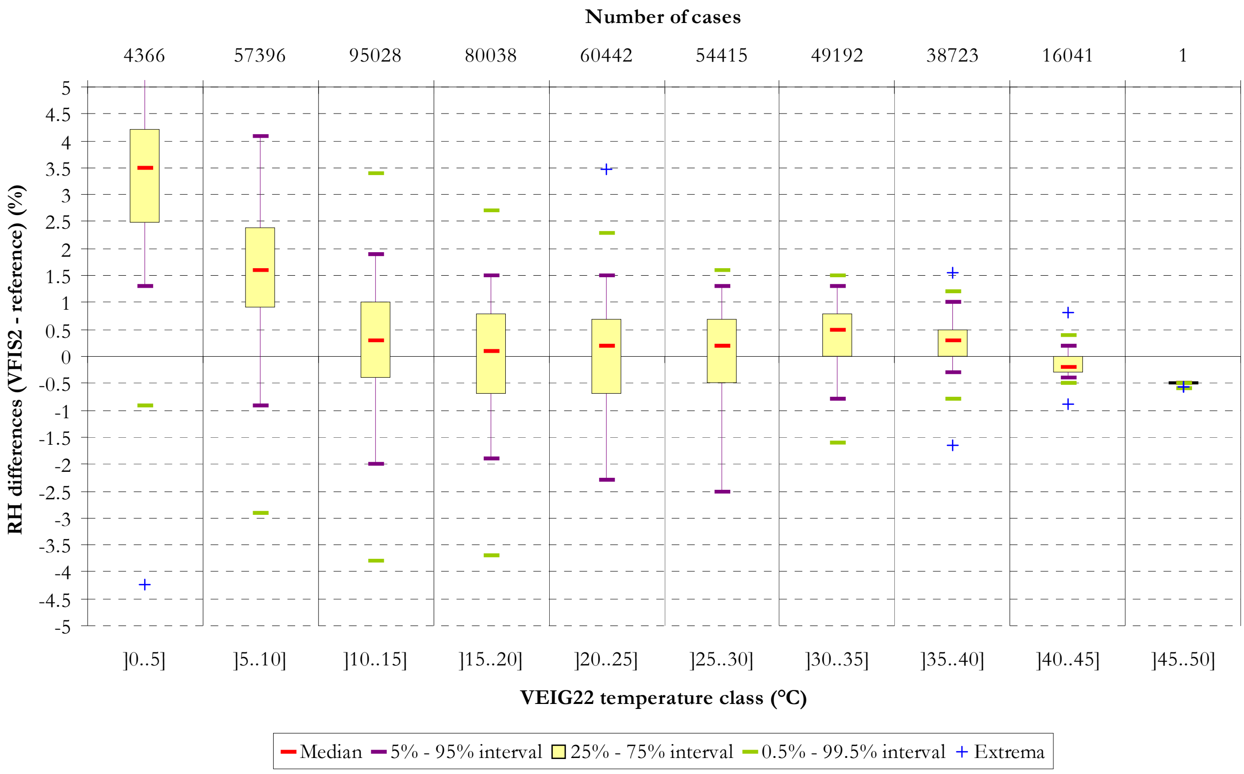


**Figure 15**

Here also, both sensors have the same behavior globally. Medians of differences decrease when temperature increases, for temperatures below 15°C. Above this value, medians level off around –2% for VFIS1, around 0% for VFIS2.

## COMBINED INFLUENCE OF TEMPERATURE AND RELATIVE HUMIDITY

The medians of differences between VFIS and UHMP reference are represented here with a contour plot. The VEIG22 temperature is on the X-axis and the reference relative humidity is on the Y-axis. Medians are used in all cases, provided that at least one data is available for both conditions on temperature and humidity considered.

The scale was chosen so as to be the same for all relative humidity sensors.

Sensor #1:

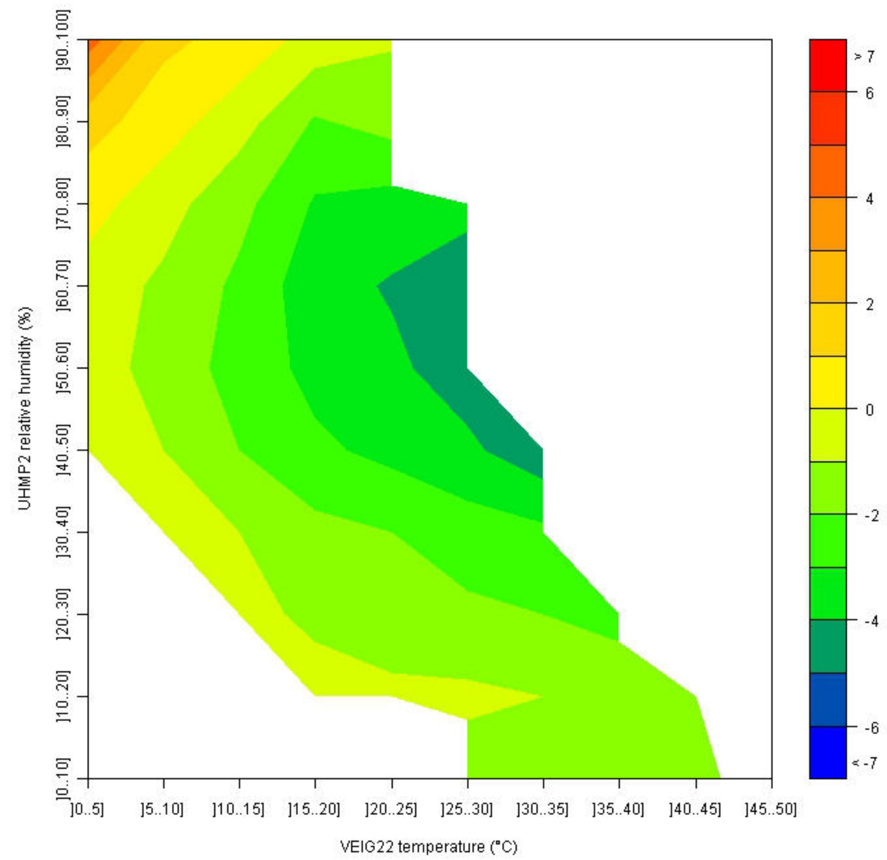


**Figure 16**

Sensor #2:

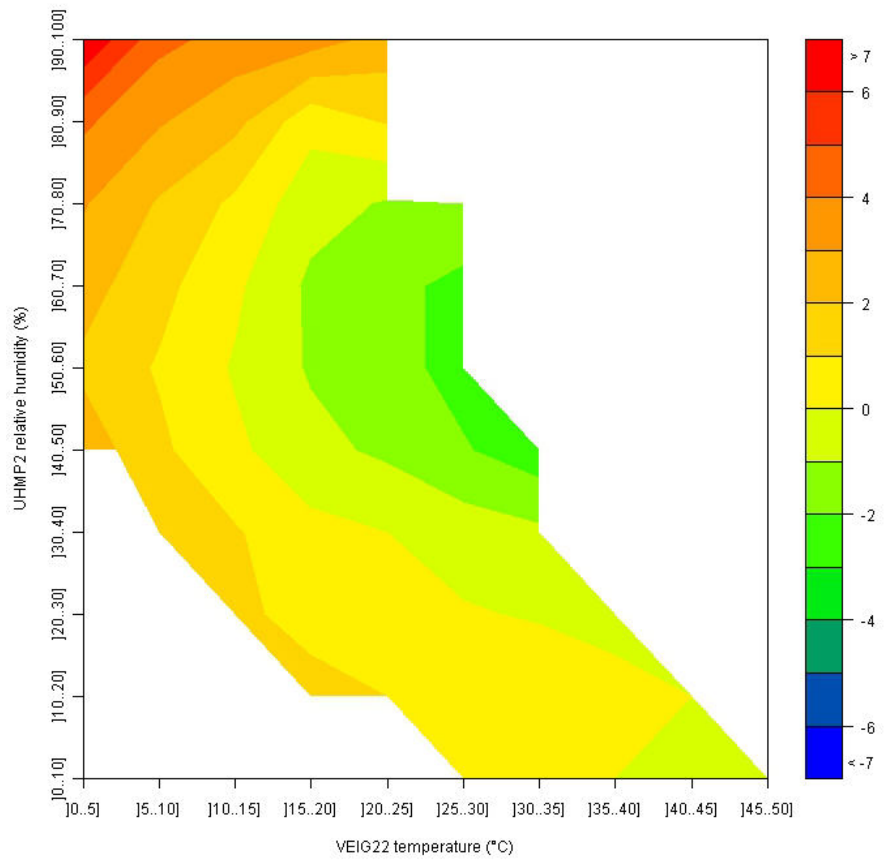


**Figure 17**

Both sensors show negative differences for temperatures between 25 and 30° and relative humidity values between 50% and 70%.

Differences are getting higher when temperature decreases and relative humidity increases.

## TIME DRIFT

The distributions of differences between VFIS and the references are plotted, using 1-minute quality checked data for the whole period of the intercomparison, by step of one month. Reference relative humidity between 20% and 50% are only considered here: this is the common range in order to have data every month, without introducing influence of humidity itself.

Sensor #1:

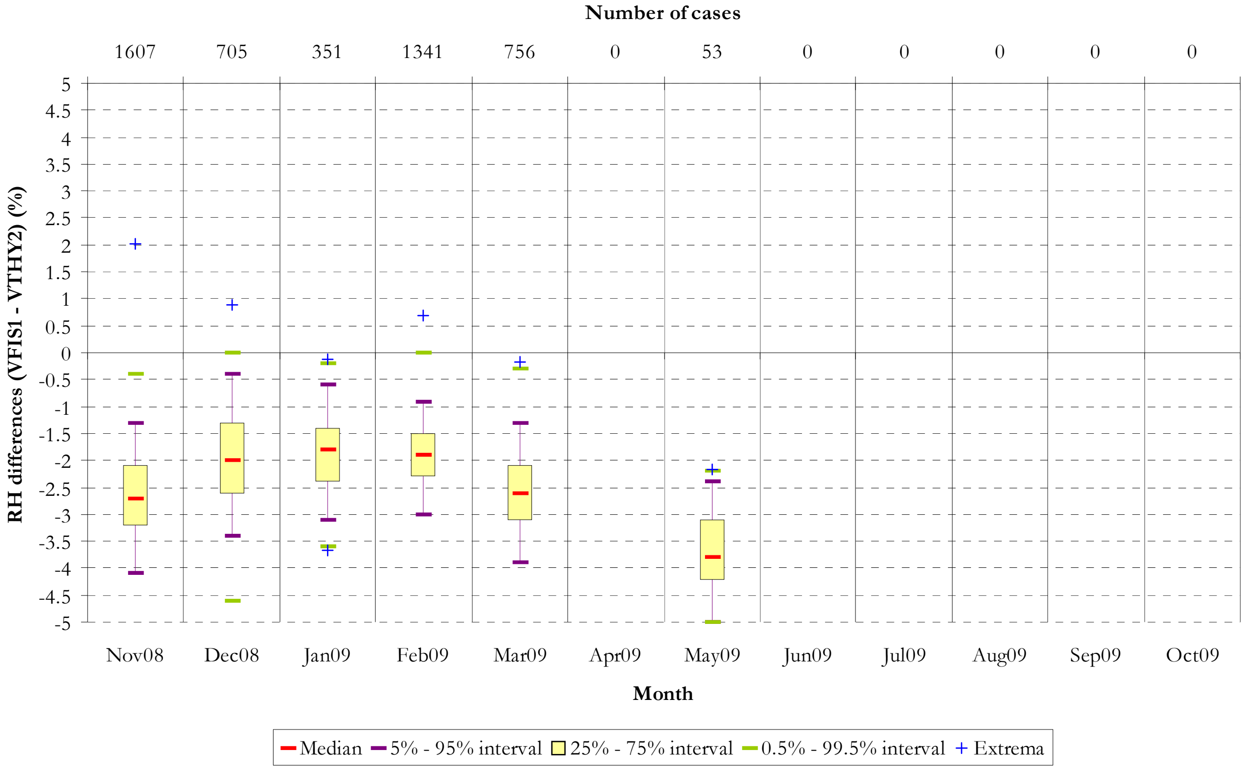


**Figure 18**

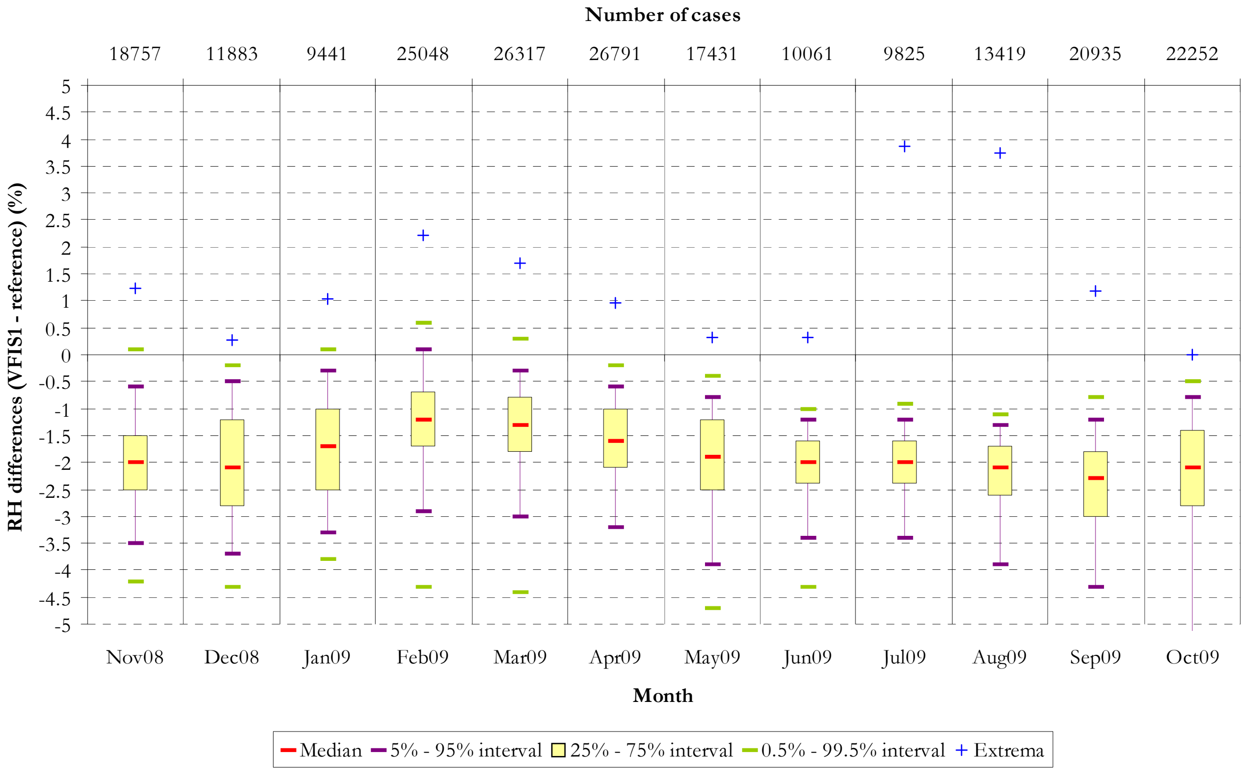


**Figure 19**

Sensor #2:

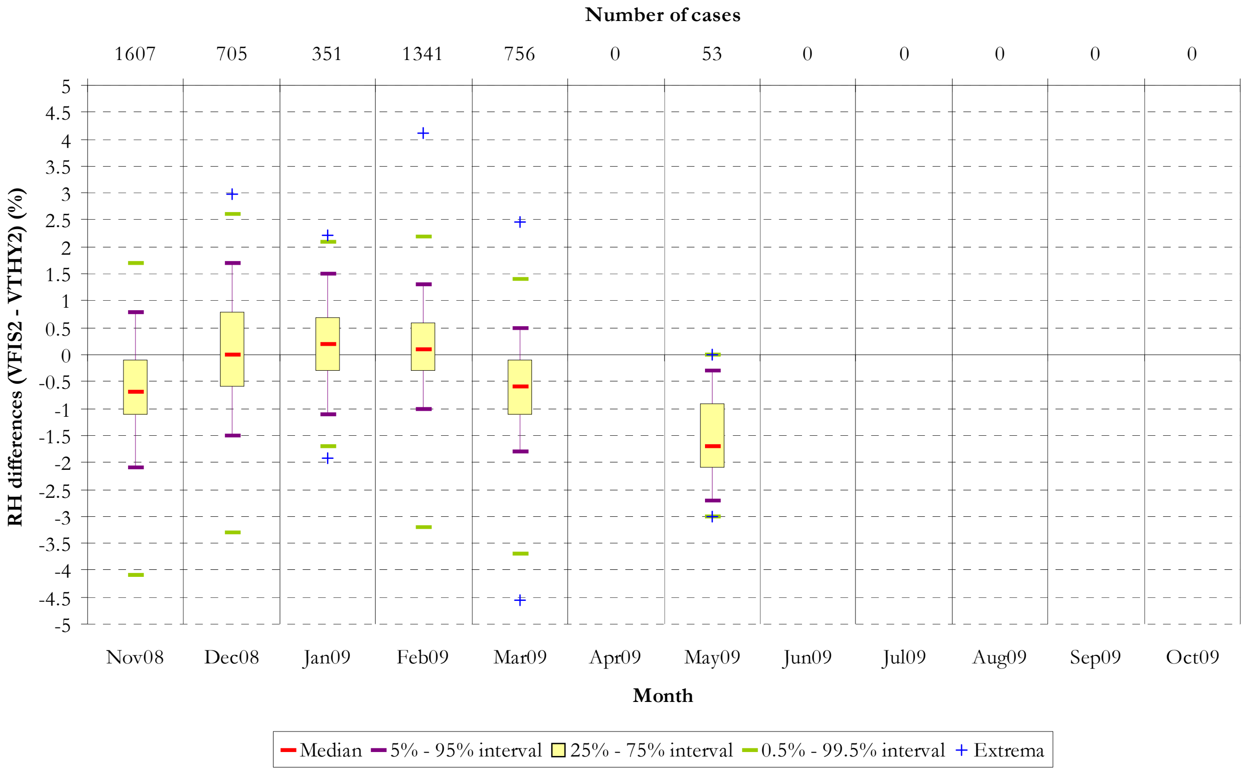


**Figure 20**

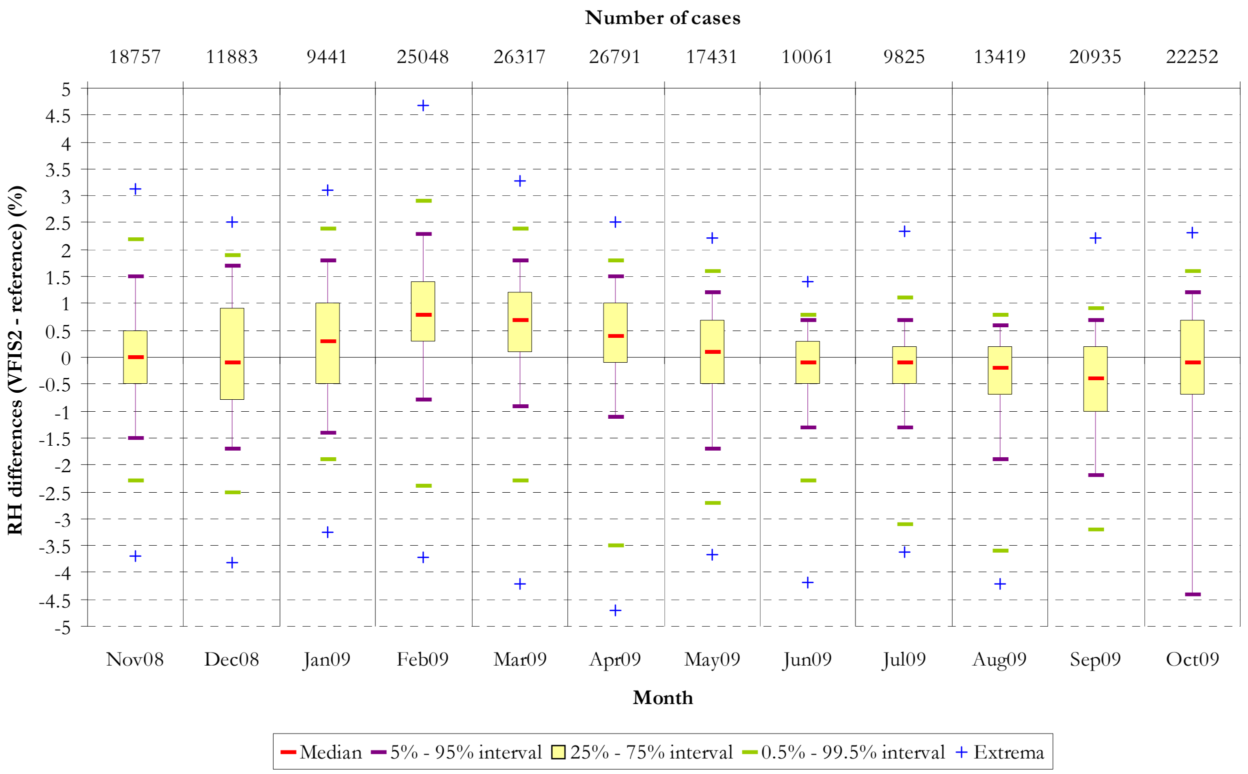


**Figure 21**

Medians of differences were quite constant during the intercomparison period, around –2% for VFIS1, around 0% for VFIS2 (within more or less 0.5 %), except in February and March 2009 (it may be an effect of temperature). Dispersion of differences remains quite stable all year long.

## QUALITY CONTROL INFORMATION

### DATA AVAILABILITY

The intercomparison period extends from the 1st of November 2008 to the 1st of November 2009. The theoretical number of 1-minute data is 525600.

The table 3 sums up the total number of data for each sensor and for each possible QC flag.

**Table 3**

| QC flag | VFIS1 | VFIS2 |
|---|---|---|
| 0 (good) | 503104 | 503113 |
| 1 (inconsistent) | 0 | 0 |
| 2 (doubtful) | 0 | 2 |
| 3 (erroneous) | 3701 | 3690 |
| 7 (missing) | 18795 | 18795 |

### MAINTENANCE

No actions done during the intercomparison period.

# HMT337 VAISALA
# – Germany –
# SVAI

## TECHNICAL SPECIFICATIONS (PROVIDED BY THE MANUFACTURER)

Dimensions: Length 9.95 cm x Diameter 1.2 cm
Principle of operation: Capacitive sensor, PT100 RTD 1/3 Class B
Accuracy: ± 1 % RH (10  90% RH) at 20°C
Power supply: 10  35 VDC

**Figure 1**

This sensor is installed in conjunction with HMT330MIK meteorological installation kit.

**Figure 2**

## OVERVIEW

Both sensors give similar results. The dispersion between them is higher when humidity increases.

About 98.5 % of the measurements were found within ±3% of the reference.

The differences with VTHY2 reference are very low and they do not vary much with humidity or temperature. The differences with UHMP2 reference are a bit greater and they vary with humidity and with temperature. It may be a characteristic of the UHMP2 reference itself.

The global shape of the two contour plots is the same for both sensors, higher differences are obtained for temperatures between 25 and 35°C and for relative humidity values between 30 and 40%.

Distributions of differences has varied along the period, but this is likely an effect of temperature. The distribution at the end of the intercomparison is not far from the one at the beginning, so these sensors did not have an important drift.

## CALIBRATION INFORMATION

Calibration in Trappes (12 Feb 2007):

**Table 1**

| Sensor | Serial number | 23°C | | | | | 40°C | | | | |
|---|---|---|---|---|---|---|---|---|---|---|---|
| | | 10% | 33% | 55% | 75% | 90% | 10% | 33% | 55% | 75% | 90% |
| SVAI1 | B4940009 | 0.3 | -0.7 | -0.4 | -1.1 | -2.6 | 0.3 | 0.8 | 3.7 | -2.3 | 2.2 |
| SVAI2 | B4940010 | -0.2 | 0.3 | -0.5 | -0.9 | -1.3 | 0.3 | 0.6 | 0.5 | 0.4 | 0.9 |

## COMPARISON OF BOTH SENSORS

The distribution of differences between SVAI1 and SVAI2 is plotted, using 1-minute quality checked data for the whole period of the intercomparison. Differences are classified according SVAI1 relative humidity.

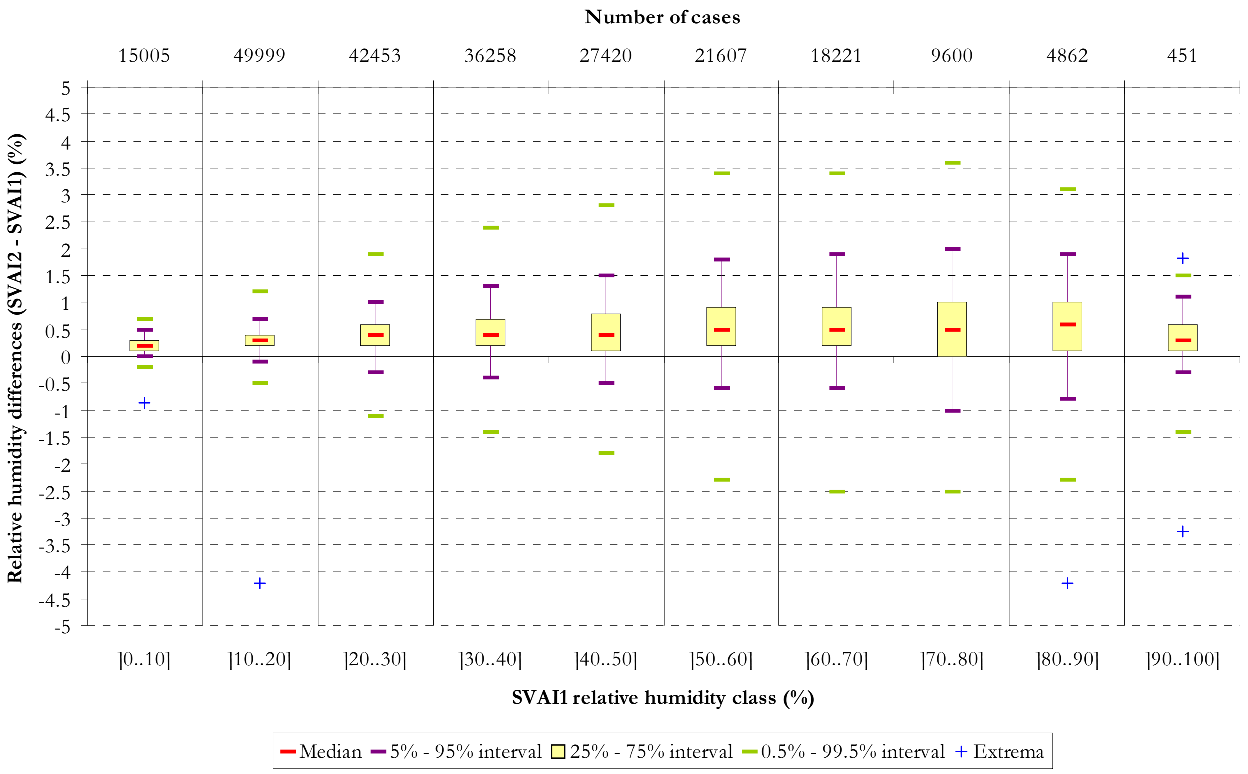


**Figure 3**

Both sensors give similar results. The dispersion between them is higher when humidity increases.

## COMPARISON WITH THE REFERENCE

Thygan sensor #2 was first chosen as the reference for humidity measurements. But it was not available after April 2009. That is why a second reference was selected, which is the average of two HMP45D probes from Vaisala, when the difference between both values is lower than 1 percentage point of relative humidity.

For more details about the choice of references for humidity measurement, please refer to part 5.5.1 of the final report.

### HISTOGRAM OF DIFFERENCES

The histograms of differences between SVAI and the references are plotted, using 1-minute quality checked data for the whole period of the intercomparison. Differences are plotted by steps of 1 %. The vertical axis is the frequency in percent for each class of differences.

Sensor #1:

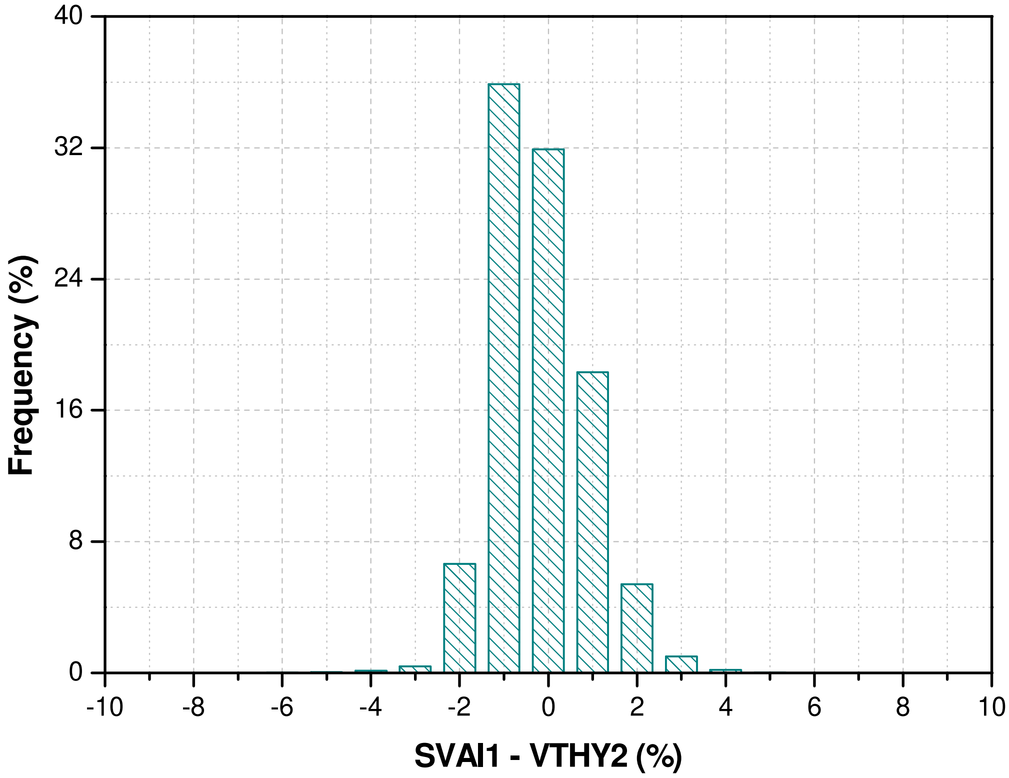


**Figure 4**

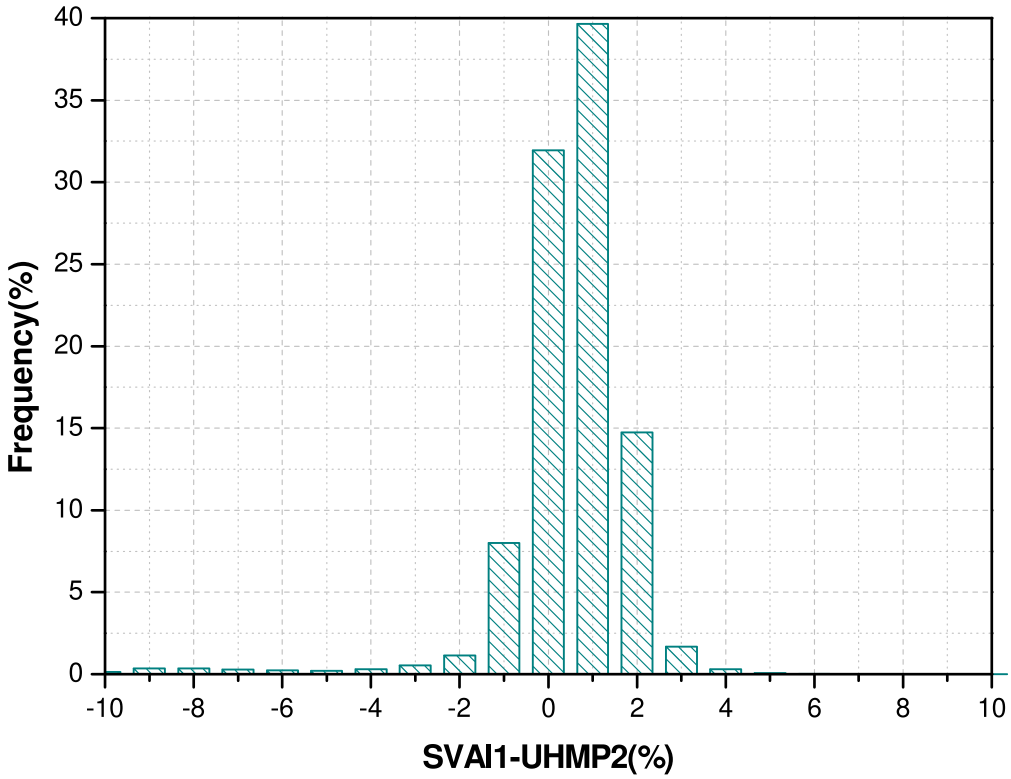


**Figure 5**

Sensor #2:

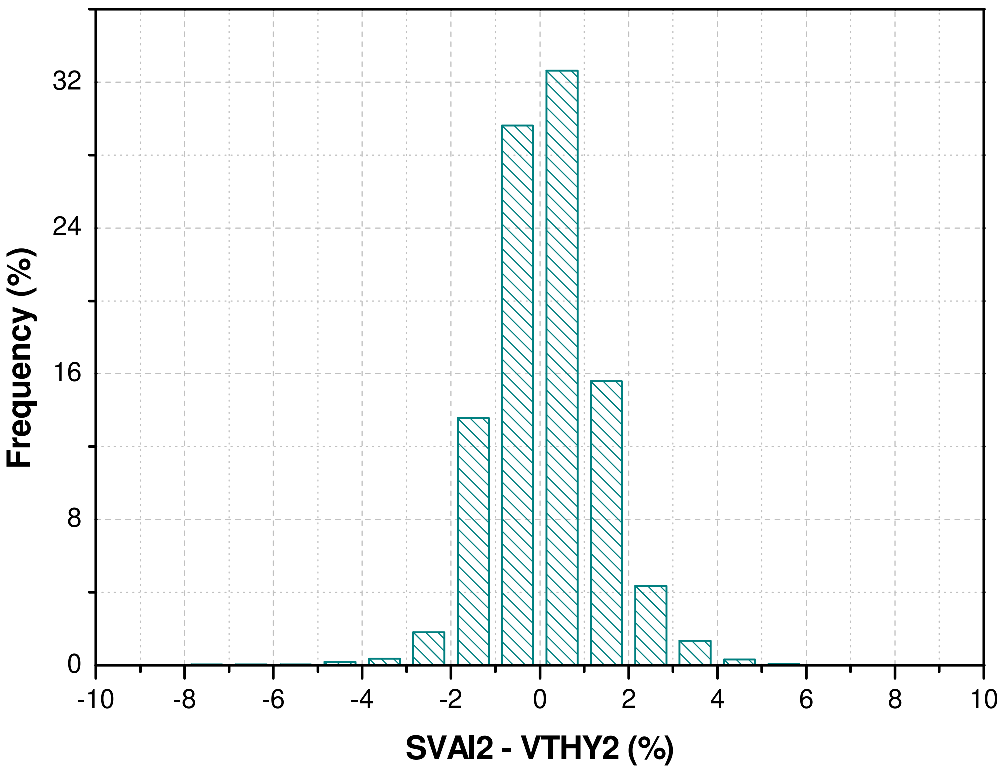


**Figure 6**

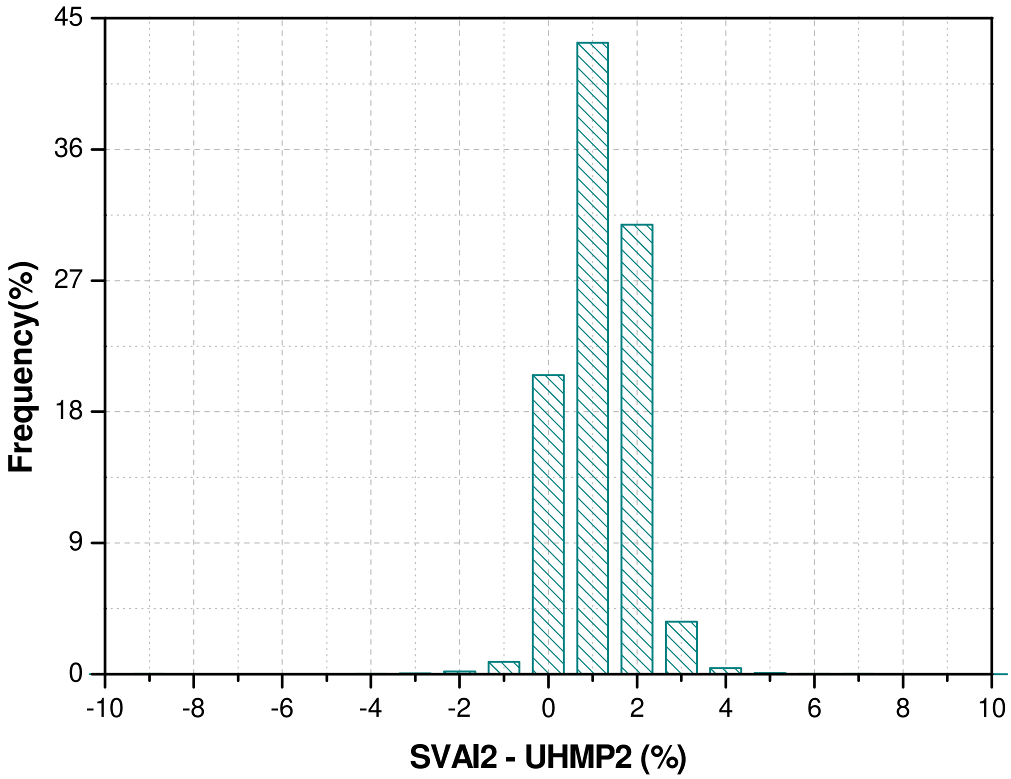


**Figure 7**

TABLE

The table 2 indicates the percentage of data that differ by less than 3 (and 6) % from the reference considered (VTHY2 or UHMP2).

**Table 2**

| | VTHY2 | | UHMP2 | |
|---|---|---|---|---|
| | [-3..3] | [-6..6] | [-3..3] | [-6..6] |
| SVAI1 | 99.1 | 100.0 | 98.9 | 99.8 |
| SVAI2 | 98.0 | 99.9 | 98.3 | 99.9 |

## INFLUENCE OF HUMIDITY

The distributions of differences between SVAI and the references are plotted, using 1-minute quality checked data for the whole period of the intercomparison. Differences are classified according the reference relative humidity.

## Sensor #1:

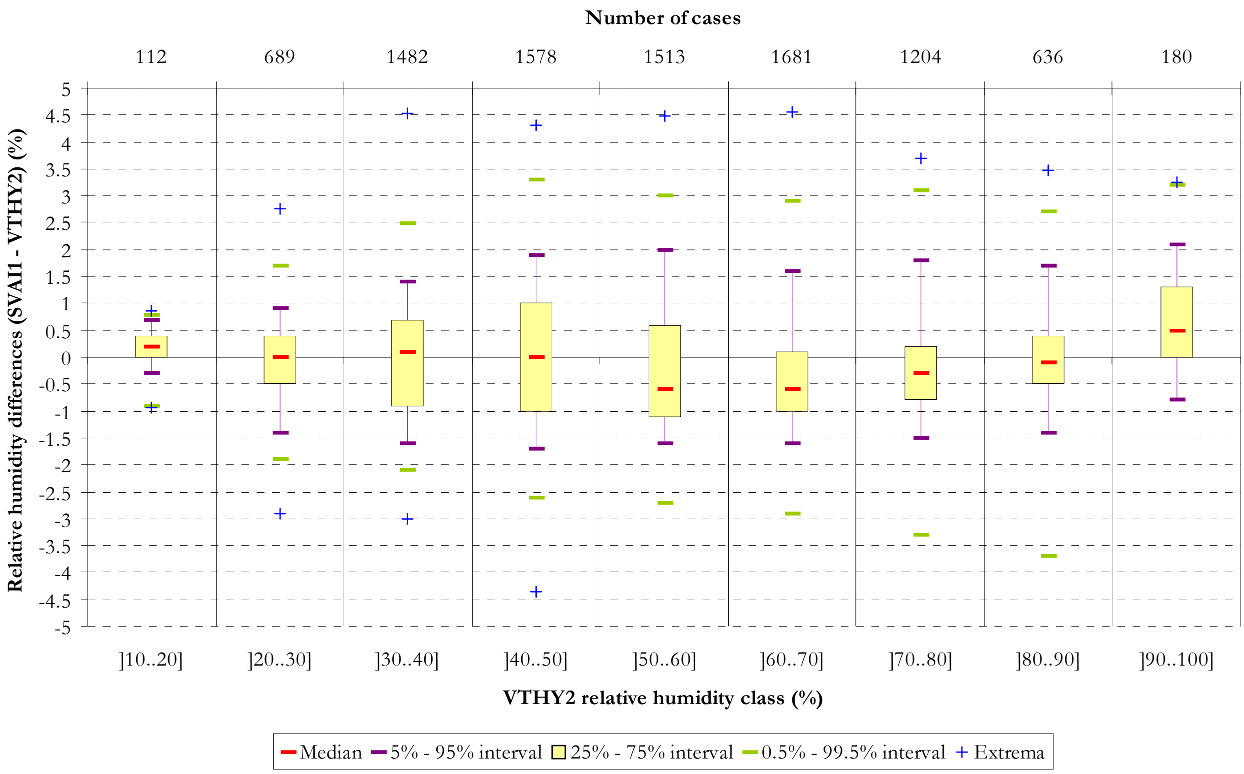


**Figure 8**

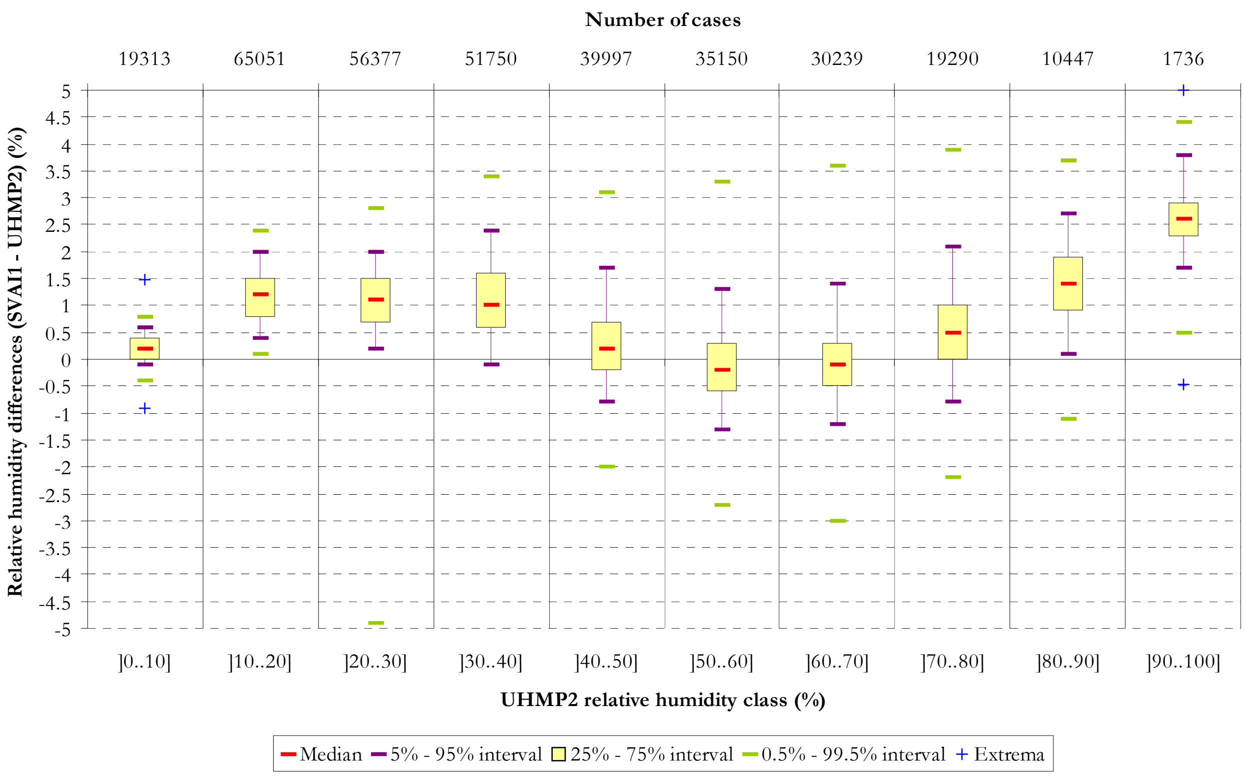


**Figure 9**

Sensor #2:

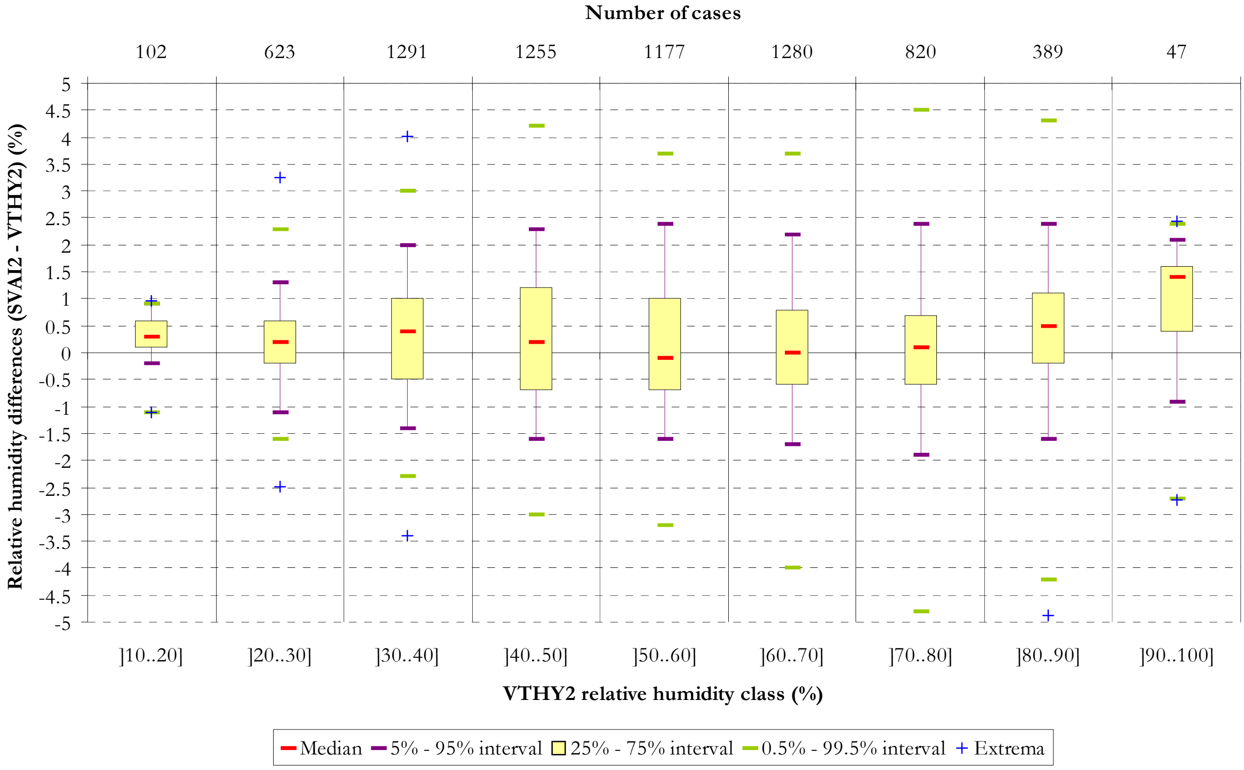


**Figure 10**

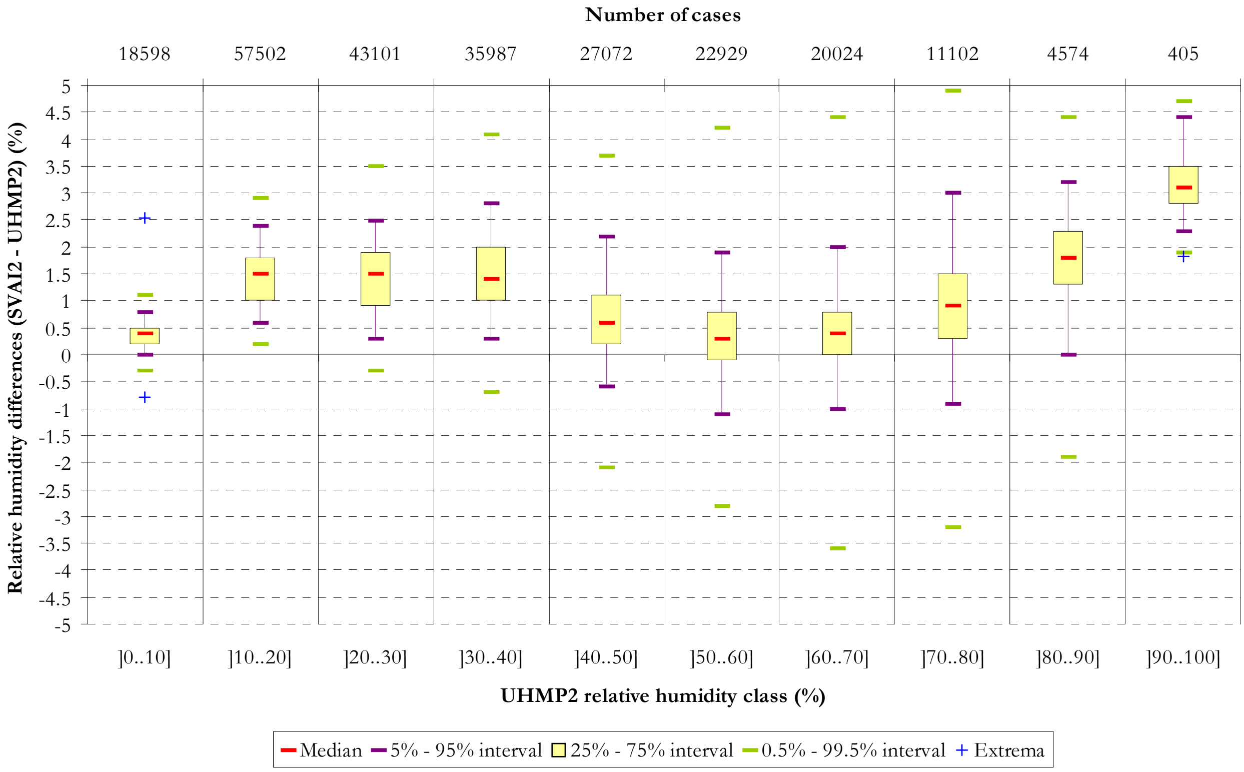


**Figure 11**

Both sensors have similar behaviour. The differences with VTHY2 reference are very low and they do not vary much with humidity. The differences with UHMP2 reference are a bit greater and they vary: they are quite low for very dry conditions, around 1.5 percentage point for humidity values between 10 and 40%, around 0.5 percentage point between 40 and 70%. For higher values of humidity, they increase up to 3 % RH.

## INFLUENCE OF TEMPERATURE

The distributions of differences between SVAI and the references are plotted, using 1-minute quality checked data for the whole period of the intercomparison. Differences are classified according VEIG22 temperature.

Sensor #1:

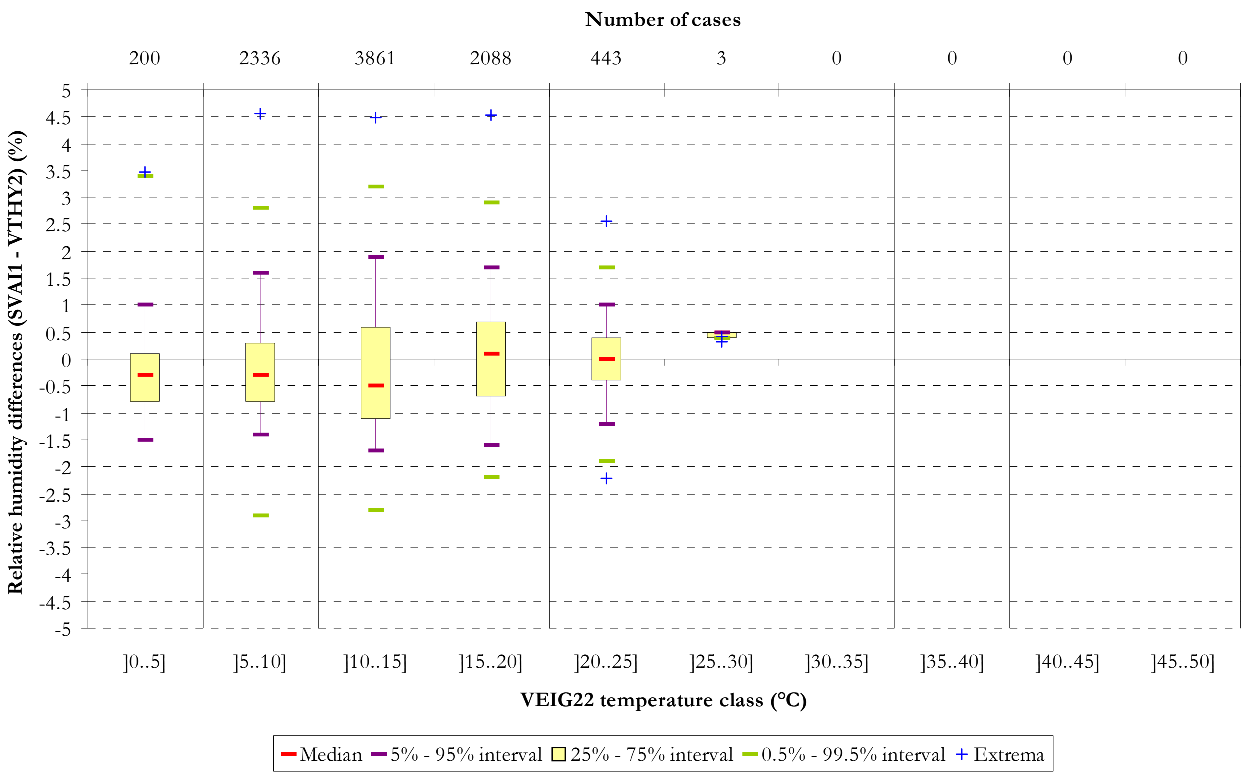


**Figure 12**

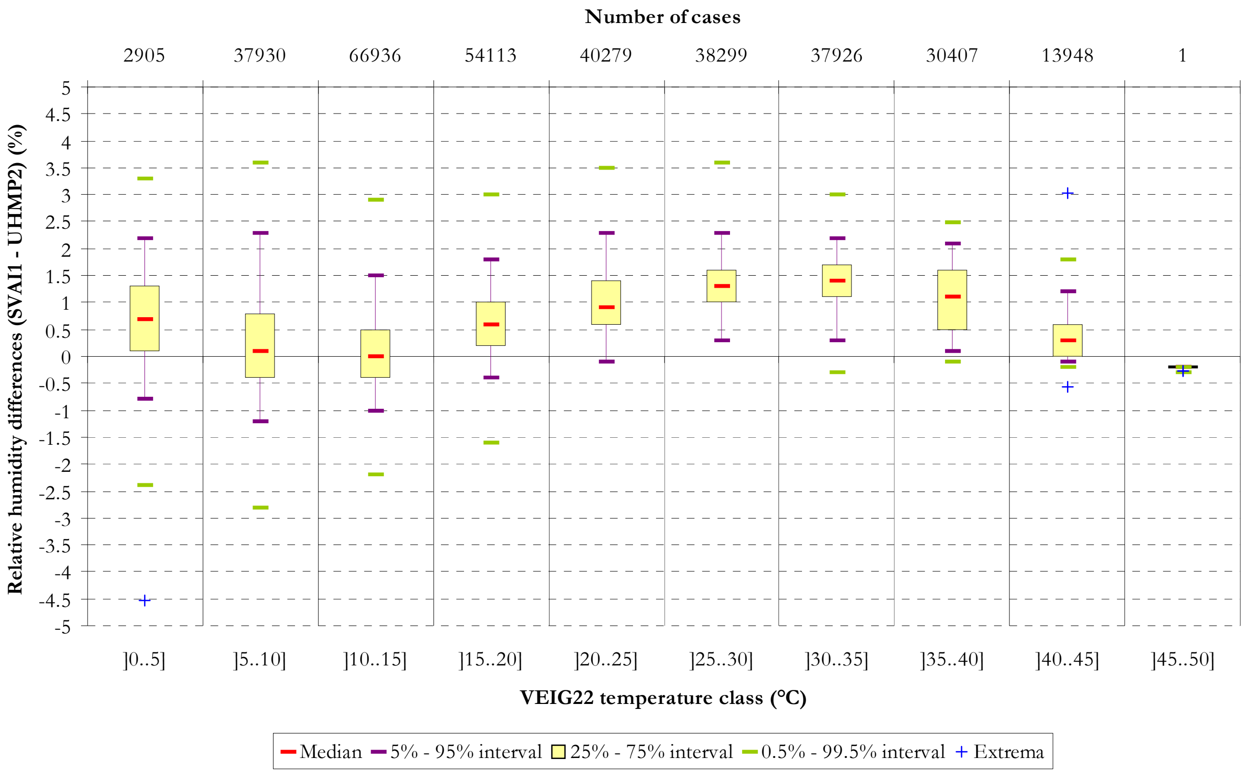


**Figure 13**

## Sensor #2:


**Figure 14**

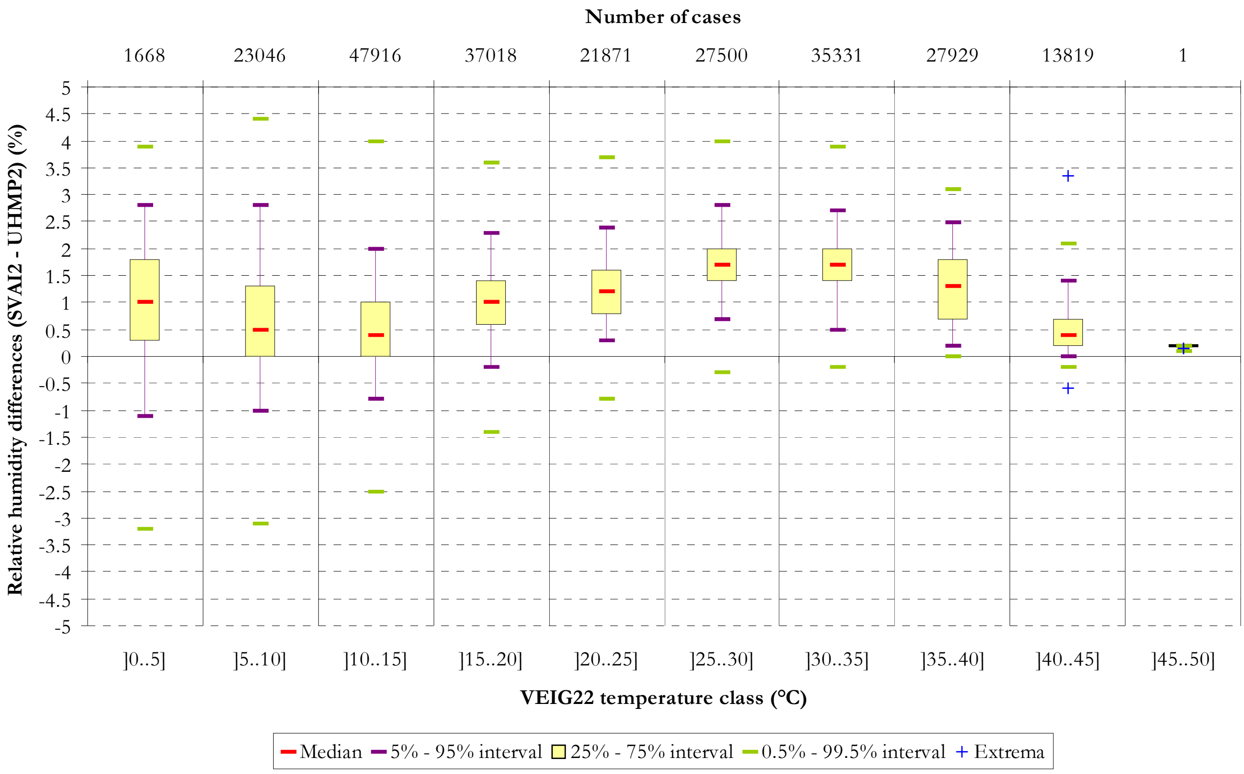


**Figure 15**

Both sensors have similar behaviour. The differences with VTHY2 reference are very low and they do not vary much with temperature. There are more variations in differences with UHMP2 reference: they are quite low for cool conditions, around 0.5 percentage point for temperatures between 5 and 10°C, around 1 to 1.5 percentage point between 15 and 40°C.

## COMBINED INFLUENCE OF TEMPERATURE AND RELATIVE HUMIDITY

The medians of differences between SVAI and UHMP reference are represented here with a contour plot. The VEIG22 temperature is on the X-axis and the reference relative humidity is on the Y-axis. Medians are used in all cases, provided that at least one data is available for both conditions on temperature and humidity considered.

The scale was chosen so as to be the same for all relative humidity sensors.

Sensor #1:

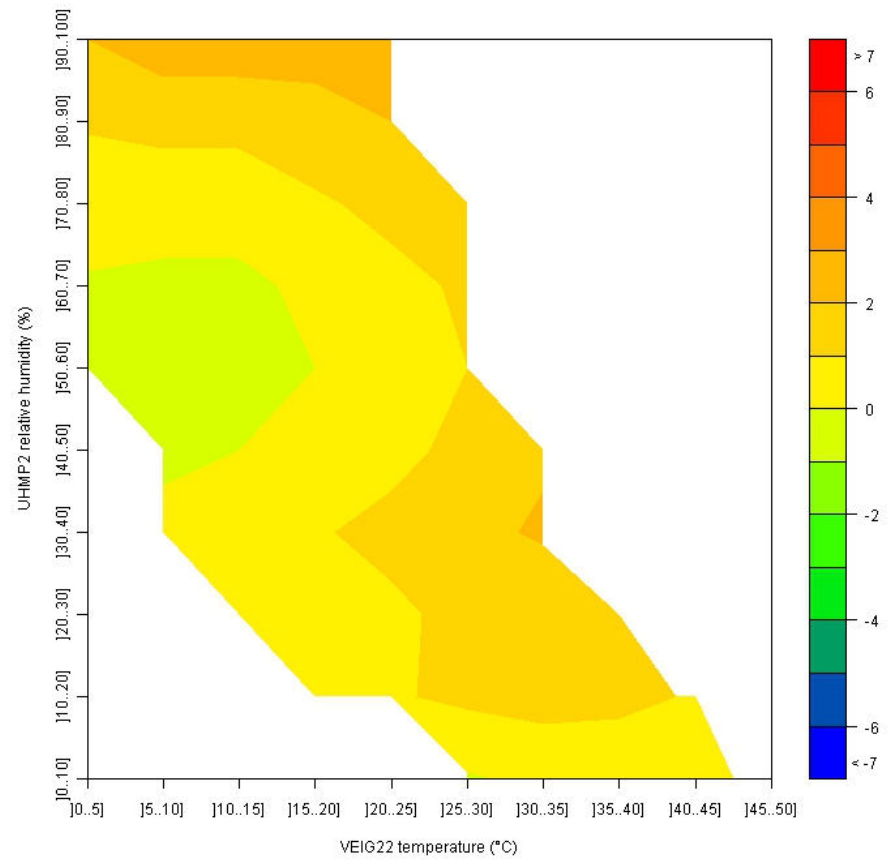


**Figure 16**

Sensor #2:

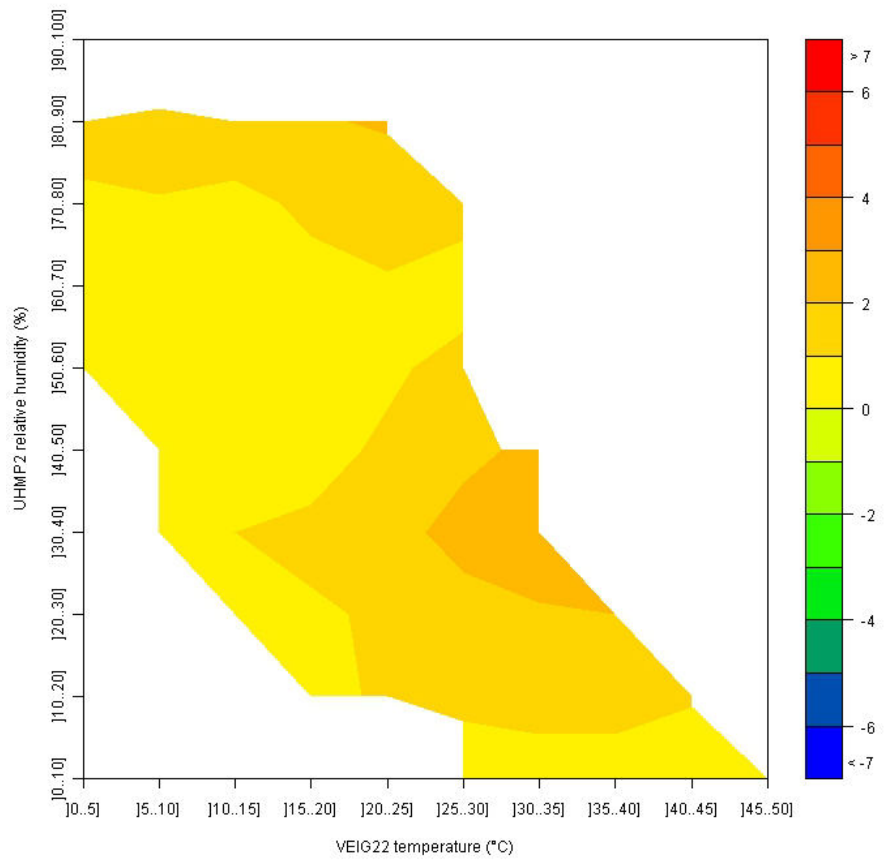


**Figure 17**

The global shape of the two contour plots is the same, higher differences are obtained for temperatures between 25 and 35°C and for relative humidity values between 30 and 40%.

## TIME DRIFT

The distributions of differences between SVAI and the references are plotted, using 1-minute quality checked data for the whole period of the intercomparison, by step of one month. Reference relative humidity between 20% and 50% are only considered here: this is the common range in order to have data every month, without introducing influence of humidity itself.

## Sensor #1:

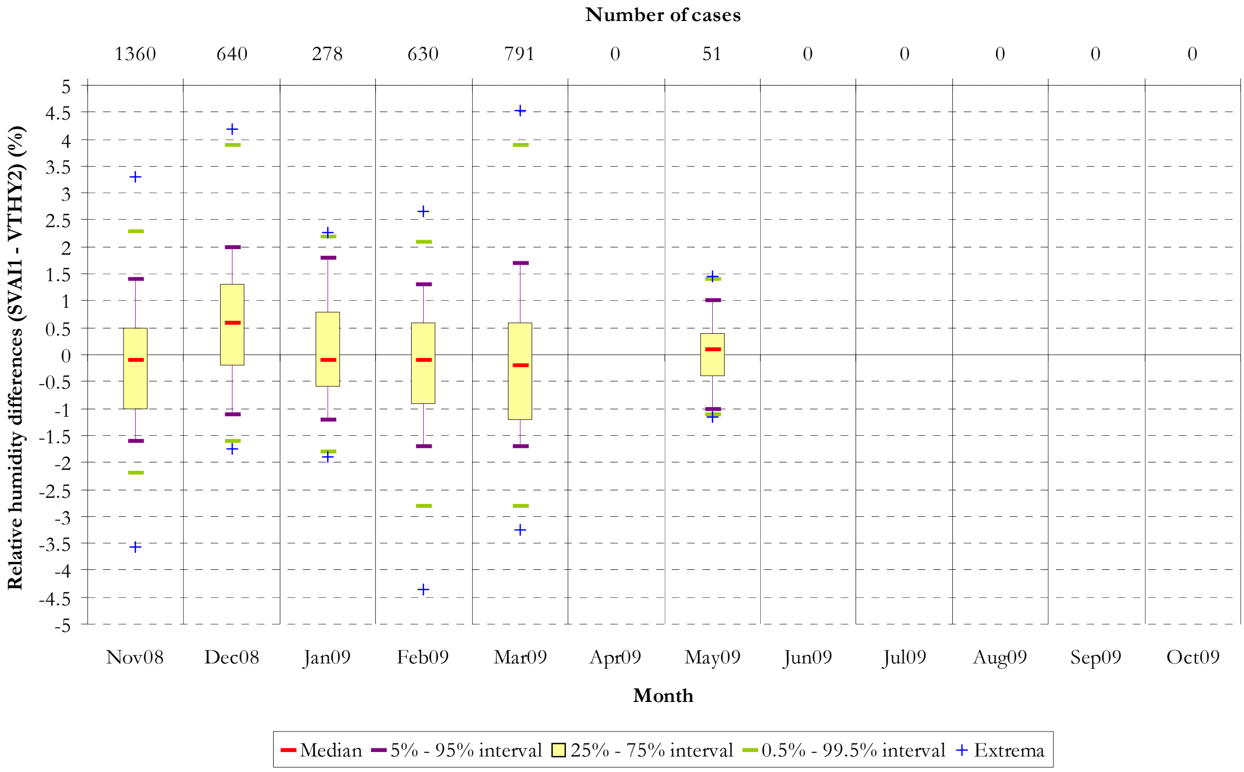


**Figure 18**

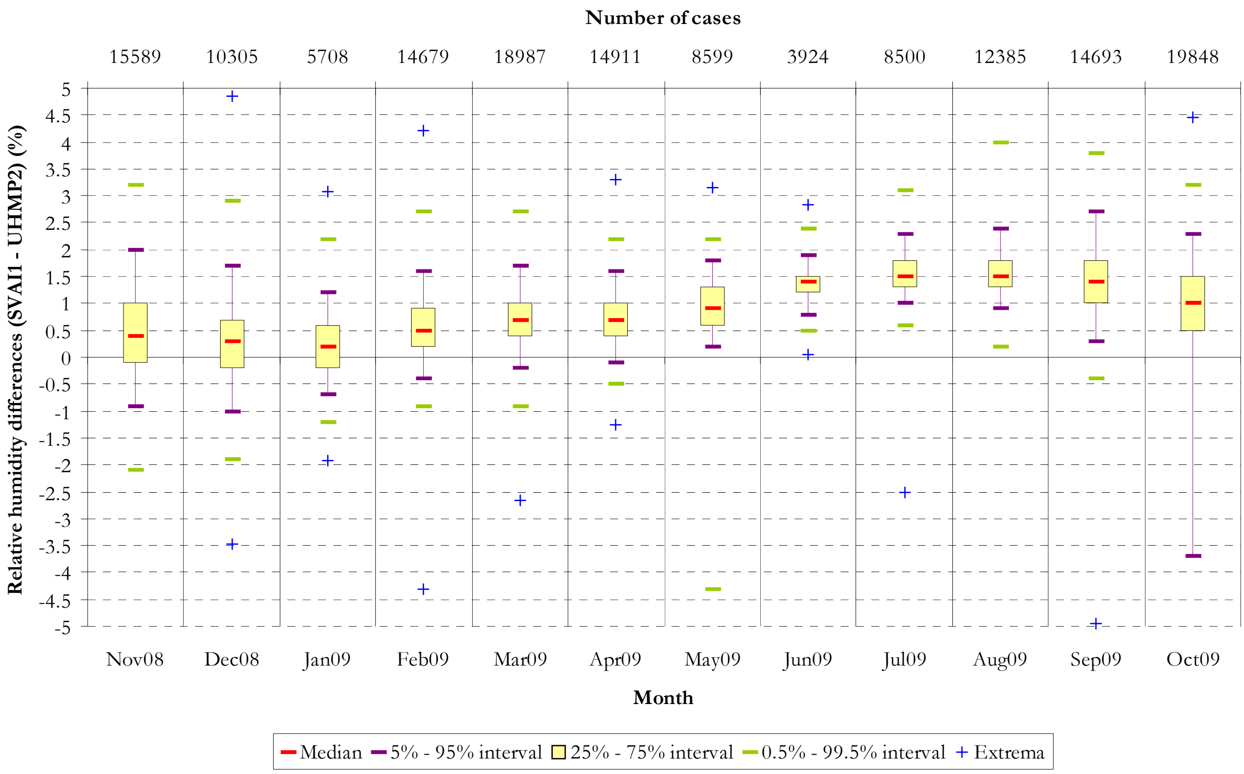


**Figure 19**

Sensor #2:

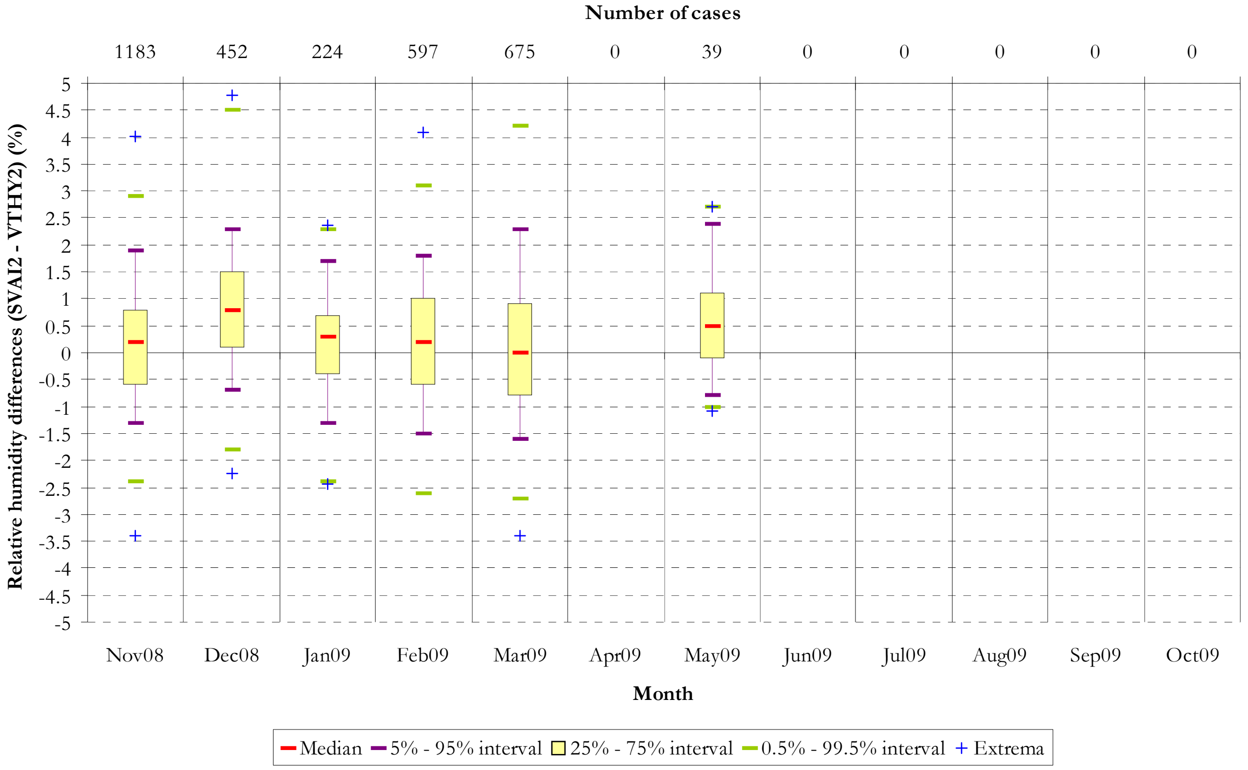


**Figure 20**

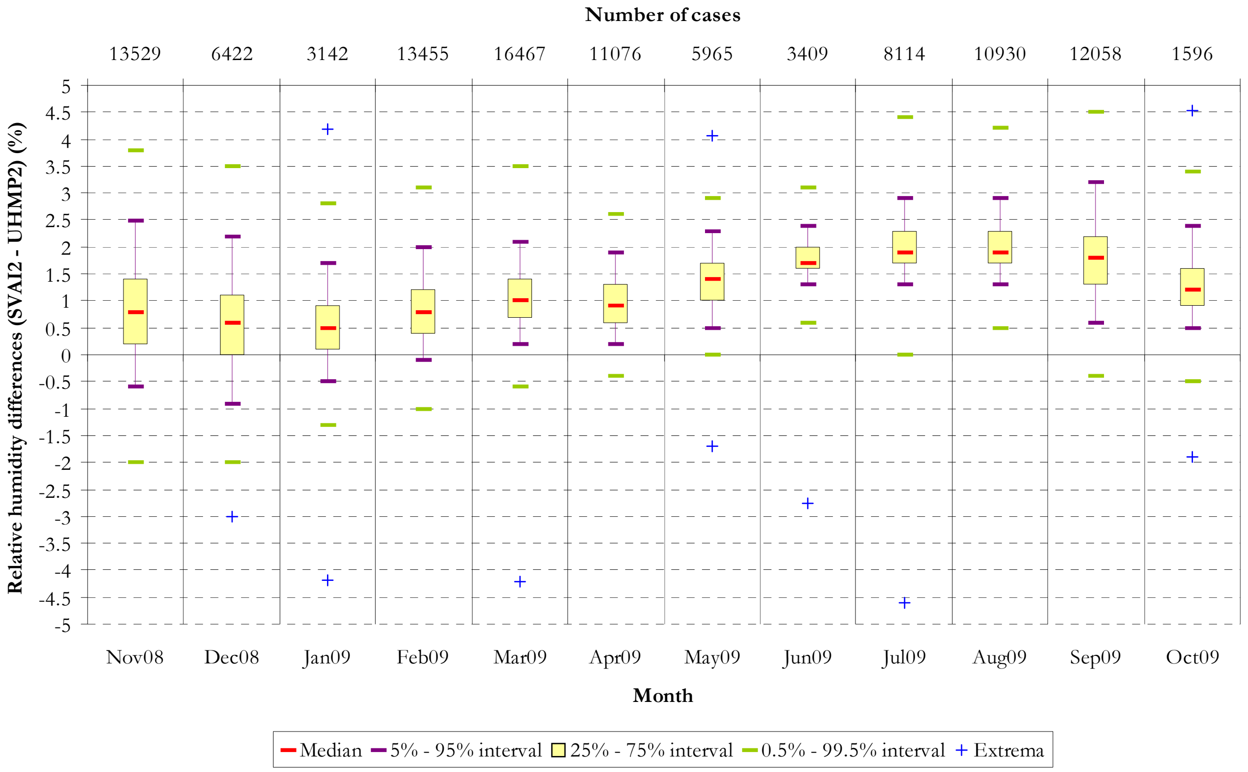


**Figure 21**

Distributions of differences has varied along the period, but this is likely an effect of temperature. The distribution at the end of the intercomparison is not far from the one at the beginning, so these sensors did not have a significant drift.

## QUALITY CONTROL INFORMATION

### DATA AVAILABILITY

The intercomparison period extends from the 1st of November 2008 to the 1st of November 2009. The theoretical number of 1-minute data is 525600.

The table 3 sums up the total number of data for each sensor and for each possible QC flag.

**Table 3**

| QC flag | SVAI1 | SVAI2 |
|---|---|---|
| 0 (good) | 360474 | 276247 |
| 1 (inconsistent) | 0 | 0 |
| 2 (doubtful) | 3 | 0 |
| 3 (erroneous) | 0 | 0 |
| 7 (missing) | 165123 | 249353 |

Serial acquisition of these sensors was done the same way for both sensors.

The main reason for missing data is frequent failures of the acquisition software.

An additional problem was encountered with sensor #1, which delivered 1-minute data. Every eleven minutes the message was not delivered.

Sensor #2 delivered 10-second data. Every eleven minutes there are 1-minute gaps in raw data. These gaps may invalid one or two 1-minute data.

Both sensors also had long interruptions with no explanation (problem of sensor or problem of data acquisition or something else ?).

### MAINTENANCE

No action done during the intercomparison period.

# HMP45D VAISALA
# – Germany –
# UHMP

## TECHNICAL SPECIFICATIONS (PROVIDED BY THE MANUFACTURER)

Dimensions: Length 30 cm x Diameter 4 cm
Principle of operation: Humicap 180 capacitive sensor
Accuracy: ± 2 % RH (10..90% RH)
Power supply: 7..30 VDC

**Figure 1**

These sensors were installed in small multiplate naturally and artificially-ventilated Eigenbrodt screens (VEIG):

**Figure 2**

## OVERVIEW

The four sensors give very close results.

98% of the measurements were found within ±3% of the Thygan reference. 99.6% of the measurements were found within ±3% of the UHMP2 reference (sensors of the same type)

For all sensors, distributions of differences with UHMP2 have very small variations and no dependency with humidity. All sensors behave the same compared to VTHY2 reference: the medians of differences are around -0.5% for humidity values less than 80%. They decrease for higher values of humidity.

Differences with both references do not depend on temperature: variations of distributions with temperature are very low.

All contour plots are very uniform with minimal deviations around the 0% RH value. No combined effect of temperature and humidity can be seen. As the secondary reference UHMP2 is based on two Vaisala HMP45D probes this result demonstrates excellent uniformity among various HMP45D probes of different production dates even when installed in different screens.

For all sensors, distributions of the end of the period look quite the same to distributions of the beginning, that means no significant drift was recorded.

## CALIBRATION INFORMATION

Calibration in Trappes (9 Jan 2007):

**Table 1**

| Sensor | Serial number | 23°C | | | | | 40°C | | | | |
|---|---|---|---|---|---|---|---|---|---|---|---|
| | | 10% | 33% | 55% | 75% | 90% | 10% | 33% | 55% | 75% | 90% |
| UHMP11 | A3810083 | 0.0 | 1.8 | 0.9 | 0.9 | 2.0 | 0.5 | 2.3 | 1.0 | 0.9 | 1.5 |
| UHMP12 | B4740049 | -0.3 | 1.4 | 0.3 | 0.5 | 1.7 | 0.0 | 2.3 | 1.6 | 2.1 | 3.1 |
| UHMP21 | A3810054 | -0.1 | 1.7 | 1.0 | 1.0 | 2.1 | 0.5 | 2.8 | 2.2 | 2.7 | 3.5 |
| UHMP22 | B4740050 | -0.3 | 1.7 | 0.6 | 0.6 | 1.8 | 0.2 | 2.4 | 1.6 | 1.8 | 2.8 |

On site calibration (June 2008):

**Table 2**

| Sensor | Serial number | 10% | 33% | 50% | 90% |
|---|---|---|---|---|---|
| UHMP11 | A3810083 | 0.1 | 1.6 | 2.3 | 1.7 |
| UHMP12 | B4740049 | -0.1 | 1.8 | 3.6 | 3.5 |
| UHMP21 | A3810054 | 0.3 | 2.4 | 4 | 4.7 |
| UHMP22 | B4740050 | -0.2 | 1.6 | 0.7 | 0.6 |

Sensors UHMP11 and UHMP12 are in the same screen.

Sensors UHMP21 and UHMP22 are in the same screen.

Due to grounding problems that affected all sensors (not at the same time), data are filtered: only data where both sensors of the same screen differ by less than 1% in absolute value, are considered.

## COMPARISON OF BOTH SENSORS

The distributions of differences between the four sensors are plotted, using 1-minute quality checked data for the whole period of the intercomparison. Differences are classified according relative humidity.

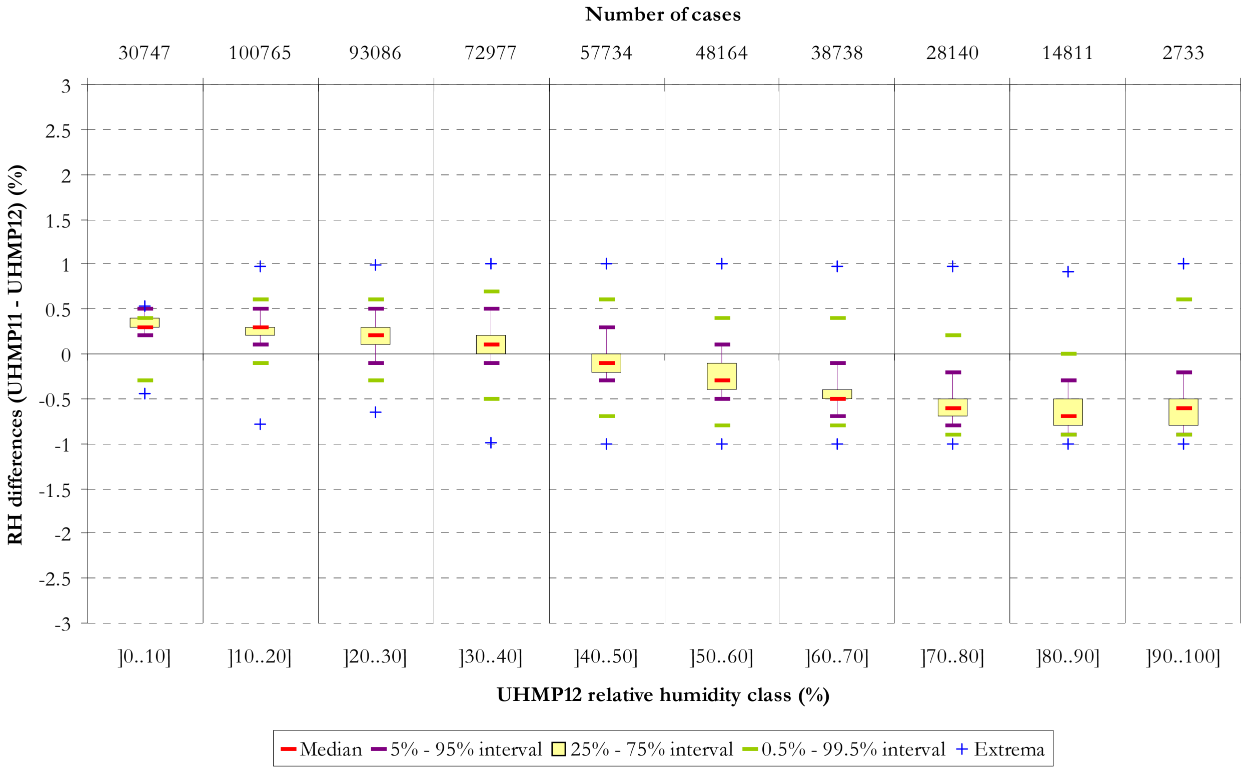


**Figure 3**

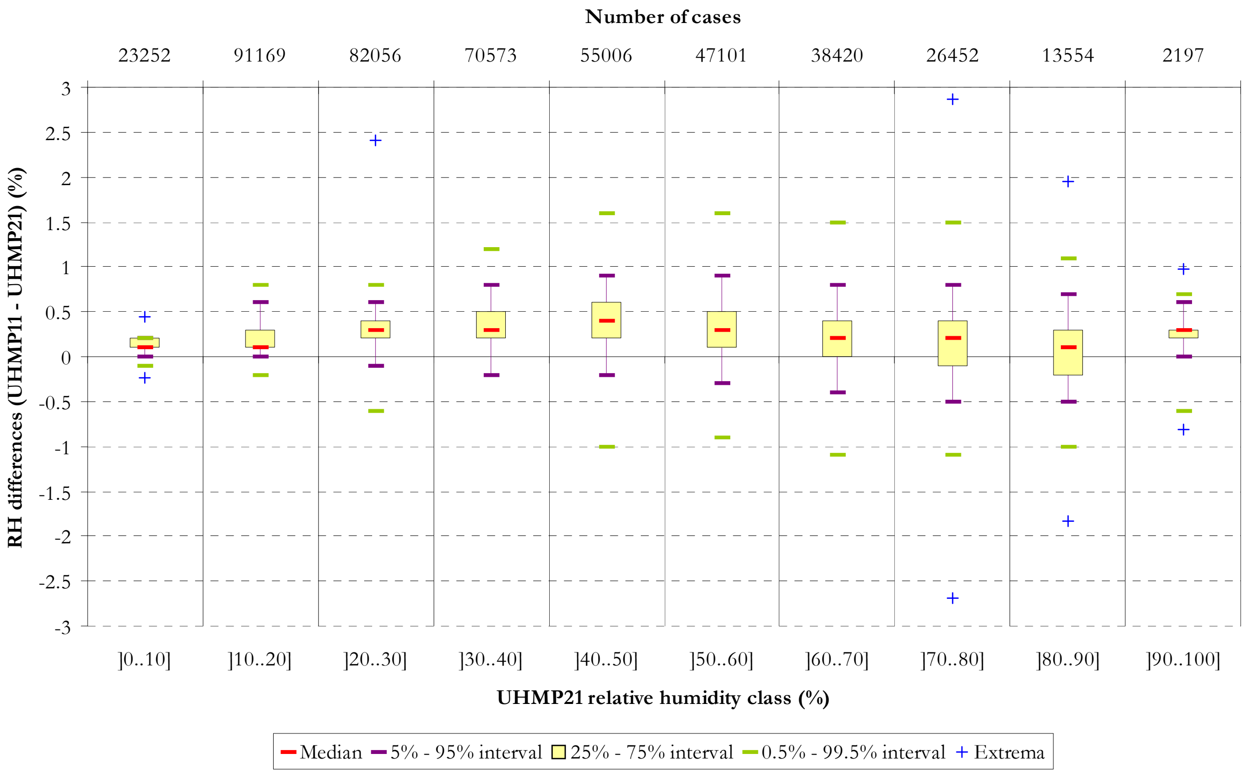


**Figure 4**

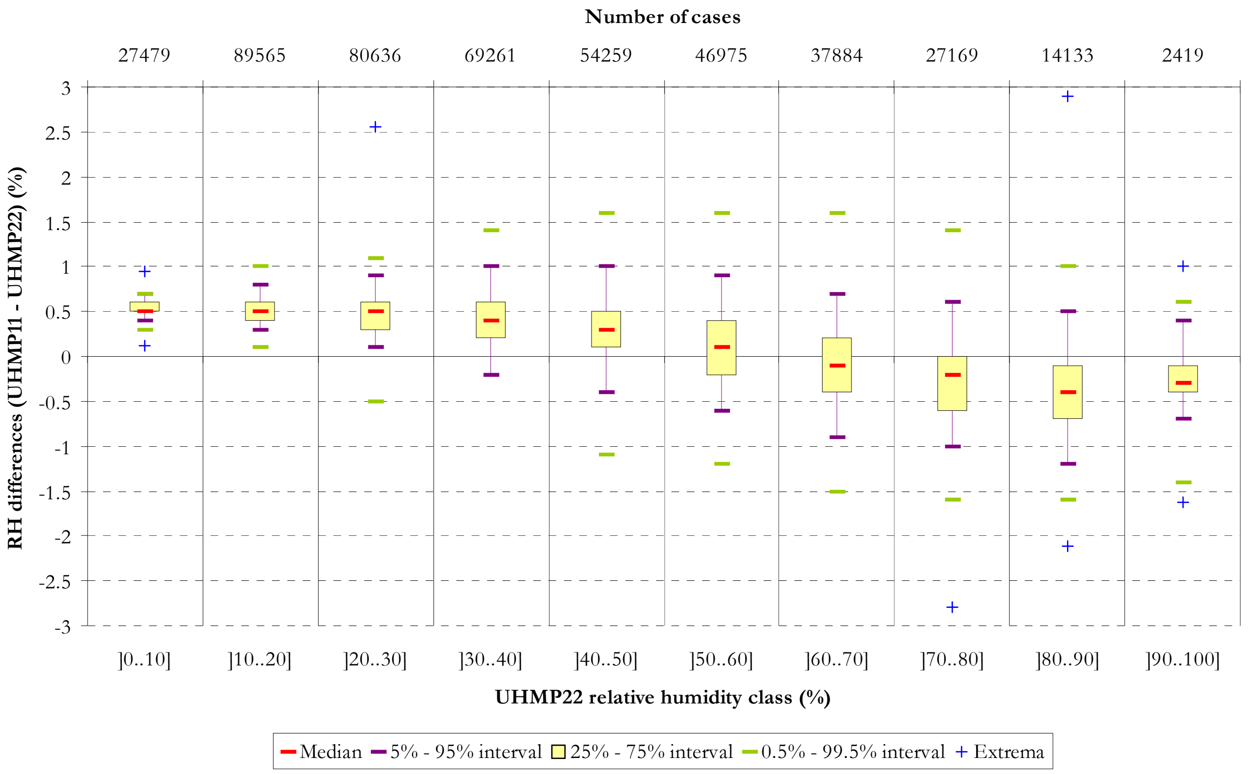


**Figure 5**

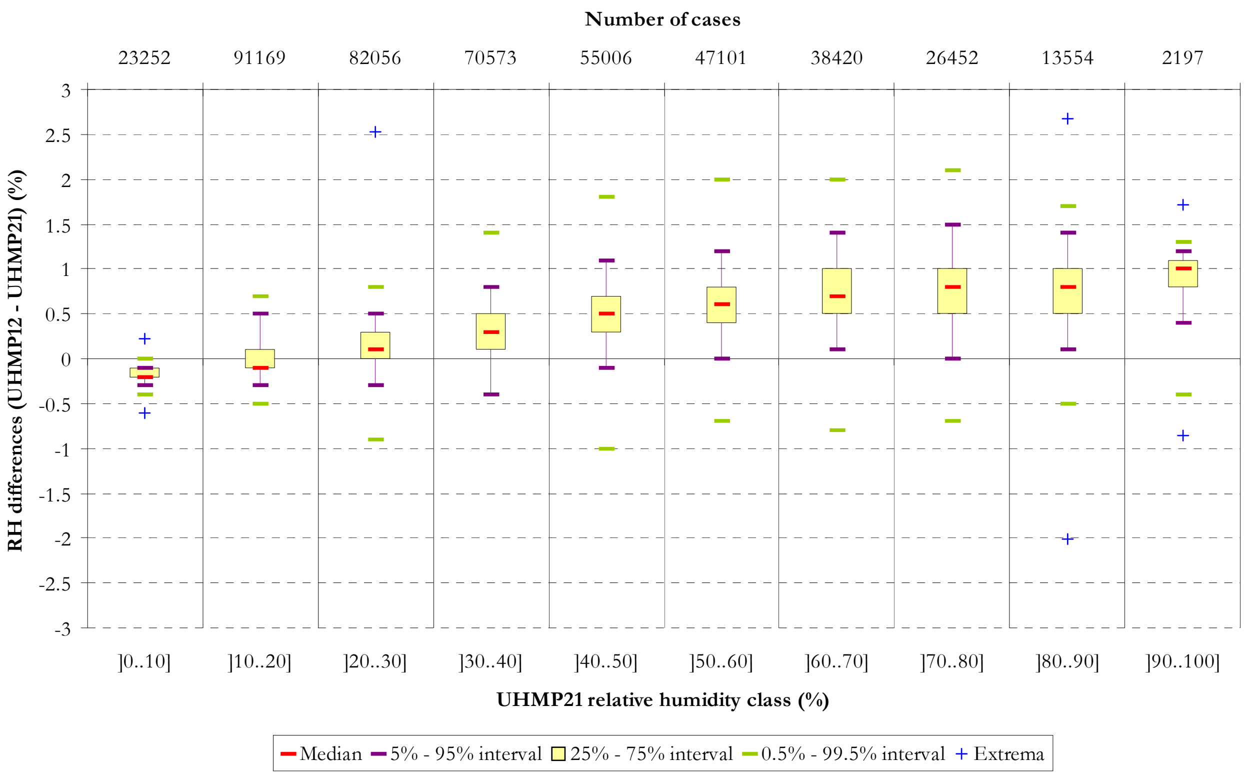


**Figure 6**

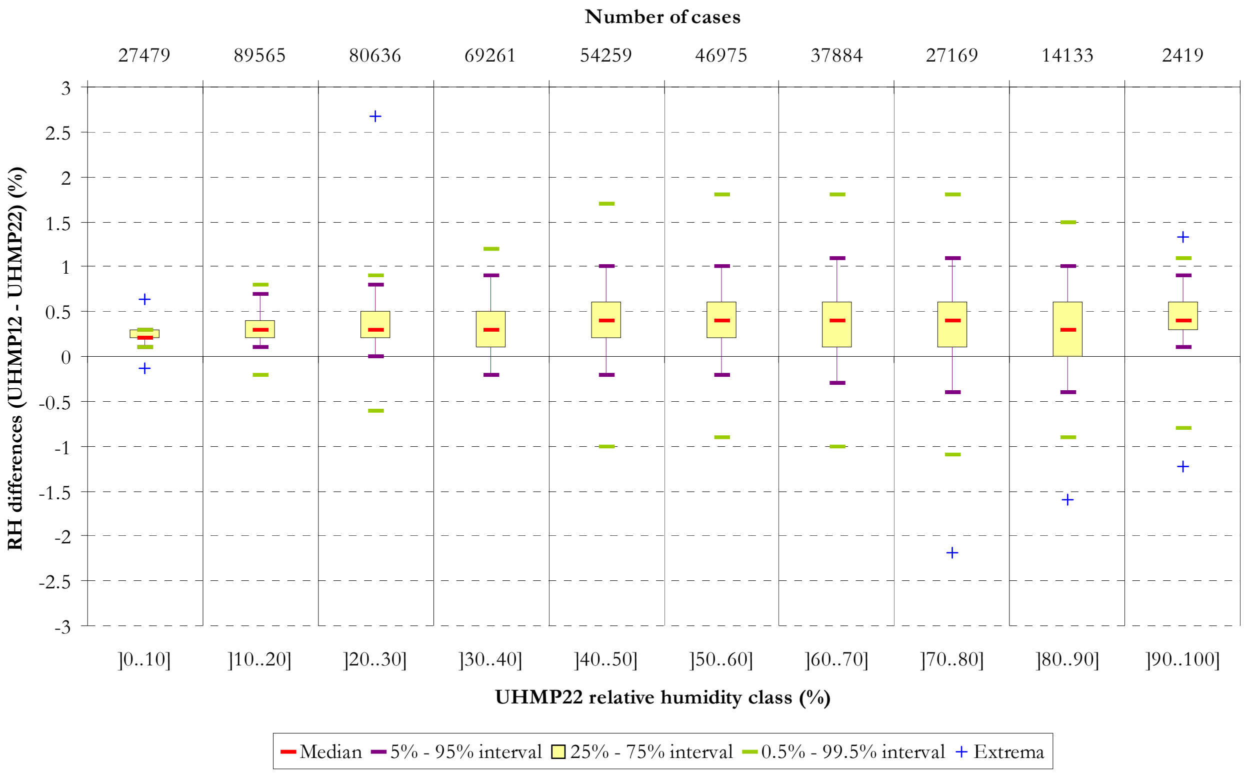


**Figure 7**

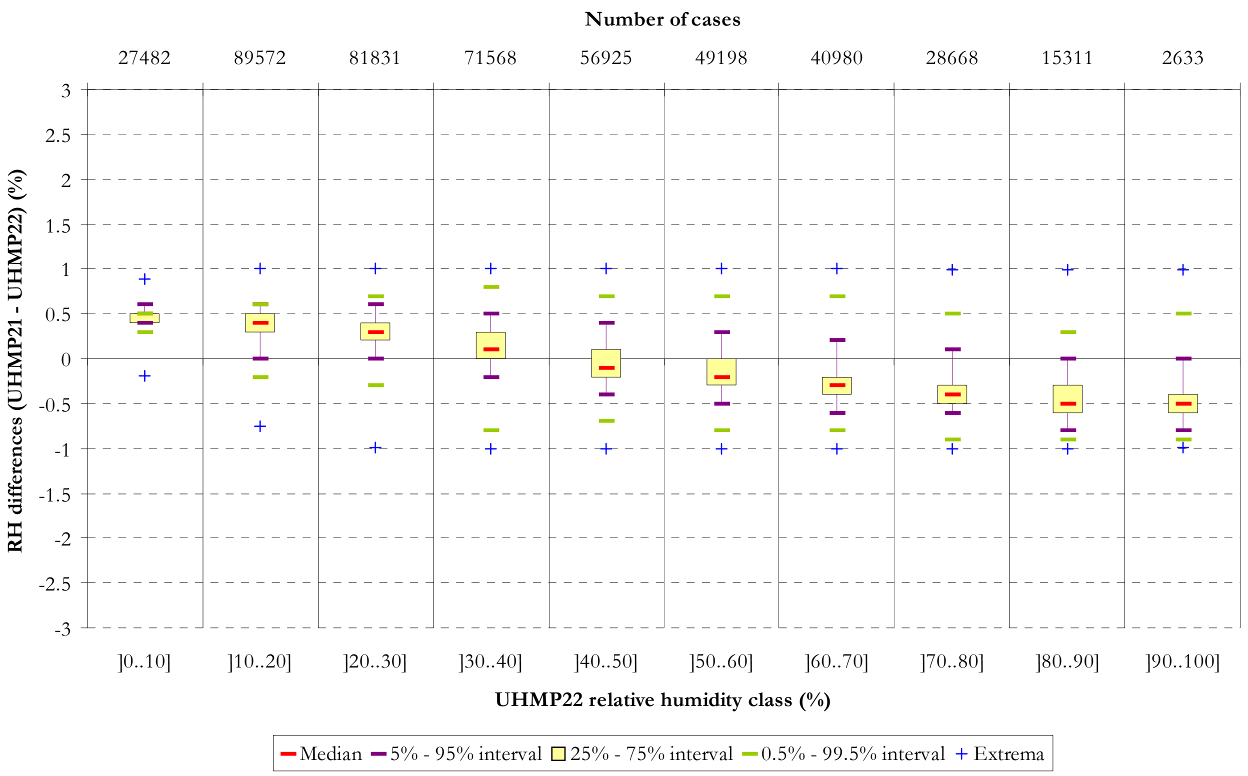


**Figure 8**

The four sensors give very close results.

## COMPARISON WITH THE REFERENCE

Thygan sensor #2 was first chosen as the reference for humidity measurements. But it was not available after April 2009. That is why a second reference was selected, which is the average of two HMP45D probes from Vaisala, when the difference between both values is lower than 1 percentage point of relative humidity.

For more details about the choice of references for humidity measurement, please refer to part 5.5.1 of the final report.

HISTOGRAM OF DIFFERENCES

The histograms of differences between UHMP and the references are plotted, using 1-minute quality checked data for the whole period of the intercomparison. Differences are plotted by steps of 1 %. The vertical axis is the frequency in percent for each class of differences.

Sensor #11:

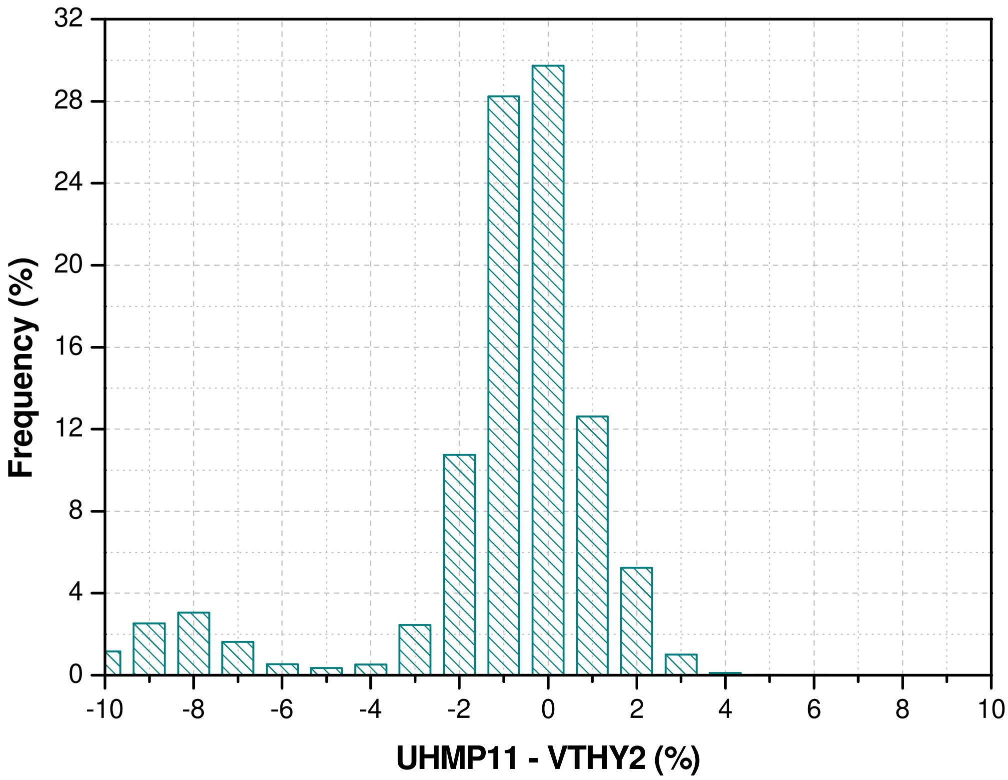


**Figure 9**

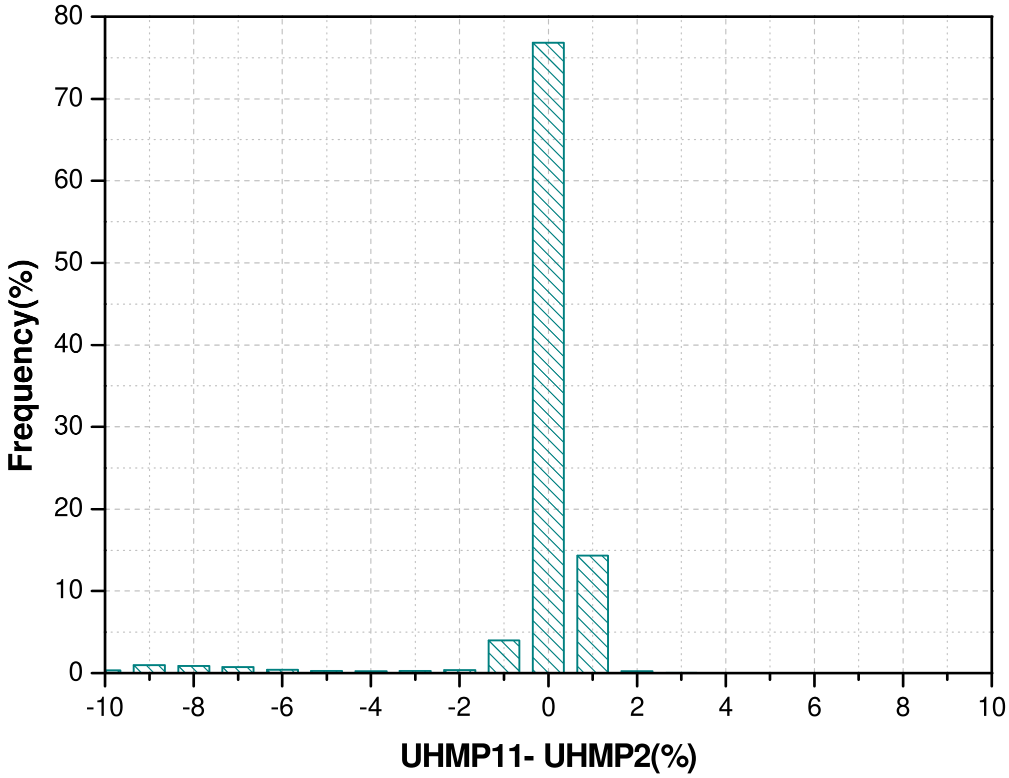
Frequency(%)
80
70
60
50
40
30
20
10
0
-10
-8
-6
-4
-2
0
2
4
6
8
10
UHMP11- UHMP2(%)

**Figure 10**

Sensor #12:

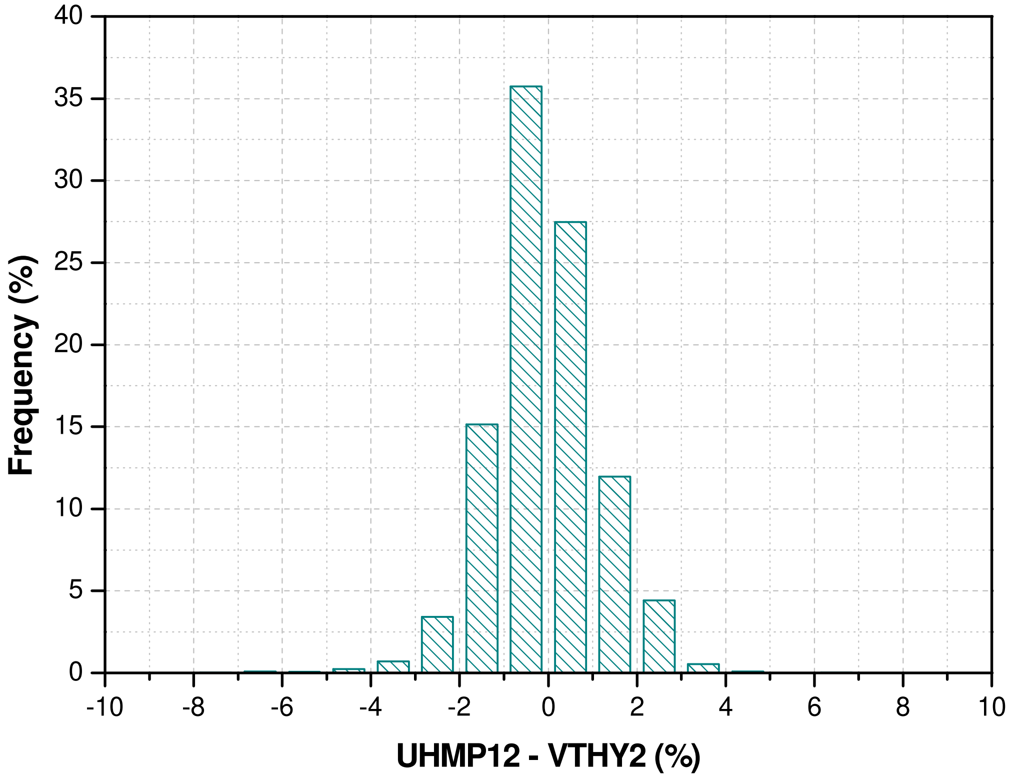


**Figure 11**

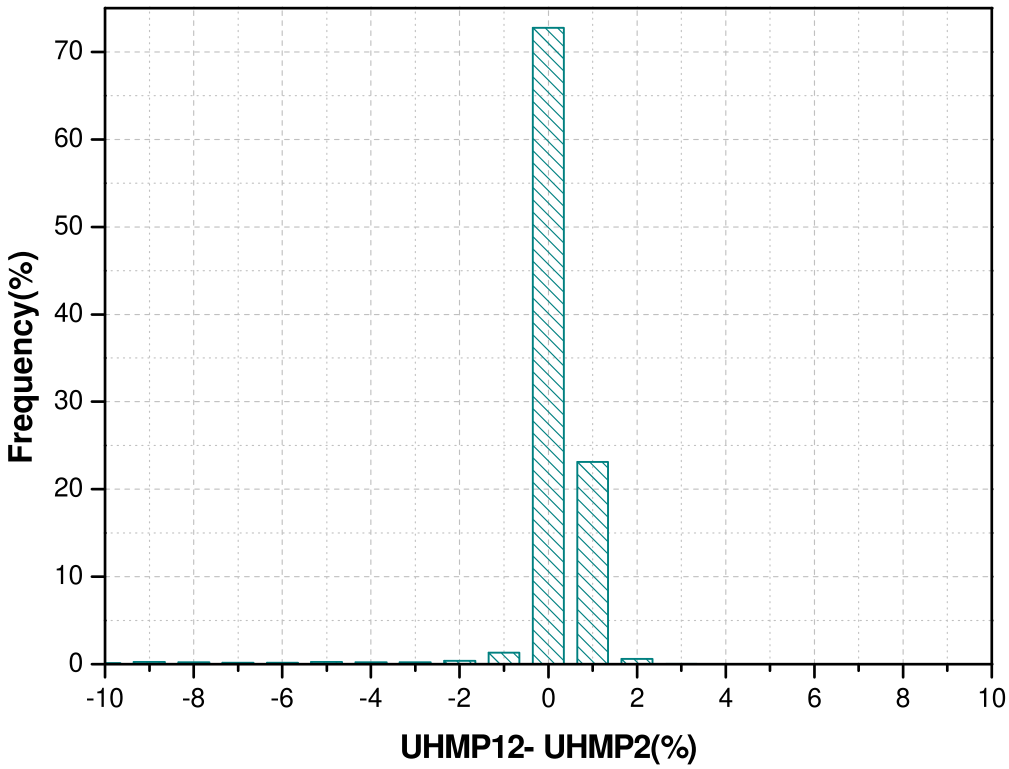


**Figure 12**

Sensor #21:

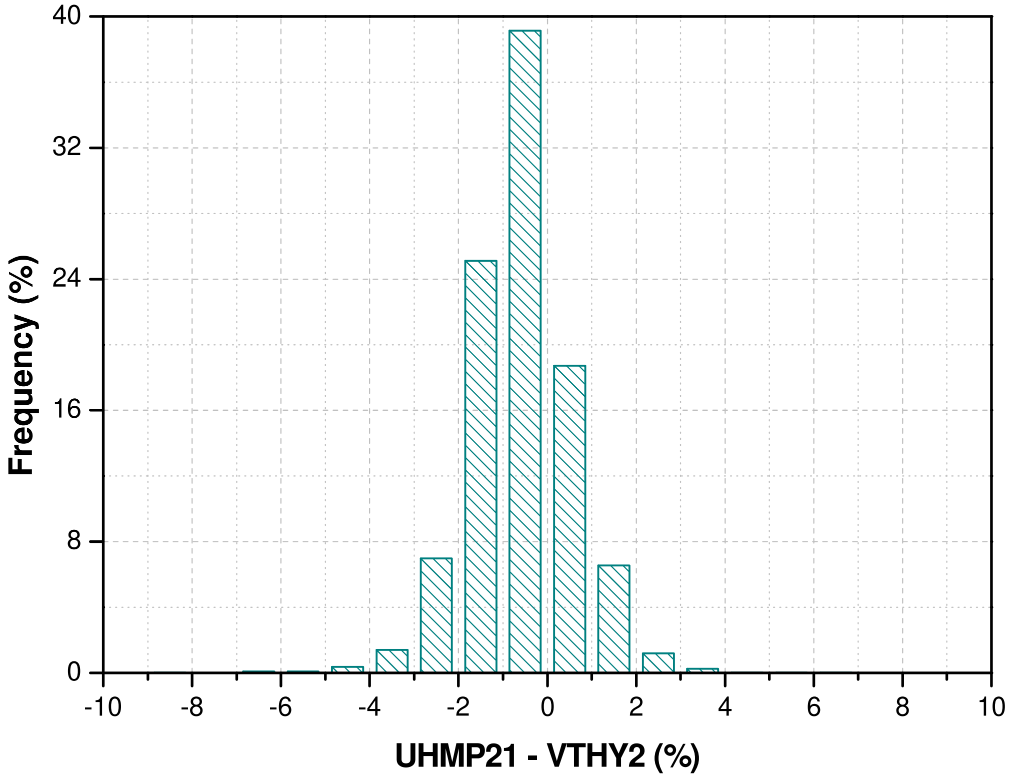


**Figure 13**

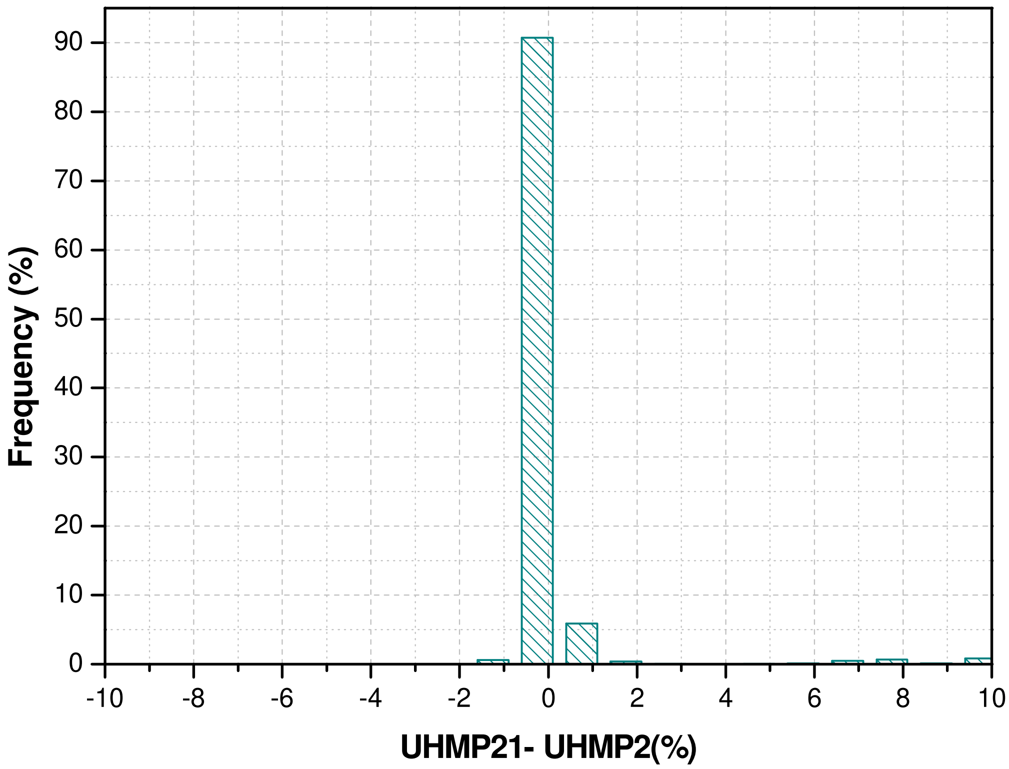
Frequency (%)
90
80
70
60
50
40
30
20
10
0
-10
-8
-6
-4
-2
0
2
4
6
8
10
UHMP21- UHMP2(%)

**Figure 14**

Sensor #22:

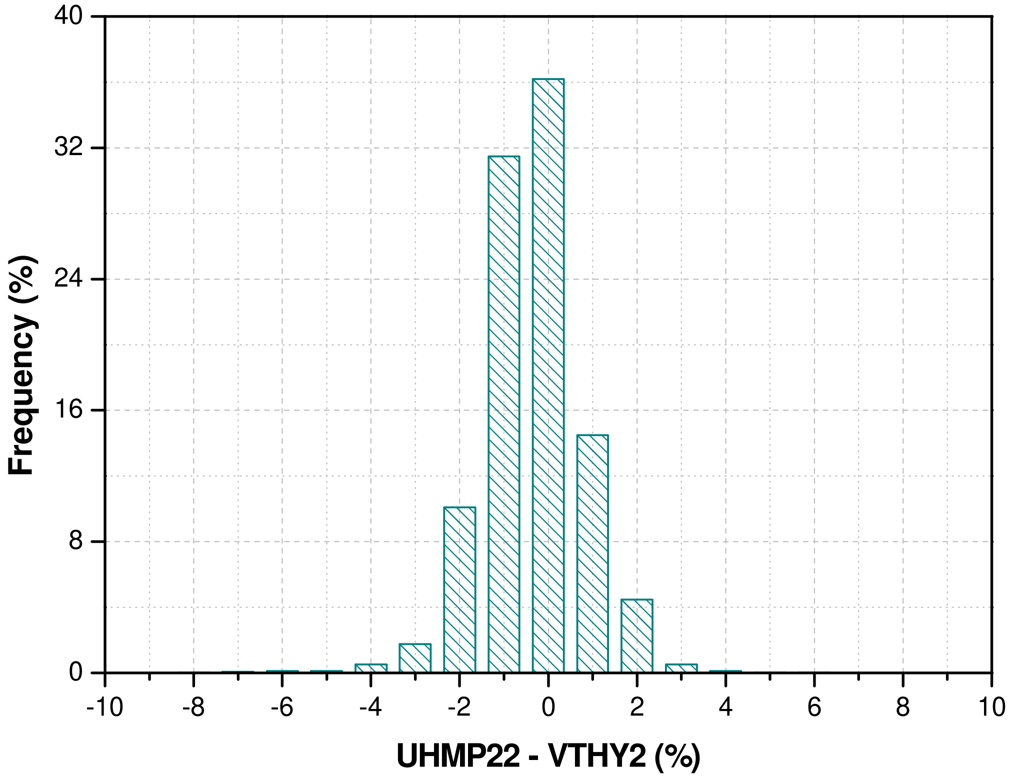


**Figure 15**

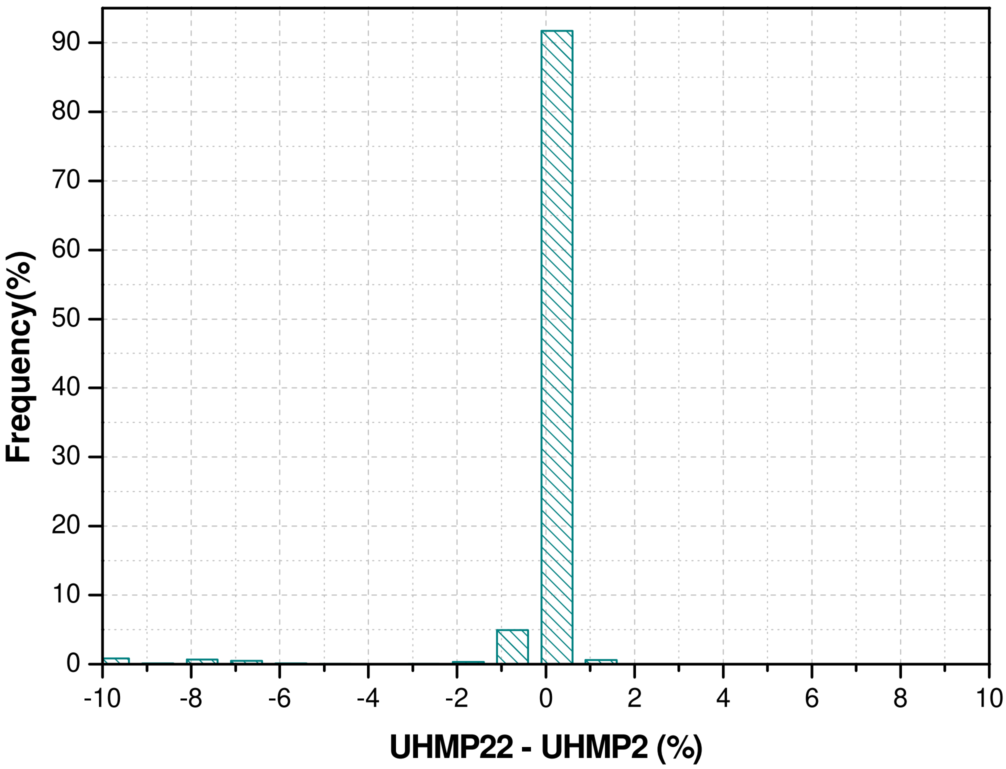


**Figure 16**

TABLE

The table 3 indicates the percentage of data that differ by less than 3 (and 6) % from the reference considered (VTHY2 or UHMP2).

**Table 3**

| | VTHY2 | | UHMP2 | |
|---|---|---|---|---|
| | [-3..3] | [-6..6] | [-3..3] | [-6..6] |
| UHMP11 | 97.8 | 99.9 | 99.6 | 99.8 |
| UHMP12 | 98.4 | 99.9 | 99.6 | 99.8 |
| UHMP21 | 97.7 | 99.9 | 99.6 | 99.8 |
| UHMP22 | 98.3 | 99.9 | 99.6 | 99.8 |

## INFLUENCE OF HUMIDITY

The distributions of differences between UHMP and the references are plotted, using 1-minute quality checked data for the whole period of the intercomparison. Differences are classified according the reference relative humidity.

Sensor #11:

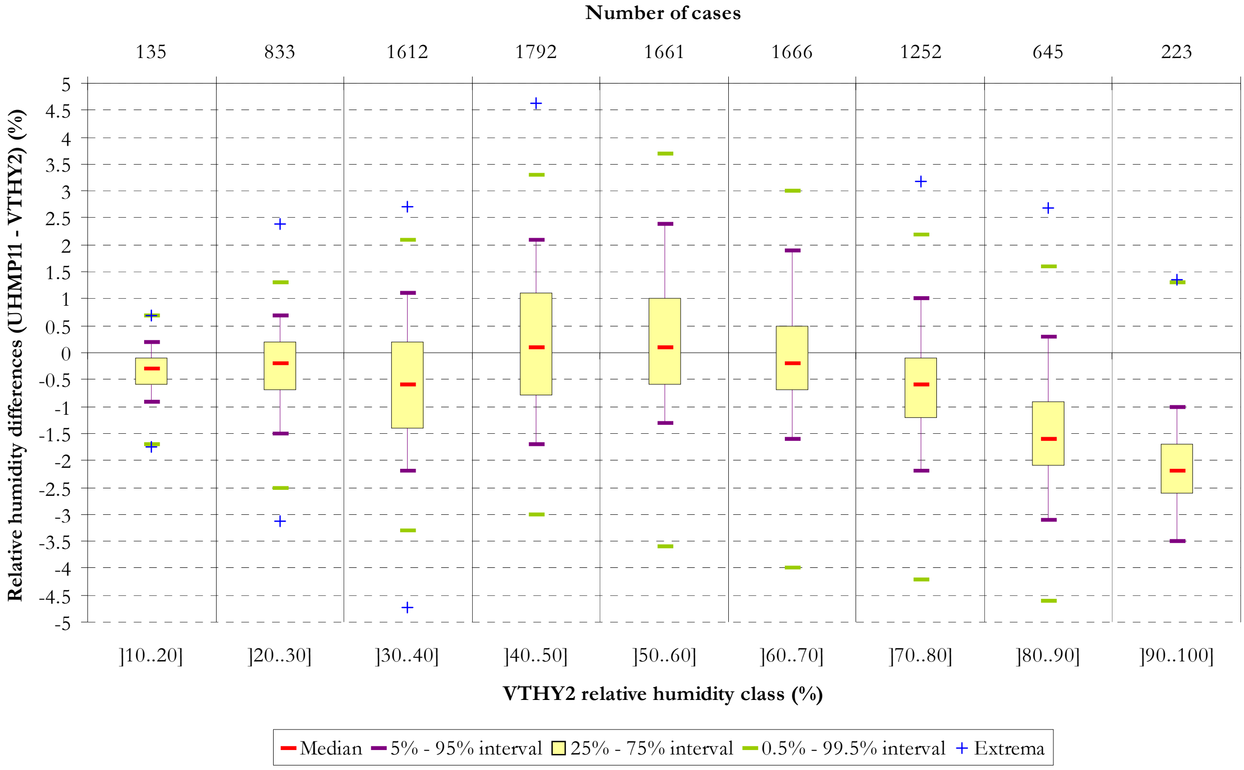


**Figure 17**

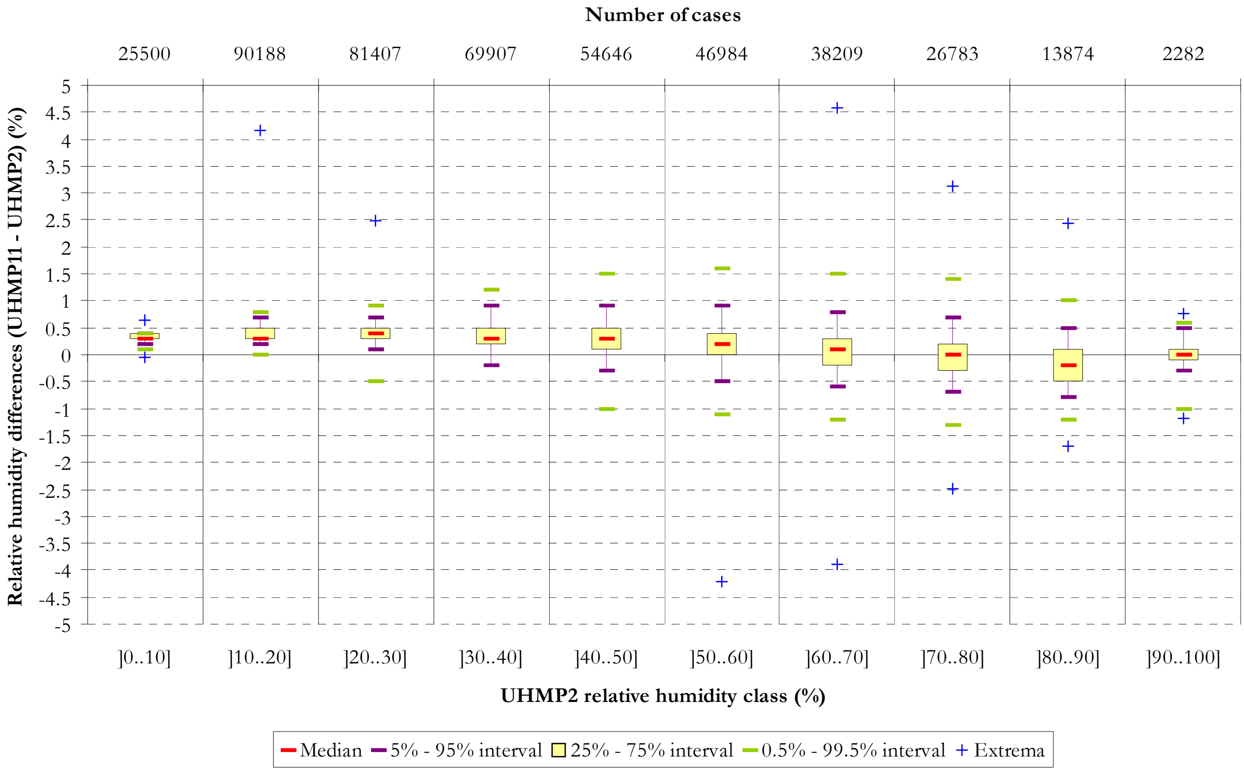


**Figure 18**

## Sensor #12:

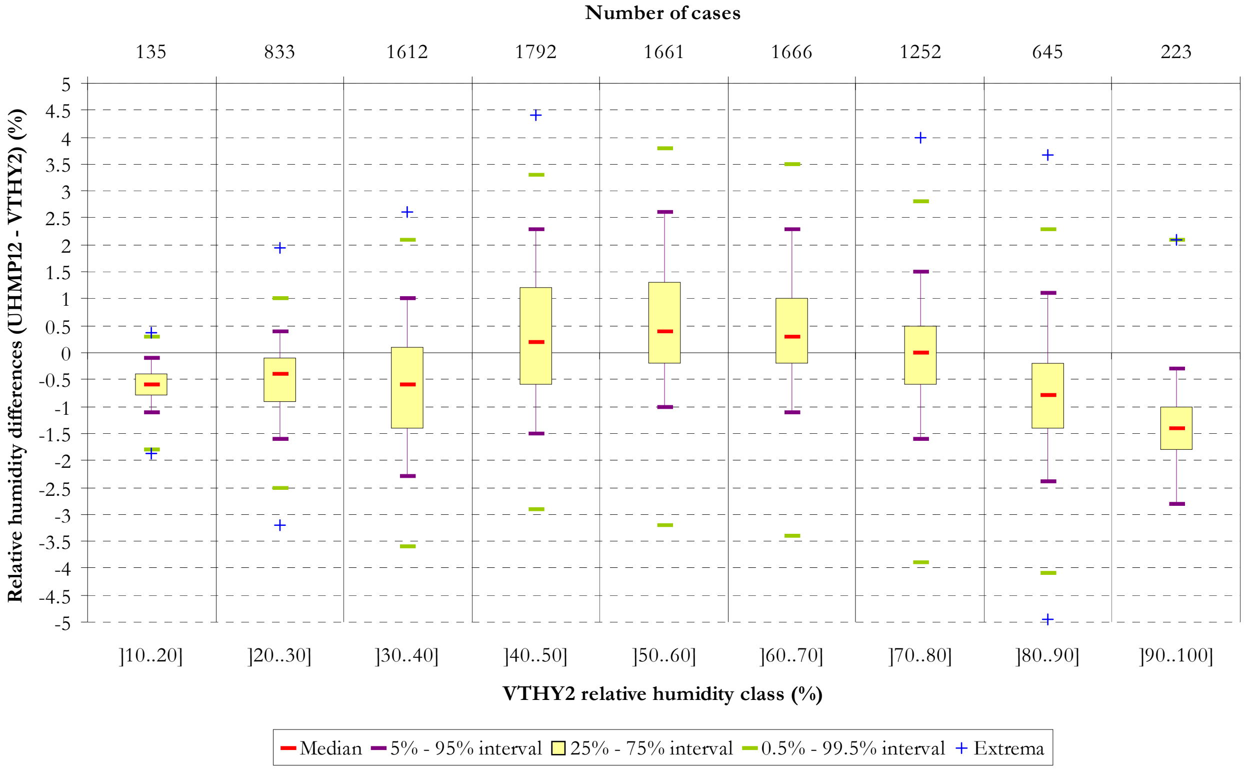


**Figure 19**

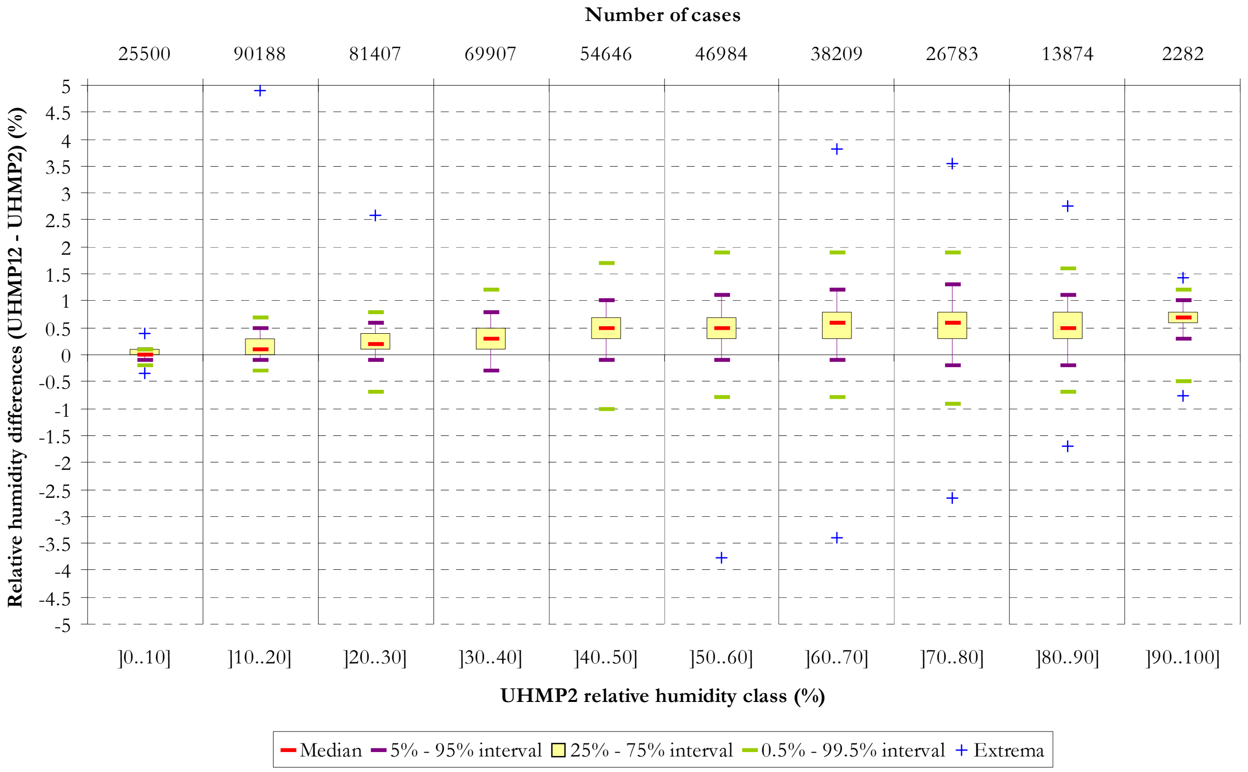


**Figure 20**

## Sensor #21:

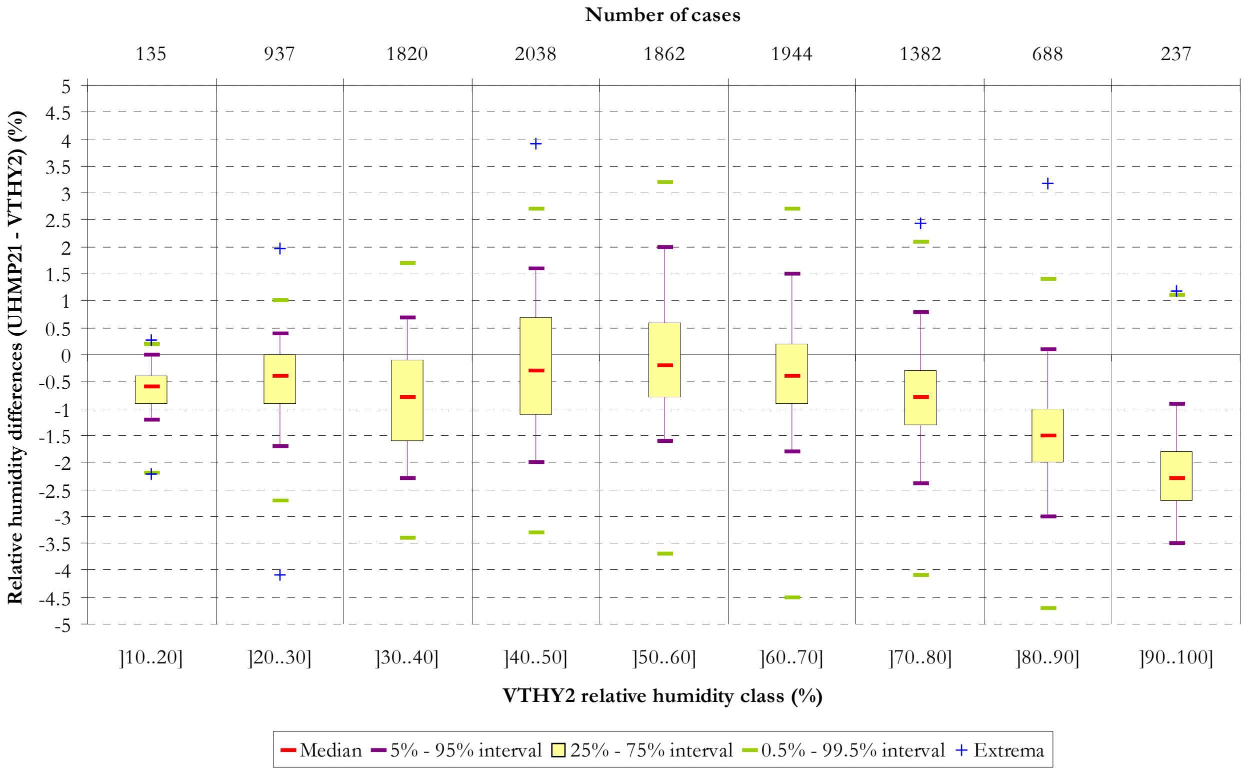


**Figure 21**

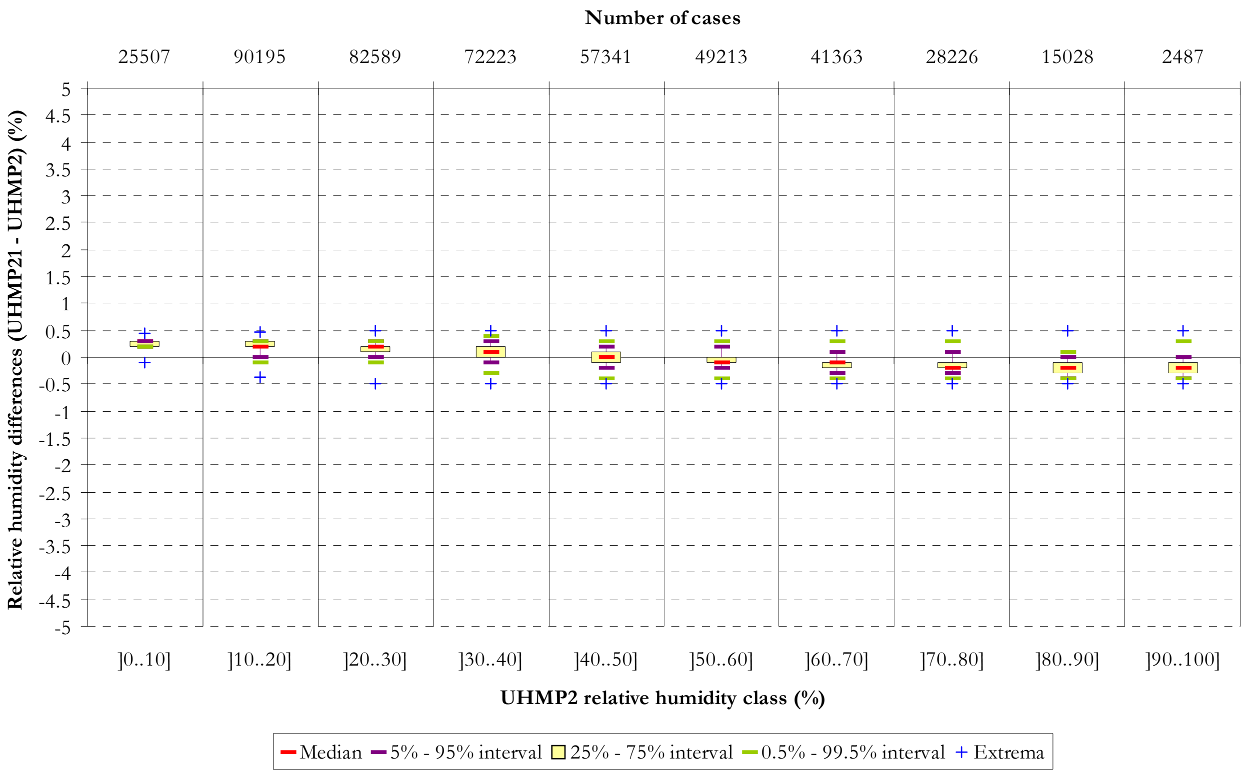


**Figure 22**

Sensor #22:

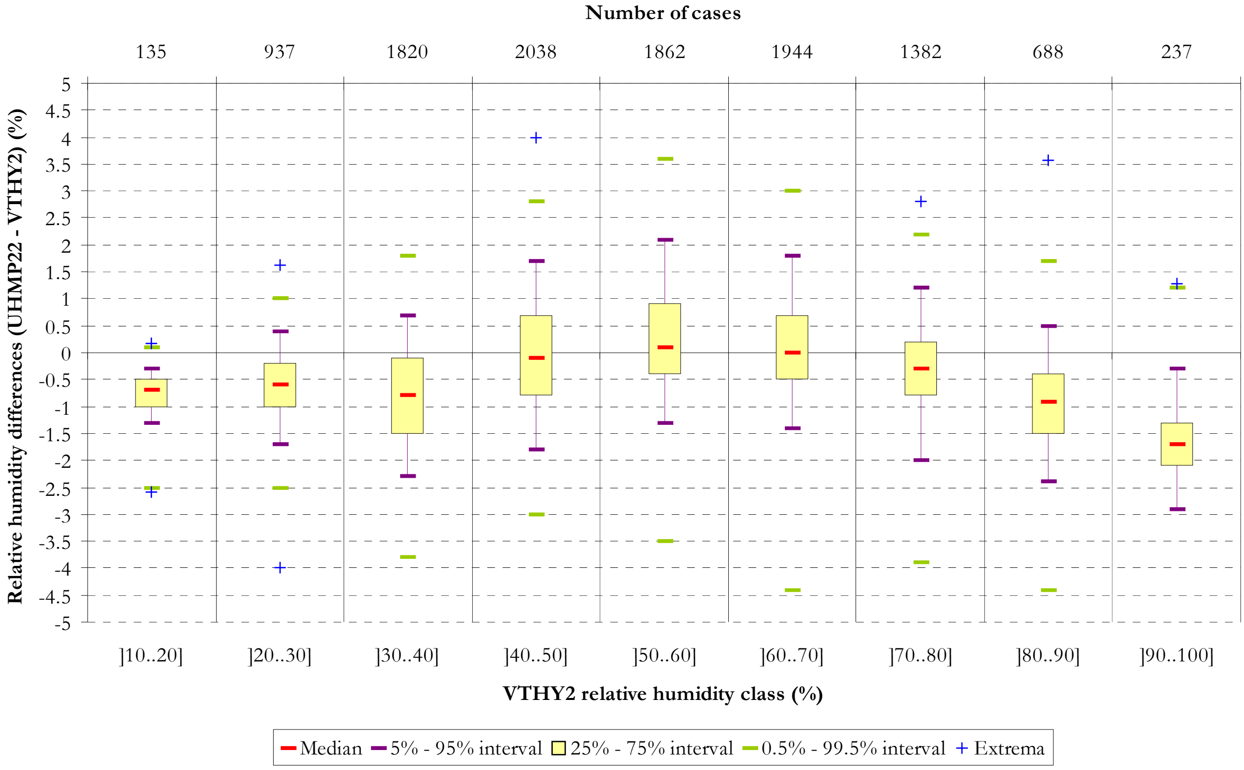


**Figure 23**

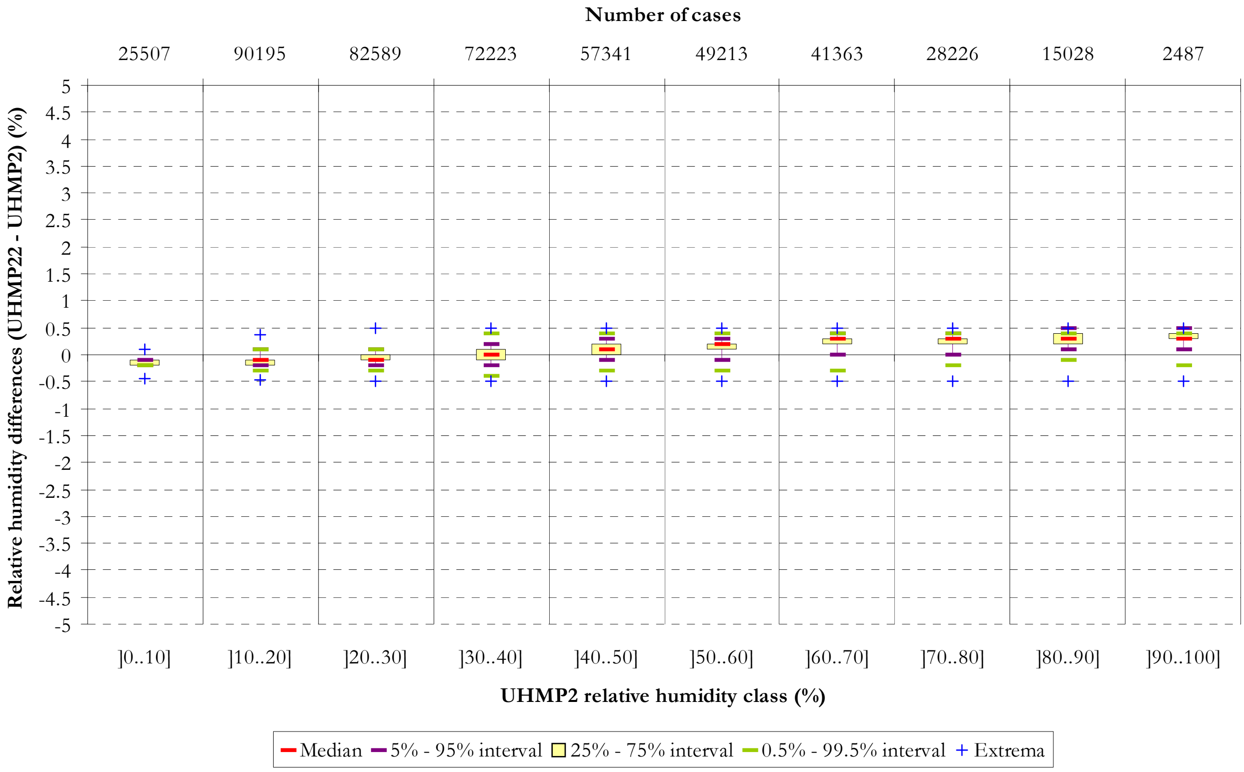


**Figure 24**

For all sensors, distributions of differences with UHMP2 have small variations, but no real dependency with humidity. All sensors behave the same compared to VTHY2 reference: the median of differences are around -0.5% for humidity values less than 80%. They decrease for higher values of humidity.

## INFLUENCE OF TEMPERATURE

The distributions of differences between UHMP and the references are plotted, using 1-minute quality checked data for the whole period of the intercomparison. Differences are classified according VEIG22 temperature.

Sensor #11:

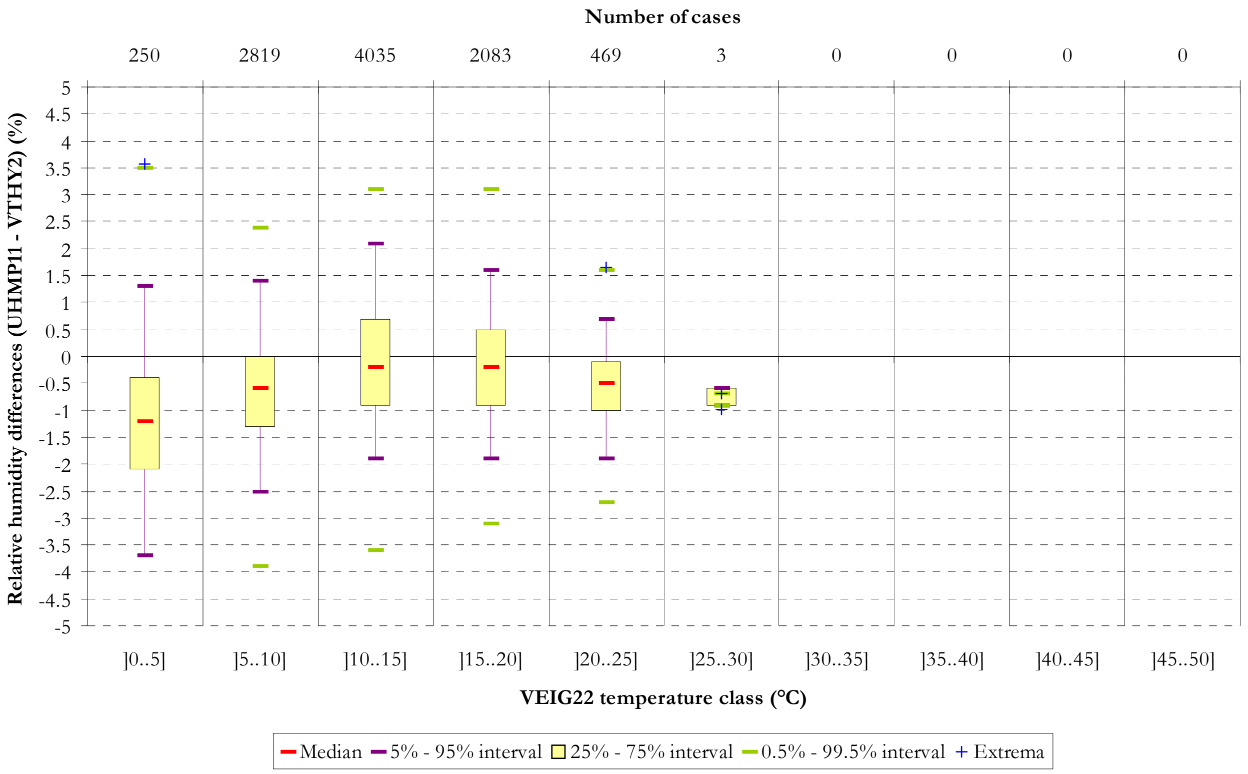


**Figure 25**

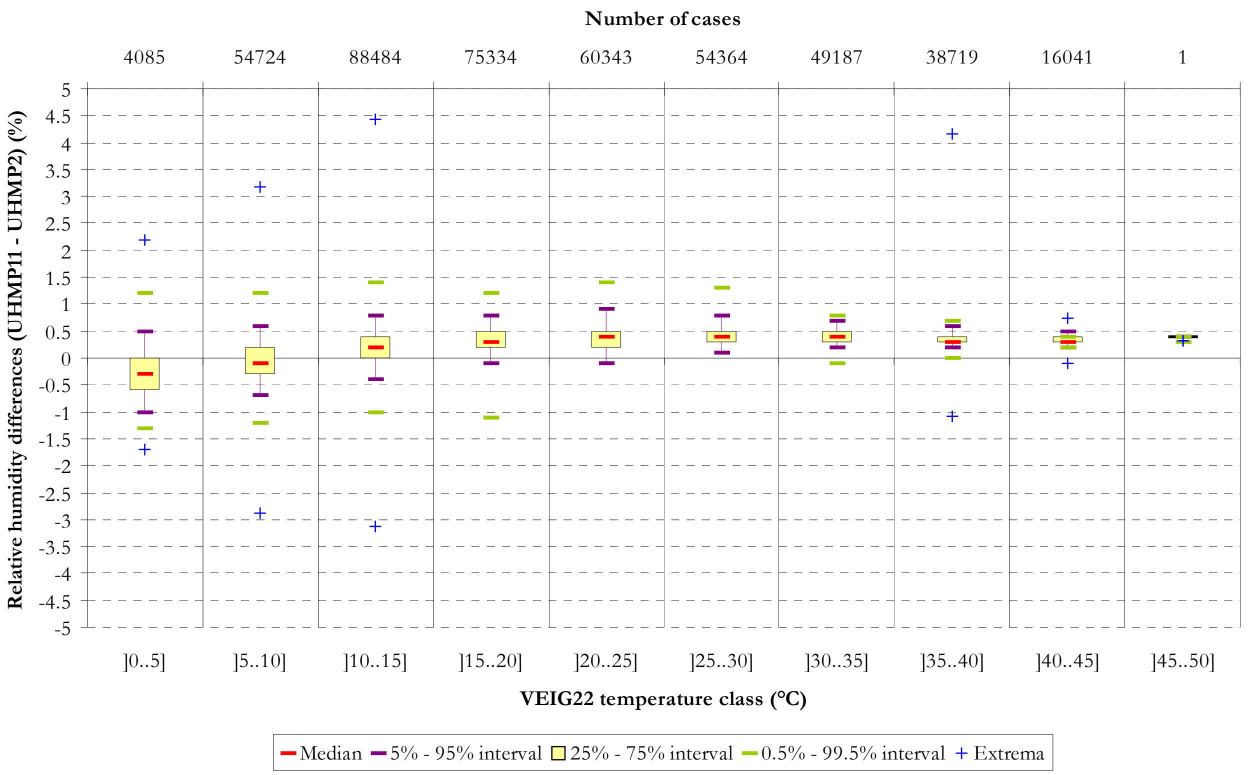


**Figure 26**

## Sensor #12:

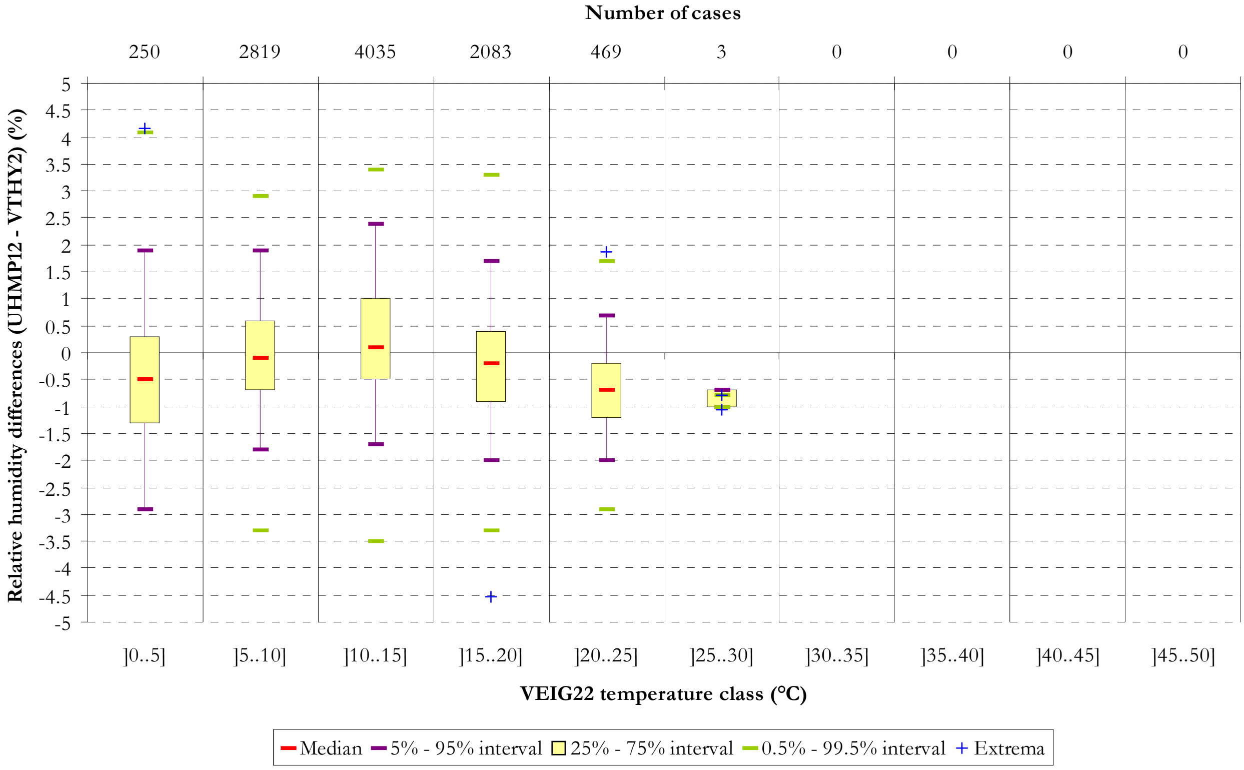


**Figure 27**

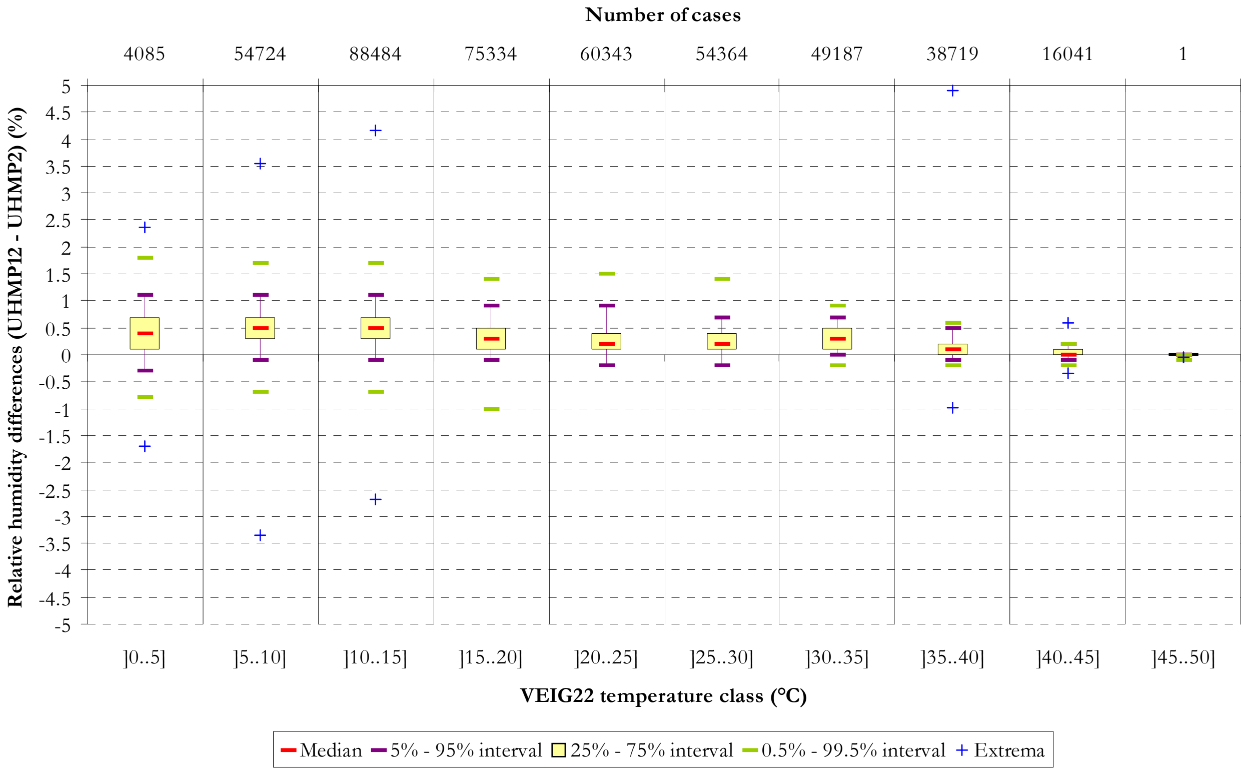


**Figure 28**

## Sensor #21:

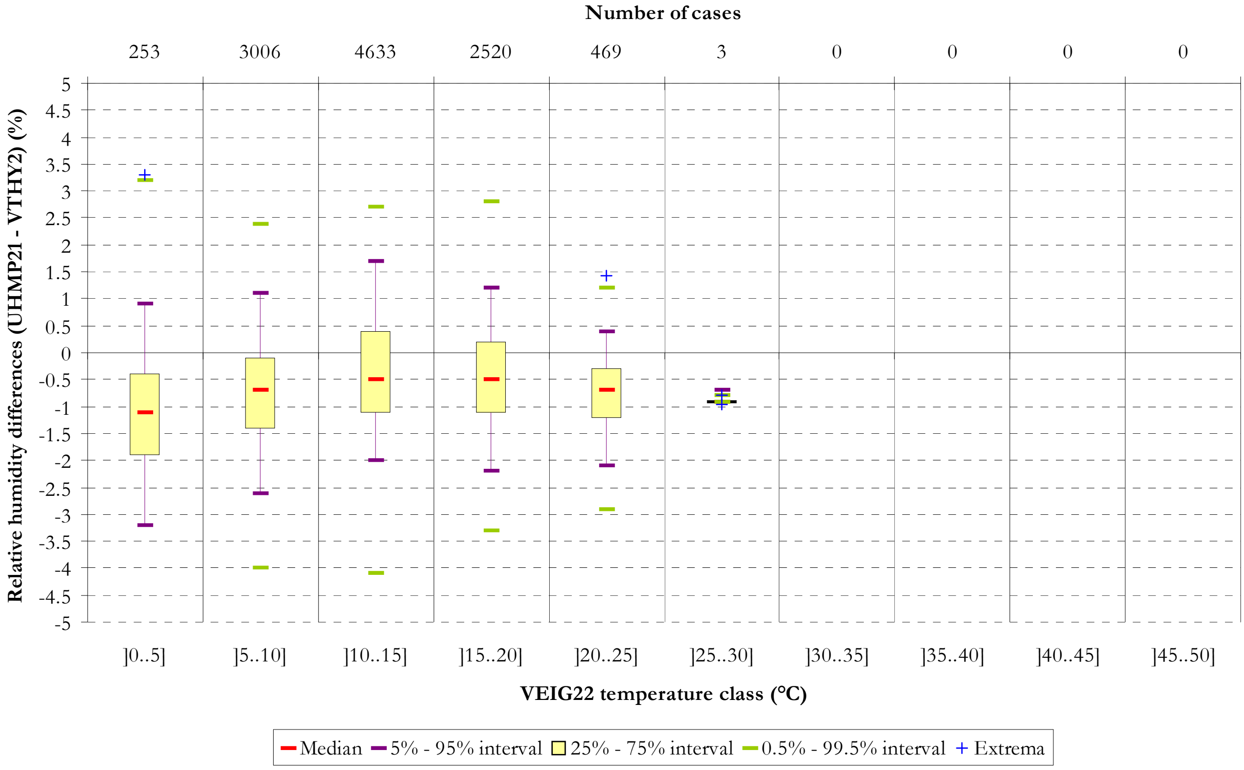


**Figure 29**

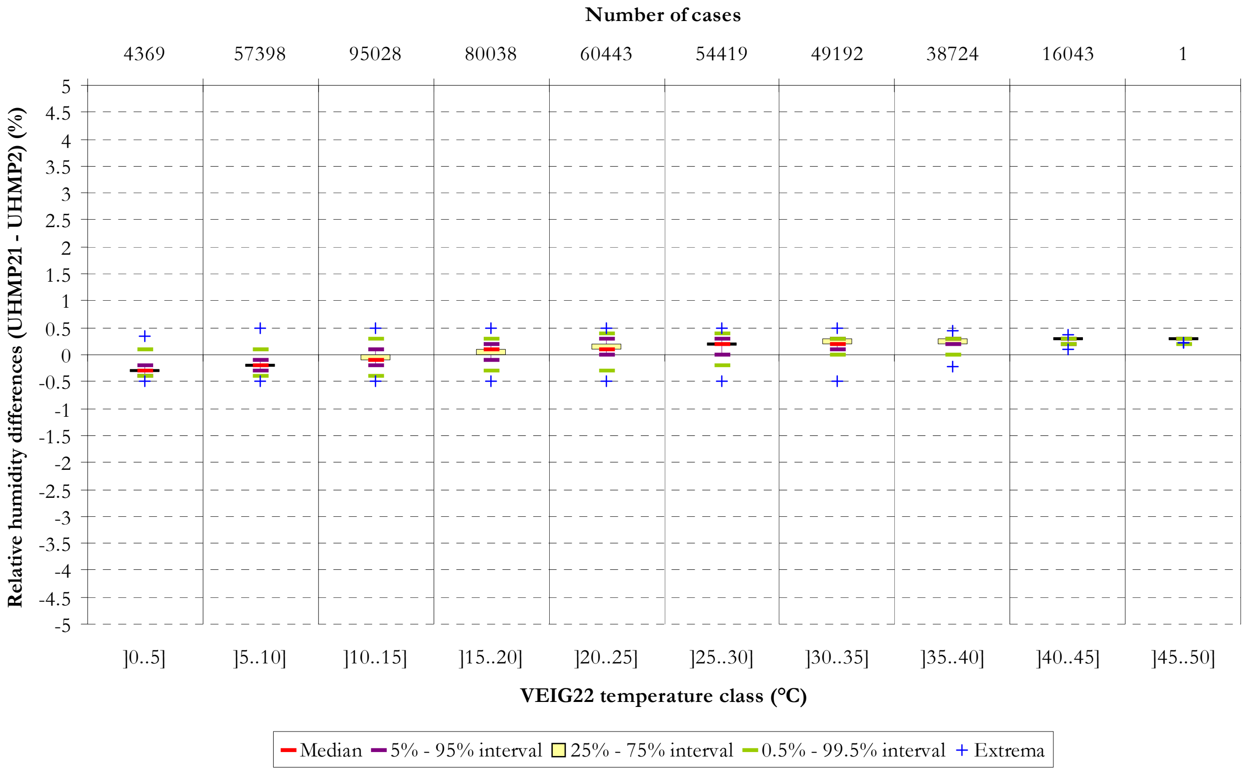


**Figure 30**

Sensor #22:

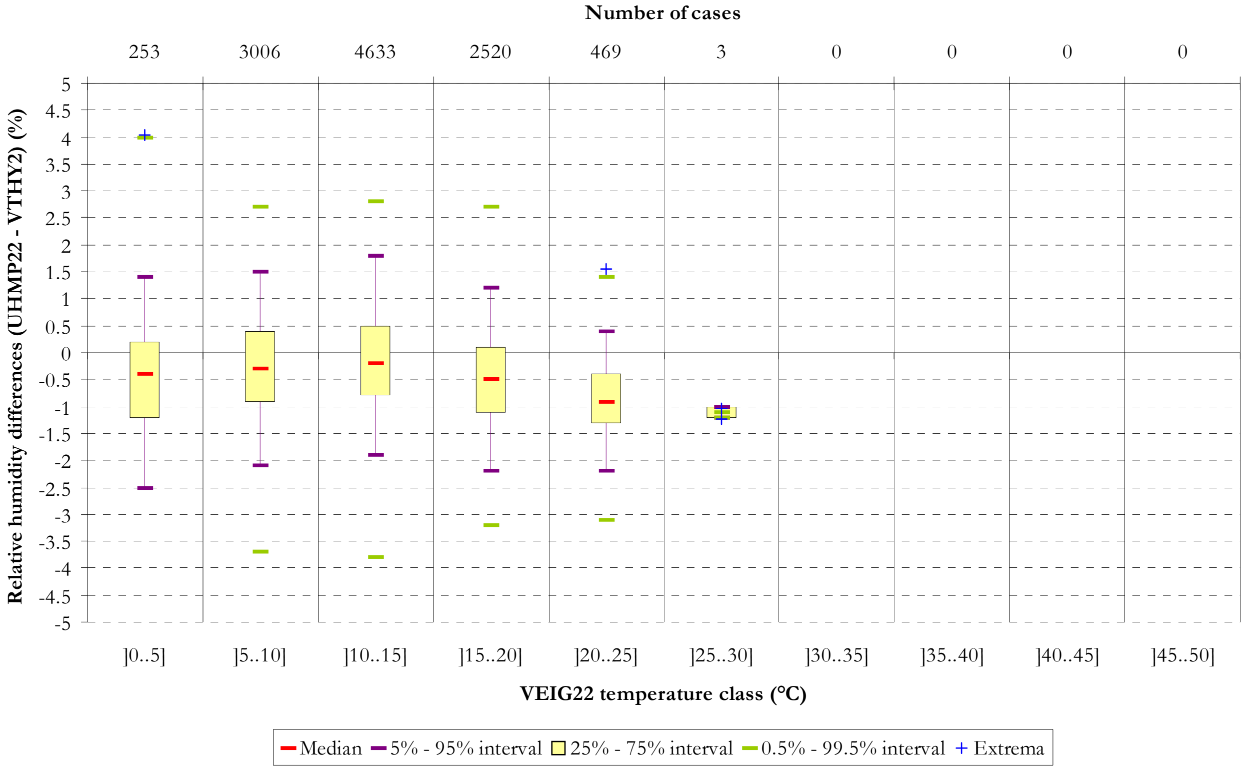


**Figure 31**

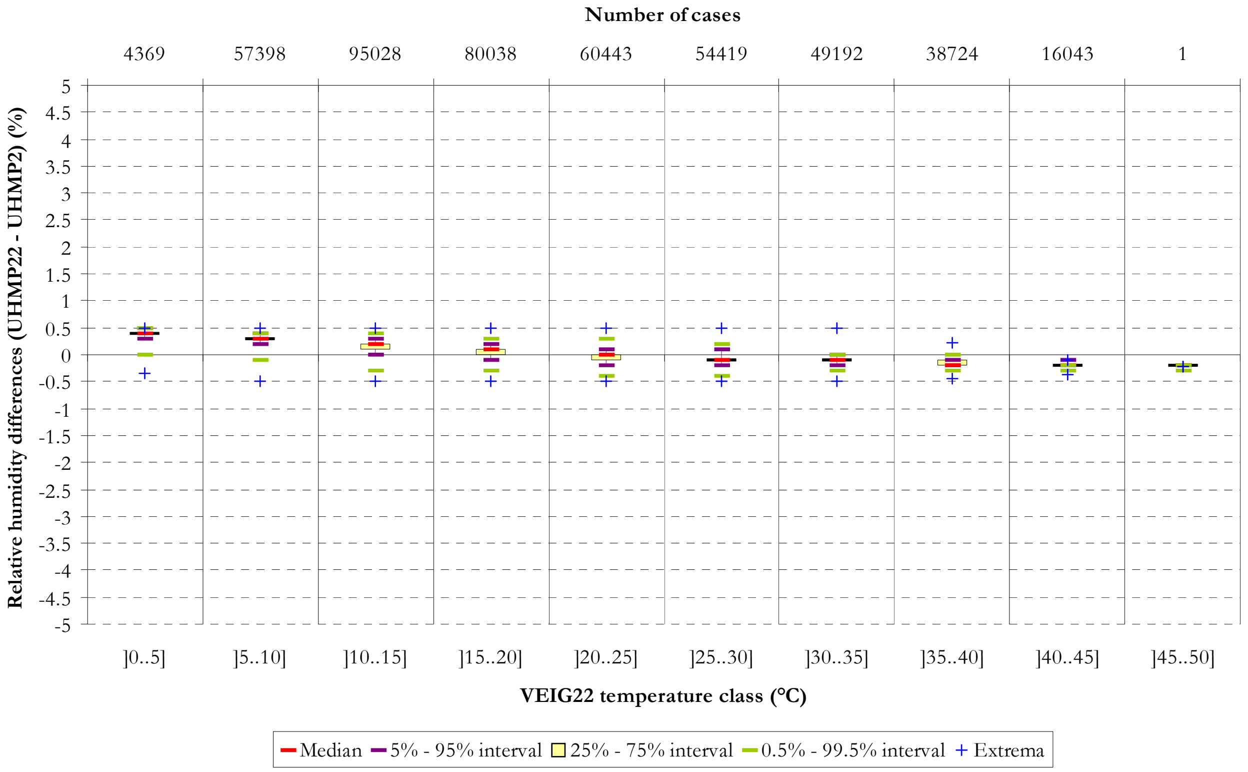


**Figure 32**

Differences with both references do not depend on temperature: variations of distributions with temperature is very low.

## COMBINED INFLUENCE OF TEMPERATURE AND RELATIVE HUMIDITY

The medians of differences between UHMP and UHMP reference are represented here with a contour plot. The VEIG22 temperature is on the X-axis and the reference relative humidity is on the Y-axis. Medians are used in all cases, provided that at least one data is available for both conditions on temperature and humidity considered.

The scale was chosen so as to be the same for all relative humidity sensors.

Sensor #11:

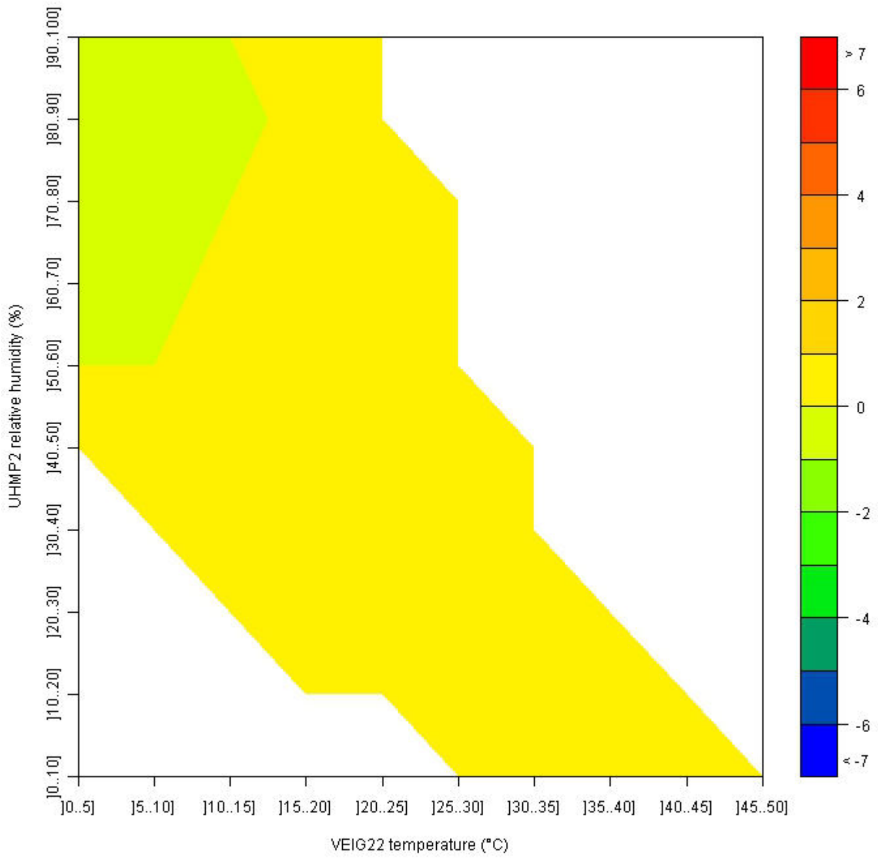


**Figure 33**

Sensor #12:

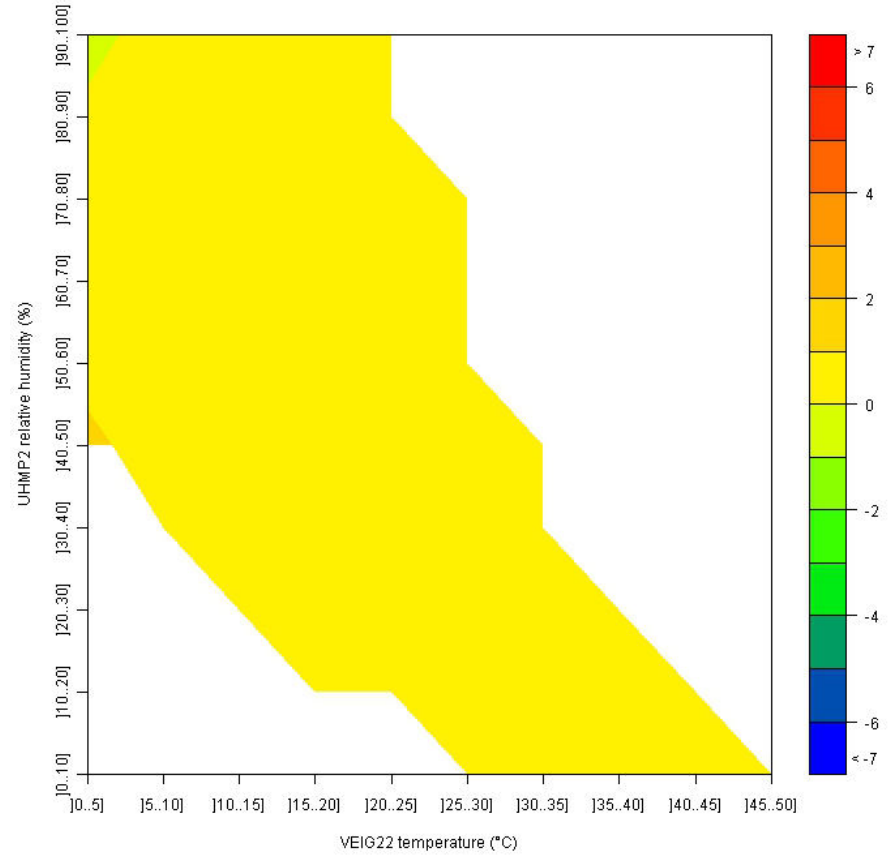


**Figure 34**

Sensor #21:

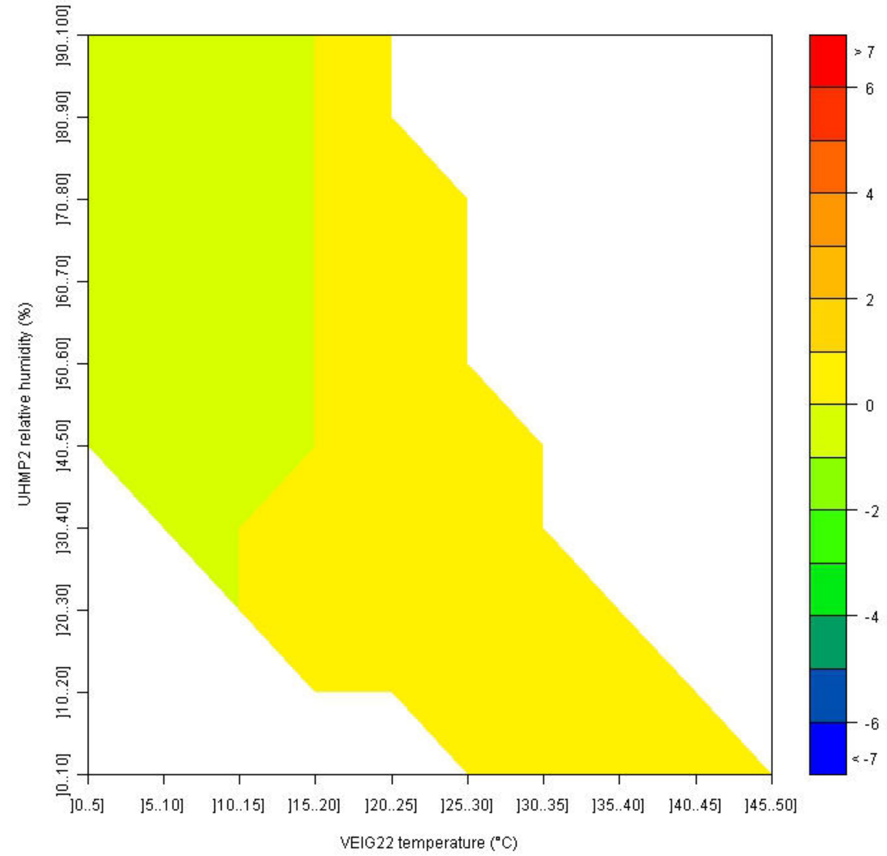


**Figure 35**

Sensor #22:

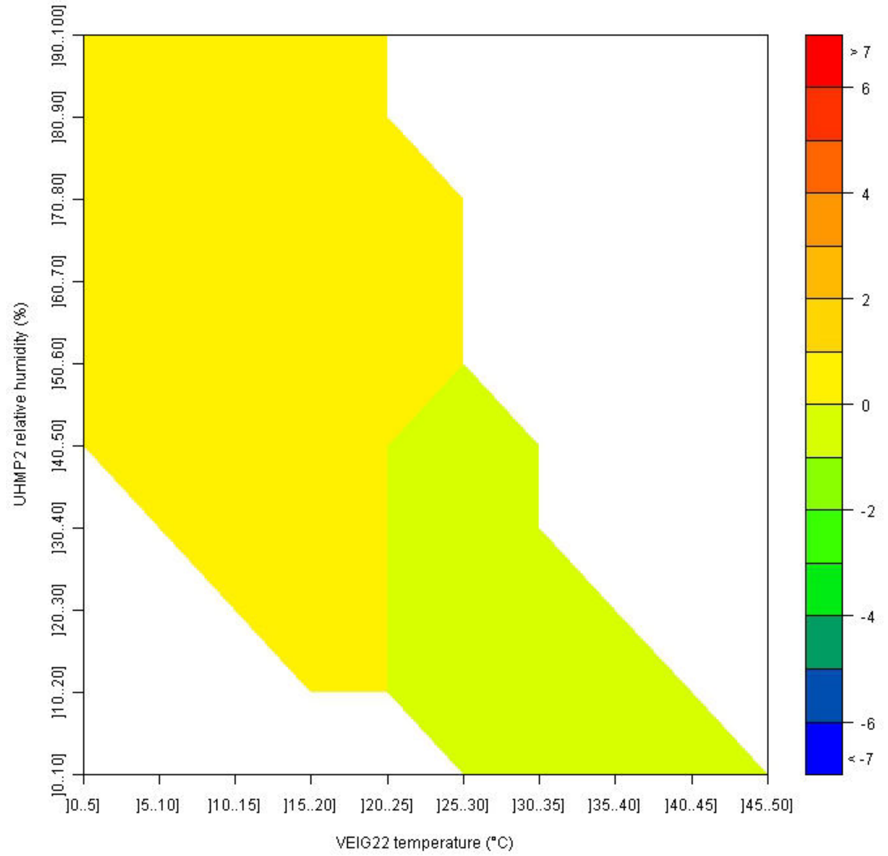


**Figure 36**

All contour plots are very uniform around the 0 value. No combined effect of temperature and humidity can be seen.

## TIME DRIFT

The distributions of differences between UHMP and the references are plotted, using 1-minute quality checked data for the whole period of the intercomparison, by step of one month. Reference relative humidity between 20% and 50% are only considered here: this is the common range in order to have data every month, without introducing influence of humidity itself.

Sensor #11:

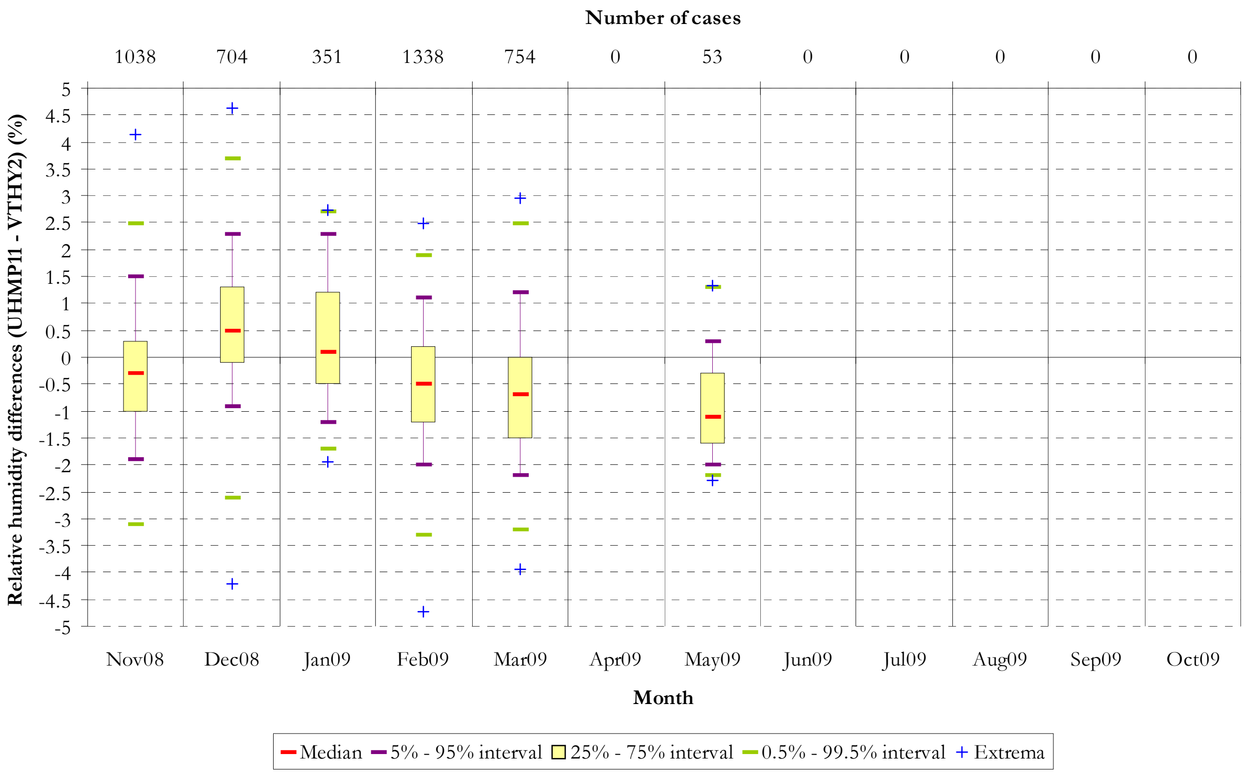


**Figure 37**

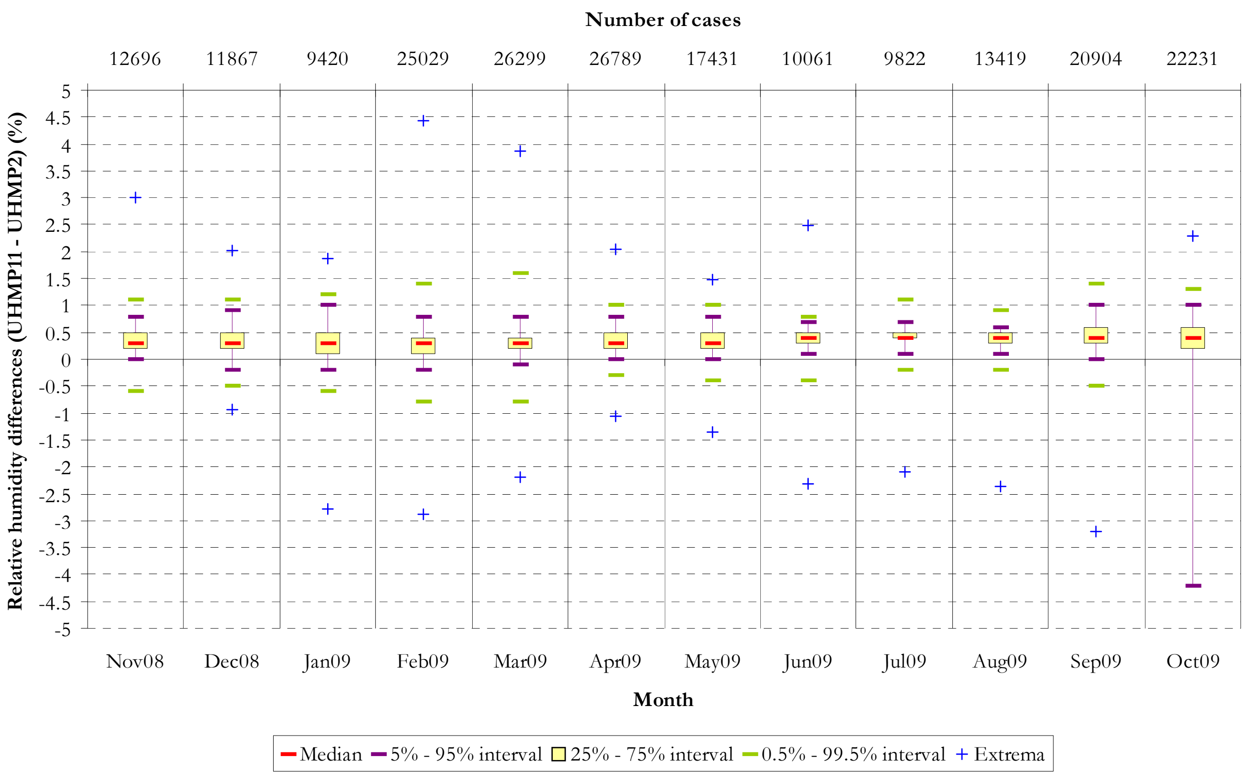


**Figure 38**

## Sensor #12:

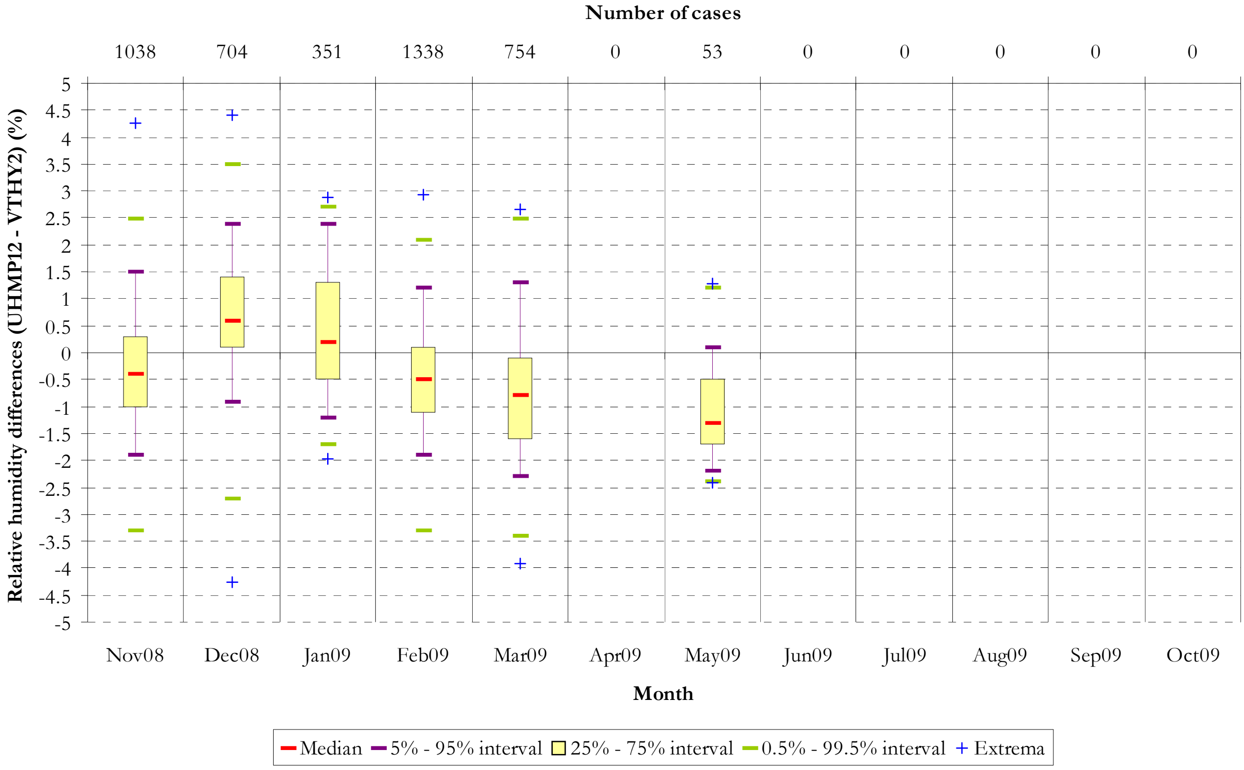


**Figure 39**

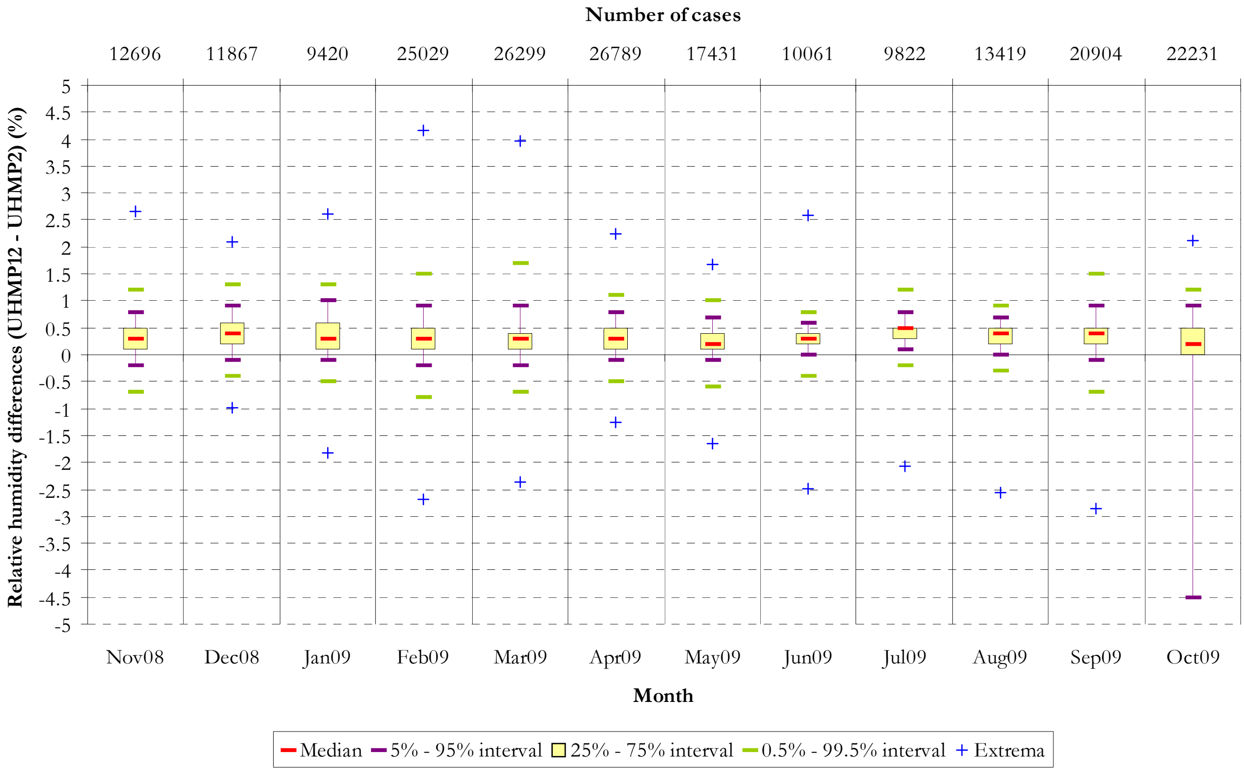


**Figure 40**

## Sensor #21:

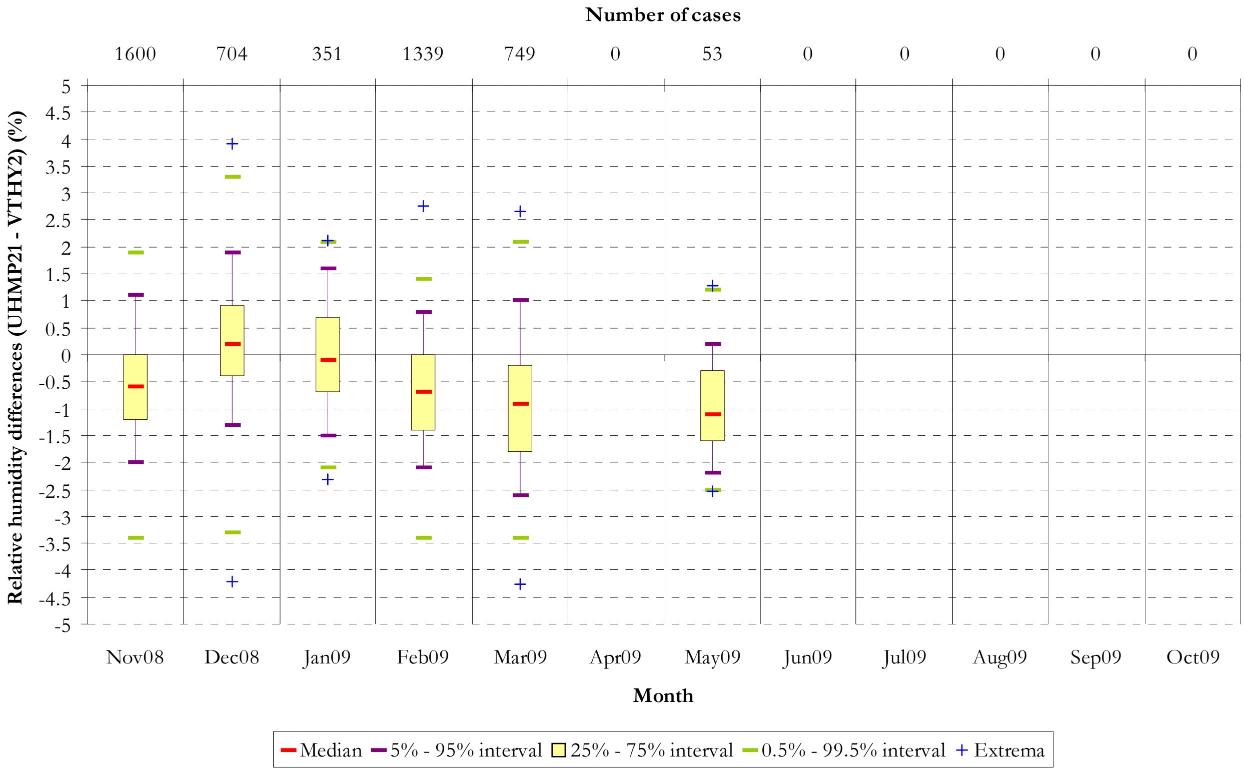


**Figure 41**

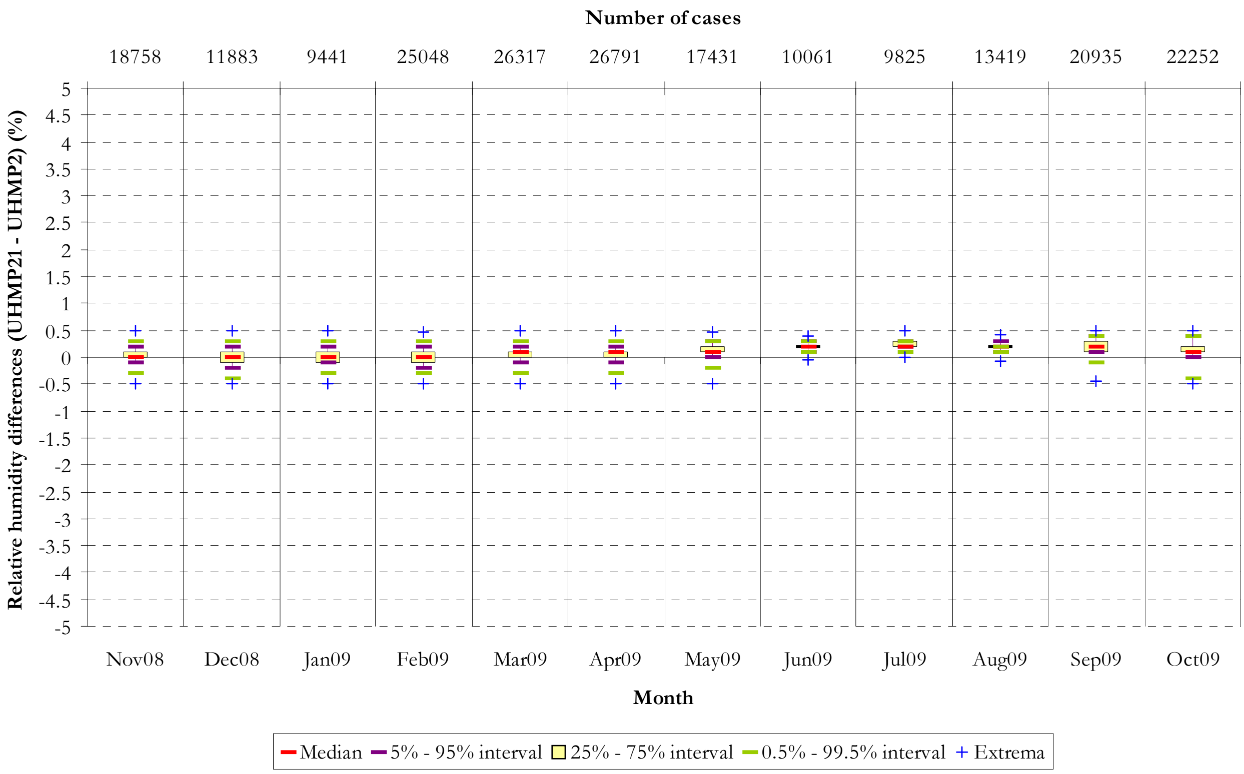


**Figure 42**

## Sensor #22:

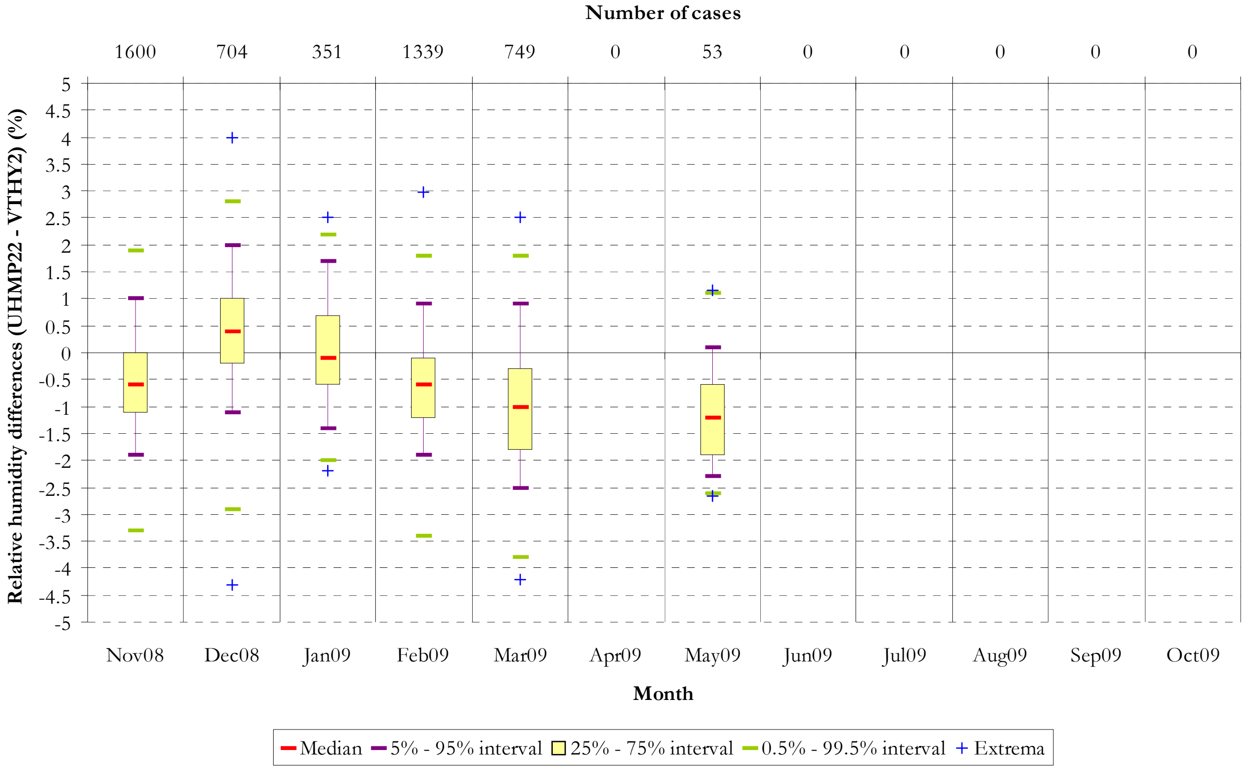


**Figure 43**

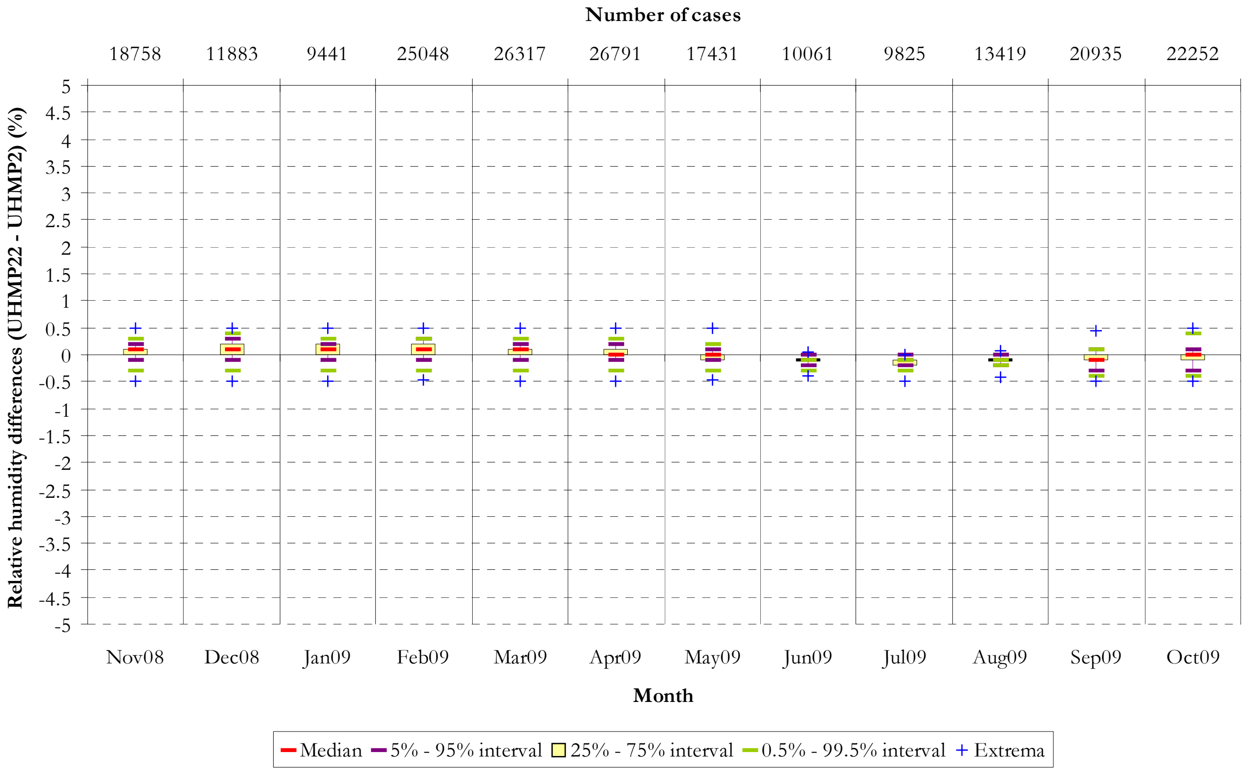


**Figure 44**

For all sensors, distributions of the end of the period look quite the same as distributions of the beginning, and this means no significant drift was recorded.

## QUALITY CONTROL INFORMATION

### DATA AVAILABILITY

The intercomparison period extends from the 1st of November 2008 to the 1st of November 2009. The theoretical number of 1-minute data is 525600.

The table 4 sums up the total number of data for each sensor and for each possible QC flag.

**Table 4**

| QC flag | UHMP11 | UHMP12 | UHMP21 | UHMP22 |
|---|---|---|---|---|
| 0 (good) | 503011 | 503026 | 503272 | 503093 |
| 1 (inconsistent) | 0 | 0 | 0 | 0 |
| 2 (doubtful) | 33 | 24 | 46 | 16 |
| 3 (erroneous) | 3761 | 3757 | 3487 | 3696 |
| 7 (missing) | 18795 | 18793 | 18795 | 18795 |

### MAINTENANCE

No action done during the intercomparison period.

# Hygrotest 6337 9742 TESTO AG
# – Germany –
# UTES

**TECHNICAL SPECIFICATIONS (PROVIDED BY THE MANUFACTURER)**

Dimensions: Length 19.6 cm x Diameter 2.1 cm

Principle of operation: capacitive humidity sensor, heated. Temperature measurement: Pt-100 with 4-wire connection

Accuracy: 2.5% RH at 25°C. Pt100 class B

Power supply: 18..28 VDC

**Figure 1**

The IOC chose to install these sensors in small multiplate naturally-ventilated Socrima screens (SSOC).

**Figure 2**

## OVERVIEW

Sensor #1 gave no measurements. The suspected reason for this fault is a problem of power supply and connection.

52 % of the measurements of sensor #2 were found within ±3% of the Thygan reference.

Sensor #2 seems to have a constant bias of 3 % with VTHY2 reference, of 4 % with UHMP2 reference. Differences with UHMP2 are a bit higher for humidity values between 20 and 40%. This bias is not explained by the laboratory and on site calibration, but these calibrations were performed a long period before the start of the intercomparison (March 2007 in laboratory).

There is an effect of temperature on differences: in particular, for temperatures between 25 and 35°C, medians of differences are around 5 %.

Sensor #2 gives higher differences for temperatures between 25 and 35°C and humidity values between 30 and 50%.

UTES2 differences with UHMP2 reference has changed by about 1.5 percentage point on the median of differences between the beginning and the end of the intercomparison. This sensor has likely drifted.

The results of UTES2 are not explained by the overestimation of the temperature in the SSOC2 screen.

## CALIBRATION INFORMATION

Calibration in Trappes (22 Dec 2006):

**Table 1**

| Sensor | Serial number | 23°C | | | | | 40°C | | | | |
|---|---|---|---|---|---|---|---|---|---|---|---|
| | | 10% | 33% | 55% | 75% | 90% | 10% | 33% | 55% | 75% | 90% |
| UTES1 | 973764 | -0.6 | -0.4 | -0.2 | 0.7 | 1.4 | -0.8 | -0.8 | -1.1 | 0.0 | 1.2 |
| UTES2 | 960104 | -0.2 | 0.2 | 0.5 | 1.2 | 1.9 | -0.4 | -0.4 | -0.5 | 0.6 | 1.4 |

On site calibration (June 2008):

**Table 2**

| Sensor | Serial number | 33% | 80% |
|---|---|---|---|
| UTES2 | 960104 | -2.65 | -0.3 |

## COMPARISON WITH THE REFERENCE

Thygan sensor #2 was first chosen as the reference for humidity measurements. But it was not available after April 2009. That is why a second reference was selected, which is the average of two HMP45D probes from Vaisala, when the difference between both values is lower than 1 percentage point of relative humidity.

For more details about the choice of references for humidity measurement, please refer to part 5.5.1 of the final report.

### HISTOGRAM OF DIFFERENCES

The histograms of differences between UTES and the references are plotted, using 1-minute quality checked data for the whole period of the intercomparison. Differences are plotted by steps of 1 %. The vertical axis is the frequency in percent for each class of differences.

Sensor #2:

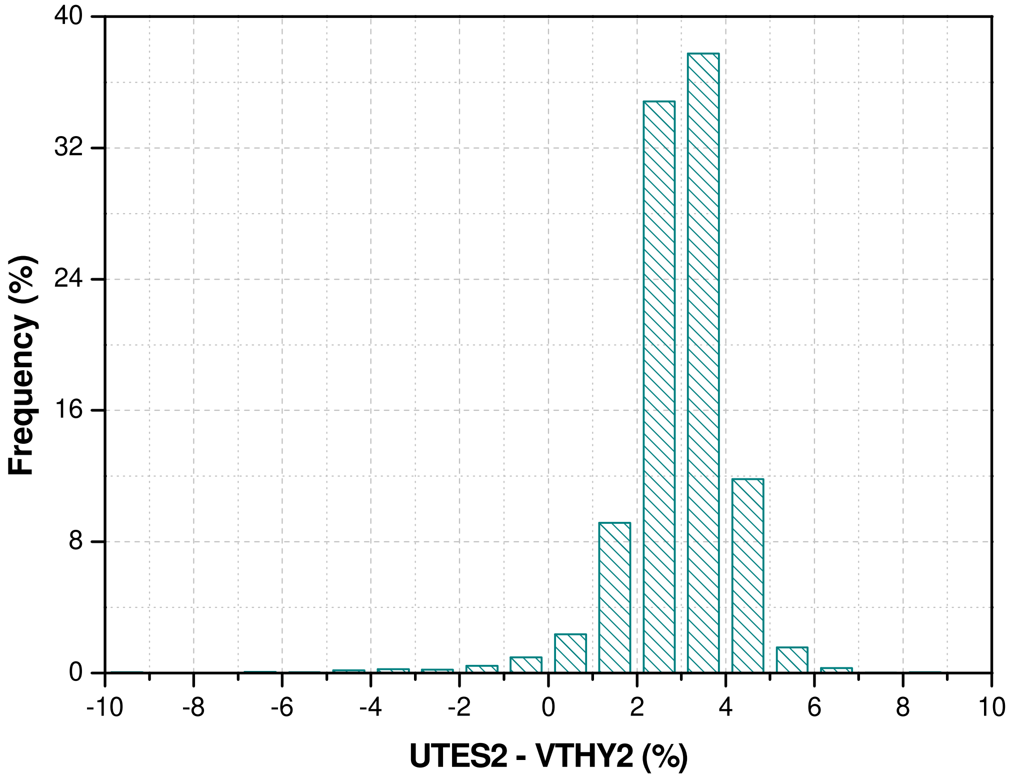


**Figure 3**

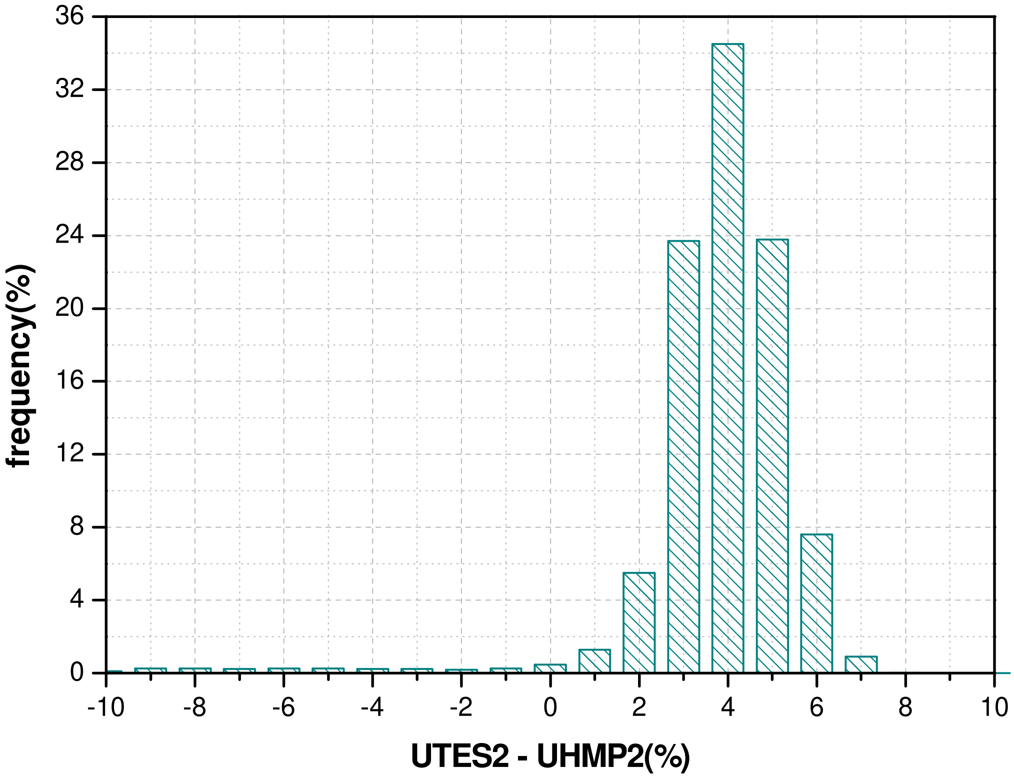


**Figure 4**

TABLE

The table 3 indicates the percentage of data that differ by less than 3 (and 6) % from the reference considered (VTHY2 or UHMP2).

**Table 3**

| | VTHY2 | | UHMP2 | |
|---|---|---|---|---|
| | [-3..3] | [-6..6] | [-3..3] | [-6..6] |
| UTES2 | 51.6 | 97.9 | 18.0 | 97.0 |

## INFLUENCE OF HUMIDITY

The distributions of differences between UTES and the references are plotted, using 1-minute quality checked data for the whole period of the intercomparison. Differences are classified according the reference relative humidity.

## Sensor #2:

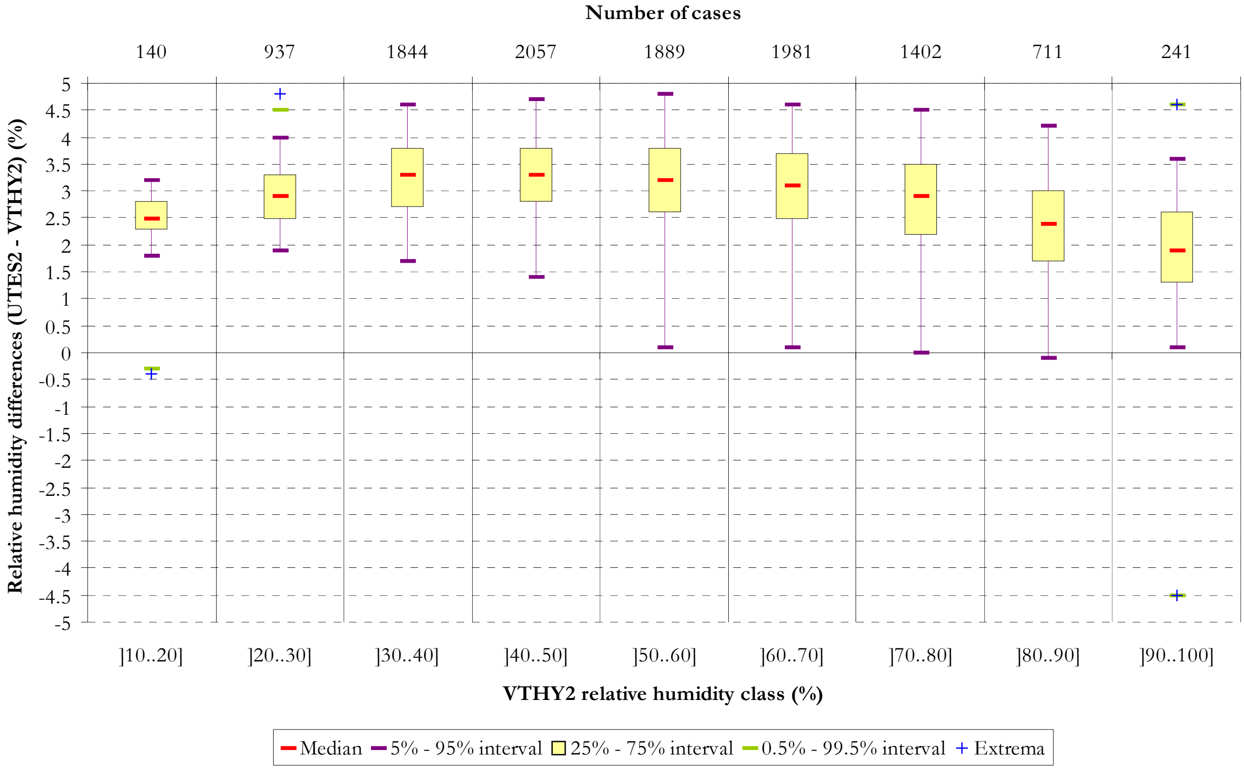


**Figure 5**

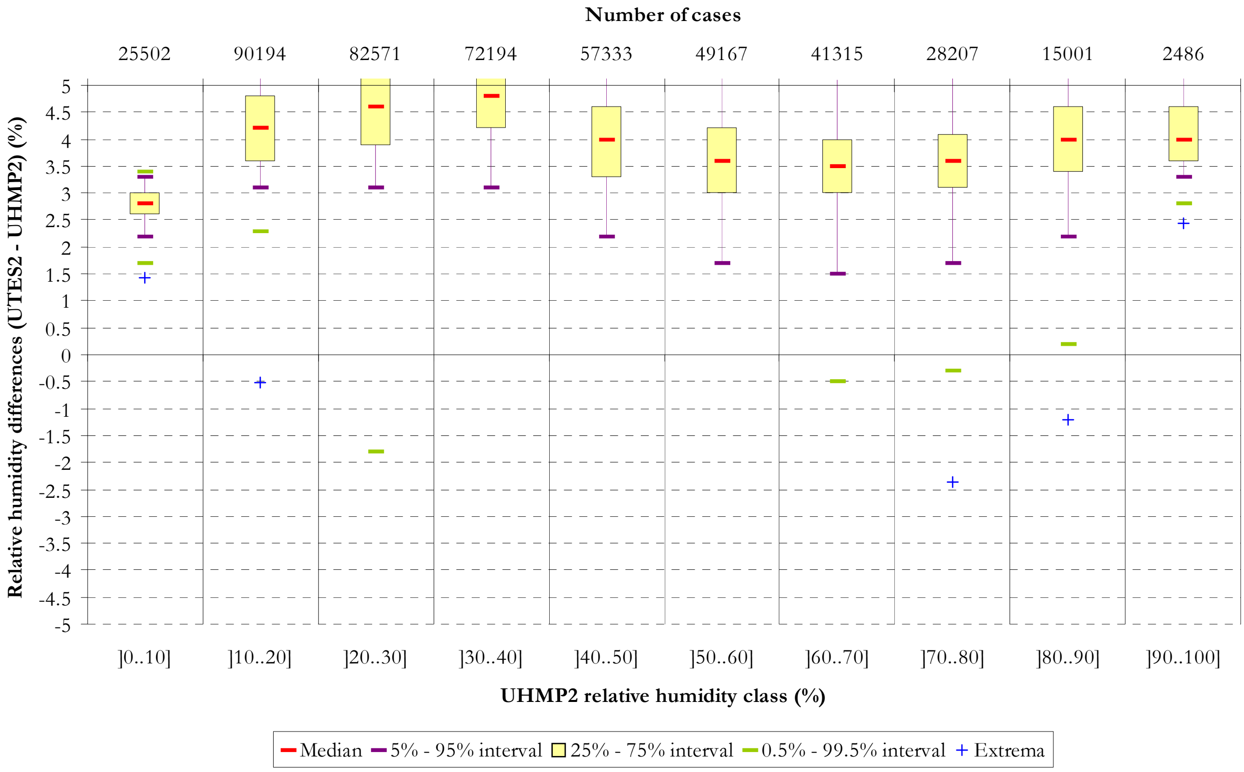


**Figure 6**

Sensor #2 seems to have a constant bias of 3 % with VTHY2 reference, of 4 % with UHMP2 reference. Differences with UHMP2 are a bit higher for humidity values between 20 and 40%.

## INFLUENCE OF TEMPERATURE

The distributions of differences between UTES and the references are plotted, using 1-minute quality checked data for the whole period of the intercomparison. Differences are classified according VEIG22 temperature.

Sensor #2:

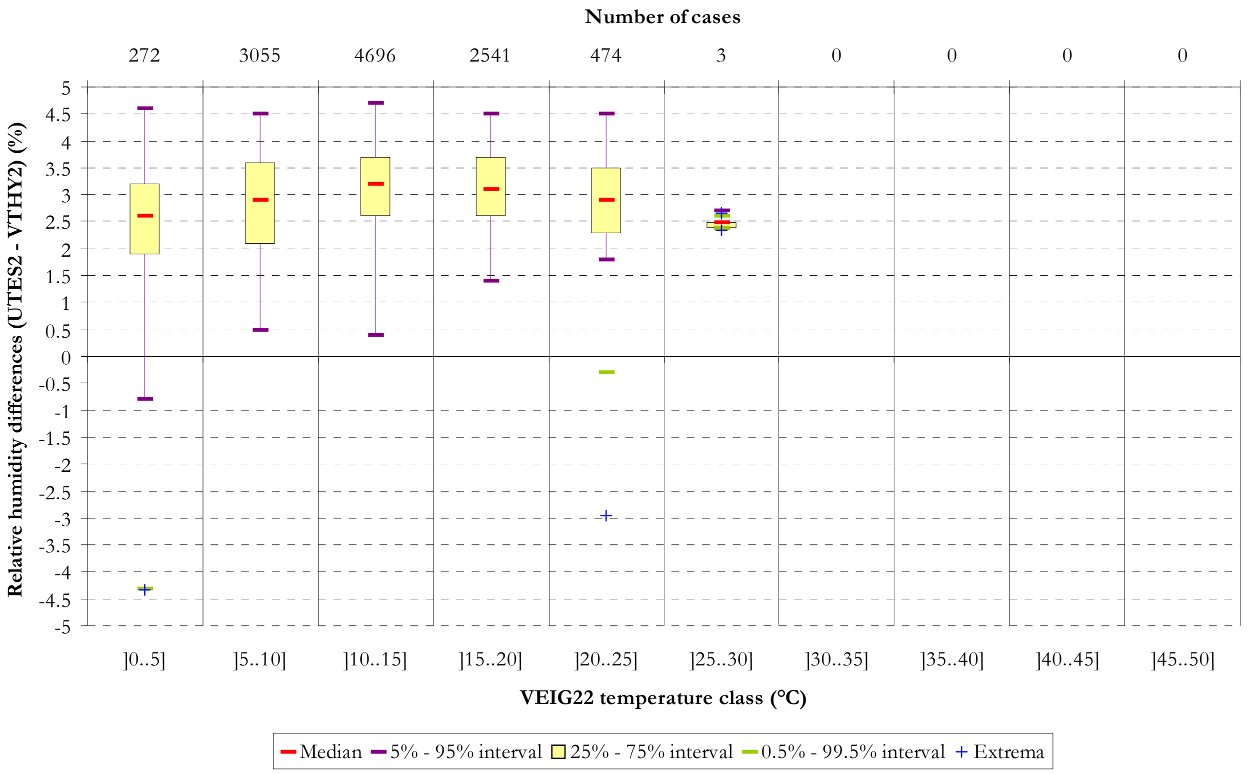


**Figure 7**

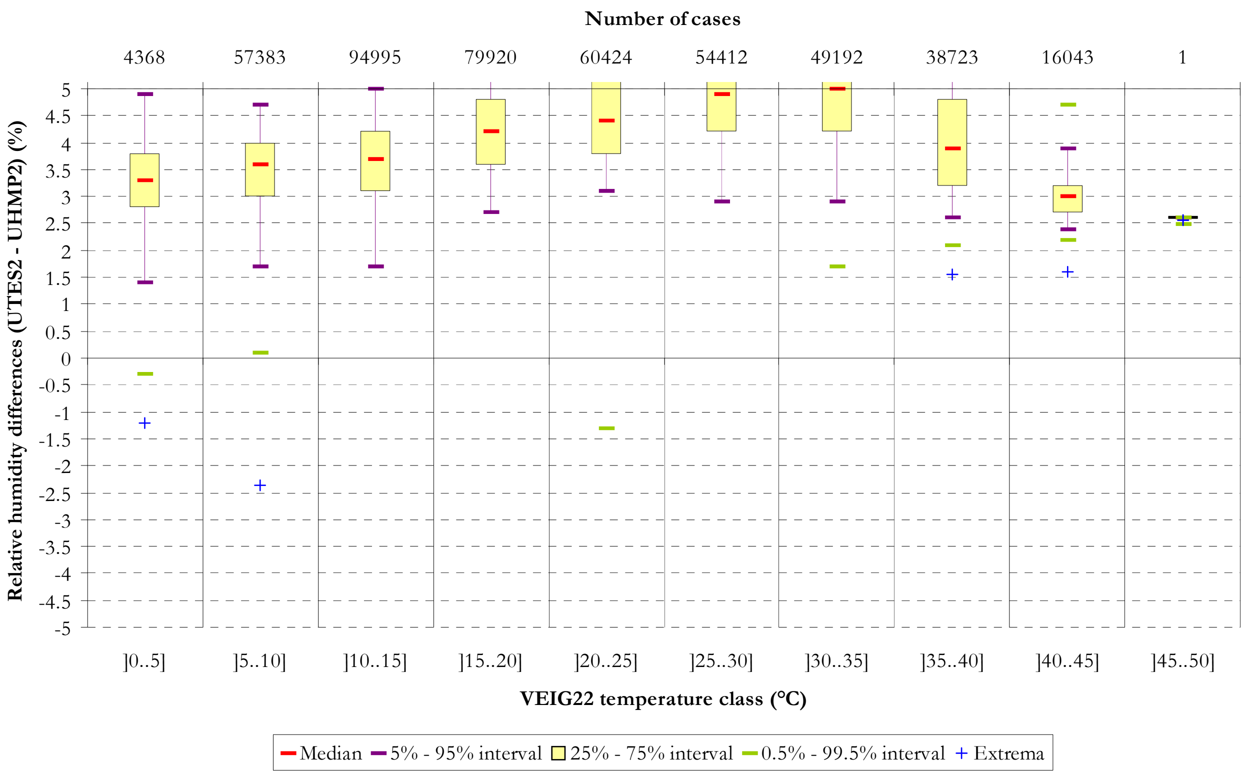


**Figure 8**

There is an effect of temperature on differences: in particular, for temperatures between 25 and 35°C, medians of differences are around 5 %. Figure 9 and figure 10 illustrate these observations. On the first one, in November 2008, the temperature (bottom curve) is quite less than 20°C, relative humidity differences (top curves) between UTES2 (green curve) and both references VTHY2 (red curve) and UHMP2 (purple curve) are around 3 %. On the second figure, with same colours, the temperature in June 2009 in much higher (between 25 and 41°C), relative humidity differences are much higher, around 6 %.

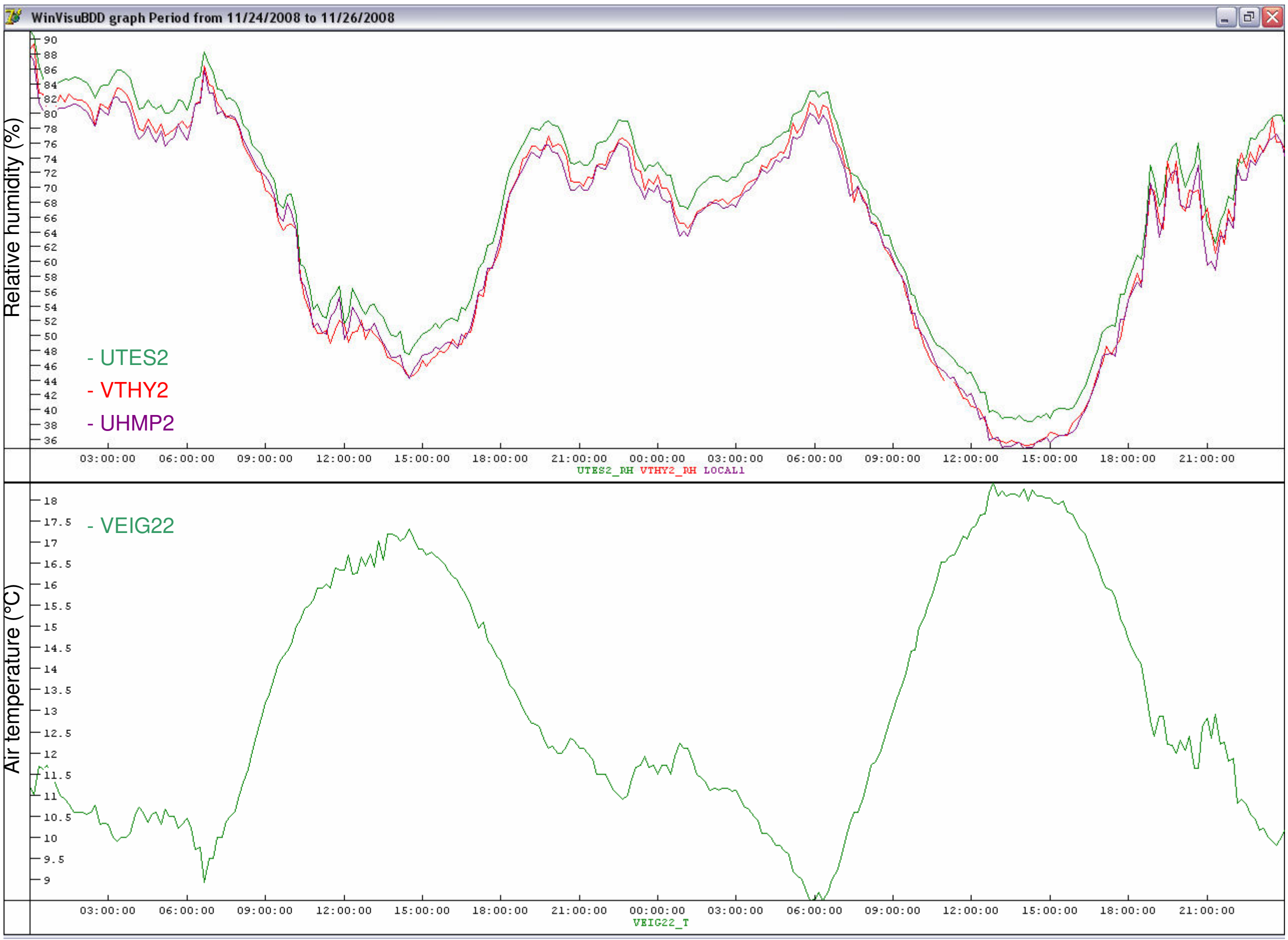


**Figure 9**

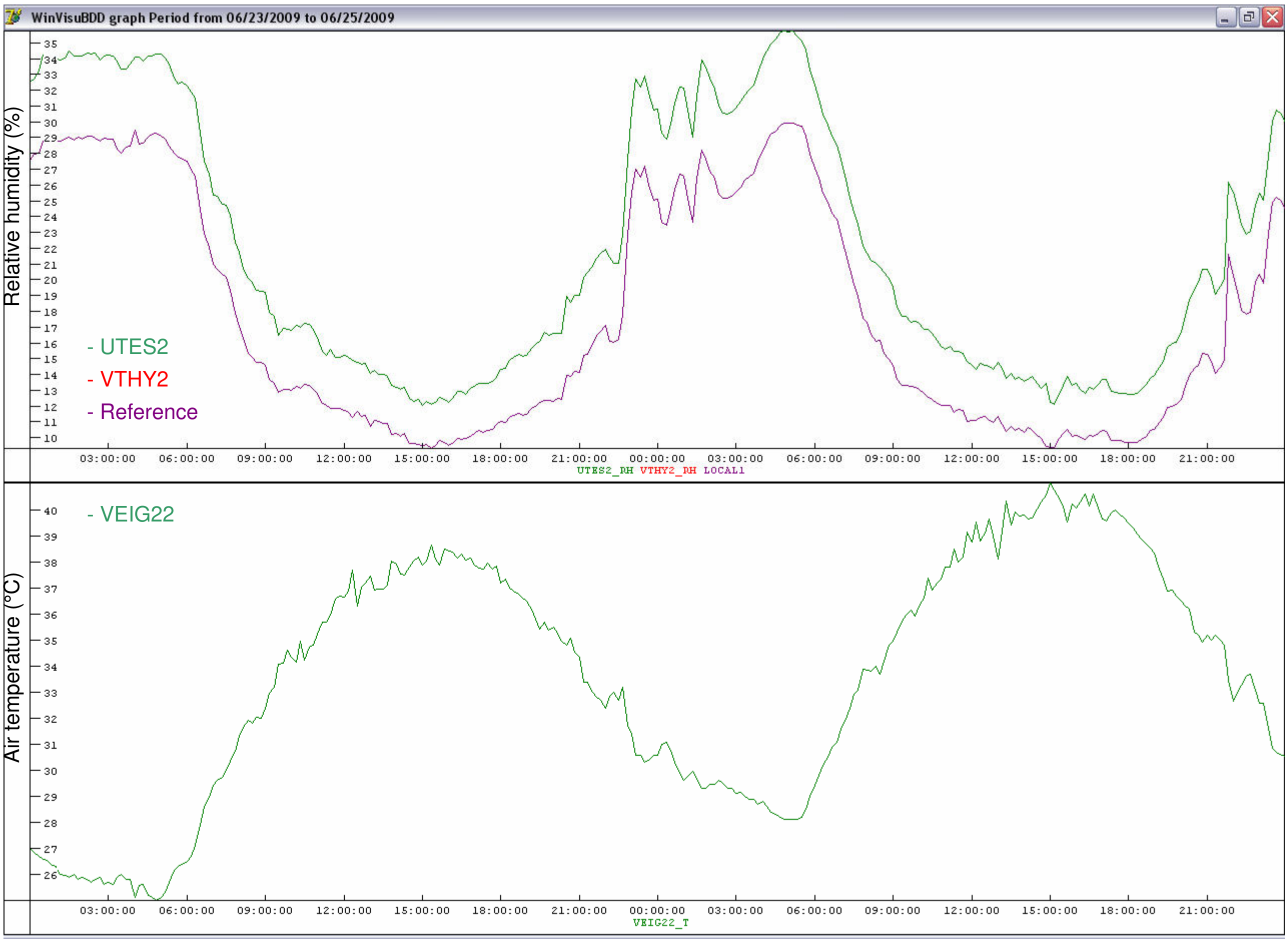


**Figure 10**

## COMBINED INFLUENCE OF TEMPERATURE AND RELATIVE HUMIDITY

The medians of differences between UTES and UHMP reference are represented here with a contour plot. The VEIG22 temperature is on the X-axis and the reference relative humidity is on the Y-axis. Medians are used in all cases, provided that at least one data is available for both conditions on temperature and humidity considered.

The scale was chosen so as to be the same for all relative humidity sensors.

Sensor #2:

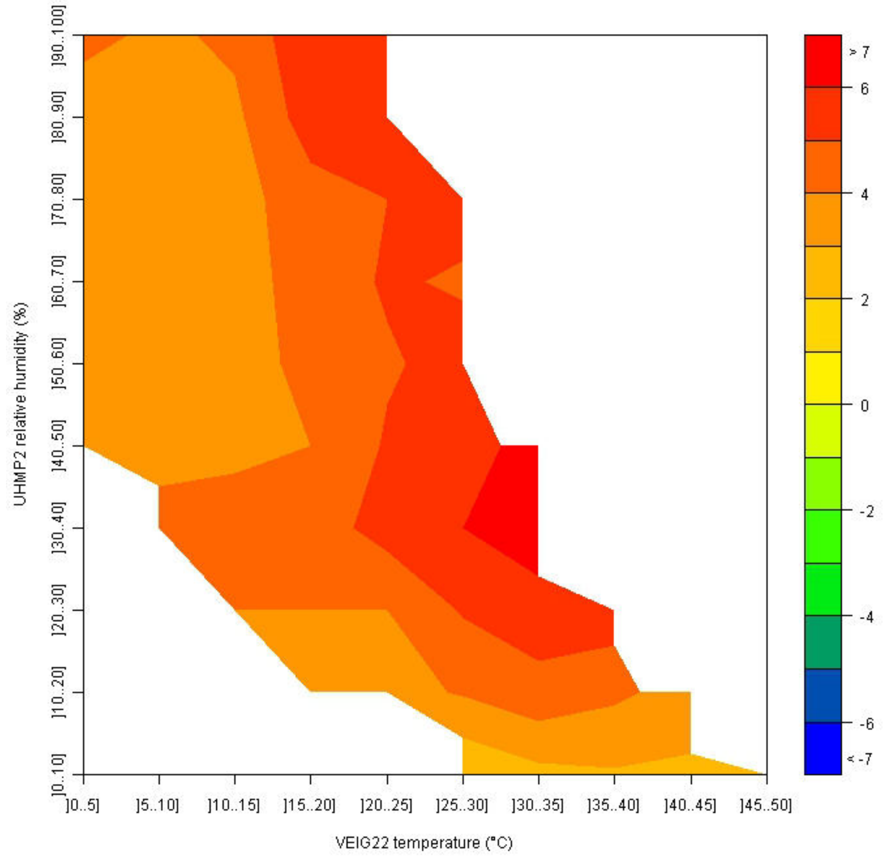


**Figure 11**

UTES2 give higher differences for temperatures between 25 and 35°C and humidity values between 30 and 50%.

## TIME DRIFT

The distributions of differences between UTES and the references are plotted, using 1-minute quality checked data for the whole period of the intercomparison, by step of one month. Reference relative humidity between 20% and 50% are only considered here: this is the common range in order to have data every month, without introducing influence of humidity itself.

## Sensor #2:

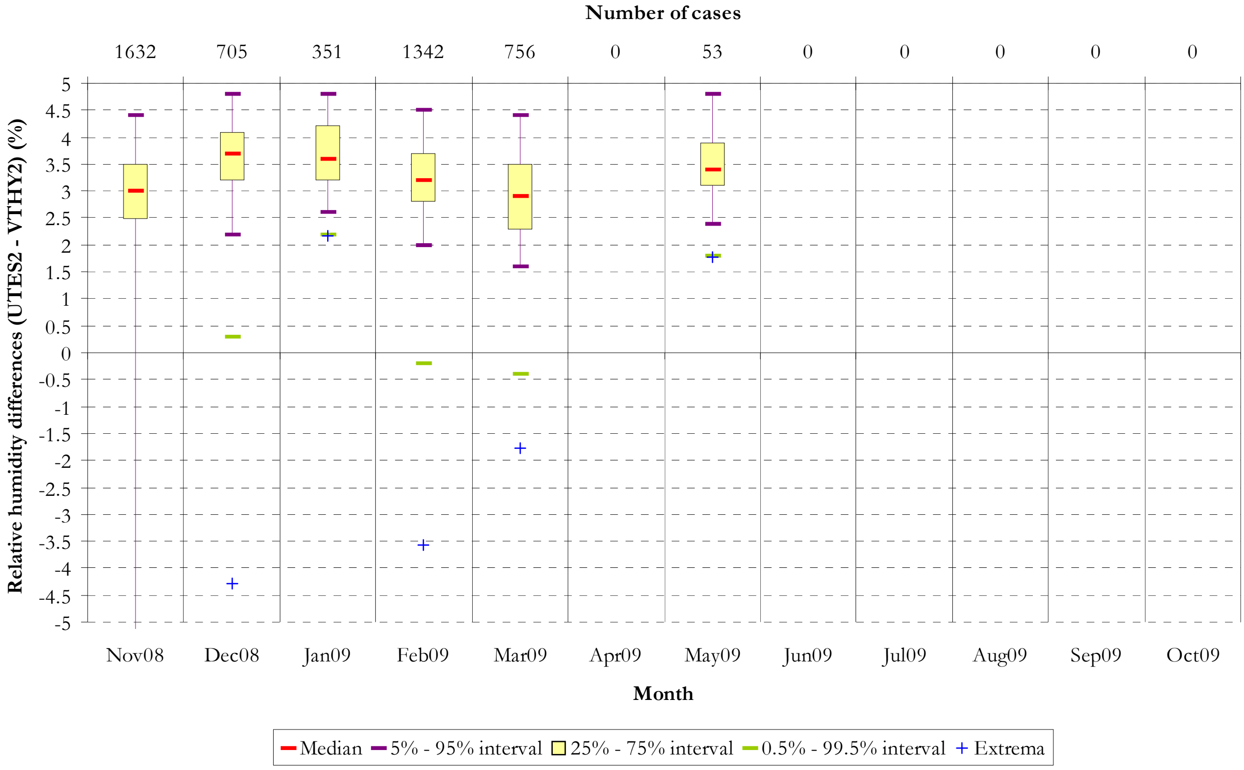


**Figure 12**

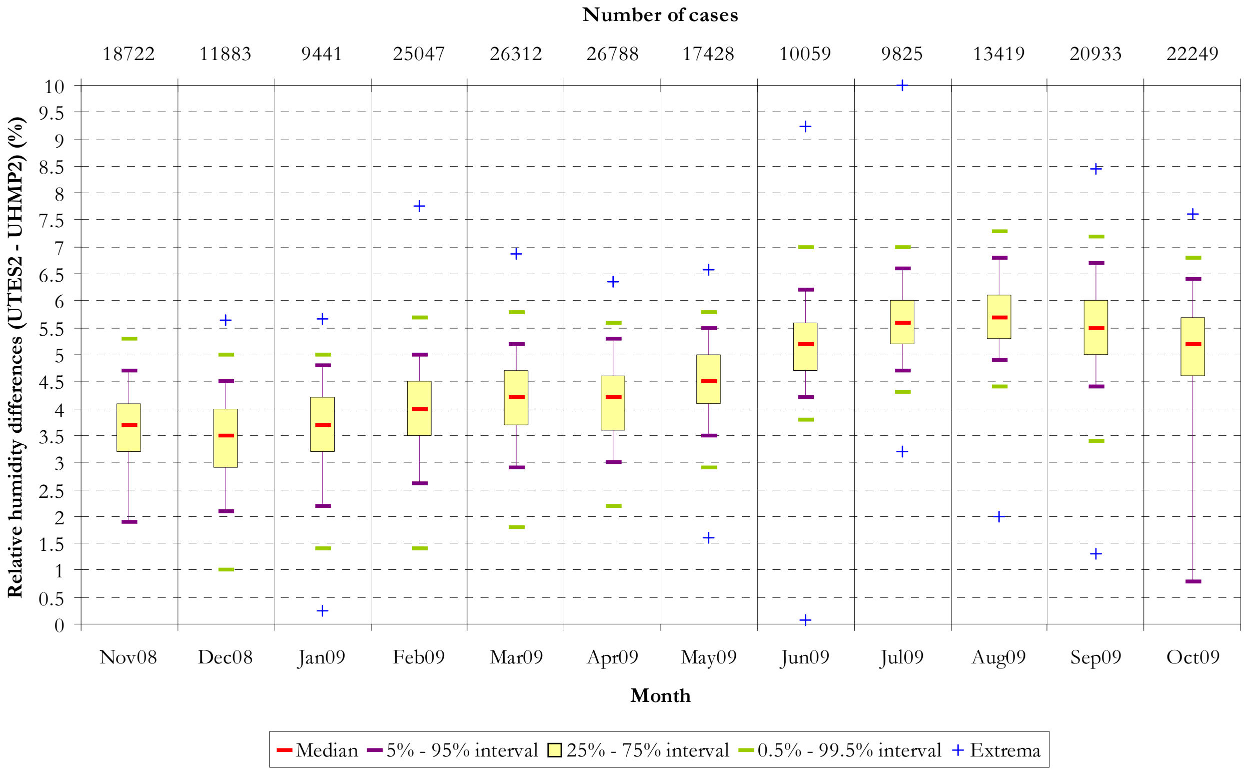


**Figure 13**

UTES2 differences with UHMP2 reference has much changed between the beginning and the end of the intercomparison: about 1.5 percentage point on the median of differences. This sensor has likely drifted.

## QUALITY CONTROL INFORMATION

### DATA AVAILABILITY

The intercomparison period extends from the 1st of November 2008 to the 1st of November 2009. The theoretical number of 1-minute data is 525600.

The table 4 sums up the total number of data for each sensor and for each possible QC flag.

**Table 4**

| QC flag | UTES1 | UTES2 |
|---|---|---|
| 0 (good) | 0 | 506069 |
| 1 (inconsistent) | 0 | 0 |
| 2 (doubtful) | 0 | 85 |
| 3 (erroneous) | 0 | 646 |
| 7 (missing) | 525600 | 18800 |

### MAINTENANCE

No actions done during the intercomparison period.

# THYGAN VTP37 METEOLABOR AG – Switzerland – VTHY

## TECHNICAL SPECIFICATIONS (PROVIDED BY THE MANUFACTURER)

Dimensions: Length 28.8 cm x Width 22.3 cm x Height 35.7 cm
Principle of operation: Heated dew point mirror
Accuracy: ± 0.15°C in the range of -20°C to 50°C and ± 0.25°C below -20°C
Power supply: 12 VDC / 48VAC
Outputs: 1 output RS485


**Figure 1**

## OVERVIEW

Both sensors give very similar results. Very large extreme values obtained between 30 and 70% occurred during two days where VTHY1 gave wrong measures. In both times, conditions were very humid, nearly saturation.

About 99 % of the measurements were found within ±3% of the reference.

The differences between both sensors is not influenced by humidity. The differences with UHMP2 reference is quite dependant of the humidity value. Especially above 80%, differences are much higher. This is consistent with UHMP2 calibration data.

No influence of temperature is detected.

Differences between Thygan sensors and UHMP2 reference are slightly greater for the ]20..30] humidity class and temperatures between 10 and 25°C.

It is not possible here to conclude about a possible time drift of one sensor to another, since there is no data at the end of the period. Differences between November 2008 and May 2009 may be to a temperature effect, because the temperature range is not the same.

## CALIBRATION INFORMATION

Calibration by manufacturer (June 2005):

**Table 1**

| Sensor | Serial number | 22°C |
|---|---|---|
| | | 50% |
| VTHY1 | 338 | 0.43 |
| VTHY2 | 339 | 0.35 |

## COMPARISON OF BOTH SENSORS

The distribution of differences between VTHY1 and VTHY2 is plotted, using 1-minute quality checked data for the whole period of the intercomparison. Differences are classified according VTHY1 relative humidity.

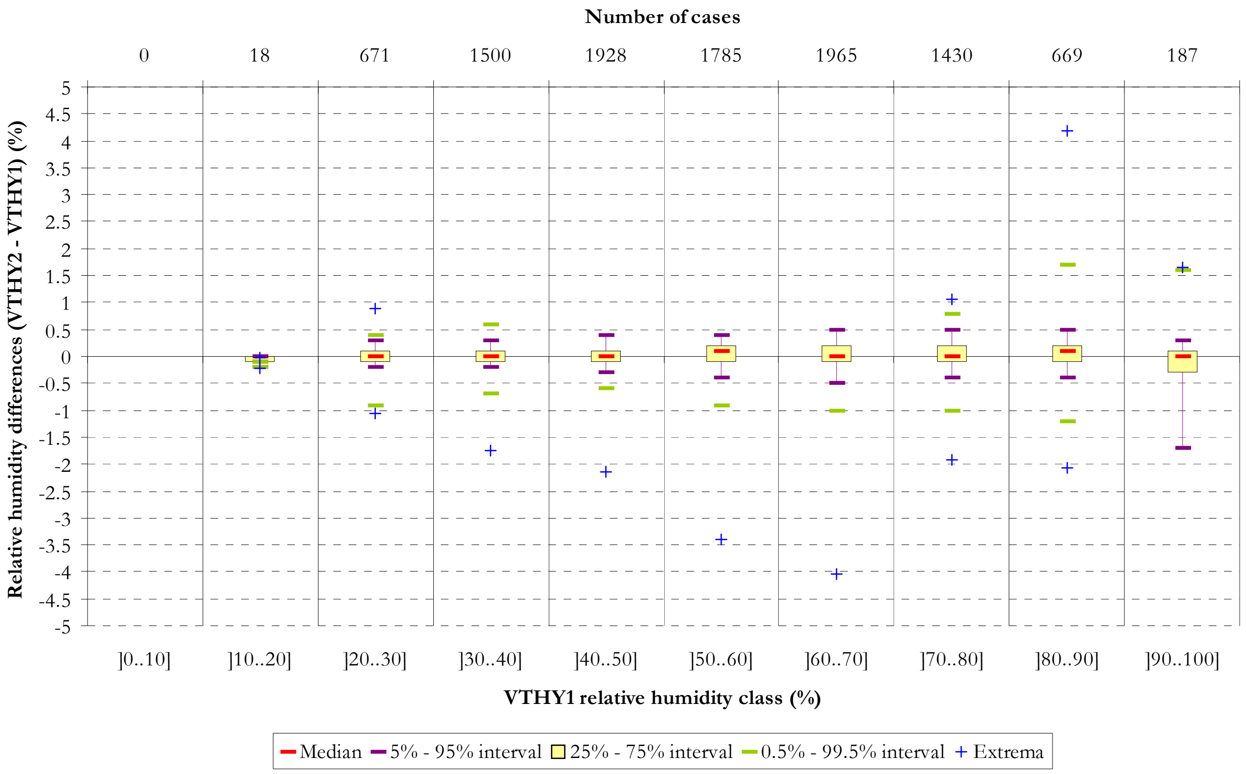


**Figure 2**

Both sensors give very similar results. Very large extreme values obtained between 30 and 70% occurred during two days where VTHY1 gave wrong measures. In both times, conditions were very humid, nearly saturation (cf. figure 3 and figure 4).

[Is there any explanation for these erroneous values? Do the sensor error codes and status indicate anything unusual?]

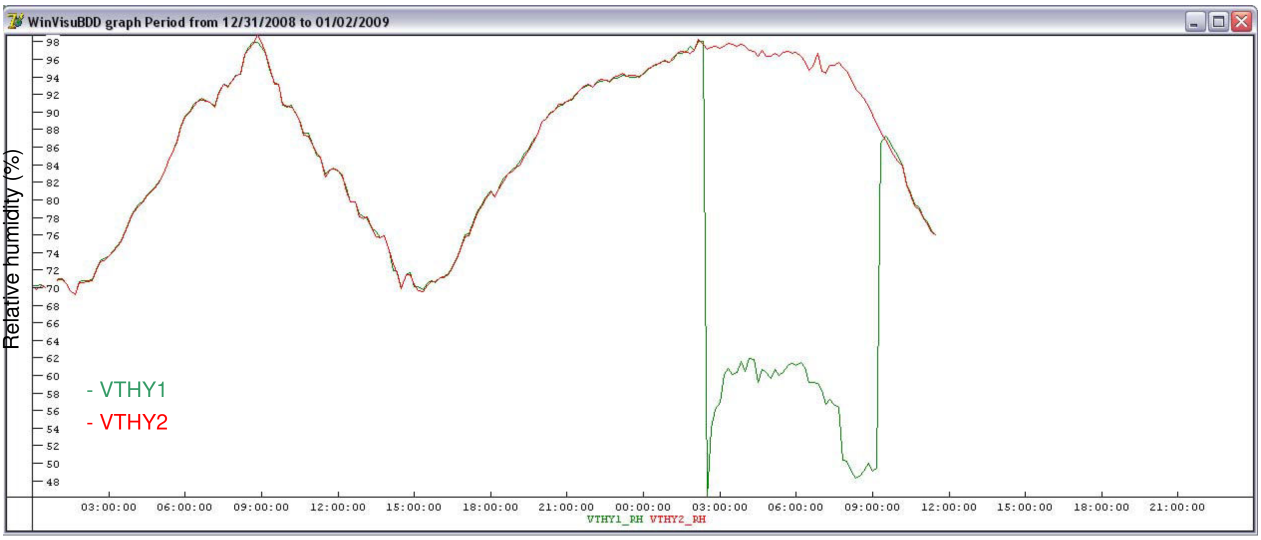


**Figure 3**


**Figure 4**

## COMPARISON WITH THE REFERENCE

Thygan sensor #2 was first chosen as the reference for humidity measurements. But it was not available after April 2009. That is why a second reference was selected, which is the average of two HMP45D probes from Vaisala, when the difference between both values is lower than 1% of relative humidity.

For more details about the choice of references for humidity measurement, please refer to part 5.5.1 of the final report.

### HISTOGRAM OF DIFFERENCES

The histograms of differences between VTHY and the references are plotted, using 1-minute quality checked data for the whole period of the intercomparison. Differences are plotted by steps of 1 %. The vertical axis is the frequency in percent for each class of differences.

Sensor #1:

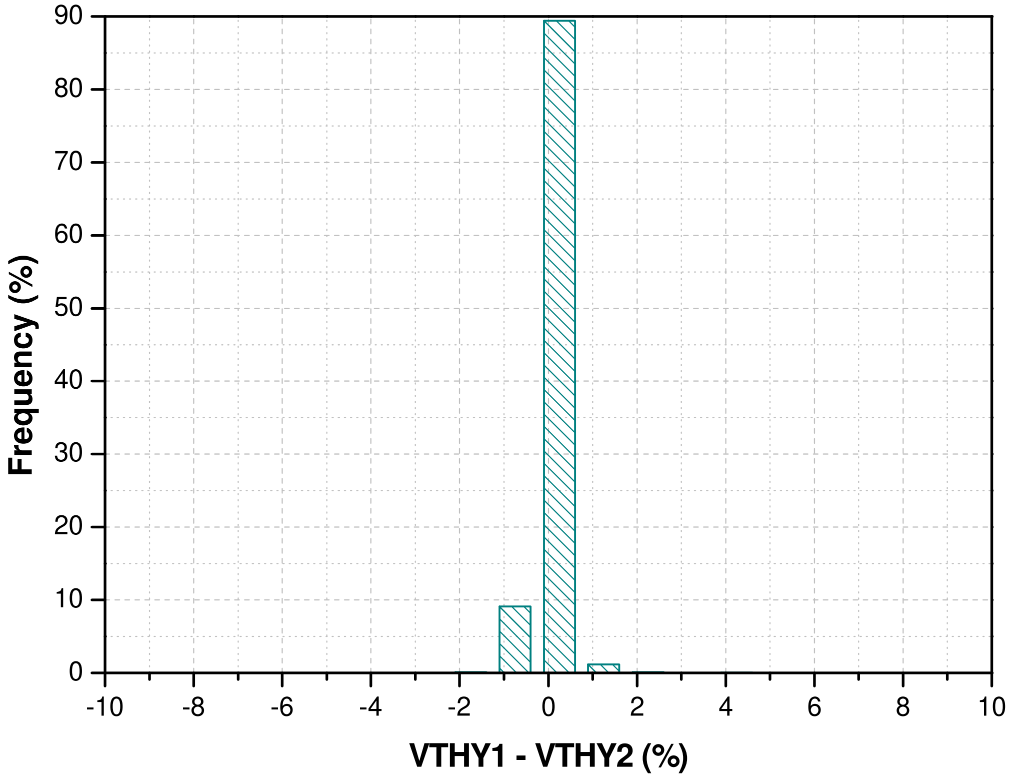


**Figure 5**

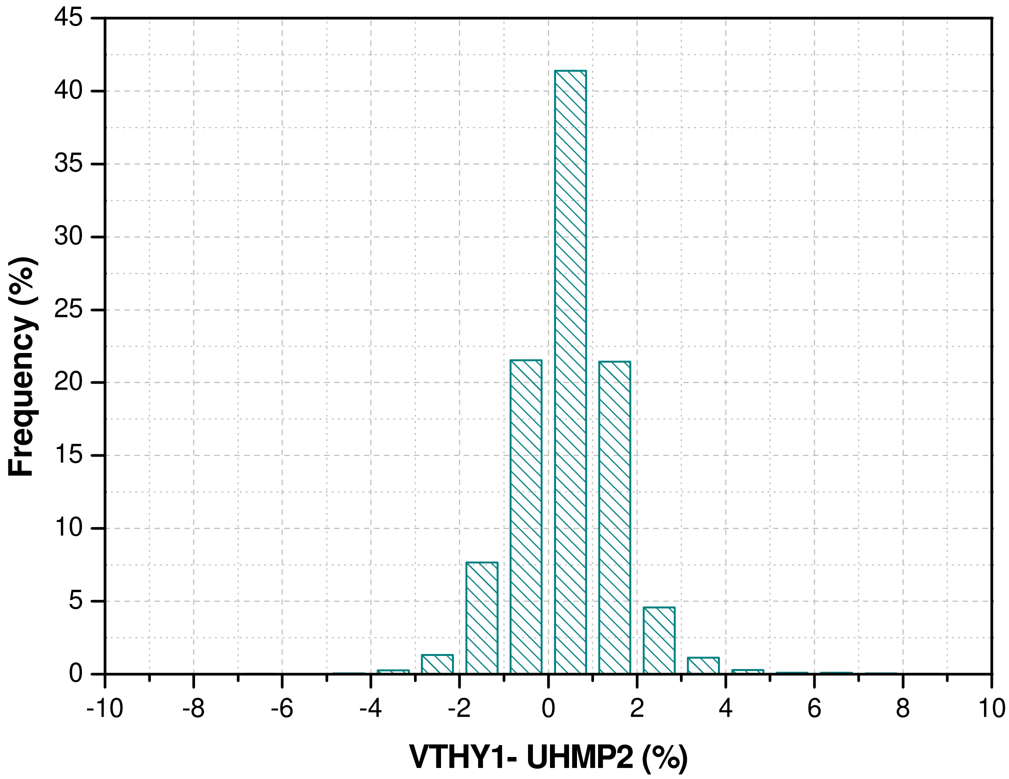
Frequency (%)
VTHY1- UHMP2 (%)
0
5
10
15
20
25
30
35
40
45
-10
-8
-6
-4
-2
0
2
4
6
8
10

Figure 6

Sensor #2:

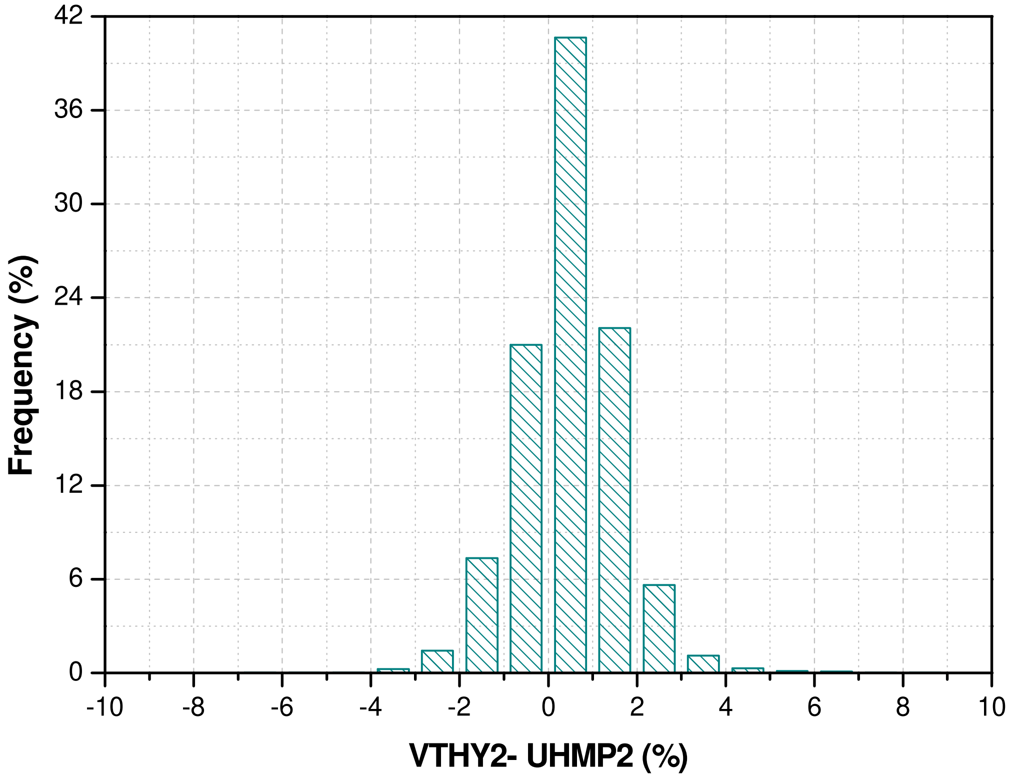


Figure 7

TABLE

The table 2 indicates the percentage of data that differ by less than 3% (and 6%) from the reference considered (VTHY2 or UHMP2).

Table 2

| | VTHY2 | | UHMP2 | |
|---|---|---|---|---|
| | [-3..3] | [-6..6] | [-3..3] | [-6..6] |
| VTHY1 | 99.4 | 99.4 | 97.8 | 99.3 |
| VTHY2 | 100 | 100 | 98.4 | 99.9 |

## INFLUENCE OF HUMIDITY

The distributions of differences between VTHY and the references are plotted, using 1-minute quality checked data for the whole period of the intercomparison. Differences are classified according the reference relative humidity.

## Sensor #1:

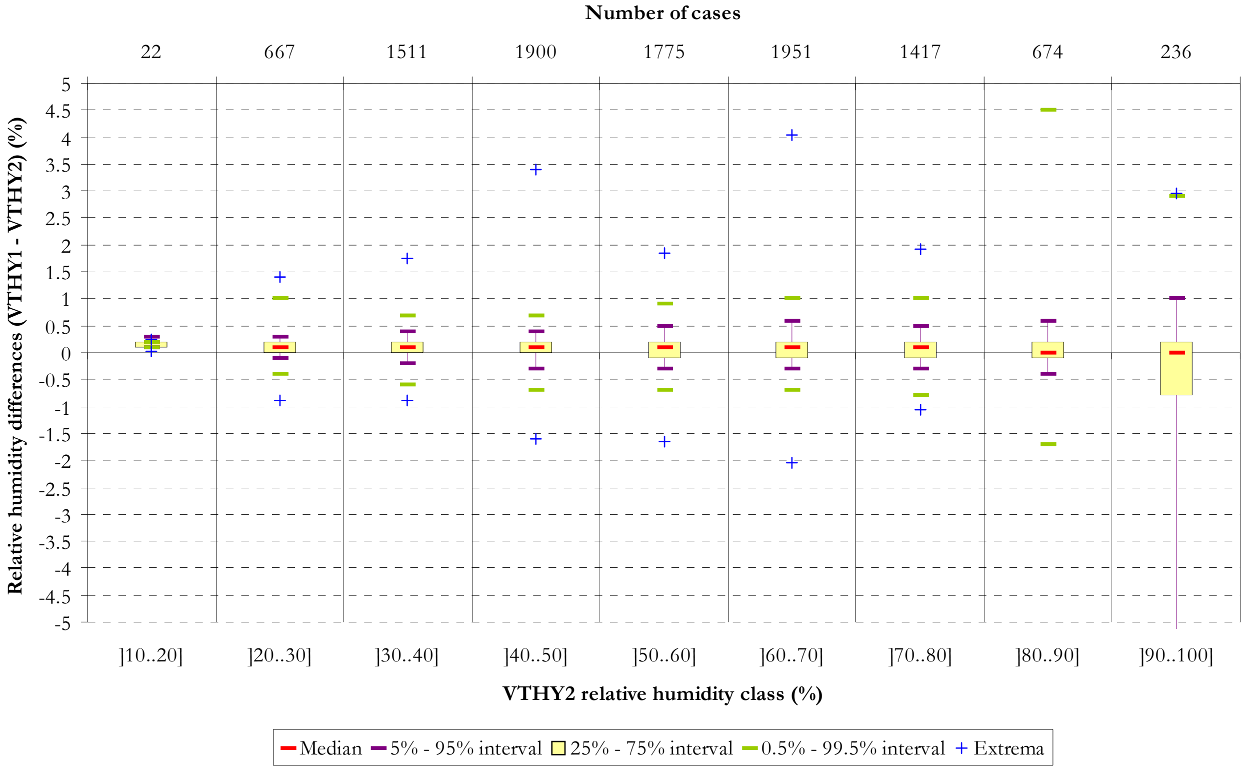


**Figure 8**

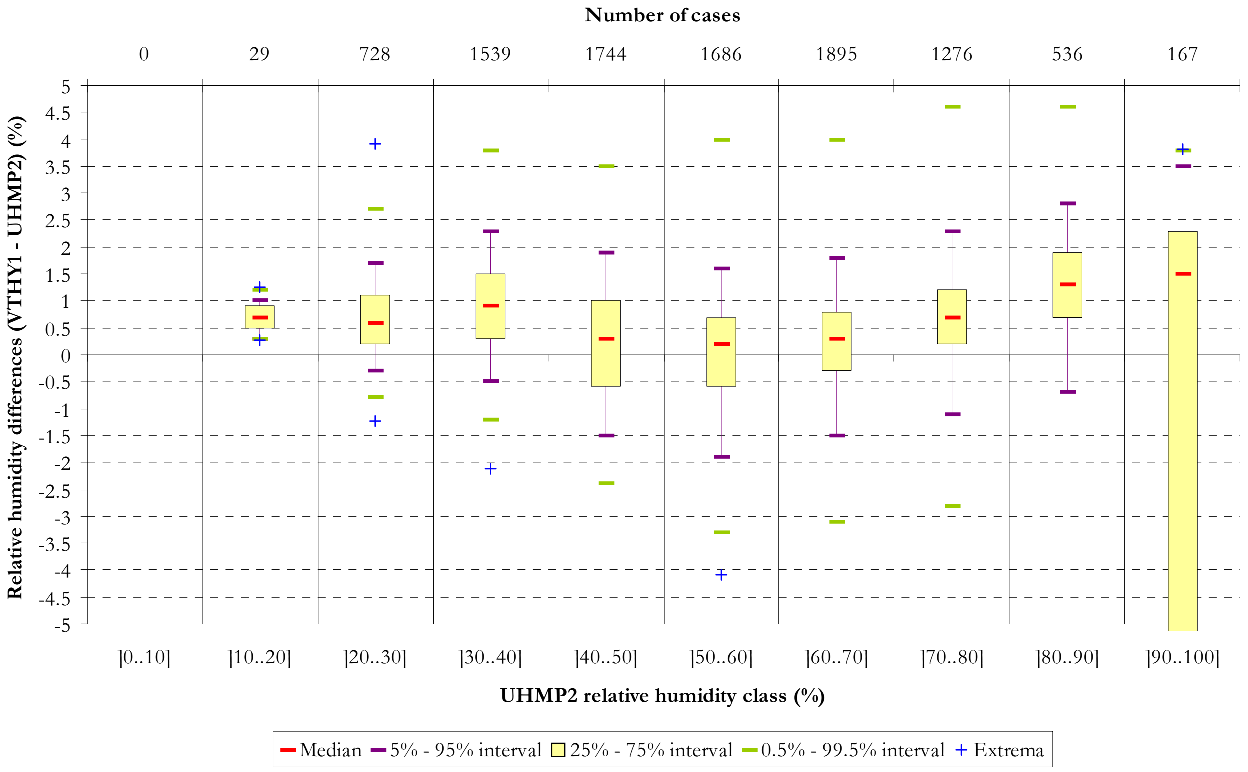


**Figure 9**

Sensor #2:

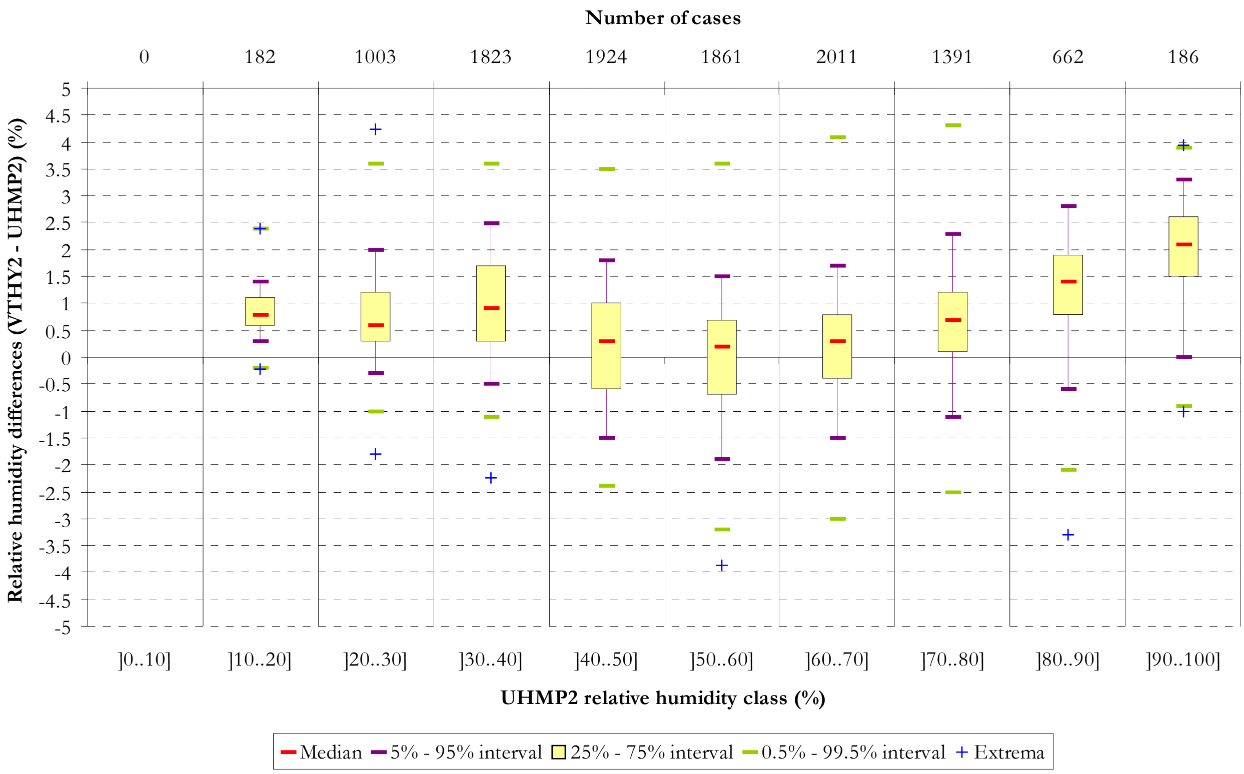


**Figure 10**

The differences between both sensors is not influenced by humidity. The very large values for VTHY1 for the class of high values are a result of the two days when this sensor underestimated humidity during saturation periods (cf. page 3).

The differences with UHMP2 reference is quite dependant of the humidity value. Especially above 80%, differences are much higher. This is consistent with UHMP2 calibration data: the two probes underestimated the reference by 1.8 and 2.1% at the (23°C,90%) calibration point.

On figure 11, the green curve is VTHY2, the red one is UHMP2 reference. During these 2 days, the UHMP2 is in agreement with VTHY2 when humidity is below 85%, but differences between both measures increases with humidity.

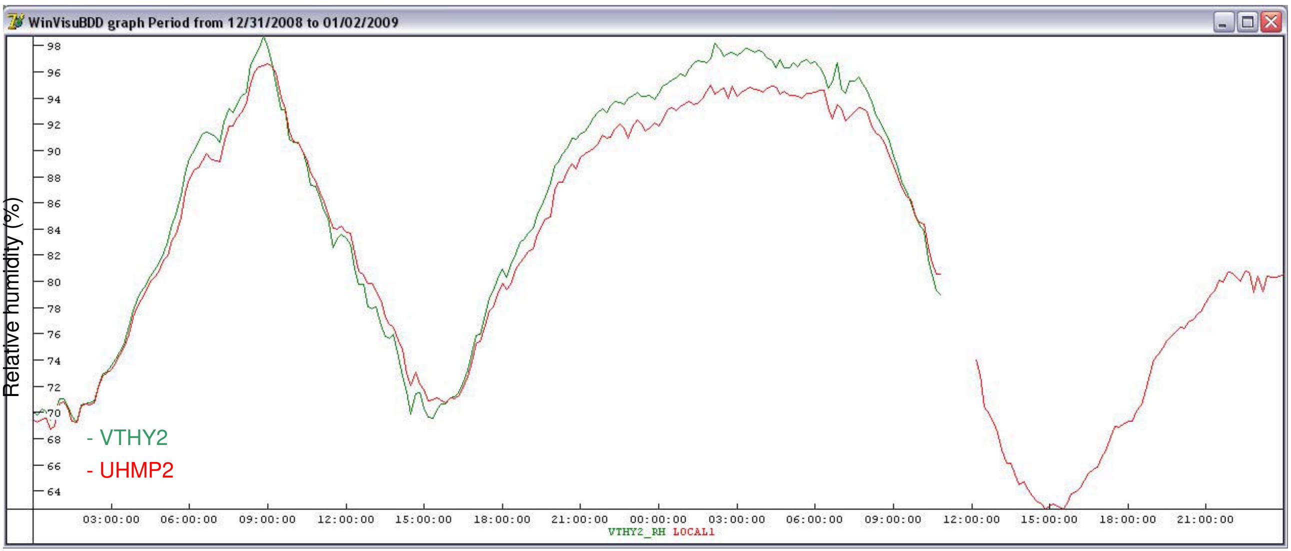


**Figure 11**

## INFLUENCE OF TEMPERATURE

The distributions of differences between VTHY and the references are plotted, using 1-minute quality checked data for the whole period of the intercomparison. Differences are classified according VEIG22 temperature.

Sensor #1:

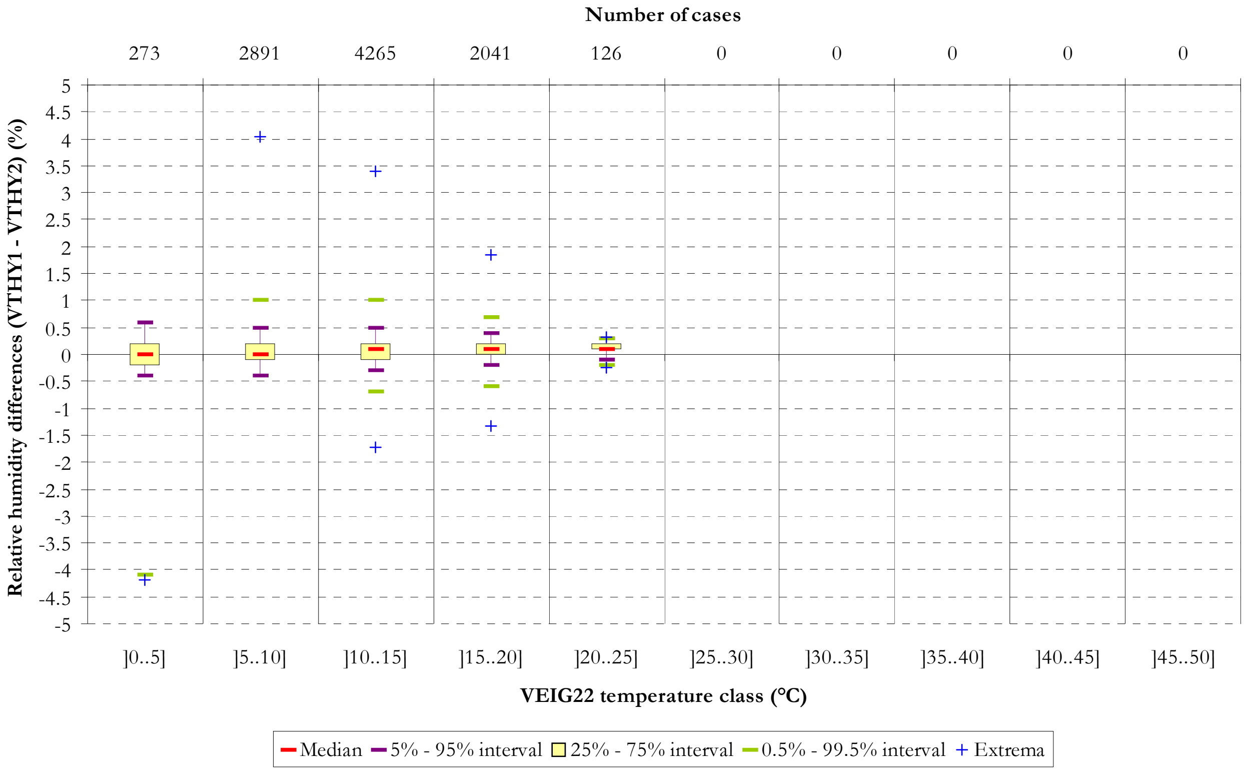


**Figure 12**


**Figure 13**

Sensor #2:

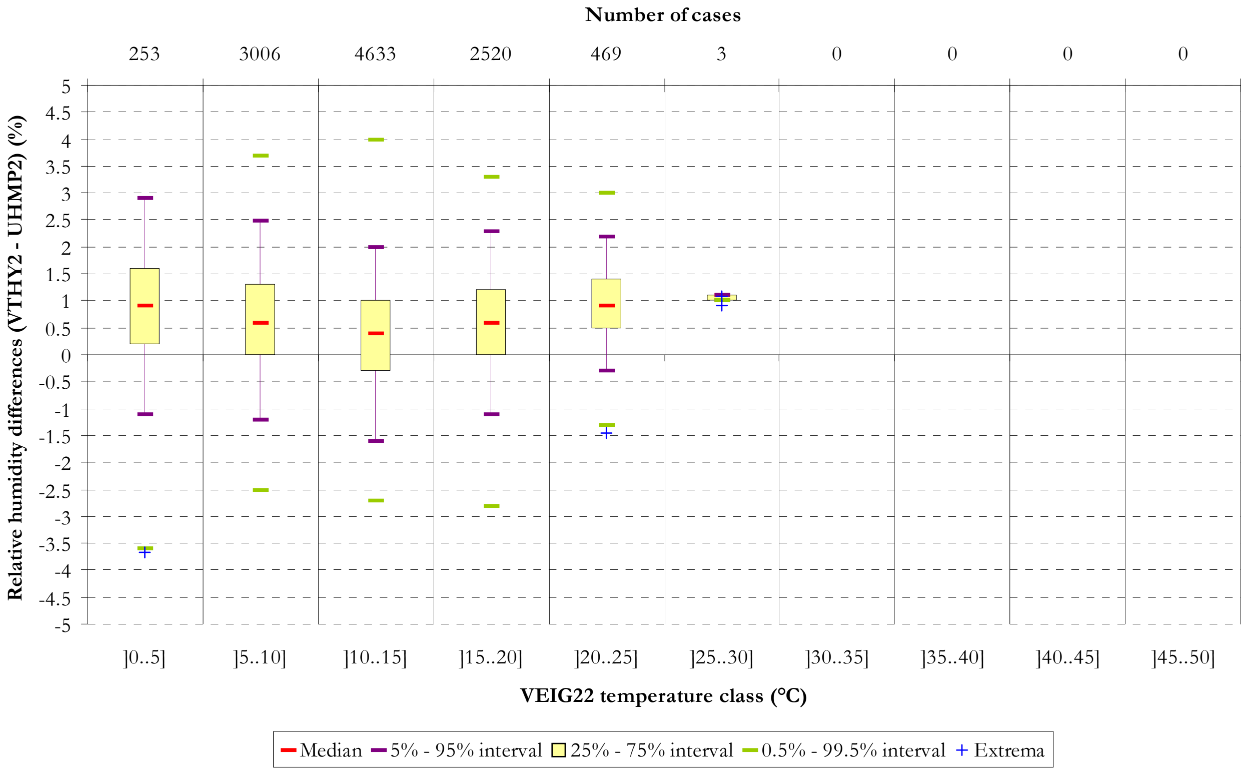


**Figure 14**

No influence of temperature is detected.

## COMBINED INFLUENCE OF TEMPERATURE AND RELATIVE HUMIDITY

The medians of differences between VTHY and UHMP reference are represented here with a contour plot. The VEIG22 temperature is on the X-axis and the reference relative humidity is on the Y-axis. Medians are used in all cases, provided that at least one data is available for both conditions on temperature and humidity considered.

The scale was chosen so as to be the same for all relative humidity sensors.

Sensor #1:

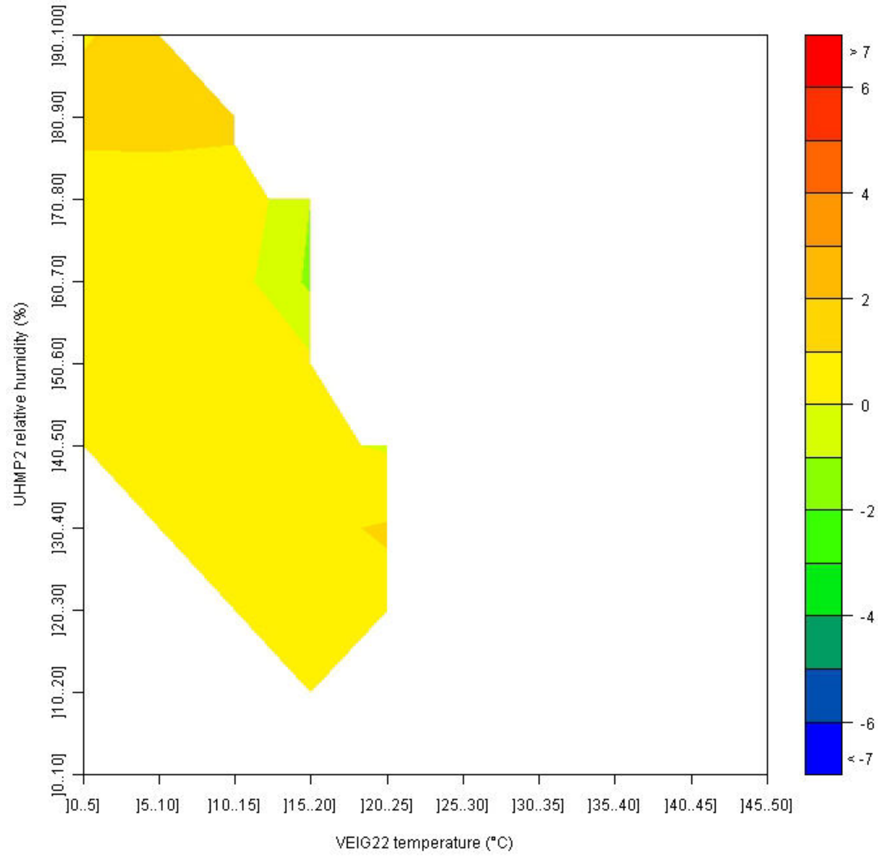


**Figure 15**

Sensor #2:

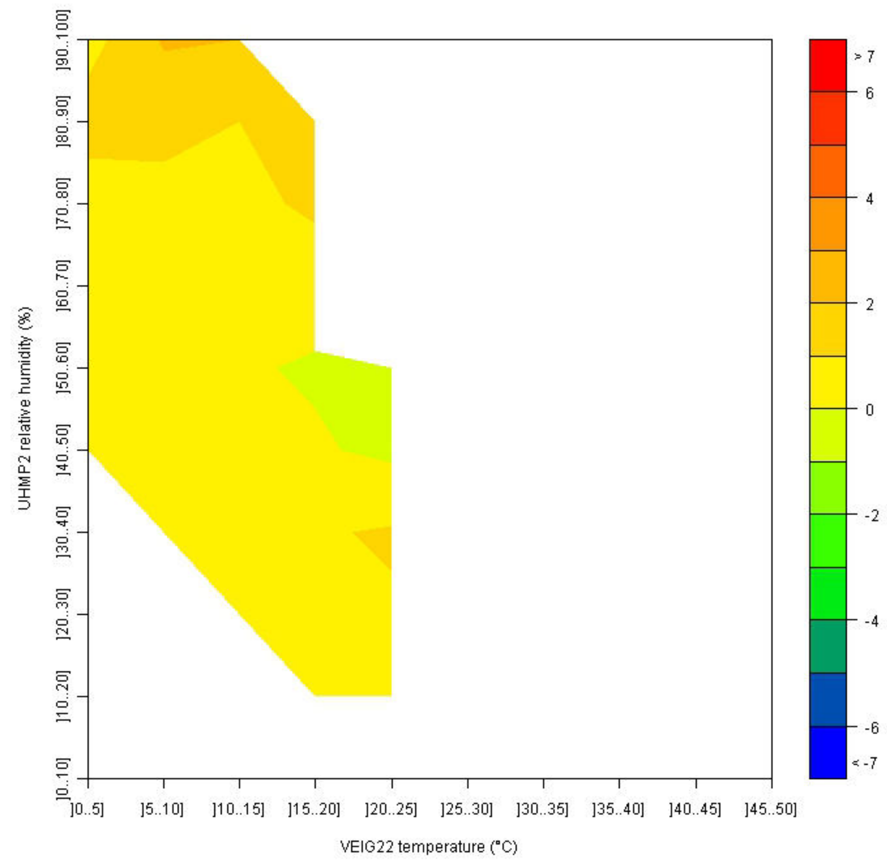


**Figure 16**

Both Thygan sensors give higher differences for high values of humidity and low temperatures. As seen before, this may be a behaviour of UHMP2 reference.

## TIME DRIFT

The distributions of differences between VTHY and the references are plotted, using 1-minute quality checked data for the whole period of the intercomparison, by step of one month. Reference relative humidity between 20% and 50% are only considered here: this is the common range in order to have data every month, without introducing influence of humidity itself.

## Sensor #1:

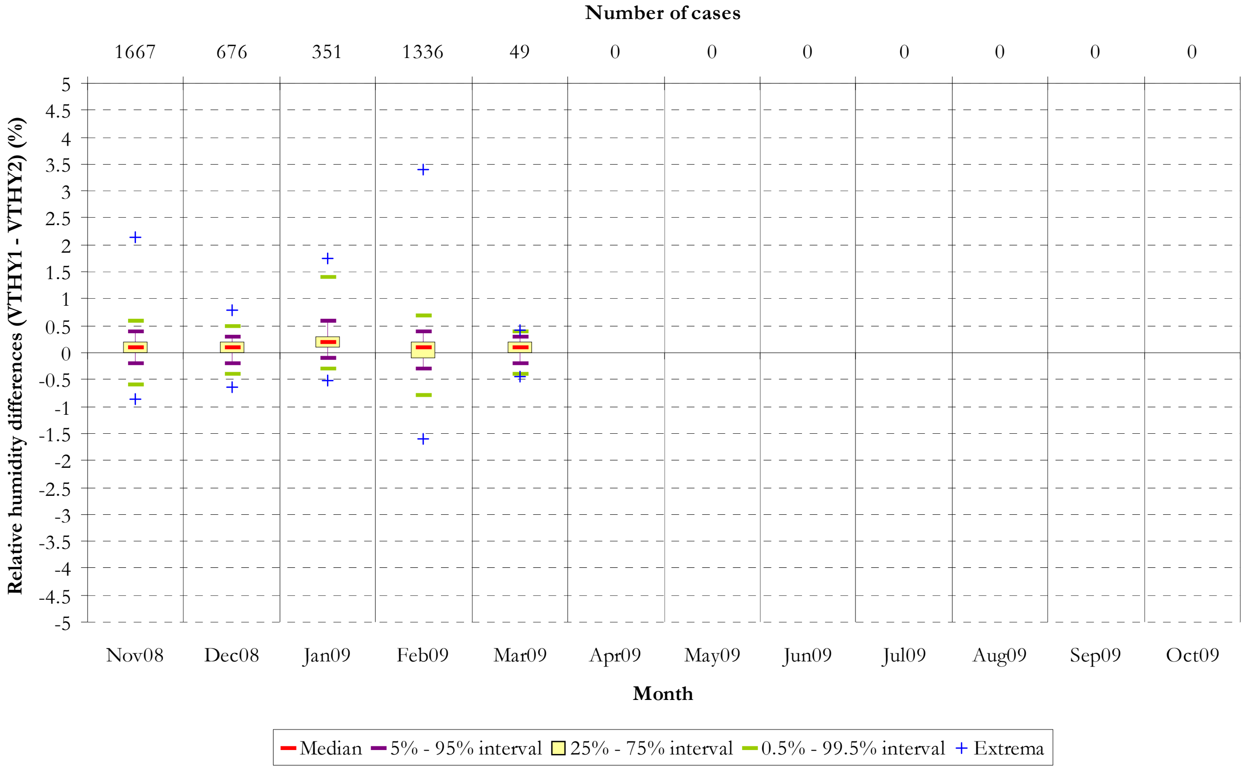


**Figure 17**

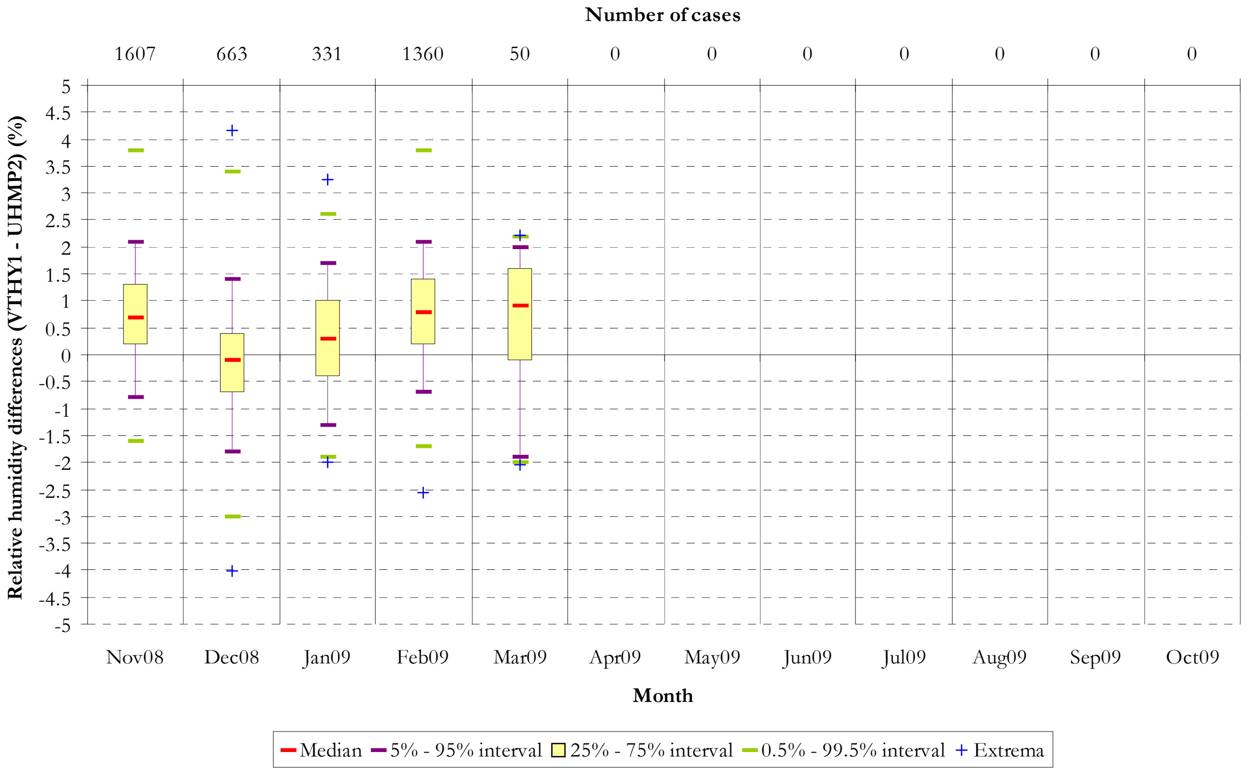


**Figure 18**

Sensor #2:

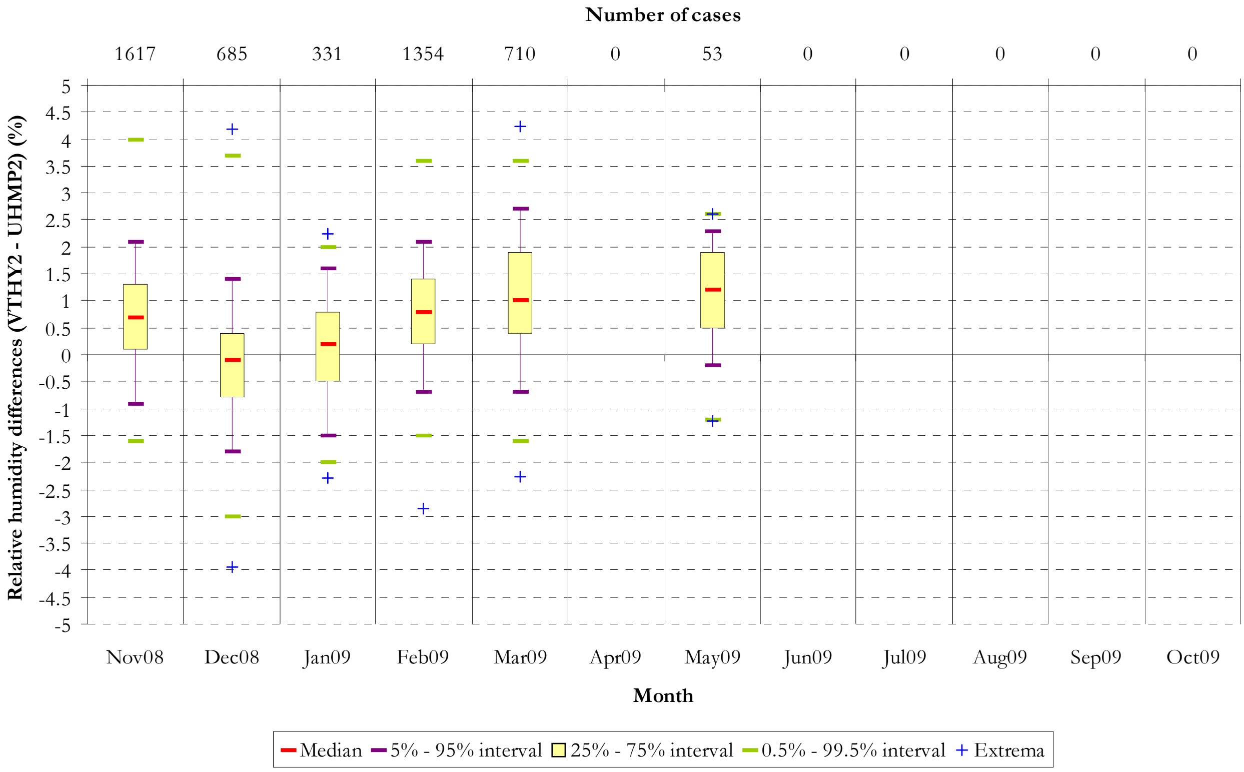


**Figure 19**

It is not possible here to conclude about a possible time drift of one sensor to another, since there is no data at the end of the period. Differences between November 2008 and May 2009 may be due to a temperature effect, because the temperature range is not the same.

## QUALITY CONTROL INFORMATION

### DATA AVAILABILITY

The intercomparison period extends from the 1st of November 2008 to the 1st of November 2009. The theoretical number of 10-minute data is 52560.

The table 3 sums up the total number of data for each sensor and for each possible QC flag.

**Table 3**

| QC flag | VTHY1 | VTHY2 |
|---|---|---|
| 0 (good) | 11693 | 11821 |
| 1 (inconsistent) | 0 | 0 |
| 2 (doubtful) | 0 | 0 |
| 3 (erroneous) | 0 | 0 |
| 7 (missing) | 40867 | 40739 |

The reasons for missing data are frequent failures of the acquisition software and the stop of transmission from Thygan sensors from May 2009

### MAINTENANCE

The acquisition software ordered for time synchronization and cleaning the mirror once per day.

Sensor #1 gave no data after the 2nd of March, 2009 at 7:00.

Sensor #2 gave no data after the 2nd of March, 2009 at 17:40.

An interface device common to the two sensors had a failure this day.

# HYGROCLIP S ROTRONIC
# – Switzerland –
# VROT

## TECHNICAL SPECIFICATIONS (PROVIDED BY THE MANUFACTURER)

Dimensions: Length 10 cm x Diameter 1.5 cm
Principle of operation: Hygromer C94 capacitive sensor, Pt100 1/3 DIN
Accuracy: ± 1 % RH/0.3K at 23°C
Power supply: 3.5..50 VDC
Outputs: 1 output 0..1V

**Figure 1**

These sensors were installed in VROT screen, provided by same manufacturer:

**Figure 2**

## OVERVIEW

The comparison between both sensors is not possible because sensor #2 gave a signal that was not correlated to humidity. The reason was unknown.

For sensor #1, 98 % of the measurements were found within ±3% of the reference.

The behaviour of VROT1 seems to depend on the relative humidity. The differences with VTHY2 references decrease when humidity increases. The differences with UHMP2 reference are stable in the humidity range of ]10..40%]. For higher humidity values until 70%, differences decrease. Above 70%, differences increase.

The differences depend on temperature: they are much higher between 15 and 35 or 40°C than for other temperatures.

The highest differences are obtained for high humidity values and temperatures between 15 and 25°C.

Distributions of differences are quite stable all year long. The last one is very similar to the first one, so no drift is detected.

## CALIBRATION INFORMATION

Calibration in Trappes (8 Mar 2007):

**Table 1**

| Sensor | Serial number | 23°C | | | | | 40°C | | | | |
|---|---|---|---|---|---|---|---|---|---|---|---|
| | | 10% | 33% | 55% | 75% | 90% | 10% | 33% | 55% | 75% | 90% |
| VROT1 | 45003016 | -1.7 | -0.1 | 0.7 | 0.7 | 1.3 | -0.7 | 0.1 | 0.7 | 1.3 | 3.1 |
| VROT2 | 45003017 | -1.4 | 0.0 | 0.6 | 0.9 | 1.2 | -0.5 | 0.1 | 0.7 | 1.1 | 2.7 |

On site calibration (June 2008):

**Table 2**

| Sensor | Serial number | 10% | 33% | 50% | 90% |
|---|---|---|---|---|---|
| VROT1 | 45003016 | -0.7 | 0.6 | 0.6 | 0.1 |
| VROT2 | 45003017 | -0.3 | 0.7 | -0.7 | 1 |

## COMPARISON OF BOTH SENSORS

The comparison between both sensors is not possible because sensor #2 gave a signal that is not correlated to humidity, as shown on figure 3.

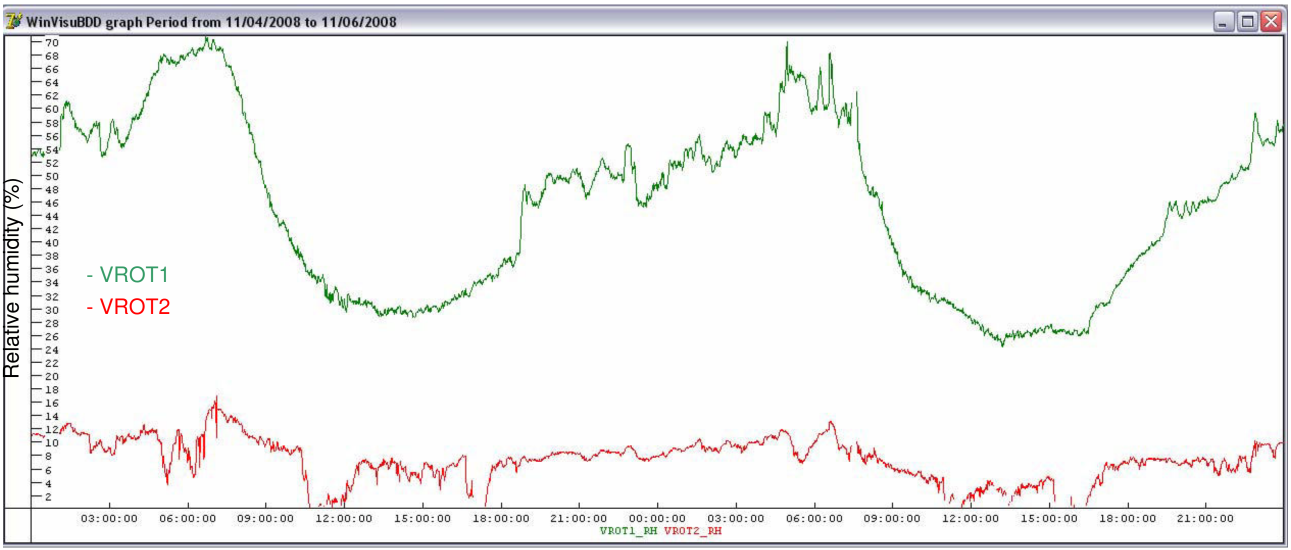


**Figure 3**

## COMPARISON WITH THE REFERENCE

Thygan sensor #2 was first chosen as the reference for humidity measurements. But it was not available after April 2009. That is why a second reference was selected, which is the average of two HMP45D probes from Vaisala, when the difference between both values is lower than 1% of relative humidity.

For more details about the choice of references for humidity measurement, please refer to part 5.5.1 of the final report.

### HISTOGRAM OF DIFFERENCES

The histograms of differences between VROT and the references are plotted, using 1-minute quality checked data for the whole period of the intercomparison. Differences are plotted by steps of 1 %. The vertical axis is the frequency in percent for each class of differences.

Sensor #1:

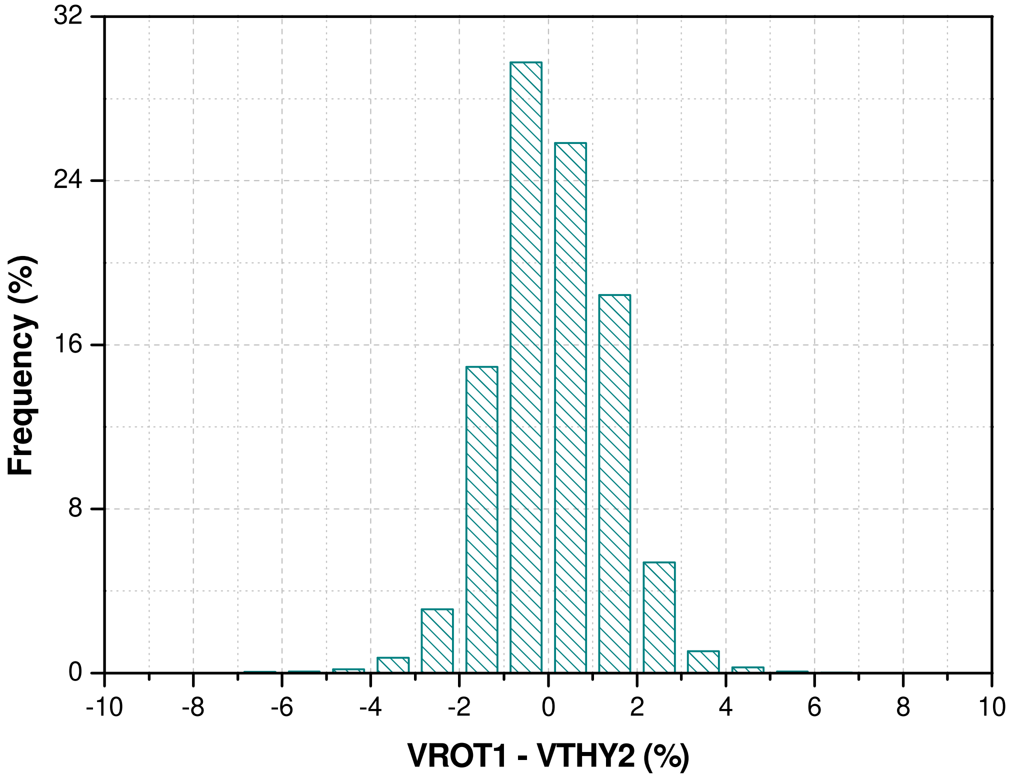


**Figure 4**

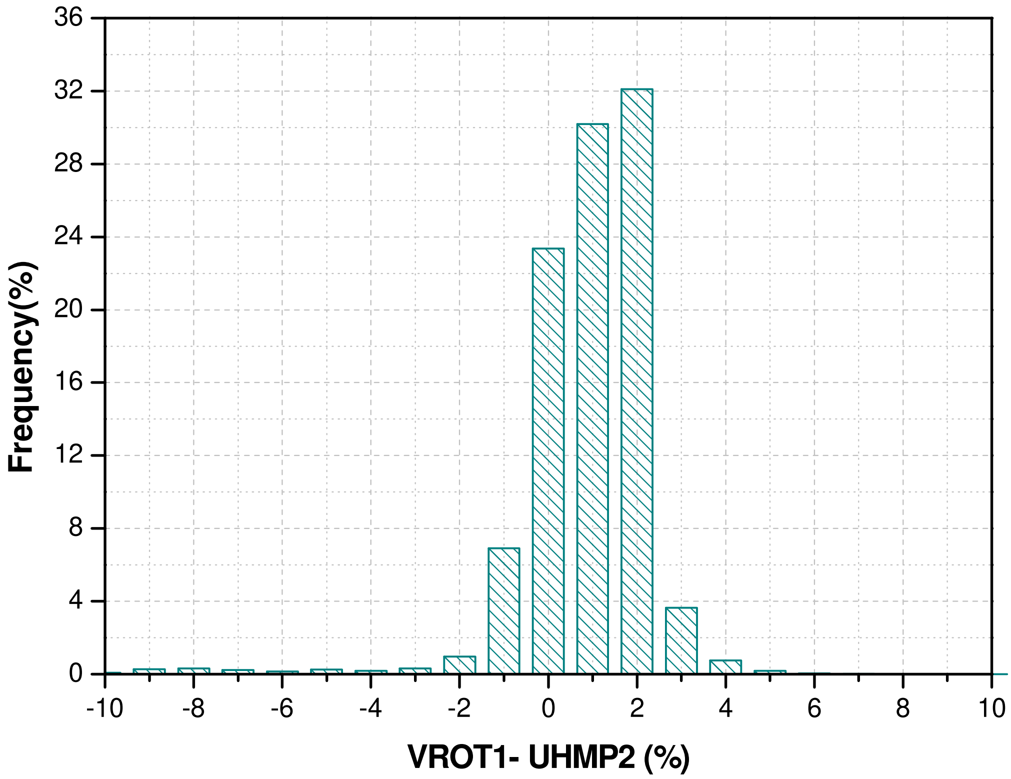


**Figure 5**

TABLE

The table 3 indicates the percentage of data that differ by less than 3% (and 6%) from the reference considered (VTHY2 or UHMP2).

**Table 3**

| | VTHY2 | | UHMP2 | |
|---|---|---|---|---|
| | [-3..3] | [-6..6] | [-3..3] | [-6..6] |
| VROT1 | 97.6 | 99.9 | 98.1 | 99.8 |

## INFLUENCE OF HUMIDITY

The distributions of differences between VROT and the references are plotted, using 1-minute quality checked data for the whole period of the intercomparison. Differences are classified according the reference relative humidity.

## Sensor #1:

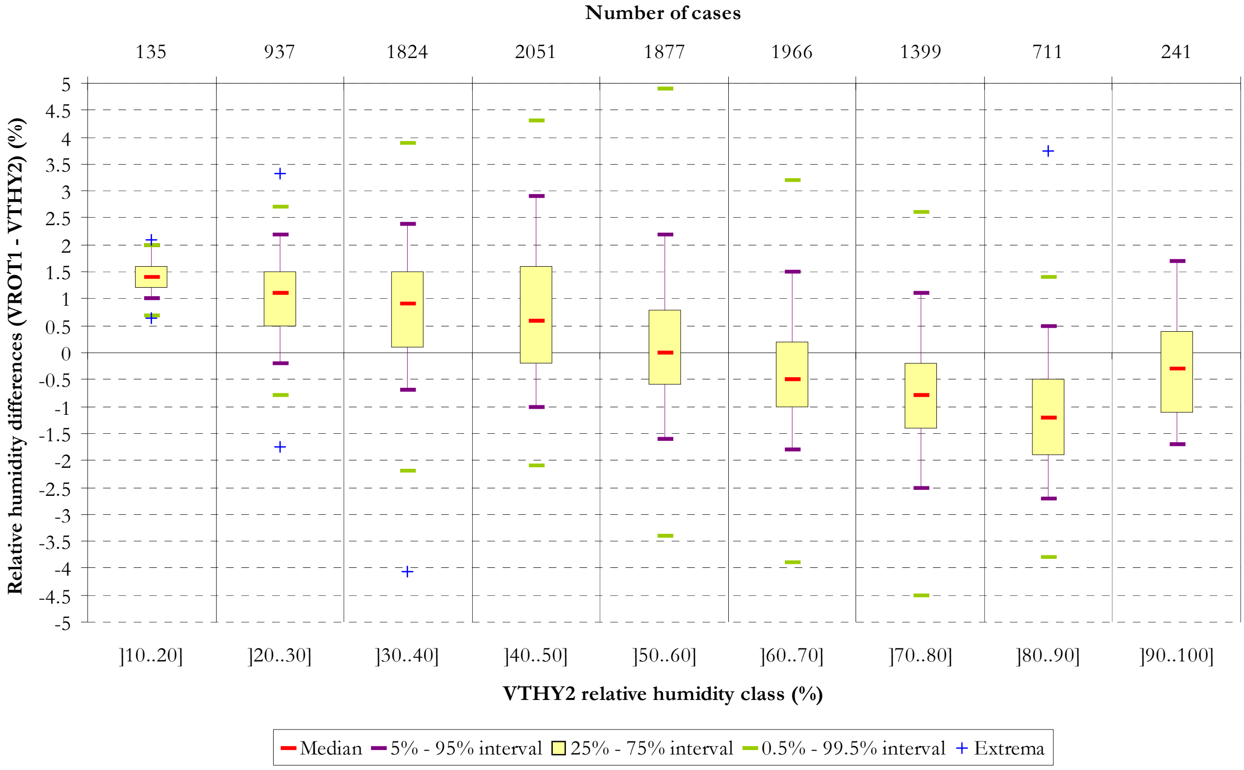


**Figure 6**

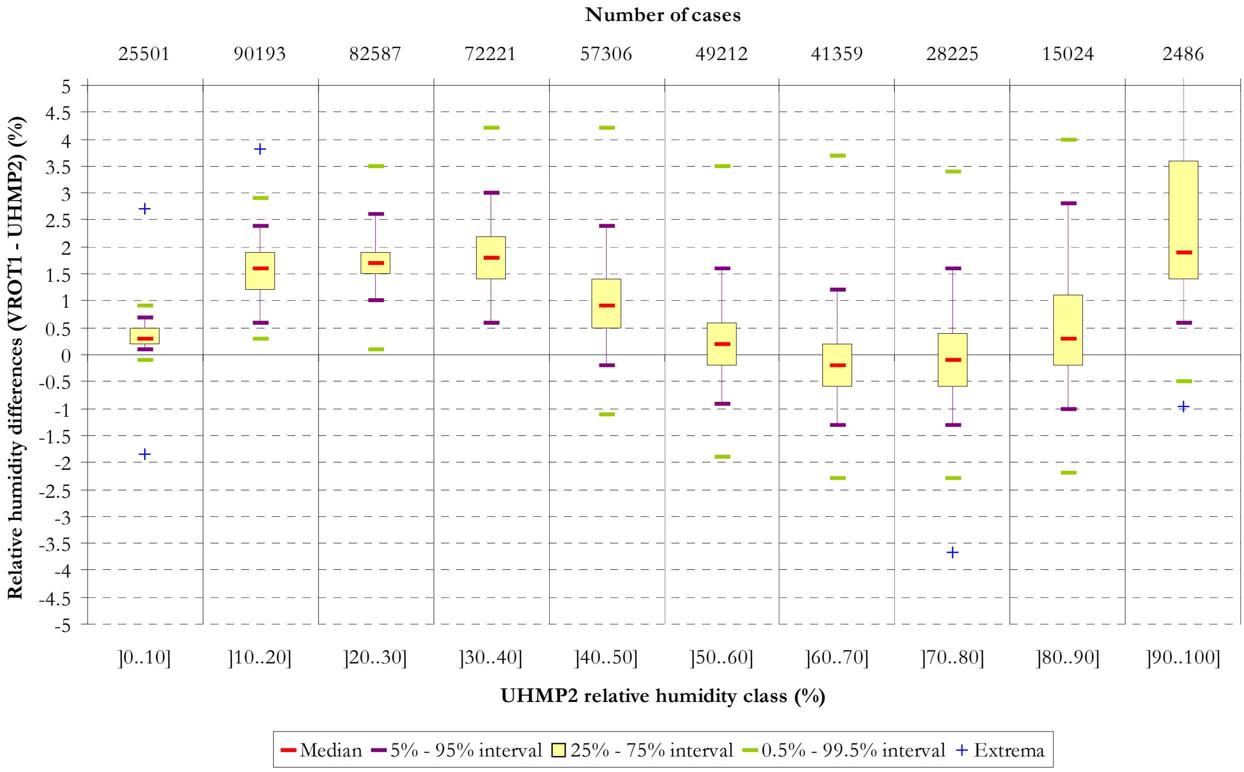


**Figure 7**

The behaviour of VROT1 seems to depend on the relative humidity. The differences with VTHY2 references decrease when humidity increases.

The differences with UHMP2 reference are stable in the humidity range of ]10..40%]. For higher humidity values until 70%, differences decrease. Above 70%, differences increase.

The high values for the last class are probably due to the UHMP2 reference that underestimates high humidity values by 2%.

## INFLUENCE OF TEMPERATURE

The distributions of differences between VROT and the references are plotted, using 1-minute quality checked data for the whole period of the intercomparison. Differences are classified according VEIG22 temperature.

Sensor #1:

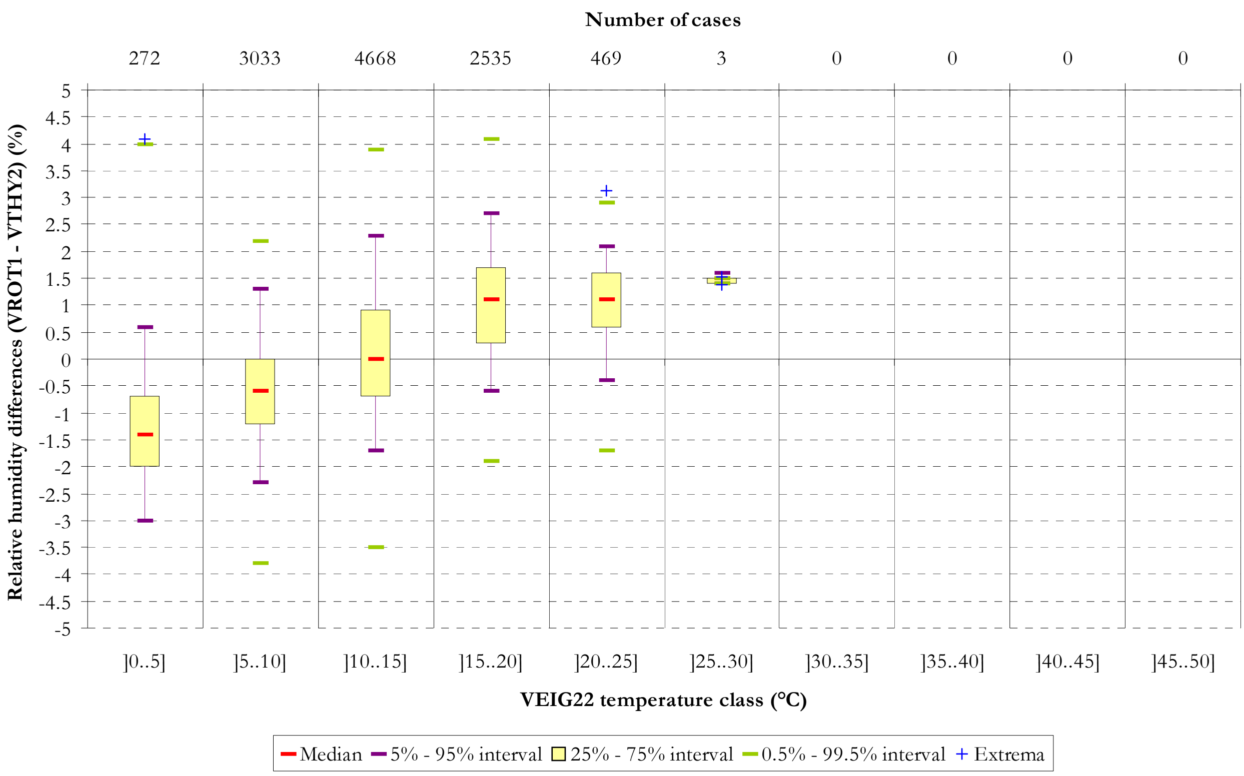


**Figure 8**

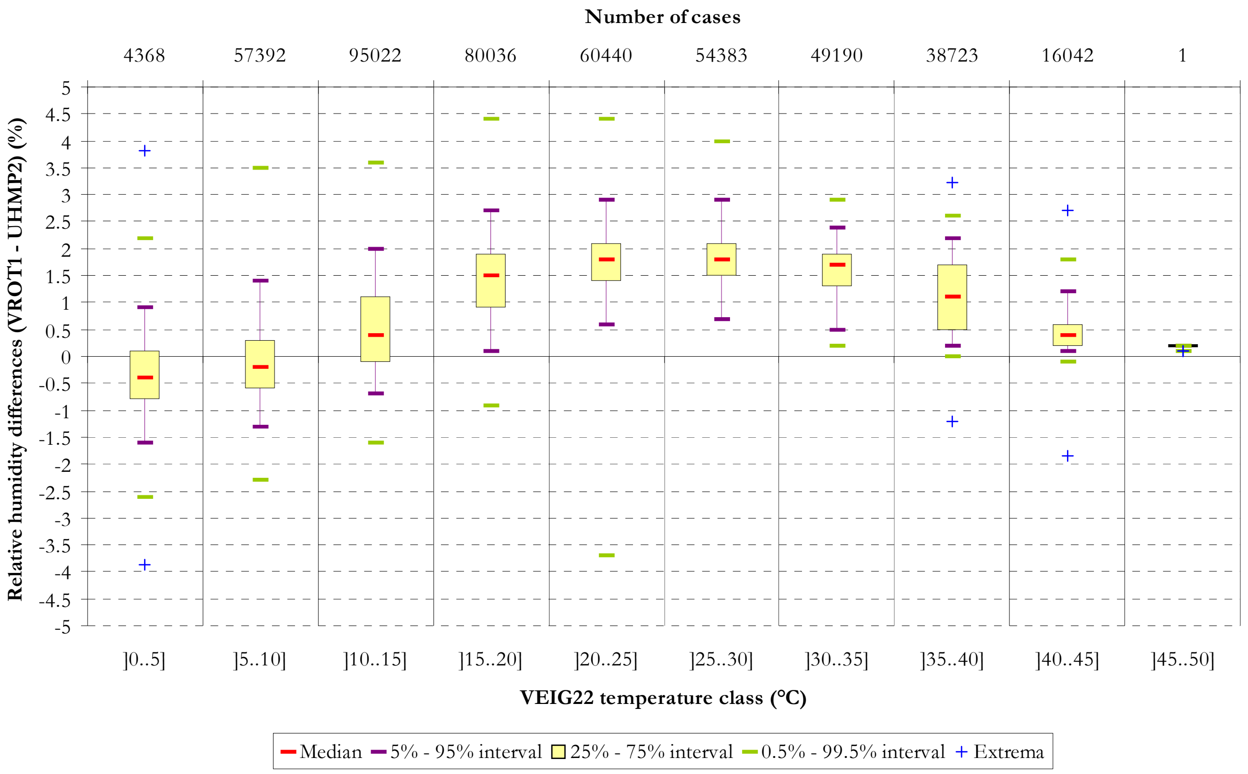


**Figure 9**

The differences depend on temperature: they are much higher between 15 and 35 or 40°C than for other temperatures. The figure 11 shows the relative humidity by VROT1 (green curve) and the UHMP2 reference (purple curve) in the top view, and, the VEIG22 temperature in the bottom view. Both humidity curves perfectly fit when temperature is below 15°C. There is a shift between them when temperature exceeds 15°C.

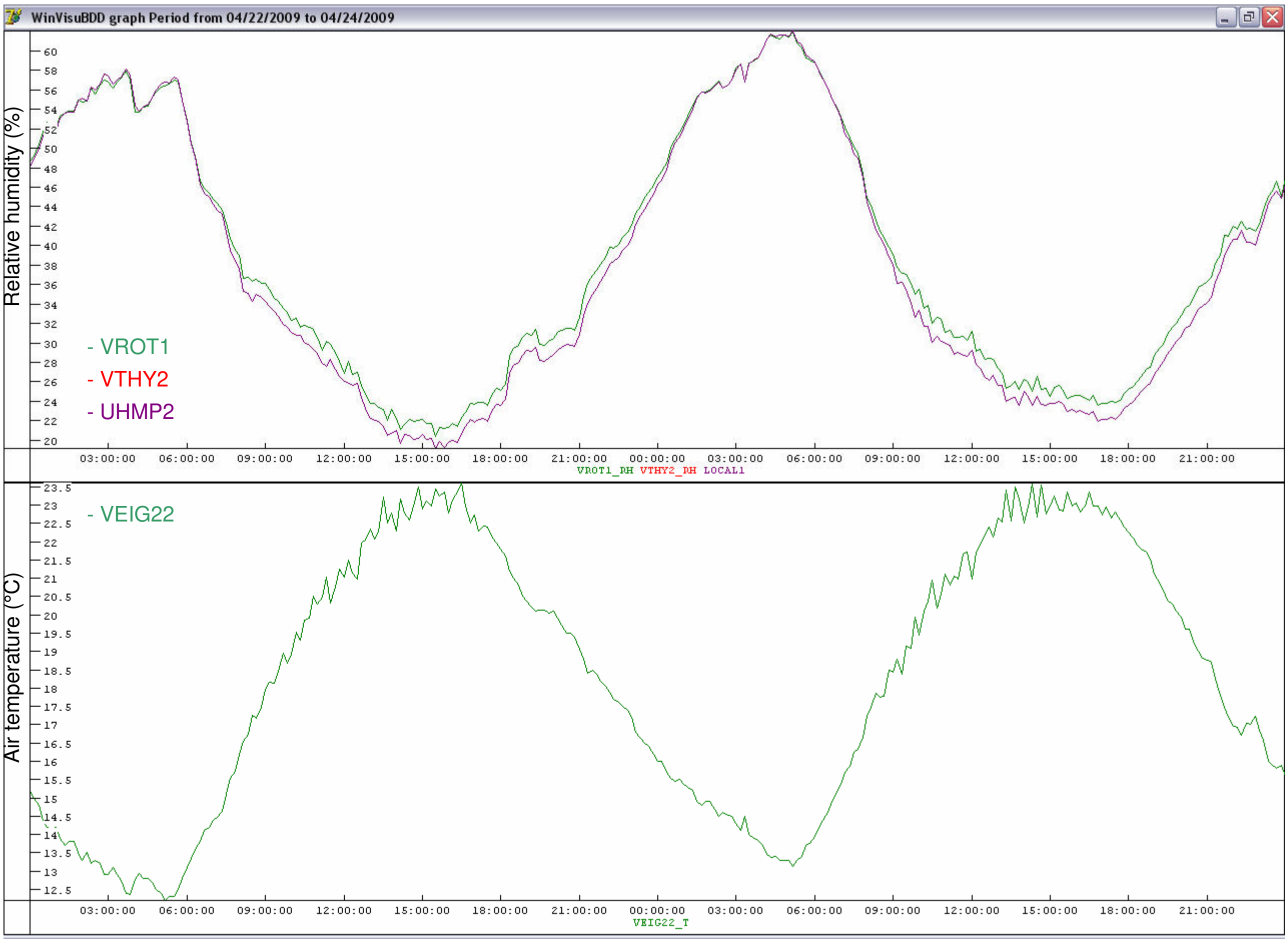


**Figure 10**

In June 2009, when temperatures are between 25 and 40°C, the curves are shifted all day long (cf. figure 11).

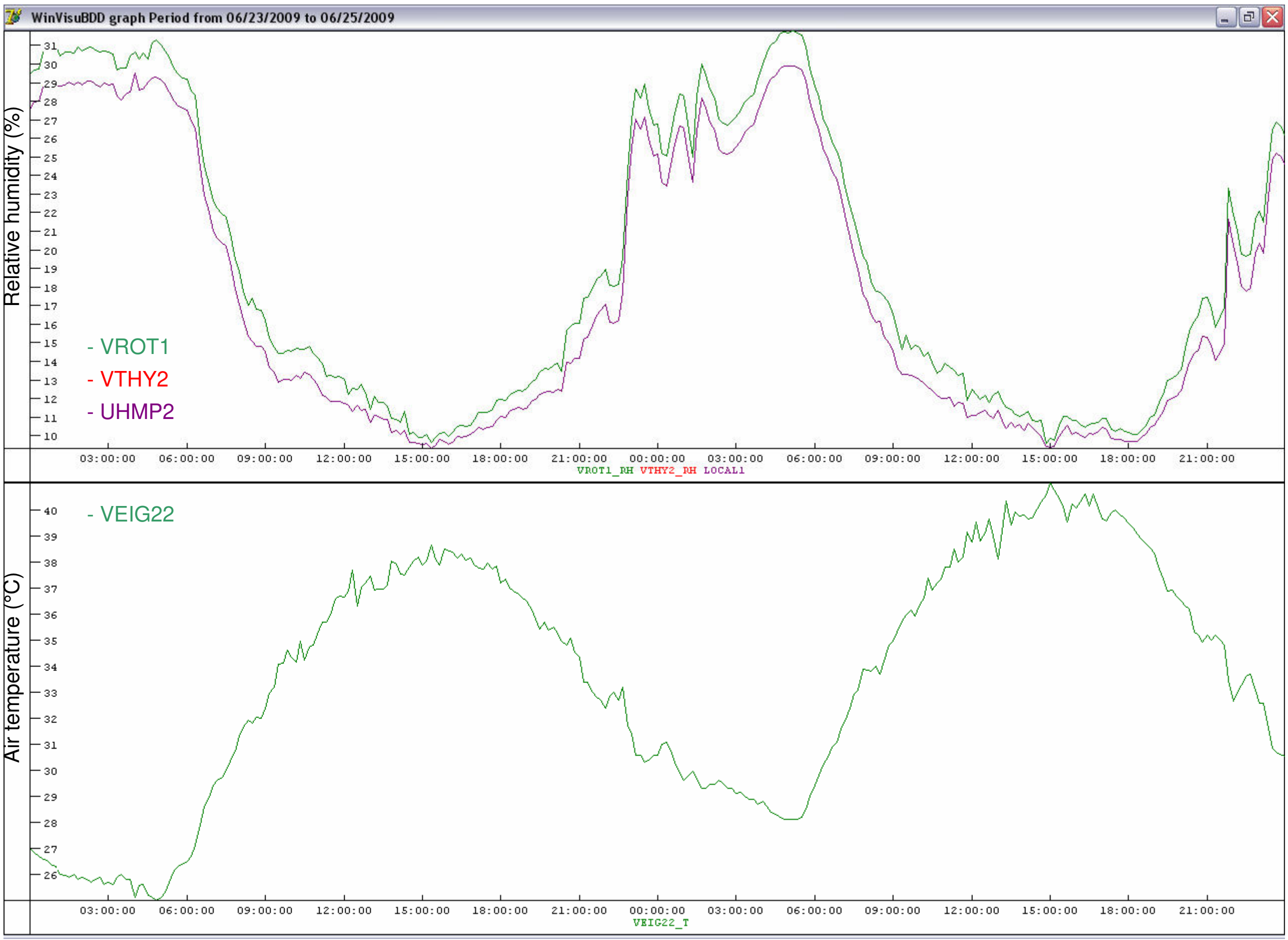


**Figure 11**

## COMBINED INFLUENCE OF TEMPERATURE AND RELATIVE HUMIDITY

The medians of differences between VROT and UHMP reference are represented here with a contour plot. The VEIG22 temperature is on the X-axis and the reference relative humidity is on the Y-axis. Medians are used in all cases, provided that at least one data is available for both conditions on temperature and humidity considered.

The scale was chosen so as to be the same for all relative humidity sensors.

Sensor #1:

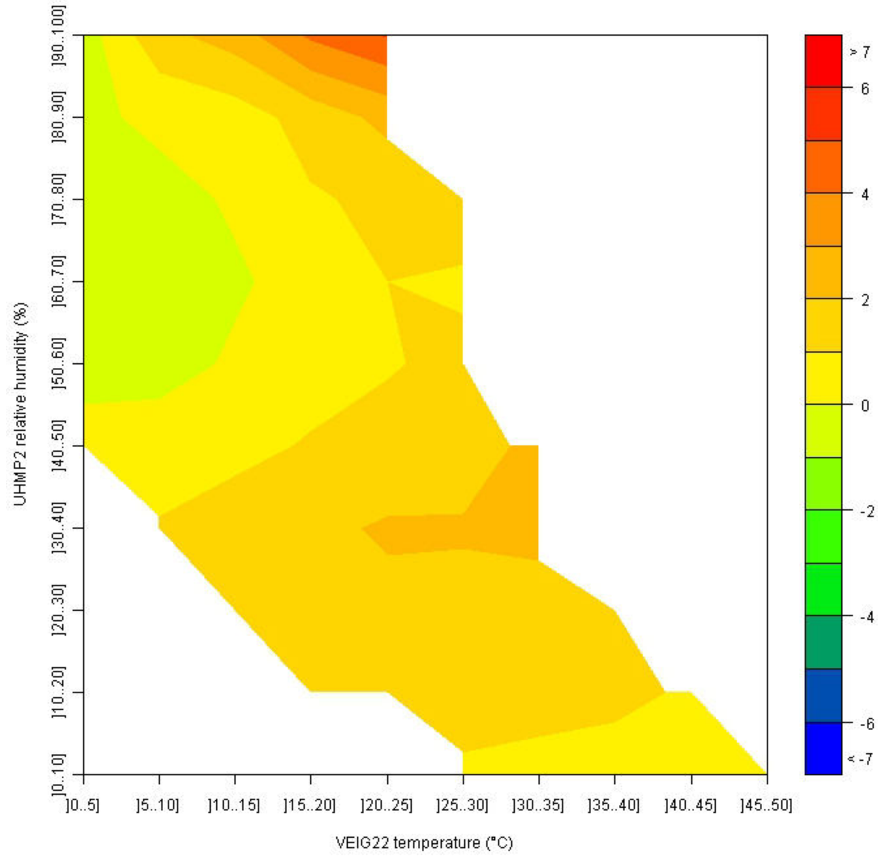


**Figure 12**

The highest differences are obtained for high humidity values and temperatures between 15 and 25°C.

## TIME DRIFT

The distributions of differences between VROT and the references are plotted, using 1-minute quality checked data for the whole period of the intercomparison, by step of one month. Reference relative humidity between 20% and 50% are only considered here: this is the common range in order to have data every month, without introducing influence of humidity itself.

Sensor #1:

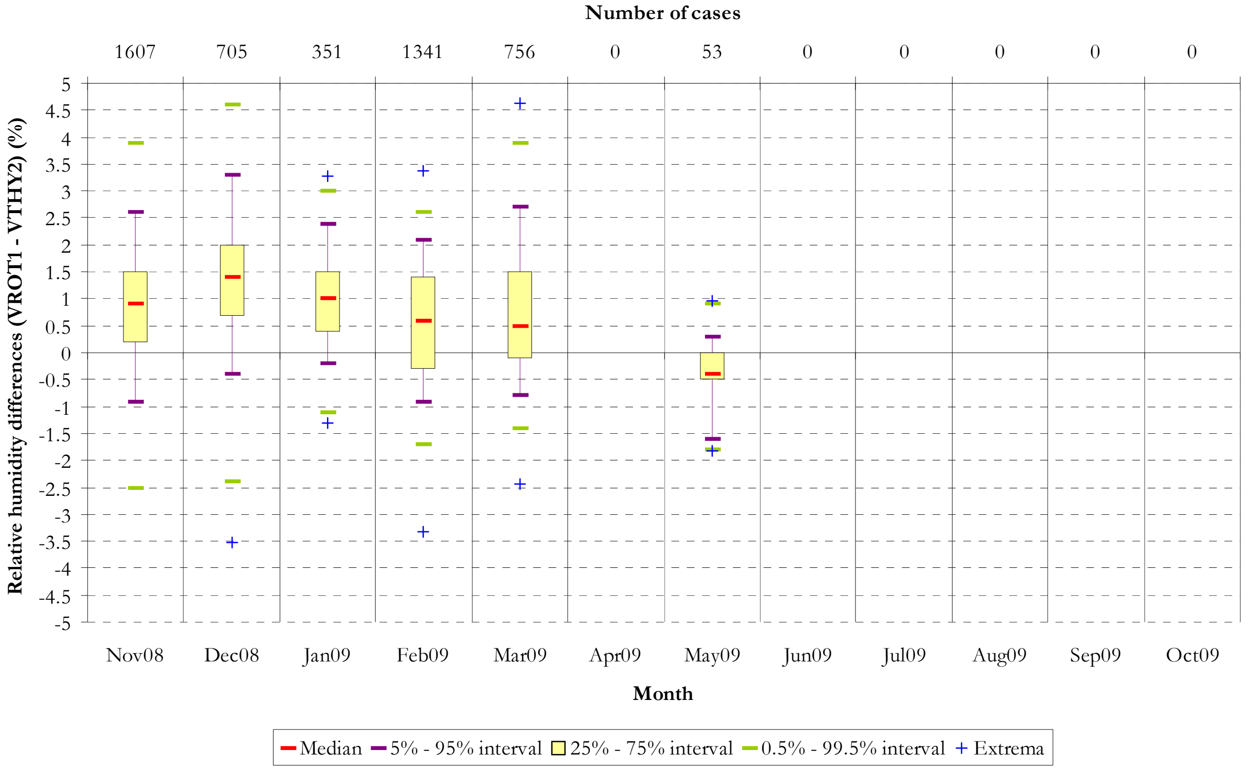


**Figure 13**

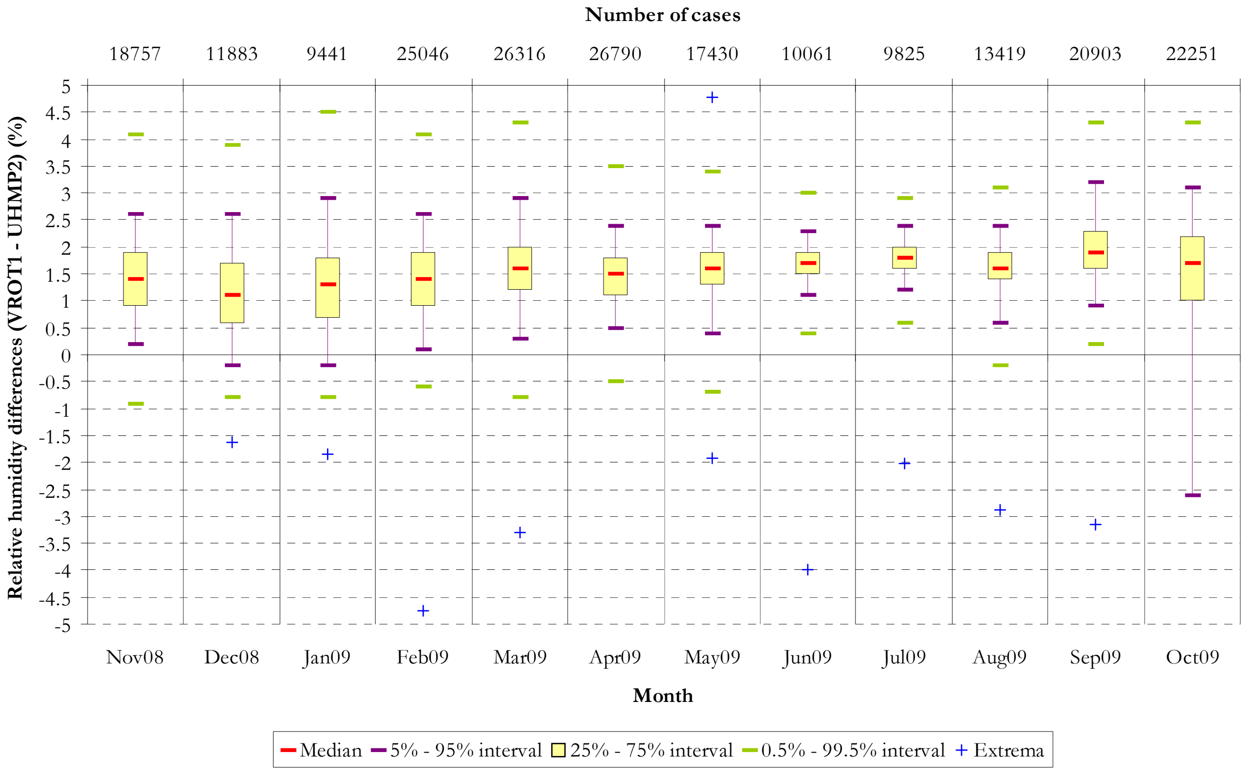


**Figure 14**

Distributions of differences are quite stable all year long. The last one is very similar to the first one, so no drift is detected.

## QUALITY CONTROL INFORMATION

DATA AVAILABILITY

The intercomparison period extends from the 1st of November 2008 to the 1st of November 2009. The theoretical number of 1-minute data is 525600.

The table 4 sums up the total number of data for each sensor and for each possible QC flag.

**Table 4**

| QC flag | VROT1 | VROT2 |
|---|---|---|
| 0 (good) | 503414 | 445162 |
| 1 (inconsistent) | 0 | 0 |
| 2 (doubtful) | 16 | 3073 |
| 3 (erroneous) | 3375 | 45417 |
| 7 (missing) | 18795 | 31948 |

MAINTENANCE

No actions done on these sensors during the intercomparison period.

# TU 20 AS CAE
# – Italy –
# SCAE

## TECHNICAL SPECIFICATIONS (PROVIDED BY THE MANUFACTURER)

Dimensions: Length 28cm x Width 28 cm x Height 27 cm
Principle of operation: capacitive sensor
Accuracy: ± 2 % RH (0…100% RH) at 25°C
Power supply: 12 V
Outputs: 1 output 0..1V


**Figure 1**

## OVERVIEW

This screen has a double shield to protect the sensors against the radiation. To improve the natural ventilation, the external shield is partly opened in one direction and must be oriented towards north (in northern hemisphere), to avoid any direct solar radiation on the internal shield.

Though this constraint was indicated in the documentation, the two sensors were mistakenly oriented towards south and the results obtained are not significant at all for the temperature measurements. The internal temperature inside the screen being not considered as valid, the internal relative humidity can be also be strongly affected (for a same dew point temperature, the relative humidity is affected by a change of the air temperature, see figure 57 in §5.5.2.1 of the main report).

Therefore, it was decided in agreement with the manufacturer to skip any data from these screens and the results, non significant at all of this equipment, are excluded from this report, both for temperature and relative humidity.